



SCUOLA
NORMALE
SUPERIORE

Ph.D. Course in Neurobiology

Ph.D. Thesis

***In Vitro* Neural Differentiation of Mouse Embryonic Stem Cells:
The Positional Identity of Mouse ES-generated Neurons
Is Affected by BMP, Wnt and Activin Signaling**

Candidate:

Michele Bertacchi

Tutor:

Federico Cremisi

*“What is perhaps the most intriguing question of all
is whether the brain is powerful enough
to solve the problem of its own creation”*

Gregor Eichele, 1992

Index

Introduction

1–Pluripotent Embryonic Stem Cells: Criteria and Definitions.....	13
2–The Emergence of the Ectoderm: Formation of the Neural Plate and Neural Tube.....	23
3–Neural Induction and Antero-Posterior Axis Formation.....	33
Progressive Determination of the Amphibian Axes: the Organizer and the Primary Embryonic Induction.....	34
The Formation of the Organizer.....	40
Molecular Mechanisms of Amphibian Axis Formation: BMP-inhibitors Mediate the Induction of Neural Ectoderm and Dorsal Mesoderm.....	43
Regional Specificity of Neural Induction.....	50
4–Mammalian Axis Formation	60
Two Signaling Centers: the Node and the Anterior Visceral Endoderm.....	60
Anterior-Posterior Patterning: Wnt, FGF and Retinoic acid Gradients.....	64
5–Tissue Architecture of the Central Nervous System: Development of the Cerebral Cortex.....	67
Cerebral organization.....	71
Cortical cell migration.....	73
6–Development of the Vertebrate Eye.....	78
Formation of the Eye Field.....	79
Cell Differentiation in the Vertebrate Eye.....	83

7–Focus on BMP.....	86
A Well-known Role in Neuralization and a Possible Role in Brain Patterning.....	86
8–An in Vitro Approach.....	89
Neural Differentiation Protocols Using Embryonic Stem Cells.....	89
Embryoid-body Based Protocols.....	90
Stromal Feeder Mediated Neural Induction	93
Neural Differentiation by Default	95
Studying Patterning Signals during Neural Differentiation in Vitro.....	97
9–Focus on Cortical Differentiation in Vitro.....	99
10–Focus on Retinal Differentiation in Vitro: high efficiency protocols, poor mechanism comprehension.....	105
11–Focus on Activin.....	112
12–Aim of research.....	117

Materials and Methods

1–Materials and Methods.....	123
Cells cultures.....	123
Neural induction.....	124
Semiquantitative real-time PCR.....	126
Immunocyto detection.....	126
BMP2 ELISA.....	127
FACS analysis.....	128
Microarray hybridization and data analysis.....	128
List of primers for Real Time RT-PCR.....	130

Markers for the study of brain patterning.....	133
--	-----

Results and Discussion

1–A Novel Neural Induction Protocol.....	139
Chemically Defined Minimal Medium (CDMM)	
Allows Efficient Neurogenesis of Embryonic Stem (ES) Cells.....	139
2–Endogenous Morphogen Expression.....	149
Mouse ES Cells Express Wnt, BMP and FGF Morphogens	
During in vitro Neural Differentiation.....	149
3–A BMP Story.....	159
Simple Neural Induction or Brain Patterning?.....	159
Effects of Noggin as a Neural Inducer in ES Cells Culture.....	160
CDMM-Differentiating ES Cells Produce and Respond to BMPs.....	164
In the Absence of Exogenous Signals, ES Cells Generate Neurons Expressing Midbrain	
Dorsal Markers.....	169
BMP Inhibition During Differentiation Supports the Expression of Telencephalic Markers.	
.....	173
4–The Making of a Cortex: Wnt vs. BMP.....	195
Efficient Corticogenesis in vitro by Double Inhibition	
of Endogenously Produced BMP and Wnt Factors.....	195
5–Anterior Brain Patterning.....	210
How to Make a Retina	
Playing with BMP, Wnt and Activin/Nodal Pathways.....	210
6–BMP and Anterior Brain Patterning.....	263
A Possible Role for BMP as a Retinal Inducer.....	263
7–Dorso-Ventral Patterning of the Diencephalon.....	269
How to Control the Dorso-Ventral Identity of Diencephalic Progenitors	
Playing with Shh Pathway.....	269

8–Terminal Differentiation of Retinal Cells.....	283
Efficient Differentiation of Retinal Cells by Prolonged Manipulation of Wnt and Activin/Nodal Pathways.....	283

Conclusions

1–Conclusions.....	295
Translating the Notion of the Default Model into an in Vitro Model of Neural Induction and Patterning.....	295
A Plastic and Handy System to Work with: ES Cells Recapitulate in vitro the Major Milestones of Brain Development in vivo.....	297
Endogenously Produced BMPs and Brain Patterning: BMP Activity Regulates Regional Differences in Embryonic Fore-Midbrain.....	299
A Novel Protocol for Cortical Induction: A Comparison with Already Established Protocols.....	301
The Inhibition of Endogenously Produced Wnts: A Must for Optimal ES Cell Cortical Conversion.....	302
What is Old and What is New: Activin as an Inducer of Retinal Identity.....	304
Retina vs. Ventral Diencephalon: Shh and Activin Switch-on Different Kinds of Rax Expression.....	307

Bibliography

1–References.....	313
--------------------------	------------

Acknowledgments

1–Special Thanks.....341

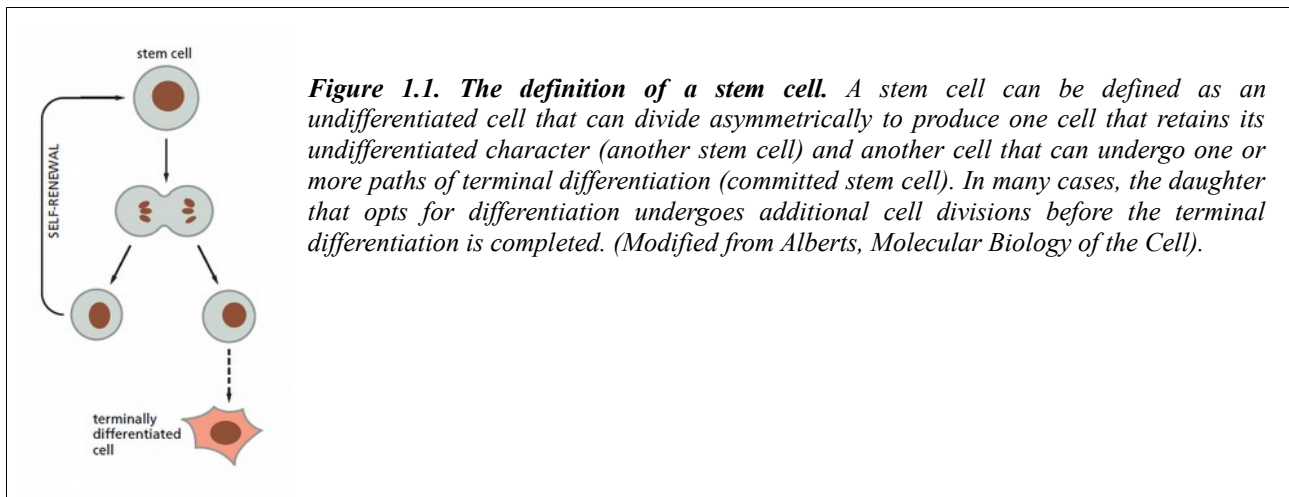


Introduction

1– Pluripotent Embryonic Stem Cells: Criteria and Definitions

Embryonic stem (ES) cells are derived from the inner cell mass (ICM) of an embryo at the blastocyst stage and have the extraordinary capacity to differentiate into every cell type of the adult body. For this reason, ES cells have been considered promising sources in cell transplantation therapies for various diseases and injuries, such as spinal cord injury, neurodegenerative diseases and myocardial infarction. In this introduction chapter, I will briefly describe the principal characteristics of embryonic stem cells, focusing on **replication capacity**, **clonality**, and **potency**.

ES cells are defined as cells that have the capacity to proliferate rapidly and self-renew, while maintaining pluripotency, which is the ability to differentiate into all cell types of the adult body. Through an asymmetric cell division, stem cells can generate daughter cells identical to their mother (*self-renewal*) as well as produce progeny with more restricted potential (*committed progenitor cells*) (**Figure 1.1**). The self-renewal capacity assures a supply of stem cells for the tissue homeostasis. However, stem cells can also divide symmetrically: in this case both daughter cells maintain the potential and the self-renewal capacity of the mother cell.



Most somatic cells cultured *in vitro* display a finite number (often less than 80 in both human and mouse cell lines) of population doublings prior to senescence or replicative arrest/differentiation. On the contrary, stem cells in culture display a seemingly unlimited **proliferative capacity**. Therefore, it is reasonable to say that a cell that can undergo more than twice this number of population doublings (160) without oncogenic transformation can be termed “capable of extensive proliferation.” In a few cases, this criteria has been met, most notably with embryonic stem (ES) cells, derived from either humans or mice, as well as with adult neural stem cells (NSCs).

A second parameter, perhaps the most important characteristic of ES cells, is the idea that stem cells are **clonogenic entities**, that is single cells with the capacity to create more stem cells (**Figure 1.2**).

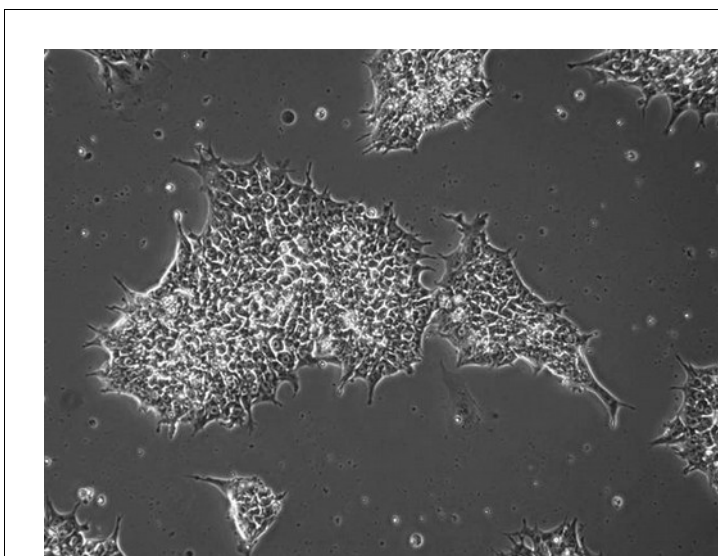
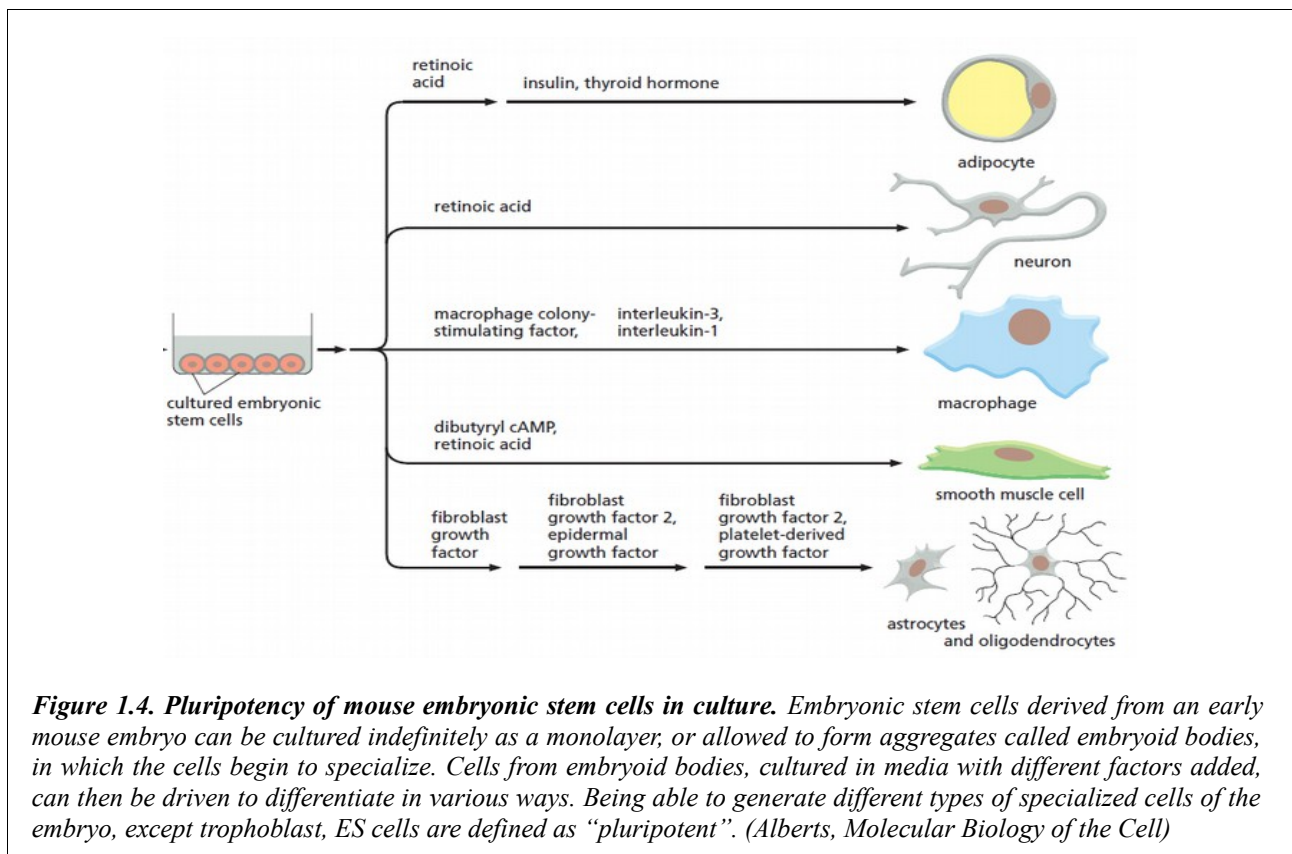
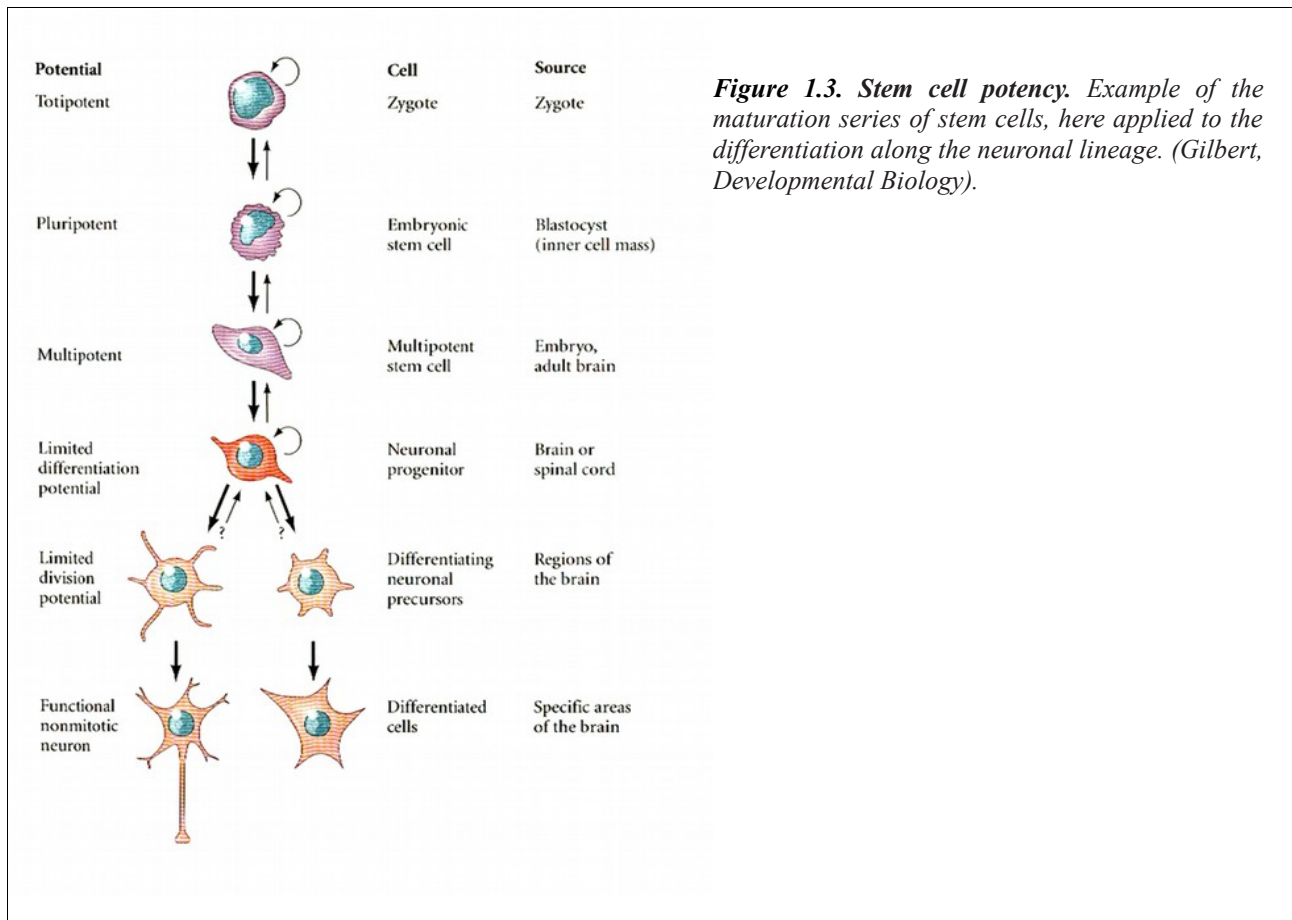


Figure 1.2. Clonality of mammalian ES cells in culture. ES cells derived from an early mouse embryo can be cultured indefinitely as a monolayer. When they reach confluence, they must be detached and replated to avoid the loss of pluripotency; single cells are able to proliferate and originate ES cell colonies (photo). A culture medium containing serum and the cytokine Leukemia Inhibitory Factor (LIF) allows to maintain embryonic stem cells in an undifferentiated state. (Image credit: <http://www.c-mtechnologies.com>).

Another characteristic that should be considered is **potency** (*Figure 1.3*), that is the ability of a particular stem cell to generate numerous different types of differentiated cells.

- In mammals, **totipotent stem cells** are capable of forming every cell in the embryo and, in addition, the trophoblast cells and the placenta. The only totipotent cells are the zygote and (probably) the first 4-8 blastomeres to form prior to compaction. By the time the zygote has reached the blastocyst stage, the developmental potential of certain cells has been restricted: the outer cells of the embryo have begun to differentiate to form the trophectoderm.
- For this reason ES cells coming from the inner cell mass of the blastocyst, being no longer able to generate the trophoblast lineage, are considered **pluripotent stem cells** and no more totipotent cells. Thus, pluripotent cells have the ability to become all the cell types of the embryo (*Figure 1.4*), except trophoblast. Some special types of pluripotent cells can be obtained from germ cells and tumors (such as teratocarcinomas).
- **Multipotent stem cells** are stem cells whose commitment is limited to a relatively small subset of all the possible cells of the body. A multipotent stem cell sits atop a lineage hierarchy and can generate multiple types of differentiated cells, each with distinct morphologies and gene expression patterns. Multipotent stem cells are usually adult stem cells, which are found in the tissues of organs after the organ has matured. These stem cells are usually involved in replacing and repairing tissues of that particular organ. The hematopoietic stem cell, for instance, can form the granulocyte, platelet, and red blood cell lineages.
- Some adult stem cells are **unipotent stem cells**, which are found in particular tissues and are involved in regenerating a particular cell type. Whereas pluripotent stem cells can produce cells of all three germ layers (as well as producing germ cells), the multipotent and unipotent stem cells can be considered committed stem cells, since they have the potential to become relatively few cell types.
- A self-renewing cell that can only produce one type of differentiated descendant (unipotent stem cell) is very similar to (and can be confused with) a **progenitor cell**. However, progenitor cells are not capable of unlimited self-renewal; they have the capacity to divide only a few times before terminal differentiation. Progenitors are typically the descendants of stem cells, only they're more constrained in their differentiation potential or capacity for self-renewal and are often more limited in both senses.



In conclusion, the basic characteristics of ES cells include self-renewal, multi-lineage differentiation both *in vitro* and *in vivo*, clonogenicity, a normal karyotype, extensive *in vitro* proliferation under well-defined culture conditions, and the ability to be repeatedly frozen and thawed.

At a molecular level, ES cells are characterized by the expression of pluripotency markers, Oct4, Nanog, Klf4 and Sox2, which have been demonstrated to be fundamental for the maintenance of an undifferentiated state. Especially Oct4 and Nanog are crucial components of the genetic circuitry necessary and sufficient to maintain ES cells in an undifferentiated state of pluripotency (Mitsui et al., 2003; **Figure 1.5**).

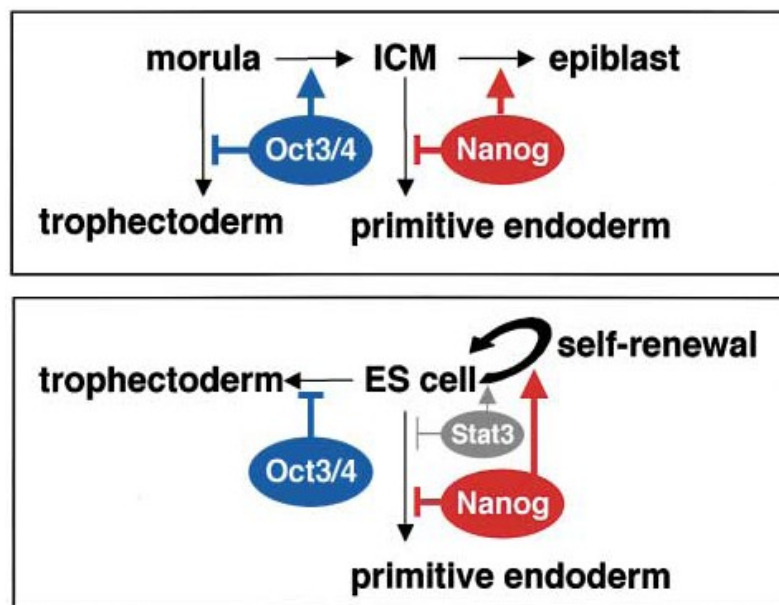


Figure 1.5: Proposed functions of Nanog and Oct4 in preimplantation embryos (upper) and ES cells (lower). Homeoprotein Nanog can maintain self-renewal and pluripotency in both ICM and ES cells independently of the LIF/gp130/Stat3 pathway. The primary function of Oct3/4 is to prevent trophectoderm differentiation of ICM and ES cells. In contrast, Nanog independently prevents differentiation into extraembryonic endoderm and actively maintains pluripotency. ES cells derived from ICM require both Oct3/4 and Nanog to prevent differentiation into trophectoderm and primitive endoderm, respectively. However, a normal expression level of these two transcription factors is not sufficient for prolonged ES cell self-renewal. Additional factor(s), such as Stat3 activated by LIF, are required to support extended maintenance of pluripotency. (Mitsui et al., 2003).

Additionally, Oct4, Klf4 and Sox2, have been demonstrated to be fundamental for the induction of pluripotency in adult somatic stem cells (*reprogramming*), to obtain induced pluripotent stem (IPS) cells (Takahashi and Yamanaka, 2006). Among other markers of an undifferentiated state, Alkaline Phosphatase (AP) and SSEA-1 are often used to evaluate pluripotency.

Mouse and human ES cells are derived directly from the inner cell mass of preimplantation embryos after the formation of the blastocyst (**Figure 1.6**). This population of cells would normally produce the epiblast and then all adult tissues. ES cells appear to be the *in vitro* equivalent of the epiblast, as they have the capacity to contribute to all somatic lineages and to produce germ line chimeras in mice.

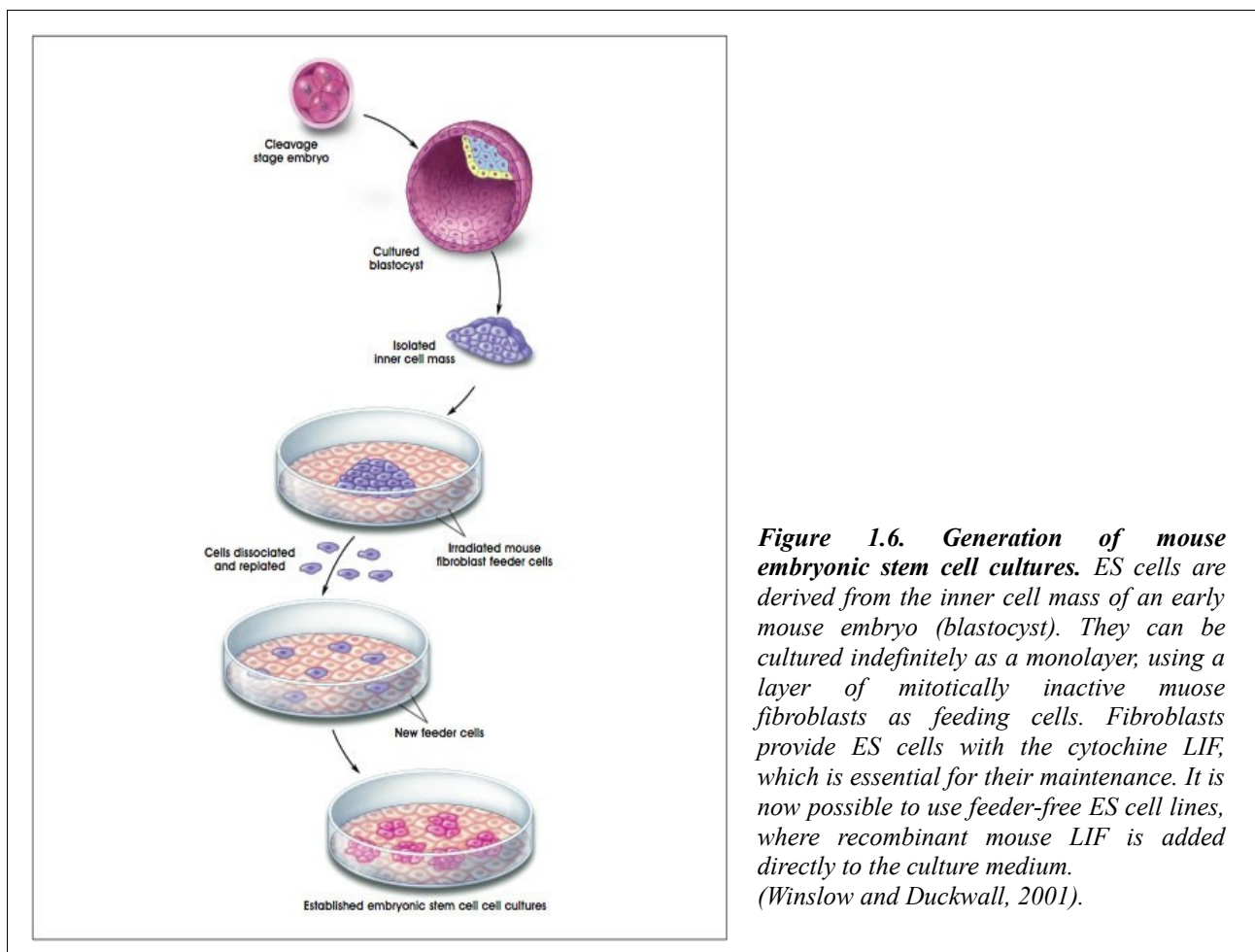


Figure 1.6. Generation of mouse embryonic stem cell cultures. ES cells are derived from the inner cell mass of an early mouse embryo (blastocyst). They can be cultured indefinitely as a monolayer, using a layer of mitotically inactive mouse fibroblasts as feeding cells. Fibroblasts provide ES cells with the cytokine LIF, which is essential for their maintenance. It is now possible to use feeder-free ES cell lines, where recombinant mouse LIF is added directly to the culture medium. (Winslow and Duckwall, 2001).

The critical *in vivo* test for pluripotency is whether the cells yield widespread, if not ubiquitous, somatic and germ line chimerism in offspring following introduction into the early embryo, either by injection into standard blastocysts or aggregation with morulae. ES cell genome can be altered during *in vitro* culture, by the addition of a cloned gene and a resistance gene for selection via antibiotic treatment, prior to injection in a host mouse embryo. For this reason, chimera generation can be considered not only a test for ES cells pluripotency, but also a useful tool for the study of genes in transgenic mice (**Figure 1.7**).

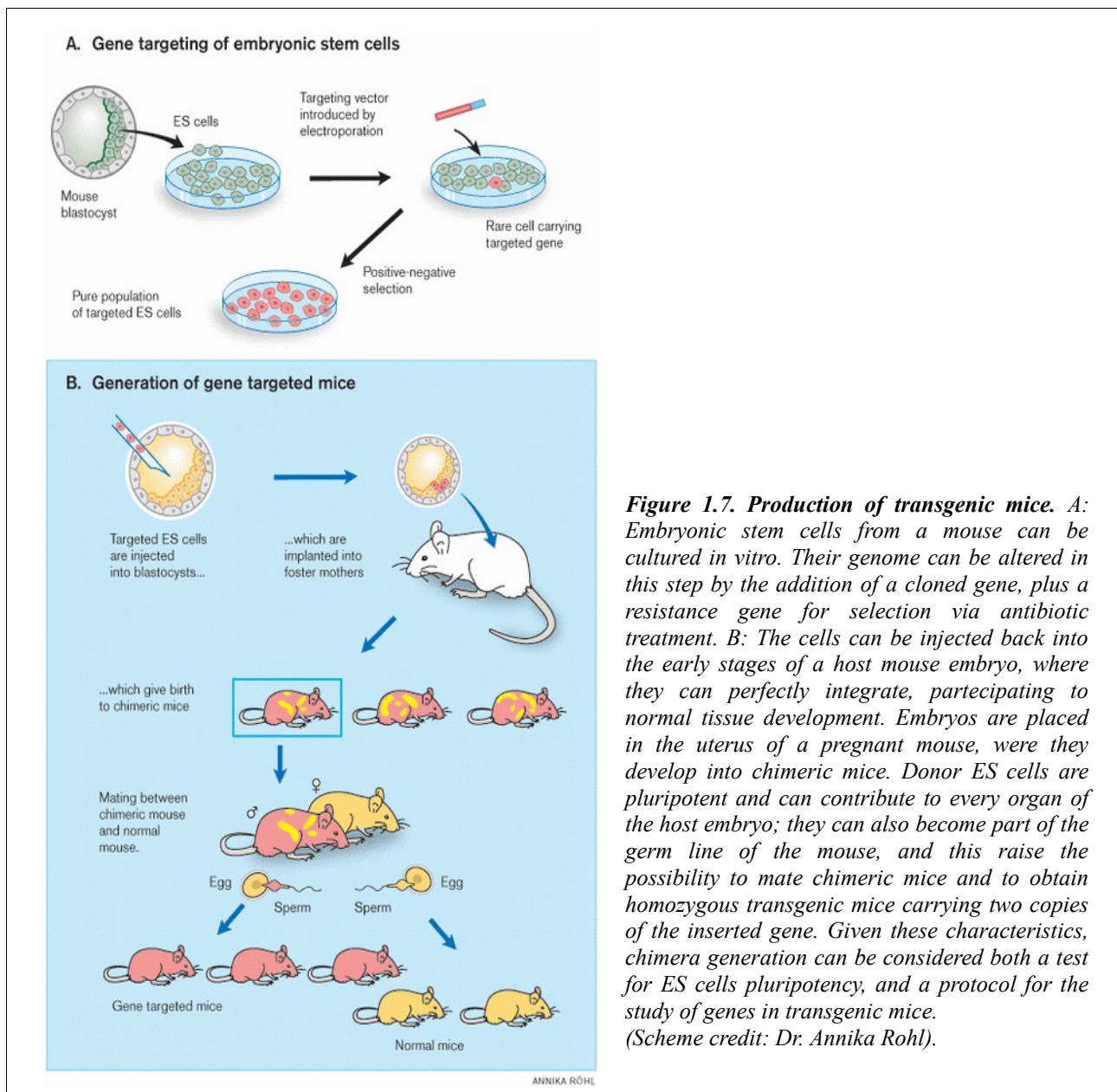
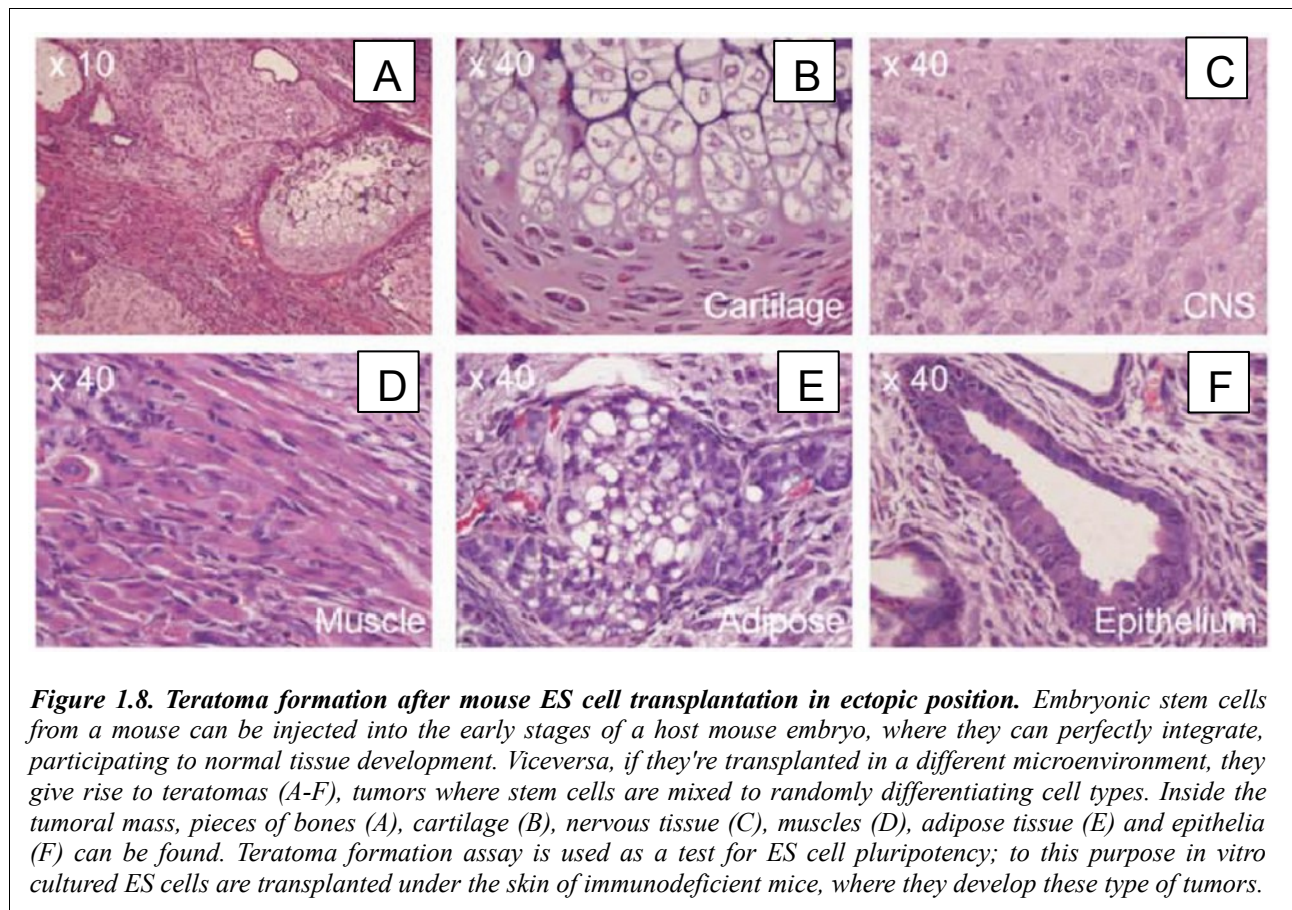


Figure 1.7. Production of transgenic mice. *A: Embryonic stem cells from a mouse can be cultured in vitro. Their genome can be altered in this step by the addition of a cloned gene, plus a resistance gene for selection via antibiotic treatment. B: The cells can be injected back into the early stages of a host mouse embryo, where they can perfectly integrate, participating to normal tissue development. Embryos are placed in the uterus of a pregnant mouse, where they develop into chimeric mice. Donor ES cells are pluripotent and can contribute to every organ of the host embryo; they can also become part of the germ line of the mouse, and this raise the possibility to mate chimeric mice and to obtain homozygous transgenic mice carrying two copies of the inserted gene. Given these characteristics, chimera generation can be considered both a test for ES cells pluripotency, and a protocol for the study of genes in transgenic mice. (Scheme credit: Dr. Annika Röhl).*

Another important assay to test ES cell pluripotency is the formation of **teratomas**. *In vitro* cultured ES cells are transplanted under the skin (ectopic graft) of histocompatible or immunosuppressed adult mice. In this case, ES cells develop a teratoma, a tumor where stem cells are mixed to randomly differentiating cell types, such as pieces of bones, nervous tissue, muscles and epithelia (**Figure 1.8**).



These criteria to test pluripotency are not appropriate for human ES cells, where chimerism cannot be tested; consequently, these cells must be tested to be able of differentiating in multiple cell types *in vitro* by using embryoid body-based differentiation protocols. Additionally, they must be tested to be able of generating teratomas when injected under the skin of immunodeficient mice; teratomas must be containing differentiated cells of all three germ layers. Moreover, as a stringent *in vivo* assessment of pluripotency is impossible, human ES cells must be shown to be positive for well-known molecular markers commonly used to characterize mouse pluripotent stem cells.

Mouse pluripotent embryonic stem (ES) cells are usually derived and maintained by using various empirical combinations of feeder cells, conditioned media, cytokines, growth factors, hormones, fetal calf serum, and serum extracts. ES-cell self-renewal is generally considered to be dependent on the activation of STAT3 by LIF (Leukemia inhibitory factor, a cytokine). ES cells cultured in serum containing medium are not homogeneous, and consist of a mixed population of Oct4-positive and Nanog-positive naïve pluripotent stem cells and Oct4-positive Nanog-negative stem cells, this latter type being already primed for differentiation (**Figure 1.9**).

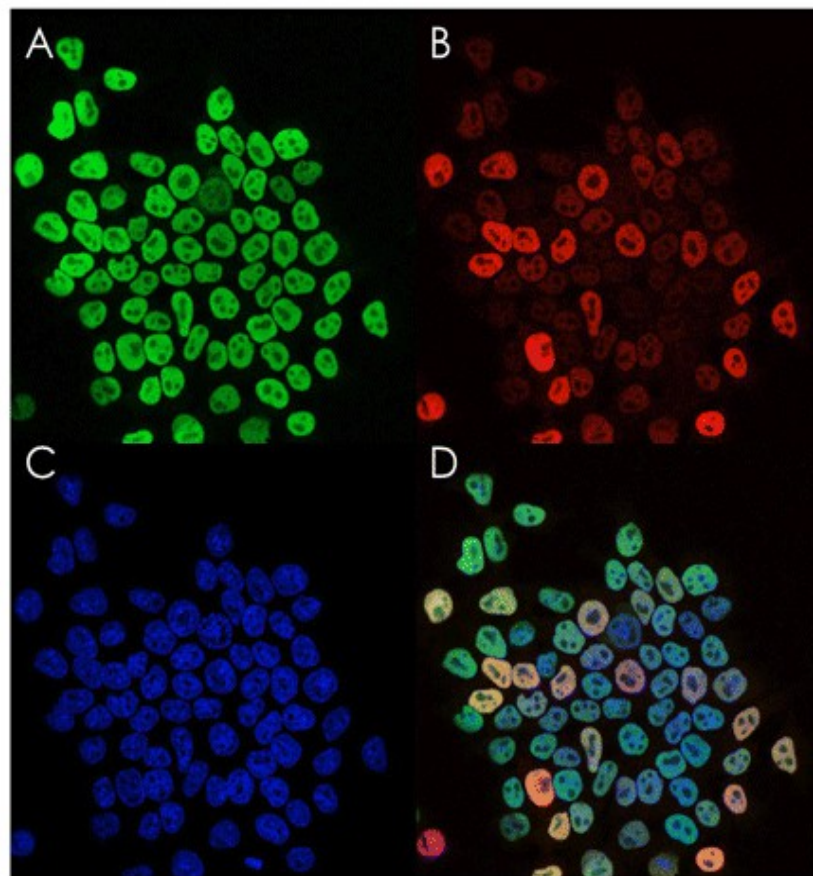


Figure 1.9. Markers of ES cell pluripotency. A-D: Immunofluorescence staining for Oct4 (A) and Nanog (B), and nuclear staining with DAPI (C); D shows an overlay of A-C. Oct4 and Nanog are crucial components of the genetic circuitry necessary and sufficient to maintain ES cells in an undifferentiated state of pluripotency. In mouse ES cells, Oct4 staining appears to be relatively homogeneous, whereas Nanog expression levels differ substantially within individual ES cells. (Image credit: Austin Smith; www.dev.biologists.org).

Austin Smith's laboratory, however, has recently revealed that ES cells have an innate program for self-replication that does not require extrinsic instruction. The authors demonstrated that ES cells in which mitogen-activated protein kinase signaling and glycogen synthase kinase-3 (GSK3) are double-inhibited are homogeneous and pluripotent when cultured in a medium containing LIF but devoid of serum. In this condition, they consist in a pure population of both Oct4 and Nanog-positive naive pluripotent stem cells (Silva et al., 2008; Ying et al., 2008).

2– The Emergence of the Ectoderm: Formation of the Neural Plate and Neural Tube

In the vertebrate embryo, after fertilization, a series of rapid cell divisions (known as cleavages) divides the fertilized egg into blastomeres. The embryo, now called blastula, then undergoes the process of gastrulation, in which the three primary or “germ” layers are formed: the mesoderm, the endoderm and the ectoderm. The fates of the vertebrate ectoderm are shown in *Figure 2.1*. Briefly, the embryo ectoderm will form the neural tissue, the neural crests and the epidermis.

The point of initiation of the gastrulation is identified on the embryo as a small invagination of the smooth surface of the blastula; this is called the blastopore. In amphibians the first cells to invaginate occur at the dorsal site of the blastopore. The involuting cells will ultimately give rise to mesodermal derivatives (muscle and bone). At this point in development, a portion of the dorsal ectoderm is specified to become neural ectoderm, and its cells become distinguishable to surface ectoderm (destined to form the skin) by their columnar appearance and by their molecular characteristics. This region of the embryo is called the **neural plate** (NP), a single-layered pseudostratified epithelium that will form the entire brain (*Figures 2.2 and 2.3*). As much as 50% of the ectoderm is included in the neural plate.

The process of neural induction and neural plate formation begins soon after gastrulation, when neural induction takes place, and the underlying dorsal mesoderm (and pharyngeal endoderm in the head region) signals the ectodermal cells above it to elongate into columnar neural plate cells (Smith and Schoenwolf, 1989; Keller et al. 1992). Subsequently, the NP is divided into domains along the antero-posterior and medio-lateral axes characterized by specific gene expression patterns, which will eventually give rise to brain structures at later stages of development. In the next Chapter, I will describe from the molecular point of view how the ectoderm is instructed to form the vertebrate nervous system and epidermis.

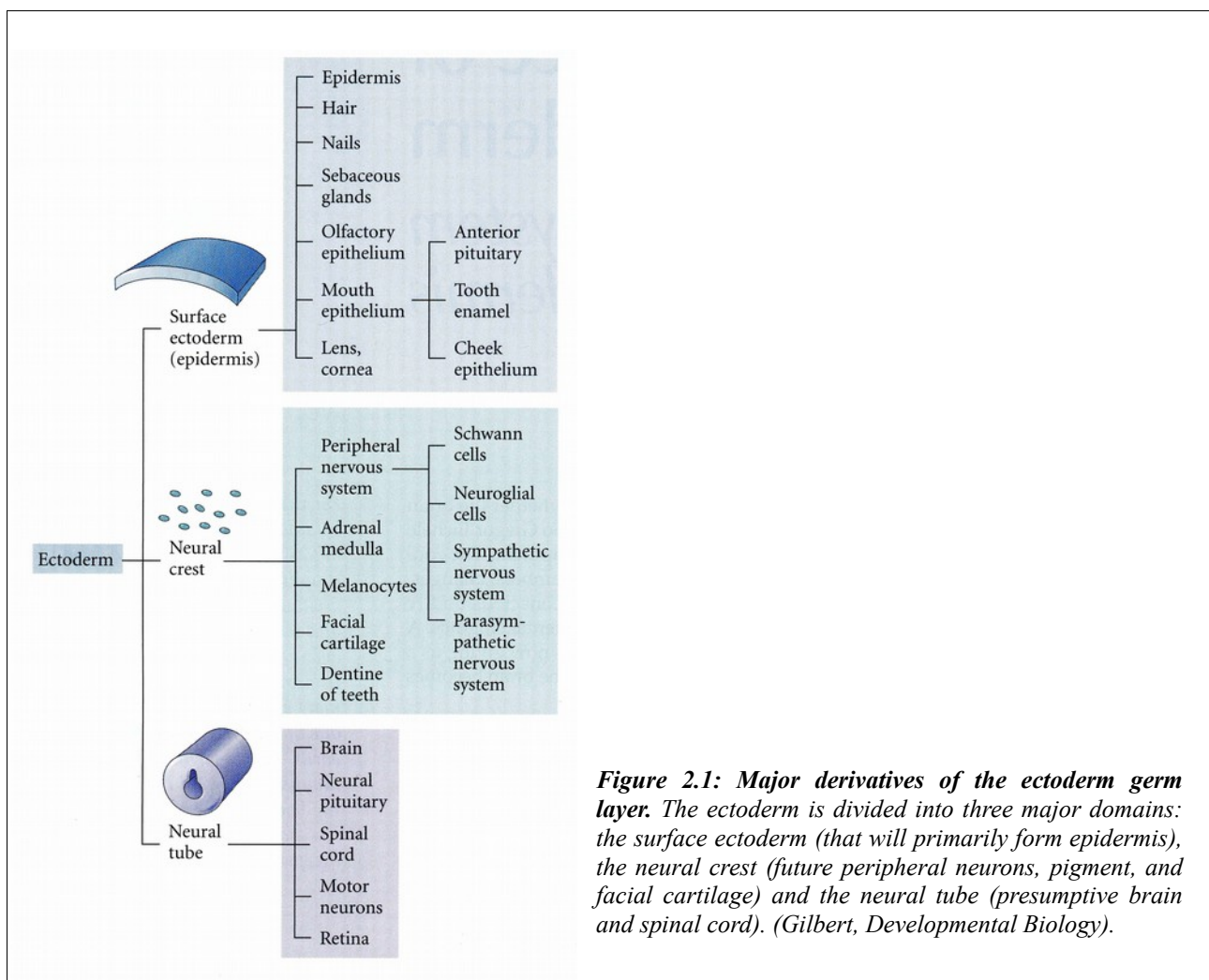


Figure 2.1: Major derivatives of the ectoderm germ layer. The ectoderm is divided into three major domains: the surface ectoderm (that will primarily form epidermis), the neural crest (future peripheral neurons, pigment, and facial cartilage) and the neural tube (presumptive brain and spinal cord). (Gilbert, *Developmental Biology*).

The neural plate is shaped by the intrinsic movements of the epidermal and neural plate regions; it lengthens along the anterior-posterior axis, narrowing itself so that subsequent bending will form a tube. In both amphibians and amniotes, the neural plate lengthens and narrows by convergent

extension, intercalating several layers of cells into a few layers. In addition, the cell divisions of the neural plate cells are preferentially in the **rostral-caudal** (anterior-posterior) direction (Jacobson and Sater, 1988; Schoenwolf and Alvarez, 1989; Sausedo et al., 1997). These events will occur even if the tissues involved are isolated.

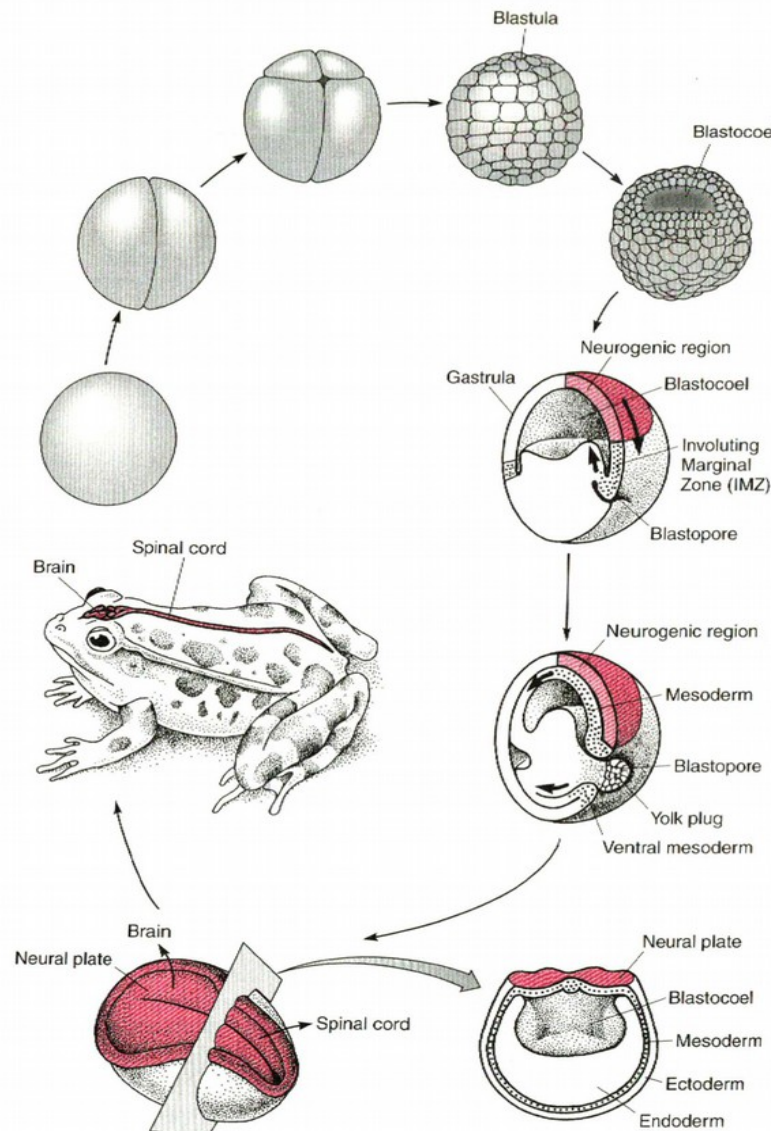
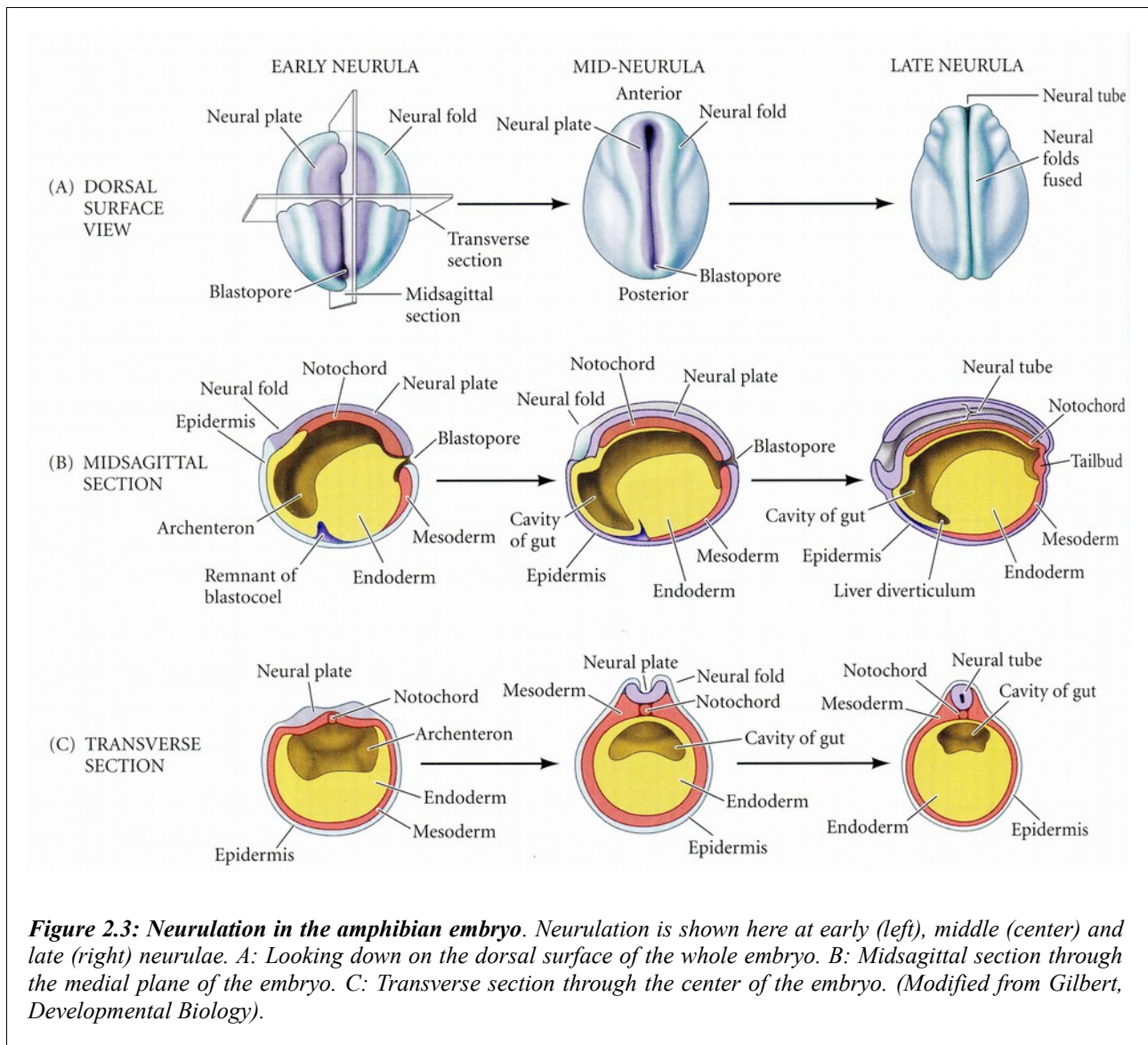


Figure 2.2: The development of the central nervous system, brain and spinal cord, in a vertebrate embryo is shown from the egg cell to the adult frog. After a series of a cleavage divisions produces a blastula, a group of cells known as the involuting marginal zone grows into the interior of the embryo at a point known as the blastopore. This process of gastrulation is shown here in two cross sections. The involuting cells will form mesodermal tissues and will induce the cells of the overlying ectoderm to develop into neural tissue, labeled here in red. After the process of neural induction, the neurogenic region is known as the neural plate and is restricted to giving rise to neural tissue. A cross section of the embryo at the neural plate stage shows the relationships between the tissues at this stage of development. The neural plate goes on to generate the neurons and glia in the adult plate and spinal cord. (Sanes, Reh, Harris; *Development of the Nervous System*).

Shortly after its formation, the neural plate begins to fold onto itself to form a tube-like structure, the **neural tube** (**Figures 2.2, 2.3** and **2.4**). This tube of cells gives rise to nearly all the neurons and glia of vertebrates. The process by which the neural plate tissue forms a neural tube, the rudiment of the nervous system, is called **neurulation**, and an embryo undergoing such changes is called a neurula (**Figure 2.3**). The neural tube forms the brain anteriorly and the spinal cord posteriorly.



There are two major ways of forming a neural tube. In the **primary neurulation**, the neural plate cells proliferate, invaginate, and pinch off from the surface to form a hollow tube. In the **secondary neurulation**, the neural tube arises from a solid cord of cells that sinks into the embryo and subsequently forms a hollow tube by cavitation. In general, the anterior portion of the neural tube is made by primary neurulation, while the posterior portion of the neural tube is made by secondary neurulation. The complete neural tube forms by joining these two separately formed tubes together (*Figure 2.4*).

The events of primary neurulation in the the frog and in the chicken are illustrated in *Figures 2.3* and *2.4*, respectively. During primary neurulation, the original ectoderm is divided into three sets of cells: (1) the internally positioned neural tube, which will form the brain and spinal cord, (2) the externally positioned epidermis of the skin, and (3) the neural crest cells. The neural crest cells form in the region that connects the neural tube and the epidermis, but then migrate elsewhere; they will generate the peripheral neurons and glia, the pigment cells of the skin, and several other cell types.

The process of primary neurulation appears to be similar in amphibians, reptiles, birds, and mammals (Gallera, 1971). Shortly after the neural plate has formed, its edges thicken and move upward to form the **neural folds**, while a U-shaped **neural groove** appears in the center of the plate, dividing the future right and left sides of the embryo (*Figures 2.3* and *2.4*). The neural folds migrate toward the midline of the embryo, eventually fusing to form the neural tube beneath the overlying ectoderm.

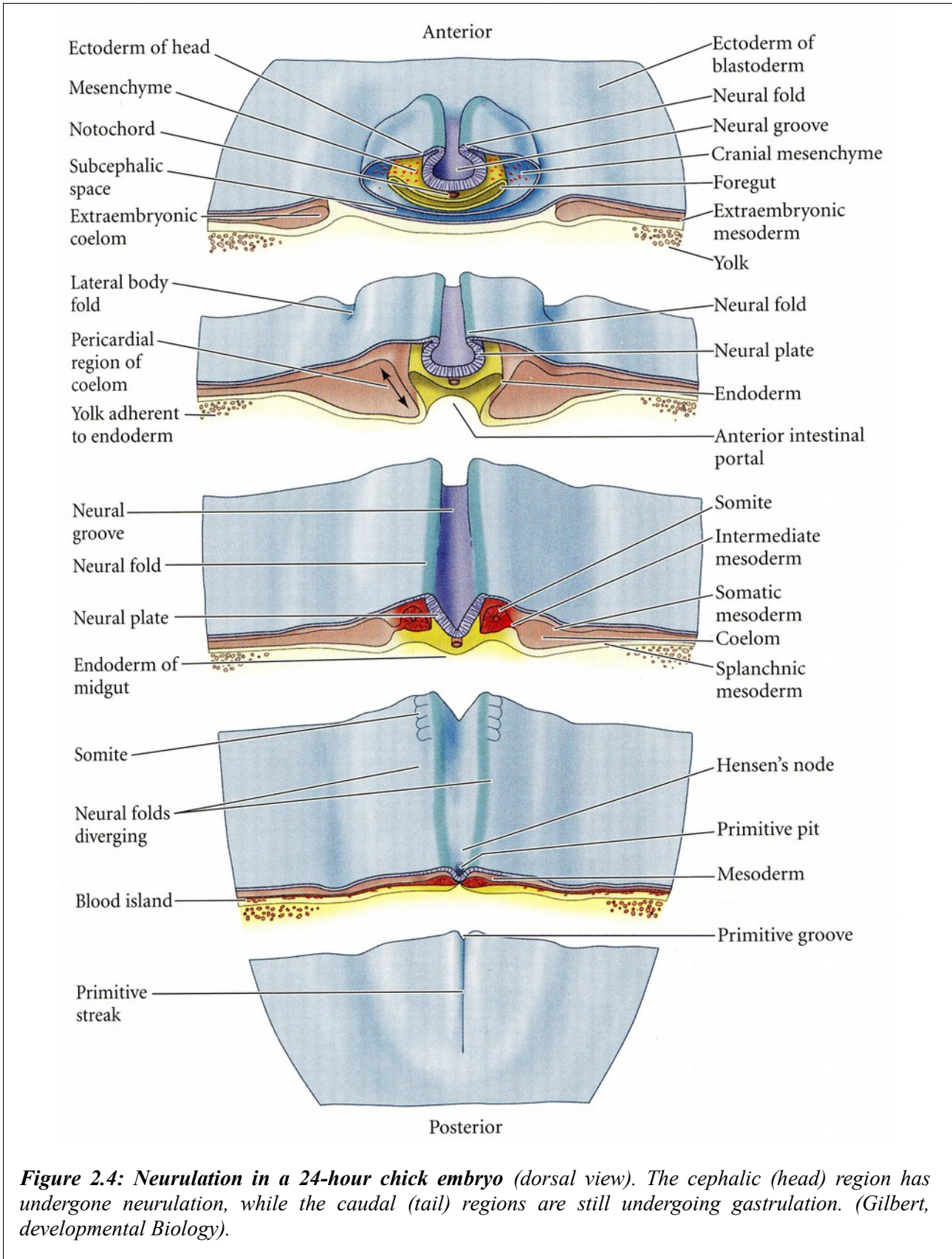
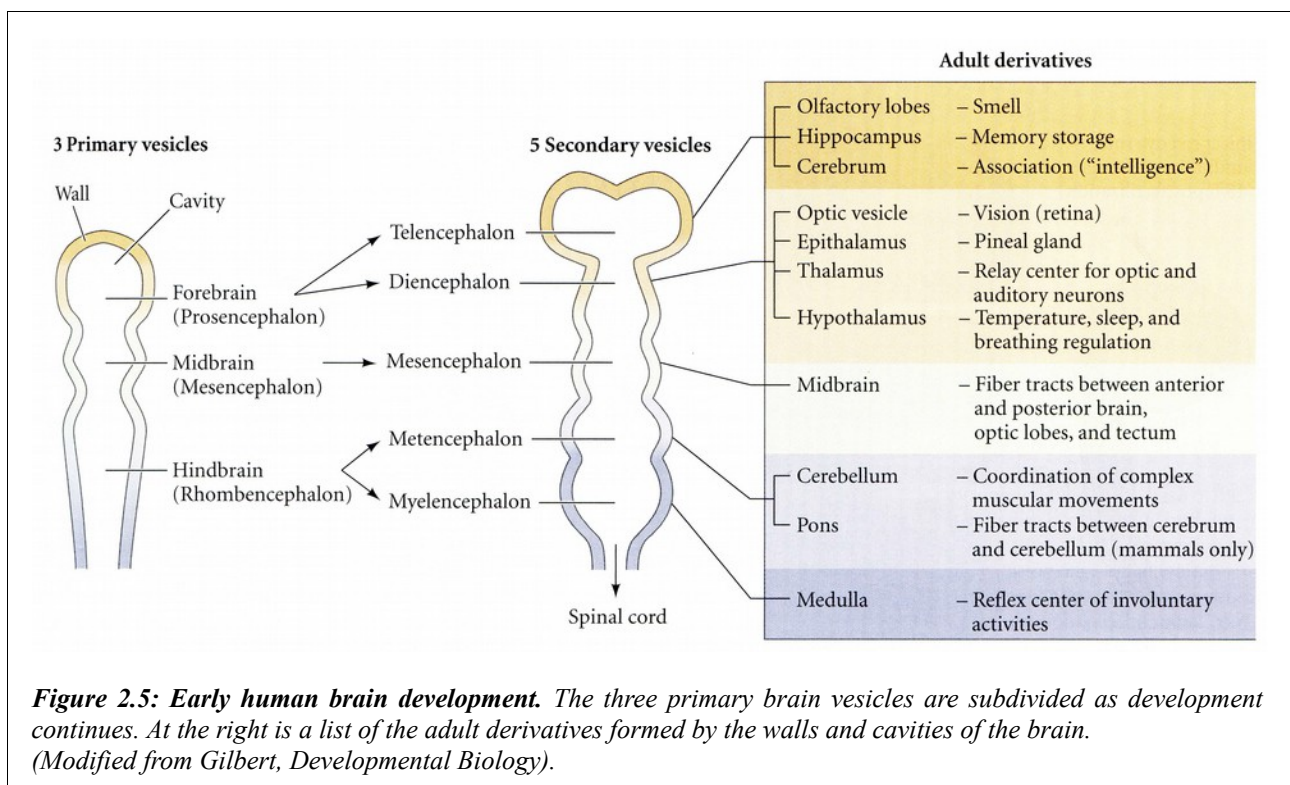


Figure 2.4: Neurulation in a 24-hour chick embryo (dorsal view). The cephalic (head) region has undergone neurulation, while the caudal (tail) regions are still undergoing gastrulation. (Gilbert, developmental Biology).

The differentiation of the neural tube into the various regions of the central nervous system occurs simultaneously in three different ways. At the anatomical level, the neural tube and its lumen form the chambers of the brain and the spinal cord. At the tissue level, the cell populations within the wall of the neural tube rearrange themselves to form the different functional regions of the brain and the spinal cord. Finally, on the cellular level, the neuroepithelial cells themselves differentiate into the numerous types of nerve cells (**neurons**) and supportive cells (**glia**) present in the body.

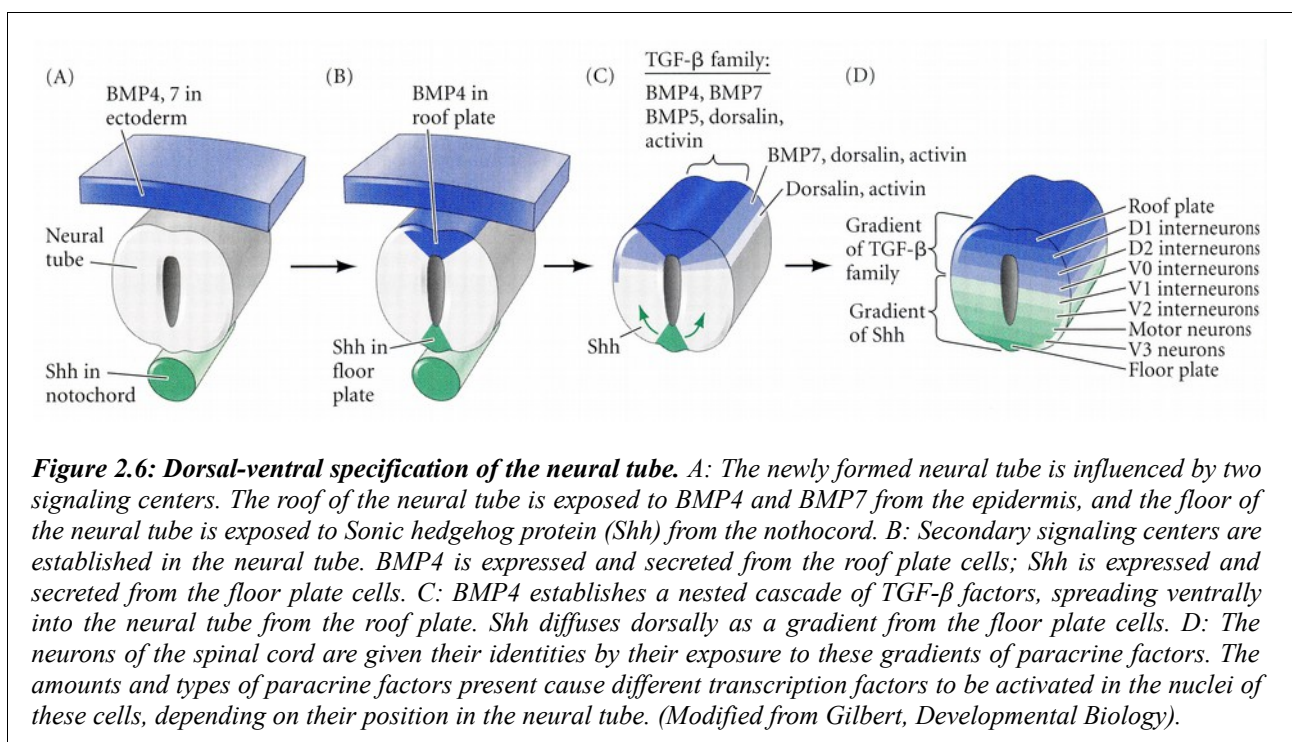
The early mammalian neural tube is a straight structure. However, even before the posterior portion of the tube has formed, the most anterior portion of the tube is undergoing drastic changes. In this region, the neural tube balloons into three primary vesicles (**Figure 2.5**): forebrain (**prosencephalon**), midbrain (**mesencephalon**), and hindbrain (**rhombencephalon**).



The prosencephalon becomes subdivided into the anterior **telencephalon** and the more caudal **diencephalon**. The telencephalon will eventually form the cerebral hemispheres, and the diencephalon will form the thalamic and hypothalamic brain regions that receive neural input from

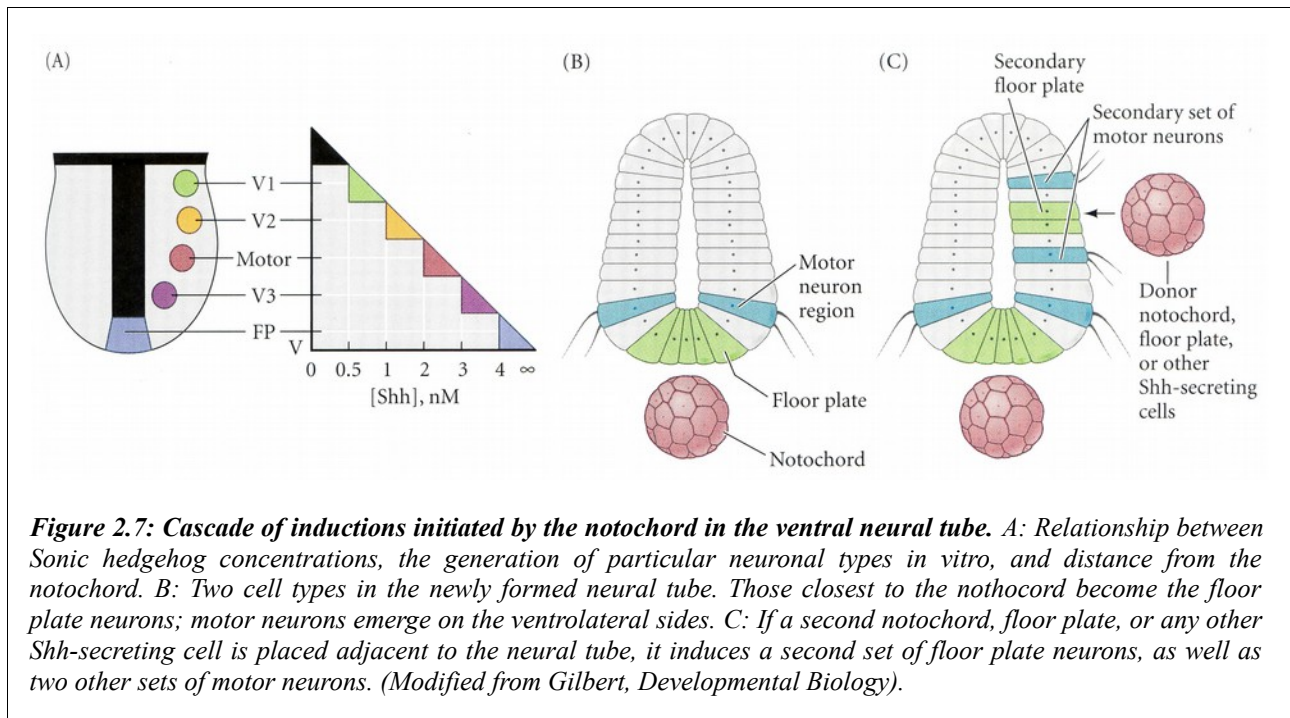
the retina. Indeed, the retina itself is a derivative of the lateral wall of the diencephalon. The mesencephalon does not become subdivided, and its lumen eventually becomes the cerebral aqueduct. The rhombencephalon becomes subdivided into a posterior **myelencephalon** and a more anterior **metencephalon**. The myelencephalon eventually becomes the medulla oblongata, whose neurons generate the nerves that regulate respiratory, gastrointestinal, and cardiovascular movements. The metencephalon gives rise to the cerebellum, the part of the brain responsible for coordinating movements, posture, and balance. The rhombencephalon develops a segmental pattern that specifies the places where certain nerves originate. Periodic swellings called **rhombomeres** divide the rhombencephalon into smaller compartments. These rhombomeres represent separate developmental “territories”: the cells within each rhombomere can mix freely within it, but not with cells from adjacent rhombomeres (Guthrie and Lumsden, 1991). Moreover, each rhombomere has a different developmental fate and will form **ganglia** clusters of neuronal cell bodies whose axons form a nerve.

The neural tube is polarized along its dorsal-ventral axis. In the spinal cord, for instance, the *dorsal* region is the place where the spinal neurons receive input from sensory neurons, while the *ventral* region is where the motor neurons reside. In the middle are numerous interneurons that relay information between them. The polarity of the neural tube is induced by signals coming from its immediate environment. The dorsal pattern is imposed by the epidermis, while the ventral pattern is induced by the notochord (**Figure 2.6**).



One agent of ventral specification of the neural tube is the **Sonic hedgehog** protein, originating from the notochord; another agent specifying the ventral neural cell types is retinoic acid, which probably comes from the adjacent somites (Pierani et al., 1999). Sonic hedgehog establishes a gradient, and different levels of this protein cause the formation of different cell types. Sonic hedgehog is initially synthesized in the notochord. The secreted Sonic hedgehog induces the medial hinge cells to become the **floor plate** of the neural tube. These floor plate cells also secrete Sonic hedgehog, which forms a gradient highest at the most ventral portion of the neural tube (Roelink et al., 1995; Briscoe et al., 1999). Those cells adjacent to the floor plate that receive high concentrations of Sonic hedgehog become the ventral (V3) neurons, while the next group of cells, exposed to slightly less Sonic hedgehog, become motor neurons (**Figure 2.6**). The next two groups of cells, receiving progressively less of this protein, become the V2 and V1 interneurons. The different concentrations of Sonic hedgehog function by causing the different groups of neurons to express different types of transcription factors. These transcription factors, in turn, activate the genes whose protein products control the cellular identity. Sonic hedgehog may also work by repressing the expression of genes encoding dorsal neural tube transcription factors, which would otherwise be expressed throughout the neural tube.

The importance of Sonic hedgehog in inducing and patterning the ventral portion of the neural tube can be shown experimentally. If notochord fragments are taken from one embryo and transplanted to the lateral side of a host neural tube, the host neural tube will form another set of floor plate cells at its sides (**Figure 2.7**). The floor plate cells, once induced, induce the formation of motor neurons on either side of them. The same results can be obtained if the notochord fragments are replaced by pellets of cultured cells secreting Sonic hedgehog (Echelard et al., 1993; Roelink et al., 1994). Moreover, if a piece of notochord is removed from an embryo, the neural tube adjacent to the deleted region will have no floor plate cells (Placzek et al., 1990; Yamada et al., 1991, 1993).



The dorsal fates of the neural tube are established by proteins of the TGF- β superfamily, especially the bone morphogenetic proteins 4 and 7, dorsalin, and activin (Liem et al., 1995, 1997). Initially, BMP4 and BMP7 are found in the epidermis. Just as the notochord establishes a secondary signaling center the floor plate cells on the ventral side of the neural tube, the epidermis establishes a secondary signaling center by inducing BMP4 expression in the **roof plate** cells of the neural tube. The BMP4 protein from the roof plate induces a cascade of TGF- β superfamily proteins in adjacent cells. Different sets of cells are thus exposed to different concentrations of TGF- β superfamily proteins at different times (the most dorsal being exposed to more factors at higher concentrations and at earlier times). The temporal and concentration gradients of the TGF- β superfamily proteins induce different types of transcription factors in cells at different distances from the roof plate, thereby giving them different identities.

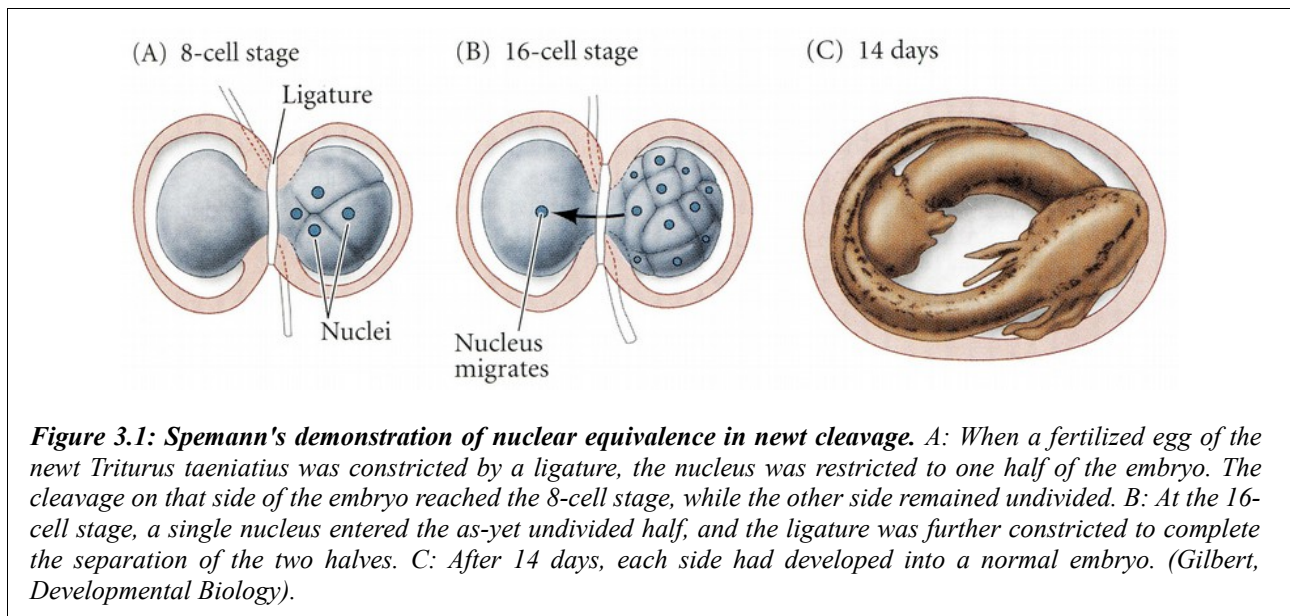
3– Neural Induction and Antero-Posterior Axis Formation

Research from the last 15 years has provided a working model for how the neural tissue is induced and specified along the anterior-posterior (A-P) axis during the early stages of embryogenesis. The study of neural plate specification, neural induction, and antero-posterior (A-P) axis formation are intimately linked. This model relies on three basic processes:

- (1) *induction of the neural plate* from naive ectoderm requires the inhibition of BMP/TGF β signaling;
- (2) induced neural tissue initially acquires an *anterior identity* (i.e., anterior forebrain);
- (3) *maintenance and expansion of the anterior forebrain depends on the antagonism of posteriorizing signals* that would otherwise transform this tissue into posterior neural fates.

Progressive Determination of the Amphibian Axes: the Organizer and the Primary Embryonic Induction

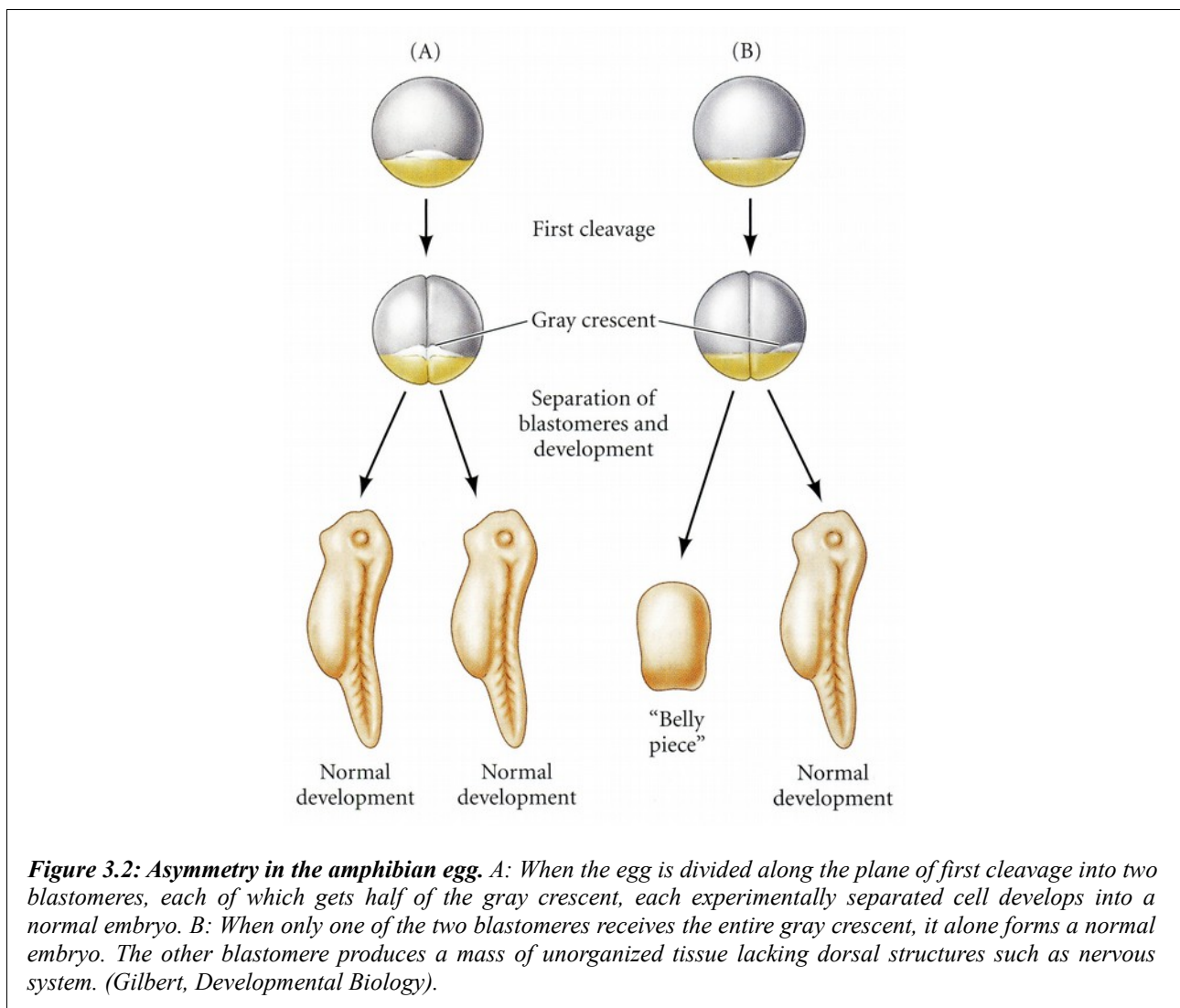
The story about the discovery of neural induction starts in 1903, when Spemann demonstrated that early newt blastomeres have identical nuclei, each capable of producing an entire larva. Shortly after fertilizing a newt egg, Spemann used a baby's hair taken from his daughter to “lasso” the zygote in the plane of the first cleavage. He then partially constricted the egg, causing all the nuclear divisions to remain on one side of the constriction. Eventually, often as late as the 16-cell stage, a nucleus would escape across the constriction into the non-nucleated side. Cleavage then began on this side, too, whereupon Spemann tightened the lasso until the two halves were completely separated. Twin larvae developed, one slightly more advanced than the other. Spemann concluded from this experiment that early amphibian nuclei were genetically identical and that each cell was capable of giving rise to an entire organism (**Figure 3.18**).



However, when Spemann performed a similar experiment with the constriction still longitudinal, but perpendicular to the plane of the first cleavage (separating the future dorsal and ventral regions rather than the right and left sides), he obtained a different result altogether.

The nuclei continued to divide on both sides of the constriction, but only the future dorsal side of the embryo gave rise to a normal larva. The other side produced an unorganized tissue mass of ventral cells, which Spemann called the *Bauchstück*, the belly piece. This tissue mass was a ball of epidermal cells (ectoderm) containing blood and mesenchyme (mesoderm) and gut cells (endoderm), but no dorsal structures such as nervous system, notochord, or somites.

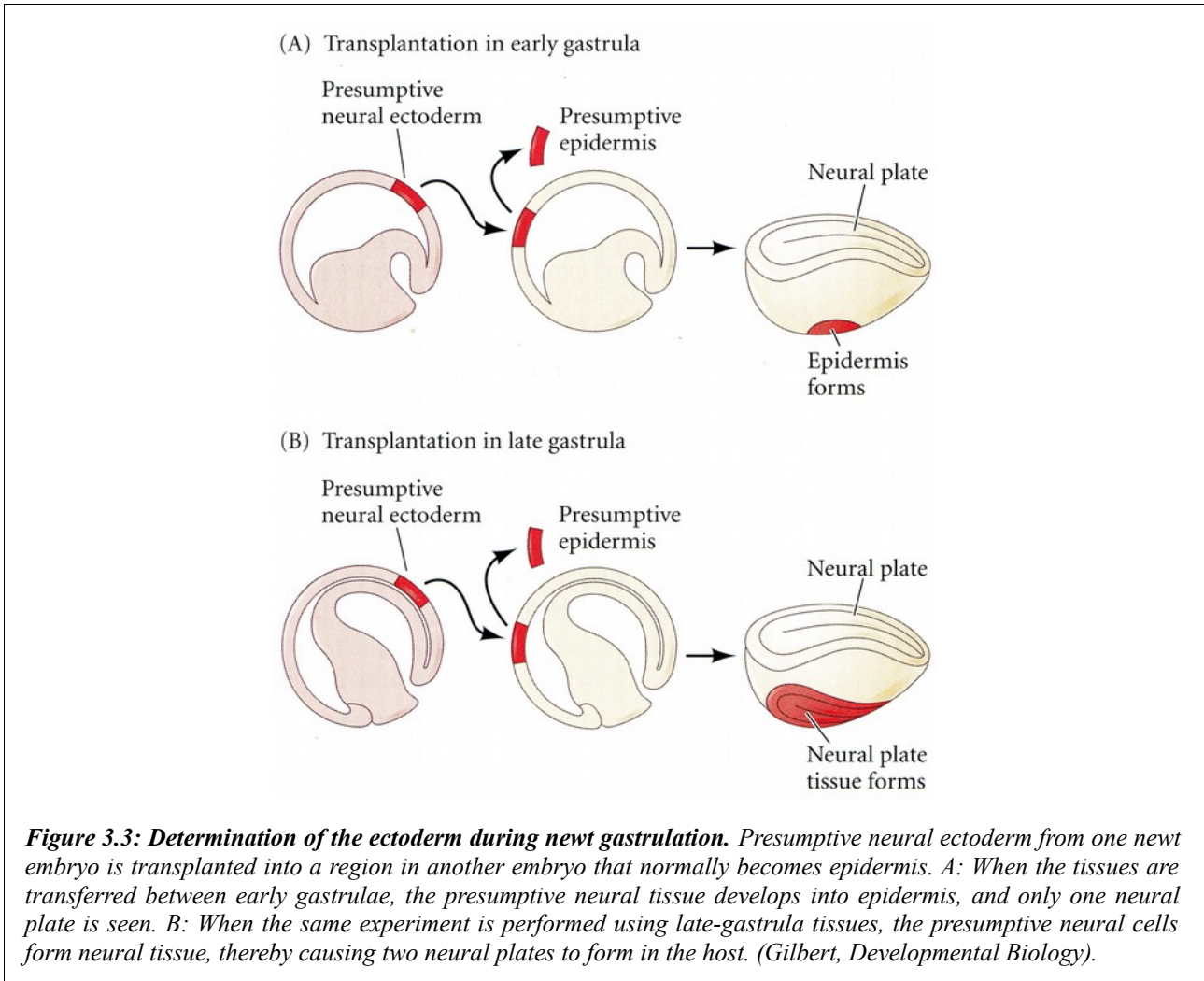
One possibility to explain why these two experiments gave different results was that when the egg was divided perpendicular to the first cleavage plane, some *cytoplasmic* substance was not equally distributed into the two halves. Fortunately, the salamander egg was a good place to test that hypothesis. There are dramatic movements in the cytoplasm following the fertilization of amphibian eggs, and in some amphibians these movements expose a gray, crescent-shaped area of cytoplasm in the region directly opposite the point of sperm entry. This area has been called the **gray crescent** (*Figure 3.2*).



Moreover, the first cleavage plane normally splits the gray crescent equally into the two blastomeres. If these cells are then separated, two complete larvae develop. However, should this cleavage plane be aberrant (either in the rare natural event or in an experiment), the gray crescent material passes into only one of the two blastomeres. Spemann found that when these two blastomeres are separated, only the blastomere containing the gray crescent develops normally (**Figure 3.2**). It appeared, then, that something in the gray crescent region was essential for proper embryonic development.

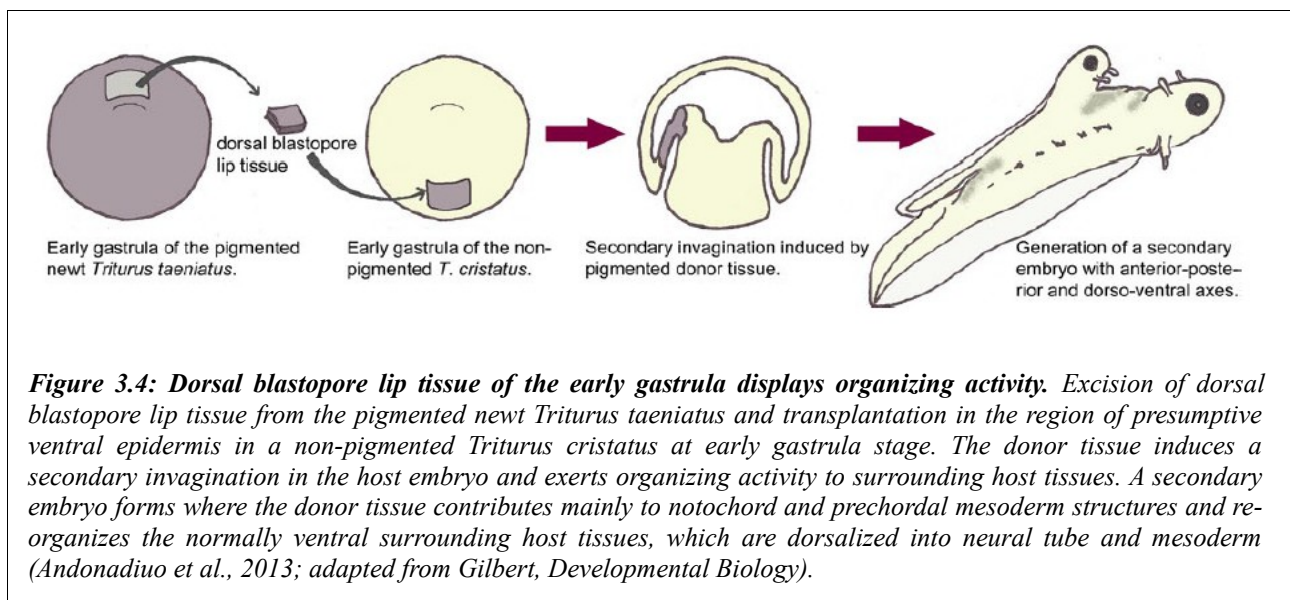
The most important clue came from the fate map of this area of the egg, because it showed that the gray crescent region gives rise to the cells that initiate gastrulation. These cells form the dorsal lip of the blastopore. The cells of the dorsal lip are committed to invaginate into the blastula, thus initiating gastrulation and the formation of the notochord. Because all future amphibian development depends on the interaction of cells rearranged during gastrulation, Spemann speculated that the importance of the gray crescent material lies in its ability to initiate gastrulation.

In 1962, Hans Spemann found that neural induction (and more in general, crucial changes in cell potency) occurred during the gastrula stage in the amphibian embryo. Spemann's demonstration involved exchanging tissues between the gastrulae of two species of newts whose embryos were differently pigmented: the darkly pigmented *Triturus taeniatus* and the non-pigmented *Triturus cristatus*. When a region of prospective neural tissue cells from an early gastrula of one species was transplanted into an area in the early gastrula of the other species and placed in a region where epidermal tissue normally formed, the transplanted cells gave rise to epidermal tissue (**Figure 3.3A**). Thus, cells of the early gastrula exhibited regulative development, because their ultimate fate depended on their location in the embryo. However, when the same transplantation experiments were performed on late gastrulae, Spemann obtained completely different results. Rather than differentiating in accordance with their new location, the transplanted cells turned out to have a determined fate. Specifically, prospective neural cells now developed into brain tissues even when placed in the region of prospective epidermis (**Figure 3.3B**). Cells were already committed to epidermal and neural fates at this stage.



Experiments by Hans Spemann and Hilde Mangold in 1924 demonstrated that an entire ectopic axis extending from the forebrain to the spinal cord could be induced in a host newt embryo by a group of cells from the dorsal blastopore lip (**Figure 3.4**). This ectopic axis was complete in that a neural tube encompassing forebrain (i.e., ectopic eyes) and spinal cord had developed over an ectopic notochord and was flanked by somites. Once again, in these experiments newt species with white or dark pigments were used to discriminate the contribution of the host and the donor tissues to the ectopic axis. When the dorsal lip of an early *T. taeniatus* gastrula was removed and implanted into the region of an early *T. cristatus* gastrula fated to become ventral epidermis (belly skin), the dorsal lip tissue invaginated just as it would normally have done (showing self-determination), and disappeared beneath the vegetal cells. The pigmented donor tissue then continued to self-differentiate into the chordamesoderm (notochord) and other mesodermal structures that normally

form from the dorsal lip. As the donor-derived mesodermal cells moved forward, host cells began to participate in the production of the new embryo, becoming organs that normally they never would have formed. In this secondary embryo, a somite could be seen containing both pigmented (donor) and unpigmented (host) tissue. Even more spectacularly, the dorsal lip cells were able to interact with the host tissues to form a complete neural plate from host ectoderm. Eventually, a secondary embryo formed, conjoined face to face with its host (**Figure 3.4**). The ectopic neural axis was comprised of mostly host cells, demonstrating that the donor cells have inducing properties. Thus, of all tissues of the early gastrula, only one had its fate autonomously determined. This self-determining tissue is the dorsal lip of the blastopore, the tissue derived from the grey crescent cytoplasm, and was named “the Organizer”.

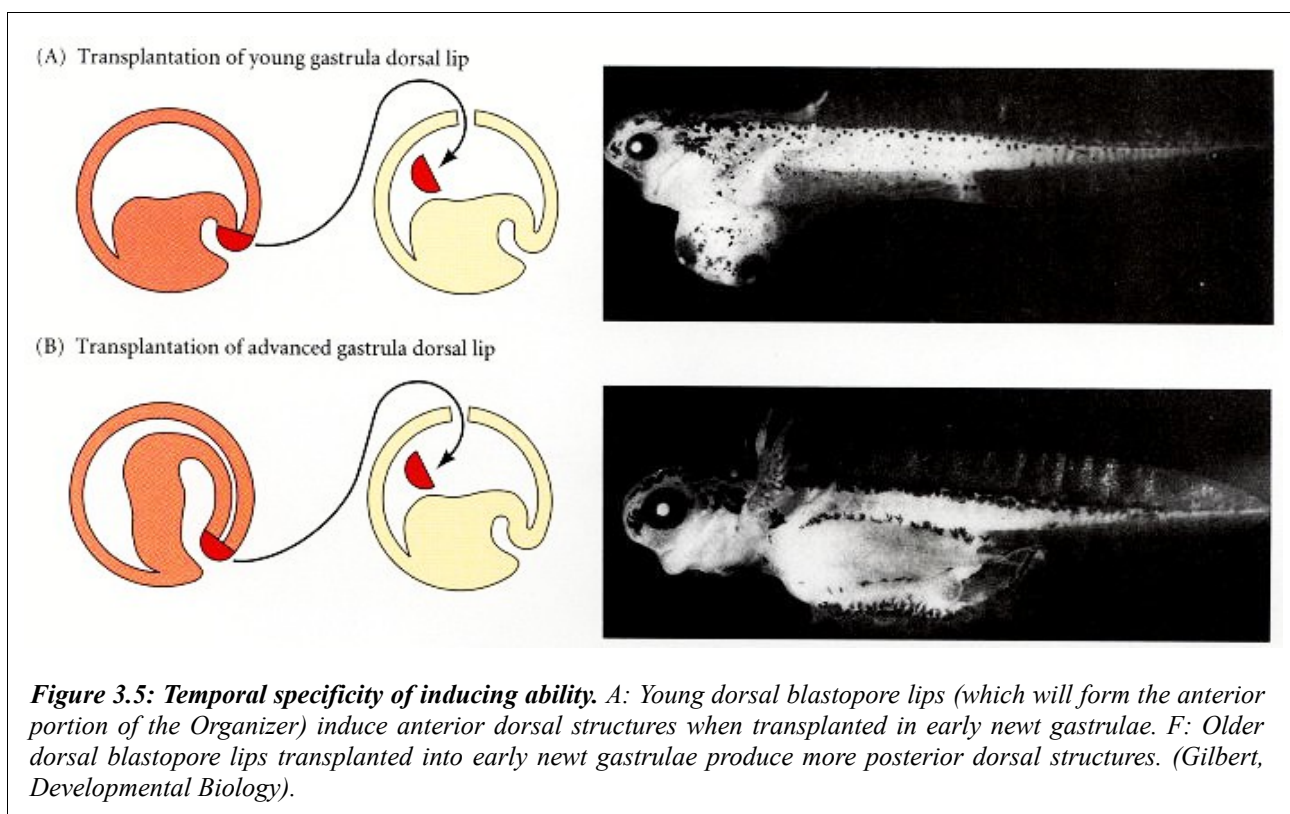


Spemann (1938) referred to the dorsal lip cells and their derivatives (notochord, prechordal mesoderm) as the **Organizer** because (1) they induced the host's ventral tissues to change their fates to form a neural tube and dorsal mesodermal tissue (such as somites), and (2) they *organized host and donor tissues into a secondary embryo with clear anterior-posterior and dorsal-ventral axes*.

He proposed that during normal development, these cells organize the dorsal ectoderm into a neural tube and transform the flanking mesoderm into the antero-posterior body axis. It is now known (thanks largely to Spemann and his students) that the interaction of the chordamesoderm and ectoderm is not sufficient to “organize” the entire embryo. Rather, it initiates a series of sequential

inductive events. Because there are numerous inductions during embryonic development, this key induction wherein the progeny of dorsal lip cells induce the dorsal axis and the neural tube is traditionally called **primary embryonic induction**.

Moreover, the abilities of the Organizer were found to be stage dependent, as dorsal blastopore lip cells from younger embryos were capable of inducing an entire ectopic neural axis (heads, eyes, brain and spinal cord), but older ones gave rise to ectopic axes lacking the eyes and the most anterior structures (**Figure 3.5**). These results show that the first cells of the Organizer to enter the embryo induce the formation of brains and heads, while those cells that form the dorsal lip of later-stage embryos induce the cells above them to become spinal cords and tails. This gave support to a model whereby the activities of the organizer can be divided into the “head” and “trunk” organizers, with early activities inducing anterior neural identity and late activities inducing only posterior neural fates.



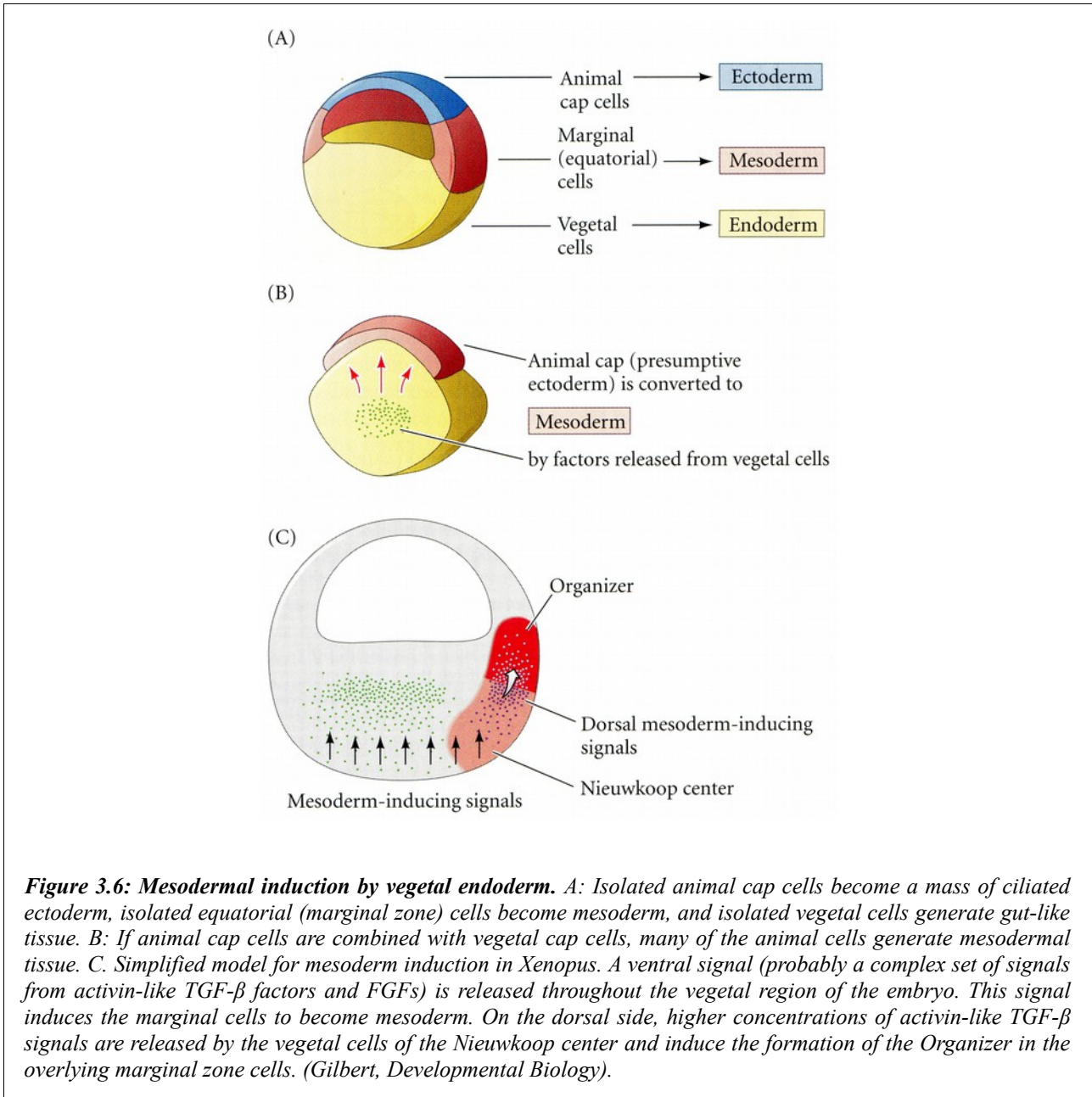
The Formation of the Organizer

The experiments of Spemann and Mangold showed that the dorsal lip of the blastopore, and the notochord that forms from it, constituted an “Organizer” that could instruct the formation of new embryonic axes. But the mechanisms by which the Organizer was constructed, and the factors being secreted from the Organizer to cause the formation of the neural tube and to create the embryo axes remained a mystery.

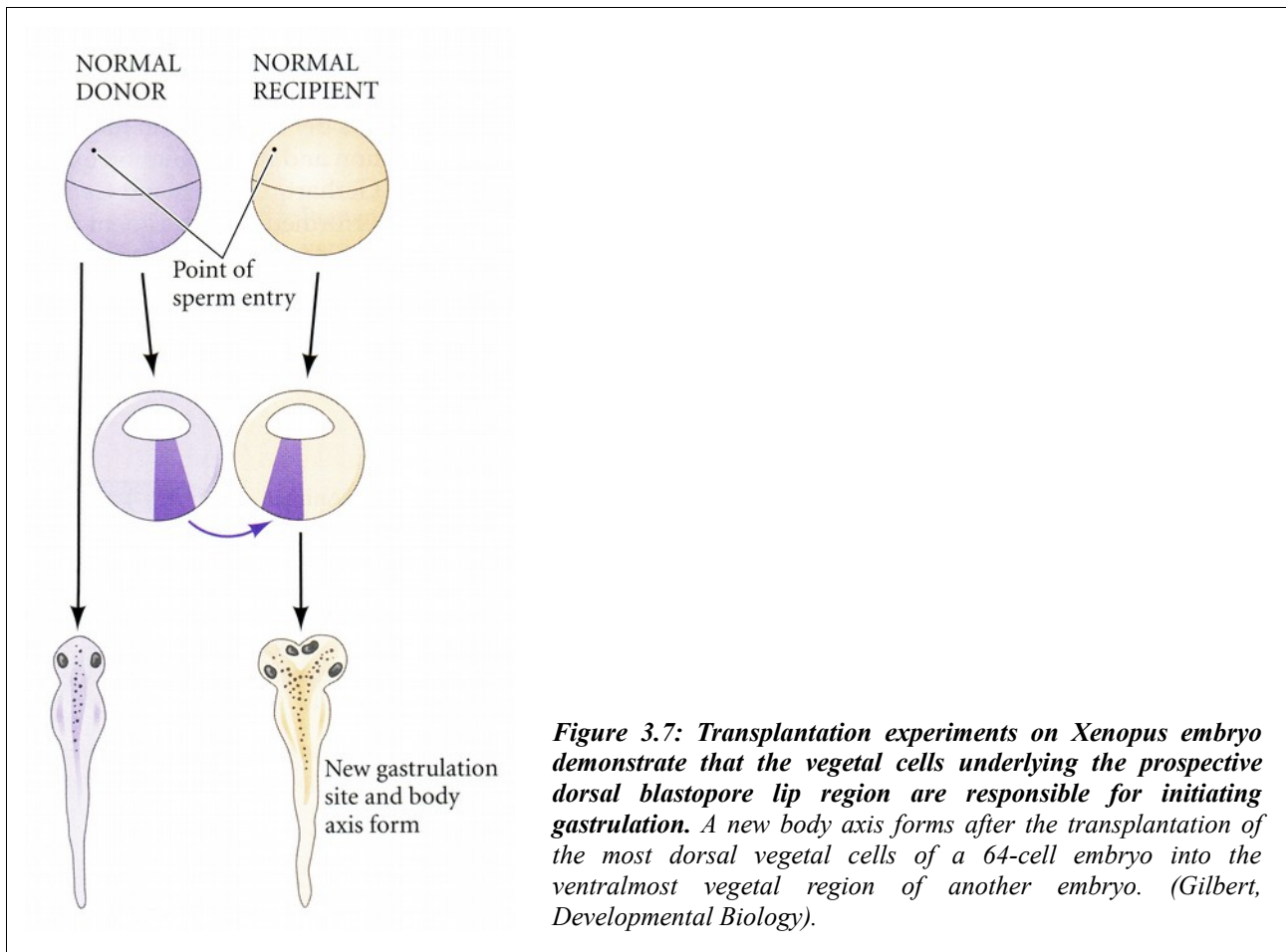
The major clue in determining how the dorsal blastopore lip obtained its properties came from the experiments of Pieter Nieuwkoop and Osamu Nakamura. These studies showed that the properties of this newly formed mesoderm (the Organizer) were induced by the vegetal (presumptive endoderm) cells beneath it.

Nakamura and his colleagues removed the equatorial cells (i.e., presumptive mesoderm) from a blastula and showed that neither the animal cap (presumptive ectoderm) nor the vegetal cap (presumptive endoderm) produced any mesodermal tissue. However, when the two caps were recombined, the animal cap cells were induced to form mesodermal structures such as notochord, muscles, kidney cells, and blood cells (*Figures 3.6A,B*).

The polarity of this induction (whether the animal cells formed dorsal mesoderm or ventral mesoderm) depended on the dorsal-ventral polarity of the endodermal (vegetal) fragment. While the ventral and lateral vegetal cells (those closer to the side of sperm entry) induced ventral (mesenchyme, blood) and intermediate (muscle, kidney) mesoderm, the dorsal-most vegetal cells specified dorsal mesoderm components (somites, notochord), including those having the properties of the organizer. These dorsal-most vegetal cells of the blastula, which are capable of inducing the Organizer, have been called the **Nieuwkoop center** (Gerhart et al., 1989) (*Figure 3.6C*).



The existence of the Nieuwkoop center was demonstrated in the 32-cell *Xenopus* embryo by transplantation and recombination experiments. First, Gimlich and Gerhart (Gimlich and Gerhart, 1984; Gimlich, 1985, 1986) performed an experiment analogous to the Spemann and Mangold studies, except that they used blastulae rather than gastrulae. When they transplanted the dorsalmost vegetal blastomere from one blastula into the ventral vegetal side of another blastula, two embryonic axes were formed (**Figure 3.7**).



Second, Dale and Slack (1987) recombined single vegetal blastomeres from a 32-cell *Xenopus* embryo with the uppermost animal cell layer of a fluorescently labeled embryo of the same stage. The dorsalmost vegetal cell, as expected, induced the animal pole cells to become dorsal mesoderm. The remaining vegetal cells usually induced the animal cells to produce either intermediate or ventral mesodermal tissues. Thus, *dorsal vegetal cells can induce animal cells to become dorsal mesodermal tissue*.

Molecular Mechanisms of Amphibian Axis Formation: BMP-inhibitors Mediate the Induction of Neural Ectoderm and Dorsal Mesoderm

While the Nieuwkoop center cells remain endodermal, the cells of the Organizer become the dorsal mesoderm and migrate underneath the dorsal ectoderm. There, the dorsal mesoderm induces the central nervous system to form. Evidence from experimental embryology showed that one of the most critical properties of the Organizer was its production of soluble factors.

Scientists were searching for molecules secreted by the Organizer and received by the ectoderm that then converted it into neural tissue. However, experimental evidences showed an opposite mechanism: The ectoderm is actually induced to become epidermal tissue by soluble morphogens called bone morphogenetic proteins (BMPs). The nervous system forms from that region of the ectoderm that is protected from this epidermal induction (Hemmati-Brivanlou and Melton, 1994, 1997). In other words, (1) the “default fate” of the ectoderm is to become neural tissue; (2) certain parts of the embryo induce the ectoderm to become epidermal tissue by secreting BMPs, and (3) the Organizer tissues act by secreting molecules that block this induction, thereby allowing the ectoderm to be “protected” by these factors and thus to become neural tissue.

Three of the major BMP-inhibitors secreted by the Organizer are Noggin, Chordin and Follistatin.

In 1992, the first of the soluble organizer molecules was isolated. Smith and Harland (1992) constructed a cDNA plasmid library from dorsalized (lithium chloride-treated) gastrulae. Messenger RNAs synthesized from sets of these plasmids were injected into ventralized embryos (having no neural tube) produced by irradiating early embryos with ultraviolet light. Those sets of plasmids whose mRNAs rescued the dorsal axis in these embryos were split into smaller sets, and so on, until single-plasmid clones were isolated whose mRNAs were able to restore the dorsal axis in such embryos (**Figure 3.8**). One of these clones contained the *noggin* gene (**Figures 3.8 and 3.9**).

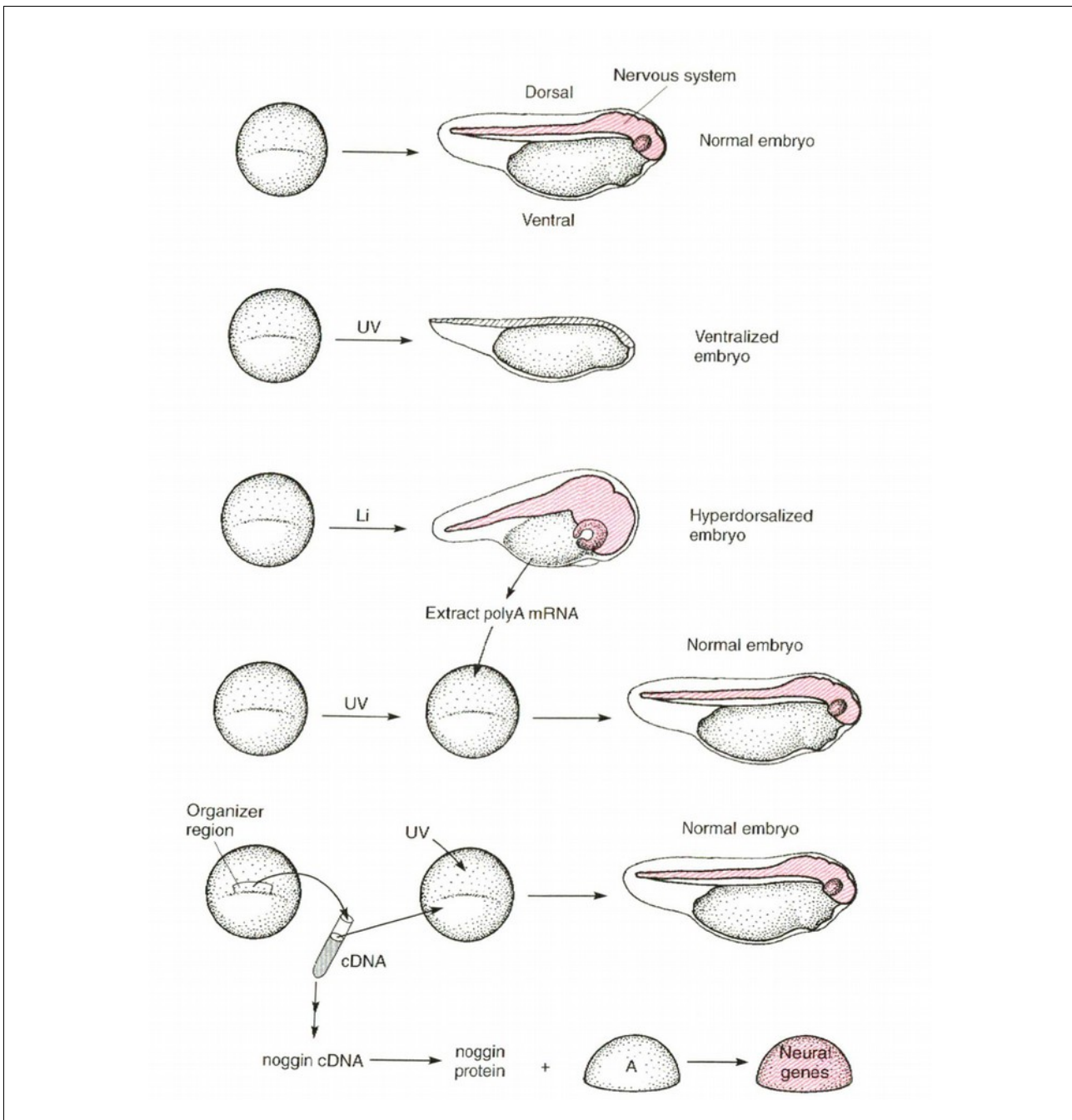


Figure 3.8: The identification of *noggin* as a neural inducer was accomplished through the use of an expression cloning strategy in *Xenopus* embryos. UV light treatment of the early embryo inhibits the development of dorsal structures by disrupting the cytoskeleton rearrangements that pattern the dorsal inducing molecules prior to gastrulation (ventralized). Lithium treatment of the early embryo has the opposite effect; the embryo develops more than normal dorsal tissue (hyperdorsalized). If messenger RNA is extracted from the hyperdorsalized embryos and injected into a UV-treated embryo, the messages encoded in the mRNA can “rescue” the UV-treated embryo and it develops relatively normally. Similarly, cDNA from the Organizer region of a normal embryo can rescue a UV-treated embryo. The *noggin* gene was isolated as a cDNA from the Organizer region that could rescue the normal development of UV-treated embryos. Subsequently, recombinant protein was made from *noggin* cDNA and shown to induce neural tissue from isolated animal caps without any induction of mesodermal genes. (Sanes, Reh and Harris; *Development of the Nervous System*).

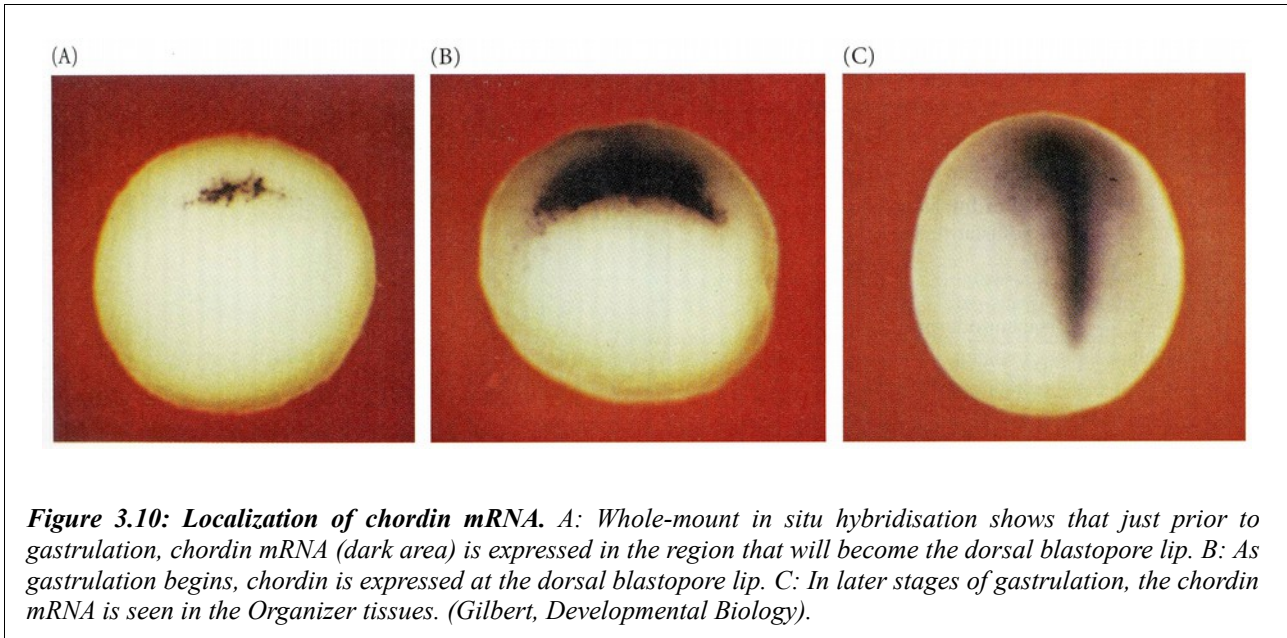


Figure 3.9: *The soluble protein Noggin dorsalizes the amphibian embryo. Figure shows the rescue of dorsal structures by Noggin protein. When *Xenopus* eggs are exposed to ultraviolet radiation, cortical rotation fails to occur, and the embryos lack dorsal structures (top). If such an embryo is injected with *noggin* mRNA, it develops dorsal structures in a dosage-related fashion (top to bottom). (Gilbert, *Developmental Biology*).*

Noggin is a secreted protein that is able to accomplish two of the major functions of the Organizer. It induces dorsal ectoderm to form neural tissue, and it dorsalizes mesoderm cells that would otherwise contribute to the ventral mesoderm. Noggin binds to BMP4 and BMP2 and inhibits their binding to receptors (Zimmerman et al., 1996). Smith and Harland (1992) have shown that newly transcribed *noggin* mRNA is first localized in the dorsal blastopore lip region and then becomes expressed in the notochord.

The second organizer protein found was **Chordin**. It was isolated from clones of cDNA whose mRNAs were present in dorsalized, but not in ventralized, embryos (Sasai et al., 1994). These clones were tested by injecting them into ventral blastomeres and seeing whether they induced secondary axes. One of the clones capable of inducing a secondary neural tube contained the *chordin* gene. The chordin mRNA was found localized in the dorsal blastopore lip and later in the

dorsal mesoderm of the notochord (**Figure 3.10**). Like Noggin, chordin binds directly to BMP4 and BMP2 and prevents their complexing with their receptors (Piccolo et al., 1996).



The mRNA for a third organizer-secreted protein, **Follistatin**, is also transcribed in the dorsal blastopore lip and notochord. Follistatin was found in the Organizer through the unexpected result of an experiment that was looking for something else. Ali Hemmati-Brivanlou and Douglas Melton (1992, 1994) wanted to see whether the protein Activin was required for mesoderm induction, so they constructed a dominant negative Activin receptor and injected it into *Xenopus* embryos. Remarkably, the ectoderm of these embryos began to express neural-specific proteins. It appeared that the Activin receptor (which also binds other structurally similar molecules such as the BMPs) normally functioned by inhibiting neural induction. When its function was blocked, all the ectoderm became neural. Follistatin, such as Noggin and Chordin, is a secreted protein capable of inhibiting BMP, and additionally able to block Activin. In 1994, Hemmati- Brivanlou and Melton proposed a “**Default model of neural induction**”: *under normal conditions, ectoderm becomes neural unless induced to become epidermal by BMPs. The Organizer functioned by producing inhibitors of anti-neuralizing factors such as BMPs and Activin.*

This model was also supported and explained by cell dissociation experiments. Three studies, by Grunz and Tacke (1989), Sato and Sargent (1989), and Godsave and Slack (1989) showed that when whole embryos or their animal caps were dissociated, they formed neural tissue. This result would

be explainable if the "default state" of the ectoderm was not epidermal, but neural, and the tissue had to be induced to have an epidermal phenotype. The Organizer, then, would block this epidermis-inducing induction by inactivating BMPs.

In *Xenopus*, the epidermal inducers are bone morphogenetic protein BMP4 and its close relatives BMP2 and BMP7. There is an antagonistic relationship between these BMPs and the Organizer (**Figure 3.11**).

If the mRNA for BMP4 is injected into *Xenopus* eggs, all the mesoderm in the embryo becomes ventrolateral mesoderm, and no involution occurs at the blastopore lip (Dale et al., 1992; Jones et al., 1992). Conversely, overexpression of a dominant negative BMP4 receptor resulted in the formation of two dorsal axes (Graff et al., 1994; Suzuki et al., 1994). In 1995, Wilson and Hemmati-Brivanlou demonstrated that BMP4 induced ectodermal cells to become epidermal. By 1996, several laboratories had demonstrated that Noggin, Chordin, and Follistatin each was secreted by the organizer and that each prevented BMP from binding to the ectoderm and mesoderm near the organizer (Piccolo et al., 1996; Zimmerman et al., 1996; Iemura et al., 1998) (**Figure 3.11**).

BMP4 is expressed initially throughout the ectodermal and mesodermal regions of the late blastula. However, during gastrulation, *bmp4* transcripts become restricted to the ventrolateral marginal zone. In the ectoderm, BMPs repress the genes (such as neurogenin) involved in forming neural tissue, while activating other genes involved in epidermal specification (Lee et al., 1995).

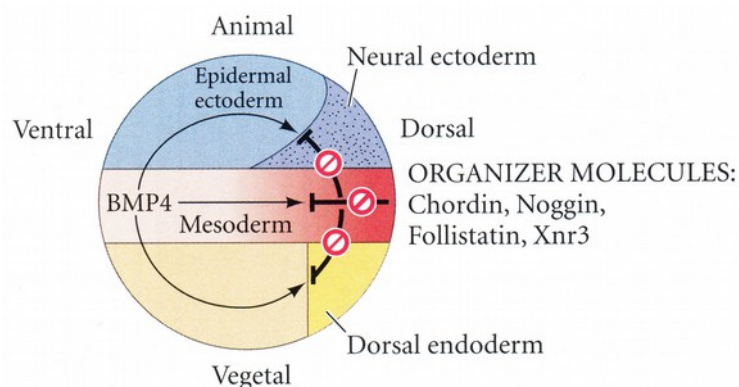
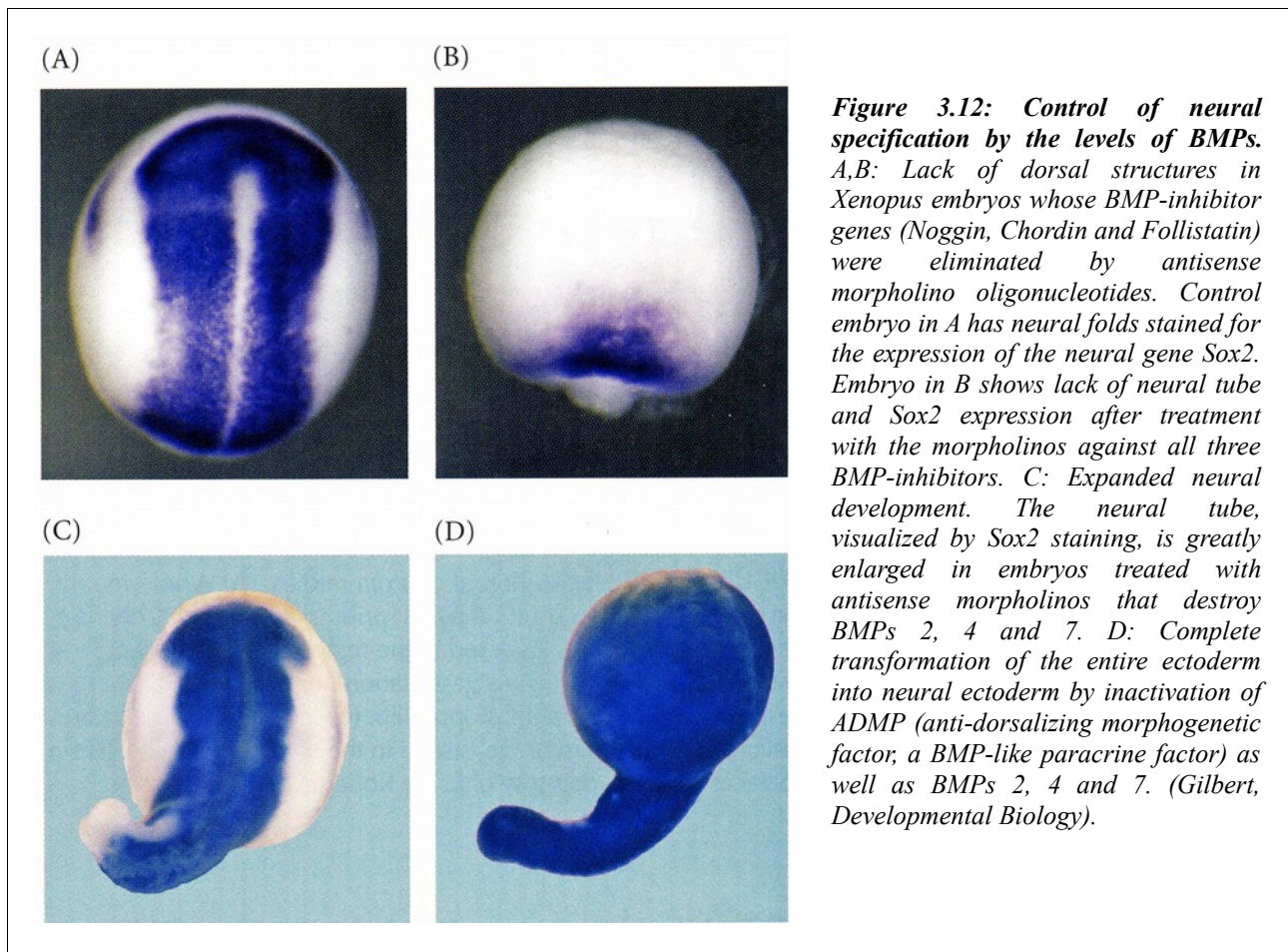


Figure 3.11: Model for the action of the Organizer. BMP4 (along with other molecules) is a powerful ventralizing factor. Organizer protein such as Noggin, Chordin and Follistatin block the action of BMP4; their inhibitory effect can be seen in all three germ layers. (Gilbert, *Developmental Biology*).

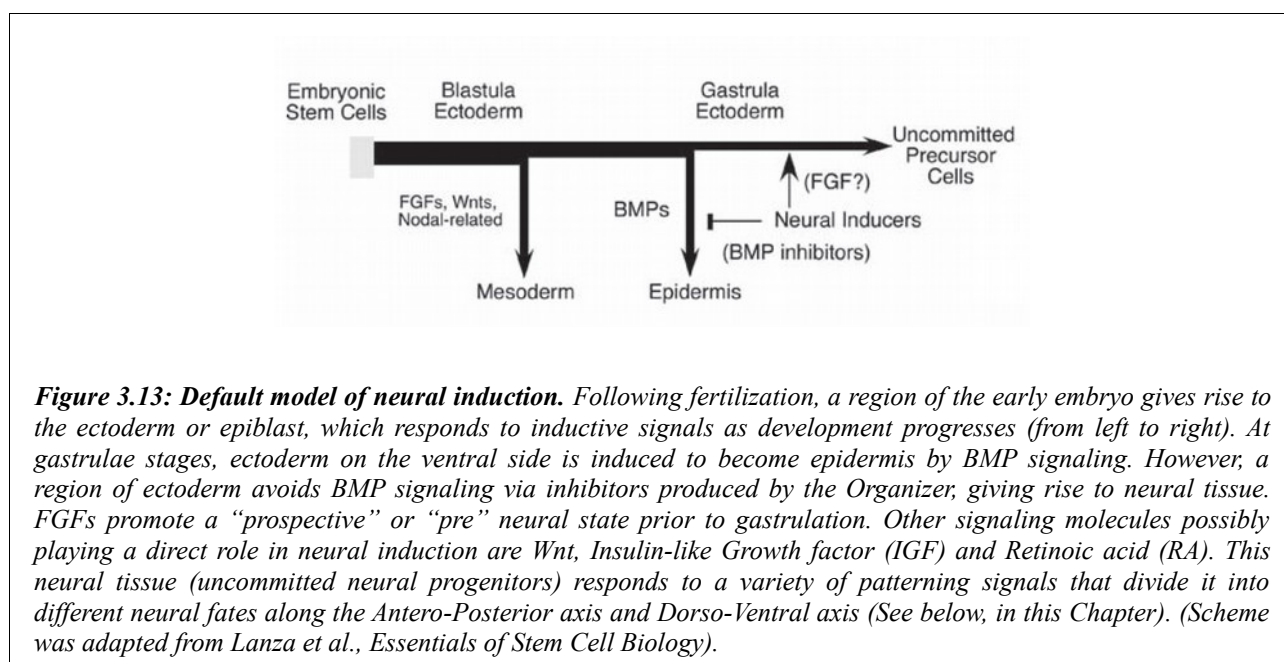
In 2005, two important sets of experiments confirmed the default model and the importance of blocking BMPs to specify the nervous system. First, Khokha and colleagues (2005) used antisense morpholinos to eliminate the three BMP antagonists (i.e., Noggin, Chordin and Follistatin) in *Xenopus*. The resulting embryos had catastrophic failure of dorsal development and lacked neural plates and dorsal mesoderm (**Figures 3.12A,B**). Second, Reversade and colleagues (2005) performed the opposite experiment by blocking BMP activity with antisense morpholinos. When they simultaneously blocked the formation of BMPs 2, 4 and 7, the neural tube became greatly expanded, taking over a much larger region of the ectoderm (**Figures 3.12C,D**). These experiments also highlighted a significant degree of functional redundancy concerning the activity of these genes.



These findings fit well with the concept that inhibition of BMP/TGF- β signaling is a prerequisite for neural induction. BMP inhibitors such as Noggin and Chordin are expressed in the vertebrate Organizers and play a role in neural induction by preventing BMP signaling. However, BMP

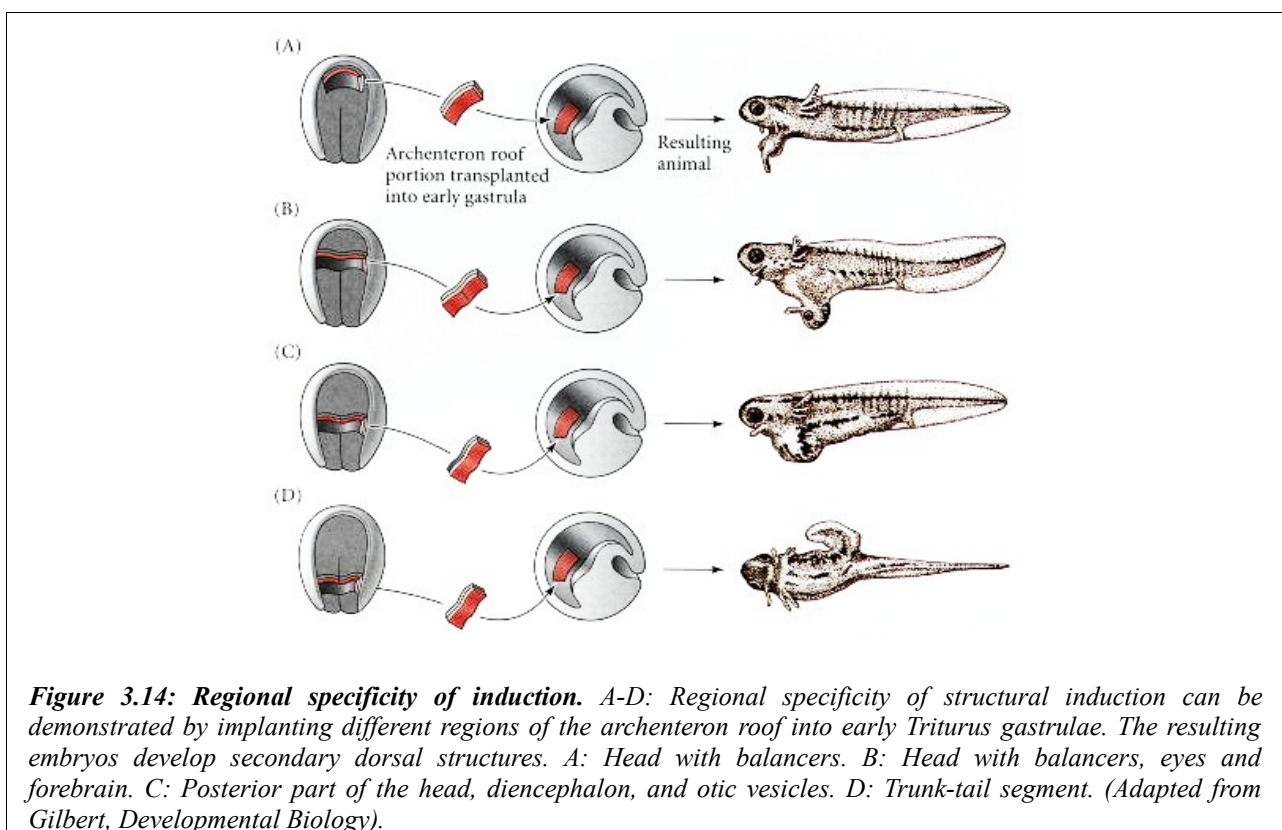
signaling appeared not to be the only player in neural induction. FGF signaling has also been involved in the initiation of neural induction. Activation of FGF signaling has been proposed to be required prior to, or independent to, the inhibition of BMP signaling. Likewise, WNT signals have also been proposed to be required for neural induction in chick embryos. However, there is also evidence suggesting that FGF signals are dispensable for the process of neural induction. FGF signaling plays multiple and often contrasting roles in the early embryo as well as in pluripotent stem cells, and conclusions may vary depending on the particular experimental conditions and the assays used. Reconciling, at least partially, these discrepancies, elegant experiments have led to propose a model by which the activation of the FGF and WNT signaling pathways inhibits BMP signaling (Andonadiou and Martinez-Barbera, 2013). Together, these studies suggest that the activation of both the FGF and WNT pathways converge with the inhibition of BMP signaling at the levels of Smad1 and reinforces the idea that BMP signaling inhibition may be a conserved requirement for neural induction.

Thus, embryonic cells appear to acquire neural potential if they avoid a series of signaling events that promote their differentiation along non-neural lineages; these and other observations led to the proposition of a process called the **Default Model for Neural Induction** (*Figure 3.13*). According to this view, BMPs play a key role by antagonizing a neural default differentiation program. Antagonists of BMP signaling such as Noggin would ensure low levels of BMPs in the presumptive neuroectoderm thus allowing neural development (See Wilson & Houart, 2004, for a review).



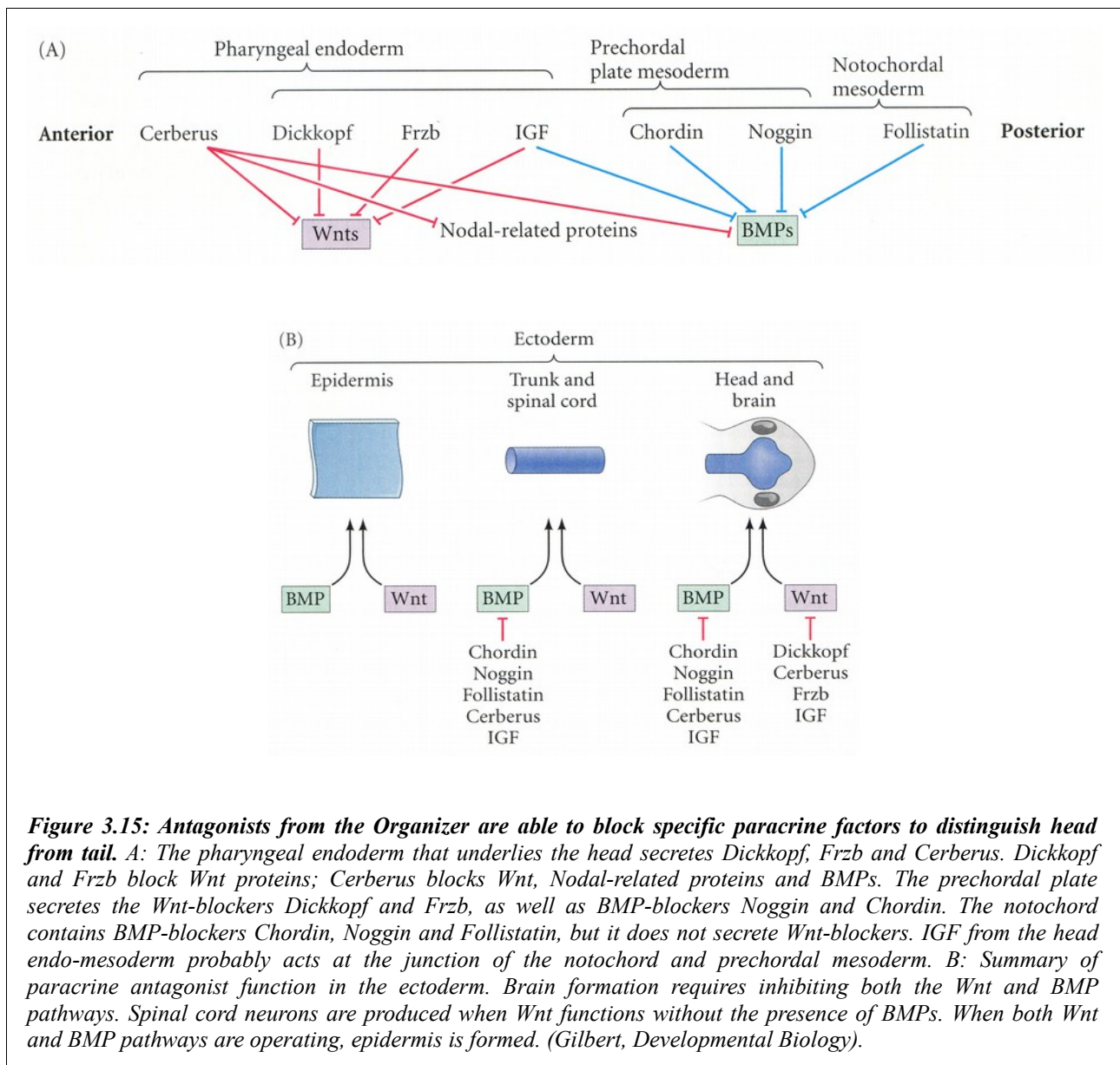
Regional Specificity of Neural Induction

One of the most important phenomena in neural induction is the acquisition of a regional identity of the newly produced neural structures. Forebrain, hindbrain and spinocaudal regions of the neural tube must be properly organized in an anterior-to-posterior direction. The Organizer tissue not only induces the neural tube, it also specifies the regions of the neural tube. This region-specific induction was demonstrated by Hilde Mangold's husband, Otto Mangold, in 1933. He transplanted four successive regions of the archenteron roof of late-gastrula newt embryos into the blastocoels of early-gastrula embryos (**Figure 3.14**). The most anterior portion of the archenteron roof (containing head mesoderm) induced balancers and portions of the oral apparatus (**Figure 3.14A**); the next most anterior section induced the formation of various head structures, including nose, eyes, balancers, and otic vesicles (**Figure 3.14B**); the third section (including the notochord) induced the hindbrain structure (**Figure 3.14C**); and the most posterior section induced the formation of dorsal trunk and tail mesoderm (**Figure 3.14D**).



Moreover, the abilities of the Organizer were found to be stage dependent, as dorsal blastopore lip cells from younger embryos were capable of inducing an entire ectopic neural axis (heads, eyes, brain and spinal cord), but older ones gave rise to ectopic axes lacking the eyes and the most anterior structures (*Figure 3.5*).

The molecules secreted by the Organizer in a regional fashion are indicated in *Figure 3.15* and described in detail in the text. The first cells involuting through the blastopore lip (the endomesoderm) induce head structures, while the next portion of involuting mesoderm (notochord) produces trunk and tail structures.



It had been thought that all the neural tissue induced by the Organizer was induced to become forebrain, and that the notochord represented the most anterior portion of the Organizer. However, the most anterior regions of the head and brain are underlain not by notochord, but by pharyngeal endoderm and head (prechordal) mesoderm. This “**endomesoderm**” constitutes the leading edge of the dorsal blastopore lip. Recent studies have shown that these cells not only induce the most anterior head structures, but that they do it by blocking the Wnt pathway as well as blocking BMP4 (**Figure 3.15**).

In 1996, Bouwmeester and colleagues showed that the induction of the most anterior head structures could be accomplished by a secreted protein called **Cerberus**. Unlike the other proteins secreted by the Organizer, Cerberus promotes the formation of the cement gland (the most anterior region of tadpole ectoderm), eyes, and olfactory (nasal) placodes. When *cerberus* mRNA was injected into a vegetal ventral *Xenopus* blastomere at the 32-cell stage, ectopic head structures were formed (**Figure 3.16**). These head structures were made from the injected cell as well as from neighboring cells. The *cerberus* gene is expressed in the pharyngeal endomesoderm cells that arise from the deep cells of the early dorsal lip, and the Cerberus protein has a triple activity, as it can bind (inhibit) both Nodal, BMPs and Xwnt8 (Glinka et al., 1997; Piccolo et al., 1999).

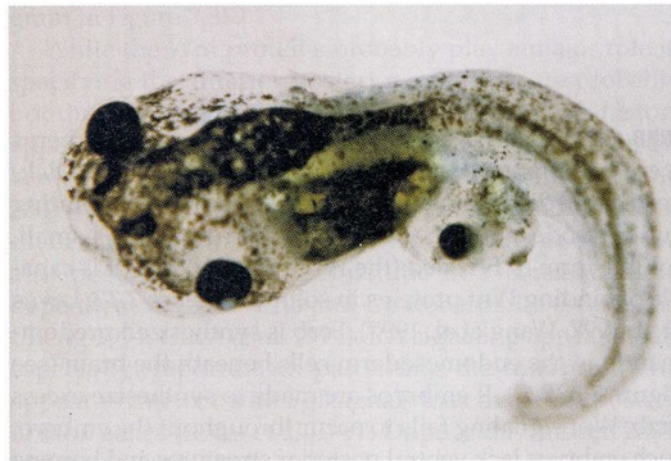
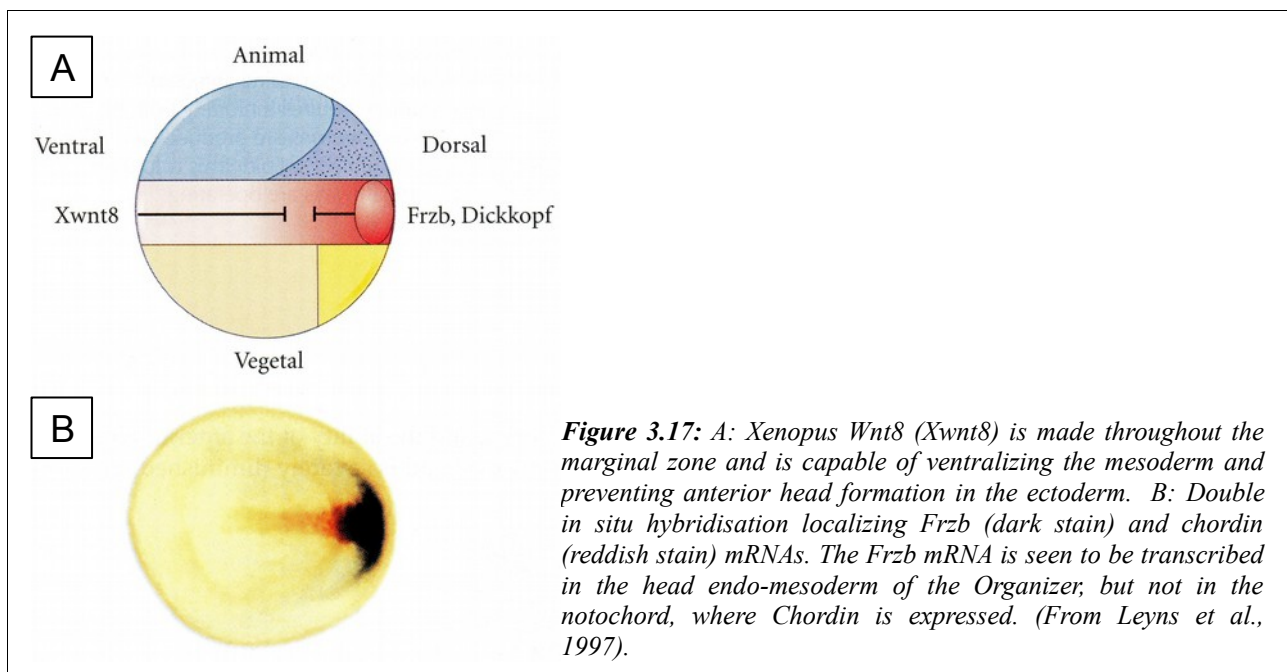


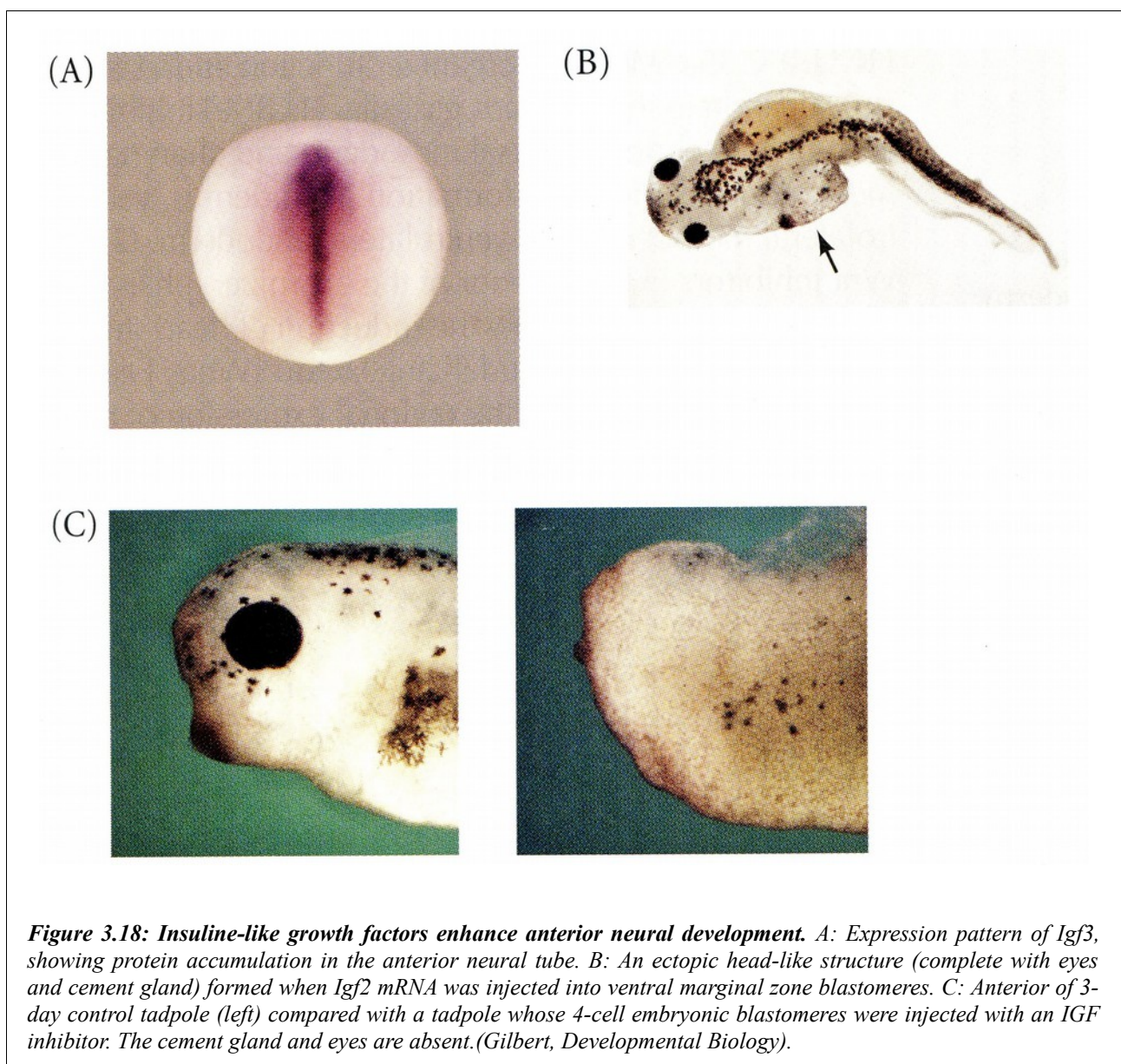
Figure 3.16: *Cerberus* mRNA injected into a single ventral vegetal blastomere of a 32-cell *Xenopus* embryo induces head structures, as well as duplicated heart and liver. The secondary eye (a single cyclopic eye) and olfactory placode can be readily seen. (Modified from Gilbert, *Developmental Biology*).

Shortly after the attributes of Cerberus were demonstrated, two other proteins, Frzb and Dickkopf, were discovered to be synthesized in the involuting endomesoderm. **Frzb** (pronounced “frisbee”) is a small, soluble form of Frizzled, the Wnt receptor, that is capable of binding Wnt proteins in solution (Leyns et al., 1997; Wang et al., 1997). It is synthesized predominantly in the endomesoderm cells beneath the head (**Figure 3.17A,B**). If embryos are made to synthesize excess Frzb, Wnt signaling fails to occur, and the embryos lack ventral posterior structures, becoming solely head. The **Dickkopf** (German; “big head”) protein also appears to interact directly with Wnt proteins in the extracellular space (**Figure 3.17A**). Injection of antibodies against Dickkopf protein into the blastocoel causes the resulting embryos to have small, deformed heads with no forebrain (Glinka et al., 1998).



Glinka and colleagues (1997) have thus proposed a new model for embryonic induction. The induction of trunk structures may be caused by the blockade of BMP signaling from the notochord. However, to produce a head, both the BMP signal and the Wnt signal must be blocked. This blockade comes from the endo-mesoderm, now considered the most anterior portion of the Organizer.

In addition to those proteins that block BMPs and Wnts by physically binding to these paracrine factors, the head region contains yet another set of proteins that prevent BMP and Wnt signals from reaching the nucleus. Pera and colleagues (2001) showed that **insuline-like growth factors (IGFs)** are required for the formation of an anterior neural tube, including the brain and sensory placodes (**Figure 3.18**). IGFs accumulate in the dorsal midline and are especially prominent in the anterior neural tube (**Figure 3.18A**). When injected into ventral mesodermal blastomeres, IGF mRNA causes the formation of ectopic heads, while blocking the IGF receptors results in the lack of head formation (**Figure 3.18B,C**). IGFs appear to work by initiating a signal transduction cascade that interferes with the signal transduction pathways of both BMPs and Wnts.



In the 1950s, evidence accumulated for the existence of two gradients in amphibian embryos: a dorsal gradient of “neuralizing” activity and a caudal gradient of “posteriorizing” activity (Nieuwkoop, 1952; Toivonen and Saxén, 1955). The neuralizing activity came from the Organizer and induced the ectoderm to be neural. The posteriorizing activity originated in the posterior of the embryo and weakened anteriorly. Recent studies have extended this model and provided candidates for the posteriorizing molecules. As predicted, the two signaling systems work independently (Kolm and Sive, 1997). Chordin, Noggin, and the other molecules discussed above constitute the neuralizing factors secreted by the Organizer. The candidates for the posteriorizing factor include FGF, Retinoic acid (RA), and Wnt factors (Wnt3a and Wnt8).

It appears that a gradient of Wnt proteins is necessary for specifying the posterior region of the neural plate (the trunk and tail; Niehrs, 2004). In *Xenopus*, an endogenous gradient of Wnt signaling is highest in the posterior and absent in the anterior. Moreover, if *Xwnt8* is added to developing embryos, spinal cord-like neurons are seen more anteriorly in the embryo, and the most anterior markers of the forebrain are absent. Conversely, suppressing Wnt signaling (by adding *Frzb* or *Dickkopf* to the developing embryo) leads to the expression of the anterior-most markers in more posterior neural cells.

Another candidate as a caudalizing factor is *Xenopus* **Wnt3a** (McGrew et al., 1995). This protein is found in the neural ectoderm of the early neurula. When ectoderm is isolated from *Xenopus* gastrulae but remains connected to the dorsal blastopore lip, the ectoderm develops an anterior-posterior array of neural markers. If the embryo is first injected with *Xwnt3a* mRNA (causing the overexpression of this protein), the anterior markers are lost.

Fibroblast growth factors are able to turn anterior neural tissue into posterior neural tissue. When early-gastrula ectoderm (which has not yet been underlain by dorsal mesoderm) was isolated and neuralized by Noggin, Chordin, or Follistatin, anterior-type neural markers were found in that tissue. However, when isolated early-gastrula ectoderm was incubated with a neural inducer plus **FGF2**, it expressed more posterior neural markers. FGF2 also induces forebrain tissue to express hindbrain-specific genes (Cox and Hemmati-Brivanlou, 1995; Lamb and Harland, 1995). Furthermore, when FGF signaling is blocked *in vivo* by a dominant negative FGF receptor, the resulting tadpoles lack their posterior segments (Amaya et al., 1991). FGF2 is probably not the natural posteriorizing FGF in *Xenopus*, since it is not secreted by the embryo at this site, and it is

not localized to any side of the embryo. However, embryonic FGF (**eFGF**, a *Xenopus* FGF similar to mammalian FGF4) is found in *Xenopus* posterior and tailbud mesoderm, and it has the same effects as FGF2 (Isaacs et al., 1992). Overexpression of eFGF up-regulates several posteriorly expressed genes, including the *Xenopus* homologue of *caudal*. These genes, in turn, encode proteins that appear to regulate the Hox genes controlling the specification of body segments along the anterior-posterior axis. This leads to the more posterior specification of the caudal nervous system (Pownall et al., 1996). Interestingly, eFGF may be induced by the posterior notochord (Taira et al., 1997).

Retinoic acid is also likely to play a role in posteriorizing the neural tube.

In vivo, Retinoic acid is synthesized from vitamin A (retinol) by the action of retinol dehydrogenases, which are expressed in the posterior regions of the embryo, but not in the anterior neural plate at the time of neural induction. In contrast, enzymes such as CYP26, a cytochrome P450 enzyme that degrades RA, is expressed at high levels in the anterior neural plate. This differential expression of synthesis and degradation enzymes is thought to create a RA signaling gradient along the AP axis (low-anterior and high-posterior).

If *Xenopus* neurulae are treated with nanomolar to micromolar concentrations of Retinoic acid (RA), their forebrain and midbrain development is impaired in a concentration-dependent fashion (**Figure 3.19**; Papalopulu et al., 1991; Sharpe, 1991). When lower concentrations are used, the actual induction of neural tissue does not appear to be inhibited, but fewer forebrain structures are produced (Durstion et al., 1989; Sive et al., 1990). Retinoic acid appears to affect both the mesoderm and the ectoderm. Ruiz i Altaba and Jessell (1991) found that anterior dorsal mesoderm from RA-treated gastrulae was unable to induce head structures in host embryos, and Sive and Cheng (1991) found that RA-treated ectoderm was unable to respond to the anterior-inducing mesoderm of untreated gastrulae. An RA gradient (tenfold higher in the posterior than in the anterior) has been detected in the dorsal mesoderm of early *Xenopus* neurulae (Chen et al., 1994). Like eFGF, retinoic acid has been shown to activate the expression of more posterior Hox genes (Cho et al., 1991; Sive and Cheng, 1991; Kolm and Sive, 1997).

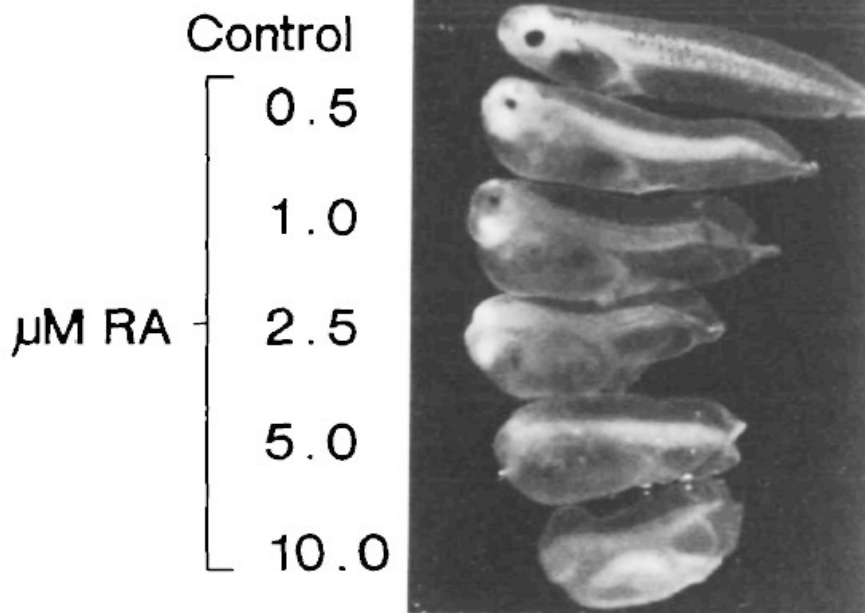
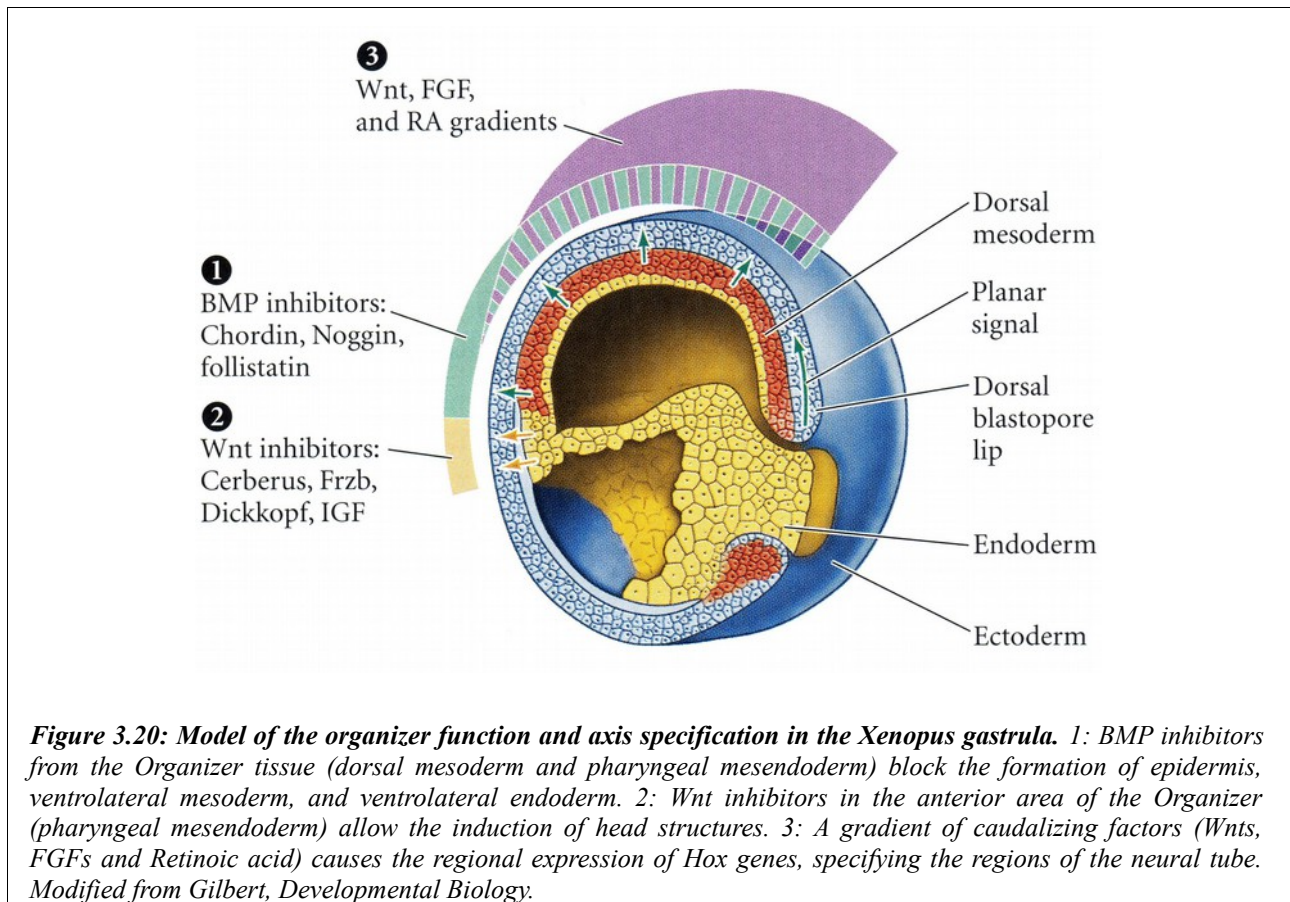


Figure 3.19: Effects of increasing doses of Retinoic acid on *Xenopus* brain development.
(Papalopulu et al., 1991).

The relationship between these three pathways of posteriorization has yet to be worked out. They may play different roles in different regions of the embryo, and they may work together. Retinoic acid has its major effect on hindbrain patterning, while eFGF is more important in the regionalization of the spinal cord (Blumberg et al., 1997; Kolm et al., 1997; Godsave et al., 1998). By interacting with FGFs, RA signaling is able to activate posterior Hox genes. Wnt3a may suppress anterior genes and be a permissive factor allowing the other two proteins to function (McGrew et al., 1997).

The basic model of neural induction, then, looks like the diagram in **Figure 3.20**.



In summary, all the above described factors (such as Wnts, Retinoic acid and FGFs) are thought to convert neuroepithelial cells from an anterior ground state to a more posterior position along the neuraxis. In many assays, whenever neural tissue is induced, it expresses transcripts that are later restricted to forebrain and midbrain territories. Expression of these “anterior markers” raises the possibility of an obligate link between induction of neural identity and acquisition of anterior character (discussed in Foley and Stern, 2001). In such a scenario, *neural inducing signals are proposed to impart both neural and anterior identity to the ectoderm while the generation of the full range of CNS structures would be the result of later events that posteriorize anterior neural tissue* (**Figure 3.21**; See Wilson and Houart, 2004 as a Review, and Beccari et al., 2013).

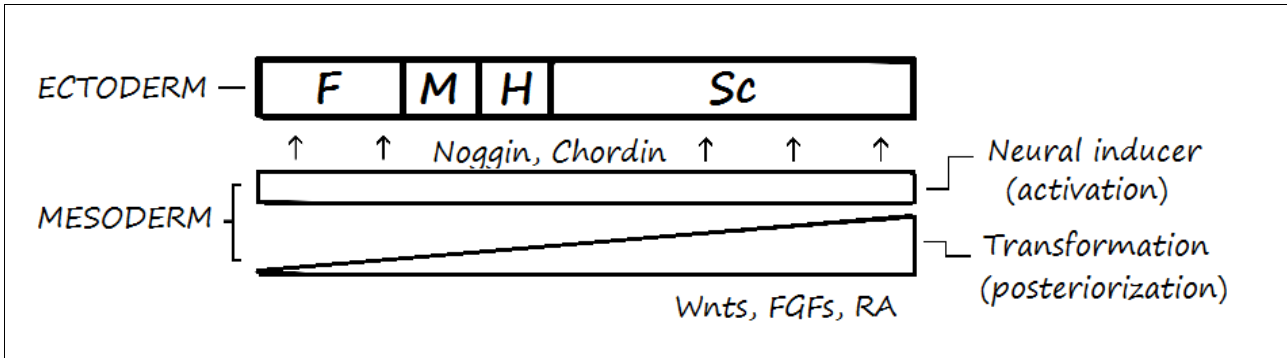
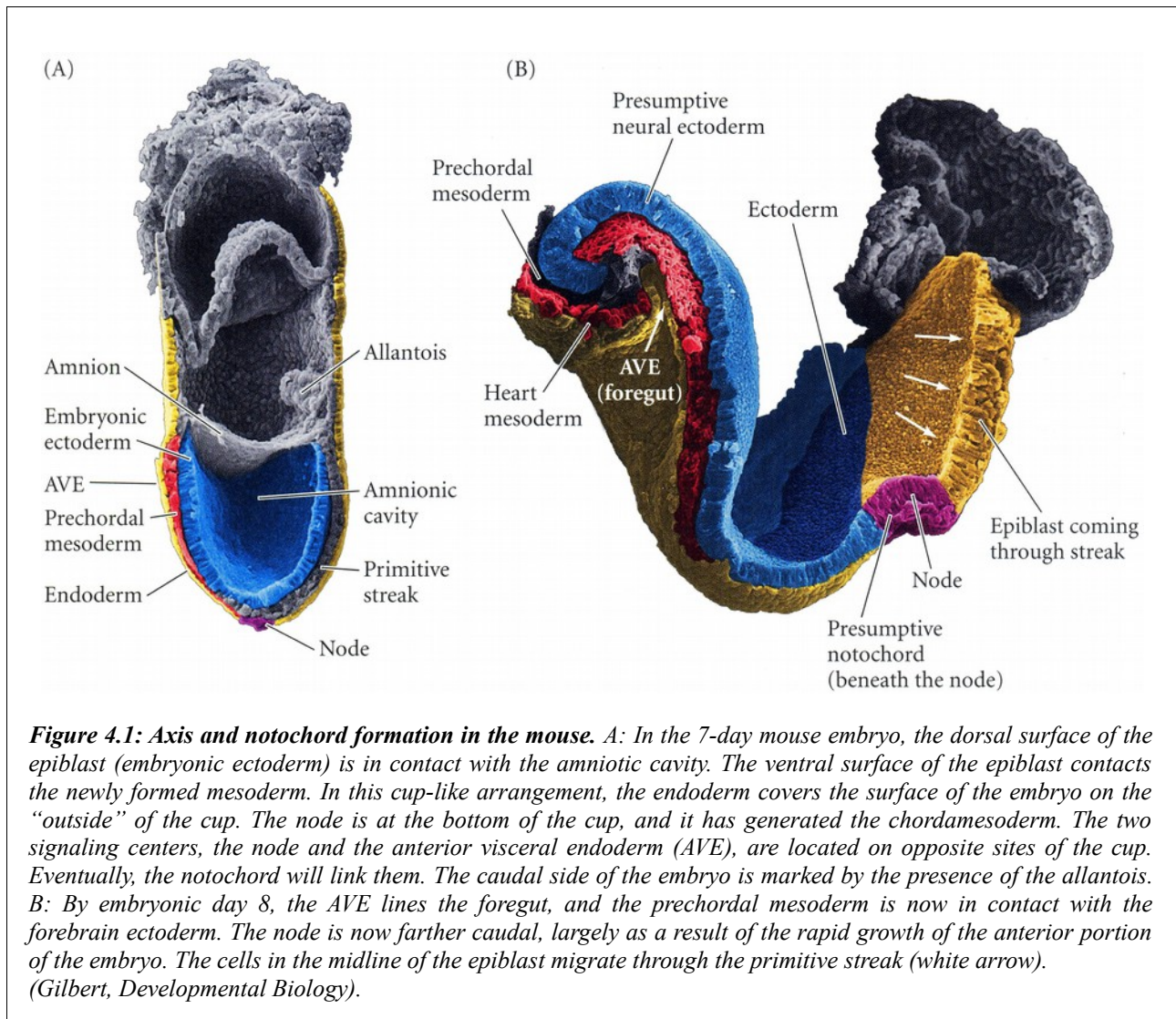


Figure 3.21: Nieuwkoop and Faber model of neural induction and A-P patterning. Much of our knowledge on neural induction and subsequent brain patterning has come from amphibian studies. This led to the development of a **two step Activation-Transformation model**: ectodermal cells initially acquire an anterior fate upon neural induction (activation), but they can subsequently be transformed into more caudal cell fates (transformation) to obtain all of the different subdomains along the A/P axis, a process referred to as caudalization. (Reviewed in Wilson and Houart, 2004).

4– Mammalian Axis Formation

Two Signaling Centers: the Node and the Anterior Visceral Endoderm

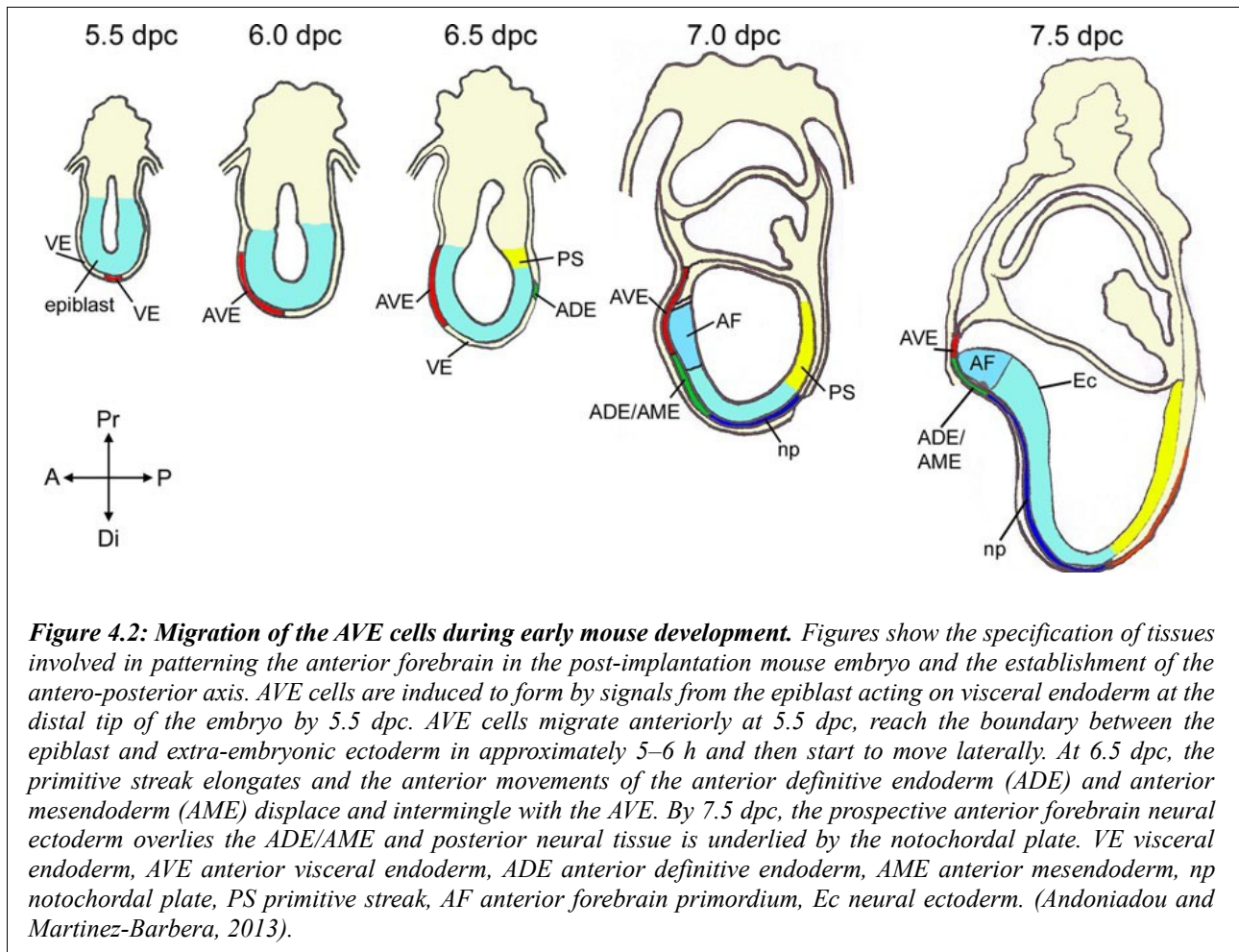
Neural induction and the formation of the anterior-posterior axis has been extensively studied in mice. The structure of the mouse epiblast is cup-shaped. The dorsal surface of the epiblast (the embryonic ectoderm) contacts the amniotic cavity, while the ventral surface of the epiblast contacts the newly formed mesoderm. In this cup-like arrangement, the endoderm covers the surface of the embryo on the “outside” of the cup (*Figure 4.1A*).



The mammalian embryo has two signaling centers: the **node** (equivalent to the amphibian Organizer) and the **anterior visceral endoderm (AVE)**; similar to the prechordal endomesoderm, the head portion of the amphibian Organizer) (**Figure 4.1B**). The node, which is positioned at the bottom of the cup in the mouse early embryo, is responsible for the specification of the body and, together with the AVE, works to form the anterior region of the embryo (Bachiller et al., 2000). The notochord forms by the dorsal infolding of the small, ciliated cells of the node. Both the mouse node and the anterior visceral endoderm express many of the genes known to be expressed in the chick and frog Organizer tissue. In mouse, the transplantation of the node led to similar results compared to the amphibian Organizer transplantation. However, it came as a surprise that the transplantation of the mouse node gave rise to an incomplete axis lacking the anterior forebrain.

This happened because the second signaling center, the AVE, was necessary together with the node for the specification of most anterior tissues.

The AVE originates from the visceral endoderm (hypoblast) that migrates forward (**Figure 4.2**).



As the AVE migrates, it secretes two antagonists of the Nodal protein, Lefty-1 and Cerberus. Lefty-1 binds to the Nodal's receptor and blocks Nodal binding, while Cerberus binds to Nodal itself. While the Nodal proteins in the epiblast activate the expression of posterior genes that are required for mesoderm formation, the AVE creates an anterior region where Nodal cannot act. The AVE also begins expressing the anterior markers that are necessary for head formation, such as transcription factors *Hesx1*, *Lim1*, *Lhx1*, *Foxa1* and *Otx2*, as well as the gene coding for the Wnt-inhibitor *Dickkopf*. *Dickkopf* is expressed both in the AVE and in the node.

Studies on mutant mice indicate that the AVE promotes anterior specification by suppressing the formation of the primitive streak (a posterior structure) by Nodal and Wnt proteins (Perea-Gomez et al., 2002). However, AVE alone cannot induce neural tissue, as the node can.

The placement of the node and the primitive streak appears to be due to the blocking of Nodal signaling by the Cerberus and Lefty-1 from AVE. The anterior visceral endoderm is established before the node, and the primitive streak always forms on the side of the epiblast *opposite* this anterior site. Once formed, the node will secrete Chordin (**Figure 4.3A**); the head process and notochord will later secrete also Noggin. These two BMP antagonists are not expressed in the AVE. While knockouts of either *noggin* or *chordin* genes did not affect development, mice missing both genes lack forebrain, nose and other facial structures (Bachiller et al., 2000; **Figures 4.3B-D**).

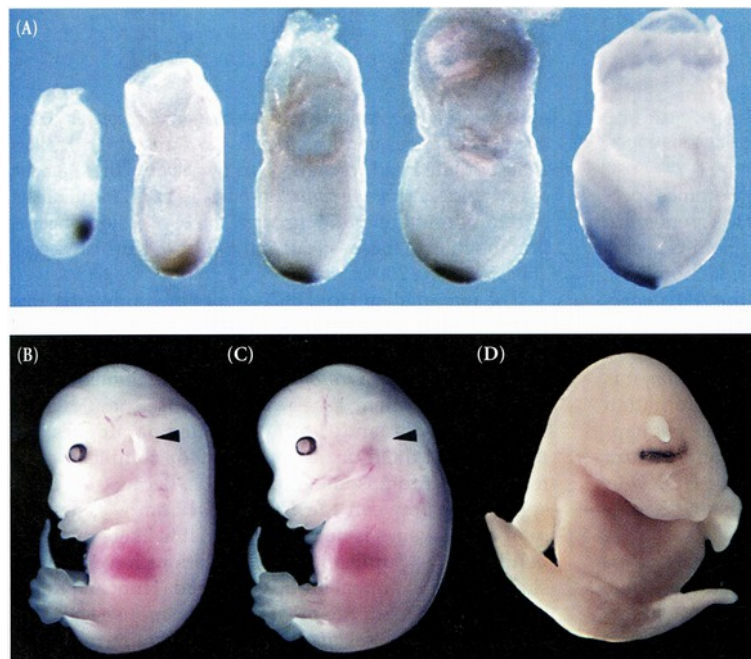


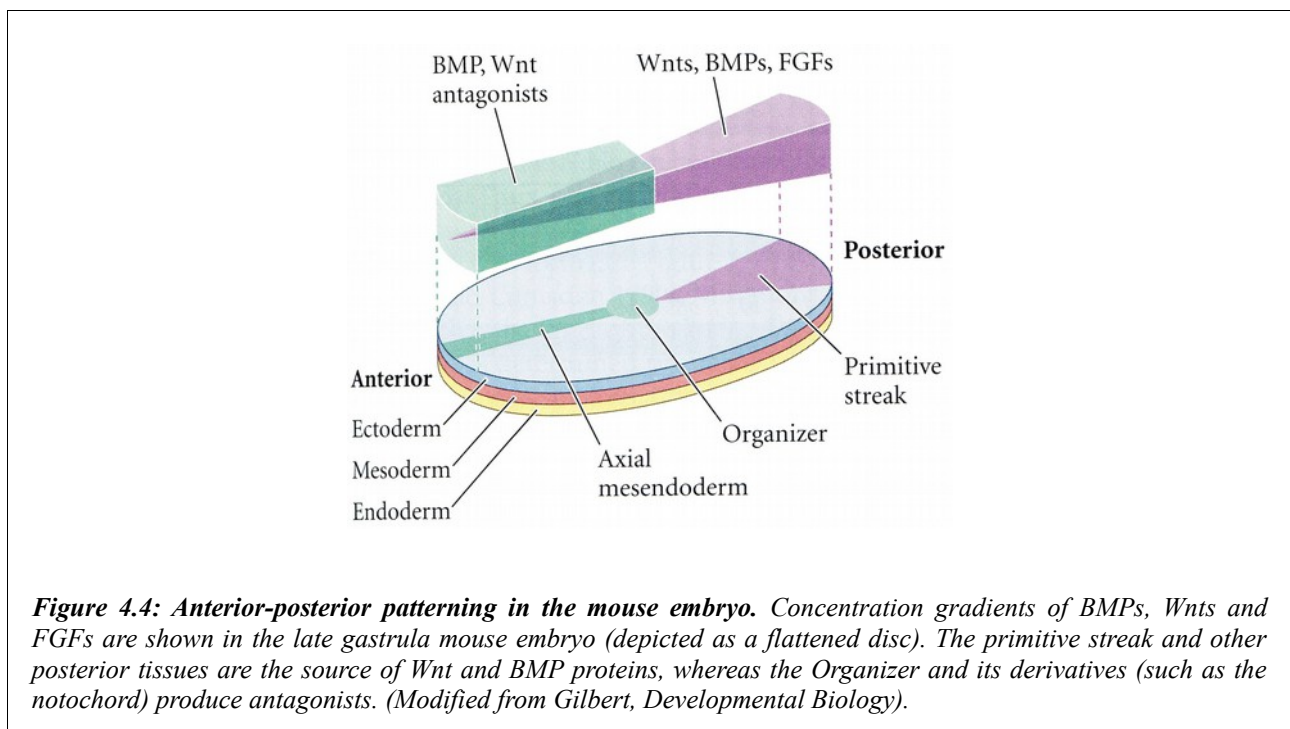
Figure 4.3: Expression of BMP antagonists in the mammalian node. A: Expression of Chordin during mouse gastrulation is seen in the anterior primitive streak, node and axial mesoderm. It is not expressed in the AVE. B-D: Phenotypes of 12.5-day embryos. B: Wild-type embryo. C: Embryo with the Chordin gene knocked out has a defective ear but an otherwise normal head. D: Phenotype of a mouse deficient in both Chordin and Noggin. There is no jaw, and there is a single centrally located eye, over which protrudes a large proboscis (nose). (Bachiller et al., 2000).

It is probable that the AVE functions in the epiblast to restrict Nodal activity, thereby cooperating with the node to promote the expression of head-forming genes in the anterior portion of the epiblast. Homozygosity for mutant alleles of any of the above-mentioned head-specific organizing genes produces mice lacking forebrain.

Anterior-Posterior Patterning: Wnt, FGF and Retinoic acid Gradients

A clear scenario emerges from what so far reported: the head region of the mammalian embryo is devoid of Nodal signaling; BMPs, FGFs and Wnts are also inhibited. The posterior region is characterized by Nodal, BMPs, Wnts, FGFs and Retinoic acid (RA). There appears to be a gradient of Wnt, BMP and FGF proteins that is highest in the posterior and that drops off strongly near the anterior region (**Figure 4.4**).

Moreover, in the anterior half of the embryo, starting at the node, there is a high concentration of antagonists that prevent BMPs and Wnts from acting (**Figure 4.4**).



The FGF8 gradient is created by the decay of mRNA: Fgf8 is expressed at the growing posterior tip of the embryo, but the FGF8 message is slowly degraded in the newly formed tissues. Thus, there is a gradient of FGF8 mRNA across the posterior of the embryo, which is then converted into an FGF8 protein gradient (**Figure 4.5**; Dubrulle and Pourquié, 2004).

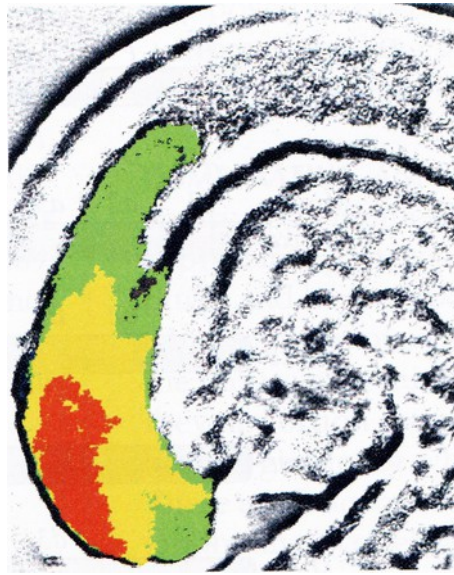
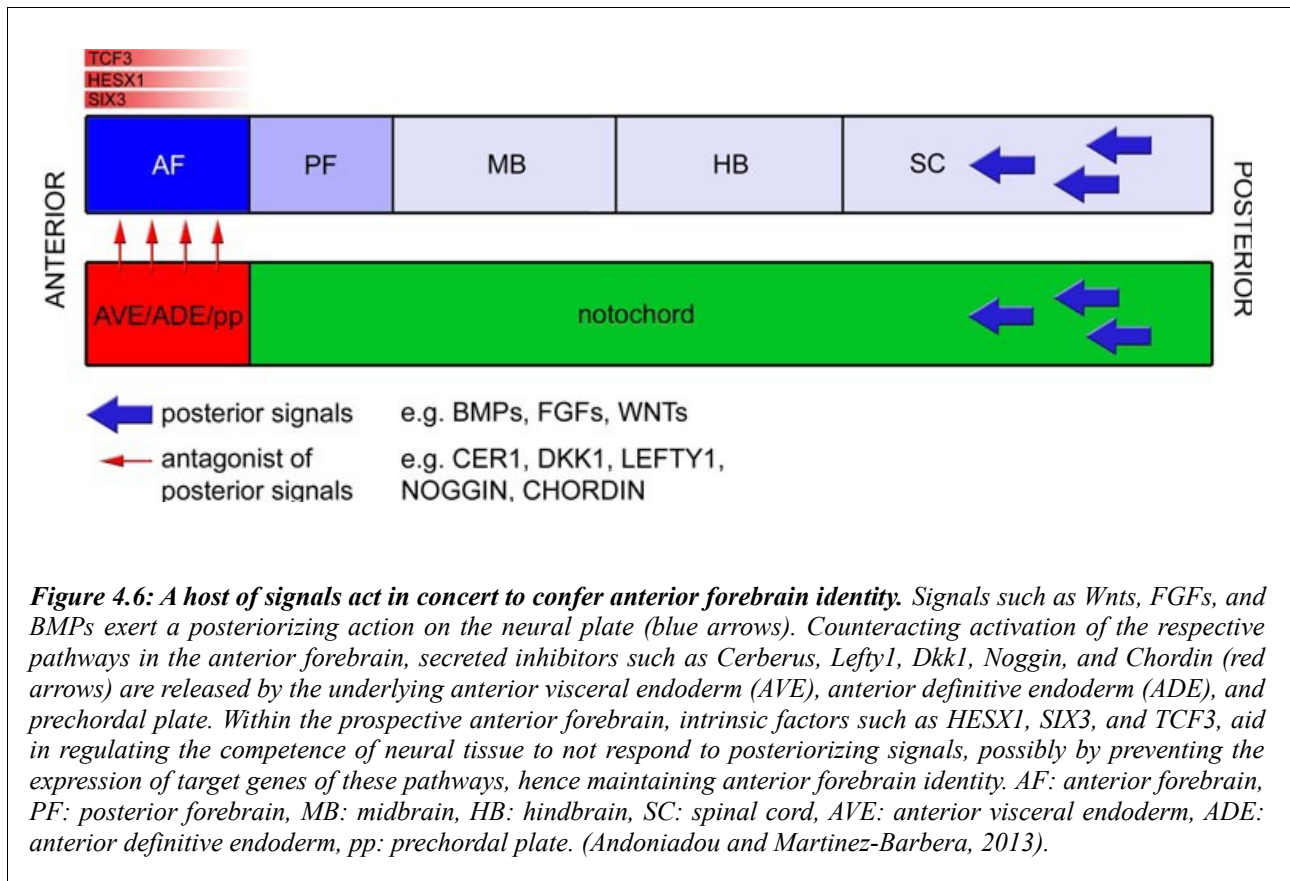


Figure 4.5: *FGF8 is expressed in the posterior tip of the gastrula and continues to be made in the tail bud. Its mRNA decays, creating a gradient across the posterior portion of the embryo. Figure shows the FGF8 gradient in the tailbud region of a 9-day mouse embryo. The highest amount of FGF8 (red) is found near the tip. The gradient was determined by in situ hybridisation of an FGF8 probe and staining for increasing amounts of time. (Dubrulle and Pourquié, 2004).*

In addition to FGFs, the late gastrula has a gradient of Retinoic acid too. RA levels are high in the posterior regions and low in the anterior portions of the embryo. This gradient (like that of frog embryos) appears to be controlled by the expression of RA-synthesizing enzymes in the embryo's posterior and RA-degrading enzymes in the anterior parts of the embryo.

The FGF gradient patterns the posterior portion of the embryo by working through the Cdx family of caudal-related genes. The Cdx transcription factors, in turn, integrate the various posteriorizing signals (Retinoic acid, FGF8 and Wnt3a) by activating and regulating the activity of Hox genes, whose expression regulates anterior-posterior patterning in all vertebrates.

In general, the **activation-transformation model** created after experiments in frogs, was found to be valid also for mammalian embryos: *Neural tissue develops anterior character unless exposed to caudalizing signals. (Figure 4.6).*

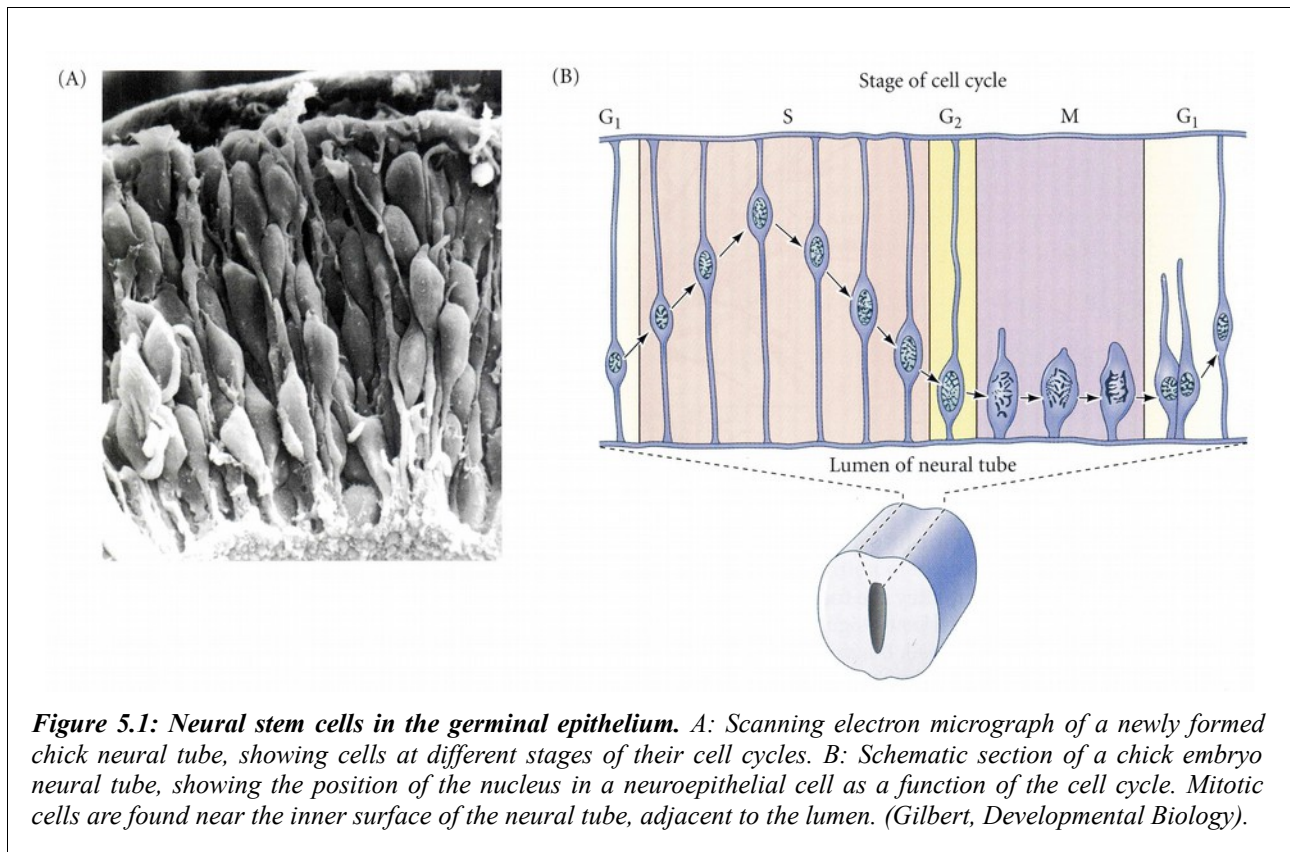


5– Tissue Architecture of the Central Nervous System: Development of the Cerebral Cortex.

The neurons of the brain are organized into layers (**cortices**) and clusters (**nuclei**), each having different functions and connections. The original neural tube is composed of a **germinal neuroepithelium**, a layer of rapidly dividing neural stem cells, one cell layer thick.

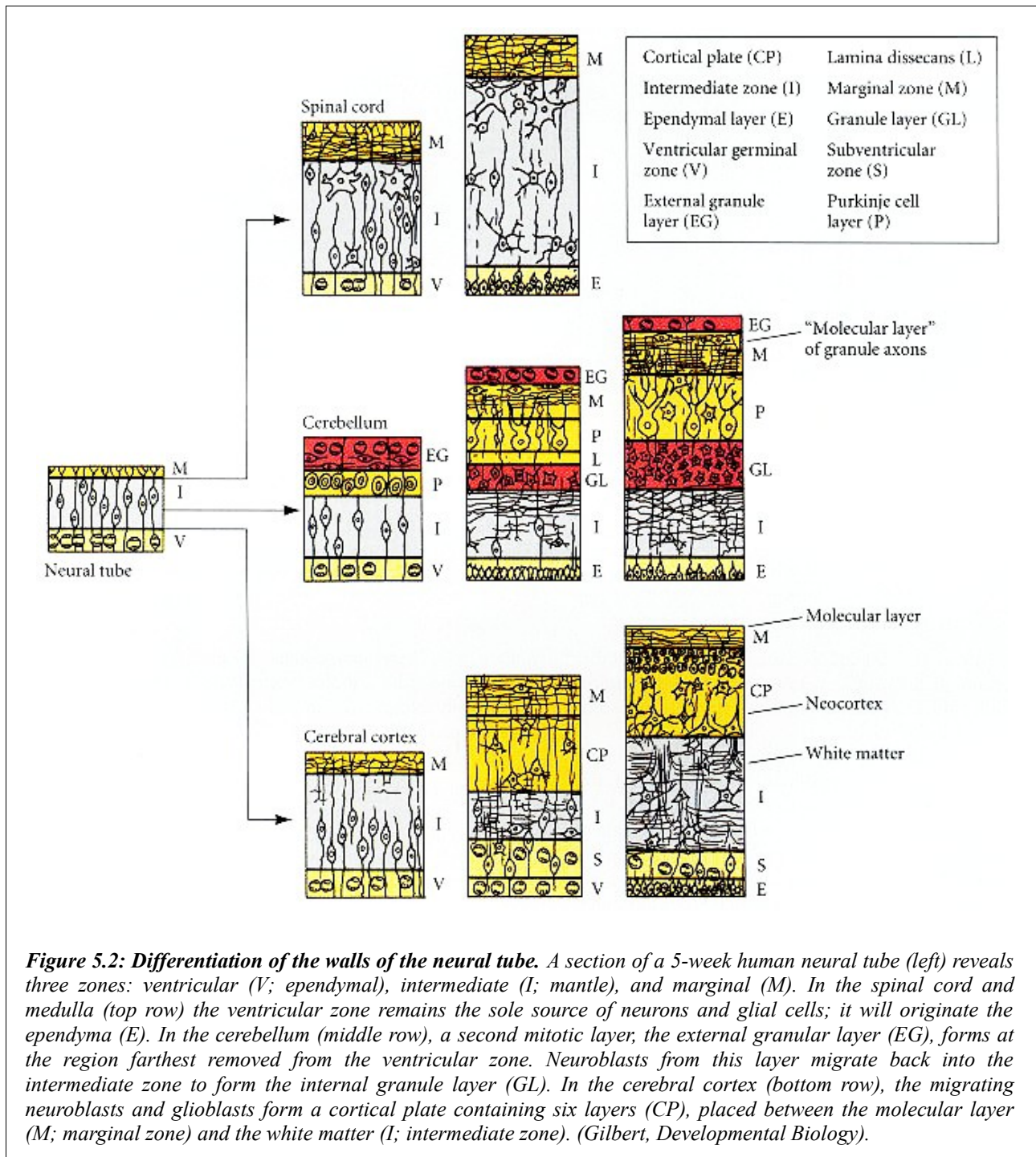
Sauer (1935) and others have shown that all the cells of the germinal epithelium are continuous from the luminal surface of the neural tube to the outside surface, but that the nuclei of these cells are at different heights, thereby giving the superficial impression that the neural tube has numerous cell layers (*Pseudostratified Neuroepithelium*) (**Figure 5.1**).

The nuclei move within their cells as they go through the cell cycle. DNA synthesis (S phase) occurs while the nucleus is at the outside edge of the neural tube, and the nucleus migrates luminally as the cell cycle proceeds (**Figure 5.1**). Mitosis occurs on the luminal side of the cell layer. If mammalian neural tube cells are labeled with radioactive thymidine during early development, 100% of them will incorporate this base into their DNA (Fujita, 1964). Shortly thereafter, certain cells stop incorporating these DNA precursors, thereby indicating that they are no longer participating in DNA synthesis and mitosis. These neuronal and glial cells then migrate and differentiate outside the neural tube (Fujita, 1966; Jacobson, 1968).



If dividing cells in the germinal neuroepithelium are labeled with radioactive thymidine at a single point in their development, and their progeny are found in the outer cortex in the adult brain, then those neurons must have migrated to their cortical positions from the germinal neuroepithelium. When a cell of the germinal neuroepithelium is ready to generate neurons (instead of more neural stem cells), the plane of cell division shifts. The neuroepithelial stem cell divides "vertically" instead of "horizontally." Thus, the daughter cell adjacent to the lumen remains connected to the ventricular surface (and usually remains a stem cell), while the other daughter cell migrates away and differentiates (Chenn and McConnell, 1995).

The time of this vertical division is the last time the migrating cell will divide, and is called that neuron's **birthdate**. Different types of neurons and glial cells have their birthdates at different times. Labeling cells at different times during development shows that cells with the earliest birthdays migrate the shortest distances. The cells with later birthdays migrate through these layers to form the more superficial regions of the cortex. Subsequent differentiation depends on the positions these neurons occupy once outside the germinal neuroepithelium (Letourneau, 1977; Jacobson, 1991).

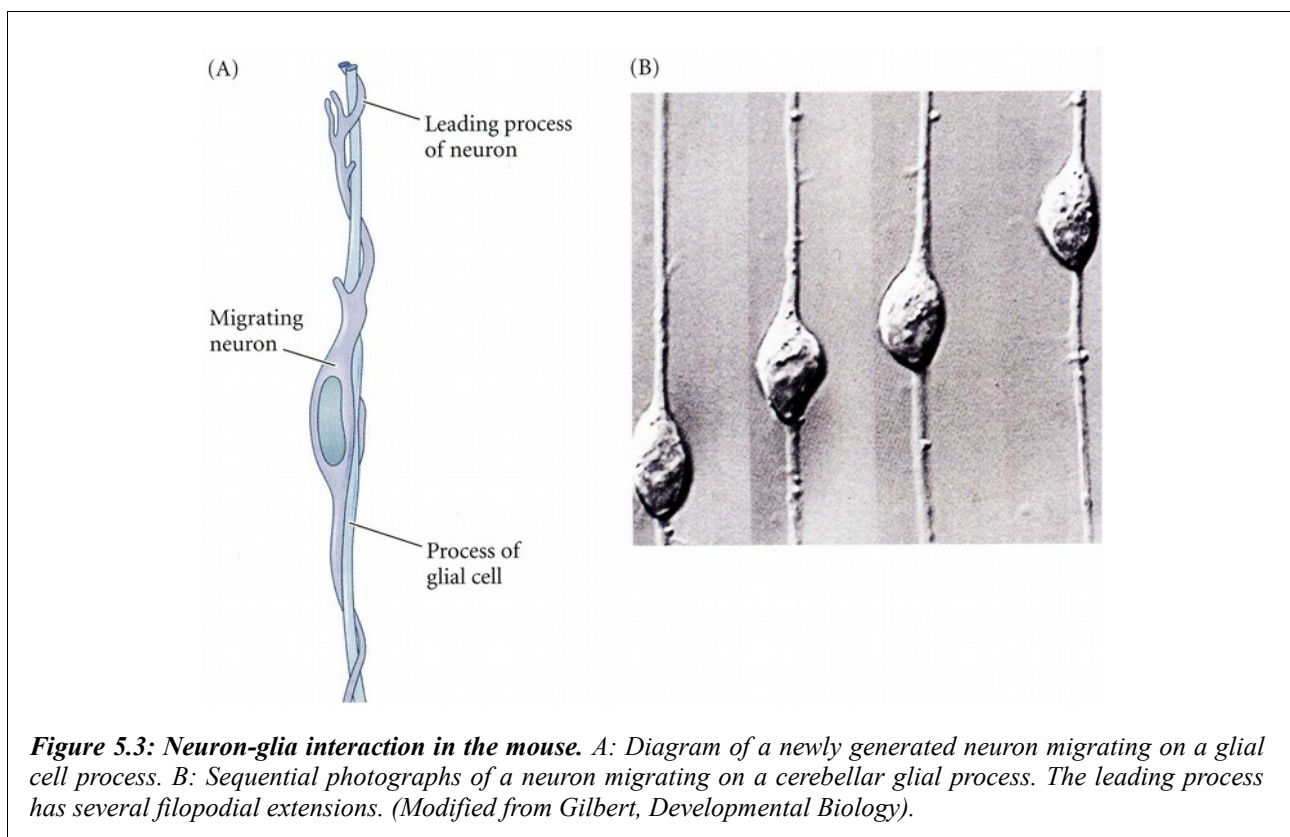


As the cells adjacent to the lumen continue to divide, the migrating cells form a second layer around the original neural tube. This layer becomes progressively thicker as more cells are added to it from the germinal neuroepithelium. This new layer is called the **mantle** (or **intermediate**) **zone**, and the germinal epithelium is now called the **ventricular zone** (and, later, the **ependyma**) (**Figure 5.2, left**). The mantle zone cells differentiate into both neurons and glia. The neurons make connections

among themselves and send forth axons away from the lumen, thereby creating a cell-poor **marginal zone**. Eventually, glial cells cover many of the axons in the marginal zone in myelin sheaths, giving them a whitish appearance. Hence, the mantle zone, containing the neuronal cell bodies, is often referred to as the **gray matter**; the axonal, marginal layer is often called the **white matter**. In the spinal cord and medulla, this basic three-zone pattern of ependymal, mantle, and marginal layers is retained throughout development (**Figure 5.2**).

In the brain, cell migration, differential neuronal proliferation, and selective cell death produce modifications of the three-zone pattern. The development of spatial organization is critical for the proper functioning of the cortices (cerebellum and cerebrum). For this to happen, the proper cells must differentiate at the appropriate place and time.

One mechanism thought to be important for positioning young neurons within the developing mammalian brain is **glial guidance** (Rakic, 1972; Hatten, 1990). In the cerebellum, the granule cell precursors travel on the long processes of the **Bergmann glia** (**Figure 5.3**; Rakic and Sidman, 1973; Rakic, 1975).



Throughout the cortex, neurons are seen to ride a “glial monorail” to their respective destinations: newly generated cortical neurons reach their destinations thanks to the radial glia. These glial cells have long processes that extend from the ventricular zone all the way to the pial surface.

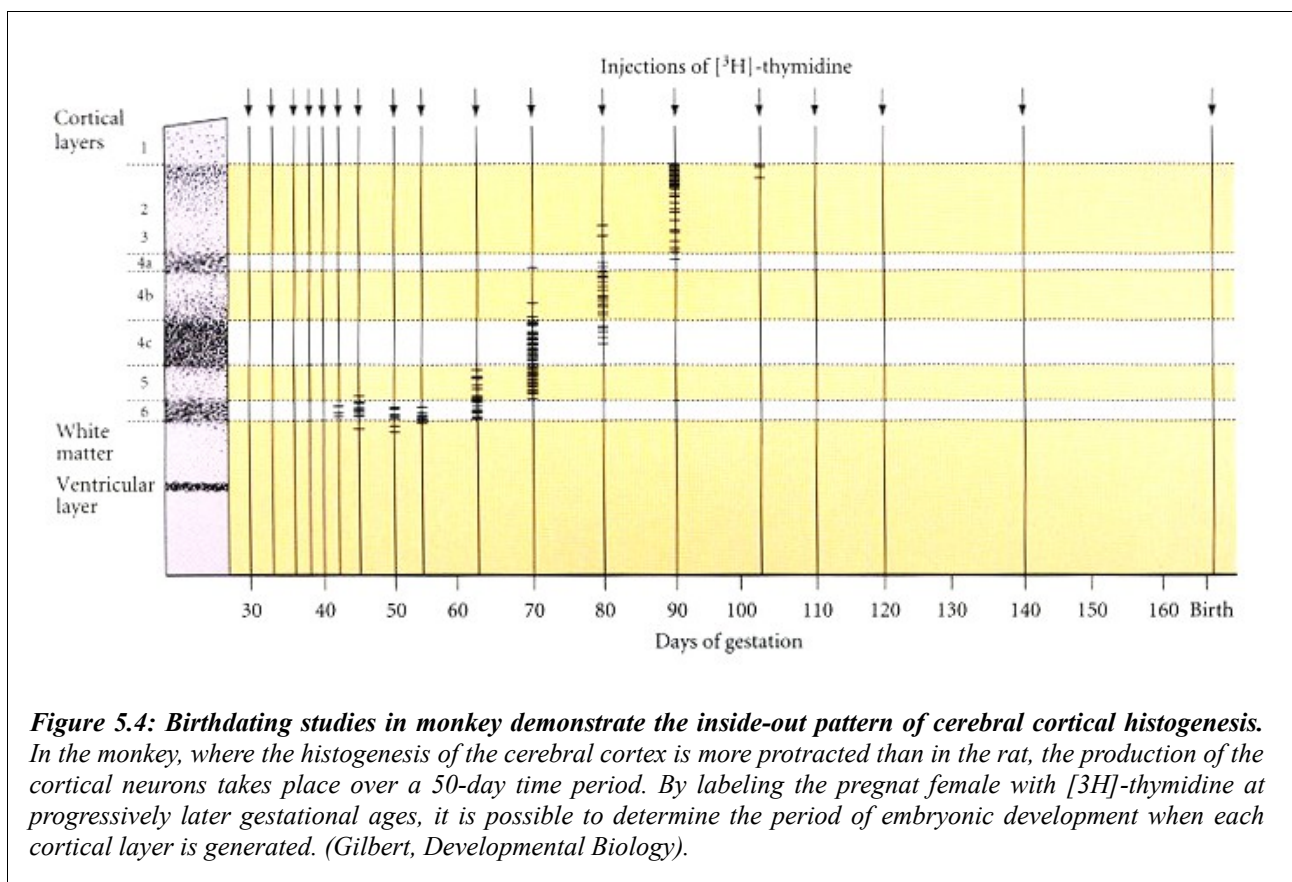
This neural-glia interaction is a complex and fascinating series of events, involving reciprocal recognition between glia and neuroblasts (Hatten, 1990; Komuro and Rakic, 1992). The neuron maintains its adhesion to the glial cell through a number of proteins, one of them an adhesion protein called **astrotactin**. If the astrotactin on a neuron is masked by antibodies to that protein, the neuron will fail to adhere to the glial processes (Edmondson et al., 1988; Fishell and Hatten, 1991).

Cerebral organization

The three-zone arrangement of the neural tube is also modified in the cerebrum. The cerebrum is organized in two distinct ways. First, like the cerebellum, it is organized vertically into layers that interact with one another (see *Figure 5.2, bottom row*). Certain neuroblasts from the mantle zone migrate on glial processes through the white matter to generate a second zone of neurons at the outer surface of the brain. This new layer of gray matter is called the **neocortex**. The specification of the neocortex is accomplished largely through the Lhx2 transcription factor, which activates numerous other cerebral genes. In Lhx2-deficient mice, the cerebral cortex fails to form (Mangale et al., 2008). The neocortex eventually stratifies into six layers of neuronal cell bodies; the adult forms of these layers are not completed until the middle of childhood. Each layer of the neocortex differs from the others in its functional properties, the types of neurons found there, and the sets of connections that they make. For instance, neurons in layer 4 receive their major input from the thalamus (a region that forms from the diencephalon), while neurons in layer 6 send their major output back to the thalamus.

Second, the cerebral cortex is organized horizontally into over 40 regions that regulate anatomically and functionally distinct processes. For instance, neurons in cortical layer 6 of the “visual cortex” project axons to the lateral geniculate nucleus of the thalamus (for vision processing), while layer 6 neurons of the auditory cortex (located more anteriorly than the visual cortex) project axons to the medial geniculate nucleus of the thalamus (for hearing).

Neither the vertical nor the horizontal organization of the cerebral cortex is clonally specified. Rather, the developing cortex forms from the mixing of cells derived from numerous stem cells. After their final mitosis, most of the neuronal precursors generated in the ventricular (ependymal) zone migrate outward along glial processes to form the **cortical plate** at the outer surface of the brain. As in the rest of the brain, those neuronal precursors with the earliest “birth dates” form the layer closest to the ventricle. Subsequent neurons travel greater distances to form the more superficial layers of the cortex. This process forms an “inside-out” gradient of development (**Figure 5.4**; Rakic, 1974).



Cortical cell migration.

The first cortical neurons to be generated migrate out of the germinal zone to form the transient **preplate**. Subsequently generated neurons migrate into the preplate and separate it into two layers: the **Cajal-Retzius layer** and the **subplate** (*Figure 5.5*). The Cajal-Retzius layer becomes and remains the most superficial layer of the neocortex, and its cells express the cell surface glycoprotein Reelin (*Figure 5.7*). The subplate remains the deepest layer through which the successive waves of neuroblasts travel to form the **cortical plate**.

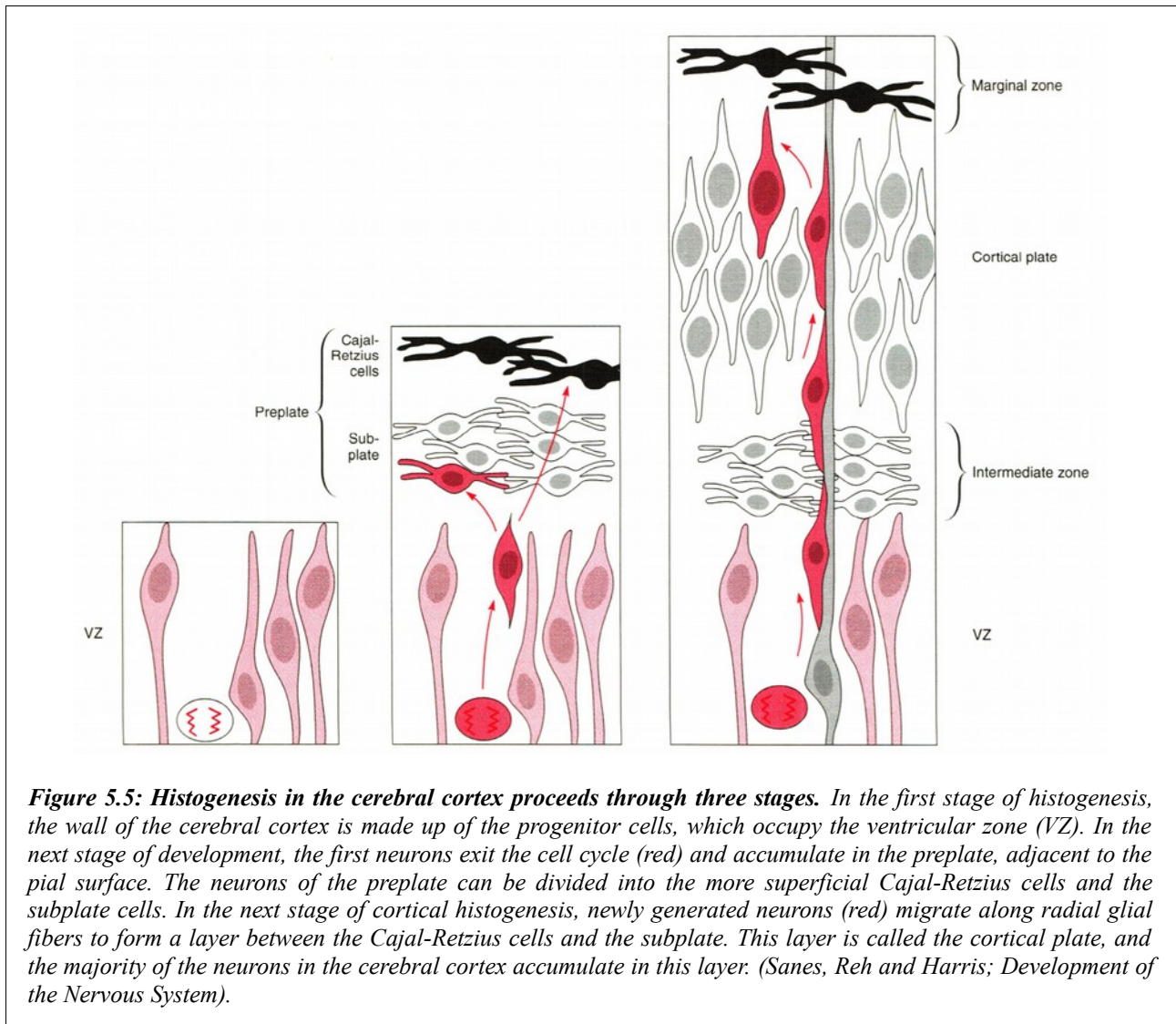
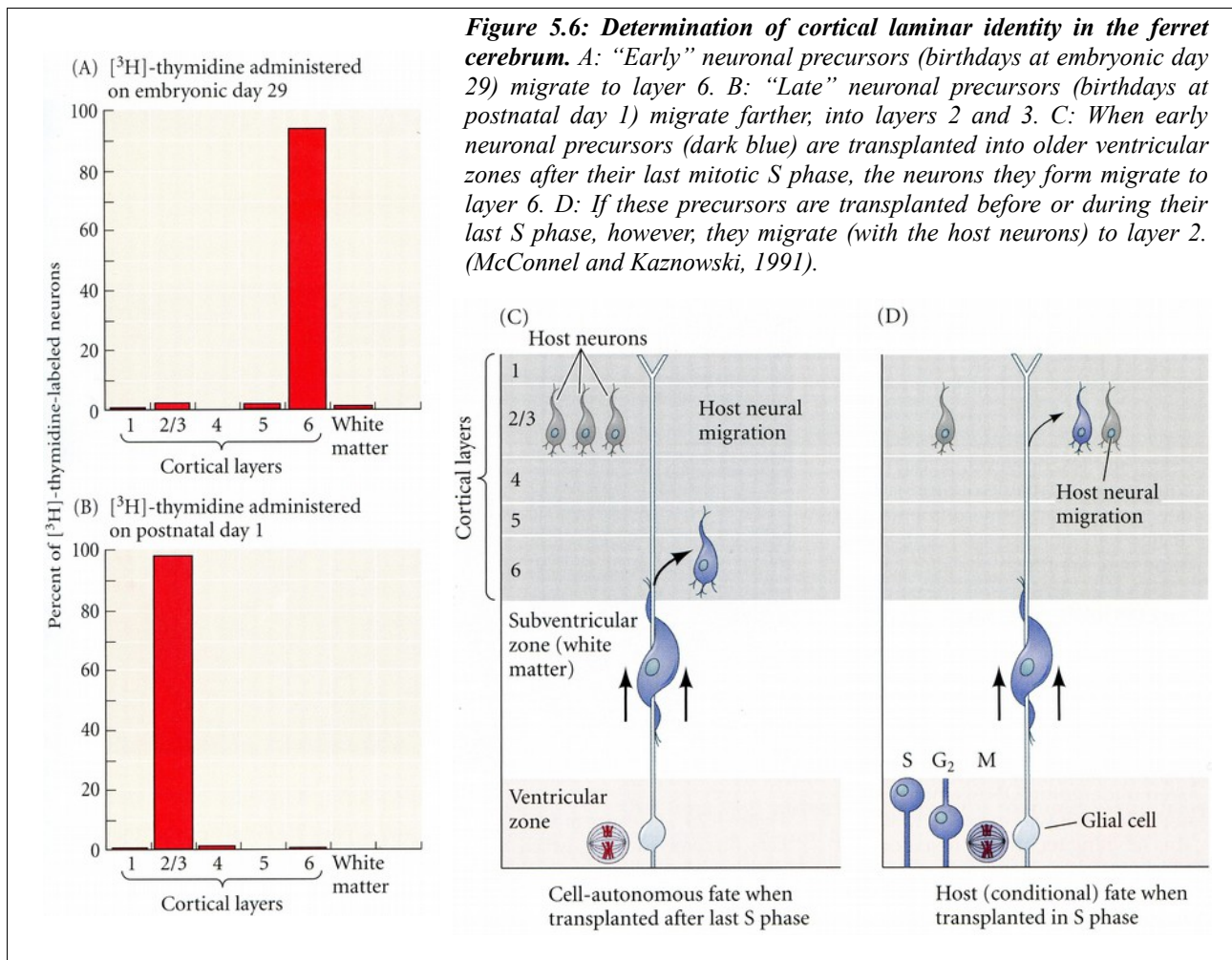


Figure 5.5: Histogenesis in the cerebral cortex proceeds through three stages. In the first stage of histogenesis, the wall of the cerebral cortex is made up of the progenitor cells, which occupy the ventricular zone (VZ). In the next stage of development, the first neurons exit the cell cycle (red) and accumulate in the preplate, adjacent to the pial surface. The neurons of the preplate can be divided into the more superficial Cajal-Retzius cells and the subplate cells. In the next stage of cortical histogenesis, newly generated neurons (red) migrate along radial glial fibers to form a layer between the Cajal-Retzius cells and the subplate. This layer is called the cortical plate, and the majority of the neurons in the cerebral cortex accumulate in this layer. (Sanes, Reh and Harris; *Development of the Nervous System*).

The Reelin-producing cells of the Cajal-Retzius layer are critical in the separation of the preplate. In Reelin-deficient mice, the preplate fails to split, and the neurons produced by the germinal layers pile up behind the previously generated neurons (instead of migrating through them). The fact that neural stem cells express Reelin, together with other proteins thought to be glial-specific, caused them to be called the *radial glial cells*.



A single stem cell in the ventricular layer can give rise to neurons (and glial cells) in any of the cortical layers (Walsh and Cepko, 1988). McConnell and Kaznowski (1991) have shown that the determination of laminar identity (i.e., which layer a cell migrates to) is made during the final cell division (**Figure 5.6**). Newly generated neuronal precursors transplanted after this last division from young brains (where they would form layer 6) into older brains whose migratory neurons are forming layer 2 are committed to their fate, and migrate only to layer 6 (**Figure 5.6A,C**). However,

if these cells are transplanted prior to their final division (during mid-S phase), they are uncommitted, and can migrate to layer 2 (**Figure 5.6B,D**). The fates of neuronal precursors from older brains are more fixed. While the neuronal precursor cells formed early in development have the potential to become any neuron (at layers 2 or 6, for instance), later precursor cells give rise only to upper-level (layer 2) neurons (Frantz and McConnell, 1996) (**Figure 5.6**). Although the molecular code of cell diversity in the cortex begins to be discovered, and more markers and effectors of different neuronal identities are emerging in the cortex (**Figure 5.7**), we still do not know exactly the molecular mechanisms that activate different programs in the cortical progenitor cell as it becomes committed.

Figure 5.7 indicates key markers for layer-specific differentiation of cortical neurons as in Gaspard et al., 2008.

Layers	Markers	Birthdate
Cajal–Retzius neurons	Reelin, calretinin, p73, TBR1	E10.5–11.5
Upper layers	SATB2, CUX1	E13.5–16.5
Deep layers	CTIP2, SOX5, OTX1, ER81, TBR1, TLE4, FOXP2	E11.5–14.5
Subplate	TBR1, calretinin, reelin	E10.5–13.5

Figure 5.7: Scheme depicting patterns of the layer-specific markers in cortical neurons, and their timing of generation *in vivo*. Key markers for layer-specific differentiation of cortical neurons are indicated. (Modified from Gaspard et al., 2008).

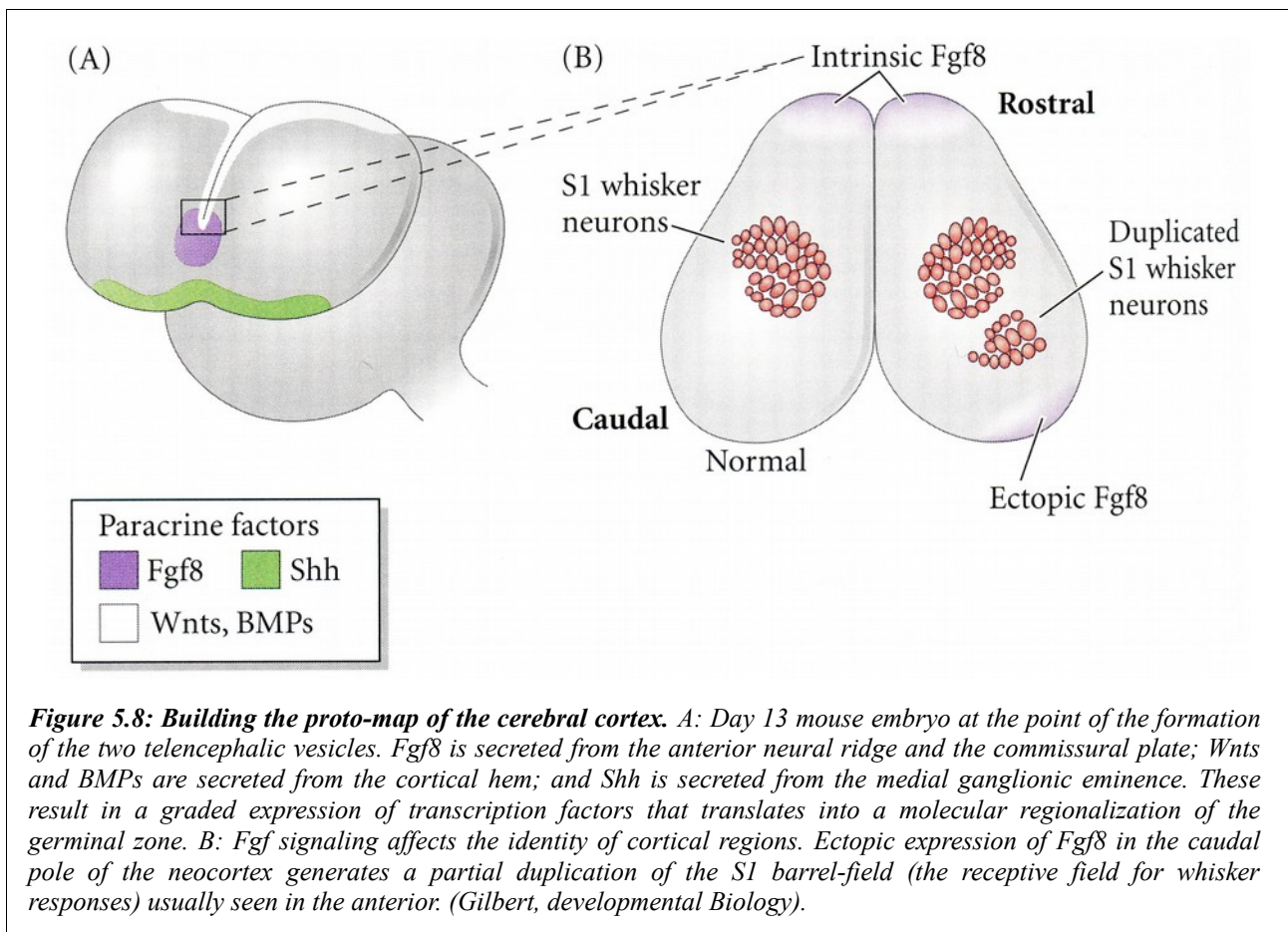
Not all neurons, however, migrate radially. O'Rourke and her colleagues (1992) labeled young ferret neurons with fluorescent dye and followed their migration through the brain. While a great majority of the young neurons migrated radially on glial processes from the ventricular zone into the cortical plate, about 12% of them migrated laterally from one functional region of the cerebral cortex into another. These observations meshed well with those of Walsh and Cepko (1992), who infected ventricular stem cells with a retrovirus and were able to stain these cells and their progeny after birth.

They found that the neural descendants of a single ventricular stem cell were dispersed across the functional regions of the cortex. Thus, the specification of the cortical areas into specific functional domains occurs after neurogenesis. Once the cells arrive at their final destination, it is thought that they produce particular adhesion molecules that organize them together as brain nuclei (Matsunami and Takeichi, 1995).

One of the major questions in developmental neurobiology is whether the different functional regions of the cerebral cortex are already specified in the ventricular region, or if specification is accomplished much later by the synaptic connections between the regions. Evidence that specification is early (and that there might be some “**proto-map**” of the cerebral cortex) is suggested by certain human mutations that destroy the layering and functional abilities in only one part of the cortex, leaving the other regions intact (Piao et al., 2004).

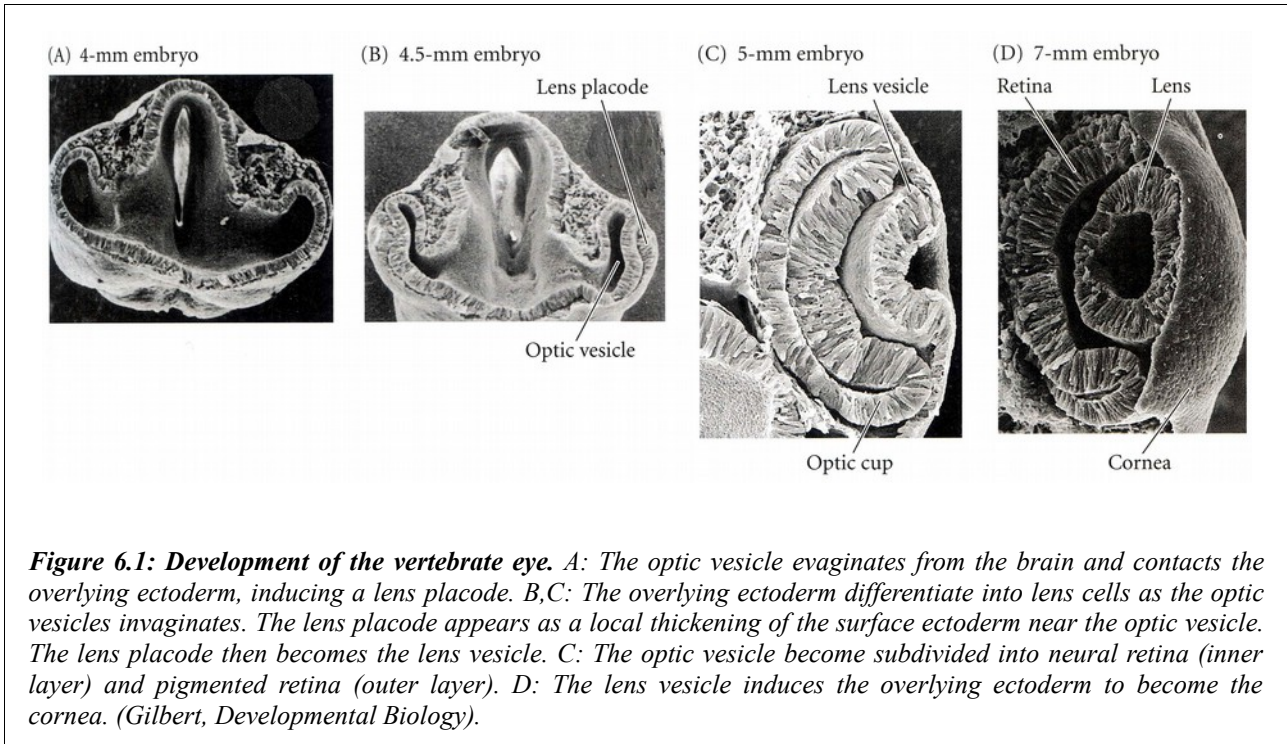
The early regionalization of the neocortex is thought to be organized by paracrine factors secreted by the epidermis and neural crest cells at the margin of the developing brain (Rakic et al., 2009). The paracrine factors induce the expression of transcription factors in the specific brain regions, which then mediate the survival, differentiation, proliferation and migration of the newly generated neurons. For instance, Fgf8 protein is secreted by the anterior neural ridge and is important for the A/P patterning of the cerebral cortex. If Fgf8 is overexpressed in the ridge, specification of the telencephalon is extended caudally, whereas if Fgf8 is ectopically added to the caudal region of the cortex, part of the caudal region of the cortex will acquire an anterior cortical fate (**Figure 5.8**).

The orphan nuclear receptor COUP-TFI is a transcription factor expressed in a caudomedial-high to rostralateral-low gradient in the developing neocortex. The rostralization of the neocortex in the absence of COUP-TFI, and the established role for COUP-TFI as a transcriptional repressor, suggest that COUP-TFI acts to specify caudal neocortical identity by repressing a rostral fate. The gradient of COUP-TFI in the developing neocortex lies in opposition to the rostral-high to caudal-low gradient of FGF signaling (**Figure 5.8**), and it is natural to ask whether these gradients regulate one another. There is good evidence that FGF signaling regulates COUP-TFI expression. The ability of FGF to repress the expression of COUP-TFI indicates that the Fgf-signaling gradient is responsible for establishing the caudal-high to rostral-low gradient of COUP-TFI in the neocortex (see Sansom and Livesey, 2009, as a Review).



6– Development of the Vertebrate Eye

The neural retina generates from the posterior part of the embryonic prosencephalon, the diencephalon, as a lateral evagination of neuroepithelium, the optic vesicle. The optic vesicle extends from the lateral walls of the diencephalon, and where it meets the head ectoderm, it induces the formation of a lens placode, which then invaginates to form the lens (*Figure 6.1*). As the optic vesicle becomes the optic cup, its two layers differentiate in different ways. The cells of the outer layer produce melanine pigment (being one of the few tissues other than the neural crest cells that can form this pigment) and ultimately become the pigmented retina. The cells of the inner layer proliferate rapidly and generate a variety of glia, ganglion cells, interneurons, and light-sensitive photoreceptor neurons. Collectively, these cells constitute the neural retina. The retinal ganglion cells are neurons whose axons send electric impulses to the brain. Their axons meet at the base of the eye and travel down the optic stalk, which is then called the optic nerve.



Formation of the Eye Field

A group of genes coding for transcription factors, Six3, Pax6, and Rx1, is expressed in the most anterior tip of the neural plate and plays a key role in specifying the retinal identity. The expression of these three genes identifies a domain that is initially single and will later split into the bilateral regions that form the optic vesicles.

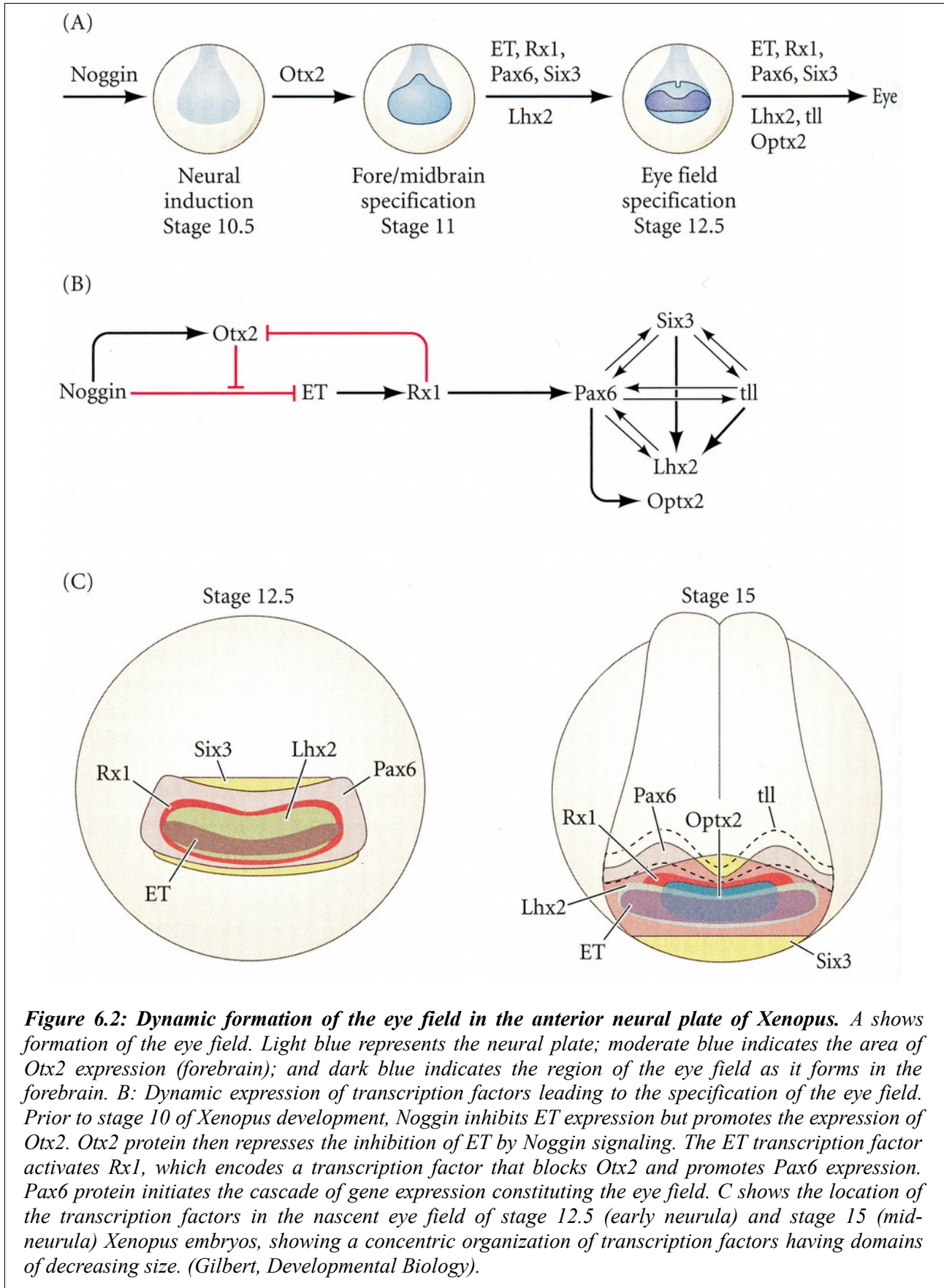
Eye formation has been studied in several organisms, but historically the amphibian eye has received the most attention. Using *in situ* hybridisation and injection of transcription factors mRNA into developing *Xenopus* embryos, Zuber and colleagues were able to outline the mechanisms by which the amphibian eye field becomes specified (**Figure 6.2**).

The formation of the eye field begins with the specification of the neural tube. The anterior portion of the neural tube, where both BMP and WNT pathways were inhibited, is specified by the expression of the Otx2 genes (**Figure 6.2A**). Noggin is especially important in blocking BMPs, as

this not only allows Otx2 expression but also inhibits expression of the transcription factor ET, one of the first proteins expressed in the eye field. However, once Otx2 protein accumulates, it blocks Noggin's ability to inhibit the ET gene, so ET protein is produced (**Figure 6.2B**).

One of the genes controlled by ET is Rx1 (called Rax in mouse), whose product helps specify the retina. Rx1 is a transcription factor that acts first by inhibiting Otx2, and second by activating Pax6, the major gene in forming the eye field in the anterior neural plate. The Pax6 protein is especially important in the specification of the lens and retina. Indeed, it appears to be a common denominator for photoreceptive cells in all *phyla*. When the mouse Pax6 gene is inserted into the *Drosophila* genome and activated randomly, *Drosophila* eyes form ectopically (Halder et al., 1995).

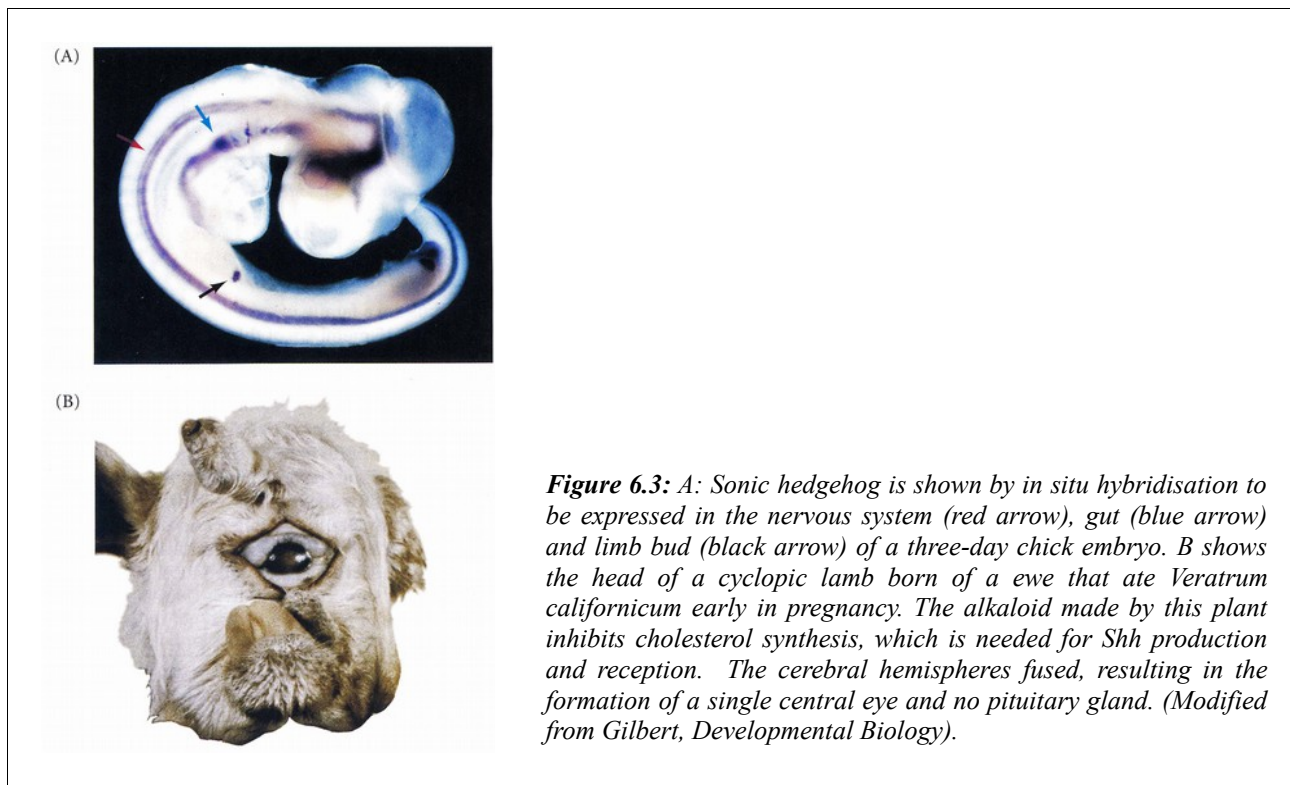
Transcription factors of the nascent eye field show a concentric organization in the anterior portion of the neural plate of the *Xenopus* embryo (neurula stage), having domains of decreasing size: Six3 > Pax6 > Rx1 > Lhx2 > ET (Zuber et al., 2003) (**Figure 6.2C**).



Pax6 is also expressed in the mouse forebrain, hindbrain and nasal placodes, but the eyes seem to be most sensitive to its absence. Humans and mice heterozygous for loss-of-function mutations in Pax6 have small eyes, while homozygous mice, humans and *Drosophila* lack eyes altogether (Jordan et al., 1992; Glaser et al., 1994; Quiring et al., 1994). In both flies and vertebrates, Pax6 protein initiates a cascade of transcription factors that mutually activate one another to constitute the eye field.

In vertebrates, separation of the single eye field into two bilateral eye fields depends on the secretion of Sonic hedgehog (Shh; **Figure 6.3**). If the mouse Shh gene is mutated, or if the processing of this protein is inhibited, the single median eye field does not split. The result is cyclopia, a single eye in the center of the face, usually below the nose (**Figure 6.3B**). Shh from the prechordal plate suppresses Pax6 expression in the center of the embryo, dividing the field in two. The phenomenon of human cyclopia also involves loss-of-function mutations that prevent Shh from functioning.

Conversely, if too much Shh is synthesized by the prechordal plate, Pax6 is suppressed in a too large area and the eyes fail to form at all.



Cell Differentiation in the Vertebrate Eye.

Rax (retinal and anterior neural fold homeobox) gene is the key gene for retinal development, and it's expressed in the eye field of the early neurula embryo (**Figure 6.4A**). Rax expression is upregulated by Otx2 protein, which specifies the anterior head region and encodes a transcription factor that activates numerous genes; among these genes are Pax6 and Six3, both of which help specify the retinal neurons. While initial expression of Pax6 and Six3 is not dependent on Rax expression, their continued expression in the retinal progenitor cells requires Rax protein. Pax6 protein is critical for specification of the retinal ganglion cells (which transmit visual information to the brain), while Six3 is necessary for coordinating the number of times retinal precursor cells divide before they differentiate.

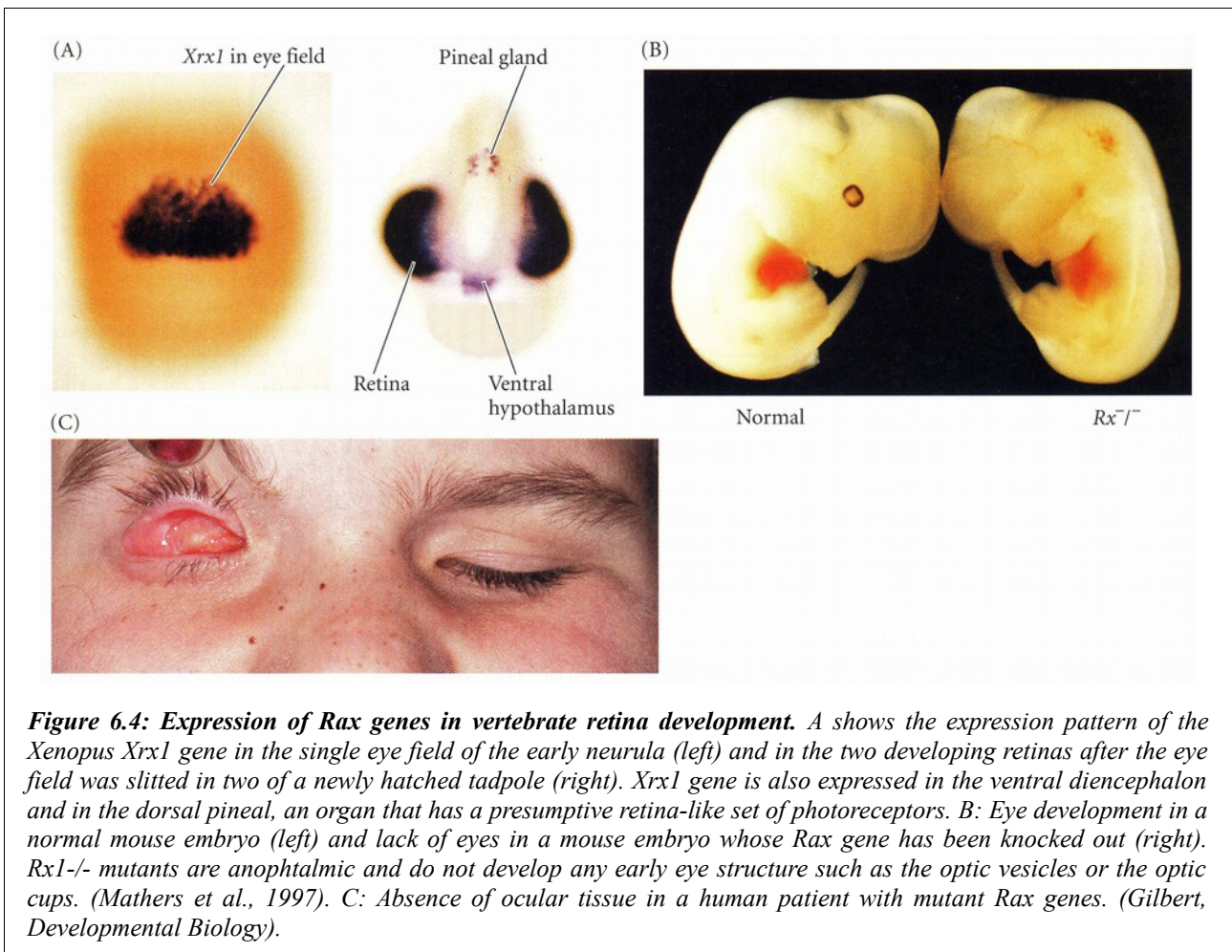


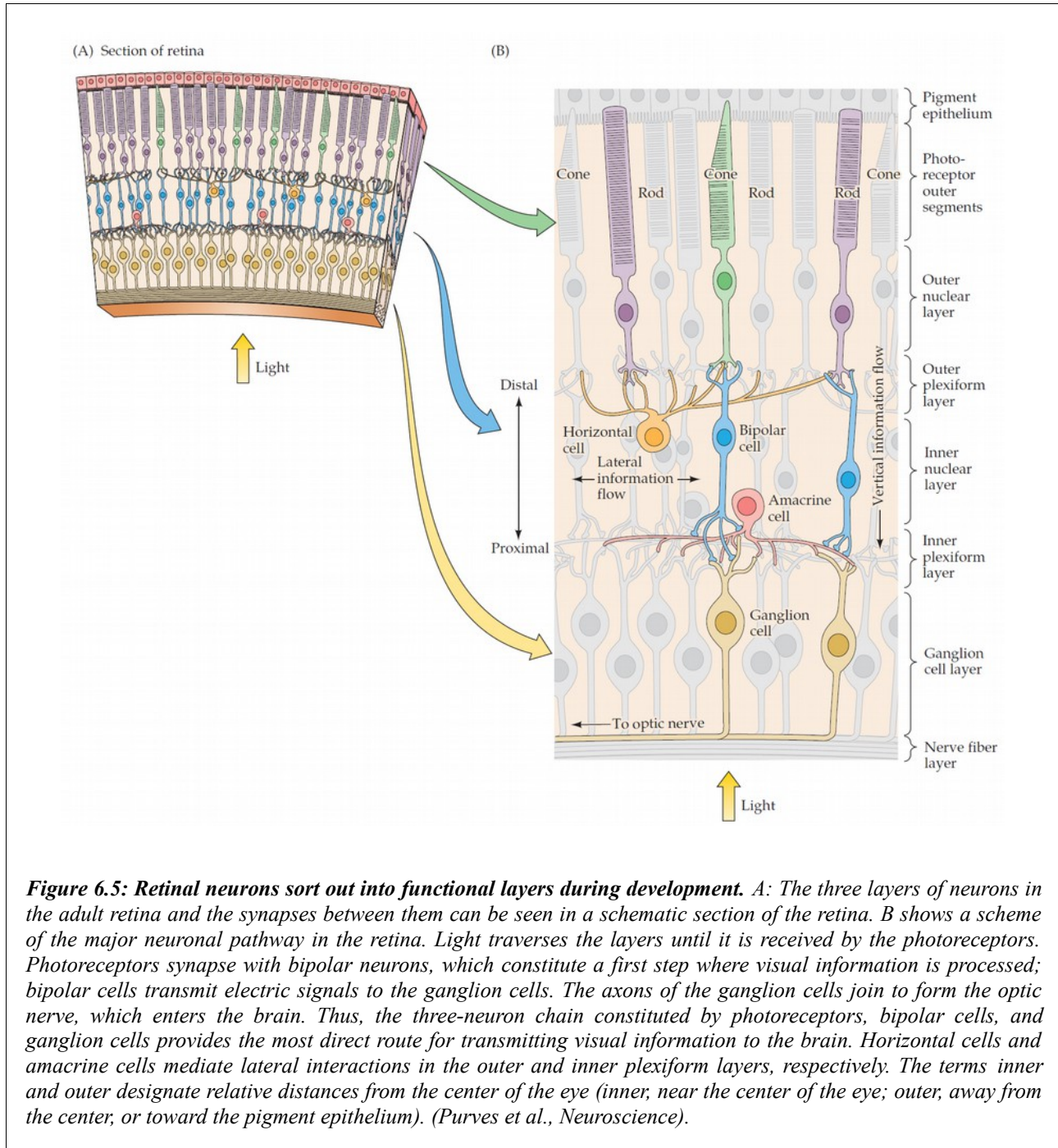
Figure 6.4: Expression of Rax genes in vertebrate retina development. A shows the expression pattern of the *Xenopus Xrx1* gene in the single eye field of the early neurula (left) and in the two developing retinas after the eye field was slitted in two of a newly hatched tadpole (right). *Xrx1* gene is also expressed in the ventral diencephalon and in the dorsal pineal, an organ that has a presumptive retina-like set of photoreceptors. B: Eye development in a normal mouse embryo (left) and lack of eyes in a mouse embryo whose Rax gene has been knocked out (right). *Rx1*^{-/-} mutants are anophthalmic and do not develop any early eye structure such as the optic vesicles or the optic cups. (Mathers et al., 1997). C: Absence of ocular tissue in a human patient with mutant Rax genes. (Gilbert, *Developmental Biology*).

As in *Xenopus*, the murine *Rax* gene is first activated in the anterior neural plate at stage E7.5, in a region that will give rise to the eyes, the pineal gland, and the diencephalon (**Figure 6.4B left**). At stage E10.5, expression of *Rax* is confined to the developing retina and the ventral forebrain. There is a uniform expression in the entire neural retina of E15.5 embryos. At later stages there is a progressive reduction of *Rax* expression in the retina, which initiates in the ganglion cells and proceeds in accordance with the loss of proliferative activity in the retinal cell layers.

Expression in the eye at stage P6.5 is restricted to photoreceptors and the inner nuclear layer; at stage P13.5 no *Rax* expression is detected (Mathers et al., 1997). *Rx1*^{-/-} human and mouse mutants are anophthalmic and do not develop any early eye structure such as the optic vesicles or the optic cups (Mathers et al., 1997) (**Figures 6.4B right** and **6.4C**), while *small eye/small eye* homozygous mutants, carrying a mutation in *Pax6*, develop anomalous optic vesicles. *Rx1*^{-/-} mutants show a gradual phenotype: in the mild phenotype the prosencephalon is present, but optic vesicles are not and the putative eye field region lacks also the expression of *Pax6*, *Otx2* and *Six3* (Zhang et al., 2000); in the severe phenotype the animals lack completely the prosencephalon and the mesencephalon seems missing to a variable extent (Mathers et al., 1997).

Like the cerebral and cerebellar cortices, the neural retina develops into a layered array of different neuronal types. These layers include the light- and color-sensitive photoreceptor cells (rods and cones); the cell bodies of the ganglion cells; and bipolar interneurons that transmit electric stimuli from rods and cones to the ganglion cells (**Figure 6.5**).

Early neuroblasts of the retina are competent to generate all seven retinal cell types. Classical studies of cell lineage tracing by retroviral vectors performed in rat showed the clonal origin of the different retinal cell types (Turner and Cepko, 1987). The key genes specifying distinct retinal cell identities, and the mechanisms by which a multipotent retinal progenitor generates different types of neurons following a temporal schedule that is conserved among vertebrates, have been described in many studies over the last two decades (reviewed in Livesey and Cepko, 2001).



7– Focus on BMP

A Well-known Role in Neuralization and a Possible Role in Brain Patterning

BMP and his antagonist Noggin are key molecules in neural conversion. The neural plate is derived from the dorsal ectoderm and induced by “Organizer” signals coming from the underlying notochord. The dominant model of neural induction is the default hypothesis. This hypothesis states that neural tissue is formed spontaneously in the absence of BMP signaling during early gastrulation, while exposure to BMP signals causes epidermal differentiation. Accordingly, signals emanating from the Organizer, essential for neural induction, are BMP inhibitors such as Chordin and Noggin (both BMP-inhibitors), Follistatin (an inhibitor of BMPs and Activin), and Cerberus (a molecule able to inhibit BMP, Wnt and Activin/Nodal).

Of particular importance in determining specific neural fates are signals that provide regional identity, both in the antero–posterior (A–P) and dorso–ventral (D–V) axis, and define domains of distinct expression of homeodomain proteins and bHLH transcription factors.

D–V identity is determined by the antagonistic action of Sonic hedgehog (Shh) secreted ventrally from the notochord and floor plate, and BMPs and WNT signals dorsally. There is ample evidence from explant and ES cell differentiation studies that confirm a concentration-dependent role of Shh to define specific progenitor domains within the neural tube. A role for BMPs in dorsal neural patterning has been suggested from explant and ES cell differentiation studies. Gain of function

studies in mice overexpressing the BMP receptors under control of the regulatory elements of the nestin gene are pointing to a role for BMPs in dorsal patterning.

However, loss-of-function studies of the BMP receptors suggest a much more limited role for BMPs in dorsal patterning. BMPs could play a role in the specification of telencephalic progenitor cells toward the most dorsal fate, the choroid plexus (Hébert et al., 2002).

Focusing on A-P patterning, the leading hypothesis of A–P axis specification states that anterior fates are the default ones during early neural induction, while FGF, WNT, and Retinoid signals actively posteriorize cell fates.

Early studies in lower vertebrates suggested that BMP factors could play a key role in anterior/posterior patterning. BMP antagonism on pluripotent cells of *Xenopus* animal caps induces cement glands, which are the most anterior ectodermal structures in *Xenopus*, and anterior brain markers such as the fore-midbrain marker *Otx2*, but not hindbrain or spinal cord markers (Hawley et al., 1995; Lamb et al., 1993; Sasai et al., 1995). Simultaneous inhibition of Wnt, Nodal and BMP by Cerberus was shown to be sufficient for head induction in *Xenopus* and also in mammals; BMP antagonism is essential for the formation of the forebrain (Piccolo et al., 1999; Yang & Klingensmith, 2006). More recent studies highlight that the BMP-inhibitor Noggin has a dose-dependent patterning effect on *Xenopus* animal caps. At lower doses, Noggin supports neuralization without the expression of diencephalic markers, which are instead activated at higher doses (Lan et al., 2009).

It was recently shown that the cell-intrinsic expression of the zinc-finger nuclear protein *Zfp521*, which is inhibited by BMPs, plays a pivotal role in promoting a default neural state of ES cells. Furthermore, a role of *Zfp521* in supporting an anterior identity of neurons generated by ES cells was hypothesized (Kamiya et al., 2011).

Moreover, in *Xenopus* embryos the specification of the forebrain requires isolation of its cells from BMP, Activin/Nodal and Wnt signaling by high concentrations of Noggin produced in cells at the anterior margin of the neural plate (Bayramov et al., 2011).

These observations suggest that *in vivo* the concentration of endogenous BMPs might be relevant in the control of the positional identity of neurons.

Concerning mouse development, it was also proposed that BMPs play a role in the regional morphogenesis of mouse dorsal telencephalon, by the control of specific gene expression, cell proliferation and local cell death (Furuta et al., 1997). Furthermore, mice that are double mutant for

the BMP antagonists Chordin and Noggin, have severe defects in the most anterior part of the brain, indicating that BMP antagonism is essential for the proper development of the anterior neurectoderm (Bachiller et al., 2000; **Figure 7.1**).



Figure 7.1: Phenotype of *Noggin-Chordin* double mutant mice. A wild-type E12.5 mouse embryo (left) can be compared to *Chd*^{-/-};*Nog*^{+/+} embryo (center) and to *Chd*^{-/-};*Nog*^{-/-} embryo (right). Single mutant shows a normal head and defective ear (arrowhead). Double mutant is showing extensive anterior deletions of forebrain, eye, nose and facial structures. White arrowhead indicates the rhombic lip (future cerebellum). (Bachiller et al., 2000).

Though the role of BMP in dorso-ventral patterning is well established, its role in A-P patterning is less clear. Early effects of BMP signaling on the anterior-posterior patterning are not well characterized. BMP role as a possible morphogen, acting not only during neural induction but also in the second step of neural patterning, has never been investigated in a systematic way.

8— An *in Vitro* Approach

Neural Differentiation Protocols Using Embryonic Stem Cells

The recent development of embryonic stem cells biology has fueled the idea that restricted progenitors or differentiated cell types can be generated *in vitro* from these pluripotent cells, and then used in a therapeutic setting to repair human tissue damaged by trauma or disease. Human ES cells successfully converted into the appropriate neural cell types might be used, for instance, to repair neural tissue that is damaged in such human conditions as Multiple Sclerosis, Parkinson's, Alzheimer's, Amyotrophic Lateral Sclerosis, or spinal cord injury. Given this goal, one approach is to apply differentiation protocols to mouse and human ES cells that mimic the extrinsic and intrinsic cues that underlie the formation of neural cell types in the embryo. Indeed, one of the more successful protocols for differentiating mouse ES cells into transplantable motor neurons is based on a systemic understanding of the developmental mechanisms that underlie the formation of the embryonic spinal cord. Similar logic has also guided subsequent attempts to differentiate ES cells into other specific classes of neurons, including retinal photoreceptors, cerebellar granular neurons, or cerebral-type neurons that use glutamate, GABA or dopamine as their principle neurotransmitter.

However, the use of ES cells in protocols of *in vitro* differentiation has in some cases reversed the logical of the experimental strategy, as ES cells differentiating in chemically defined media can

serve as a model to dissect the signals required to specify distinct fates of differentiation, bypassing the use of a whole embryo. This might be a winning strategy, for instance, when aiming at investigating the role of a specific growth factor in a well defined temporal window of embryonic development. In fact, blocking or inducing the signaling of a given factor by adding its agonist or antagonist to the medium of a cell culture at a specific time of *in vitro* differentiation is much easier than targeting the same signaling *in vivo*.

There are at least three main strategies for the neural induction of ES cell *in vitro*: (1) mimicking the environment that produces neurectoderm in the embryo by providing appropriate cell-cell interactions and signals through embryoid body (EB)-based systems; (2) depriving the ES cells of both cell-cell interactions and signals by low density culture in serum-free medium, evoking a default mechanism for NSC differentiation into neural fates; and the (3) stromal feeder mediated neural induction.

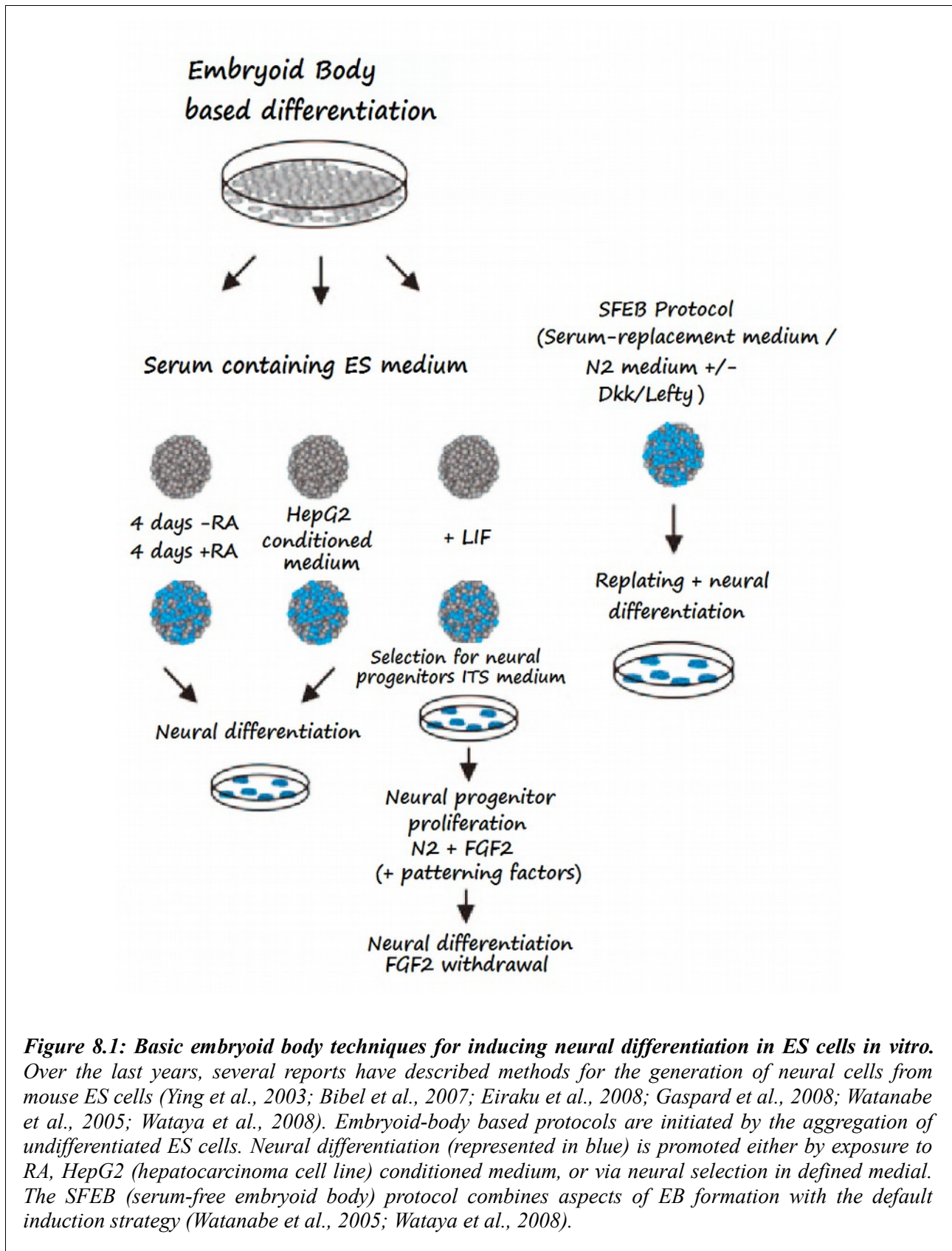
Some protocols combine aspects of the first two approaches, promoting cell-cell interactions to facilitate formation of all three primary germ layers followed by neural lineage-specific selection under defined conditions. (See as a review Cai and Gabel, 2007).

Embryoid-body Based Protocols

EBs are formed by aggregation of ES cells in suspension culture (**Figure 8.1**). The interaction of cells within the EB causes cell differentiation, mimicking early embryonic development processes that include the induction of early extraembryonic endoderm and various aspects of gastrulation. EBs thus represent a useful assay to generate derivatives of all three germ layers *in vitro*. Various modifications of the basic protocol have been developed to drive neural induction, and to select and expand EB-derived neural precursors.

The first EB-mediated neural differentiation protocol was based on exposure to Retinoic acid (RA) for four days, following four days of EB formation in the absence of RA (so called 4/4 protocol). In addition to neural induction, RA treatment also exhibits a strong caudalizing effect on A–P patterning mediated through activating the Hox gene cascade (Aubert et al., 2002; Verani et al., 2007).

An alternative EB-based strategy is the exposure to conditioned medium derived from a hepatocarcinoma cell line (HepG2), which appears to directly induce neuroectodermal fate. Accordingly, HepG2-treated aggregates do not express endodermal or mesodermal markers, but appear to give rise directly to neural progeny. The active component within HepG2-conditioned medium is not known, although data suggest that at least two separable components are responsible for this activity.



A third EB-based strategy makes use of neural-selective growth conditions. EB progeny is kept under minimal growth conditions in serum-free medium containing insulin, transferrin and selenite (ITS medium). Under these conditions, most EB-derived cells die and a distinct population of immature cells emerges that expresses increasing levels of the intermediate filament Nestin. These Nestin-positive precursors can be replated and directed towards various neuronal and glial fates using a combination of patterning, survival and lineage promoting factors.

The most recent variation of an EB-like differentiation protocol is the so-called SFEB (serum-free EB) protocol by Yoshiki Sasai's Lab. The SFEB approach is distinct from other EB-based strategies, as it does not involve a gastrulation-equivalent intermediate stage but directly yields neural progeny in the absence of serum or other inducing signals. Therefore, SFEB-based protocols combine ES cell aggregation with the default neural induction concept discussed below. SFEB-based protocols are particularly attractive for generating anterior neural fates, such as cortical or ventral forebrain fates. However, variations of this approach can be adapted to the derivation of many neuron types, including spinal motoneurons.

Stromal Feeder Mediated Neural Induction

Bone marrow-derived stromal cell lines have been used for many years to support the growth of undifferentiated hematopoietic stem cells. Over the last 10 years, it has become evident that several stromal cell lines also exhibit neural-inducing properties in co-culture with mouse ES cells (**Figure 8.2**). Stromal cell lines with the highest efficiencies of neural induction are typically at the pre-adipocytic stage of differentiation and are isolated from the bone marrow (e.g., PA-6, MS5, S17) or from the aorta-gonad-mesonephros (AGM) region. The molecular nature of this stromal-derived inducing activity remains unknown. However, the efficiency and robustness of neural induction using stromal feeder approaches is high compared with alternative protocols, and differentiation can be directed towards specific regional fates in response to extrinsic factors, despite the fact that these protocols have been particularly useful for the derivation of midbrain dopamine neurons from ES cells.

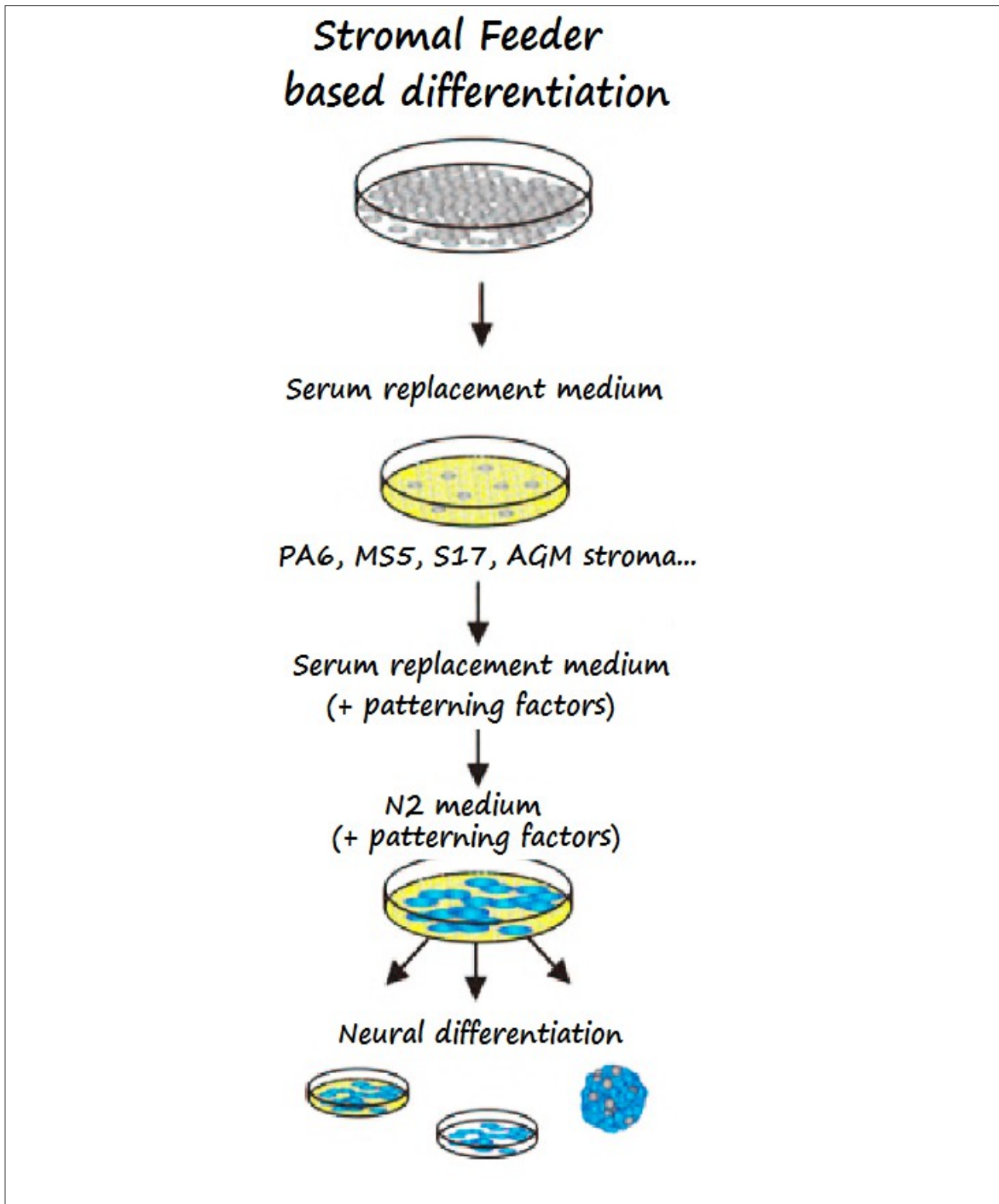


Figure 8.2: Basic techniques for stromal feeder-induced neural differentiation in embryonic stem cells *in vitro*. Neural differentiation is represented in blue. Stromal feeder mediated differentiation is obtained upon plating undifferentiated ES cells at low density on stromal feeder cell lines derived from the bone marrow of the aorta-gonad-mesonephros region of the embryo. Serum-free conditions are required throughout the protocol. Conditions can be readily adapted to achieve neural subtype-specific differentiation for a large number of CNS cell types. Classic studies made use of PA6 and MS5 cell mediated differentiation (Kawasaki et al., 2000; Barberi et al., 2003).

Neural Differentiation by Default

Different methods exist to generate neural cells from mouse ES cells and more and more evidence is found in favor of the default model of neural induction in this system as well (**Figure 8.3**): co-culture-free direct neural differentiation protocols are based on the default hypothesis: the absence of signals in primitive ectodermal cells will lead to neural differentiation. This can be obtained by culturing embryonic stem cells in serum-free conditions (free of the many growth factors present in serum) and at relatively low cell density (to limit the cell to cell signaling). Several neural induction approaches in mouse and human ES cells have been developed based on this approach (Tropepe et al. 2001; reviewed in Munoz-Sanjuan & Brivanlou 2002; Bouhon et al. 2005; Smukler et al. 2006). Under these conditions, rapid expression of neural markers is observed in the few surviving colonies.

Tropepe et al. were the first to show that ES cells cultured in chemically defined serum-free and feeder layer-free low density culture conditions readily acquire a neural identity, originating Nestin-positive neural precursors. The marker Nestin was strongly expressed after only 4 hours of culture in their protocol. However, the cells expressing neural markers were reported to represent a “primitive” neural progenitor population, distinct from fully committed neural progeny.

Direct adherent monolayer culture conditions (with no aggregation step) have been developed for neural induction of mouse and human ES cells in the presence of N2 medium supplemented with B27 and FGF2. One example of this is the mono-adherent culture method in a defined serum-free medium, N2B27 that leads to more than 70% Sox-1 (an early pan-neurectoderm marker) expressing cells by day 4 (Ying et al. 2003a). However, these protocols need to be validated critically, addressing the contribution of neural induction versus selective survival of spontaneously differentiating neural progeny.

Most recent work in human ES cells suggests that adherent monolayer cultures can be developed that are extremely efficient at driving neural induction under simple serum-free conditions in the presence of inhibitors that block both the BMP and TGF β /Activin branch of SMAD signaling.

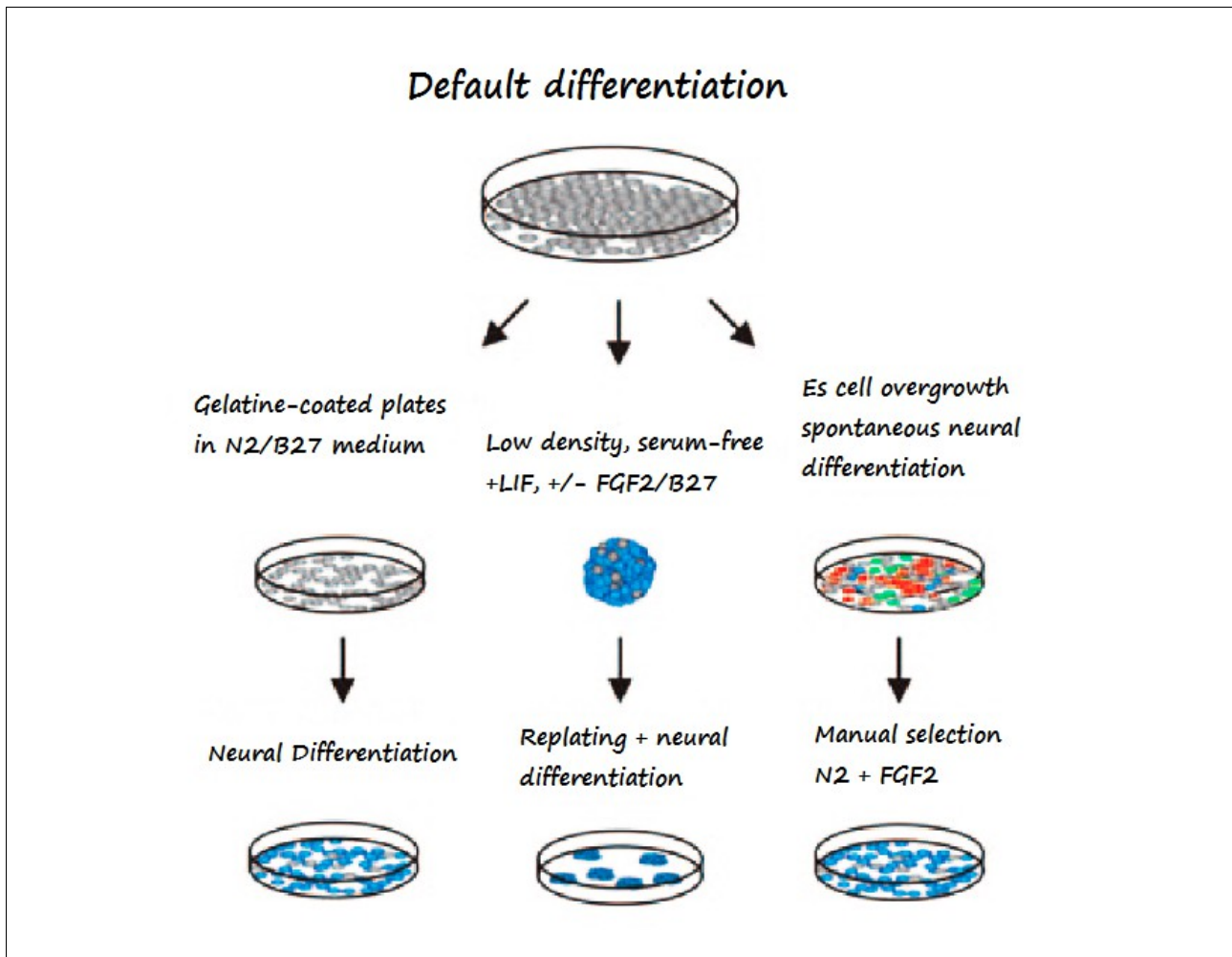


Figure 8.3: Basic techniques for inducing neural differentiation in embryonic stem cells in vitro, by exploiting an intrinsic default differentiation program. Neural differentiation is represented in blue. Default differentiation: neural differentiation is achieved by reducing endogenous BMP signals via plating cells at low density under minimal medium conditions (Ying et al., 2003a), or in the presence of the BMP antagonist Noggin. Neurally-committed cells can also be mechanically isolated and propagated from plates exhibiting spontaneous neural differentiation after overgrowth of ES cells.

Studying Patterning Signals during Neural Differentiation *in Vitro*

The dissection of diffusible signals that orchestrate neural induction and regulate regional brain patterning has recently been made easier by the study of embryonic stem cells (ES cells) *in vitro* differentiation. The fundamental strategy for achieving neuronal subtype specification is based on mimicking patterning events that define A–P and D–V patterning *in vivo*.

Spontaneous differentiation into neurons occurs rapidly on neural induction of mouse ES cells, and several recent reviews have examined the conditions required to produce specific neuronal and glial subtypes. First of all, neuronal subtype specification can be influenced by the mode of neuronal induction. This is particularly the case for direct neural induction protocols using Retinoic Acid: in addition to neural induction, RA treatment also exhibits a strong caudalizing effect on A–P patterning. Using defined growth media, it has been possible to investigate the diffusible factors that affect the anterior-posterior (A/P) as well as the dorso-ventral (D/V) identity of *in vitro* generated neurons. Among these, not only Retinoic Acid (RA), but also BMPs, Wnts, Fibroblast Growth Factors (FGFs) and Sonic Hedgehog (SHH) have been described (Chatzi et al., 2011; Eiraku et al., 2008; Gaspard & Vanderhaeghen, 2010; Hendrickx et al., 2009; Li & Lee, 1993; Watanabe et al., 2005).

Addition of caudalizing signals, such as retinoic acid (RA) or FGF2 can promote a spinal cord identity and subsequent production of motor neurons (Wichterle et al., 2002), whereas addition of Wnt and Nodal antagonists promotes production of telencephalic progenitors (Watanabe et al., 2005).

The following protocol, concerning the derivation of midbrain dopamine neurons, provides a classic example of how developmental pathways can be harnessed to direct ES cell fate *in vitro*. Derivation of midbrain dopamine neurons from ES cells has been of particular interest, due to the clinical potential for dopamine neuron transplants in Parkinson's disease. Protocols for the dopaminergic differentiation of mouse ES cells are based on studies in explants that identified FGF8 and Shh as critical factors in midbrain dopamine neuron specification. Consistently, they found that treatment with FGF8 and Sonic Hedgehog promote production of ventral midbrain precursors and subsequent differentiation of dopaminergic neurons (Lee et al., 2000; Barberi et al., 2003). The effect of

Shh/FGF8 on ES-derived neural precursors was first described using an EB-based five-step differentiation protocol. Under these conditions, up to 34% of all neurons expressed tyrosine hydroxylase (TH), the rate-limiting enzyme in the synthesis of dopamine. A further increase in dopamine neuron yield (nearly 80% of all neurons expressing TH) was obtained in Nurr1 overexpressing ES cells. Midbrain dopaminergic differentiation was also obtained using co-culture of ES cells on the stromal feeder cell line (PA6) with 16% of all neurons expressing TH in the absence of Shh and FGF8. These results were initially interpreted as PA6 exhibiting a specific patterning action that promotes dopamine neuron fate. However, later studies demonstrated that neural precursors induced on stromal feeders can be shifted in A–P and D–V identity, and reach a yield of up to 50% of all neurons expressing TH without a need for transgenic Nurr1 expression.

9– Focus on Cortical Differentiation *in Vitro*

The cerebral cortex is the most complex structure in the mammalian brain, and displays many different neuronal subtypes. This complexity is established sequentially, starting with the differentiation of the cortical primordium in the most anterior area of the brain (the Forebrain).

Forebrain identity is thought to constitute a primitive pattern of neural identity: The anterior default fate is retained through the inhibition of caudalizing morphogen signals, such as Wnt and FGF factors, according to the two step activation-transformation model (see Introduction, Chapter 3).

The forebrain then undergoes further patterning along the dorso–ventral axis, mainly through the induction of ventral identity by sonic hedgehog (Shh), secreted from the ventral neural tube and underlying tissue, and through the reinforcement of a dorsal identity by BMP and Wnt signaling. This leads to the specification of the two main populations of cortical neurons, pyramidal neurons (generated from the dorsal part of the telencephalon) and interneurons (generated ventrally).

A next level of complexity emerges through the specification of different subtypes of cortical neurons that will populate specific cortical layers; every neuron subtype exhibits specific patterns of gene expression and connectivity. This specification follows a coordinated temporal pattern: Neurons from different layers are generated sequentially, but the underlying mechanisms remain poorly known. As a general rule, neurons that will populate deep cortical layers are generated early, followed later by neurons that will constitute superficial cortical layers.

Gaspard et al. have showed that mouse embryonic stem cells, cultured at low density without any morphogen, recapitulate *in vitro* the major milestones of cortical development (**Figure 9.1**). In their hands, ES cells need treatment with Cyclopamine, a Shh-inhibitor, to efficiently generate cortical neurons. They lead to the sequential generation of a diverse repertoire of neurons that display most salient features of genuine cortical pyramidal neurons, both from the molecular and electrophysiological point of view (**Figure 9.1**). When grafted into the cerebral cortex, these neurons correctly develop patterns of axonal projections corresponding to a wide range of cortical layers.

From the technical point of view, in Gaspard's protocol ES cells were plated at low density on gelatin-coated dishes and cultured in a chemically defined minimal medium devoid of morphogens or serum derivatives. Cyclopamine treatment was performed from day 2 to day 10 of differentiation. For longer differentiation, neural progenitors were re-plated at day 14 on polylysine/laminin in N2B27 medium. This kind of approach (neural differentiation of ES cells in minimal medium devoid of serum) and the final outcome (anterior cortical differentiation) strongly supports the default hypothesis for anterior neural development.

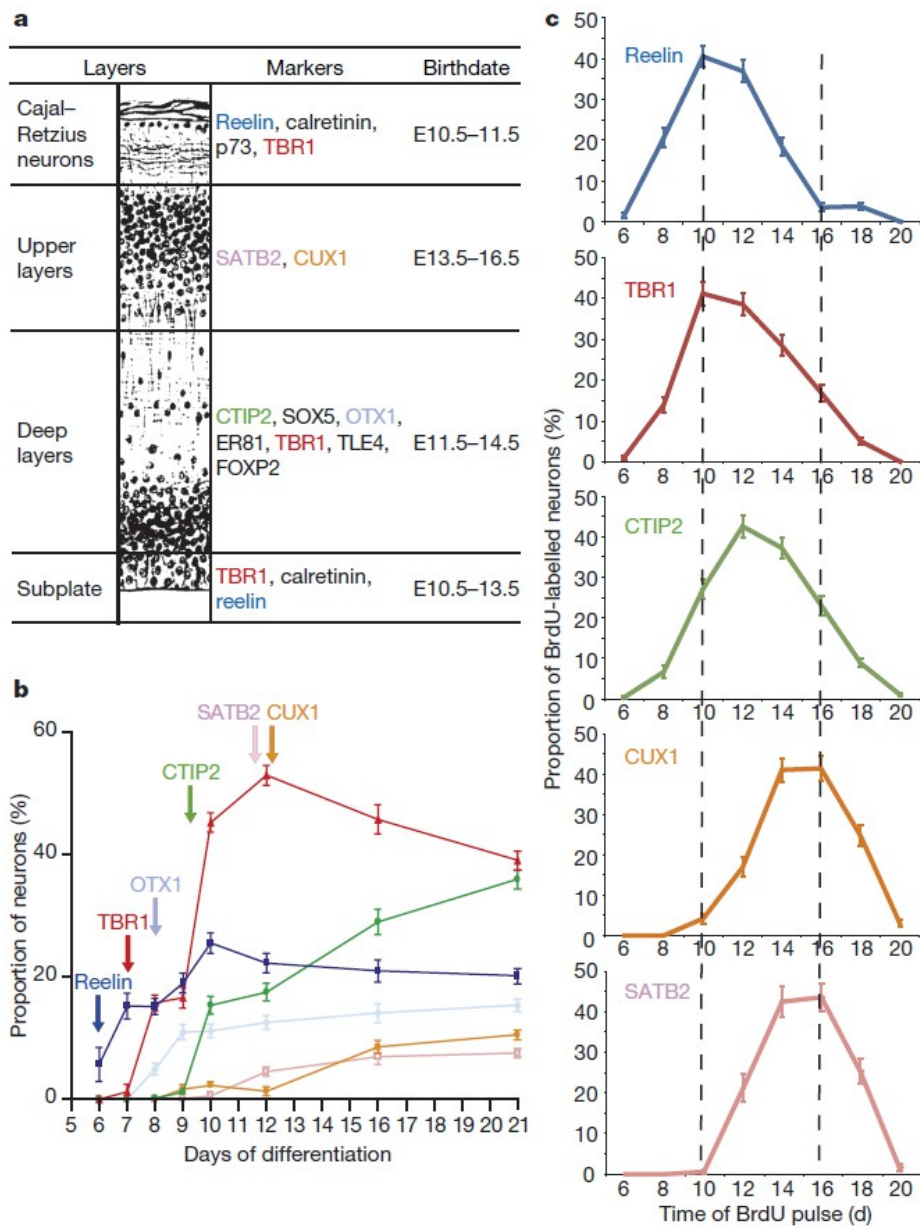
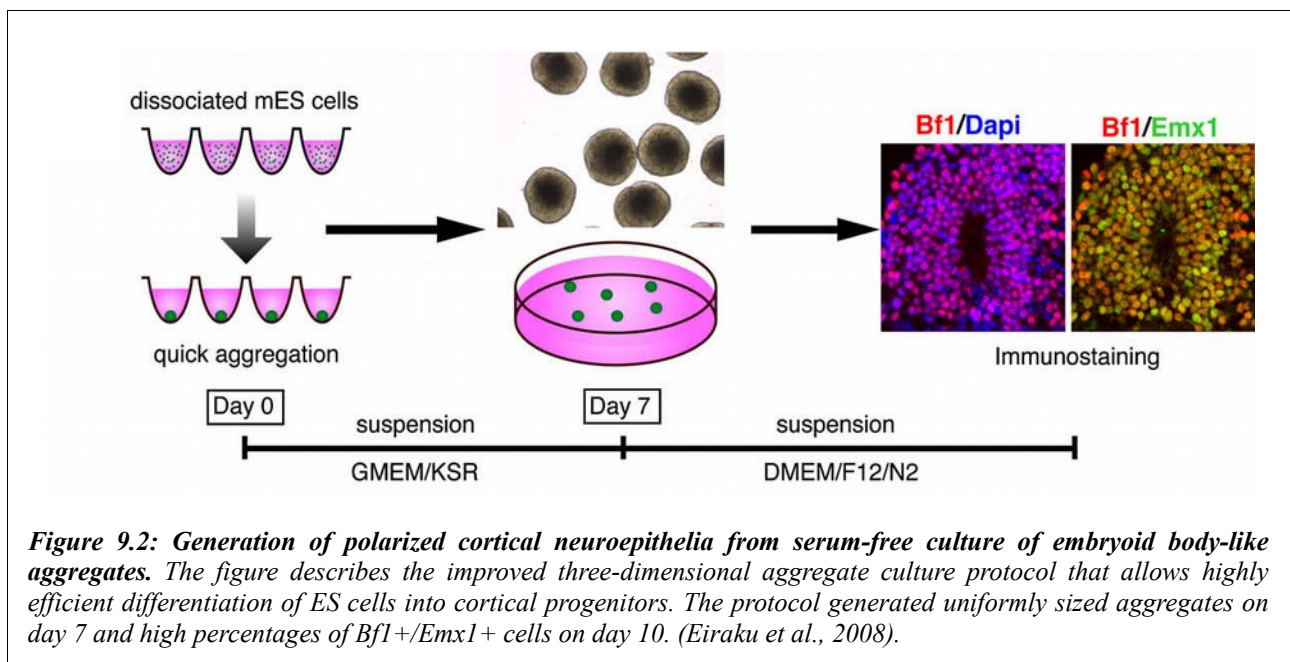


Figure 9.1: Corticogenesis from ES cells using Gaspard's protocol. With this differentiation protocol, ES cells differentiate into multipotent cortical progenitors that follow the major milestones of cortical development, including the sequential generation of neurons displaying distinct layer-specific identities. This sequential generation of cells is similar to the in vivo development. *A*: Scheme depicting patterns of the layer-specific markers in cortical neurons, and their timing of generation in vivo. *B*: Evolution in time of the proportion of β -Tubulin-III-positive neurons expressing layer-specific markers in chemically defined minimal medium, plus Shh-inhibition by Cyclopamine. Colored arrows indicate the first day of appearance of each marker. *C*: Birthdating analysis. Cultures were pulse-labeled with BrdU for 24 h at various time points (*x* axis). Cultures were stopped by the Authors at day 21, and the proportion of BrdU fully labeled nuclei was quantified among β -Tubulin-III-positive neurons expressing each specific marker. (Gaspard et al., 2008).

In Sasai's lab, Eiraku et al. not only obtained cortical neurons *in vitro* from mouse ES cells, but also developed a three-dimensional aggregation culture (serum-free culture of embryoid body-like aggregates; SFEB culture) for the self-organized generation of apico-basally polarized cortical tissues (**Figure 9.2**). The generated cortical neurons are functional, transplantable and capable of forming proper long-range connections *in vivo* and *in vitro*.

Furthermore, their protocol can be considered very plastic in terms of responsiveness to exogenously added morphogens: As an example, the majority of the SFEB-induced telencephalic progenitors express the pallial marker Pax6, but Shh treatment suppresses Pax6 and induces the expression of sub-pallial markers such as Nkx2.1. Furthermore, the regional identity of the generated pallial tissues can be selectively sub-specified into olfactory bulb, rostral and caudal cortices, hem, and choroid plexus by the secreted patterning factors FGF, Wnt, and BMP.

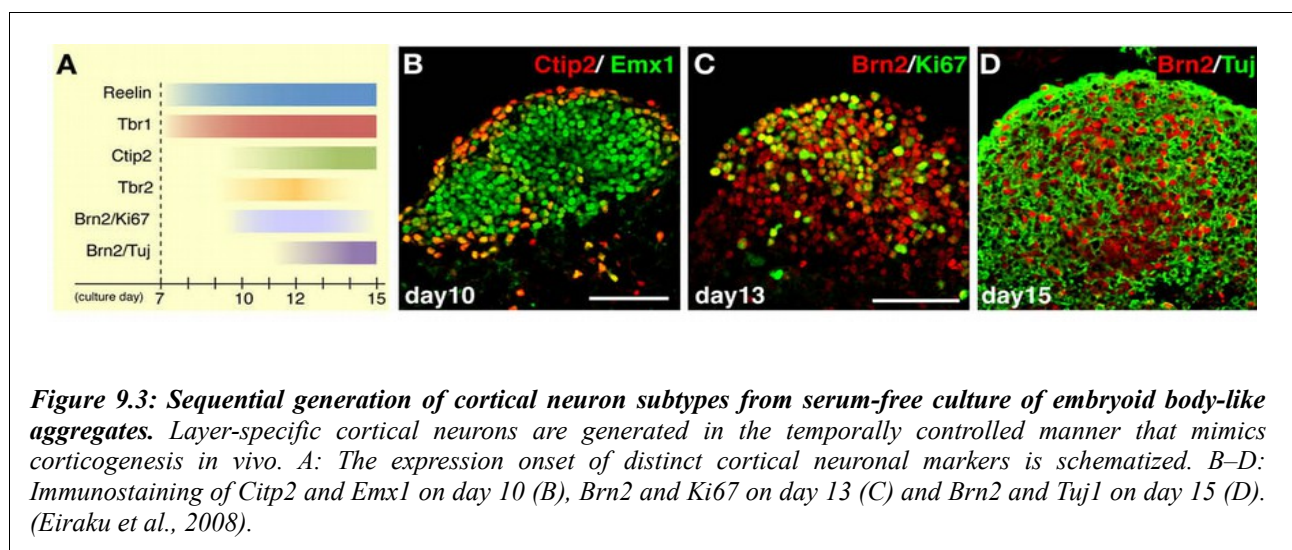
In this case, dissociated ES cells were quickly reaggregated and then cultured in suspension in KSR containing medium, supplemented with the Wnt-inhibitor Dkk-1 and the Activin/Nodal-inhibitor Lefty-1. This suggested that efficient ES cell anteriorization could be obtained by Wnt signaling inhibition, during culture in a minimal medium where serum is replaced by KSR.



The Authors state that neural differentiation in the SFEB culture occurs tissue-autonomously and does not require extrinsic inducers. Despite of this statement, the culture medium includes some morphogens, whose exact role/effect is not described by the Authors. The Activin-inhibitor Lefty-1 could contribute to avoid mesoderm induction and facilitate neural conversion of embryoid body-like aggregates. The medium was also supplemented with Wnt-inhibitor Dkk-1, probably to protect a default anterior fate of differentiating ES cells.

SFEB-cultured mouse ES cells differentiated into Bf1 (FoxG1)⁺ telencephalic progenitors at high frequency. In dissociation culture, the SFEBq-induced neural progenitors (dissociated on day 12) differentiated into Tuj1⁺ postmitotic neurons expressing characteristic cortical markers such as Emx1 (82% positive cells) and vGlut1 (83% positive cells), as well as CamKIIa and GluR1.

SFEB-cultured mouse ES cells also expressed subtype-specific markers such as Tbr1, Ctip2, and Brn2. Again, the protocol showed the *in vivo*-mimicking birth order of distinct layer-specific cortical neurons (**Figure 9.3**).



Although very efficient, the two protocols by Gaspard et al. and by Eiraku et al. are exposed to some criticisms.

First, in Gaspard's protocol ES cells are cultured at very low density (1.000 cells per cm² at the beginning of the protocol); this situation is artificial and cannot be found in nature, where embryonic stem cells always differentiate together with neighboring cells and tissues. This could lead to the selection of a surviving subpopulation inside the culture. We do not know if this could be responsible for the strong endogenous Shh expression/production and for the unusual need to block

Shh pathway (by Cyclopamine treatment) to obtain a default (anterior and dorsal) neural differentiation fate.

Second, Eiraku's protocol makes use of embryoid bodies. The formation of a three-dimensional structure is interesting, however this could also lead to the uncontrolled generation of intrinsic gradient of autocrine factors produced by differentiating cells themselves. A 3D structure could also obstacle the treatments with exogenous morphogens added to culture medium. Additionally, KSR (knock-out serum replacement supplement) was used in Eiraku's protocol during neural induction; the composition of this patented supplement is not completely known, and its possible contribution to neural tissue patterning has never been thoroughly investigated.

Notably, in both protocol a detailed investigation on endogenous production of diffusible morphogens is almost completely missing. Gaspard's protocol includes a treatment with Cyclopamine, but the authors never investigated in detail the expression/secretion of endogenous Shh, nor the reason for this anomalous expression inside their culture system. Eiraku's protocol focuses on setting-up the exogenous addition of reagents, never asking which endogenous factors are the differentiating cells possibly producing.

Overall, the two protocols focus on the “cortical outcome” of ES cell differentiation, but fail to investigate the biological mechanisms underlying this phenomenon, or the production of endogenous morphogens possibly influencing it.

10– Focus on Retinal Differentiation *in Vitro*: high efficiency protocols, poor mechanism comprehension

Diversification during neural patterning is particularly complex in the forebrain (Telencephalon + Diencephalon), where cells in nearby locations within the early neural plate become differentially specified to give rise to structures such as the cerebral cortex (telencephalon) and the retina (diencephalon). The eye morphogenetic field (or “Eye field”) is located in the diencephalon and is demarcated by the expression of the key retinal gene *Rax* (called *Rx* in lower vertebrates, *Rx1* in *Xenopus laevis*; see Introduction, Chapter 6). The eye field give rise to an epithelial vesicle evaginating laterally from the diencephalon; subsequently, its distal portion invaginates to form a cup-like structure, the optic cup, which develops into the outer layer (the future pigmented epithelium) and inner layer (the neurosensory organ) of the retina.

Several reports have described ES cell specification to retinal fate (Hicks and Courtois, 1992; Lamba et al., 2006; Ikeda et al., 2005; Kelley et al., 1994; Levine et al., 1997). Moreover, following the generation of human embryonic stem cells and that of human induced pluripotent stem cells, it has proved possible, as in the mouse, to direct their differentiation towards the retinal lineage and generate both retinal pigmented epithelium (RPE) and retinal neurons (Lamba et al., 2006; Osakada et al., 2008; Lamba et al., 2010). Some experiments not only produced retinal precursors *in vitro*, but successfully used these cells to restore vision in blind mice after transplantation (MacLaren et al., 2006; Lamba et al., 2009). However, in one of these works retinal cells were not produced using embryonic stem cells, but were obtained from early postnatal mouse eyes; this option is not optimal for future therapeutic application in humans because of ethical problems (MacLaren et al., 2006). Furthermore, the existing protocols have been mainly focused on cell-type production (especially concerning Rhodopsin-positive photoreceptor cells) and were based on empirical combinations of culturing media and growth factor treatments. To date, few existing studies have focused on the molecular mechanisms leading to retinal fate specification (Lupo et al., 2013). Very often, the final differentiation of ES cells into retinal progenitors and/or fully differentiated retinal cells has been achieved by co-culture experiments, where differentiating ES cells are cultured together with retinal tissues obtained from embryos (Ikeda et al., 2005; Lamba et al., 2006); in such experiments, the dissection of instructive signals acting on ES cell differentiation is far from easy.

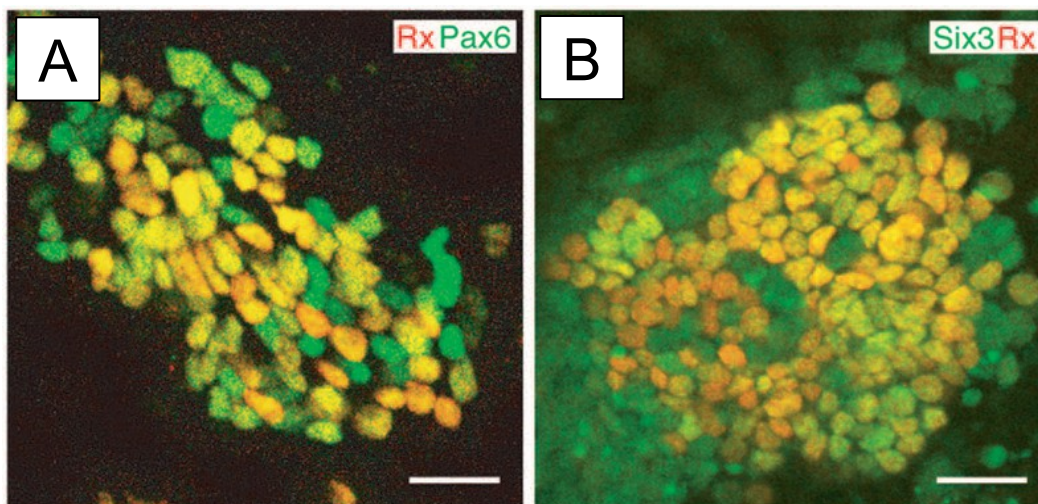


Figure 10.1: Efficient generation of Rax⁺/Pax6⁺/Six3⁺ retinal precursors from mouse ES cells by serum-free culture of embryoid body-like aggregates. The figure shows immunocytochemical analysis of cells cultured with Dkk, Lefty, FCS, and Activin. The majority of colonies contained significant numbers of Rax-positive cells. Induced Rax-positive cells (in red) frequently co-expressed Pax6 (green in A) and Six3 (green in B). Scale bar: 20 micrometers. (Ikeda et al., 2005).

Bona fide Rax⁺/Pax6⁺ retinal precursors were generated *in vitro* from ES cells by Yoshiki Sasai's Lab (**Figure 10.1A**; Ikeda et al., 2005). The Authors reported for the first time the efficient generation of neural retinal precursors, capable of producing photoreceptors. The first step was to obtain Six3-positive rostral forebrain cells; this was followed by the attempt to switch-on the expression of the eye field marker Rax, together with other transcription factors (Pax6 and Otx2) which are co-expressed with Rax in retinal precursors *in vivo* (**Figure 10.1A,B**). Retinal progenitors obtained *in vitro* by Sasai's Lab were able to differentiate into photoreceptor cells when co-cultured for longer periods (up to 17 days) with dissociated neural retina cells.

From the technical point of view, the protocol consisted in a three-dimensional aggregation culture (serum-free culture of embryoid body-like aggregates; SFEB culture; **Figure 10.2**) similar to that used for the formation of polarized cortical tissues. Cell aggregates were cultured in GMEM containing 5% KSR, supplemented with Activin/Nodal-inhibitor Lefty-1 and Wnt-inhibitor Dkk-1, to promote (presumably, because this was not indicated by the Authors) ES cell neuralization and anterior fate specification, respectively. FCS was added to medium starting from day 3, and was followed by exogenous Activin addition at day 4. Floating cell aggregated were re-plated at day 5 on polylysine/laminin/fibronectin coated culture slides and allowed to differentiate for longer periods.

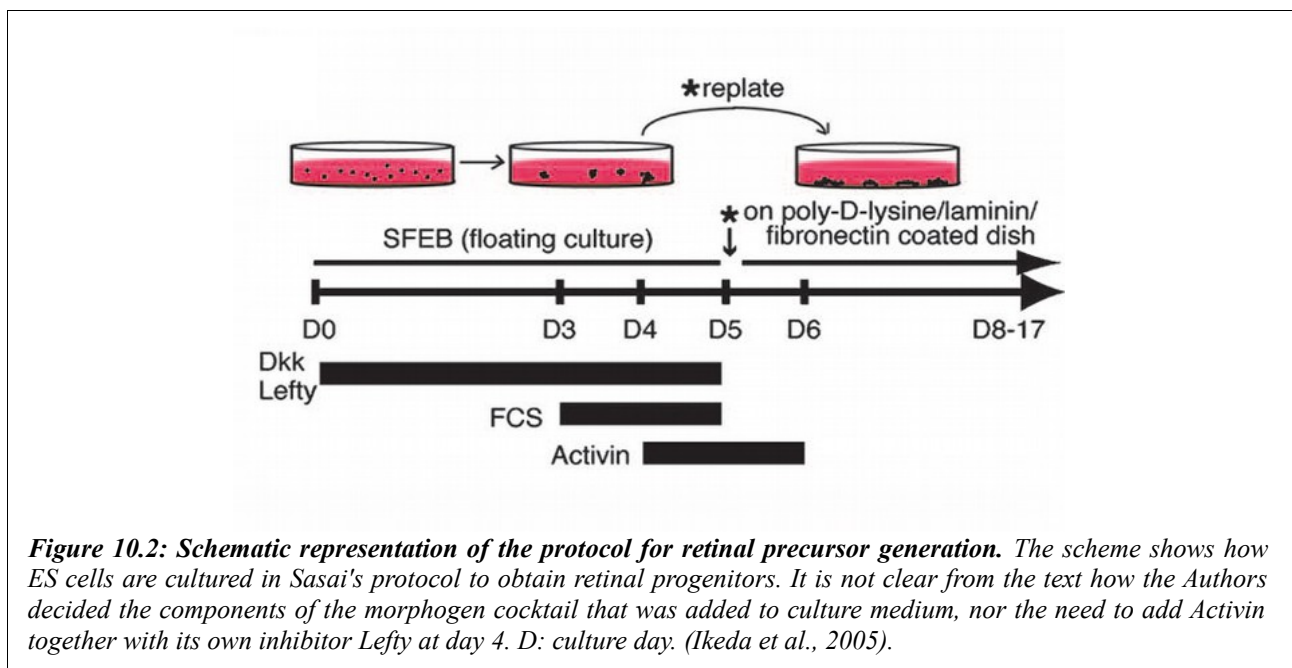


Figure 10.2: Schematic representation of the protocol for retinal precursor generation. The scheme shows how ES cells are cultured in Sasai's protocol to obtain retinal progenitors. It is not clear from the text how the Authors decided the components of the morphogen cocktail that was added to culture medium, nor the need to add Activin together with its own inhibitor Lefty at day 4. D: culture day. (Ikeda et al., 2005).

In 2011, Yoshiki Sasai's Lab developed a new astonishing protocol for retinal differentiation *in vitro*. The Authors reported the autonomous formation of the optic cup (retinal primordium) structure from a serum-free three-dimensional culture of mouse ES cell aggregates (**Figure 10.3**). Embryoid bodie-like aggregates differentiated into Rax-positive retinal epithelium, which spontaneously formed a structure reminiscent of the optic cup, with a proximal pigment epithelium and a distal neural retina. The distal portion progressively folded inward and then generated a stratified neural retina tissue. The formed Rax-positive tissues were also positive for Pax6 and Chx10, and this was consistent with retinal marker expression *in vivo*.

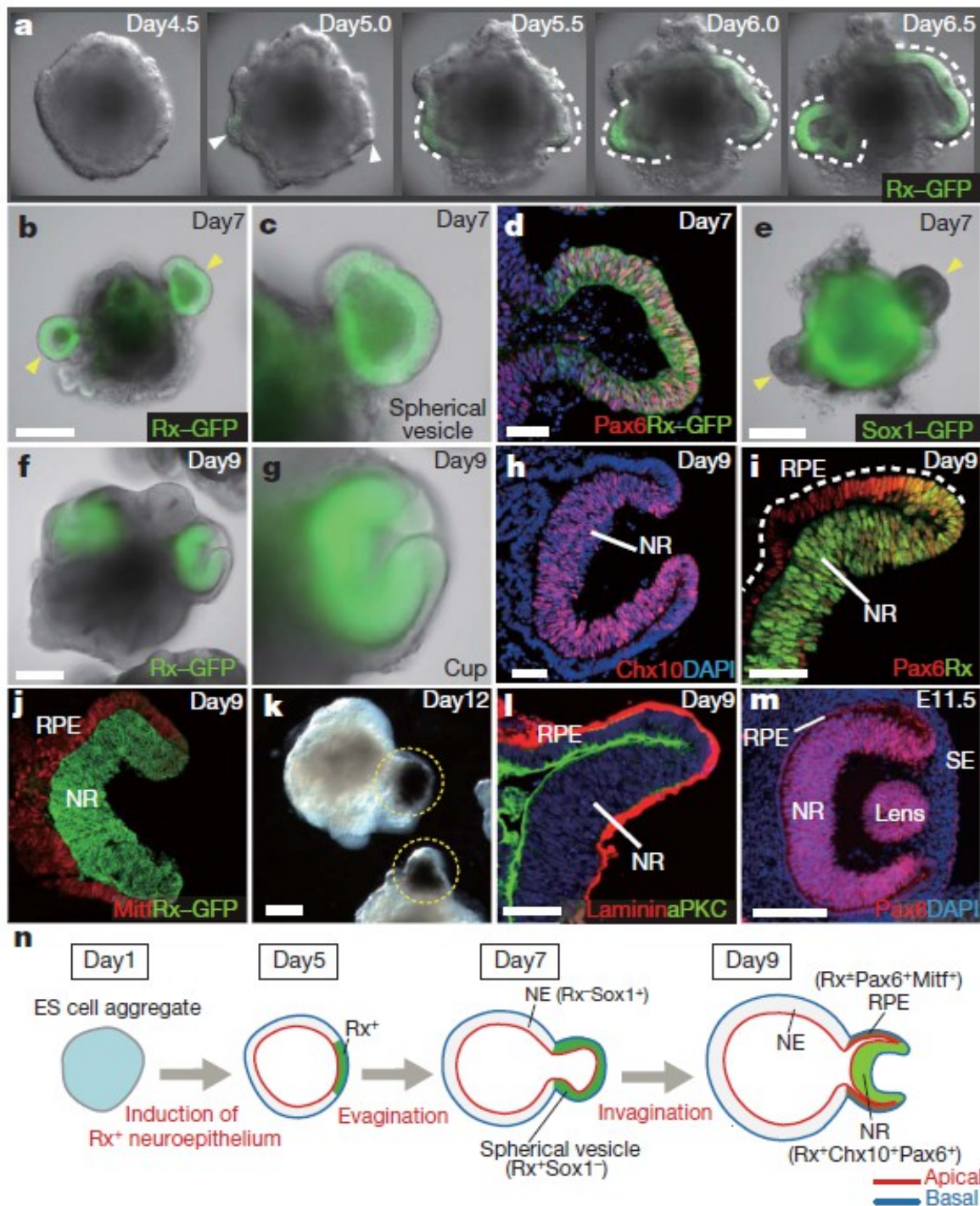


Figure 10.3: Self-formation of an optic-cup-like structure in 3D culture of ES cell aggregates. A-E: SFEBq/matrigel culture. Self-formation of vesicles expressing Rax-GFP (A-C) and Pax6 (D), but not Sox1-GFP (E). F-I: Rax-GFP1 eye-cup structures on day 9 (strongly and weakly in the neural retina (NR) and RPE portions, respectively). H,I: The inner portion strongly expressed Chx10 (H) and Rax and moderately expressed Pax6 (I) on day 9. J,K: The outer epithelial shell of the cup expressed Mitf (J; day 9) and accumulated pigment on day 12 (K). L: The apical marker aPKC and laminin1 basement membrane. M: E11.5 mouse eye. N: Schematic of optic-cup self-formation. SE, surface ectoderm. Scale bars: 200 μ m (B, E-F, K), 50 μ m (D, H, I, L), 100 μ m (M). (Eiraku et al., 2011).

When isolated and cultured for 10-14 days of differentiation, the Rax⁺ tissues spontaneously formed large, continuous epithelial structures with clear stratification, reminiscent of the early postnatal retina. Multiple layers of distinct cellular components consisted of photoreceptors (Rhodopsin⁺ and Recoverin⁺), ganglion cells (Brn3⁺ and Calretinin⁺), bipolar cells (Chx10⁺), horizontal cells (Calbindin⁺), amacrine cells and Muller glia cells. These cellular subtypes were spatially arranged into the correct apical-basal order as seen *in vivo*, and were generated with the right temporal order (as seen by birth-dating analysis with BrdU incorporation; **Figure 10.4**).

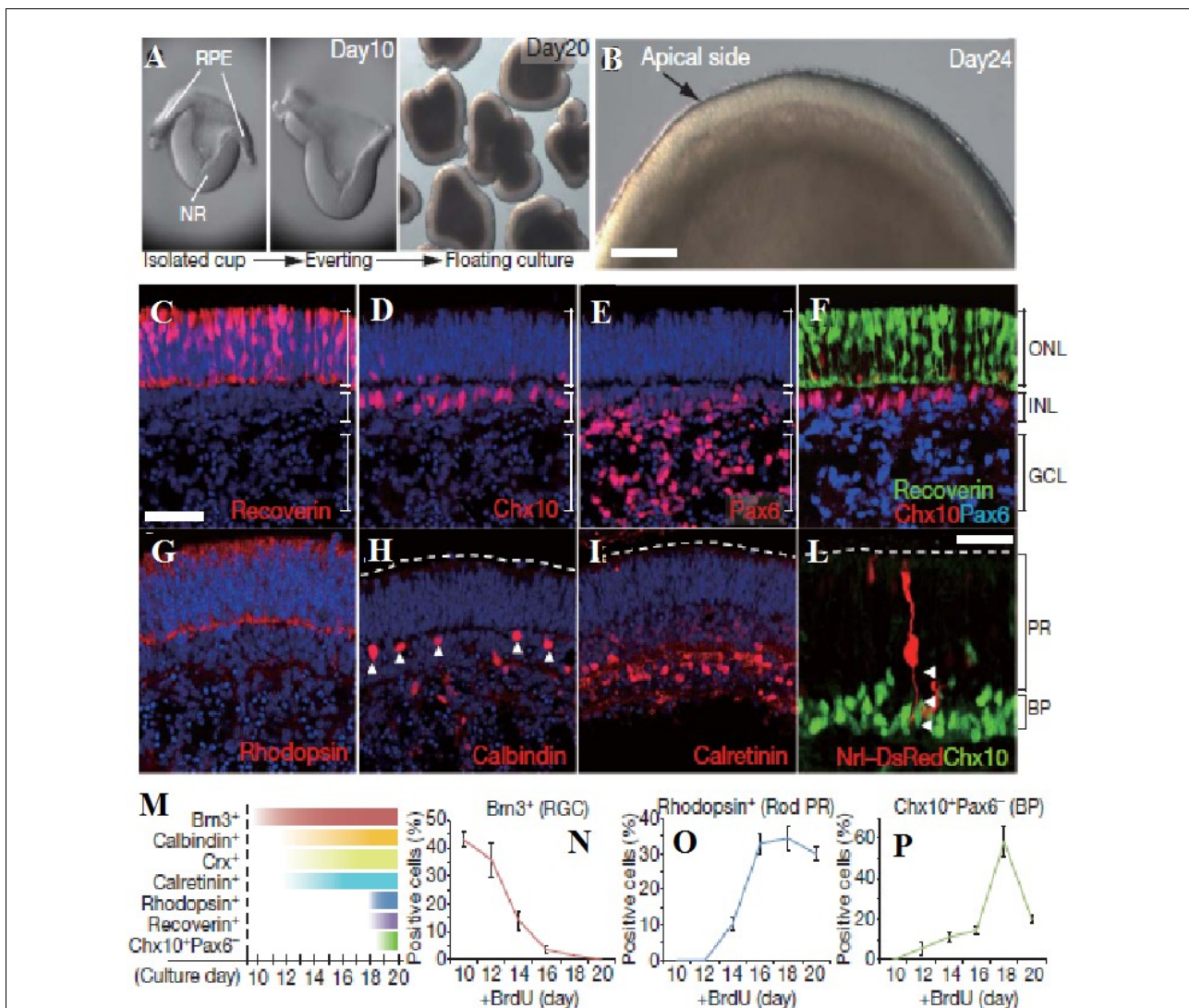


Figure 10.4: Generation of stratified neural retina tissues from ES-cell-derived invaginated epithelia. *A:* Isolation of the optic cups from the SFEBq aggregates at day 10 (*A*; left). Eversion of the RPE hinge occurring after excision (*A*; middle). Floating tissues on day 20 are shown (*A*; right). *B:* Uniformly extending retinal epithelium in day 24 culture. *C-L:* Neural retina markers in cross-sections on day 24. BP, bipolar cells; GCL, ganglion cell layer; INL, inner nuclear layer; ONL, outer nuclear layer; PR, photoreceptors. *L:* pNrl-DsRed2 was electroporated (apically) on day 16, and analysed on day 24. *M:* Temporal expression profile of neural retina markers. *N-P:* BrdU was incorporated on the given day and the BrdU-retaining cell types were analysed on day 24. (Eiraku et al., 2011).

From the technical point of view, the procedure consisted in dissociating and quickly re-aggregating ES cells in GMEM supplemented with 1.5% KSR.

Matrigel (or alternatively Laminin/Entactin/Nodal) was added at day 1. Differentiating ES cells were incubated under 40% O₂ and 5% CO₂ conditions. For long-term neural retina culture, medium consisted in DMEM/F12 supplemented with N2 + 10% FBS + 0.5 μM all-*trans* retinoic acid (RA) + 1 mM L-aurine.

To sum up, Sasai's Lab shared with the scientific community two important ES cell differentiation protocols for the generation of retinal cells *in vitro*. Especially the second - more recent - protocol, is really interesting and opens up new avenues for the transplantation of artificial retinal tissue sheets, rather than simple cell grafting. However, as in the case of cortical differentiation protocols showed in the previous Chapter, again the Authors have been mainly focused on cell-type production, rather than on the molecular mechanisms leading to cell fate specification. The experimental procedures and the culture media always seemed to be chose empirically, testing different combinations of morphogens, and the exact role for each molecule used during differentiation was not precisely dissected. As an example of the confusion generated by this approach, one should notice that the culture medium of the first protocol (**Figure 10.2**), contained the Activin/Nodal inhibitor Lefty from day 0 to day 5 of differentiation, followed by Activin itself starting from day 4, with an unexplainable overlapping of this two opposite treatments during the third day of culture. The Authors do not explain the need for this anomalous overlapping.

Furthermore, both protocols made use of supplements whose composition and possible contribution to retinal differentiation were not investigated, as KSR (knock-out serum replacement supplement) and Fetal Bovine Serum (whose composition and morphogen content is far from being simple and well-defined).

While much information can be found about A/P neural patterning of differentiating ES cells and about cortical fate acquisition, the regulation of forebrain regionalization remains poorly understood (Wilson and Houart, 2004; Beccari et al., 2013). The molecular mechanisms controlling the diversification of the presumptive telencephalon and the eye field has not been elucidated so far. The use of a different scientific approach, focusing not only on the final outcome of the protocol but especially on the systematic analysis of signaling pathways and molecular mechanisms required for retinal differentiation, will be essential to gain new insights on retinal development.

11– Focus on Activin

The formation of three germ layers (endoderm, mesoderm and ectoderm) is the most important event in early vertebrate development. Classical studies showed that Activin plays a pivotal role in the induction of mesodermal and endodermal tissues.

Xenopus laevis animal cap assay can be used to reproduce the *in vivo* induction of amphibian tissues in order to investigate the differentiation processes that occur in normal embryonic development. Animal caps explants (which are made of pluripotent stem cells, similar to mouse ES cells) are treated with morphogens, then the differentiation fate is investigated by RT-PCR, immunohistochemistry or *in situ* hybridisation. By performing animal cap assays, Activin was found to be a potent inducer of various types of mesodermal and endodermal tissue (**Figures 11.1** and **11.2**).

Dissociated animal cap cells express different genes when exposed to Activin, whose effects were found to be dose-dependent (**Figure 11.1**).

- Without any treatment (culture in saline solution), animal cap cells became epidermal cells (expressing keratin).
- At low/moderate concentrations of Activin, animal cap cells switched-on the expression of

the key gene for mesodermal induction, Brachyury, and also expressed genes that characterize the posterior and lateral plate mesoderm (XIHbox6, Xhox3). They developed ventral mesoderm derivatives such as blood cells.

- At moderate/high concentrations, Activin triggered the differentiation of dorsal mesoderm derivatives: beating heart, pronephros, pancreas and cartilage can be induced by microsurgical manipulation and simultaneous treatment with high Activin doses and other factors (Ariizumi and Asashima, 2001; Okabayashi and Asashima, 2003).
- At high doses, Activin induced the Organizer genes to become expressed (Gilbert, *Developmental Biology*; Okabayashi and Asashima, 2003), driving the differentiation of the dorsal-most mesoderm of the embryo, the Notochord. The cells became vacuolated and expressed notochord markers such as Mz15 and low amounts of Goosecoid. (After Green et al., 1992.)
- Adding other factors to Activin also produced interesting results, such as the development of endodermal tissues. The addition of Retinoic acid to the concentration of Activin that usually induces the formation of notochord, for example, will cause the formation of kidney tubules. When insulin-like growth factor is added to the concentration of Activin that can produce muscles, ear and eye vesicles form.

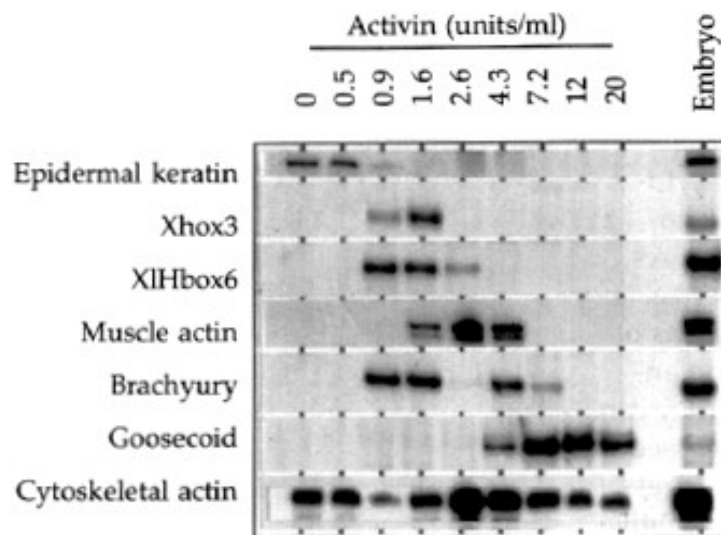


Figure 11.1: Dissociated animal cap cells express different genes when exposed to different concentrations of *Activin*. At low concentrations, they become epidermal cells (expressing keratin). However, after a sharp threshold, they begin expressing genes that characterize the posterior and lateral plate mesoderm (*XIHbox6*, *Xhox3*, *Brachyury*). If exposed to higher concentrations of *Activin*, the cells express notochord markers such as *Mz15* and low amounts of *Goosecoid*. (After Green et al., 1992).

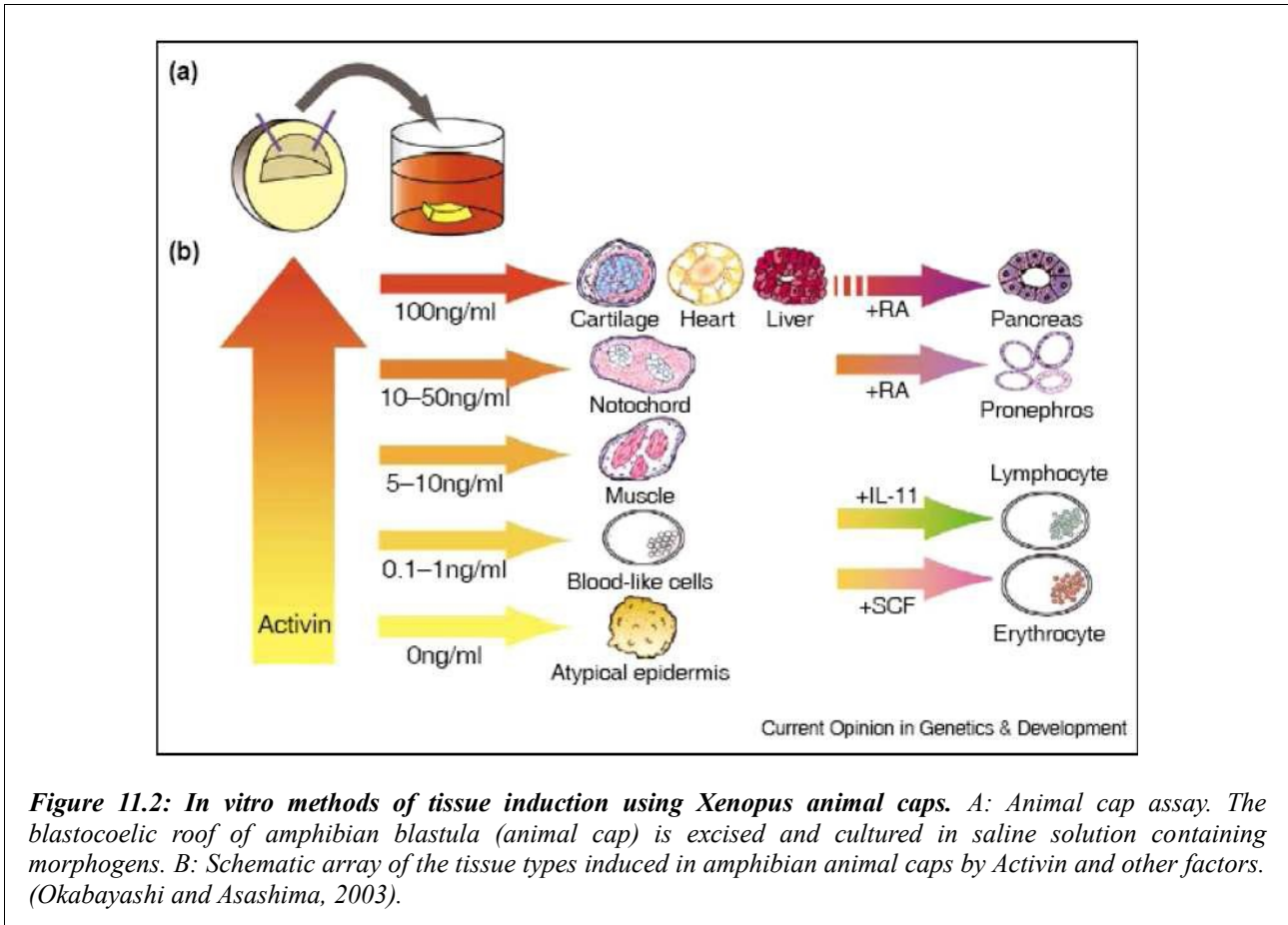
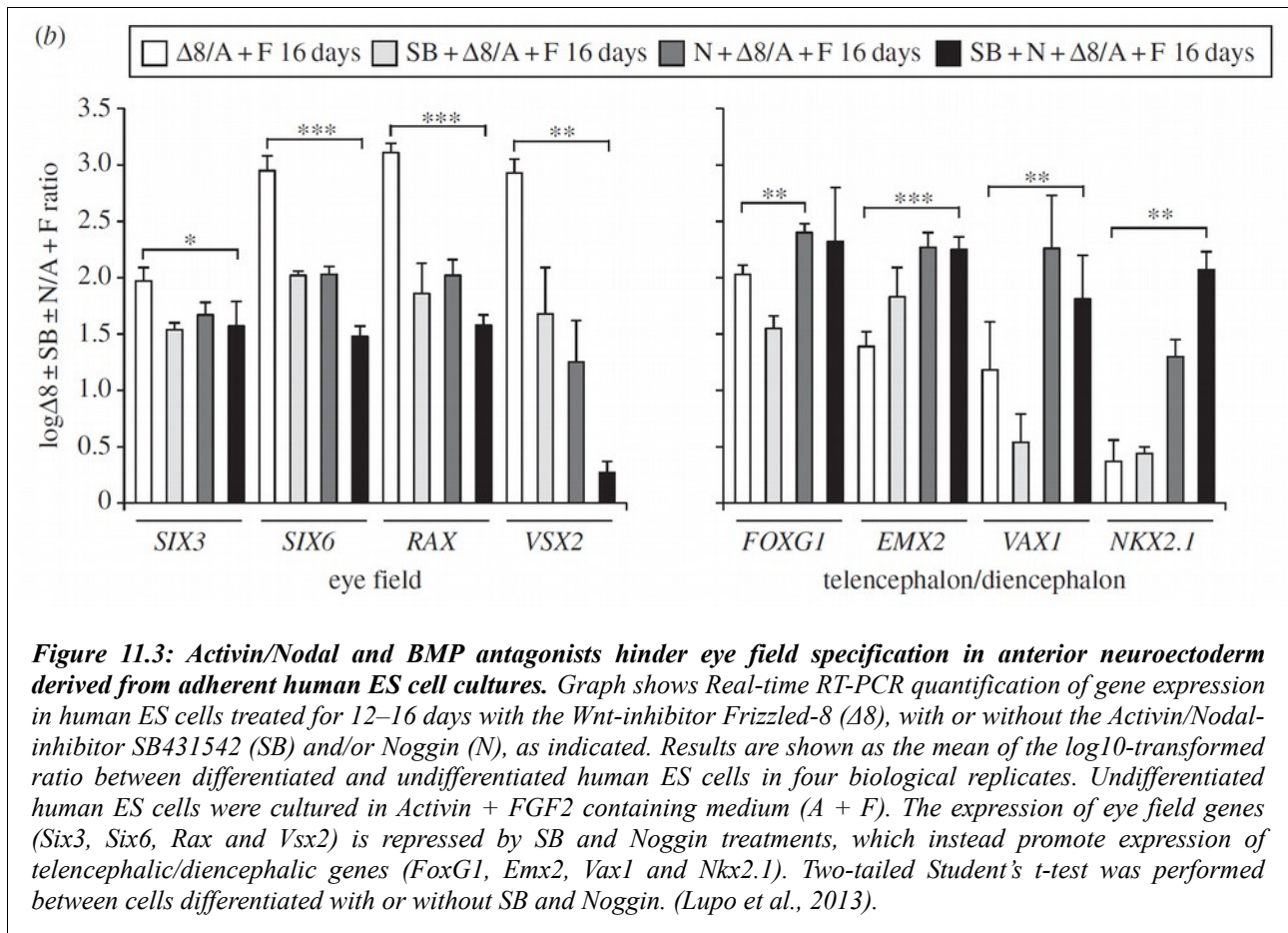


Figure 11.2: In vitro methods of tissue induction using *Xenopus* animal caps. A: Animal cap assay. The blastocoelic roof of amphibian blastula (animal cap) is excised and cultured in saline solution containing morphogens. B: Schematic array of the tissue types induced in amphibian animal caps by Activin and other factors. (Okabayashi and Asashima, 2003).

Activin is now principally employed in mammalian ES cell differentiation protocols as an efficient inducer of both mesodermal identity (Cerdan et al., 2012) and endodermal identity (Teo et al., 2012; Iwao et al., 2013; Vosough et al., 2013) during mammalian ES cell differentiation *in vitro*. Additionally, Activin was found to have a role in maintenance of stem cell pluripotency (Tomizawa et al., 2013; Sakaki-Yumoto et al., 2013).



In summary, Activin plays important roles in the maintenance of stem cell pluripotency and in stem cell differentiation (for the induction of mesodermal/endodermal tissues). Some new studies suggest that Activin could play additional roles in ES cell patterning during neural differentiation. To date, few evidence has been provided for a possible role of Activin as an inducer of retinal identity. A cue in this direction has been given by Sasai's Lab (Ikeda et al., 2005); their protocol for the *in vitro* generation of retinal progenitors makes use of Activin-A in the culture medium. Unfortunately, the experimental procedures described in this work did not allow to infer neither the exact role for each of molecules used nor the temporal competence of cells to specifically respond to the different signals. In particular, the role of Activin in patterning neural fate toward a retinal identity was not dissected. A detailed comparison between cells treated with Activin and cells differentiated in absence of it, for example, was completely missing.

Conversely, Lupo et al. showed the importance of both BMP and Activin/Nodal signaling for the induction of eye field genes in differentiating human ES cells, separately investigating their

contribution and time of action on the transcription of early retinal markers (Lupo et al., 2013; **Figure 11.3**). They found that levels of Activin/Nodal and BMP signaling have a marked influence on forebrain patterning and that the inhibition of these pathways represses expression of eye field genes (**Figure 11.3**).

The regulation of forebrain regionalization remains poorly understood (Wilson and Houart, 2004). In particular, the molecular mechanisms controlling the diversification of the presumptive telencephalon and the eye field have not been elucidated so far. The systematic analysis of signaling pathways (such as Wnt, BMP, and Activin/Nodal pathways) and the study of their early contribution for the patterning of the forebrain will be essential to gain new insights on cortical and retinal development.

12– Aim of research

The aim of this work was to directly show the endogenous production of morphogens (BMP, Wnt, FGF and Activin/Nodal factors) by differentiating ES cells and to characterize their effects on the differentiation and positional identity of ES cell-generated neurons, focusing on cortical and retinal differentiation.

The use of factor-free chemically defined media has allowed for the investigation of the differentiation fate of ES cells in the absence of exogenous signals, showing that it is predominantly neural (Tropepe et al., 2001, Gaspard et al., 2008; 2009). The first step in my work was to set up a **novel neural differentiation protocol, using chemically defined minimal medium, suitable to study the default differentiation identity of mouse ES cells and to unravel the possible production of endogenous factors during neural differentiation.** I therefore established an *in vitro* differentiation protocol that minimizes exogenous signals, and analyzed ES cell differentiation by performing RT-PCR, immunohistochemistry and genome-wide expression analysis. I created a new efficient neuralization protocol, where ES cells cultured in the absence of any added morphogen efficiently differentiate into neuronal cells, which is consistent with previous observations (Cai and Gabel, 2007; Smukler et al., 2006).

The absence of morphogens inside the culture medium does not assure a completely morphogen-free system. We reasoned that ES cells could express and produce morphogens such as Wnts, BMPs, FGFs and Activin/Nodal during neural differentiation *in vitro*. These molecules could actively affect ES cell neuralization and positional identity. I therefore investigated for the production of endogenous morphogens by RT-PCR analysis at different time points in our protocol, and I found that **mouse ES cells express different morphogens during neural differentiation *in vitro*, especially BMPs, Wnts and FGFs. These morphogens could act in an autocrine or paracrine way, affecting ES cell differentiation and the acquisition of distinct positional identities.**

Effects of factors endogenously produced by ES cells on their neural differentiation have been suggested. BMPs sustain self-renewal and inhibit neural differentiation of ES cells (Ying et al., 2003). The BMP-inhibitors Noggin and Chordin triggers *in vitro* neuronal differentiation of mammalian ES cells cultured in growth factor-free chemically defined medium (Chambers et al., 2009; Gratsch & O'Shea, 2002). Additionally, Activin/Nodal-inhibitors are often used to drive ES cell neural differentiation (and at the same time to inhibit mesodermal differentiation) (Ikeda et al., 2005). Wnt-inhibitors (such as Dkk-1) are exploited to protect the anterior default differentiation fate of differentiating ES cells (Eiraku et al., 2008; Ikeda et al., 2005; Verani et al., 2007; Nicoleau et al., 2013). These data suggest that ES cells produce, and are sensitive to, BMPs, Wnts and Activin/Nodal factors with an autocrine/paracrine mechanism. However, to our knowledge, there is no direct measurement of BMP, Wnt and Activin/Nodal production by differentiating ES cells.

At first, I decided to focus on BMP and to test if endogenously produced BMP factors could affect ES cell neuralization and/or the regional identity of ES cell-generated neurons. I found that **BMP-inhibitor Noggin, in addition to its known role as neural inducer, plays a major role in establishing an anterior, cortical fate.** Blocking the BMP pathway by Noggin or by other inhibitors selectively affects the A/P positional identity of the generated neurons. Control ES cells, differentiated with our protocol, spontaneously acquired a mesencephalic differentiation fate, while at the highest doses of Noggin-treatment that I tested, the fate of neurons produced by ES cells was predominantly dorsal telencephalic. These neurons have a gene expression profile that clusters with that of early cerebral cortical cells and express telencephalic differentiation markers. In summary, Noggin acted at two distinct levels of ES cell differentiation: it strengthened their spontaneous neural differentiation in a minimal medium, and it strongly induced a telencephalic/cortical identity.

Having defined the role of BMP in fate choice between forebrain (predominantly cortex) and midbrain, we then asked whether endogenously produced Wnts could contribute to mask an intrinsic cortical fate of neuralizing ES cells. Double BMP/Wnt inhibition showed an even stronger down-regulation of midbrain genes and more efficient up-regulation of cortical genes, compared to single treatments, suggesting a synergistic effect of BMP and Wnt pathway inhibition for the acquisition of a cortical fate. All in all, we concluded that **Wnt inhibition plays a fundamental role in establishing an anterior, telencephalic (in our case, cortical) fate during ES cell neural differentiation *in vitro***, consistently with previous findings (Eiraku et al., 2008; Ikeda et al., 2005; Verani et al., 2007; Nicoleau et al., 2013).

While many information can be found about A/P neural patterning of differentiating ES cells and about cortical fate acquisition, regulation of forebrain regionalization remains poorly understood. The molecular mechanisms controlling the diversification of the presumptive telencephalon and the eye field have not been elucidated so far (Wilson and Houart, 2004; Andonadiou et al., 2013). As the final goal of my project, I decided to exploit the plasticity of my protocol and the previously acquired information on ES cell differentiation, to steer stem cell fate choice between telencephalon (cortex) and diencephalon (retina). In particular, I studied how the **manipulation of Activin/Nodal signaling can lead to a further patterning inside the forebrain, triggering retinal specification at the expense of cortical differentiation**. I found that a low dose (10 ng/ml) of Activin was able to drive the expression of retinal markers Rax, Six3, Pax6, Otx2 and Six6, some of which were previously shown to play a fundamental role as eye field transcription factors (Zuber et al., 2003). At the same time, Activin could inhibit the expression of cortical (Emx2 and FoxG1) and midbrain (En1 and Irx3) genes.

Activin retinal inducing action was exerted only on cells that previously acquired a forebrain fate via Wnt-inhibition or double Wnt/BMP-inhibition; Activin was not effective as a retinal inducer when used alone. This suggests that a previous anteriorization to a forebrain fate was necessary to acquire the competence to respond to Activin-mediated retinal induction, consistently to what happens in *in vivo* development (Zuber et al., 2003).

Our experiments (this Thesis and Bertacchi et al., manuscript in preparation) are the first description and full characterization of an **Activin new role as inducer of retinal identity at the expense of a more anterior, telencephalic one, on mouse ES cells**.

Additionally, I found that different morphogens were able to switch-on Rax expression: while Activin was able to induce the formation of Pax6/Rax double positive cells, which can be

considered as *bona fide* retinal progenitors, SAG (Shh-agonist) was driving efficient Rax co-expression together with Nkx2.1 and Vax1, which is consistent with a ventral diencephalic identity (rostral hypothalamus cells; Wataya et al, 2008; Ikeda et al., 2005). Notably, Shh-agonist was able to induce the expression of Rax only if used in combination with Wnt-inhibitor. This suggested that only *anteriorized* forebrain cells were competent to respond to Shh-mediated Rax induction. I concluded that **different morphogens (such as Activin and Shh) are able to switch-on Rax expression, in the context of anterior forebrain-like cells.**



Materials and Methods

1– Materials and Methods

Cells cultures

Murine embryonic stem (ES) cell lines E14Tg2A (passages 25-38), 46C (transgenic Sox1-GFP ES cells kindly provided by A. Smith, University of Cambridge, UK, passages 33-39) and K/1-EB5 (transgenic Rax-GFP ES cells kindly provided by Y. Sasai, Riken Center, Japan) were cultured on gelatin-coated tissue culture dishes at a density of 40,000 cells/cm². ES cell medium, which was changed daily, contained GMEM (Sigma), 10% Fetal Calf Serum, 2mM Glutamine, 1mM sodium Pyruvate, 1mM non-essential amino acids, 0.05mM β -mercaptoethanol, 100 U/ml Penicillin/Streptomycin and 1000 U/ml recombinant mouse LIF (Invitrogen), the latter avoiding the need of a feeder cell layer. Cells were passaged using Trypsin dissociation and re-plated at a dilution of 1:3 to 1:4, to avoid cell confluence and to maintain pluripotency.

RAW 264.7 (mouse leukemic monocyte macrophage cell line, kindly supplied by Diana Boraschi, Institute of Medical Biotechnology, CNR of Pisa) were cultured in Dulbecco's modified Eagle's Medium with 4mM L-glutamine and 4.5 g/L glucose, supplemented with 10% fetal bovine serum. Cells were split every two days at a confluence of approximately 10% ($1 \cdot 10^6$ and $3 \cdot 10^6$ cells in 100-mm and 150-mm plates, respectively) and grown to a confluence of approximately 80%.

Mouse mesenchymal stromal cells (MSCs) primary cultures (kindly supplied by Cristina Magli, CNR of Pisa) were established from B6D2F1 (BDF1) mice (Charles River) as described (Nadri et al., 2007).

Mouse neuronal primary cultures or paraformaldehyde-fixed brain slices to test antibodies were obtained from wild-type mice as described (Malatesta et al., 2000).

Neural induction

We recently published the full description of the neural induction protocol used in this Thesis (Bertacchi et al., 2013). Chemically defined minimal medium (CDMM) for neural induction consisted of DMEM/F12 (Invitrogen), 2mM Glutamine, 1mM sodium Pyruvate, 0.1mM non-essential amino acids, 0.05mM β -mercaptoethanol, 100 U/ml Penicillin/Streptomycin supplemented with N2/B27 (no vitamin A; Invitrogen). Protocol outline is shown in **Figure 1.1**.

- **Step-I:** dissociated ES cells were washed with DMEM/F12, aggregated in agar-coated culture dishes (65,000 cells per cm²) and cultured as floating aggregates in CDMM for 2 days. The second day 75% of CDMM was renewed.
- **Step-II:** ES cell aggregates were dissociated and cultured in adhesion (65,000 cells per cm²) on Poly-ornithine (Sigma; 20 μ g/ml in sterile water, 24 hours coating at 37°C) and natural mouse Laminin (Invitrogen; 2.5 μ g/ml in PBS, 24 hours coating at 37°C) for 4 days, changing CDMM daily. In some cases, Step-II was further prolonged up to a maximum of 8 days of culture without any re-dissociation and re-plating.
- **Step-III:** After a second dissociation, ES cells were cultured 4 additional days in CDMM devoid of B27 supplement to drive terminal differentiation, using the same type of seeding density and coated surface. Serum employed for Trypsin inactivation was carefully removed by several washes in DMEM/F12.

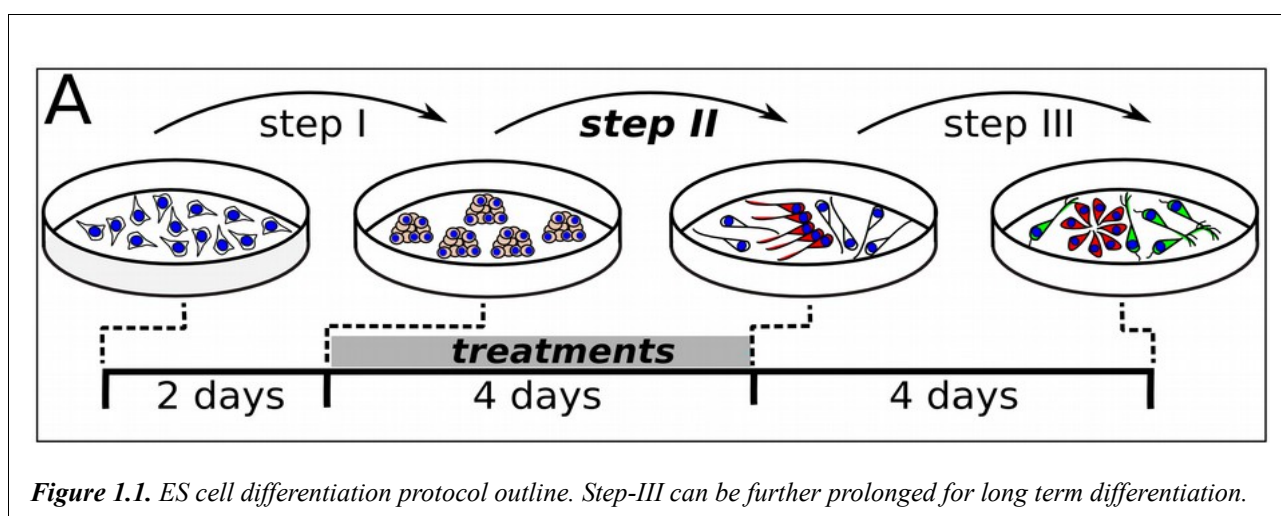


Figure 1.1. ES cell differentiation protocol outline. Step-III can be further prolonged for long term differentiation.

The following factors were tested by addition during Step-II: Recombinant Mouse Noggin (R&D; ranging from 5 nM to 400 nM), Recombinant Human/Mouse/Rat Activin-A (R&D; ranging from 1 ng/ml to 100 ng/ml), BMP4 (R&D; 50 ng/ml), Recombinant Mouse BMPRIA/Fc Chimera (R&D; 3.75 nM and 37.5 nM), Dorsomorphin (Sigma-Aldrich; 5 μ M), Retinoic Acid (Sigma-Aldrich; 0.1 to 10 μ M), Cyclopamine (Sigma-Aldrich; 5 μ M), SAG (Santa Cruz Biotechnology; 100/150 nM), SB431542 (Sigma-Aldrich; 10 μ M), IWR-1-endo (Calbiochem; 5/10 μ M). Cell viability and proliferation, which were monitored by trypan blue exclusion test and cell counting, respectively, were not significantly affected by most common treatments (**Figure 1.3** and **Figure 1.2**).

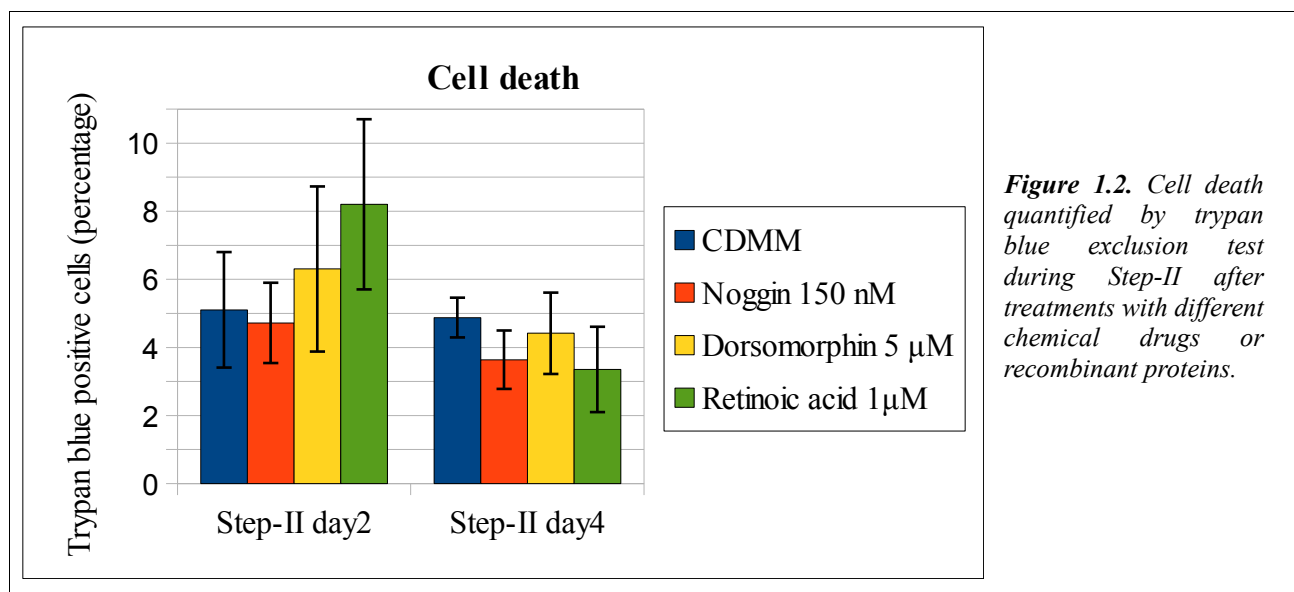


Figure 1.2. Cell death quantified by trypan blue exclusion test during Step-II after treatments with different chemical drugs or recombinant proteins.

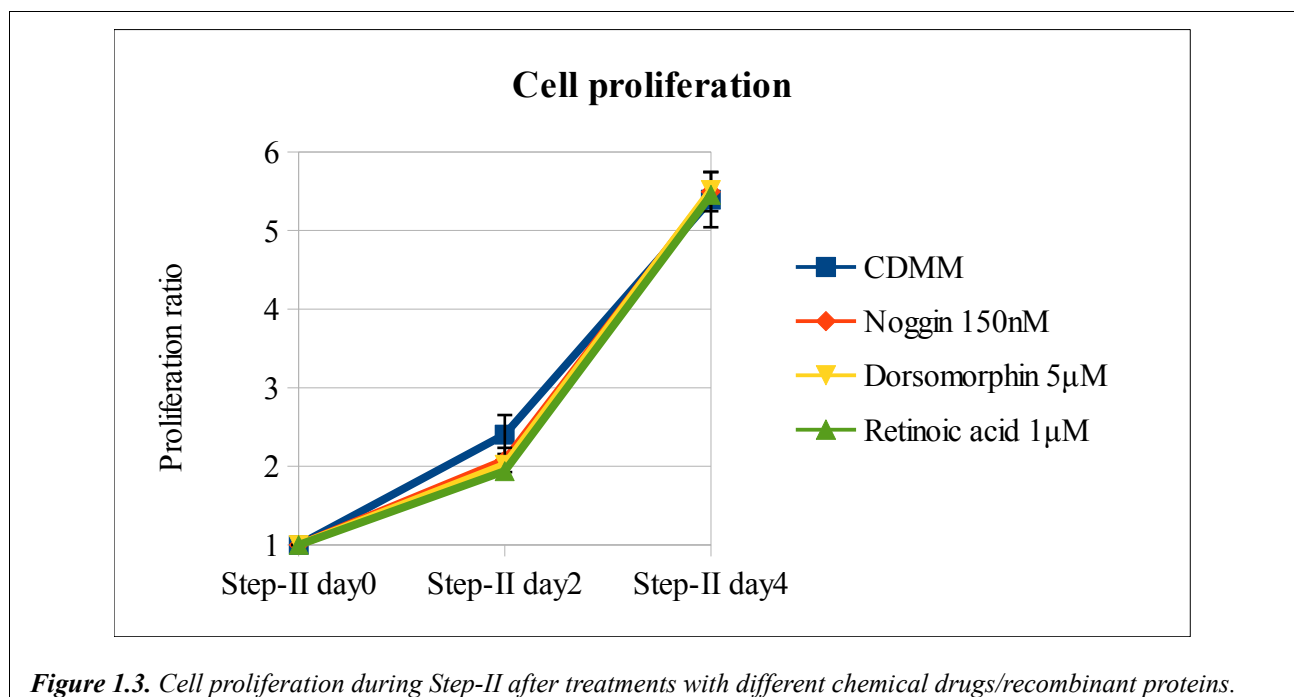


Figure 1.3. Cell proliferation during Step-II after treatments with different chemical drugs/recombinant proteins.

Semiquantitative real-time PCR

Total RNA was extracted from ES cells or tissue samples with NucleoSpin RNA II columns (Macherey-Nagel). ES cells from at least two-three different wells of 24-well plates / 6-well plates were always pooled together to compensate for variability in cell seeding. RNA quantity and RNA quality were assessed with Nanodrop and gel electrophoresis. For each sample, 200/500 ng of total RNA were reverse-transcribed. Amplified cDNA was quantified using GoTaq qPCR Master Mix (Promega) on Rotor-Gene 6000 (Corbett) with the primers listed in **Table 1**, at the end of this Chapter. Amplification take-off values were evaluated using the built-in Rotor-Gene 6000 *relative quantitation analysis* function, and relative expression was calculated with the $2^{-\Delta\Delta C_t}$ method, normalizing to the housekeeping gene β -Actin. Standard errors were obtained from the error propagation formula as described in (Nordgård et al., 2006) and statistical significance was probed with randomization test, taking advantage of REST Software (Pfaffl et al., 2002).

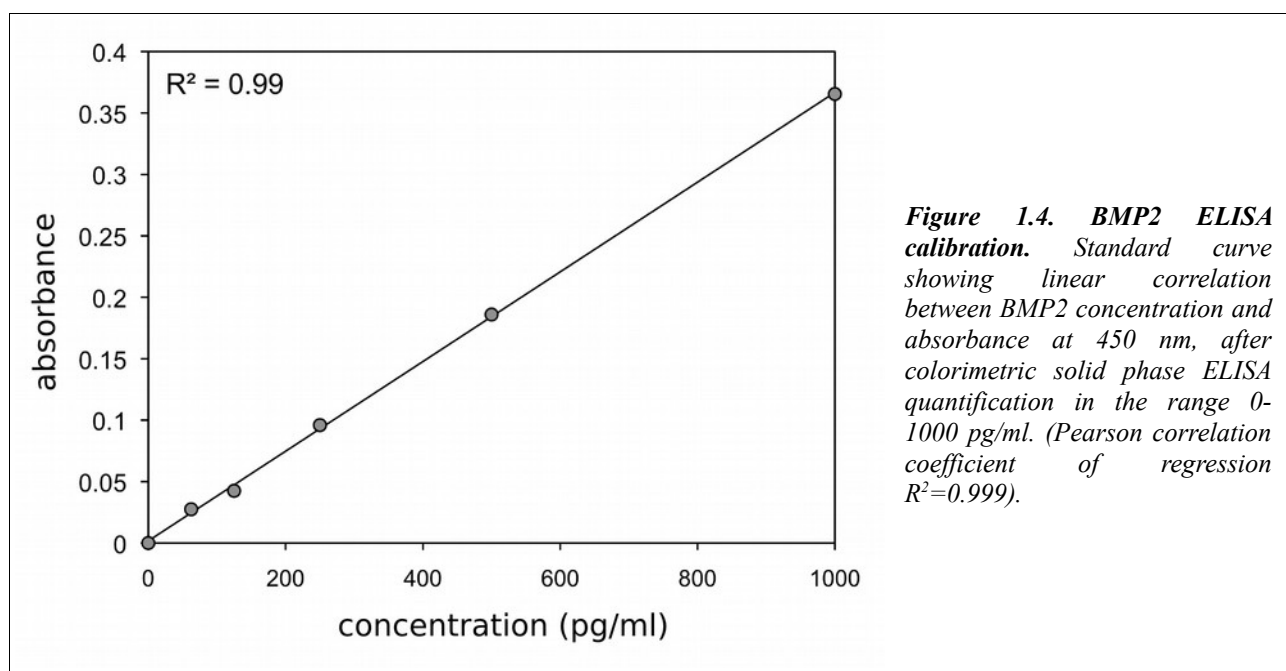
ImmunocytoDetection

Cells prepared for immunocytoDetection experiments were cultured on Poly-ornithine/Laminin coated round glass coverslips. Cells were fixed using 2% paraformaldehyde for 10-15 minutes, washed twice with PBS, permeabilized using 0.1% Triton X100 in PBS and blocked using 0.5% BSA in PBS. Primary antibodies used for microscopy included Oct3/4 (1:200; Santa Cruz DBA), Nanog (1:300; Novus Biologicals), acetylated N-Tubulin (1:500; Sigma), Neuronal Class III β -Tubulin (1:500; Covance), Doublecortin (1:500; Abcam), Musashi-1 (1:200; Cell Signaling), Nestin (1:200; Millipore), Synaptophysin (1:100; Santa Cruz DBA), α -Internexin (1:100; Santa Cruz DBA), phospho-Smad1/5/8 (1:100; Millipore), FoxG1 (1:200; Abcam), Tbr1 (1:400; Millipore), Satb2 (1:200; Abcam), Ctip2 (1:400; Abcam), GFP (rabbit polyclonal; 1:1,000; Invitrogen), GFP (chicken polyclonal; 1:1,000; Aves Lab), Rhodopsin (1:1,000; Sigma), vGlut2 (1:300; Abcam), GAD65 (1:500; Chemicon), Pax6 (1:400; Covance), Nkx2.1 (1:400; Abcam) and GFAP (1:100; Dako). Primary antibodies were incubated 2 hours at room temperature; cells were then washed three times with PBS (10' each). Alexa Fluor 488 and Alexa Fluor 568 anti-guinea pig, anti-goat,

anti-mouse, anti-rabbit or anti-chicken IgG conjugates (Molecular Probes, 1:500) were incubated 1 hr at RT in PBS containing 0.1% Triton X100 and 0.5% BSA for primary antibody detection, followed by three PBS washes (10' each). Nuclear staining was obtained with DAPI. The protocol varied for Tbr1, Satb2, Ctip2 and FoxG1, which antibodies were incubated over-night at 4°C using 0.3% Triton X100.

BMP2 ELISA

Cells were seeded into 24-wells and cultured as described. When cells reached 70-80% confluence, each well was washed with PBS, and fresh medium (DMEM/F12 containing 2mM Glutamine and 1mM sodium Pyruvate) was replaced. After 24h, supernatant was collected, centrifuged (10,000 g, 5') to remove particulates and assayed for BMP2 content with a commercially available ELISA kit (Quantikine, BMP-2 Immunoassay, R&D Systems, Minneapolis, MN USA), according to the manufacturer's instructions. This assay could measure BMP-2 concentrations as low as 50 pg/ml in a linear range (Pearson correlation coefficient of linear regression $R^2=0.999$, see **Figure 1.4**). A 1.2% cross-reactivity was observed with 50 ng/mL recombinant human BMP-4. BMP-2 concentrations of triplicate samples were determined from the optical densities at 450 nm in relation to standard curves of the recombinant antigen provided in the kit.



FACS analysis

Adherent cells were detached by trypsinization, washed and resuspended in PBS at RT, then analyzed with a FACSCalibur cytometer (BD). At least 10,000 events per sample were collected. Data were processed with the free software WinMDI 2.9 (The Scripps Research Institute).

Microarray hybridization and data analysis

Cortex, midbrain and hindbrain were dissected from n=3 mouse embryos (C57BL/6 strain) at embryonic day (E)16. Total RNA was extracted with NucleoSpin RNA II columns (Macherey-Nagel). RNA from three different sets of experiment was pooled. RNA quality was assessed with Agilent Bioanalyzer RNA 6000 Nano kit; 500 ng of RNA were labeled with One Color Quick amp labeling kit (Agilent), purified and hybridized overnight onto an Agilent Mouse Gene Expression Microarray chip (4x44K v2) before detection, according to the manufacturer's instructions. Three slides were hybridized with Noggin-treated ES cell RNA and two slides were hybridized with RNA from all the other conditions. Agilent DNA Microarray scanner was used for slide acquisition and spot analysis was performed with Feature Extraction software (Agilent).

For GSEA analysis, genes differentially expressed between Noggin treatment and CDMM (Supplemental **Table 2**), or between RA treatment and CDMM (Supplemental **Table 3**; fold-change greater or equal than 2), were analyzed by the GeneSpring GX11.0 software using BROAD Gene Ontology collection (C5; www.broadinstitute.org/gsea). A complete GSEA list with enrichment scores of gene sets with q-value <0.3 is shown in Supplemental **Table 4** (On-line material; Bertacchi et al., 2013).

To select a gene-set representing the anterior-posterior regionalization of the developing brain, we compared gene expression profiles of E16 cortex and hindbrain using Genespring GX11.0 software

(Agilent). A set of 592 genes with an absolute fold-change greater or equal than 10 ($p < 0.05$) was selected (see Supplemental **Table 5**, on-line material; Bertacchi et al., 2013). Significance of the data was proven by one-way ANOVA and Tukey *post hoc* test with Bonferroni correction for multiple comparisons. The content of this set of genes was explored by hierarchical clustering and Principal Component analysis, taking advantage of Cluster software (Eisen et al., 1998). Single linkage algorithm was employed for hierarchical clustering. Trees were generated using absolute correlation for genes and Euclidean distance for arrays, and visualized with java TreeView (Saldanha, 2004).

List of primers for Real Time RT-PCR.*Table 1: List of primers.*

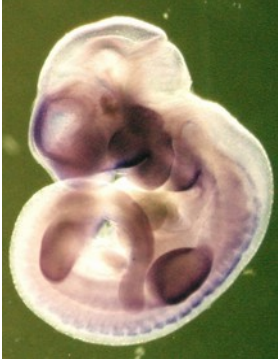


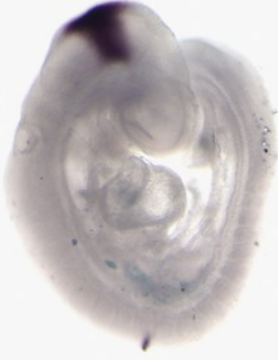




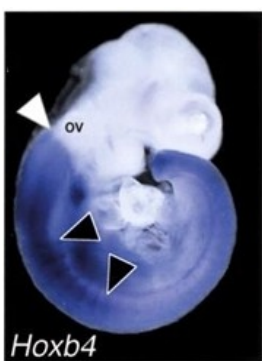
Name		5'-3' sequence	Amplicon (bp)
Activin-A	sense	AGGGCCGAAATGAATGAAC	
Activin-A	antisense	ACTTCTGCACGCTCCACTAC	
BMP2	sense	ACACAGGGACACACCAACCAT	125
BMP2	antisense	TGTGACCAGCTGTGTTTCATCTTG	
BMP4	sense	TTCCTGGTAACCGAATGCTGA	114
BMP4	antisense	CCTGAATCTCGGCGACTTTTT	
BMP6	sense	GGTGACGGCTGCTGAGTT	
BMP6	antisense	GGGTGTCCAACAAAATAGGTC	
BMP7	sense	GATTTACAGCTGGACAACGAG	108
BMP7	antisense	GGGCAACCCTAAGATGGACAG	
BMPR1a	sense	GCAAGGATTCACCGAAAGCCCAG	122
BMPR1a	antisense	GCTGCCATCAAAGAACGGACCTA	
BMPR1b	sense	TGGGTGCGTGAAAGATGGAGACC	187
BMPR1b	antisense	ACCGTAGAGTGAAACACAGAGGGA	
Bsx1	sense	AGAGGCCACGTCGTTTTTC	
Bsx1	antisense	GCACCCTAGAGGCCAGAGA	
CaM-Kinase-IIa	sense	CAATATCGTCCGACTCCATG	178
CaM-Kinase-IIa	antisense	CATCTGGTGACAGTGTAGC	
Crx	sense	ACCAGGCTGTCCCATACTCA	198
Crx	antisense	TCGCCCTACGATTCTTGAAC	
Ctip2	sense	CCCGACCCTGATCTACTCAC	
Ctip2	antisense	CTCCTGCTTGGGACAGATGC	
Dlx2	sense	TGGGCTCCTACCAGTACCAC	
Dlx2	antisense	TGGCTTCCCGTTCACTATTC	
Emx2	sense	GGCTAGAGCACGCTTTTGAG	199
Emx2	antisense	CACCGGTTAATGTGGTGTGT	
En1	sense	AGTGGCGGTGGTAGTGGA	232
En1	antisense	CCTTCTCGTTCCTTTTCTTCTTT	
FGF15	sense	GTTTACCGCTCCTTCTTTG	
FGF15	antisense	TCTACATCCTCCACCATCCTG	
FGF4	sense	TCTTCGGTGTGCCTTTCTTT	
FGF4	antisense	CACTCGGTTCCCCTTCTTG	
FGF5	sense	GTCAATGGCTCCCACGAA	
FGF5	antisense	TGGAATCTCTCCCTGAACTTACA	
FGF8	sense	TTGGAAGCAGAGTCCGAGTT	
FGF8	antisense	ATACGCAGTCTTGCCCTTG	
FoxG1	sense	CGACCCTGCCCTGTGAGT	107
FoxG1	antisense	GGAAGAAGACCCCTGATTTTG	









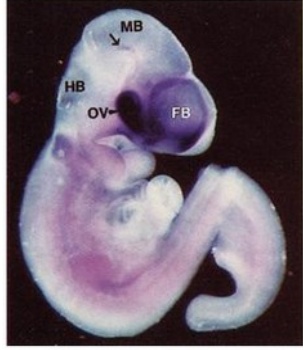
FoxH1	sense	CGCCACAACCTTTCTCTAA	
FoxH1	antisense	GGAATCAGGCTCACATCCAC	
Gata4	sense	GGAAGACACCCCAATCTCG	75
Gata4	antisense	CATGGCCCCACAATTGAC	
GFAP	sense	GGAGAGGGACAACCTTTGCAC	164
GFAP	antisense	CCAGCGATTCAACCTTTCTC	
HoxB4	sense	AAAGAGCCCGTCGTCTACC	102
HoxB4	antisense	AGTGTTAGGCGGTCCGAGAG	
HoxB9	sense	GAAGGAAGCGAGGACAAAGA	188
HoxB9	antisense	AGATTGAGGAGTCTGGCCACT	
Id1	sense	CRACTACATCAGGGACCTGCA	143
Id1	antisense	GAACACATGCCGCCTCGG	
Irx3	sense	AGTGCCTTGGAAGTGGAGAA	108
Irx3	antisense	CGAGGAGAGAGCTGATAAGACC	
LEF1	sense	TCAAATAAAGTGCCCGTGGT	
LEF1	antisense	GGGGTAGAAGGTGGGGATT	
Lhx2	sense	CTACCCCAGCAGCCAAAAGA	
Lhx2	antisense	CCTGCCGTAAAAGGTTGC	
Lhx8	sense	AAACACGTCAGTCCCAACCA	
Lhx8	antisense	ACGTAGGCAGAATAAGCCATTT	
NCAM	sense	AGGAGAAATCAGCGTTGGAG	182
NCAM	antisense	CGATGTTGGCGTTGTAGATG	
Nestin	sense	TGTCCCTTAGTCTGGAAGTGG	199
Nestin	antisense	GGGGAAGAGAAGGATGTTGG	
NF-L	sense	CCATGCAGGACACAATCAAC	184
NF-L	antisense	CTACCCACGCTGGTGAAACT	
Nkx2.1	sense	CAATGAGGCTGACGCCCCCG	131
Nkx2.1	antisense	GAAGTGGGTTTCTGTCTGAGCG	
Nodal	sense	GAGGGCGAGTGTCTTAACC	
Nodal	antisense	ATGCTCAGTGGCTTGGTCTT	
Oct4	sense	TCAGCTTGGGCTAGAGAAGG	150
Oct4	antisense	GGCAGAGGAAAGGATACAGC	
Otx2	sense	CCACTTCGGGTATGGACTTG	128
Otx2	antisense	GGTCTTGGCAAACAGAGCTT	
Pax6	sense	CCTCCTTCACATCAGGTTCC	189
Pax6	antisense	CATAACTCCGCCCATTCCT	
SatB2	sense	CATGAGCCCTGGTCTTCTCT	
SatB2	antisense	AACTGCTCTGGGAATGGGTG	
Shh	sense	CAGAGGGAACGAACGAGCCGA	193
Shh	antisense	CACCAGCAGCGAGGAAGCAAGGAT	


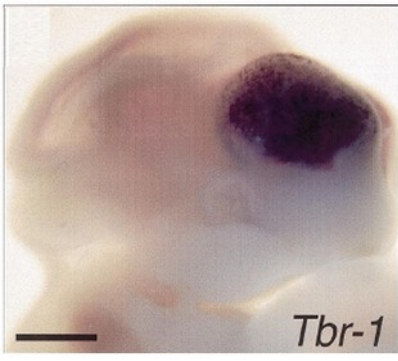

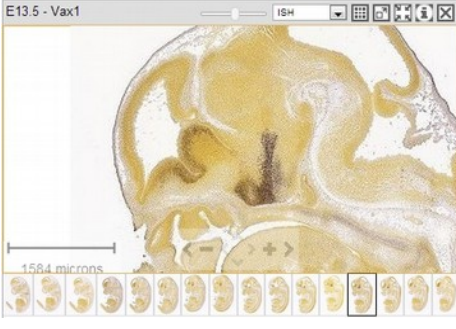


Six3	sense	TCAACAACCCCACCACCACCTACT	105
Six3	antisense	CACCTCTTTTATGCTTTCTGCCCCGC	
Six6	sense	CAAAAACCGCAGACAAAGAGA	
Six6	antisense	GTCGCTGGATGTGATGGAG	
Sox2	sense	ACTTTTGTCCGAGACCGAGA	122
Sox2	antisense	CTCCGGGAAGCGTGTACTTA	
T	sense	TACACACCACTGACGCACACGG	
T	antisense	GCAGCCCCCTTCATACATCGGAG	
Tbr1	sense	CGCCCTCCTCCATCAAATCCATCG	155
Tbr1	antisense	GCAGTTCCTTCGCAGTCCCGC	
Tbx3	sense	ACAAGCGGGGTACAGAGATG	
Tbx3	antisense	ACCATCCACCGAGAGTTGTG	
TGF- β 2	sense	GTTCAGGGTCTTCCGCTTG	
TGF- β 2	antisense	CCTCCGCTCTGGTTTTTCAC	
TGF- β 3	sense	GGGTTACTATGCCAACTTCTGCT	
TGF- β 3	antisense	CCTCTGGGTTCAGGGTGTT	
Vax1	sense	GAGAAATCATCCTGCCCAA	
Vax1	antisense	GTATTGGCAACGCTGGAAC	
WNT1	sense	ACAGCAACCACAGTCGTCAG	
WNT1	antisense	TCGTGGAGGAGGCTATGTT	
WNT3	sense	ATCTTTGGGCCTGTCTTGG	
WNT3	antisense	TGGCCCCTTATGATGTGAGT	
WNT4	sense	GCGTAGCCTTCTCACAGTCC	
WNT4	antisense	CACGCCAGCACGTCCTTAC	
WNT5a	sense	AGGAGTTCGTGGACGCTAGA	
WNT5a	antisense	AGGCTACATCTGCCAGGTTG	
WNT5b	sense	ACTGACGCCAACTCCTGGT	
WNT5b	antisense	ACTCTCTGATGCCCGTCTTG	
Wnt7b	sense	ATGCCCGTGAGATCAAAAAG	163
Wnt7b	antisense	CGGAACTTAGGTAGCGTGGT	
WNT8b	sense	CGTGTGCGTTCCTTAGTCACTT	
WNT8b	antisense	CAACGGTCCCAAGCAAAC	
WNT9a	sense	GGGACAACCTCAAGTACAGCA	
WNT9a	antisense	GGTTTCCACTCCAGCCTTTA	
Zfp521	sense	GAGCGAAGAGGAGTTTTTGG	
Zfp521	antisense	AGTTCCAAGGTGGAGGTCAC	
β -Actin	sense	AATCGTGCGTGACATCAAAG	177
β -Actin	antisense	AAGGAAGGCTGGAAAAGAGC	
β -Tubulin-III	sense	TTCTGGTGGACTTGGAACCT	186
β -Tubulin-III	antisense	ACTCTTCCGCACGACATCT	

Markers for the study of brain patterning

Table 2: Most important genes used as markers for the study of brain patterning. All images were found on-line on Allen Developing Mouse Brain Atlas (developingmouse.brain-map.org) and/or on Edinburgh Mouse Atlas Project (emouseatlas.org/emap), as indicated.

		
<p>Ctip2 Cortex E stage 10.5 EMAP Edinburgh Mouse Atlas</p>	<p>Ctip2 Cortex (medium-late generated neurons) E stage 13.5 Allen Mouse Atlas</p>	<p>Emx2 Forebrain (Cortex) E stage 10.5 EMAP Edinburgh Mouse Atlas</p>
		
<p>En1 Midbrain - Hindbrain E stage 9.5 EMAP Edinburgh Mouse Atlas</p>	<p>En1 Midbrain - Hindbrain E stage 13.5 Allen Mouse Atlas</p>	<p>FoxG1 Forebrain E stage 13.5 Allen Mouse Atlas</p>
		
<p>Gad65 Gabaergic neurons E stage 13.5 Allen Mouse Atlas</p>	<p>Gata4 Extraembryonic Endo-Mesoderm E stage 7.5 EMAP Edinburgh Mouse Atlas</p>	<p>HoxB4 Hindbrain – Spinal cord E stage 10.5 EMAP Edinburgh Mouse Atlas</p>

		
<p>Otx2 Midbrain – Retina E stage 11.5 EMAP Edinburgh Mouse Atlas</p>	<p>Otx2 Midbrain – Retina E stage 13.5 Allen Mouse Atlas</p>	<p>Pax6 Neural tissue (Anterior, Dorsal and Retina) E stage 10.5 EMAP Edinburgh Mouse Atlas</p>
		
<p>Pax6 Neural tissue (Cortex and Retina) E stage 11.5 Allen Mouse Atlas</p>	<p>Rax Forebrain E stage 8.7 EMAP Edinburgh Mouse Atlas</p>	<p>Rax Diencephalon (Ventral + Retina) E stage 10.5 EMAP Edinburgh Mouse Atlas</p>
		
<p>SatB2 Cortex (late generated neurons) E stage 15.5 Allen Mouse Atlas</p>	<p>Shh Ventral nervous tissue E stage 9.5 EMAP Edinburgh Mouse Atlas</p>	<p>Six3 Forebrain (Retina) E stage 9.5 EMAP Edinburgh Mouse Atlas</p>

	 <p style="text-align: right;"><i>Tbr-1</i></p>	
<p>Six6 Retina E stage 10.5 EMAP Edinburgh Mouse Atlas</p>	<p>Tbr1 Cortex E stage 10.5 EMAP Edinburgh Mouse Atlas</p>	<p>Tbr1 Cortex (early generated neurons) E stage 13.5 Allen Mouse Atlas</p>
		
<p>Vax1 Forebrain (Ventral) E stage 13.5 Allen Mouse Atlas</p>	<p>vGlut2 Glutamatergic neurons E stage 15.5 Allen Mouse Atlas</p>	<p>Wnt7b Forebrain (Cortex) E stage 9.5 EMAP Edinburgh Mouse Atlas</p>



Results and Discussion

1– A Novel Neural Induction Protocol

Chemically Defined Minimal Medium (CDMM)

Allows Efficient Neurogenesis of Embryonic Stem (ES) Cells.

In order to measure the endogenous production of morphogens during differentiation, and to investigate the default positional identity of neurons generated from ES cells, we established a culture method that allows neurogenesis minimizing the influence of exogenous signals.

This method consists of a three-step procedure of culture in a chemically defined minimal medium (CDMM; see Materials and Methods; *Figure 1.1*) devoid of serum or morphogens but allowing cell survival by insulin.

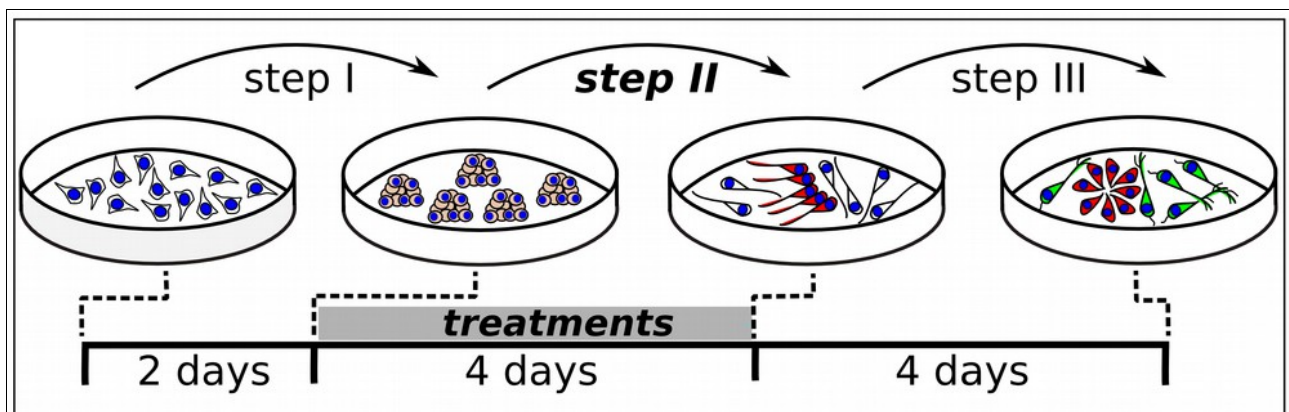


Figure 1.1: Three-step protocol of ES cell neuronal differentiation. ES cell differentiation protocol outline.

Undifferentiated mouse embryonic stem cells are the starting point of the protocol. The condition of pluripotency can be tested by immunostaining of the crucial stem cell markers, Oct4 and Nanog (**Figure 1.2**).

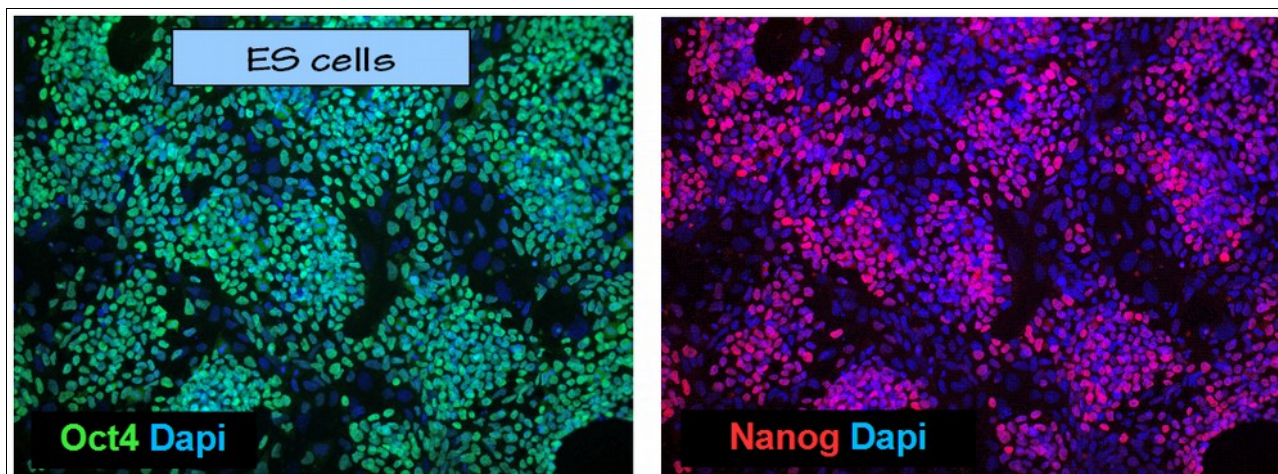


Figure 1.2: *Oct4 (green) and Nanog (red) immunocytochemical detection of undifferentiated ES cells cultured in serum- and LIF-containing medium. In our culture, the vast majority of cells were positive to Oct4 staining; Nanog showed a strong signal only in a subset of Oct4-positive cells. This heterogeneity of serum-cultured ES cells is consistent with Austin Smith's Lab observation (Silva et al., 2008).*

Upon LIF and serum withdrawal, dissociated ES cells were initially grown as aggregates (**Figure 1.3**) in CDMM for 2 days. This step (Step-I), which minimizes cell death, follows a procedure adapted from previously described methods (Bibel et al., 2007; Lee et al., 2000; Watanabe et al., 2005). As many protocols use serum-containing medium (SCM) during ES cell aggregation, we assayed also this condition in the preliminary set-up of our protocol. As additional control, we used undifferentiated ES cells cultured in LIF+serum (ES cell medium).

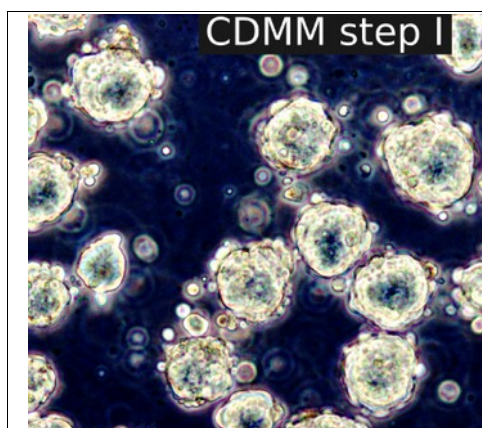
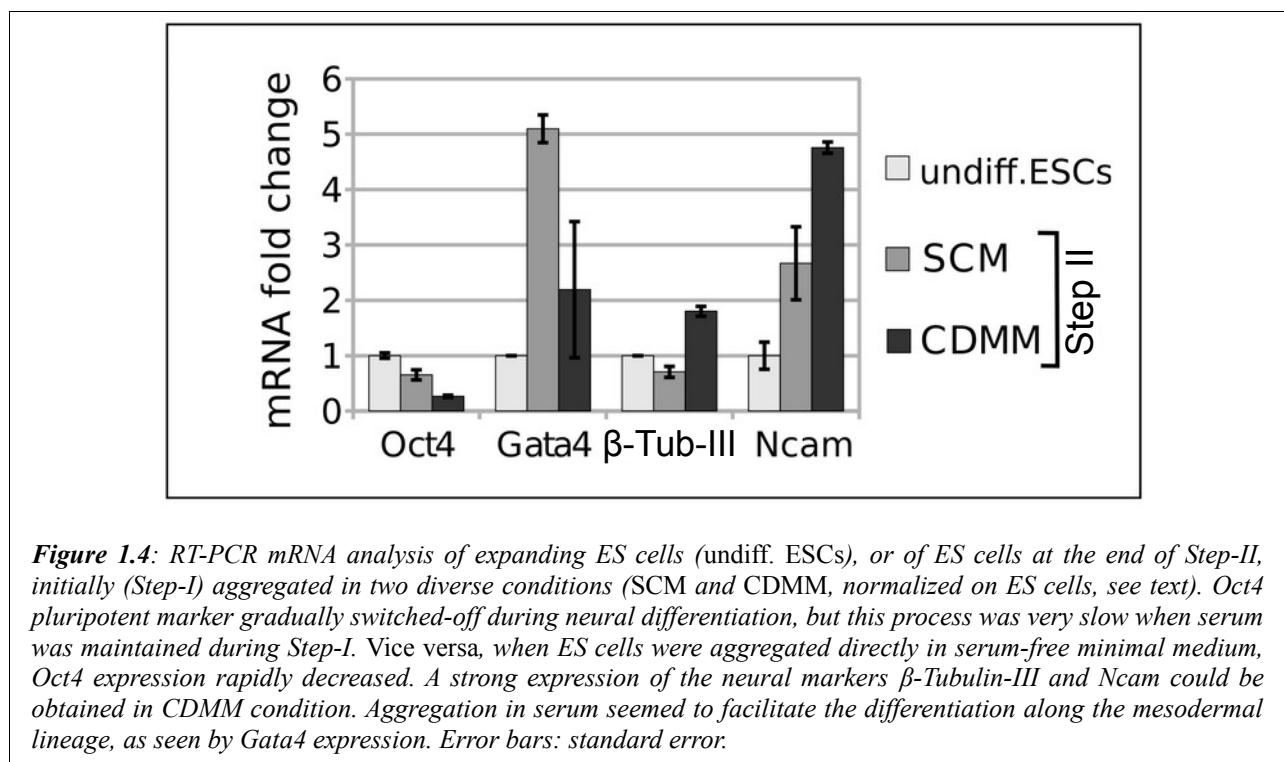


Figure 1.3: *ES cell aggregates at Step-I. Undifferentiated embryonic stem cells are trypsinized and replated in suspension on an agar-coated surface, where they form embryoid body-like aggregates. Step-I reaggregation can be performed in serum-containing medium (SCM) or directly in chemically defined minimal medium (CDMM); this difference will influence subsequent neural induction efficiency, see below in the text.*

ES cell aggregates were subsequently dissociated and cultured in adhesion for 4 days on Poly-oronhitine/Laminin-coated wells in CDMM (Step-II). All additional treatments (e.g. Noggin, chemical drugs, etc), when applied, were performed during this step (**Figure 1.1**), unless specified. During Step-II, ES cells turned off the expression of the stem cell marker Oct4 (Niwa et al., 2000) and activated the expression of the pan-neuronal markers β -Tubulin-III and Ncam, as seen by RT-PCR (**Figure 1.4**). This activation was higher in ES cells aggregated in CDMM than in ES cells aggregated in SCM, as the latter still expressed high levels of Oct4 and activated the mesodermal marker GATA4 (**Figure 1.4**).



At the end of Step-II, immunostaining showed much higher expression of the neural progenitor cell marker Musashi-1 (Okano et al., 2005) and robust down-regulation of Oct4 in ES cells cultured in CDMM (**Figure 1.5A**) compared to ES cells cultured in SCM (**Figure 1.5B**). This was consistent with RT-PCR data.

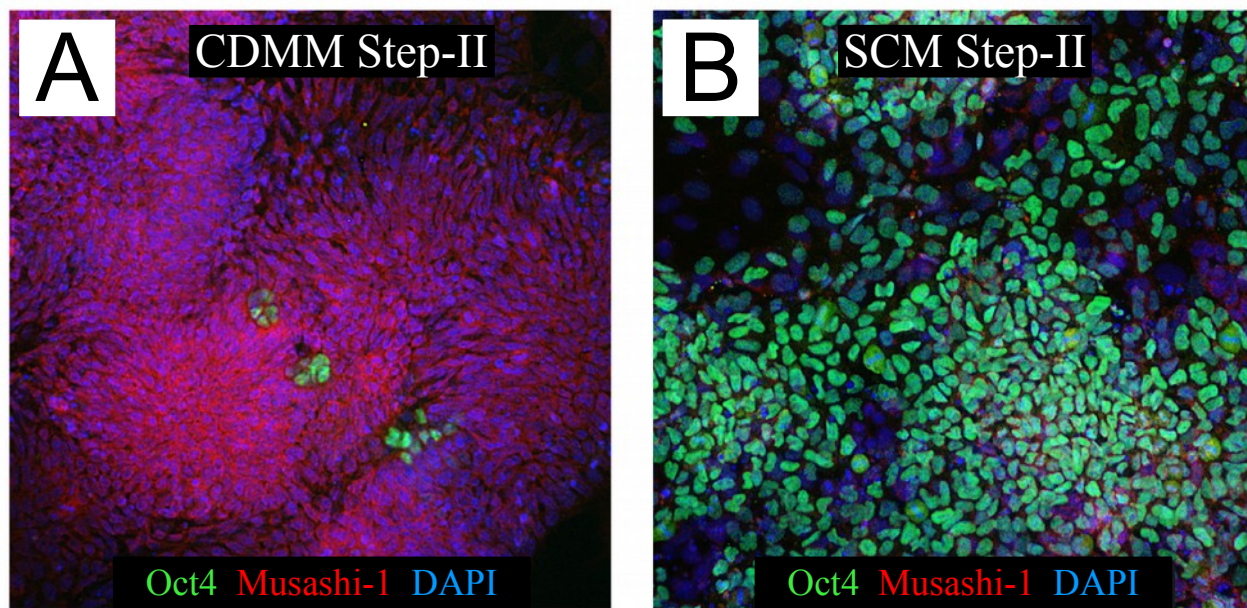


Figure 1.5: Oct4 (green) and Musashi-1 (red) immunocytochemistry of ES cells at the end of Step-II. The figures clearly show the difference of the neuralization efficiency after CDMM (A) or SCM (B) aggregation at Step-I. The direct reaggregation of mouse embryonic stem cells in a minimal medium allows fast and efficient neural conversion.

Whereas ES cells aggregated in CDMM started expressing β -Tubulin-III at Step-II, ES cells aggregated in SCM failed to show β -Tubulin-III labeling (**Figure 1.6A,B**). Similar results were obtained when analyzing ES cell aggregates cultured for 5 days (**Figure 1.6C,D**). Our observations indicate that aggregation (Step-I) in the absence of serum facilitates loss of stem cell pluripotency and induces rapid neural differentiation (as evaluated at the end of Step-II).

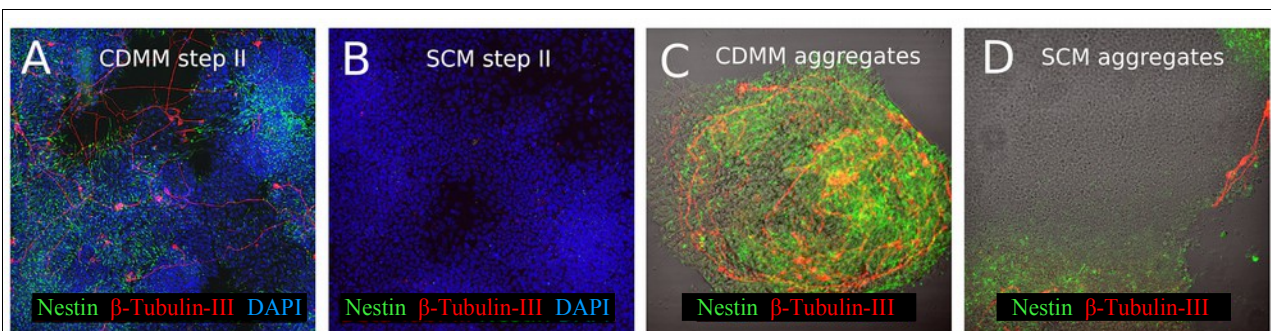


Figure 1.6: Nestin (green) and β -Tubulin-III (red) immunocytochemistry of ES cells during neural conversion. A-D show β -Tubulin-III and Nestin immunocytochemistry identifying neurons and neural progenitor cells, respectively, in ES cells aggregated (Step-I) in CDMM (A,C) or SCM (B,D) and then differentiated in CDMM. Cells were analyzed at the end of Step-II (A,B) or after 5 days of culture as aggregates (C,D).

After a second dissociation, cells were cultured for 4 days in CDMM. This additional step (Step-III) allowed cells to undergo terminal differentiation. Notably, the presence of serum during Step-I profoundly affected the fate of cells produced at the end of Step-III, as the ratio of neural progenitor cells immunostained by Nestin antibody was lower in cells aggregated in SCM ($8\pm 4.8\%$) compared to cells aggregated in CDMM ($44.3\pm 8.7\%$; **Figure 1.7A-C**).

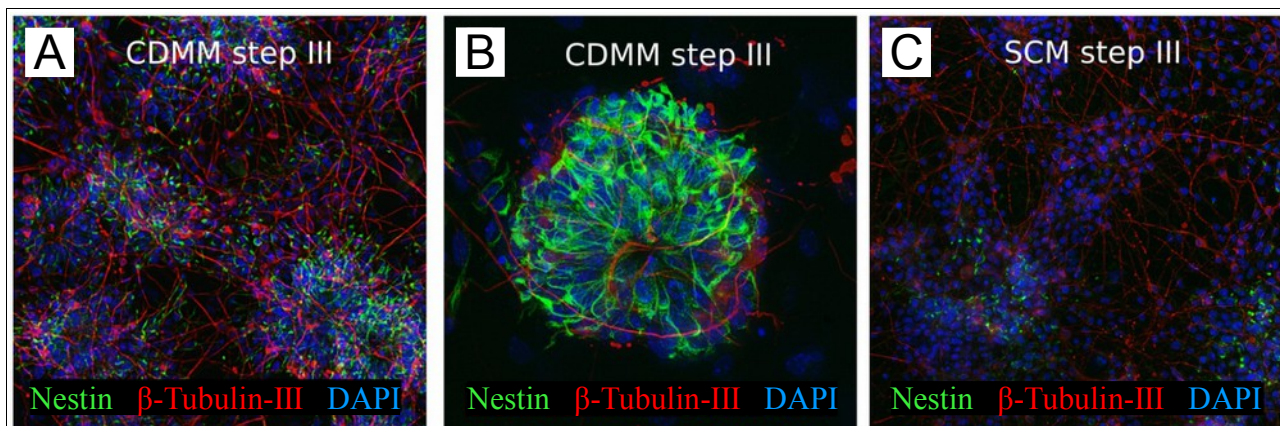


Figure 1.7: Nestin (green) and β -Tubulin-III (red) immunocyto detection of ES cells at the end of Step-III. Nestin-positive neural progenitors formed rosette-like structures at the end of Step-III, which are typical of neural progenitors *in vitro*. Again, the neural differentiation efficiency seemed strongly improved by early serum removal.

Consistently, mRNA expression of Nestin and of pan-neuronal markers Ncam and β -Tubulin-III, at the end of Step-III, was significantly lower in cells that were aggregated in SCM than in cells that were aggregated in CDMM (**Figure 1.8**).

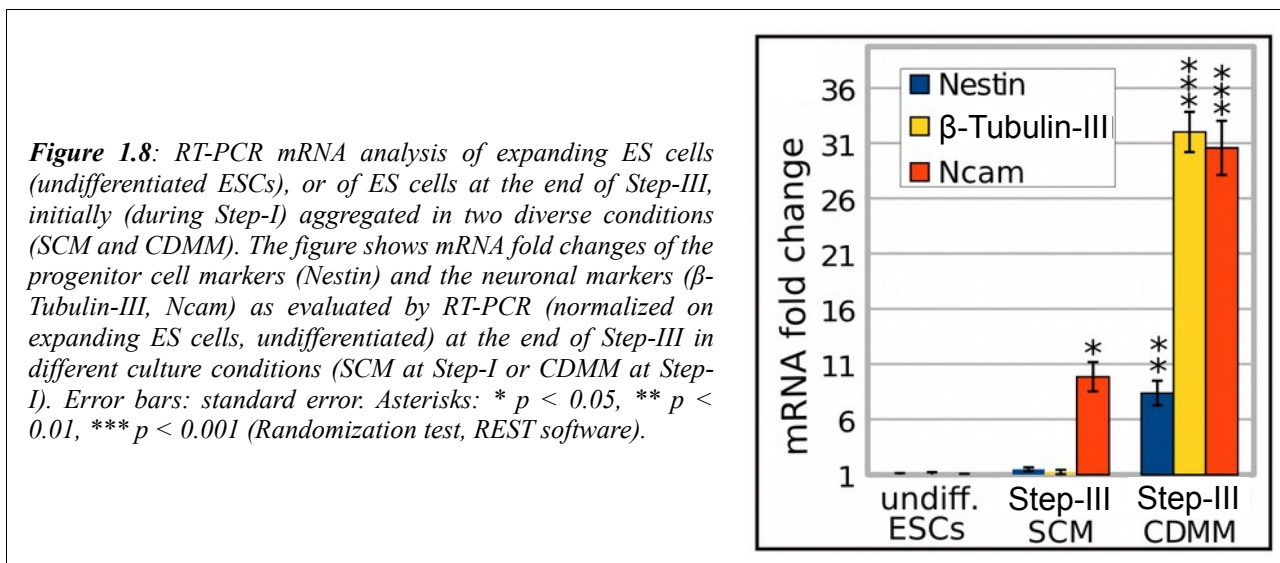


Figure 1.8: RT-PCR mRNA analysis of expanding ES cells (undifferentiated ESCs), or of ES cells at the end of Step-III, initially (during Step-I) aggregated in two diverse conditions (SCM and CDMM). The figure shows mRNA fold changes of the progenitor cell markers (Nestin) and the neuronal markers (β -Tubulin-III, Ncam) as evaluated by RT-PCR (normalized on expanding ES cells, undifferentiated) at the end of Step-III in different culture conditions (SCM at Step-I or CDMM at Step-I). Error bars: standard error. Asterisks: * $p < 0.05$, ** $p < 0.01$, *** $p < 0.001$ (Randomization test, REST software).

Moreover, cells cultured in CDMM formed rosette-like structures at the end of Step-III, which are typical of neural progenitors *in vitro* (Zhang et al., 2001; **Figure 1.7B**), and generated high proportions of neuronal cells immunostained by anti-acetylated-Tubulin (Ntub, **Figure 1.9A**) and β -Tubulin-III antibodies (**Figure 1.9B**).

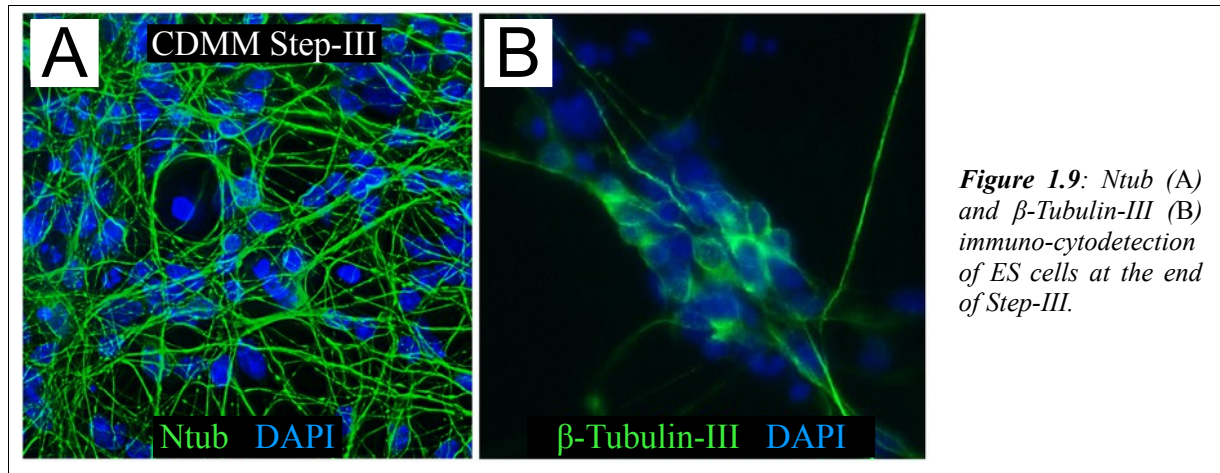


Figure 1.9: Ntub (A) and β -Tubulin-III (B) immuno-cytodetection of ES cells at the end of Step-III.

We further characterized the nature of the differentiated ES cells by immunocytochemical detection. Neuronal morphology was heterogeneous, as we found multipolar cells, pyramidal-like cells, bipolar and unipolar cells (**Figure 1.10**).

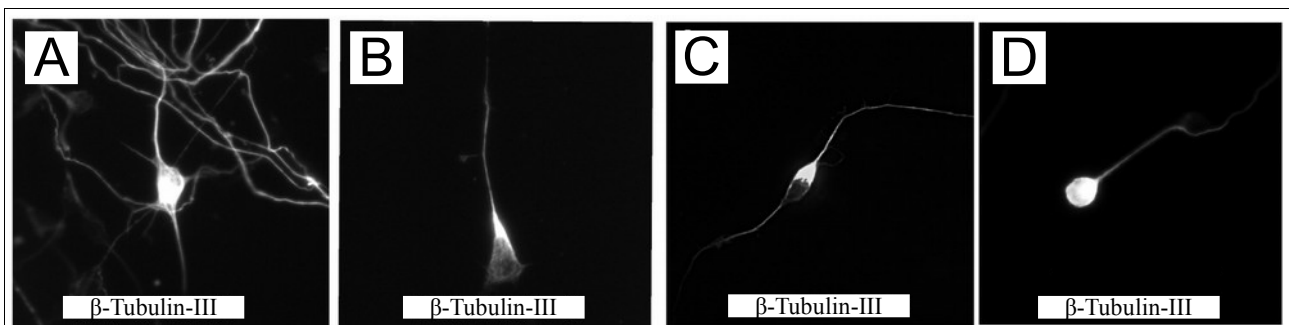
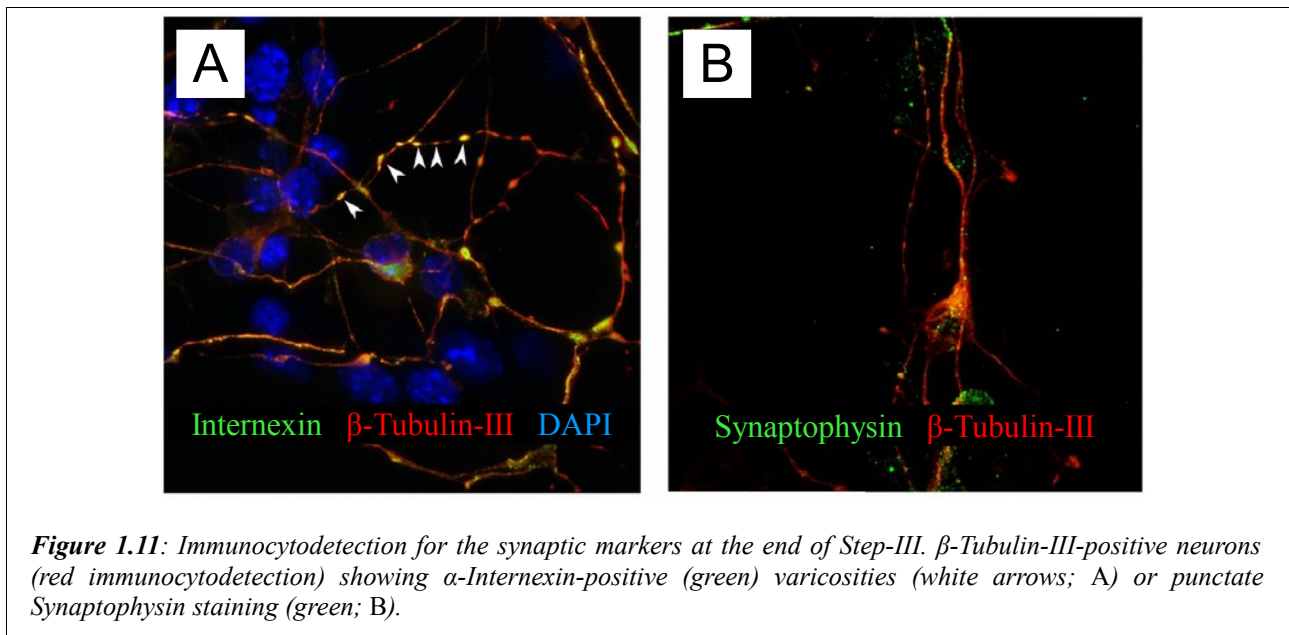


Figure 1.10: Immunocytochemical detection for β -Tubulin-III-positive neurons at the end of Step-III. A-D, Examples of β -Tubulin-III marked multipolar (A), pyramidal-like (B), bipolar (C) and unipolar (D) neurons, respectively.

ES cell-generated neurons showed processes with varicosities positive to the neuronal intermediate filament α -Internexin that are typical of neurons forming synapses (**Figure 1.11A**). Moreover, ES cell-derived neurons showed a punctate staining of the synaptic marker Synaptophysin (**Figure 1.11B**).

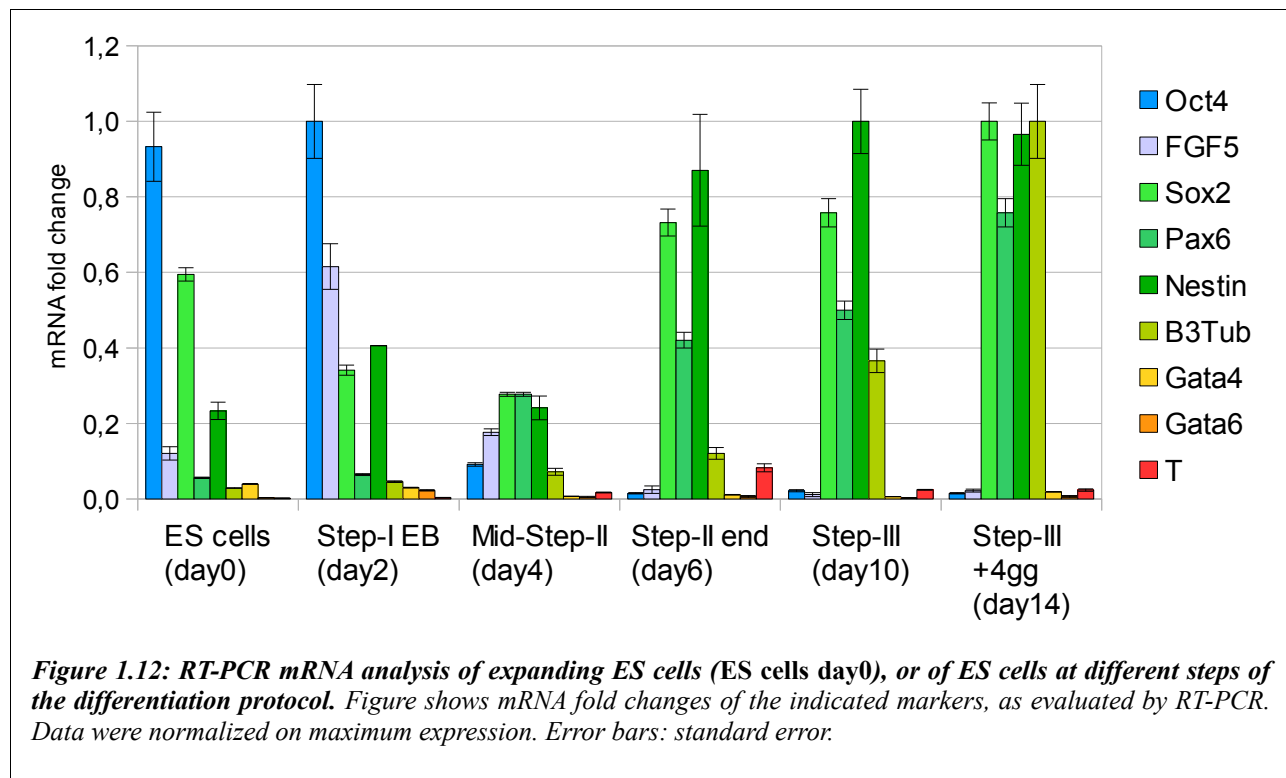


We failed to detect GFAP-positive cells by immunostaining; GFAP mRNA levels were very low compared to the levels of P0 embryonic cortex, as evaluated by RT-PCR (not shown). This is consistent with an early differentiation state of the cells, as gliogenesis is the latest step in ES cell neural differentiation protocols (Gaspard et al., 2008).

To better outline the neuralization process in our protocol, we decided to evaluate by RT-PCR the expression of the pluripotency markers Oct4 and Sox2, the epiblast marker FGF5, the neural progenitor markers Nestin and Pax6, and the marker of differentiating/differentiated neurons β -Tubulin-III, at different time points of the protocol as indicated in **Figure 1.12**. Additionally, we evaluated the expression of the mesoderm markers T (Brachiury) and Gata4, to test for possible presence of mesodermal cells in our neural differentiation protocol.

Oct4 was strongly down-regulated between Step-I and Step-II, as differentiation started. Sox2, which is considered both an embryonic stem cell pluripotency marker and a neural progenitor marker, behaved consistently with this definition, being strongly expressed by undifferentiated ES cells and by neural progenitors. Nestin and Pax6 expression became strong during Step-II, while β -Tubulin-III expression increased at Step-III. The expression of the meso/endodermal cell markers (Gata4, Gata6 and T) was almost undetectable, suggesting again that the vast majority of ES cells in our protocol adopted a neural fate, without mesodermal or endodermal “contamination” inside our neural differentiation system.

On the contrary, Gata4 was strongly up-regulated by initial (Step-I) ES cell aggregation in serum-containing medium (SCM), as showed at the beginning of this section (see **Figure 1.4**).



The results of RT-PCR analysis showed that the neural progenitor marker Nestin was strongly expressed in our protocol especially at the end of Step-II. Immunodetection of the stem cell or the neuronal cell markers during Step-II confirmed RT-PCR data. Nestin labeling appeared at the second day of Step-II (mid-Step-II; **Figure 1.13A**) and reached very high levels at the end of this step (end of the fourth day of Step-II; **Figure 1.13B**). This indicated a strong neuralization process occurring during the second half of Step-II and leading to a cell culture enriched of neural progenitors.

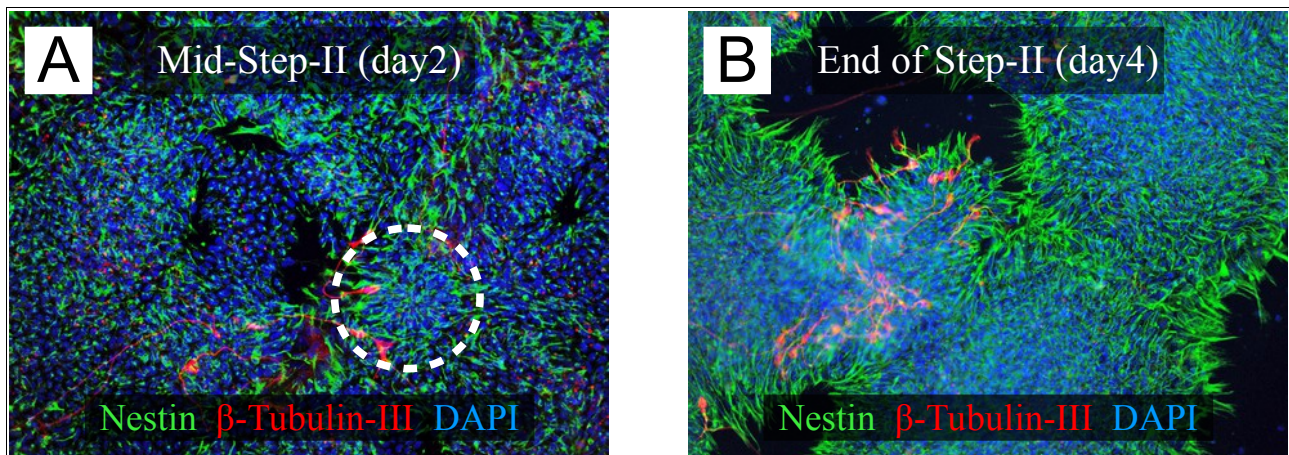


Figure 1.13: Nestin (green) and β -Tubulin-III (red) immunocyto detection of ES cells at mid-Step-II (A) and at the end of Step-II (B). Neural progenitors can be efficiently visualized by strong Nestin staining (green). Neural rosettes (encircled by white dashed lines in **Figure A**) were formed by polarized Nestin-positive progenitor cells and appeared at mid-Step-II (at the end of Step-II day2; A) and dramatically increased in number during the second half of this step (B).

To confirm the appearance of neural progenitors during Step-II in our protocol, we took advantage of a Sox1-GFP knock-in ES cell line (46C, Ying et al., 2003), analyzing GFP expression by flow cytometry (**Figure 1.14**). The analysis of differentiating 46C ES line at different time points showed how Sox1-positive neural progenitors appear at mid-Step-II (35.3% of total cells) and peak at the end of Step-II (86.8%).

These data prompted us to always focus on Step-II for any treatment designed to study early patterning of neuronal progenitors. For this reason, as already stated before, all additional treatments (e.g. Noggin, Activin and chemical drugs), when applied, were performed starting from the second day of Step-II.

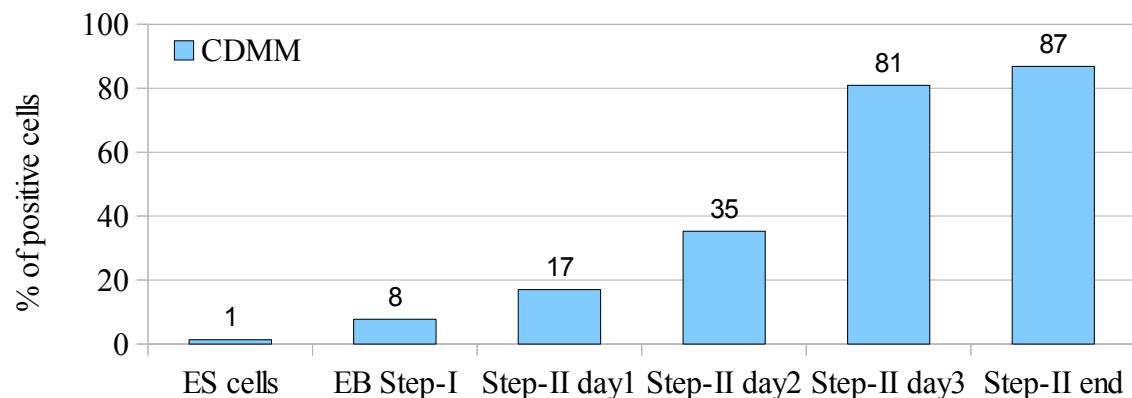


Figure 1.14: Sox1-GFP expression analysis by flow cytometry during neural differentiation. Neural progenitor percentage can be quantified using a ES cell line where the GFP coding region is inserted near the promoter of the neural marker Sox1 (ES line 46C, kindly provided by Austin Smith). At the end of Step-II, the vast majority (up to 90%) of cells is expressing GFP under the control of Sox1 promoter.

We concluded that a short exposure to serum in the first days of differentiation cultures (Step-I) inhibits the acquisition of a neuronal fate and that ES cells cultured in the absence of any added morphogen efficiently differentiate into neuronal cells, which is consistent with previous observations (Gaspard et al., 2008; Smukler et al., 2006).

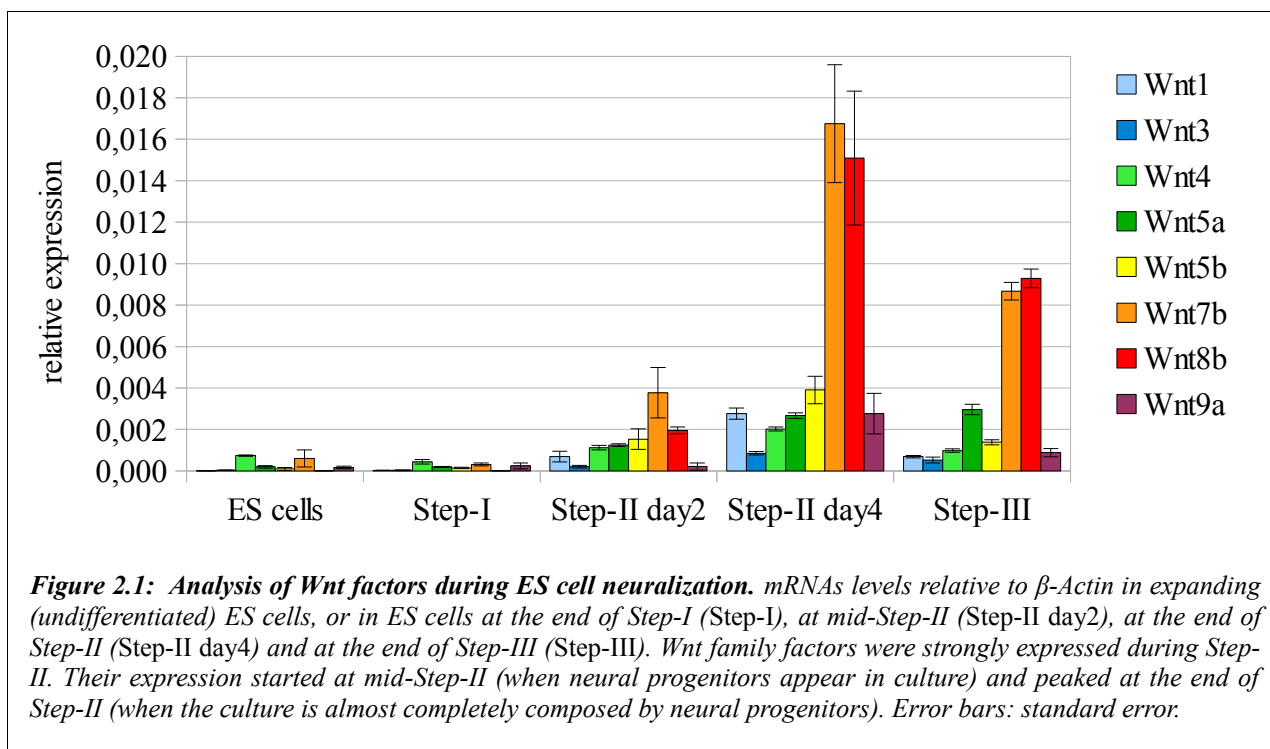
2– Endogenous Morphogen Expression

Mouse ES Cells Express Wnt, BMP and FGF Morphogens During *in vitro* Neural Differentiation.

Although our method of ES cell neuralization minimizes the influence of exogenous signals, the absence of morphogens inside the culture medium do not ensure a completely morphogen-free system. We reasoned that ES cells could express and produce morphogens such as Wnts, BMPs, FGFs and Activin/Nodal during neural differentiation *in vitro*. These molecules could actively affect ES cell neuralization and positional identity.

We investigated the production of morphogen by RT-PCR analysis at different time points in our protocol.

Wnt family factors showing high levels of expression are showed in **Figure 2.1**. Members of the Wnt family were expressed starting from the second day of Step-II, and Wnts expression peaked at the end of Step-II. Notably, this was clearly correlated with the appearance of neural progenitors inside the culture: As previously showed by immunocyto detection, by RT-PCR and by cell sorting, Nestin- and Sox1-positive neural progenitors appeared at mid-Step-II (see Results, **Figures 1.6-1.8; 1.12-1.14**). Wnt7b and Wnt8b were the most expressed Wnt morphogens in our culture system.



To identify the cell type (mitotic vs post-mitotic) responsible for the expression and production of morphogens inside the culture, we exploited the pyrimidine analog Aracytin (Arabinofuranosyl Cytidine, or AraC; 5 μ M) to kill all mitotically active cells (Grant et al., 1998) and obtain neuron enriched-, neural progenitor-free cultures. Cells were differentiated until Step-III+4 days, then cultures were treated for two days with AraC. The effect of AraC treatment on cell populations was analyzed by immunocytochemistry and by RT-PCR. Compared to control cells, AraC treated cell cultures showed a strong reduction of Nestin-positive or Musashi1-positive neural rosettes (**Figure 2.2** and data not shown). Nestin staining was detected only on few surviving isolated neural progenitor cells. After AraC treatment, the cellular population was almost completely composed by clusters of β -Tubulin-III-positive neurons (**Figure 2.2B**).

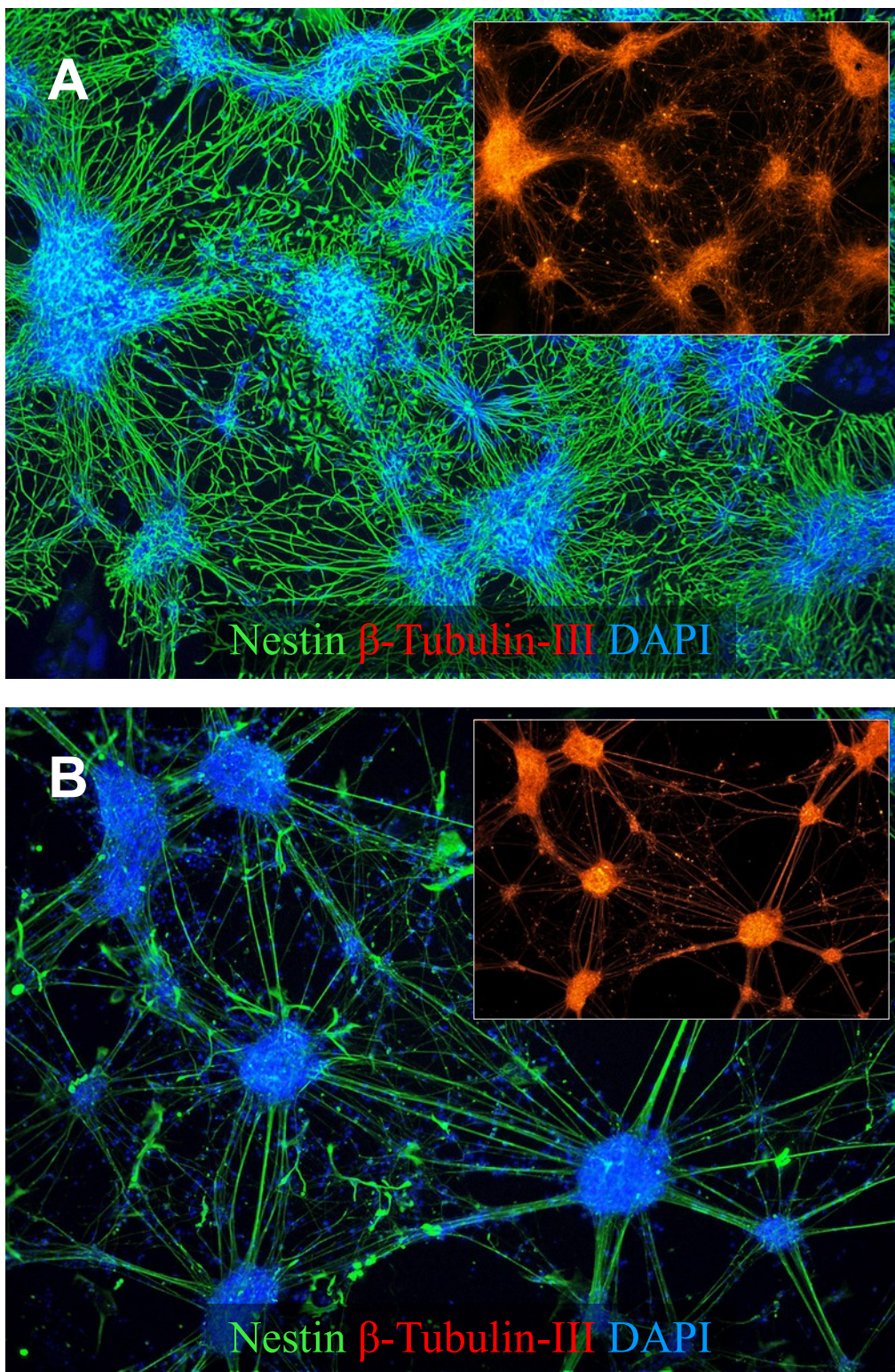
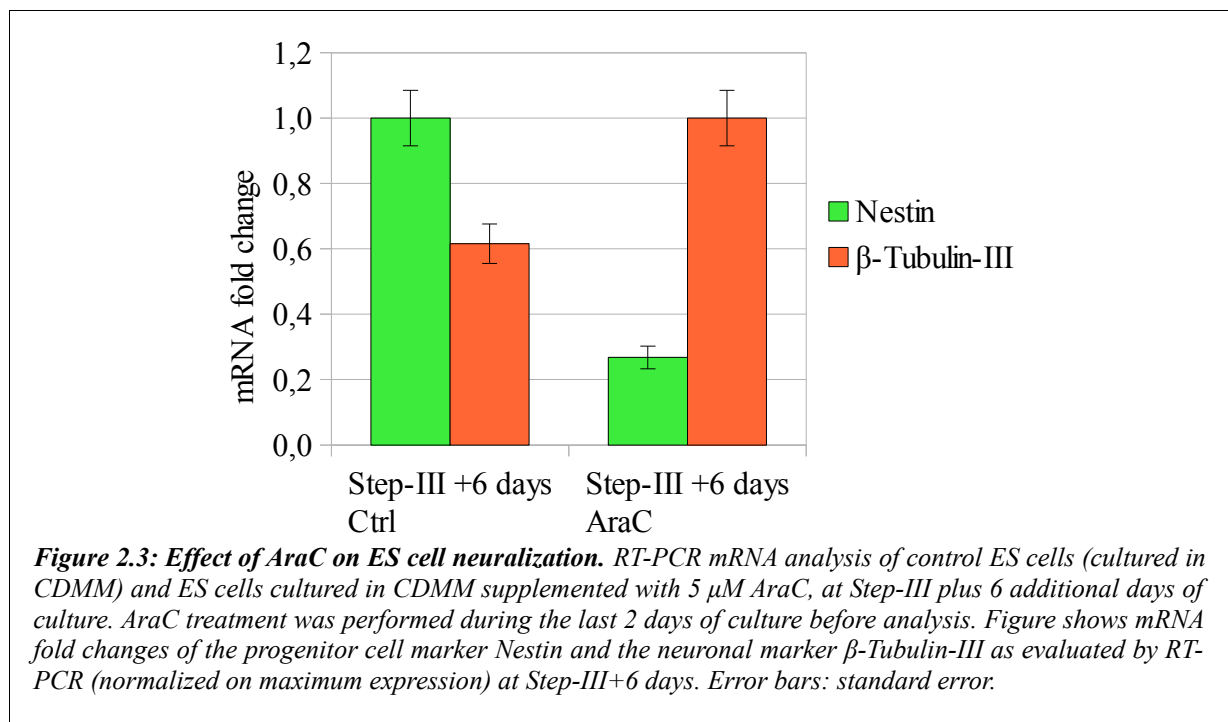
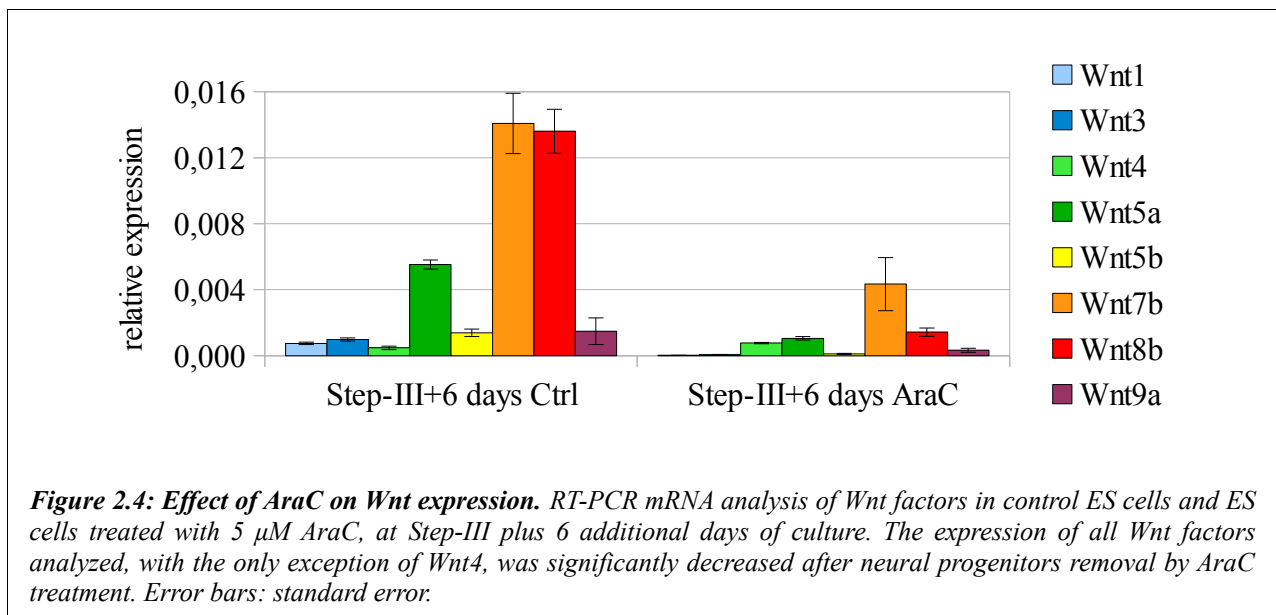


Figure 2.2: Effect of AraC on ES cell neuralization. Immunocytochemical detection shows Nestin (green) and β -Tubulin-III (red; insets) positive cells at Step-III+6 days. A) Control ES cells (cultured in CDMM) originated a mixed population of both Nestin-positive neural progenitors, often organized to form neural rosettes, and β -Tubulin-III-positive neurons. B) Cultures treated for 2 days with 5 μ M AraC were mainly made of β -Tubulin-III-positive post-mitotic cells and showed few Nestin-positive neural progenitors.

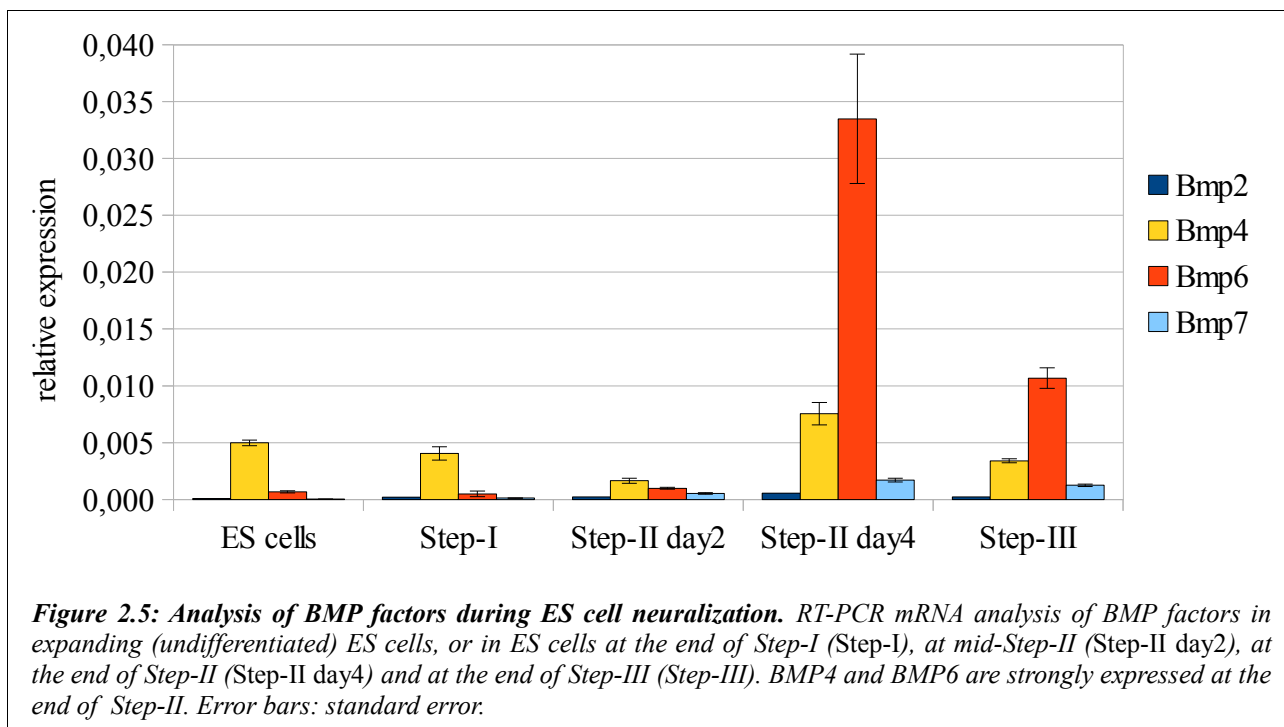
The effect of AraC treatment was confirmed by RT-PCR analysis: AraC-treated cells expressed high levels of β -Tubulin-III mRNA and showed a strong decrease of Nestin mRNA expression, compared to control CDMM-cultured cells (**Figure 2.3**). Data suggested that AraC treatment could efficiently eliminate Nestin-expressing cells and enrich the culture in β -Tubulin-III-expressing cells.



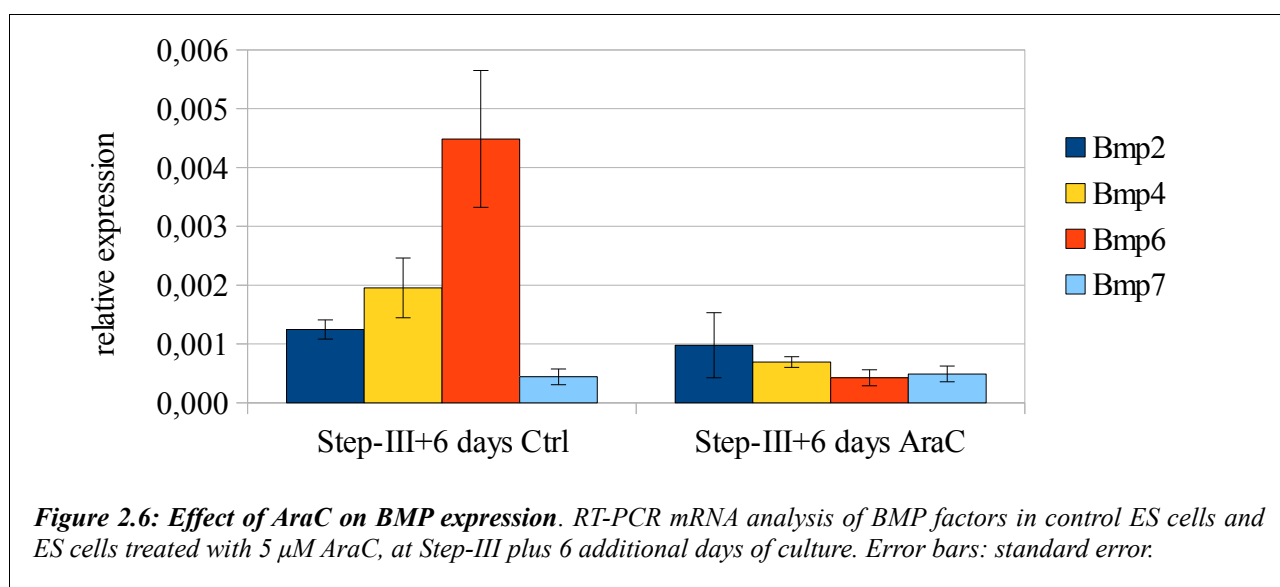
RT-PCR analysis allowed us to compare morphogen expression between control Step-III+6 days culture and AraC-treated (neural progenitor-depleted and neuron-enriched) culture. The expression of all Wnt factors analyzed, with the only exception of Wnt4, was significantly decreased after neural progenitors removal by AraC treatment (**Figure 2.4**). Thus, our results suggest that Wnt factors are expressed preferentially by Nestin-positive neural progenitors. These observations, together with the temporal coincidence of the appearance of Wnt mRNA expression and of Nestin-positive neural progenitors, strongly suggests that neural progenitors are the cell type responsible for Wnt morphogen expression inside our culture system.



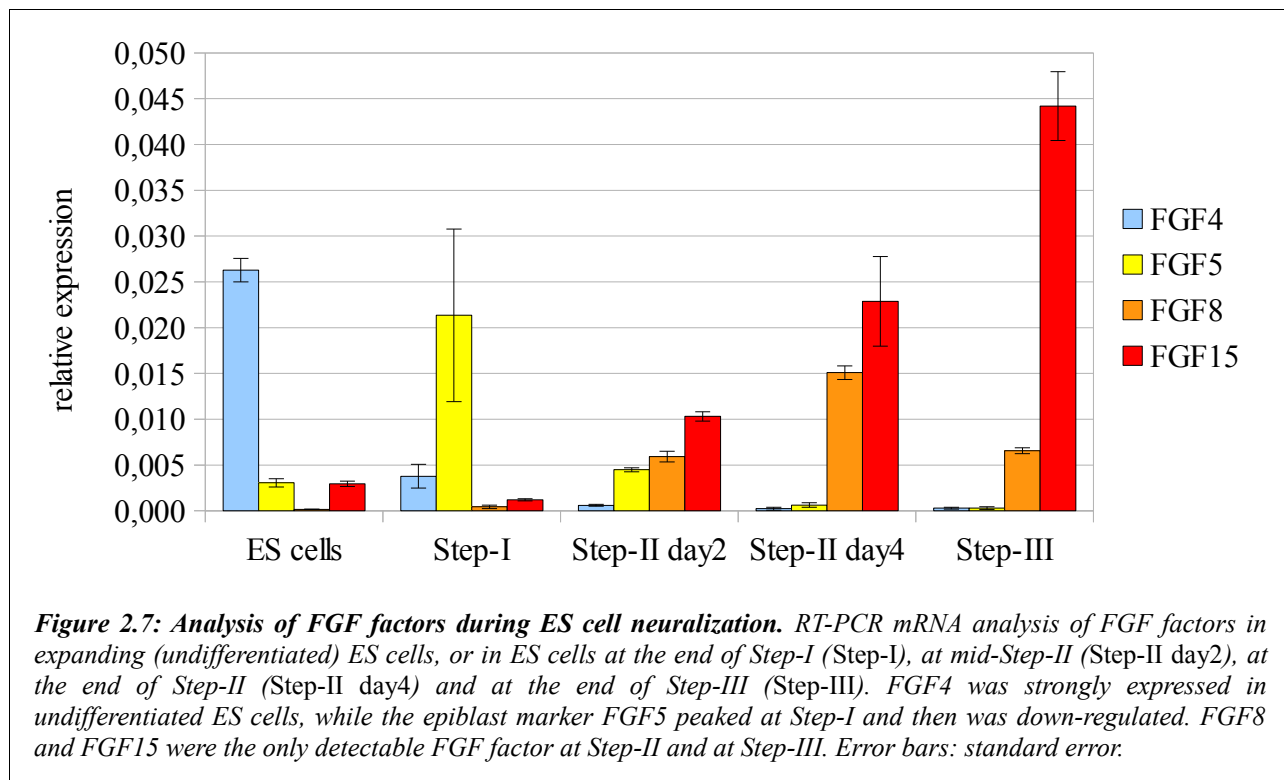
A similar analysis was performed to investigate the expression of endogenous BMP factors. ES cells showed detectable expression levels of BMP2 and BMP7, and very high expression levels of BMP4 and BMP6 (**Figure 2.5**). Other BMP factors were expressed at very low levels or were not expressed at all (data not shown). BMP4 expression was high in undifferentiated ES cells, consistently with previous findings (Silva et al., 2008), and its expression peaked again during Step-II. BMP2, BMP6 and BMP7 showed high levels of expression at Step-II and at Step-III.



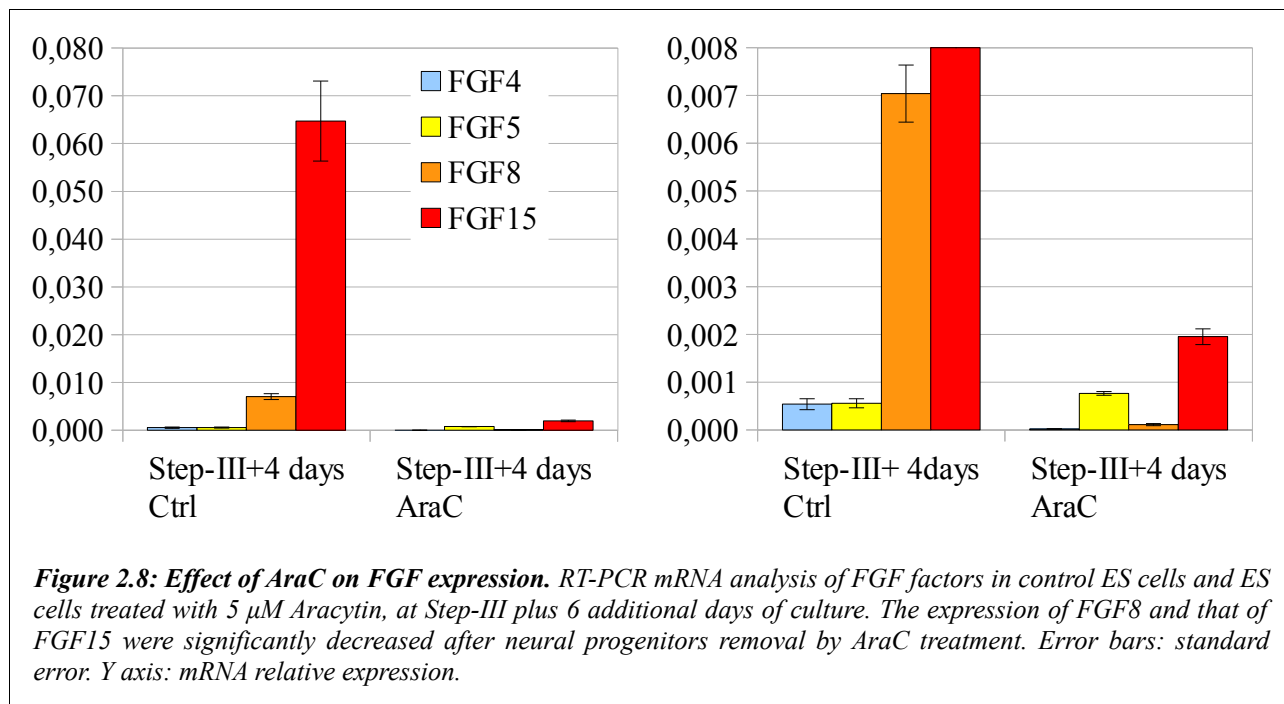
Again, AraC treatment allowed us to test if endogenous BMP morphogens were produced mainly by neural progenitors or by differentiated neurons. RT-PCR analysis showed that the expression of BMP4 and BMP6 was significantly decreased after neural progenitors removal by AraC treatment. This suggested that neural progenitors were the major responsible for the expression and production of BMP4 and BMP6. On the contrary, BMP2 and BMP7 appeared to be expressed at similar levels by both neural progenitors and neurons (**Figure 2.6**).



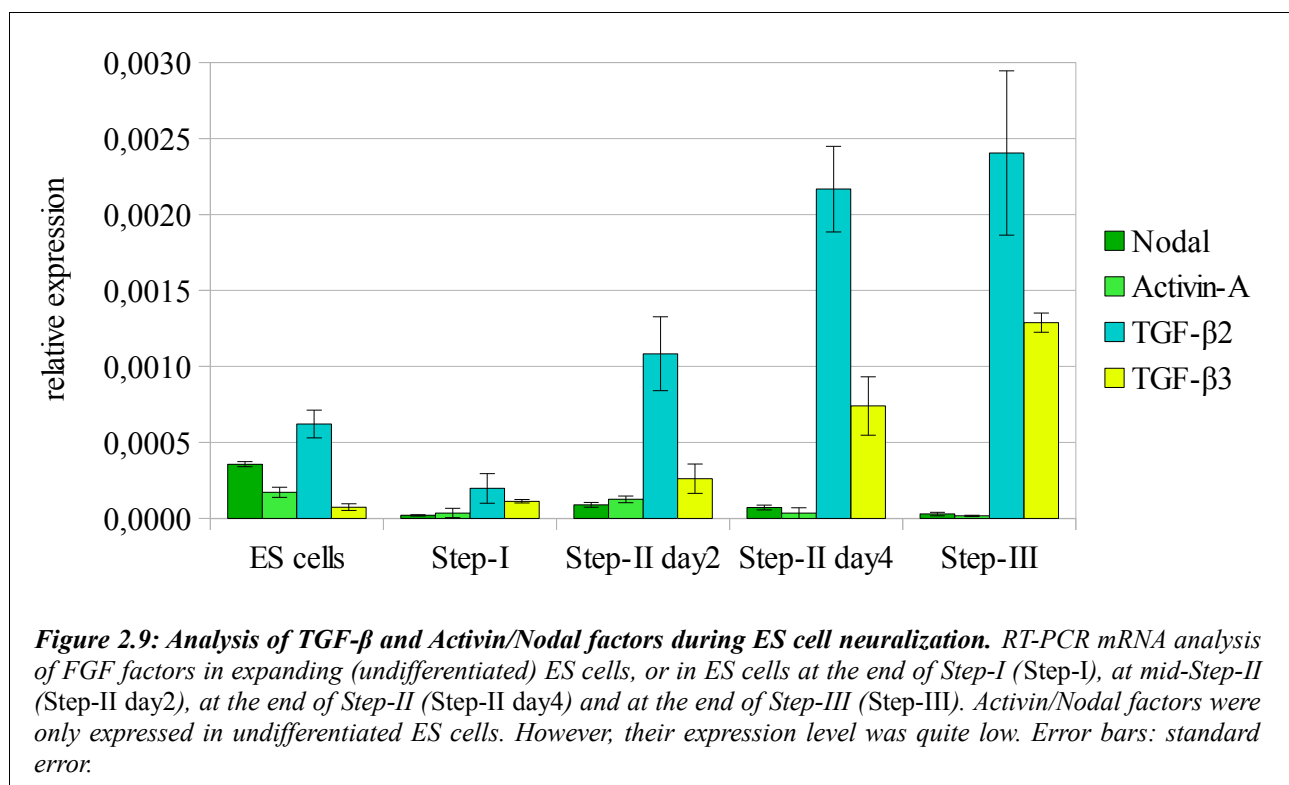
FGF factors were expressed at different time points in our neuronal differentiation culture (**Figure 2.7**). FGF4 expression was higher in undifferentiated ES cells, consistently with its role in ES cells self-renewal and lineage commitment (Silva et al., 2008). FGF5 appeared at Step-I, during embryoid bodies formation. This is not surprising, as FGF5 is considered a *bona fide* marker of the embryonic epiblast, an early tissue type derived from the inner cell mass in mammalian blastocyst. The only FGF morphogens expressed at detectable levels at Step-II and Step-III were FGF8 and FGF15, whose expression increased gradually during Step-II (ES cell neuralization). FGF8 expression then decreased, while FGF15 expression continued to increase.



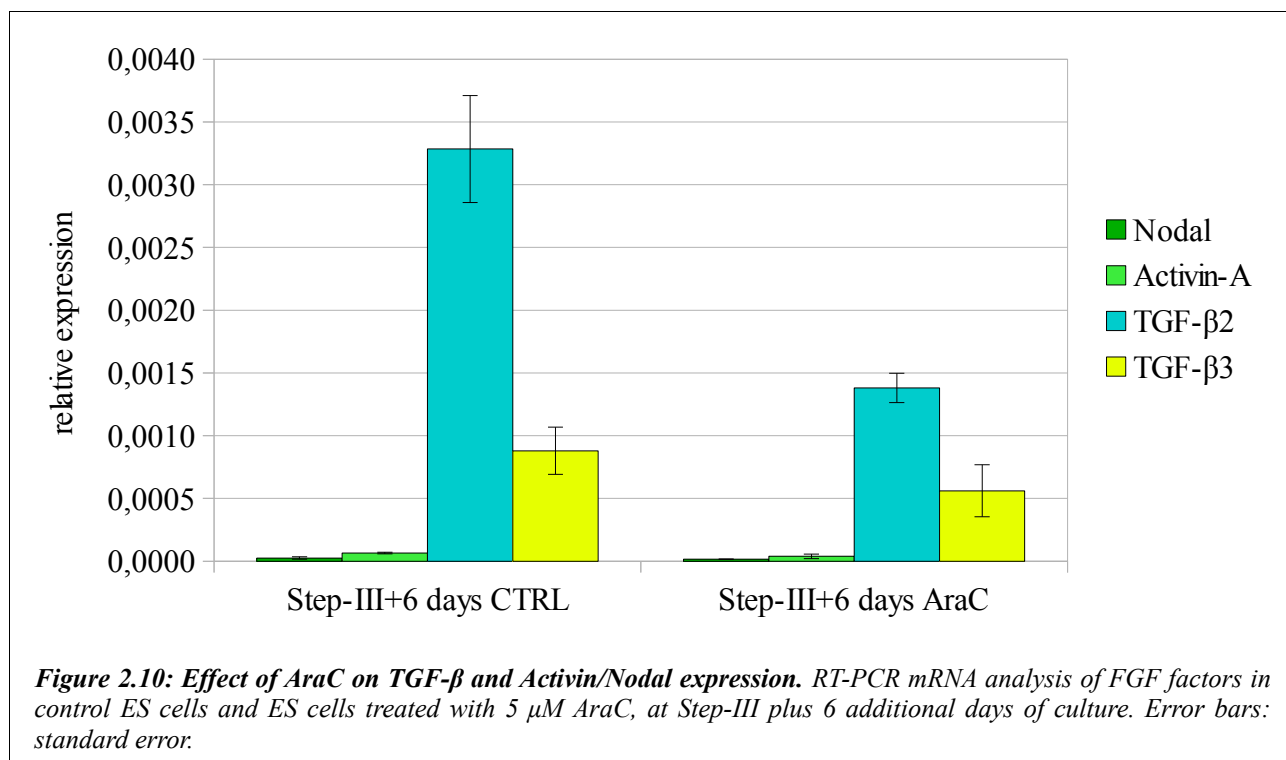
AraC treatment showed that FGF factors expressed during Step-II and Step-III (FGF8 and FGF15), were produced mainly by neural progenitors (**Figure 2.8**).



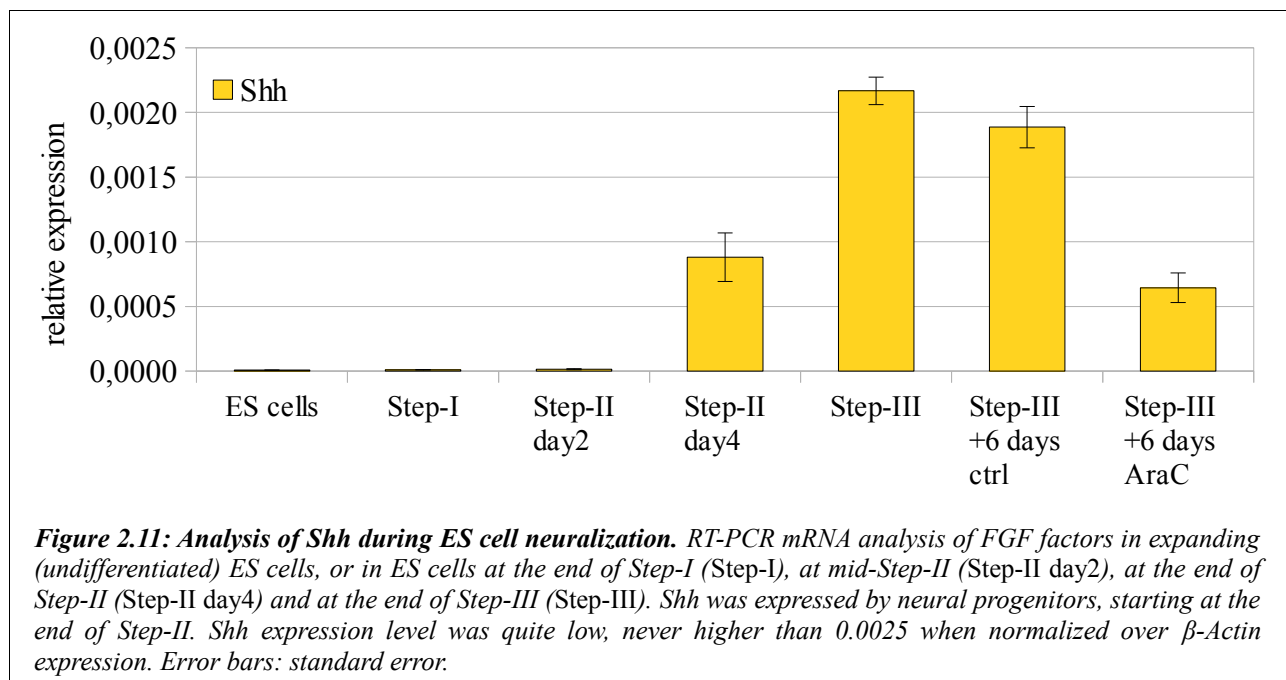
We then measured the expression of TGF- β and Activin/Nodal family of morphogens (**Figure 2.9**). Nodal and Activin-A were expressed, even if at very low levels, by undifferentiated ES cells, while TGF- β 2 and TGF- β 3 were expressed by differentiating cells. Notably, the expression level of these molecules is quite low. **Figure 2.9** shows normalization over β -Actin; Activin/Nodal and TGF- β mRNA level was never higher than 0.0025, which was from 10-fold to 20-fold lower when compared to BMP, Wnt and FGF expression levels showed before.



AraC treatment showed that TGF- β 2 and TGF- β 3 were produced mainly by neural progenitors (**Figure 2.10**). Activin/Nodal factors were not detectable at Step-III+6 days.



Finally, we concluded our analysis by measuring the expression of Shh, which was expressed, even if at very low levels, by differentiating ES cells (**Figure 2.11**). Neural progenitors removal by AraC treatment showed that Shh was produced mainly by neural progenitors (**Figure 2.11**).



Taken all together, these data suggest that mouse ES cells express different morphogens during neural differentiation *in vitro*, especially BMPs, Wnts and FGFs. Thus, the concept of *chemically defined minimal medium* must be carefully addressed: Even when using a *morphogen-free* culture medium, differentiating cells could be expressing themselves high amounts of different active molecules. These morphogens could act in an autocrine or paracrine way, affecting ES cells differentiation and positional identity acquisition.

3– A BMP Story

Simple Neural Induction or Brain Patterning?

ES cells cultured in the absence of any added morphogen efficiently differentiate into neuronal cells (Results, Chapter 1). Even when differentiated in a chemically defined, *morphogen-free* culture medium, mouse ES cells expressed themselves different morphogens during neural differentiation *in vitro*, especially BMPs and Wnts. These morphogens could act in an autocrine or paracrine way, affecting ES cell differentiation and positional identity acquisition. We therefore asked whether endogenously produced BMP could affect ES cell neuralization and/or the regional identity of ES cell-generated neurons.

Effects of Noggin as a Neural Inducer in ES Cells Culture.

The ability of the BMP-antagonist Noggin to support neuronal differentiation of ES cells has been reported in different *in vitro* differentiation protocols (Chiba et al., 2005; Gratsch & O'Shea, 2002; McNeish et al., 2010). We thus decided to start our study by testing the well known ability of Noggin to function as a neural inducer also in our culture condition. Consistently, we found that adding increasing doses of Noggin (5 nM to 400 nM) to CDMM during Step-II supported the expression of the pan-neuronal markers Ncam and Pax6, as compared to cells grown in CDMM without Noggin (**Figure 3.1A**).

At the end of Step-III, ES cells treated with Noggin during Step-II slightly increased the expression of Doublecortin (Dcx, a general neuroblast marker; Knoth et al., 2010) and of acetylated-Tubulin (Ntub, pan-neuronal marker) compared to ES cells cultured in CDMM (Ctrl; **Figure 3.1B,C**).

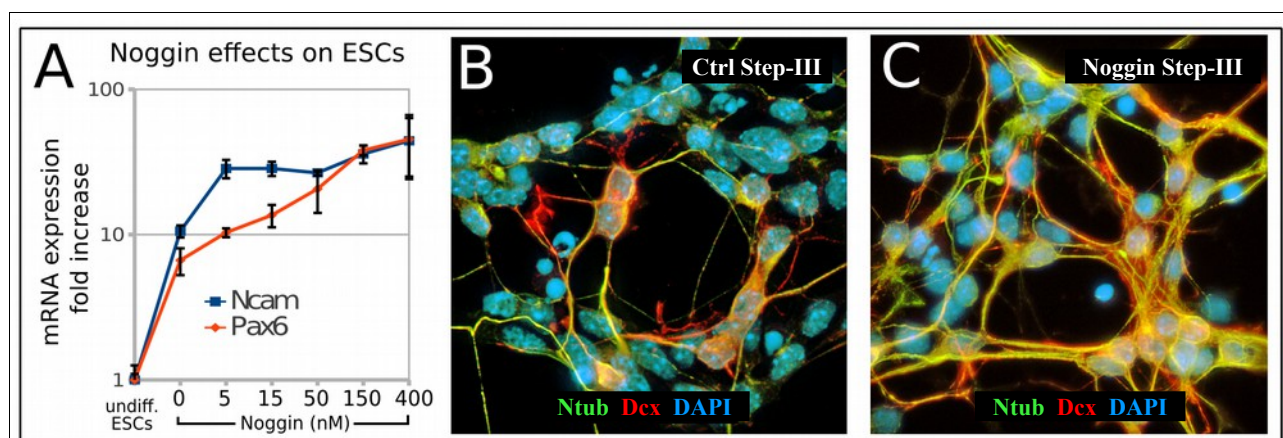
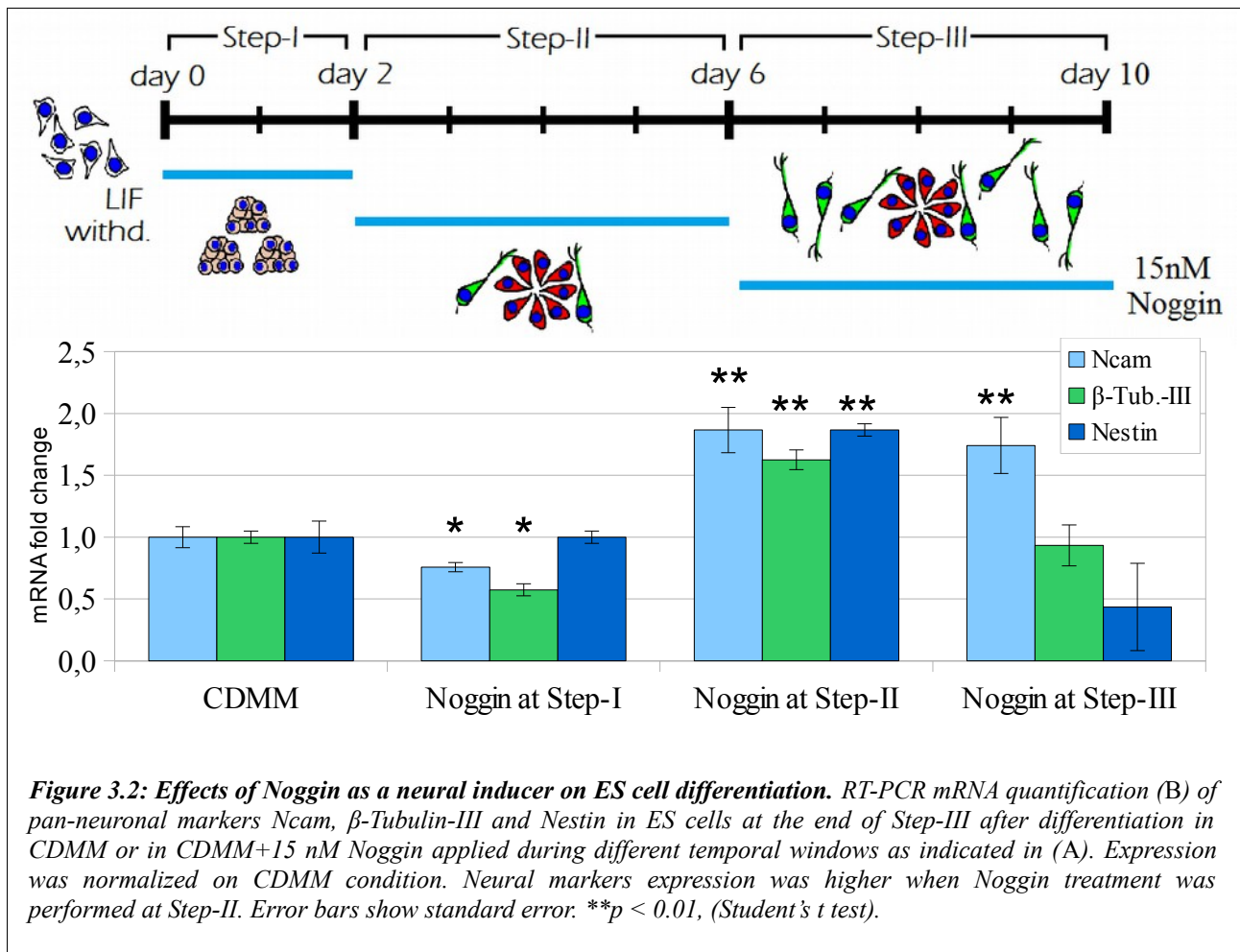


Figure 3.1: Effects of Noggin as a neural inducer on ES cell differentiation. (A): RT-PCR mRNA quantification of pan-neuronal markers Ncam and Pax6 in expanding (undifferentiated) ES cells and ES cells at the end of Step-III after differentiation in CDMM (0) or in CDMM+5–400 nM Noggin (expression normalized on undifferentiated ES cells). Error bars show standard error. (B), (C): Doublecortin (Dcx, red) and acetylated-Tubulin (Ntub, green) immunocytochemical detection of ES cells at the end of Step-III after differentiation in CDMM (Ctrl, B) or in CDMM containing 150 nM Noggin (C). ESCs: ES cells.

Notably, Noggin did not significantly affect pan-neuronal markers expression when added at Step-I or III, as evaluated by RT-PCR (**Figure 3.2**), except Ncam, that was induced by treatment at Step-III.



We directly compared the neural inducing activity of Noggin to SCM (differentiation in Serum Containing Medium, see Results, Chapter 1) and CDMM (differentiation in Chemically Defined Minimal Medium) conditions, as percentage of neural progenitors generated by ES cells. We took advantage of a Sox1-GFP knock-in ES cell line (46C, Ying et al., 2003), analyzing GFP expression by flow cytometry. This analysis showed that CDMM culture condition induced a massive increase of Sox1-GFP positive neural progenitors at mid-Step-II (day2; 68.2%) compared to SCM condition (14.4%), whereas Noggin (400 nM) induced a modest, although significant, increase compared to CDMM (78.1%; **Figure 3.3**). A similar trend was observed also at early-Step-II (end of day 1; SCM, 6.4%; CDMM, 27.9%; Noggin, 31.1%; not shown).

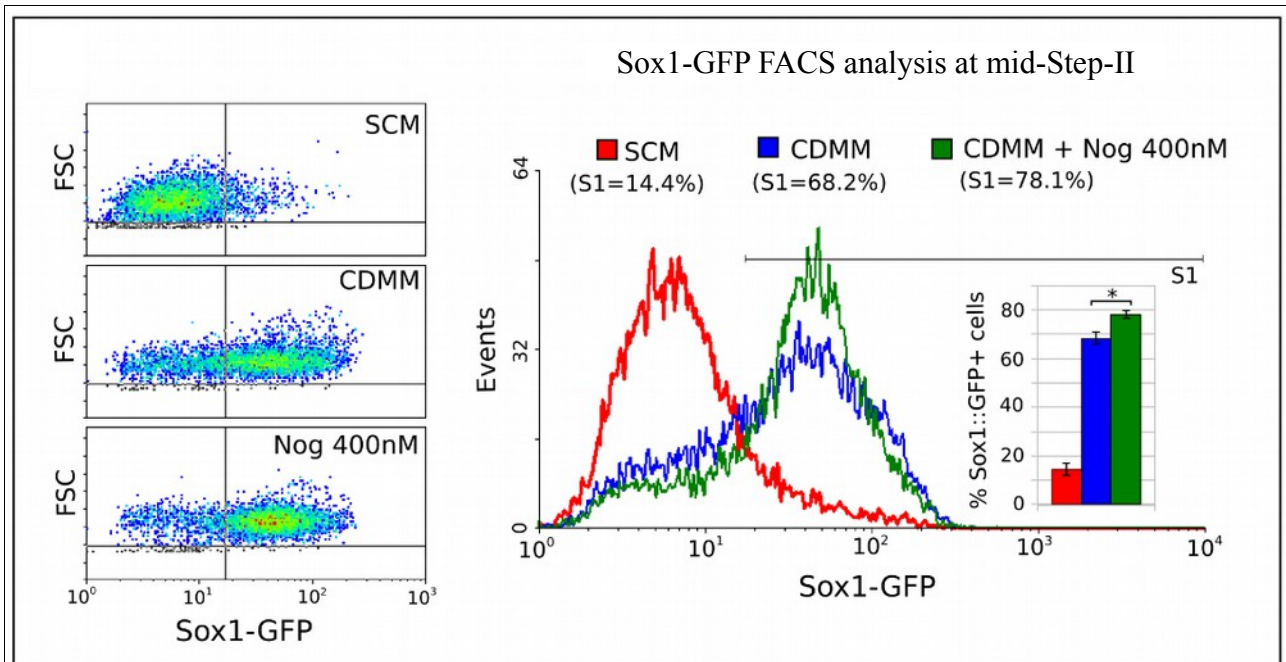


Figure 3.3: Flow-cytometry analysis of Sox1-GFP ES cells at day2 of Step-II after culture in different conditions. SCM: ES cells were aggregated (Step-I) in serum-containing medium and differentiated (2 days, Step-II) without serum. CDMM: both ES cell aggregation (Step-I) and differentiation (2 days, Step-II) were carried out without serum. CDMM+Nog 400 nM: as CDMM condition, plus Noggin treatment during the first two days of Step-II. Error bars show standard error; *** $p < 0.001$ (two-tailed Student's t test).

Ratios of Sox1-GFP positive neural progenitors obtained in the different culture conditions was consistent with a differential expression of the key transcription factor of neural commitment *Zfp521*, whose expression was highest in cultures with Noggin (400 nM; **Figure 3.4**).

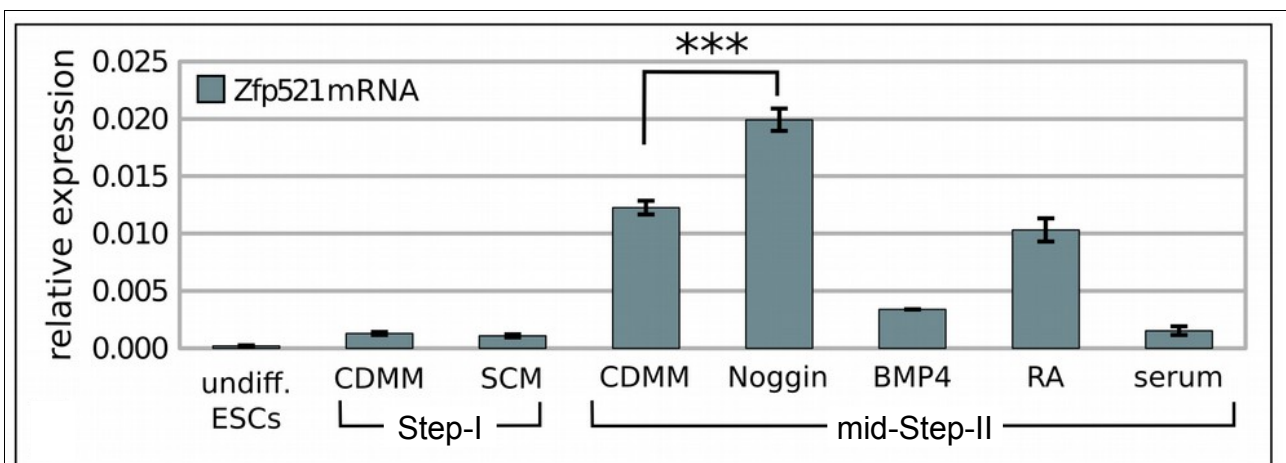


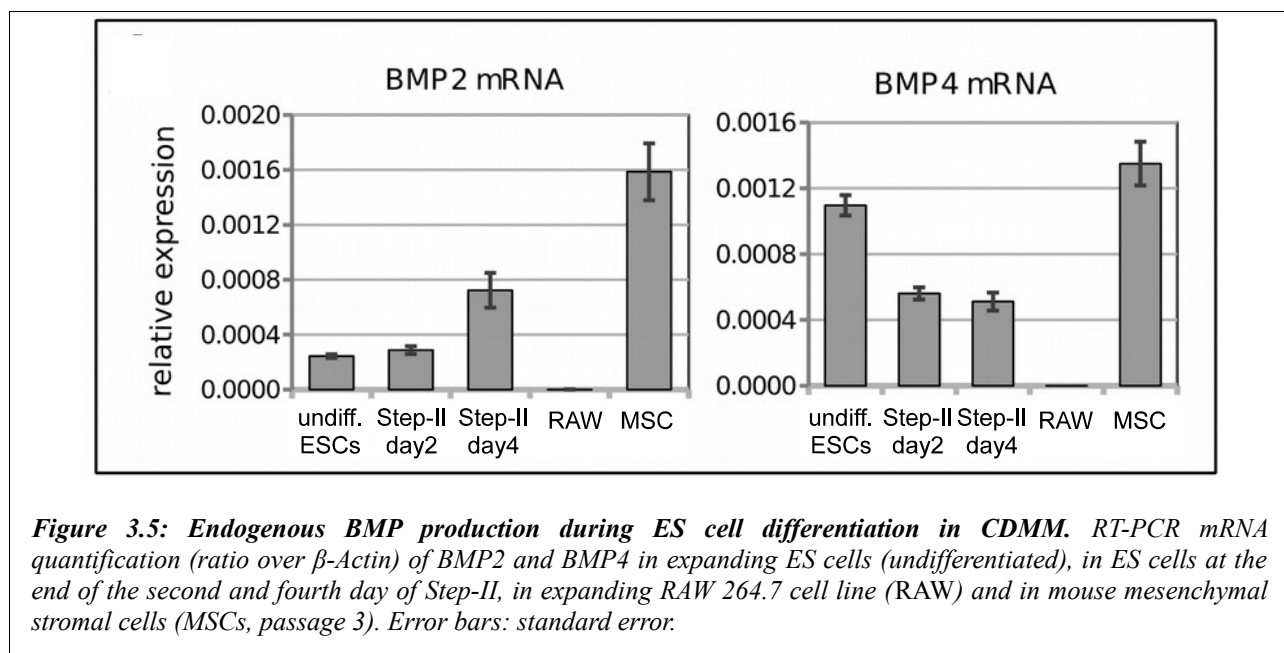
Figure 3.4: RT-PCR mRNA quantification (ratio over β -Actin) of *Zfp521* at different time points and after culture in different conditions, as indicated; treatments with Noggin (400 nM), BMP4 (50 ng/ml), RA (10 nM) and serum (10%) were performed at Step-II. Error bars show standard error; * $p < 0.001$ (two-tailed Student's t test).**

We concluded that the majority of ES cells cultured in CDMM become neural progenitors at Step-II and established CDMM culture condition as control for subsequent investigations on BMP inhibition. We also demonstrated that Noggin can further increase neuronal differentiation of ES cells in our *in vitro* differentiation protocol, as it does in many differentiation protocols already available in the scientific literature.

CDMM-Differentiating ES Cells Produce and Respond to BMPs.

As Noggin affects ES cell neuralization, but BMPs were not added to culture medium, we assayed for the presence of BMPs that were endogenously produced by ES cells during differentiation. As described in Results, Chapter 2, ES cells showed detectable expression levels of BMP2 and BMP7, and very high expression levels of BMP4 and BMP6, during neural differentiation. We focused our attention on BMP factors that can efficiently be sequestered by Noggin: BMP2 and BMP4; BMP7 can also be sequestered by Noggin, but with lower affinity. We analyzed their mRNA expression levels in proliferating ES cells, in CDMM-differentiating ES cells (during Step-II), in cells that express high BMP levels (primary mouse mesenchymal stromal cells, MSCs) or in cells that express low BMP2/4 levels (macrophage cell line RAW 264.7; Ralph & Nakoinz, 1977).

We found that both undifferentiated and differentiating ES cells express high BMP2, BMP4 (**Figure 3.5**) and BMP7 levels (see Results, Chapter 2; and data not shown). Notably, ES cells transcribe BMP2/4/7 also at Step-II, when Noggin addition to CDMM exerts its effect on neuronal differentiation.



Moreover, ELISA showed that CDMM-differentiating ES cells secrete approximately 50% of the BMP2 protein secreted by MSCs, but almost ten times more than the amount secreted by RAW cells (**Figure 3.6**).

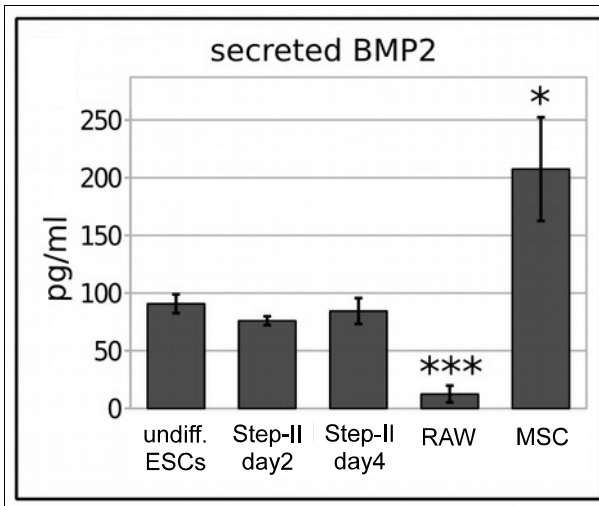


Figure 3.6: Secreted BMP2 quantification by ELISA in expanding ES cells (undifferentiated ESCs), ES cells at mid-Step-II, ES cells at the end of Step-II, expanding RAW 264.7 cell line (RAW) and mouse mesenchymal stromal cells (MSCs). Error bars: standard error. * $p < 0.05$, *** $p < 0.001$ (two-tailed Student's t test).

We found that CDMM-differentiating ES cells during Step-II express functional BMP receptors. In fact, ES cells at Step-II expressed higher levels of BMPR1a-b mRNA than MSCs, which depend on the binding of BMP2/4 to BMPR1a-b receptors for osteoblastogenesis (Abe et al., 2000) (**Figure 3.7**).

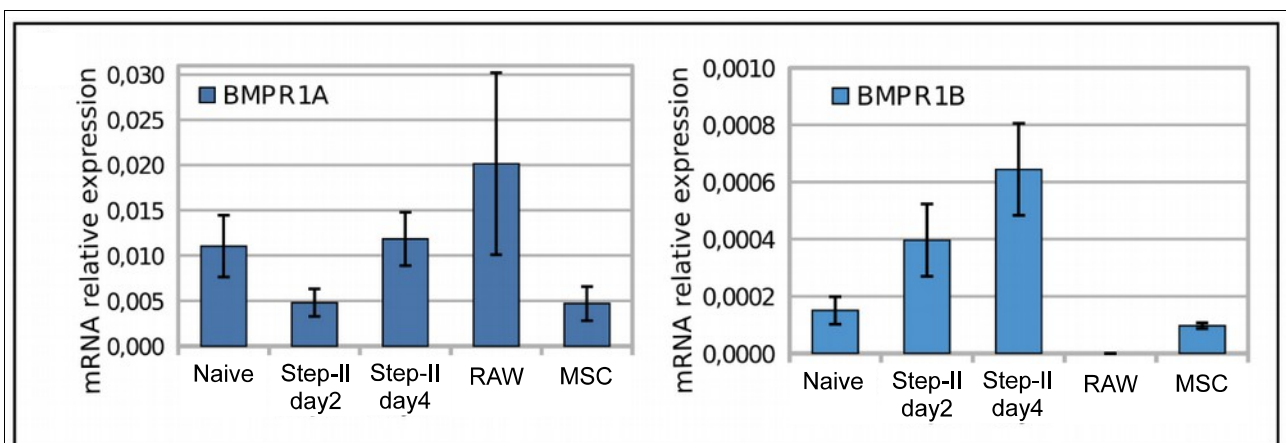
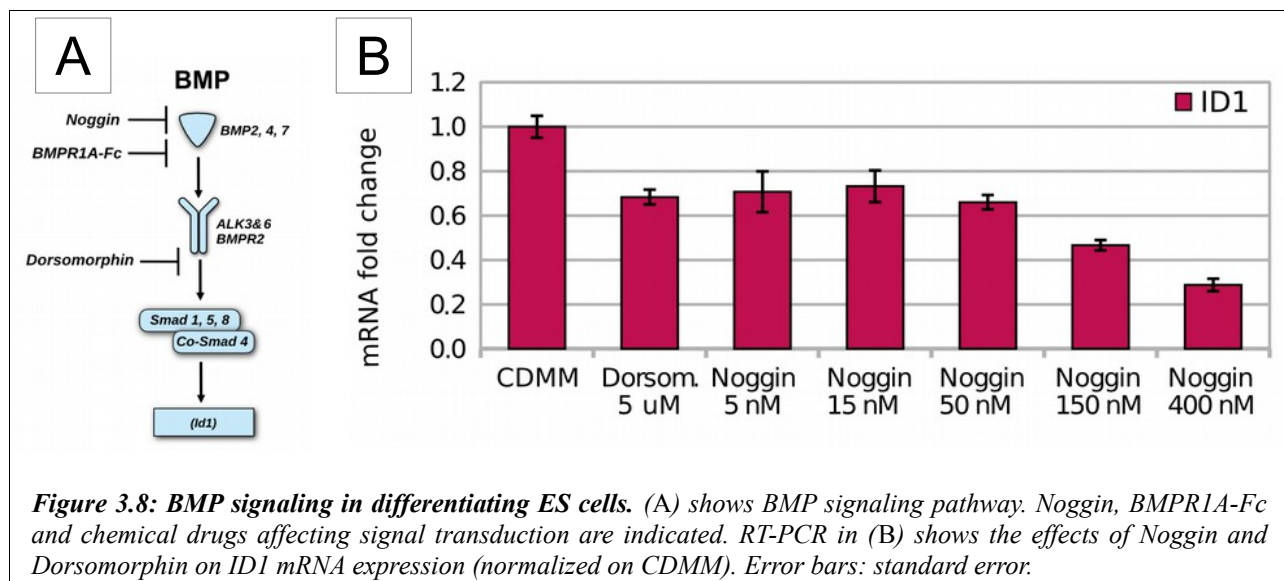


Figure 3.7: BMP receptor expression in differentiating ES cells. RT-PCR analysis shows mRNA relative expression of BMP receptors 1A and 1B in ES cells at different steps of differentiation, MSC and RAW cells (ratio over β -Actin). Error bars: standard error. Naive: undifferentiated ES cells.

Interestingly, Noggin decreased the expression of ID1, a downstream effector of the BMP-responsive pathway (Hollnagel et al., 1999) in a dose-dependent manner (**Figure 3.8**). This is in line with the ability of Noggin to block the BMP-responsive pathway in ES cells.



To test if endogenously produced BMPs were active on cultured cells, we further investigated the activation of intracellular transduction pathway in response to BMP signaling by analyzing SMAD1/5/8 phosphorylation (phospho-SMAD, **Figure 3.9A-F**). Undifferentiated ES cells were used as a positive control (**Figure 3.9D**). Most nuclei of both undifferentiated ES cells and ES cells at Step-II in different conditions showed phospho-SMAD immunostaining, with different degrees of intensity. **Figure 3.9E** shows the distribution of the immunostaining intensity, while **Figure 3.9F** reports the mean immunostaining intensity. We found that control CDMM-differentiating ES cells show intermediate levels of the phosphorylated form of SMAD1/5/8 during Step-II, as compared to ES cells in other culture conditions (**Figure 3.9A,F**). This confirms the presence of an endogenous BMP production and activity. Acute 5-hr treatment with Noggin (400 nM) or BMP4 (50 ng/ml) during Step-II significantly decreased or increased SMAD phosphorylation, respectively (**Figure 3.9B-E**). The pattern of phospho-SMAD immunodetection showed that virtually all cells responded to BMP4 addition (**Figure 3.9C**).

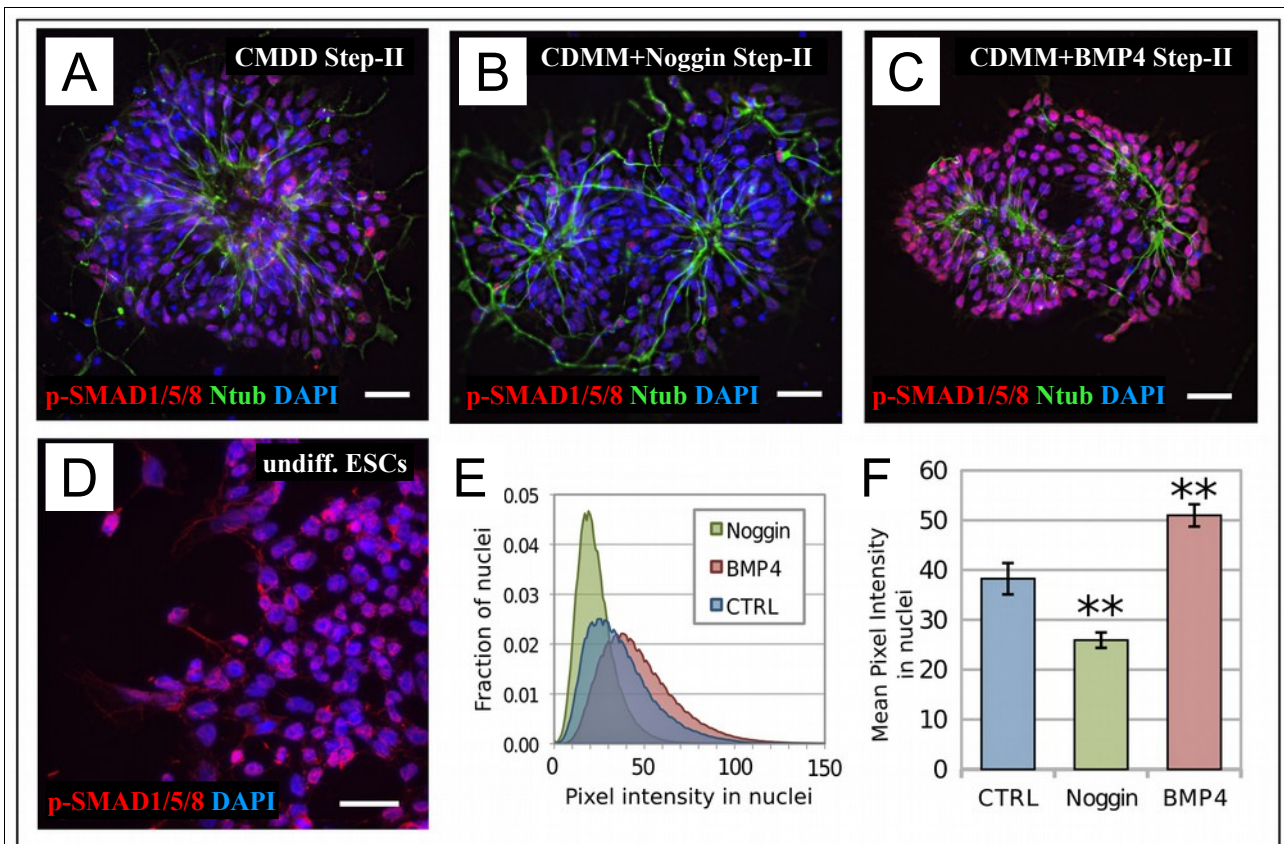
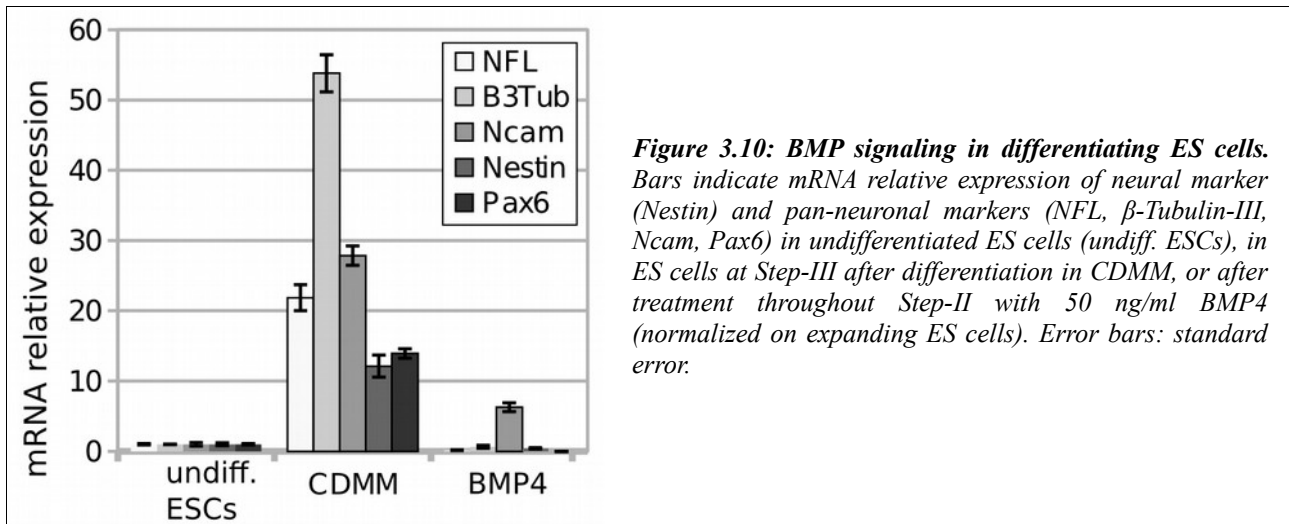


Figure 3.9: Endogenous BMP production and BMP activity during ES cell differentiation in CDMM. (A)-(C): Ntub (green) and phospho-SMAD1/5/8 immunocytochemistry (nuclear red staining over DAPI nuclear counterstaining) in ES cells at Step-II (day2) in CDMM (A), 5 h after the addition of 400 nM Noggin to CDMM (B) and 5 h after the addition of 50 ng/ml BMP4 to CDMM (C). (D), Phospho-SMAD1/5/8 immunocytochemistry (red staining over DAPI) in undifferentiated ES cells (undiff. ESCs). Scale bars 30 μ m. (E), (F): Pixel intensity distribution (fraction of nuclei with given pixel intensity (E) and mean pixel intensity (F) of immunodetection in nuclei as in ((A)-(D)), respectively. Error bars standard error; * $p < 0.05$, ** $p < 0.01$, *** $p < 0.001$ (Student's t test).

Consistently, BMP4 added exogenously to CDMM throughout Step-II (50 ng/ml), dramatically repressed the expression of the pan-neuronal markers Nestin, NFL, β -Tubulin-III and Pax6, (**Figure 3.10**), thus confirming the ability of ES cells to specifically respond to BMP signaling during Step-II.



Our data thus show that ES cells produce and are sensitive to BMPs during neuronal differentiation *in vitro*.

In the Absence of Exogenous Signals, ES Cells Generate Neurons Expressing Midbrain Dorsal Markers.

In order to investigate the effect of endogenous BMPs on ES cell positional identity, we characterized our control culture (ES cell differentiated in CDMM), by analyzing the expression of FoxG1 (Xuan et al., 1995), Wnt7b (Parr et al., 1993), Six3 (Oliver et al., 1995), Otx2 (Acampora et al., 1998) and En1 (Wurst et al., 1994) genes at the end of Step-III. These genes display an ordered (A/P) expression that covers the most anterior aspect of forebrain (FoxG1, Emx2), entire forebrain (Six3), forebrain/midbrain (Otx2) and midbrain (En1). We also analyzed the expression of HoxB4 (Ramirez-Solis et al., 1993) and HoxB9 (Chen & Capecchi, 1997), which mark hindbrain and spinal cord, respectively (**Figure 3.11A**).

We compared the mRNA levels of these genes in CDMM-differentiated ES cells to the mRNA levels found in cortex (rostral-dorsal forebrain), mesencephalon (midbrain), rhombencephalon (hindbrain), spinal cord of embryonic day16 (E16) mouse and undifferentiated ES cells. Compared to mouse brain, CDMM-differentiated ES cells expressed very high levels of Otx2 and En1, low levels of Wnt7b and Six3, and very low levels of both telencephalic (FoxG1) and posterior markers (HoxB4 and HoxB9) (**Figure 3.11B**).

As ES cells cultured in CDMM failed to express high levels of hindbrain/spinal cord specific genes, we wanted to assay for their ability to turn on these genes upon induction with the posteriorizing factor RA. As expected, ES cells treated with RA during Step-II, and analyzed at the end of Step-III, turned on the posterior markers HoxB4 and HoxB9 and down-regulated the anterior markers FoxG1, Six3 and Otx2 in a dose-dependent fashion (**Figure 3.12**).

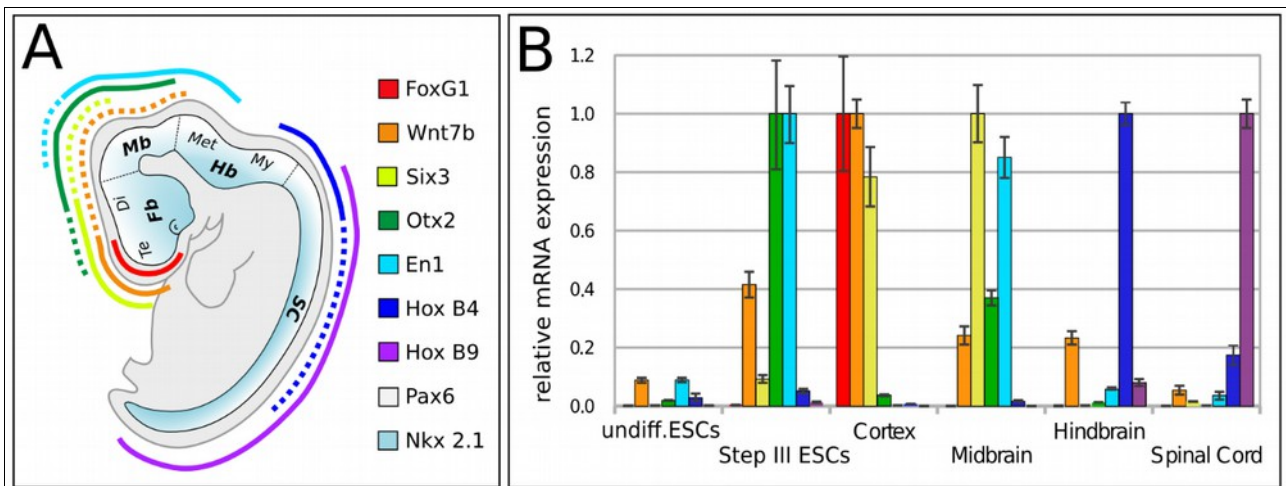


Figure 3.11: Regional identity of ES cells differentiated in CDMM. (A): A/P (color code) and D/V (white-cyan code) patterning of mouse embryo as identified by the expression of key patterning genes, elaborated from EMAP (<http://www.emouseatlas.org>; see Materials and Methods) and articles cited in text. Fb forebrain, Mb midbrain, Hb hindbrain, SC spinal cord, Te telencephalon, Di diencephalon, Met metencephalon, My myelencephalon. (B) shows mRNA relative expression of A/P genes (as evaluated by RT-PCR, normalized on maximum expression) in brain tissues of E16 embryos, undifferentiated ES cells (undiff. ESCs) and ES cells at the end of Step-III (Step-III ESCs).

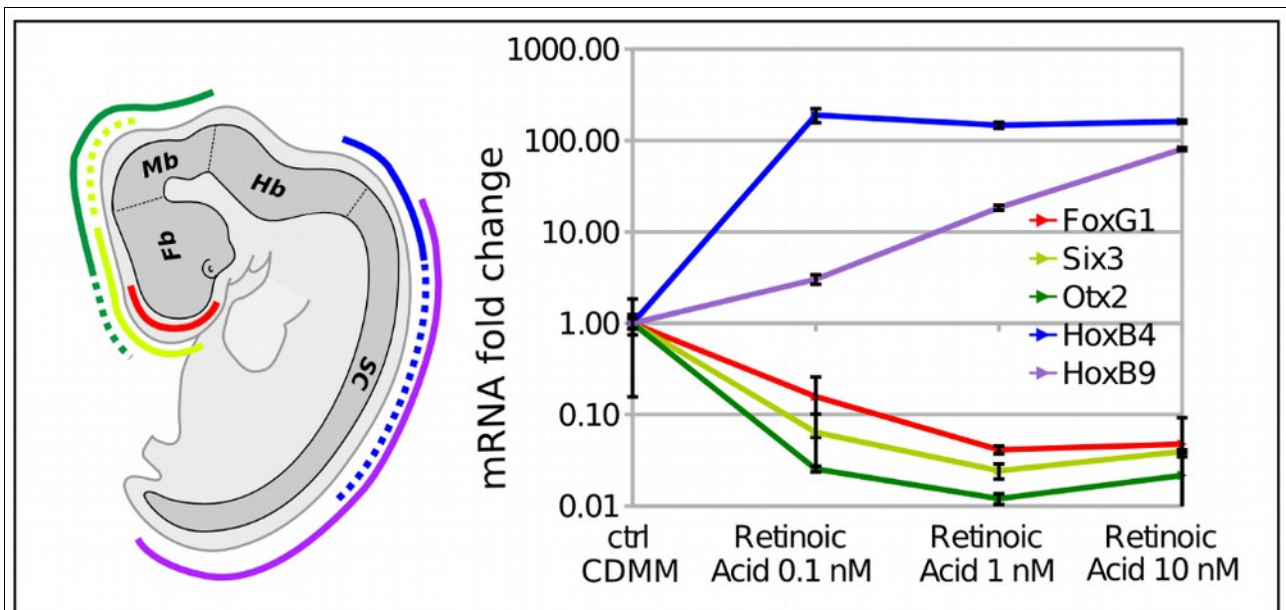
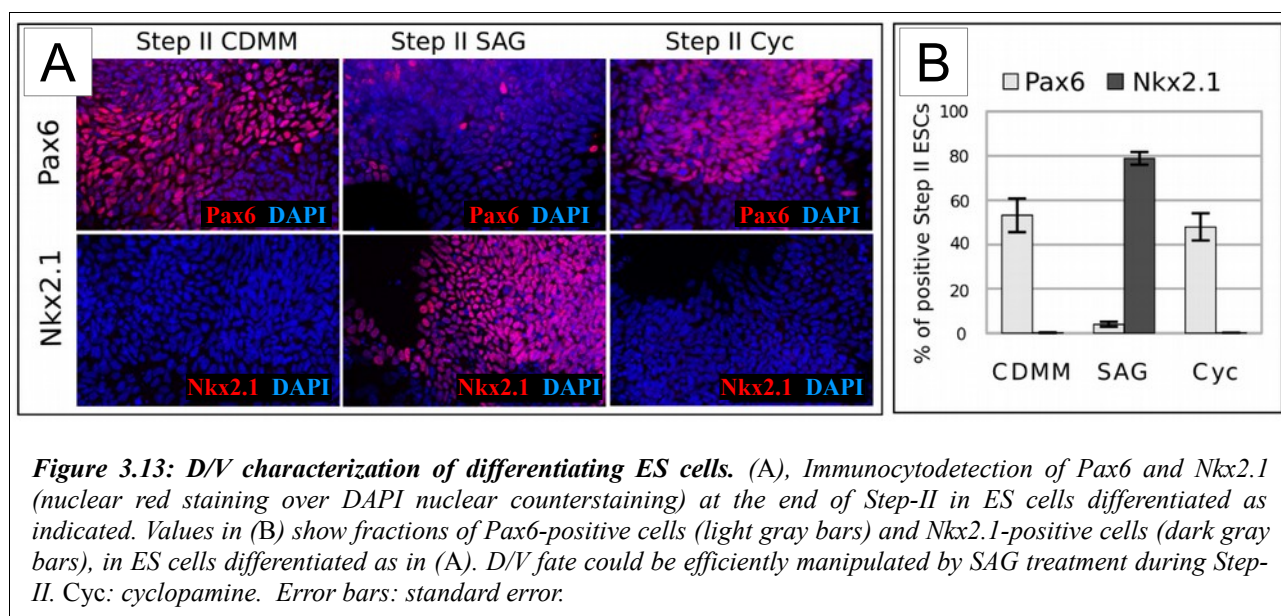


Figure 3.12: A/P characterization of differentiating ES cells. A/P (color code) patterning of mouse embryonic brain, identifying the regions of gene expression. Values indicate mRNA expression fold changes in ES cells at the end of Step-III after exposure to different RA concentration throughout Step-II, as evaluated by RT-PCR (expression normalized on control, Ctrl CDMM). This indicates that, in our protocol, RA treatment is able to posteriorize the neural progenitor fate, switching-on the expression of specific Hox genes in a dose-dependent manner.

We then analyzed the dorso-ventral (D/V) identity of ES cell-generated neural progenitors at the end of Step-II by comparing the relative ratios of cells expressing the dorsal marker Pax6 (Stoykova & Gruss, 1994) or the ventral marker Nkx2.1 (Pera & Kessel, 1997). A large fraction (53.1±7.6%) of control CDMM ES cells expressed Pax6 protein and virtually no cells expressed Nkx2.1 protein (**Figure 3.13A,B**). As the Pax6/Nkx2.1 D/V gradient is generated in response to a gradient of Sonic Hedgehog (Shh) activity (Briscoe et al., 2000), we assayed the effects of a Shh agonist (SAG, DeCamp et al., 2000) or of a Shh antagonist (Cyclopamine; Taipale et al., 2000) on ES cells. Drugs were added to CDMM throughout Step-II. SAG treatment dramatically repressed Pax6 (3.9±1.1%) and activated Nkx2.1 protein expression in a very large fraction of cells (79±2.9%), whereas Cyclopamine affected neither Pax6 nor Nkx2.1 (**Figure 3.13A,B**). The experiment showed how ES cells spontaneously differentiate into Pax6-positive neural progenitors with our protocol. D/V fate could be efficiently manipulated by SAG treatment during Step-II. RT-PCR analysis confirmed these results (**Figure 3.14**).



Notably, the lack of any effect of Cyclopamine is consistent with the observation that Step-II ES cells produced very low level of endogenous Shh (**Figure 3.15**).

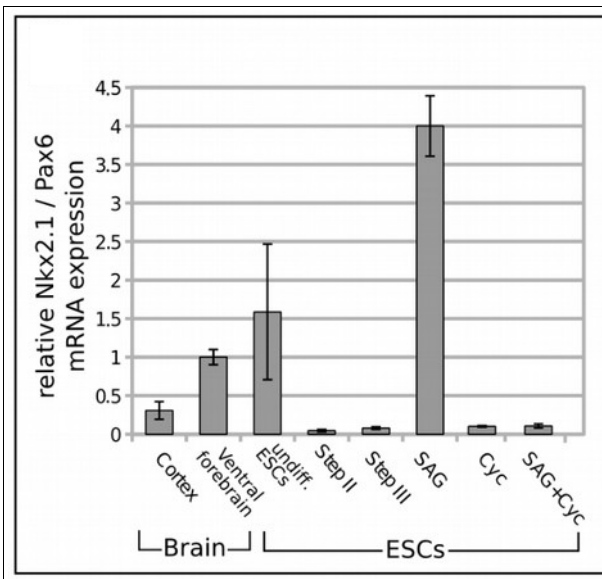


Figure 3.14: D/V characterization of differentiating ES cells. Graph shows V/D index, calculated as Nkx2.1/Pax6 mRNA ratio measured by RT-PCR at different time points and in different culture conditions or brain regions, as indicated (expression normalized on ventral forebrain level). The high variability of Nkx2.1/Pax6 mRNA ratio in undifferentiated ES cells is due to the very low levels of expression of Nkx2.1 and Pax6 mRNA in these cells. Undiff. ESCs: undifferentiated ES cells.

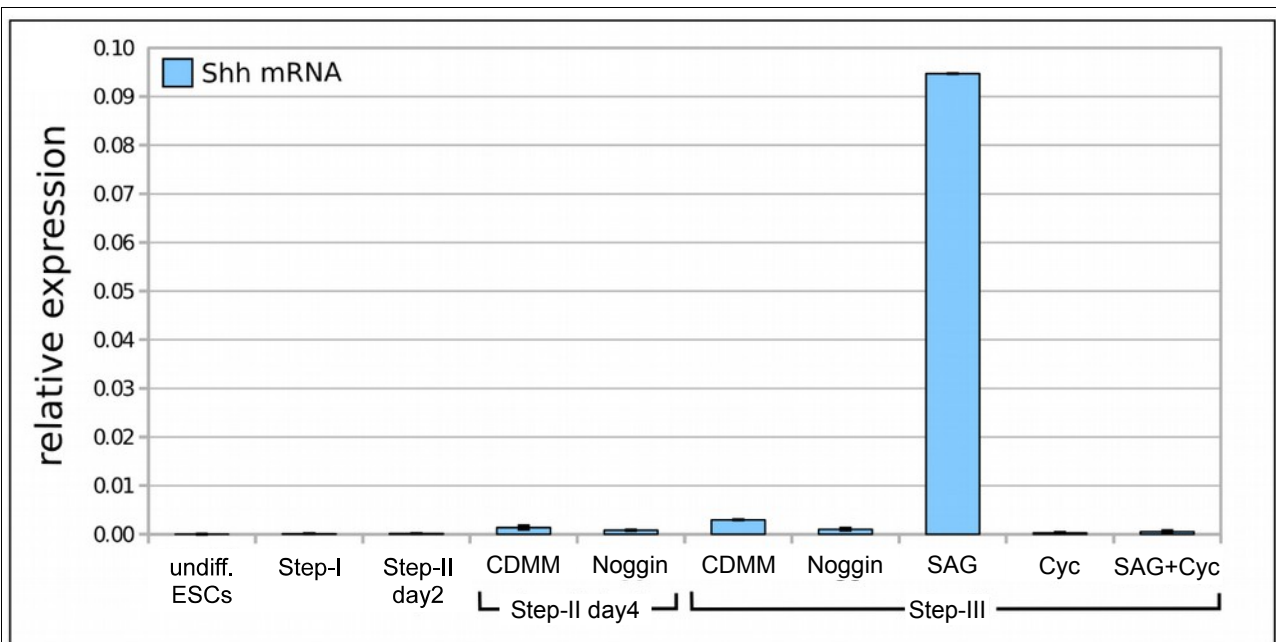


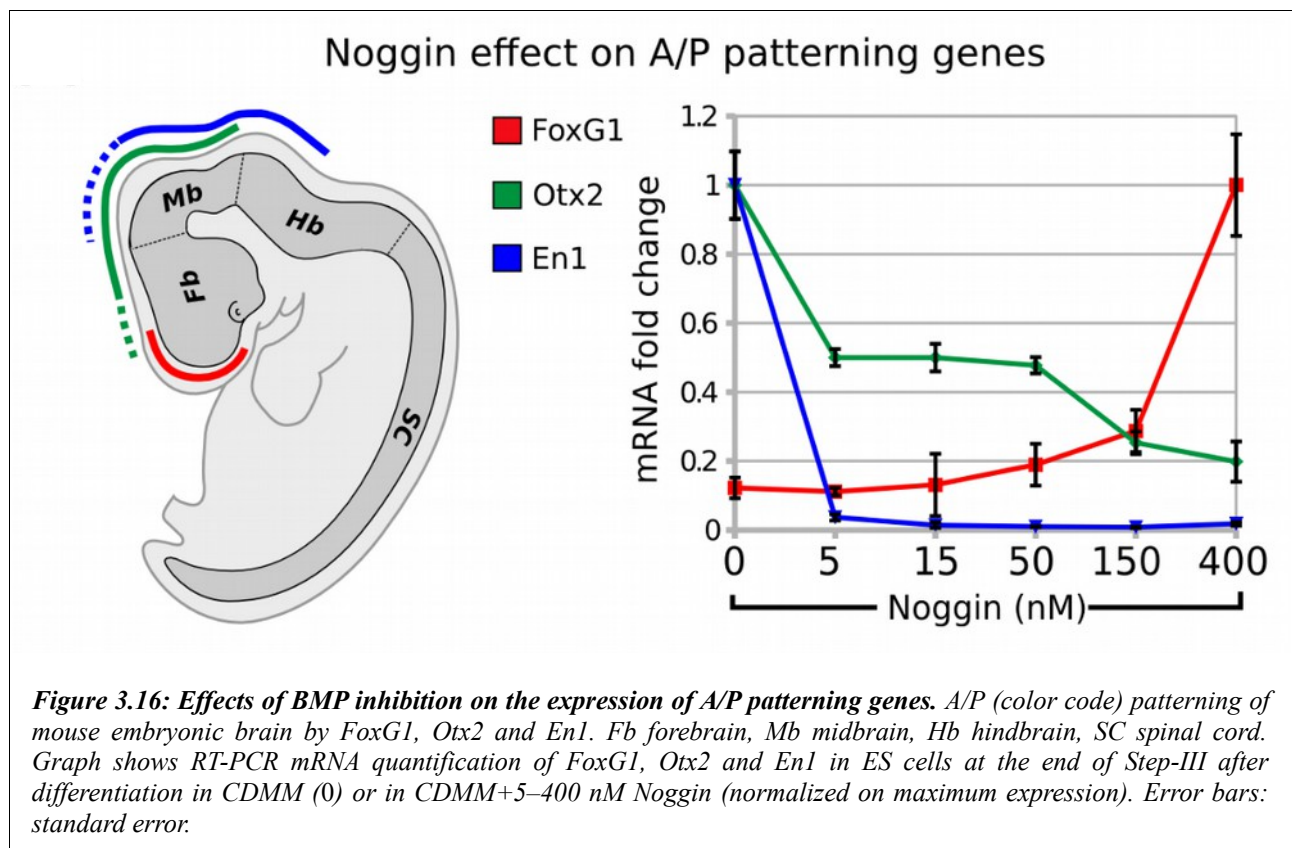
Figure 3.15: D/V characterization of differentiating ES cells. Graph shows RT-PCR analysis of Shh relative expression in ES cells at different times of differentiation and in different culture conditions, as indicated (ratio over β -Actin). Undiff. ESCs: undifferentiated ES cells; Noggin: Noggin 400 nM; SAG: Shh agonist (100 nM); Cyc: Cyclopamine 10 μ M. Error bars: standard error.

These data suggest that in our protocol of differentiation ES cells mostly adopt a midbrain dorsal identity when cultured in CDMM. However, the protocol is plastic enough to respond to treatments with morphogens, and differentiating cells can modulate the expression of A/P and D/V markers accordingly to treatments.

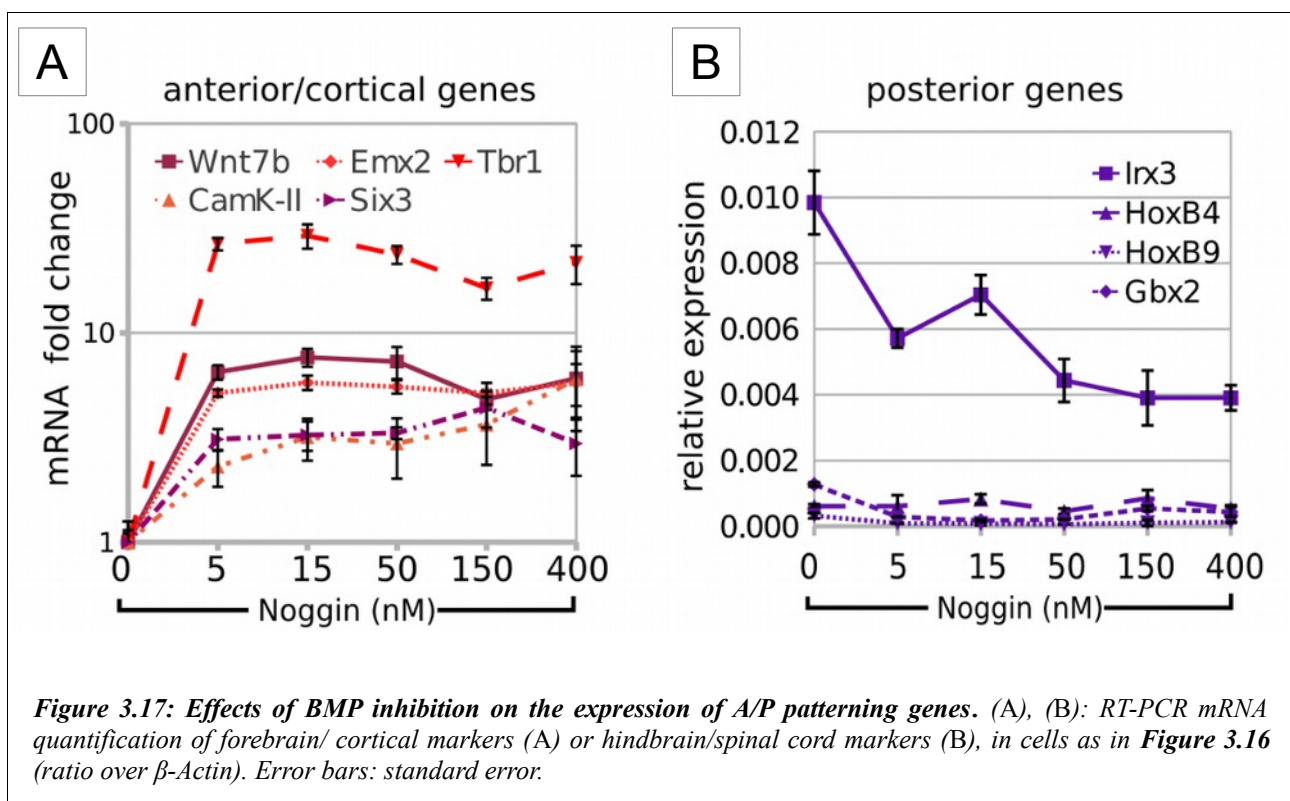
BMP Inhibition During Differentiation Supports the Expression of Telencephalic Markers.

Our *in vitro* differentiation protocol allows efficient neural conversion of ES cells, originating neural progenitors that predominantly show a midbrain/dorsal identity. BMP factors are produced endogenously by differentiating cells, and BMP inhibition by Noggin treatment can further increase neuronal differentiation of ES cells in our culture system.

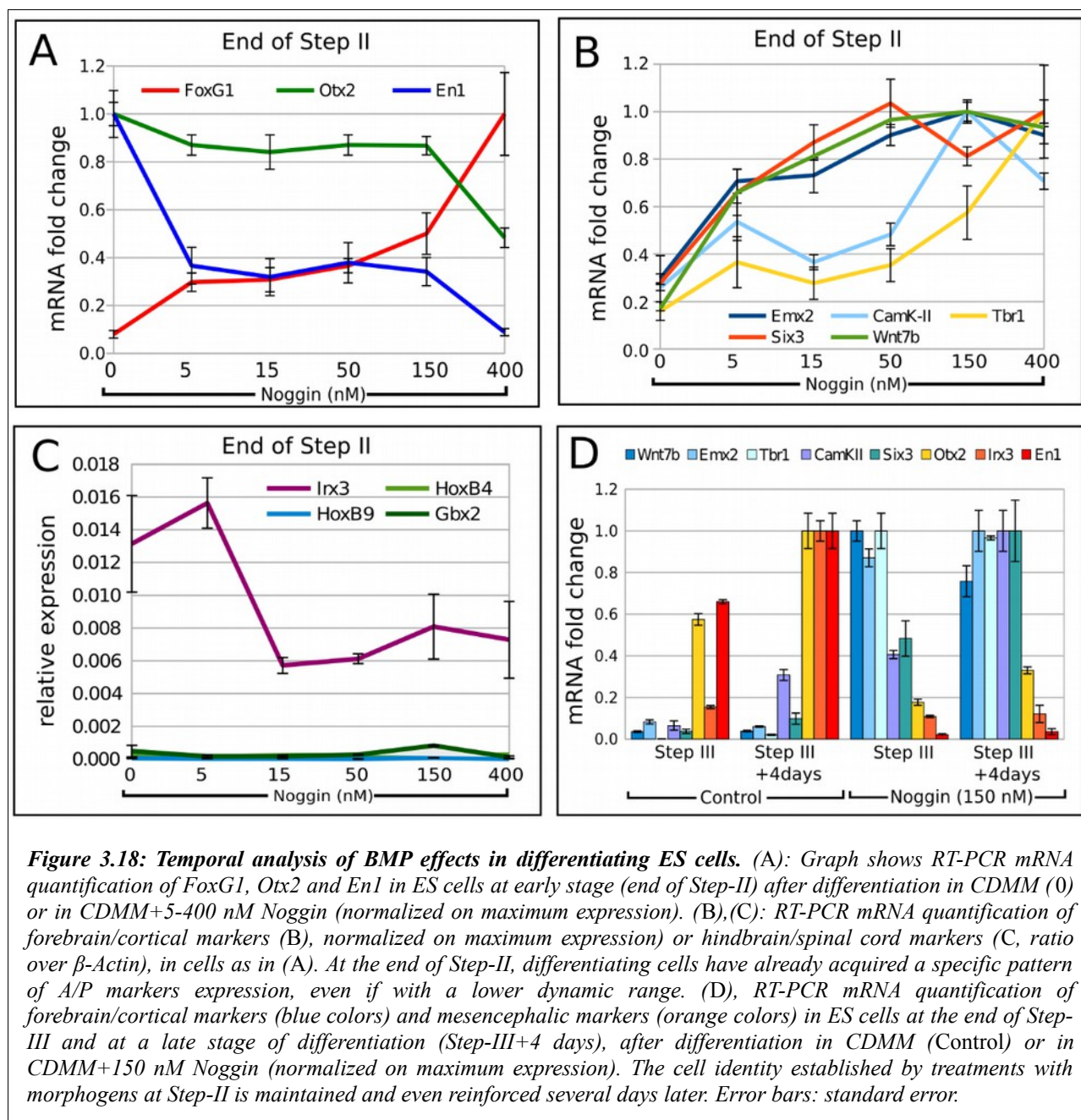
We subsequently investigated if endogenously produced BMPs can affect not only neuralization, but also the regional identity of ES cell-generated neurons. To this purpose, we analyzed the expression of specific A/P markers after treatment with Noggin. Compared to control, the treatment with increasing doses of Noggin (5 to 400 nM) during Step-II induced the telencephalic marker FoxG1 and repressed the more posterior markers Otx2 and En1 in a dose-dependent manner, as evaluated at the end of Step-III (**Figure 3.16**).



Moreover, Noggin induced the expression of Wnt7b (a forebrain marker; Parr et al., 1993), Six3 (prosencephalic marker), Emx2 (early cortical marker; A. Simeone et al., 1992), Tbr1 and α -CamK-II (late cortical markers; Bulfone et al., 1995; Kinney et al., 2006; **Figure 3.17A**), and repressed the expression of the posterior marker Irx3, which is present in caudal diencephalon, midbrain and more posterior regions (Bosse et al., 1997; **Figure 3.17B**). Noggin was ineffective on the hindbrain/spinal cord markers Gbx2, HoxB4 and HoxB9, leaving their low expression levels almost unchanged (**Figure 3.17B**).



The same positional markers were analyzed at earlier or later times of differentiation (end of Step-II or Step-III+4 days, respectively; **Figure 3.18**). As similar results were obtained, we excluded the possibility that the effect of Noggin on positional identity may be the result of an enhancement/acceleration in neural fate induction. On the contrary, we concluded that differentiating ES cells acquire a specific A/P fate after treatments with morphogens (always performed at Step-II) and maintain their identity along the differentiation, without losing their positional memory.



To confirm the specificity of action of Noggin, we used the chimeric protein BMPR1A-Fc, a BMP inhibitor that binds to a BMP epitope outside the region recognized by Noggin (Keller et al., 2004; **Figure 3.19**) and Dorsomorphin, a selective inhibitor of the BMP type I receptors ALK2, ALK3 and ALK6 that blocks BMP-mediated SMAD1/5/8 phosphorylation (Yu et al., 2008; **Figure 3.8A**).

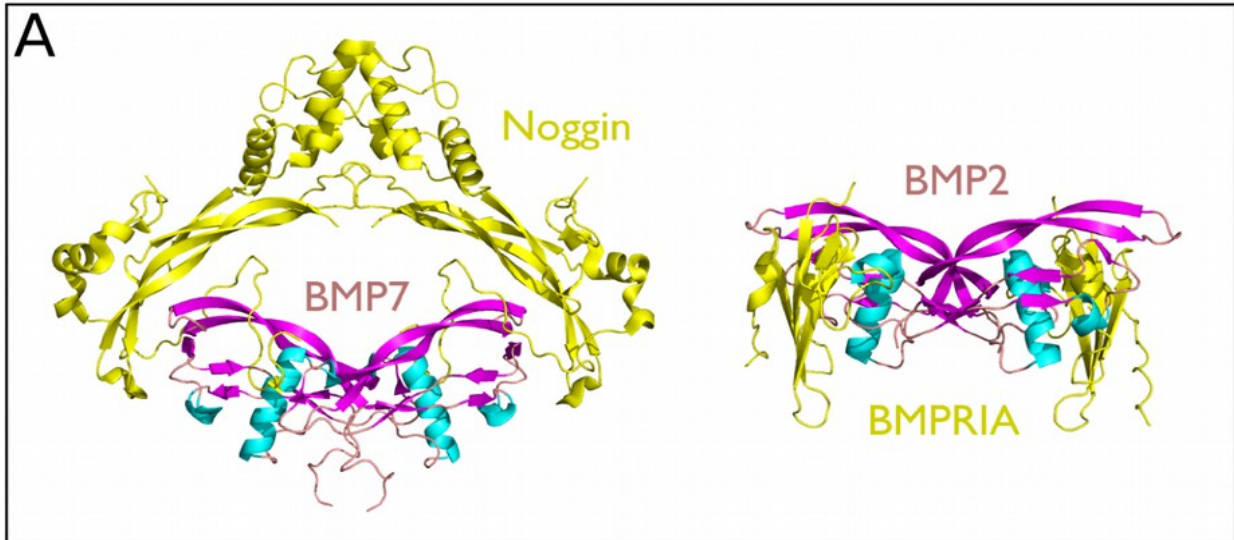


Figure 3.19: BMPR1A-Fc protein structure. Protein three-dimensional structures rendered with Pymol (<http://www.pymol.org/>). Molecular coordinates of Noggin-BMP7 and BMPR1A-BMP2 complexes, as submitted by Groppe et al., (2002) and Keller et al. (2004), were found in Protein Data Bank (<http://www.pdb.org/>).

BMPR1A-Fc induced an increase of Sox1-GFP positive neural progenitors at mid-Step-II (day2; 77.6%; **Figure 3.20**) that is comparable to the increase induced by Noggin (78.1%; **Figure 3.3**).

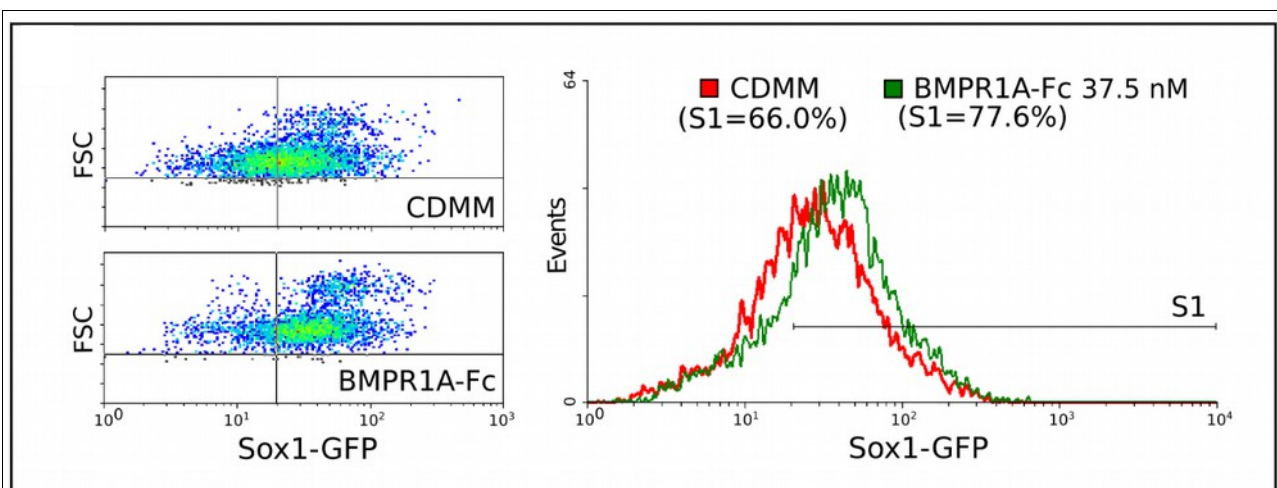


Figure 3.20: BMPR1A-Fc protein mimics Noggin effect on ES cell neuralization. Flow-cytometry analysis of Sox1-GFP ES cells at day2 of Step-II after culture in CDMM, or CDMM+37.5 nM BMPR1A-Fc.

Dorsomorphin or BMPR1A-Fc treatment during Step-II mimicked Noggin action also by inhibiting ID1 expression (**Figure 3.21A,B**), by supporting FoxG1 expression and by repressing Otx2 and En1 (**Figure 3.22A,B**).

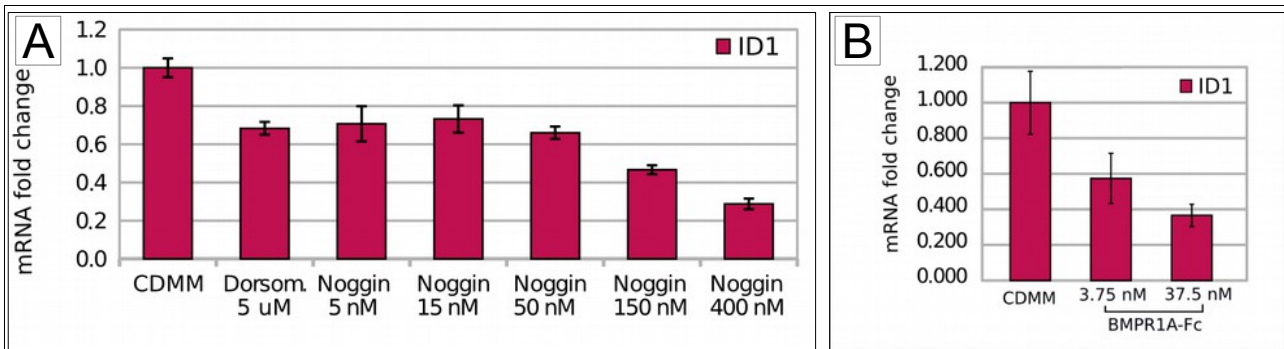


Figure 3.21: Dorsomorphin and BMPRIA-Fc mimic Noggin effects on ES cell differentiation. RT-PCR in (A) shows the effects of Noggin and Dorsomorphin on *ID1* mRNA expression (normalized on CDMM). The chemical drug mimics the effect of intermediate Noggin doses on *ID1* expression. (B) shows the effects of BMPRIA-Fc treatment on *ID1* mRNA expression, as evaluated by RT-PCR analysis (normalized on CDMM).

The specificity of BMPs in affecting ES cell differentiation fate is also suggested by the effects exerted by treatment at Step-II with SB431542. While Dorsomorphin selectively inhibits the BMP2/4 pathway, SB431542 suppresses the Activin/TGF- β receptors ALK4, ALK5 and ALK7 and prevents BMP-independent, Activin/TGF- β mediated, SMAD2/3 phosphorylation (**Figure 3.23**; Chambers et al., 2009). Compared to Noggin and Dorsomorphin, SB451243 acted by repressing, rather than by inducing, FoxG1, slightly inhibited En1 and left Otx2 expression almost unchanged (**Figure 3.22A**).

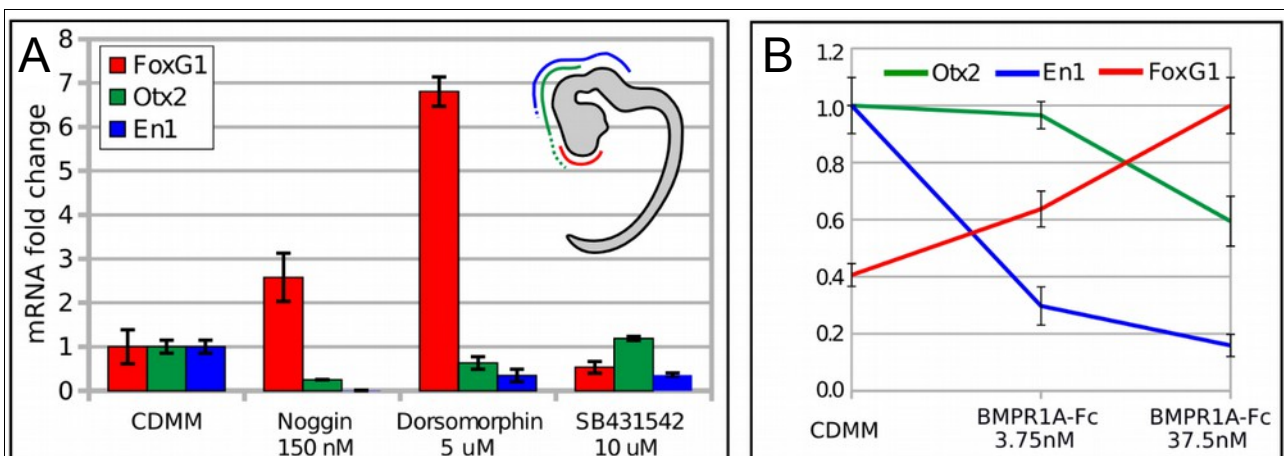


Figure 3.22: Dorsomorphin and BMPRIA-Fc mimic Noggin effects on ES cell differentiation. Bars in (A) show mRNA fold change of A/P patterning genes in ES cells at Step-III after differentiation in different culture conditions (normalized on CDMM). Drugs were added throughout Step-II. (B) shows the effects of treatment during Step-II with BMPRIA-Fc on FoxG1, Otx2 and En1 expression, as evaluated by RT-PCR at the end of Step-III. Error bars: standard error.

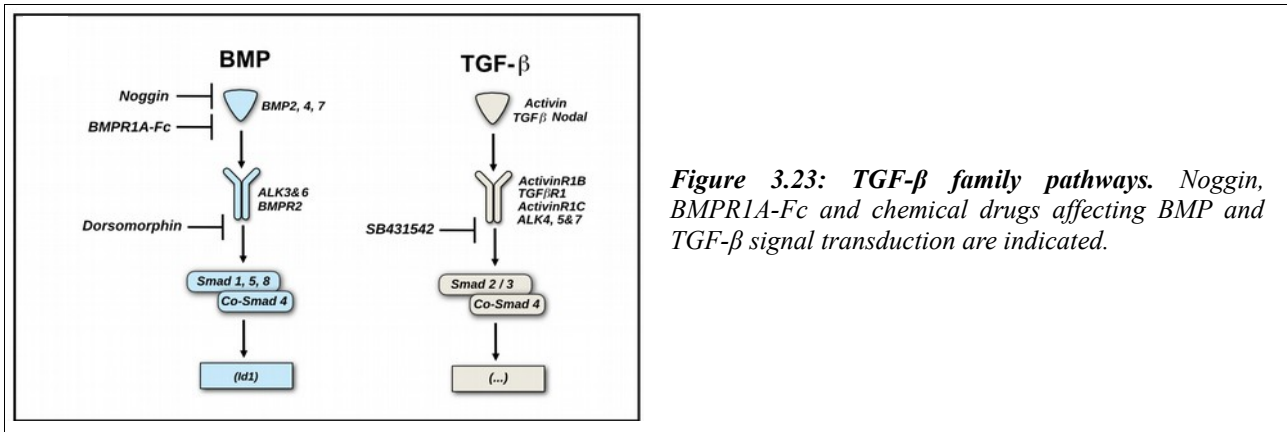


Figure 3.23: TGF- β family pathways. Noggin, BMPRIA-Fc and chemical drugs affecting BMP and TGF- β signal transduction are indicated.

Our results indicate that the inhibition of endogenously produced BMPs alters the A/P positional identity of the ES cell-generated neurons. BMP-inhibition induces a mixed population of neural progenitor cells and differentiated neurons expressing cortical markers.

We further investigated the nature of cells generated by Noggin-treated ES cells. At the end of Step-II we found 79.2% Nestin-positive neural progenitors in CDMM-differentiating ES cells, while Noggin treatment (150 nM) increased this ratio to 90.5%. Notably, of the Nestin-positive progenitors in CDMM cultures only 1.2% were positive for FoxG1, which labels telencephalic neuronal progenitors (Regad et al., 2007), while Noggin treatment (150 nM) increased this ratio to 18.2% (**Figure 3.24A-C**).

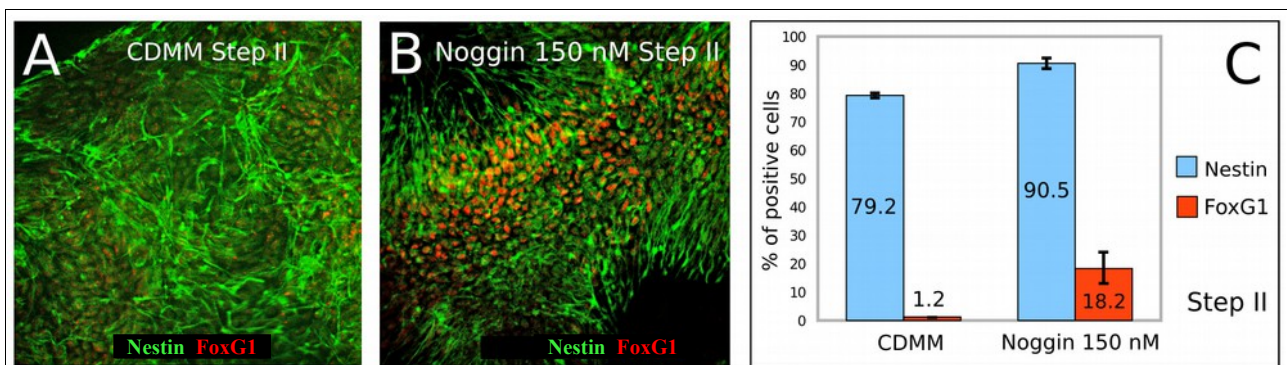


Figure 3.24: Effects of BMP inhibition on ES cell neural conversion and cell fate acquisition. (A)-(C): double immunocytochemistry of Nestin (green) and FoxG1 (red) at the end of Step-II in ES cells cultured in CDMM (A) or in CDMM+Noggin (150 nM, B). FoxG1-positive cells were always co-labeled by Nestin. Numbers in (C) show ratios of Nestin positive cells among total cells (light blue bars), or ratios of FoxG1-positive cells among Nestin-positive cells (red bars). This experiment suggests that Noggin treatment can anteriorize cell fate in a direct way, rather than simply increasing neural conversion. Error bars: standard error.

This implies that the removal of serum from our culture is *per se* sufficient to induce a high degree of neuralization and therefore the majority of ES cells in CDMM become neural progenitors also in the control condition (without Noggin). Noggin induced only a slight increase of neural progenitor ratio compared to control (79.2% Nestin-positive neural progenitors in CDMM-differentiating ES cells, 90.5% after Noggin treatment), while supporting a dramatic increase of cells expressing the telencephalic marker FoxG1 (See **Figure 3.24B**). Although significant, the small increase in neural progenitors induced by high doses of Noggin cannot explain the dramatic increase of telencephalic cells, and this clearly demonstrates that BMP inhibition is necessary to acquire a telencephalic identity. These results suggest a novel mechanism, whose molecular nature is still unknown, by which BMPs endogenously produced by differentiating ES cells directly act on the positional identity of the neural progenitors they spontaneously generate in a minimal medium.

The ratio of β -Tubulin-III positive neurons in cultures treated with Noggin (400 nM) was slightly higher than the ratio in control cultures at the end of Step-III (**Figure 3.26A**). In both conditions, the majority of cells negative for β -Tubulin-III staining were Nestin-positive progenitors (not shown). To define the biochemical identity of differentiated neurons, we performed an immunocytochemistry experiment exploiting vGlut2 (glutamatergic neurons) and GAD65 (GABAergic neurons) antibodies; both antibodies were tested on mouse brain slices and mouse primary cultures of neuronal cells. (See as an example GAD65 staining on neuronal primary cultures obtained from P0 striatum; **Figure 3.25A**). vGlut2 staining appeared with a punctate distribution along β -Tubulin-III-positive axons and soma, consistently with a vesicular localization inside the cell (**Figure 3.25B**).

Both control and Noggin-treated ES cells generated high ratios of vGlut2-positive glutamatergic neurons (**Figure 3.26A,B**), whereas the ratios of GAD65-positive GABAergic neurons either in control or in Noggin-treated ES cells were lower (**Figure 3.26A,C**). Noggin induced the expression of a number of genes coding for the isoforms of receptors for many different neurotransmitters, including GABA (**Table 3**); GABA receptors are strongly expressed on pyramidal cortical neurons *in vivo*.

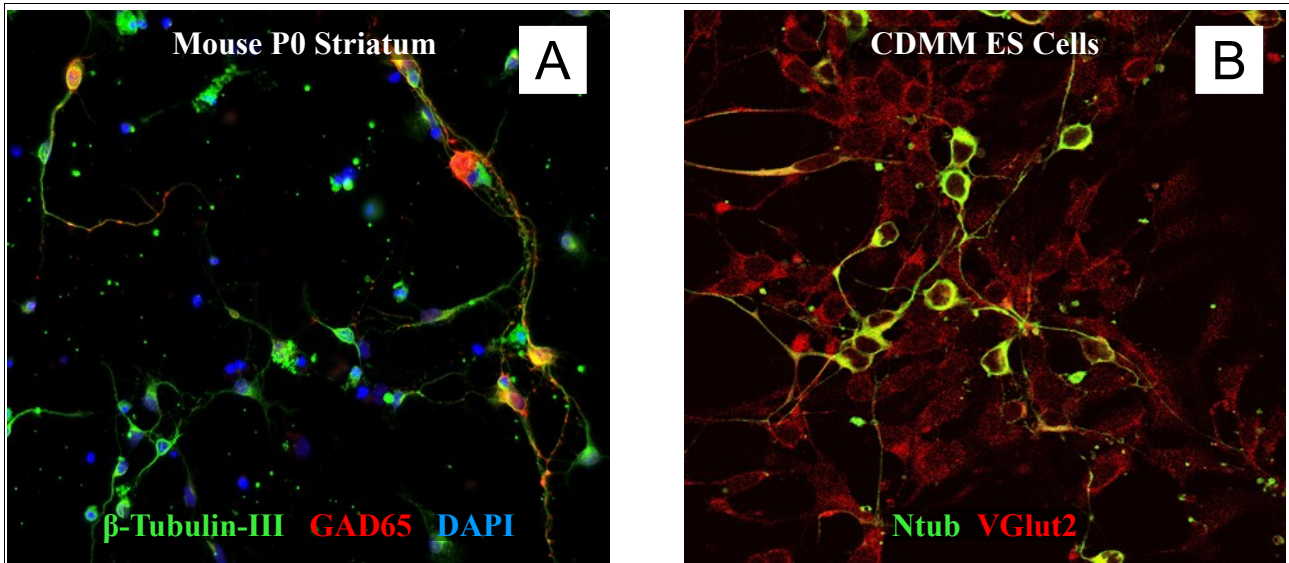


Figure 3.25: GAD65 and Vglut2 immunocytochemistry. (A) shows immunocytochemistry of β -Tubulin-III (green) and GAD65 (red) on primary cultures obtained from a P0 mouse striatum after 5 days of culture in CDMM. (B) shows immunocytochemistry of acetylated-Tubulin (green) and VGlut2 (red) at the end of Step-III in control ES cells cultured in CDMM.

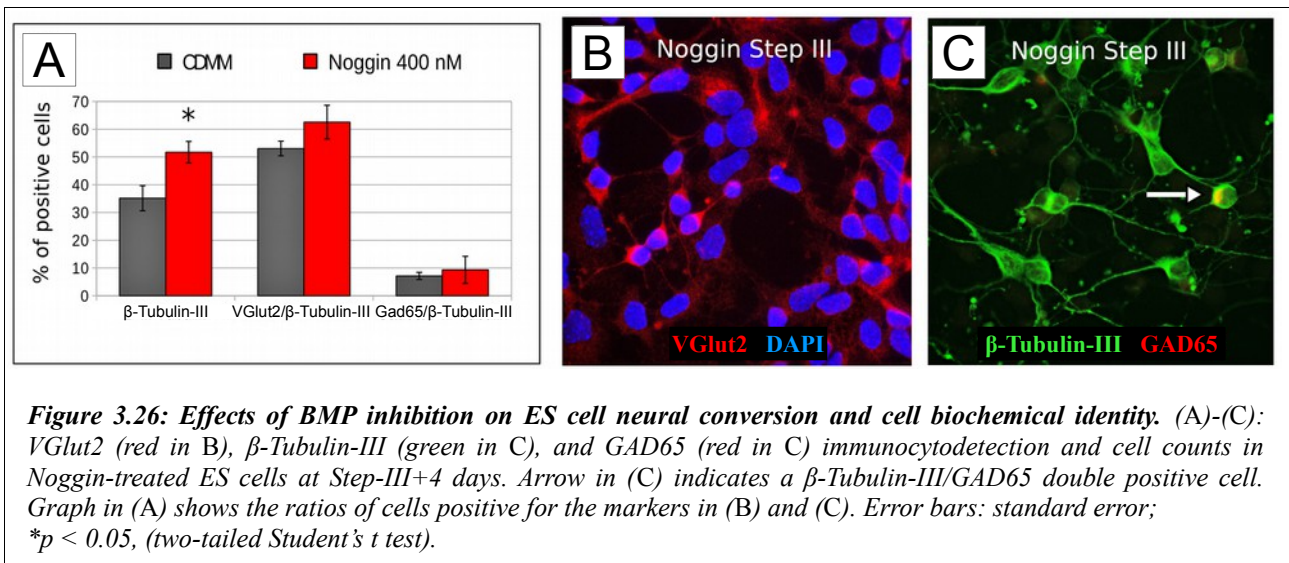


Figure 3.26: Effects of BMP inhibition on ES cell neural conversion and cell biochemical identity. (A)-(C): VGlut2 (red in B), β -Tubulin-III (green in C), and GAD65 (red in C) immunocytochemistry and cell counts in Noggin-treated ES cells at Step-III+4 days. Arrow in (C) indicates a β -Tubulin-III/GAD65 double positive cell. Graph in (A) shows the ratios of cells positive for the markers in (B) and (C). Error bars: standard error; * $p < 0.05$, (two-tailed Student's t test).

Expression fold change of genes coding for the neuronal receptorial apparatus after Noggin treatment				
See Materials and Methods for details				
GeneName	FoldChange	Regulation	SystematicName	Description
Adora1	4,15	Up	NM_001008533	ref Mus musculus adenosine A1 receptor (Adora1), transcript variant 1, mRNA [NM_001008533]
Adra2a	3,31	Up	NM_007417	ref Mus musculus adrenergic receptor, α 2a (Adra2a), mRNA [NM_007417]
Adrb1	2,2	Up	NM_007419	ref Mus musculus adrenergic receptor, β 1 (Adrb1), mRNA [NM_007419]
Chrb2	2,11	Up	NM_009602	ref Mus musculus cholinergic receptor, nicotinic, β polypeptide 2 (neuronal) (Chrb2), mRNA [NM_009602]
Cnr1	3,13	Up	NM_007726	ref Mus musculus cannabinoid receptor 1 (brain) (Cnr1), mRNA [NM_007726]
Gabrg2	6,92	Up	NM_008073	ref Mus musculus gamma-aminobutyric acid (GABA-A) receptor, subunit gamma 2 (Gabrg2), transcript variant 1, mRNA [NM_008073]
Gabra2	4,43	Up	NM_008066	ref Mus musculus gamma-aminobutyric acid (GABA-A) receptor, subunit α 2 (Gabra2), mRNA [NM_008066]
Gabrg2	4,08	Up	AK049857	gb Mus musculus adult male hippocampus cDNA, RIKEN full-length enriched library, clone:C630004C13 product:gamma-aminobutyric acid (GABA-A) receptor, subunit gamma 2, full insert sequence. [AK049857]
Gabra4	3,3	Up	NM_010251	ref Mus musculus gamma-aminobutyric acid (GABA-A) receptor, subunit α 4 (Gabra4), mRNA [NM_010251]
Gabra5	2,46	Up	NM_176942	ref Mus musculus gamma-aminobutyric acid (GABA-A) receptor, subunit α 5 (Gabra5), mRNA [NM_176942]
Gabra2	2,33	Up	AK048165	gb Mus musculus 16 days embryo head cDNA, RIKEN full-length enriched library, clone:C130038H23 product:gamma-aminobutyric acid (GABA-A) receptor, subunit α 2, full insert sequence [AK048165]
Gabrb3	2,09	Up	NM_008071	ref Mus musculus gamma-aminobutyric acid (GABA-A) receptor, subunit β 3 (Gabrb3), transcript variant 1, mRNA [NM_008071]
Gabrb1	2,03	Up	NM_008069	ref Mus musculus gamma-aminobutyric acid (GABA-A) receptor, subunit β 1 (Gabrb1), mRNA [NM_008069]
Gla2	3,53	Up	NM_183427	ref Mus musculus glycine receptor, α 2 subunit (Gla2), mRNA [NM_183427]
Grm1	6,51	Up	NM_016976	ref Mus musculus glutamate receptor, metabotropic 1 (Grm1), transcript variant 1, mRNA [NM_016976]
Grm8	3,57	Up	NM_008174	ref Mus musculus glutamate receptor, metabotropic 8 (Grm8), mRNA [NM_008174]
Grin3a	2,45	Up	ENSMUST00000076674	ens glutamate receptor ionotropic, NMDA3A Gene [Source:MGI (curated);Acc:Grin3a-002] [ENSMUST00000076674]
Grik2	2,35	Up	NM_010349	ref Mus musculus glutamate receptor, ionotropic, kainate 2 (β 2) (Grik2), transcript variant 2, mRNA [NM_010349]
Grik1	2,25	Up	NM_146072	ref Mus musculus glutamate receptor, ionotropic, kainate 1 (Grik1), transcript variant 1, mRNA [NM_146072]
Gria2	2,18	Up	NM_013540	ref Mus musculus glutamate receptor, ionotropic, AMPA2 (α 2) (Gria2), transcript variant 2, mRNA [NM_013540]
Grik4	2,1	Up	NM_175481	ref Mus musculus glutamate receptor, ionotropic, kainate 4 (Grik4), mRNA [NM_175481]
Grid2	2	Up	AK032669	gb Mus musculus 10 days neonate cerebellum cDNA, RIKEN full-length enriched library, clone:6530411F08 product:glutamate receptor, ionotropic, delta 2, full insert sequence. [AK032669]
Grin2c	2,9	Down	NM_010350	ref Mus musculus glutamate receptor, ionotropic, NMDA2C (epsilon 3) (Grin2c), mRNA [NM_010350]

Table 3

To investigate in detail the nature of cells generated by Noggin-treated ES cells, at the end of Step-III we analyzed at the cellular level the expression of FoxG1, which marks telencephalic progenitors, and Tbr1, which expression specifically identifies a sub-set of cortical neurons (Cajal-Retzius cells, subplate cells and glutamatergic neurons of the deep layers of the cerebral cortex; Hevner et al., 2001; the antibody was tested on a P7 mouse brain slice as positive control).

We decided to compare the expression of the two proteins in control cells and in cells differentiated in the presence of high doses of Noggin (150 and 400 nM). We also included some control treatment: cells treated with the chemical compound Dorsomorphin (5 μ M), cells ventralized with Shh agonist SAG (100 nM) and cells posteriorized by RA treatment (10 μ M) during Step-II. We found that, compared to control (**Figure 3.27A,E**), ES cells treated at Step-II with Noggin produced a higher ratio of both FoxG1-positive (**Figure 3.27B,D**) and Tbr1-positive cells at Step-III (**Figure 3.27F,H**).

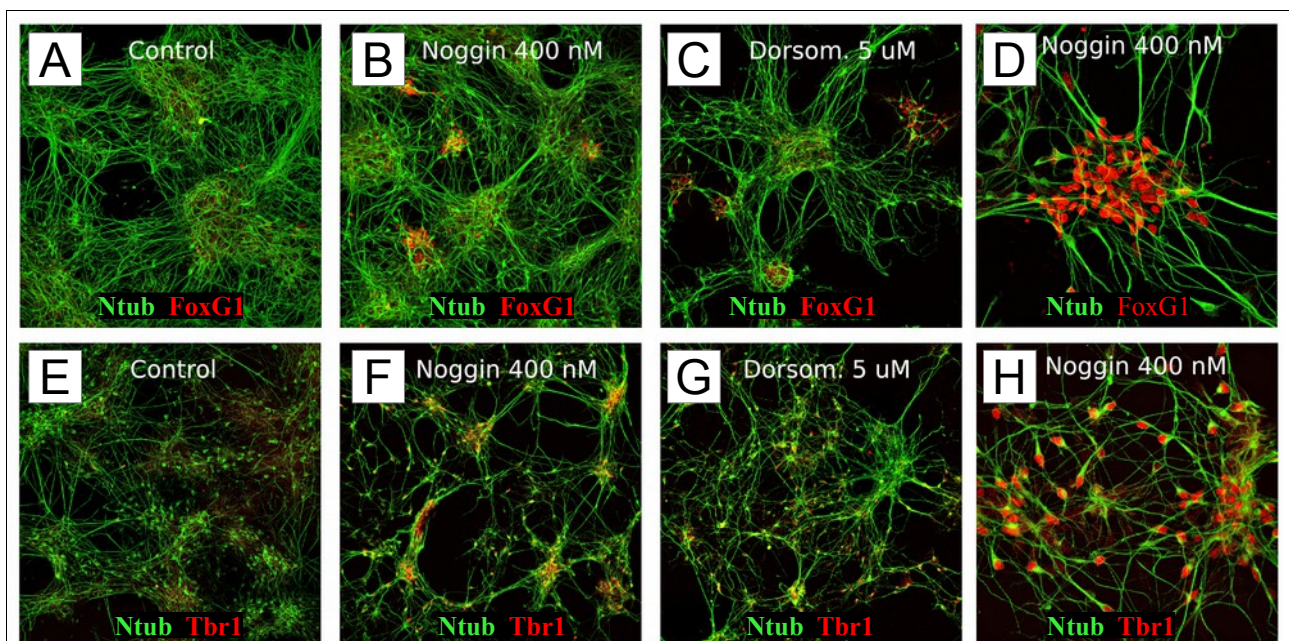
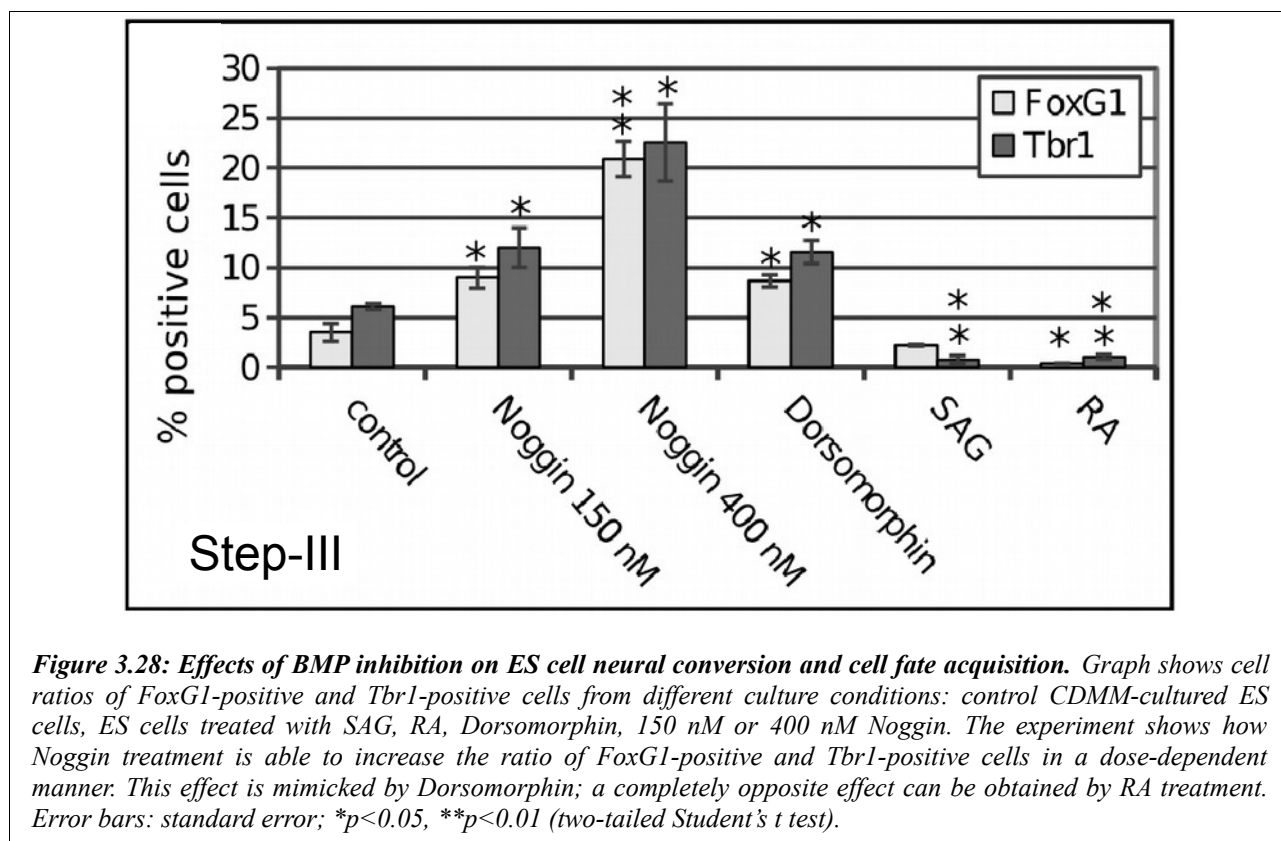


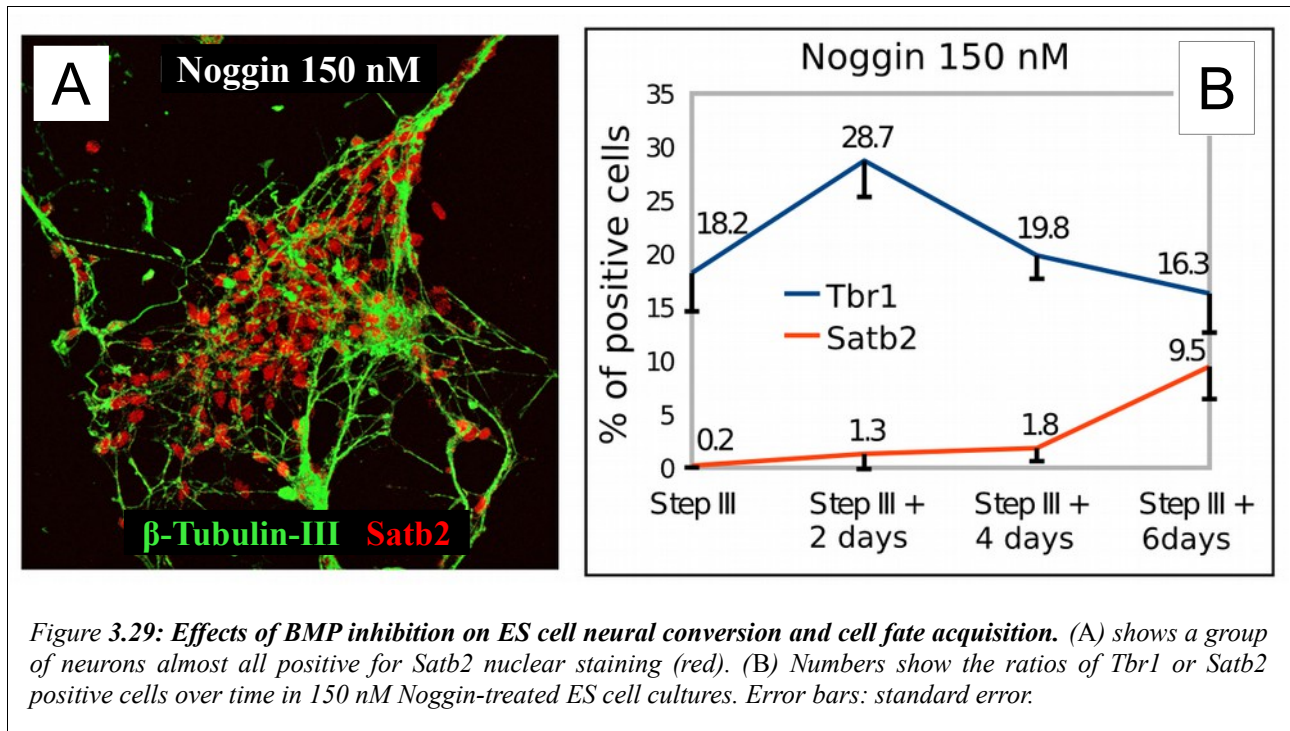
Figure 3.27: Effects of BMP inhibition on ES cells neural conversion and cell fate acquisition. (A)-(H): Immunocytochemistry of FoxG1 (red in A-D), Tbr1 (red in E-H) and acetylated-Tubulin (green in A-H) in ES cells at the end of Step-III after differentiation in CDMM (Control; A,E), CDMM plus Noggin (400 nM; B,D,F,H) and Dorsomorphin (5 μ M; C,G).

Consistently, the expression of both proteins was induced by Dorsomorphin and repressed by RA (**Figure 3.27C,G** and **Figure 3.28**). Ventralization induced by SAG inhibited Tbr1 expression and left FoxG1 expression almost unchanged (**Figure 3.28**).



Notably, Noggin-induced expression of Tbr1, which marks earlier cortical neurons, was followed by the activation of Satb2 (**Figure 3.29**), which labels late-generated cortical neurons of layers 2/3. To obtain late-generated neurons, cells were cultured for a longer period (up to a total of 18 days); N2 medium used for Step-III was gradually replaced with N2B27 starting from Step-III+4 days, to promote cell survival in long-term culture.

These results suggest that Noggin-treated ES cells follow a differentiation schedule similar to that of *in vivo* cortical neurons (**Figure 3.29B**), as previously reported by another group studying *in vitro* cortical differentiation (Gaspard et al., 2008).

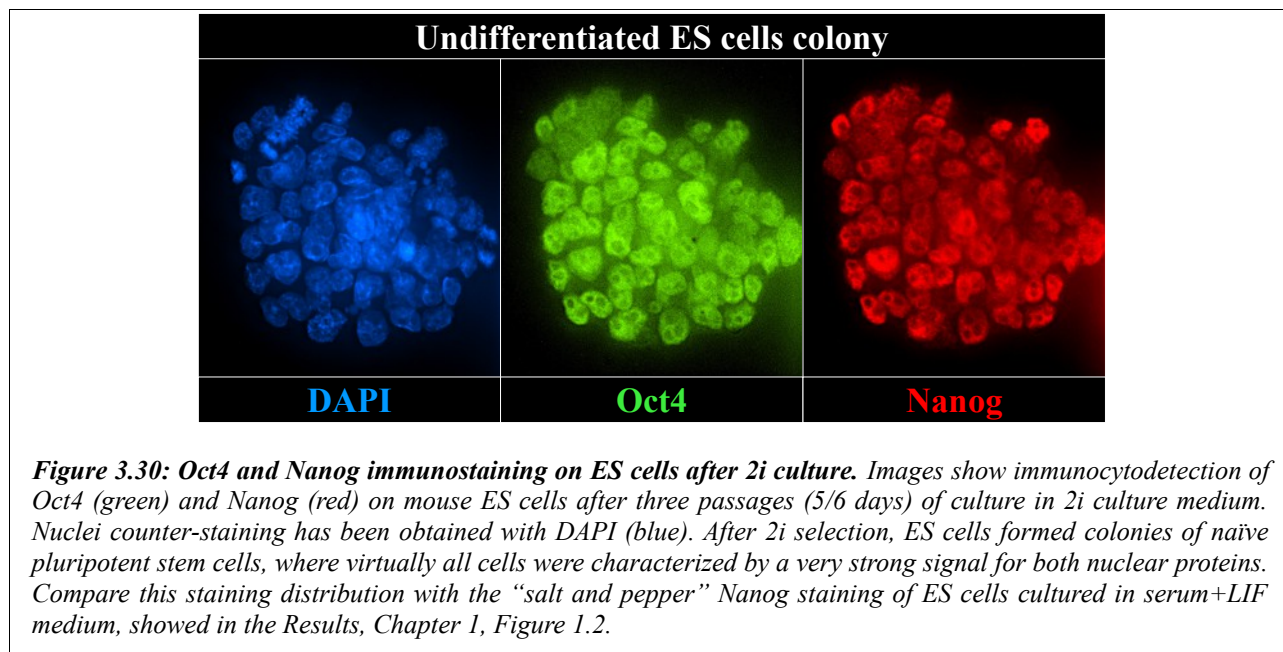


Recent reports showed how ES cells cultured in serum-containing medium are not homogeneous, and consist of a mixed population of Oct4-positive and Nanog-positive naïve pluripotent stem cells and Oct4-positive Nanog-negative stem cells, this latter type being already primed for differentiation (Silva et al., 2008). The authors demonstrated that ES cells in which mitogen-activated protein kinase signaling and glycogen synthase kinase-3 (GSK3) are double-inhibited are homogeneous and pluripotent when cultured in a medium containing LIF but devoid of serum, and consist in a pure population of both Oct4 and Nanog-positive naïve pluripotent stem cells (2i ES cells; Silva et al., 2008; Ying et al., 2008).

We considered the possibility that Noggin acts by selecting cells committed to a cortical identity, which might be already present in the heterogeneous situation of ES cell cultures maintained in serum+LIF. We thus assayed the effect of Noggin on ES cells selected in the absence of signals that might influence their differentiation potential; to this purpose we performed key experiments using ES cells cultured in 2i medium as starting material (2i ES cells).

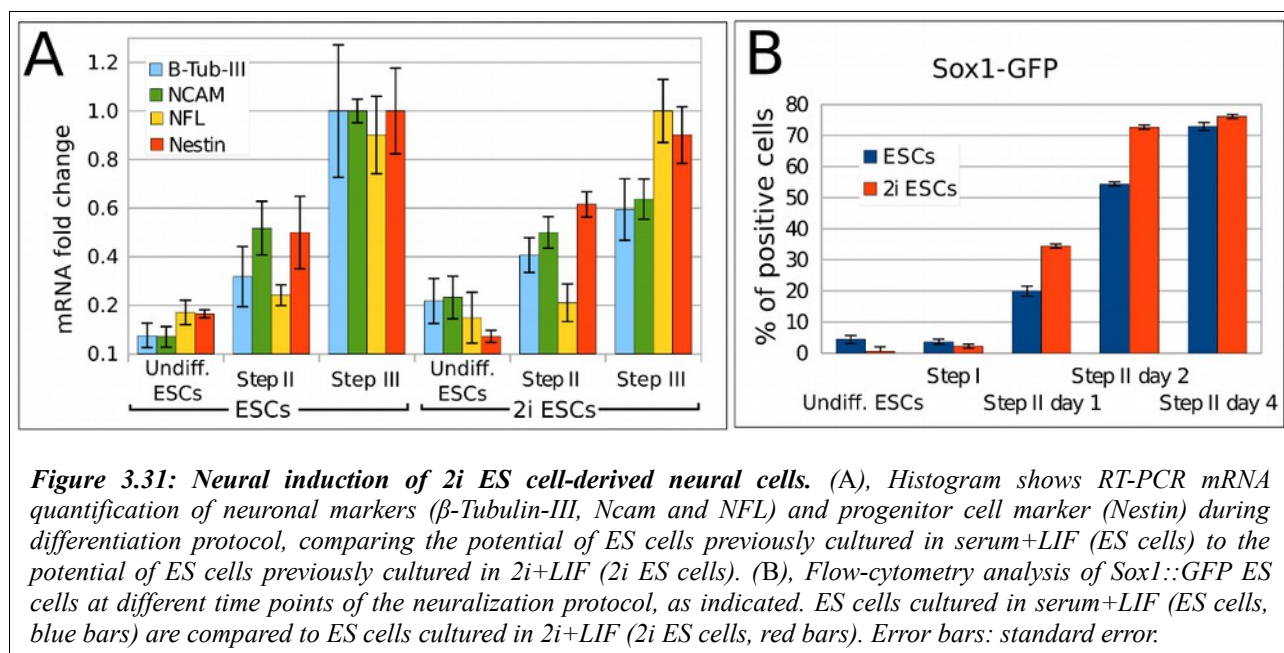
The effect of 2i culture was controlled by Oct4 and Nanog immunocytochemistry (**Figure 3.30**). ES cells cultured in 2i medium for three passages formed colonies of naïve pluripotent stem cells as showed in Ying et al., 2008, characterized by a very strong signal for both nuclear proteins. The

effect of culture in 2i medium and the signal homogeneity of 2i cultured colonies (**Figure 3.30**) can be easily appreciated by comparison with the heterogeneous situation of serum-cultured cells showed in Results, Chapter 1, Figure 1.2.



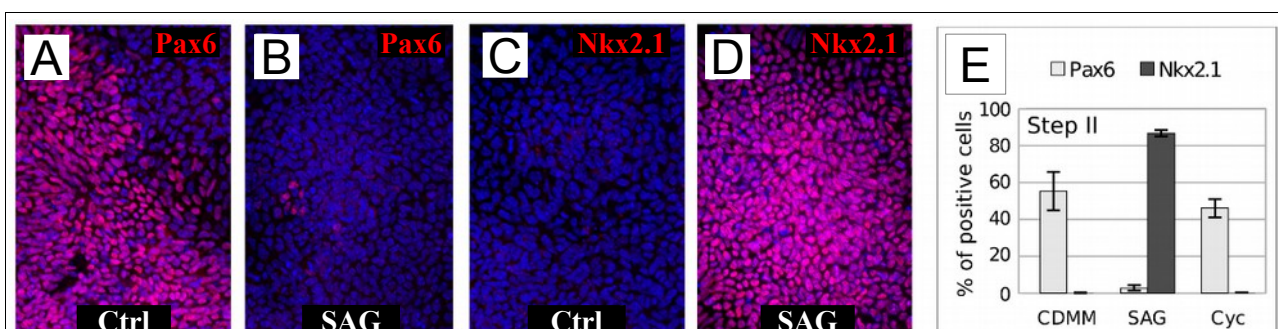
We started the analysis by comparing the neuralization potential of ES cells previously cultured in serum+LIF (ES cells) to the potential of ES cells previously cultured in 2i+LIF (2i ES cells). RT-PCR mRNA quantification of neuronal markers (β -Tubulin-III, Ncam and NFL) and progenitor cell marker (Nestin) during differentiation protocol, showed no significant difference in the expression of these markers between ES cells and 2i ES cells, except for the expression of Ncam, which was slightly lower at Step-III in 2i ES cells (64%) compared to ES cells (**Figure 3.31A**).

Flow-cytometry analysis of Sox1::GFP ES cells at different time points of the neuralization protocol showed how Sox1-driven GFP is almost not expressed in undifferentiated 2i ES cells and expressed at low levels in undifferentiated ES cells, it is activated earlier in 2i ES cells compared to ES cells by the differentiation protocol and it is expressed at similar levels at the end of Step-II. This is consistent with a higher homogeneity and a faster neuralization of 2i ES cells compared to ES cells (**Figure 3.31B**). We concluded that in our protocol, 2i ES cells neuralization was slightly faster than the neuralization of ES cells maintained in serum+LIF (**Figure 3.31**).

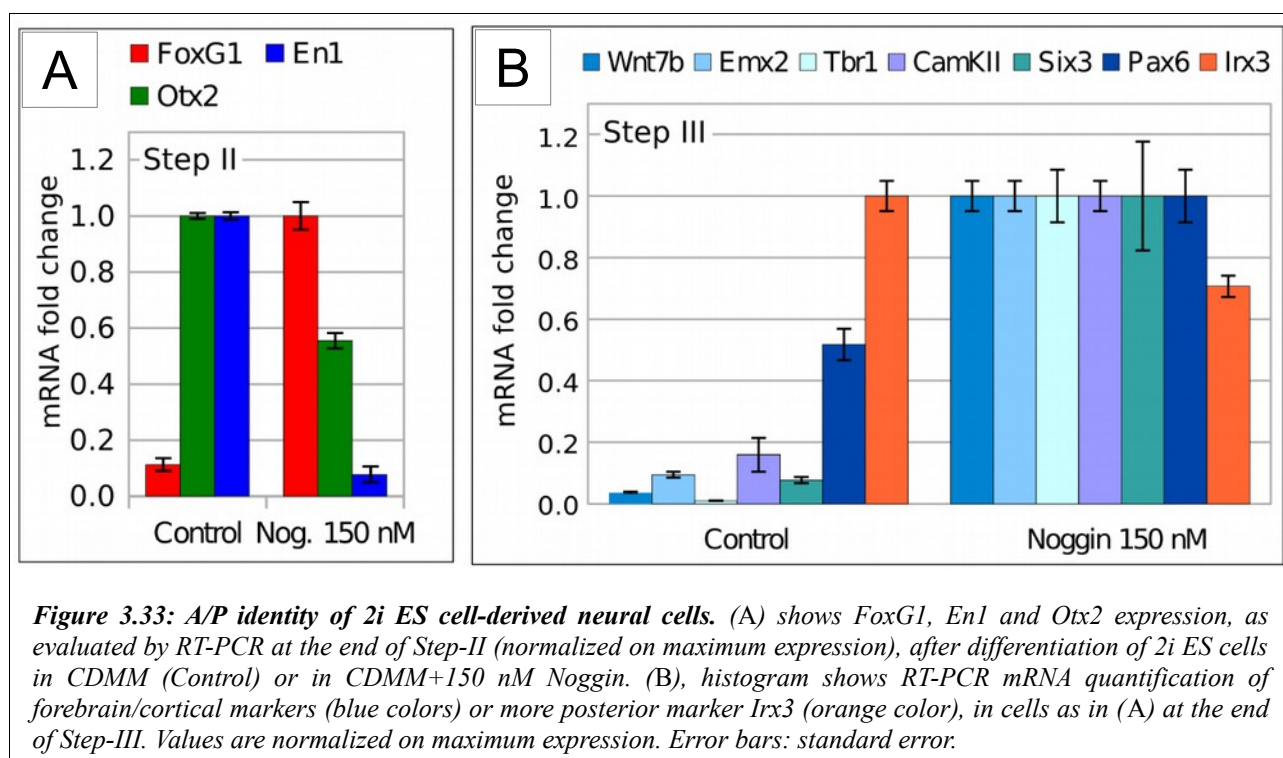


However, the expression of A/P and D/V markers in neural cells obtained by 2i ES cells was comparable to the expression in neural cells obtained by ES cells cultured in serum (Figure 3.32).

Immunocytochemistry of Pax6 (Figure 3.32A,B) and Nkx2.1 (Figure 3.32C,D) at the end of Step-II in 2i ES cells differentiated in CDMM (control), in CDMM+SAG and in CDMM+Cyclophamine resulted in fractions of Pax6-positive cells and Nkx2.1-positive cells very similar to those obtained with ES cells cultured in serum (see Figure 3.13A,B).

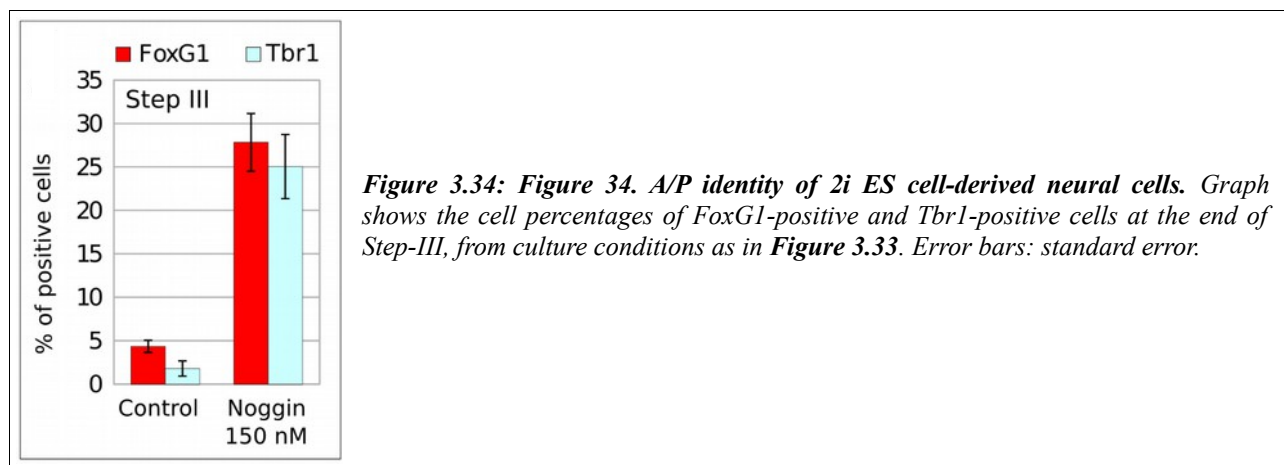


Concerning A/P patterning, we evaluated the expression of forebrain/cortical markers (FoxG1, Wnt7b, Emx2, Tbr1, CamKII, Six3 and Pax6) or of more posterior markers (En1, Irx3 and Otx2) by RT-PCR at the end of Step-II, after differentiation of 2i ES cells in CDMM (Control) or in CDMM plus 150 nM Noggin (**Figure 3.33**). We basically obtained the same results previously observed using ES cells cultured in serum.



Moving at a protein level, cell percentages of FoxG1-positive and Tbr1-positive cells at the end of Step-III, from control CDMM cells and cells differentiated with 150nM Noggin, were similar to previous experiments (**Figure 3.34**).

For this reason, we can exclude that our results might be influenced by some heterogeneity of the starting ES cell population due to culture and amplification in serum-containing medium.



Going back to serum-cultured ES cells, we decided to characterize the identity of Noggin-treated cells in more detail by comparing their global gene expression profiles to the profiles of ES cells differentiated in other culture conditions, or to the profiles of embryonic brain regions. To this purpose, we performed microarray hybridization (see Materials and Methods).

As RA is a potent inducer of neuronal differentiation (Guan et al., 2001), we compared its action to that of Noggin on ES cell differentiation. We analyzed gene expression profiles using Gene Set Enrichment Analysis (GSEA). GSEA is a computational method which allows to identify, within predefined groups of genes (gene sets associated with particular cellular functions) whether a significant enrichment of regulated genes occurs when comparing two conditions (Subramanian et al., 2005). **Figure 3.35** shows gene ontology categories implicated in neuronal function/differentiation and cell cycle control. The color heat map displays gene set enrichment scores for Noggin-treated (400 nM) versus control ES cells (first column) and for RA-treated (10 μ M) versus control ES cells (second column). Comparing Noggin to RA reveals that both molecules induce highly concordant effects, as seen by the up-regulation of gene sets associated to neuronal differentiation and by the repression of gene sets related to cell proliferation and cell cycle progression.

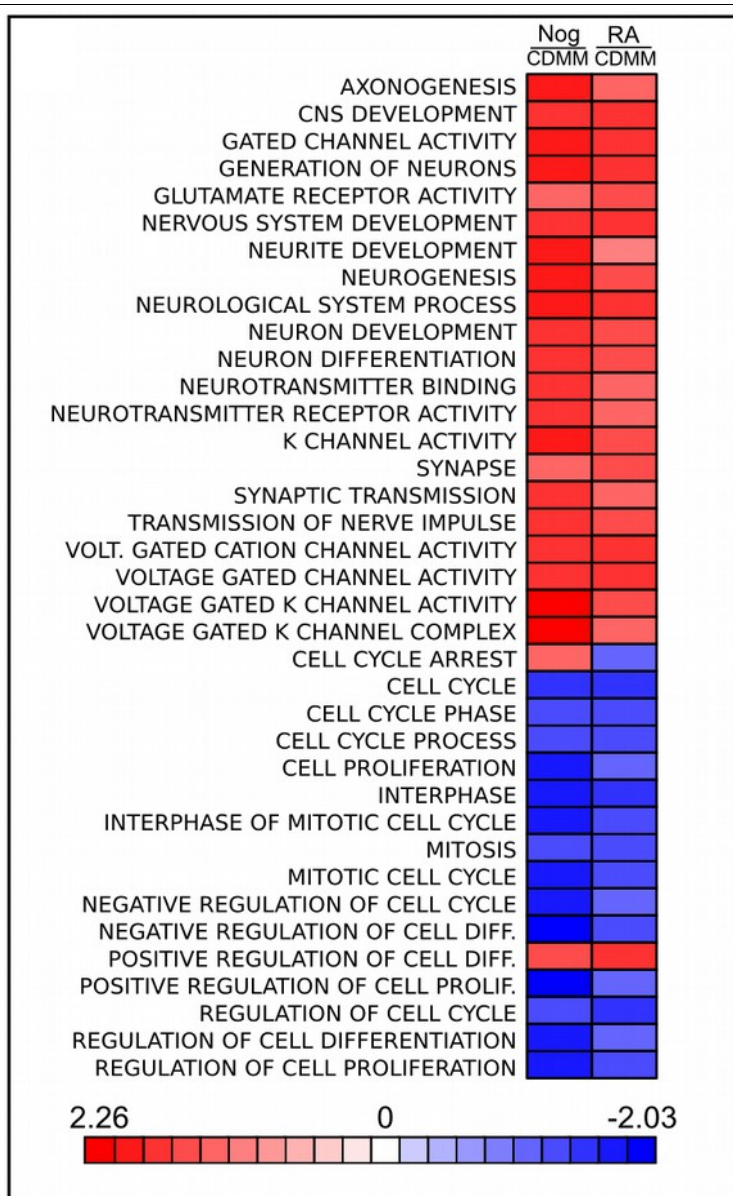
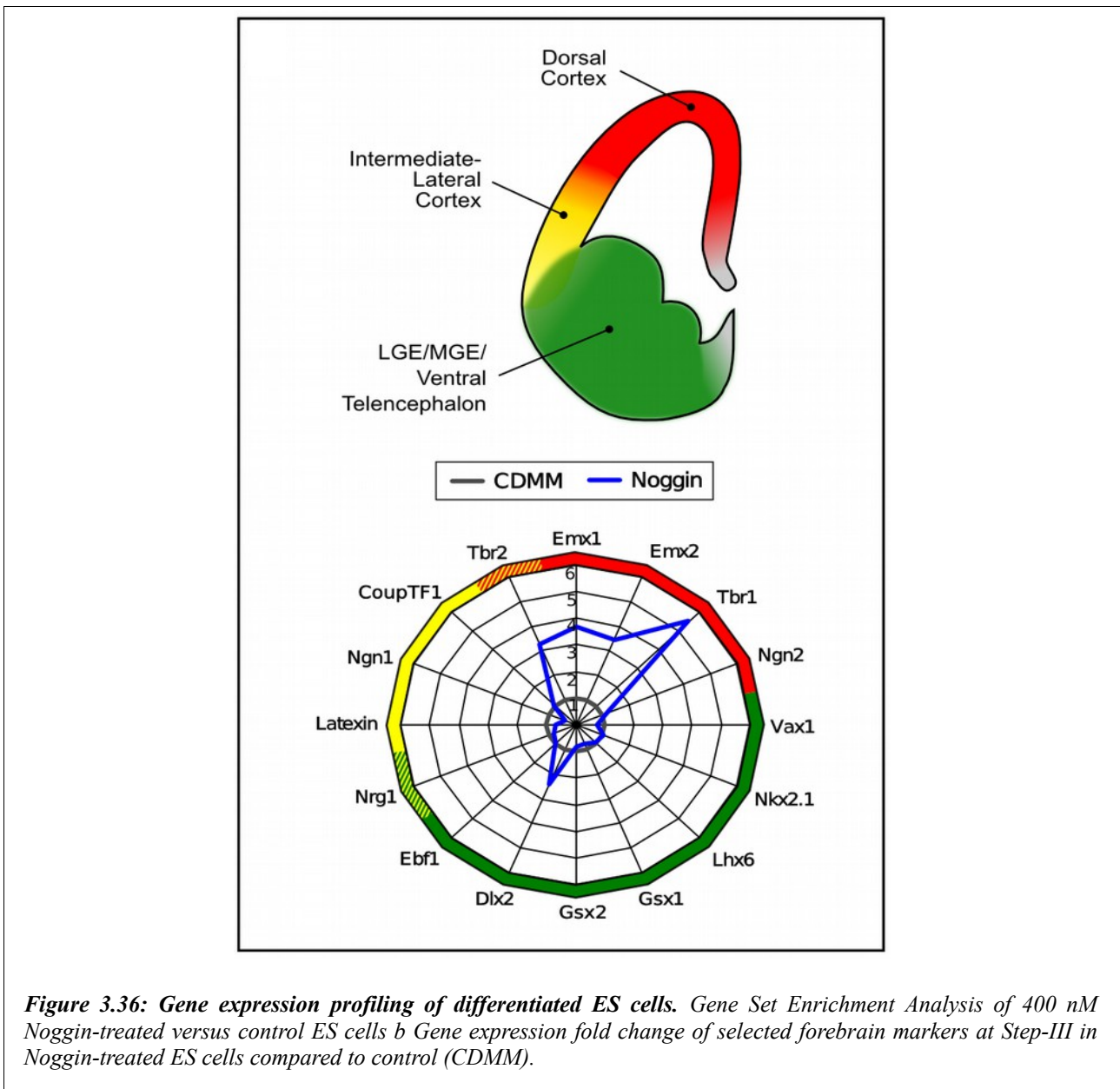


Figure 3.35: Gene expression profiling of differentiated ES cells. Gene Set Enrichment Analysis of 400 nM Noggin-treated versus control ES cells (Nog/ CDMM, first column) and 10 μ M RA-treated versus control ES cells (RA/CDMM, second column), filtered for neuronal function/differentiation and control of cell cycle. Heat map color scale indicates gene set enrichment scores.

We then investigated the effect of Noggin on positional identity. Noggin induced the expression of a number of dorsal-telencephalic markers and left almost unchanged the expression of intermediate-lateral or ventro-basal markers. This was evaluated by comparing the mRNA expression profile of ES cells treated with Noggin (400 nM) to that of control (CDMM-differentiating ES cells; **Figure 3.36**).



To study the effects of Noggin and RA on anterior/posterior (A/P) identity of ES cells, we selected a predefined subset of developmental genes known to pattern the A/P axis of the CNS (See Materials and Methods), and we analyzed their expression, using RA treatment as a control for posteriorization of ES cells. A number of these genes were coherently regulated in Noggin-treated ES cells and E16 cortex, or in RA-treated ES cells and E16 hindbrain, suggesting a certain similarity of treated ES cells and corresponding brain regions (**Figure 3.37**).

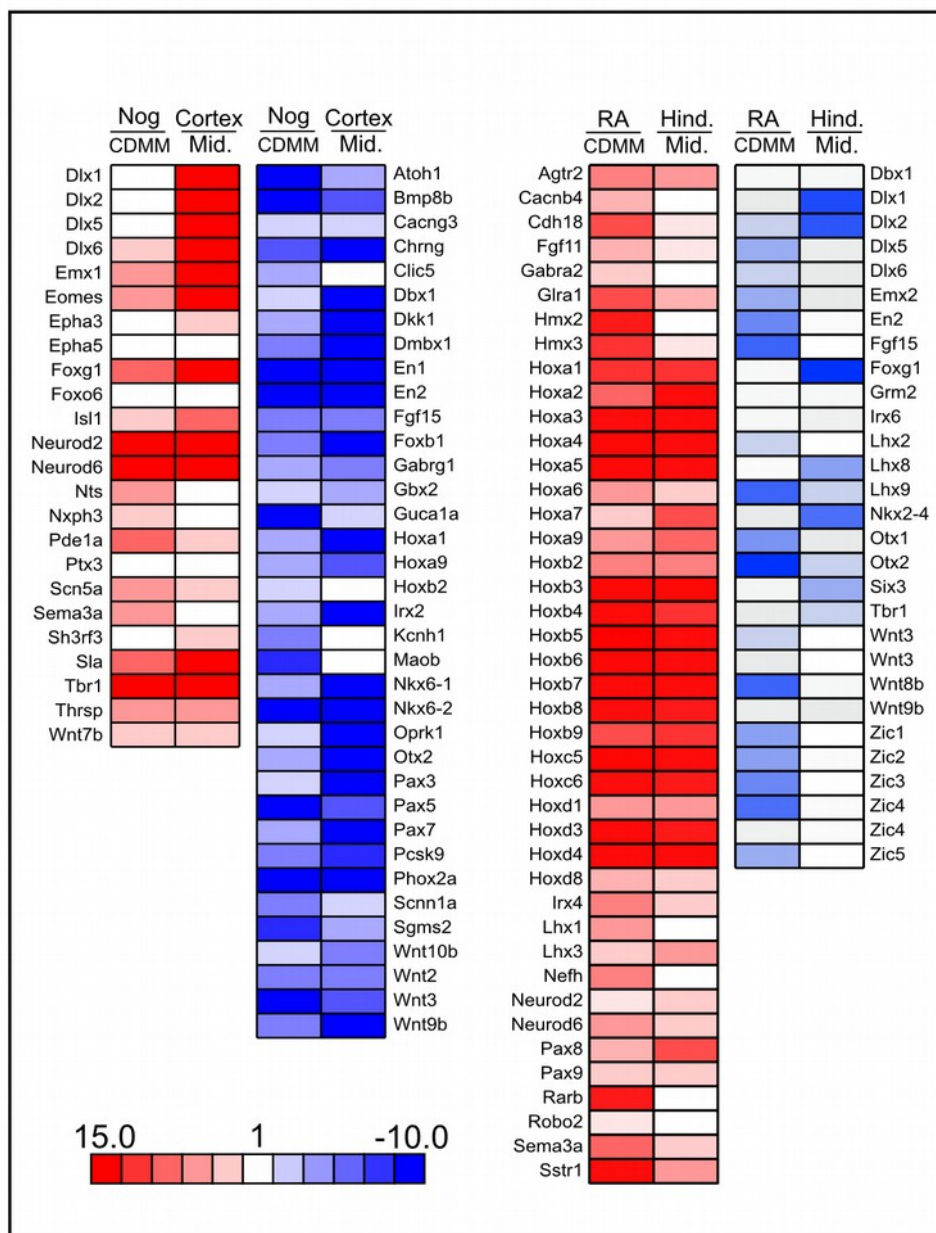


Figure 3.37: Gene expression clustering of ES cells and E16 brain tissues. Expression profiling of a predefined subset of developmentally expressed genes known to pattern the A/P axis of the central nervous system (CNS). The figure shows a heat map of the expression analysis of such genes, which are differentially regulated in Noggin-treated cells compared to control (Nog/CDMM) and in E16 cortex compared to E16 midbrain (Cortex/Mid.), or that are differentially regulated in RA-treated cells compared to control (RA/CDMM) and in hindbrain compared to E16 midbrain (Hind/Mid.). Some of these genes were coherently regulated in Noggin treated ES cells and E16 cortex, or in RA treated ES cells and E16 hindbrain, suggesting a similar identity of treated ES cells and corresponding brain regions.

To further characterize ES cell positional identity, we extracted a list of genes that are differentially expressed along the A/P axis of developing brain. We chose 592 genes that were differentially expressed between E16 cortex and E16 hindbrain with absolute fold-change greater than, or equal to, 10 fold. This gene set was first analyzed by Principal Component Analysis (PCA) to assay the effect of Noggin on ES cell positional identity. PCA is an unbiased method of analysis that projects data variability on a reduced number of orthogonal axes, such that the first axis captures the highest degree of variance in gene expression (Component 1), and subsequent axes (Component 2, ... ,n) correspond to successively decreasing variance. The Components capturing the highest degrees of variance identify the qualities mostly discriminating among data populations.

Figure 3.38 shows a plot of the first two Principal components, which account for 64.15% (Component 1) and for 18.64% (Component 2) of variance between samples. Component 2 discriminates ES cells (cyan items) from brain tissues (orange items). As expected by the nature of gene set selection, Component 1 discriminates the A/P identity (dashed lines in **Figure 3.38**). Notably, Noggin-treated ES cells have more positive values on Component 1 than control ES cells, confirming the anteriorizing effect of BMP inhibition. As an internal control of the analysis, RA-treated ES cells show an opposite trend, consistently with RA posteriorizing effect.

The same gene selection of 592 genes was used for hierarchical gene clustering analysis (see Materials and Methods) of either Noggin-treated or RA-treated ES cells, with the three brain regions (**Figure 3.39** and **Figure 3.40**). We found that the gene expression profile of Noggin-treated ES cells clustered with that of cerebral cortex (0.44 correlation factor), whereas the RA profile clustered with midbrain/hindbrain profile, although with a lower extent (0.14 correlation factor).

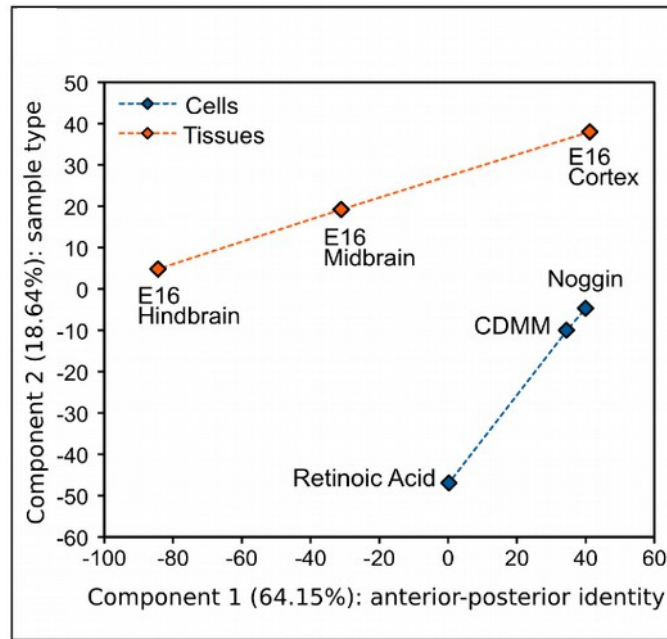


Figure 3.38: Gene expression profiling of differentiated ES cells. Principal component analysis of ES cells and E16 brain regions (see text for details).

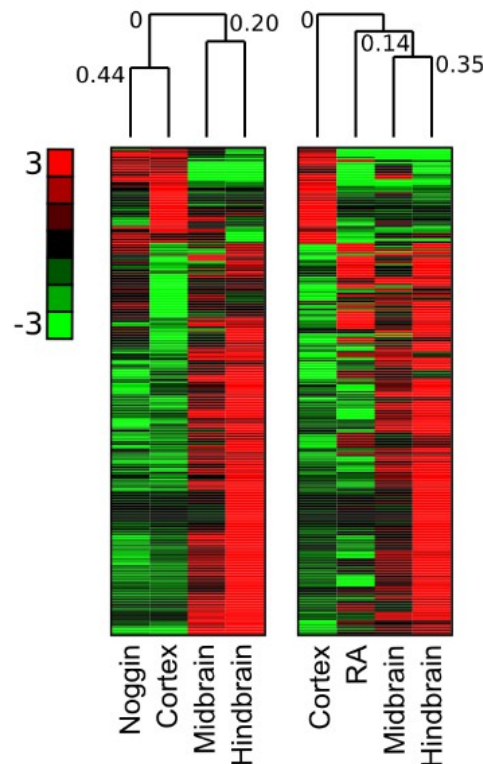


Figure 3.39: Gene expression profiling of differentiated ES cells. Hierarchical gene clustering analysis of ES cells and E16 brain regions. The first 390 genes are shown (complete clustering is displayed in **Figure 3.40**). Numbers over the branching report Euclidean distance correlation. Heat map color scale indicates normalized gene expression.

Regions of high concordance between the differentiated ES cells and the corresponding brain region are shown in **Figure 3.40** and correspond to known genes of A/P patterning, including those genes whose expression was analyzed by RT-PCR.

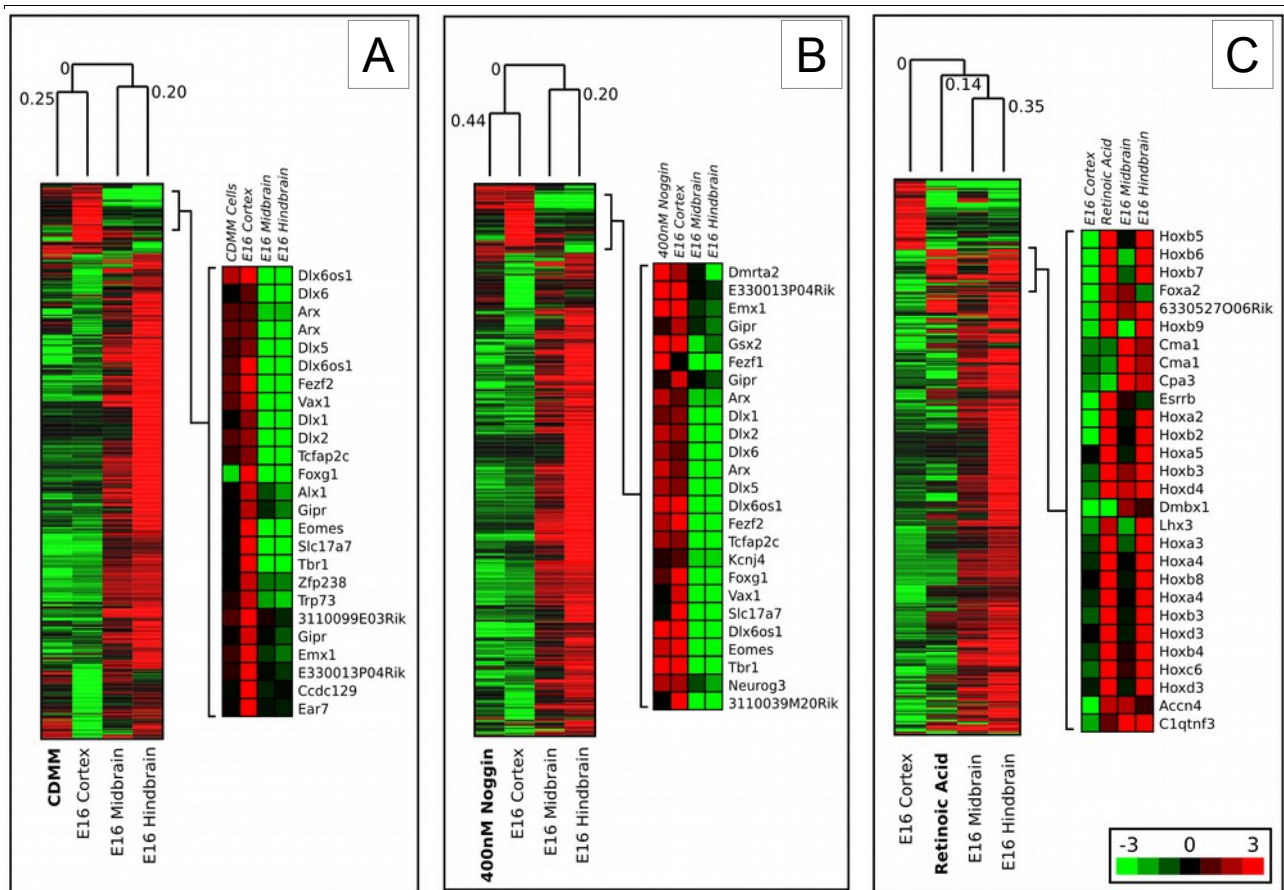


Figure 3.40: Gene expression clustering of ES cells and E16 brain tissues. A-C, Hierarchical gene clustering analysis of ES cells at Step-III, after differentiation in defined culture conditions, and E16 brain regions. Numbers over the branching report Euclidean distance correlation. Enlarged aspects indicated by brackets are regions of high concordance between differentiated ES cells and the corresponding brain region. Genes shown in these enlarged regions are mainly developmental genes whose expression patterns the CNS A/P axis and that significantly contributed to the clustering. Heat map color scale indicates normalized gene expression.

We concluded that Noggin, in addition to its known role as neural inducer, plays a major role in establishing an anterior, cortical fate.

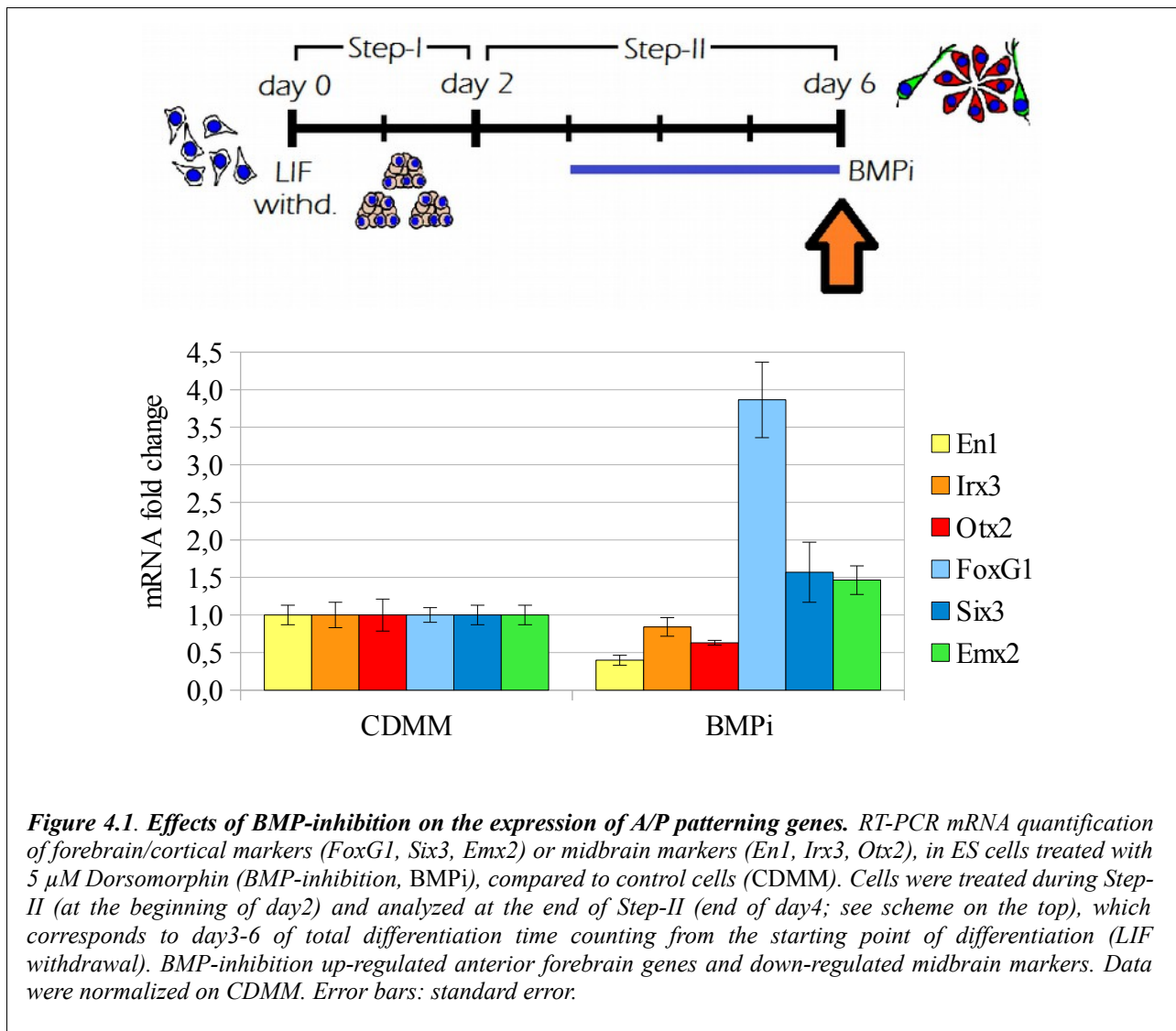
4– The Making of a Cortex: Wnt vs. BMP

Efficient Corticogenesis *in vitro* by Double Inhibition of Endogenously Produced BMP and Wnt Factors.

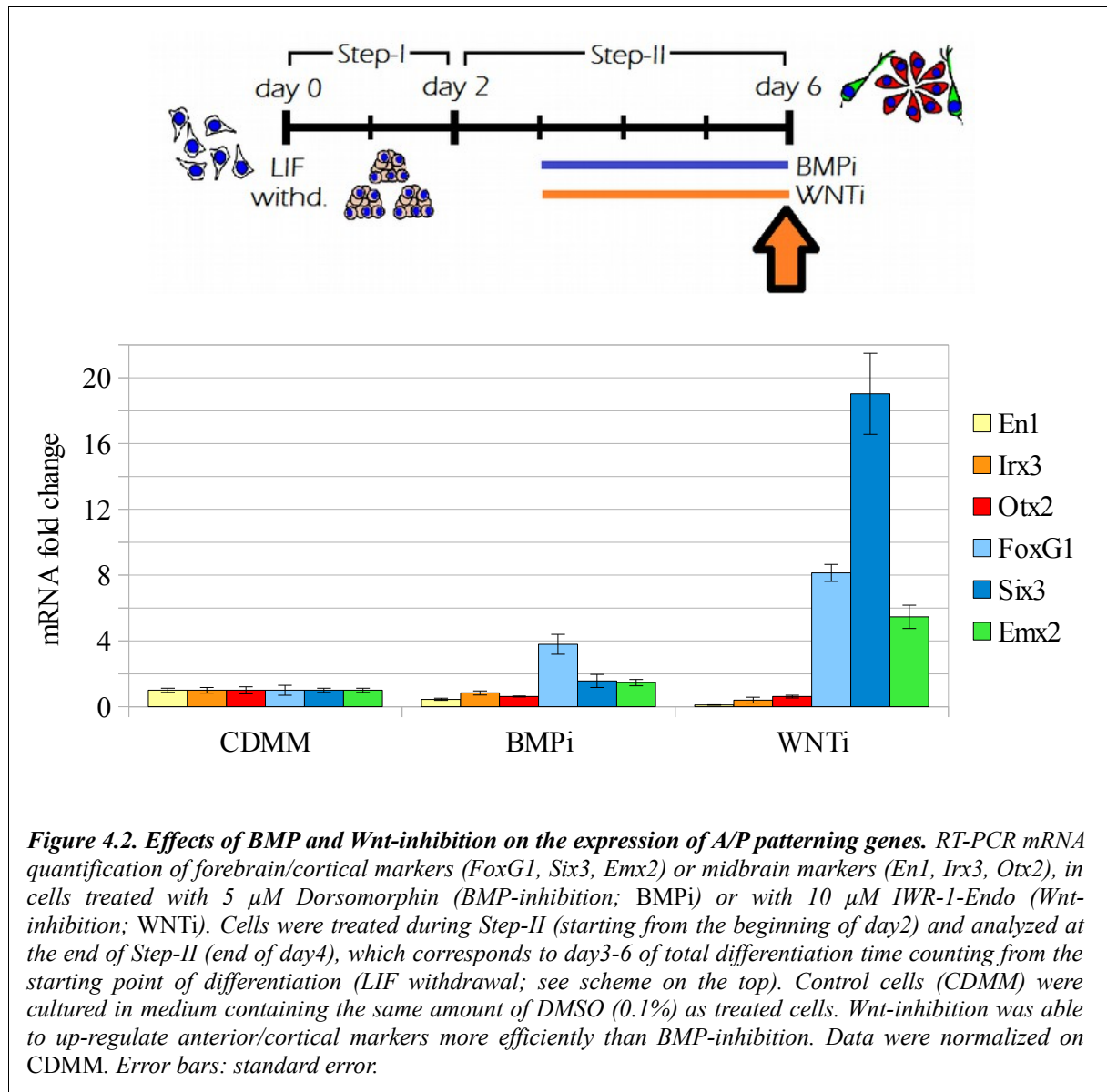
We showed that mouse ES cells express different morphogens during neural differentiation *in vitro*, especially BMPs and Wnts (Results, Chapter 2). We demonstrated that endogenously produced morphogens can affect ES cell regional fate acquisition; Noggin-mediated BMP-inhibition was necessary and sufficient to acquire a telencephalic identity in our culture system (Results, Chapter 3). We then asked whether endogenously produced Wnts could contribute to pattern neuralizing ES cells, by masking an intrinsic telencephalic differentiation fate.

As showed before (Results, Chapter 3), we characterized our control culture (ES cells differentiated in CDMM), by analyzing the expression of genes that display an ordered (A/P) expression that covers the most anterior area of forebrain (FoxG1, Emx2), entire forebrain (Six3), forebrain/midbrain (Otx2) and midbrain (En1). Data suggested that in our protocol of differentiation ES cells mostly adopt a midbrain / dorsal identity when cultured in CDMM. Compared to control, BMP-inhibition mediated by Noggin or by the chemical drug Dorsomorphin induced the telencephalic marker FoxG1 and repressed the more posterior markers Otx2 and En1, as evaluated at the end of Step-III (See Results, Chapter 3, **Figure 3.16**). We repeated this analysis at the end of

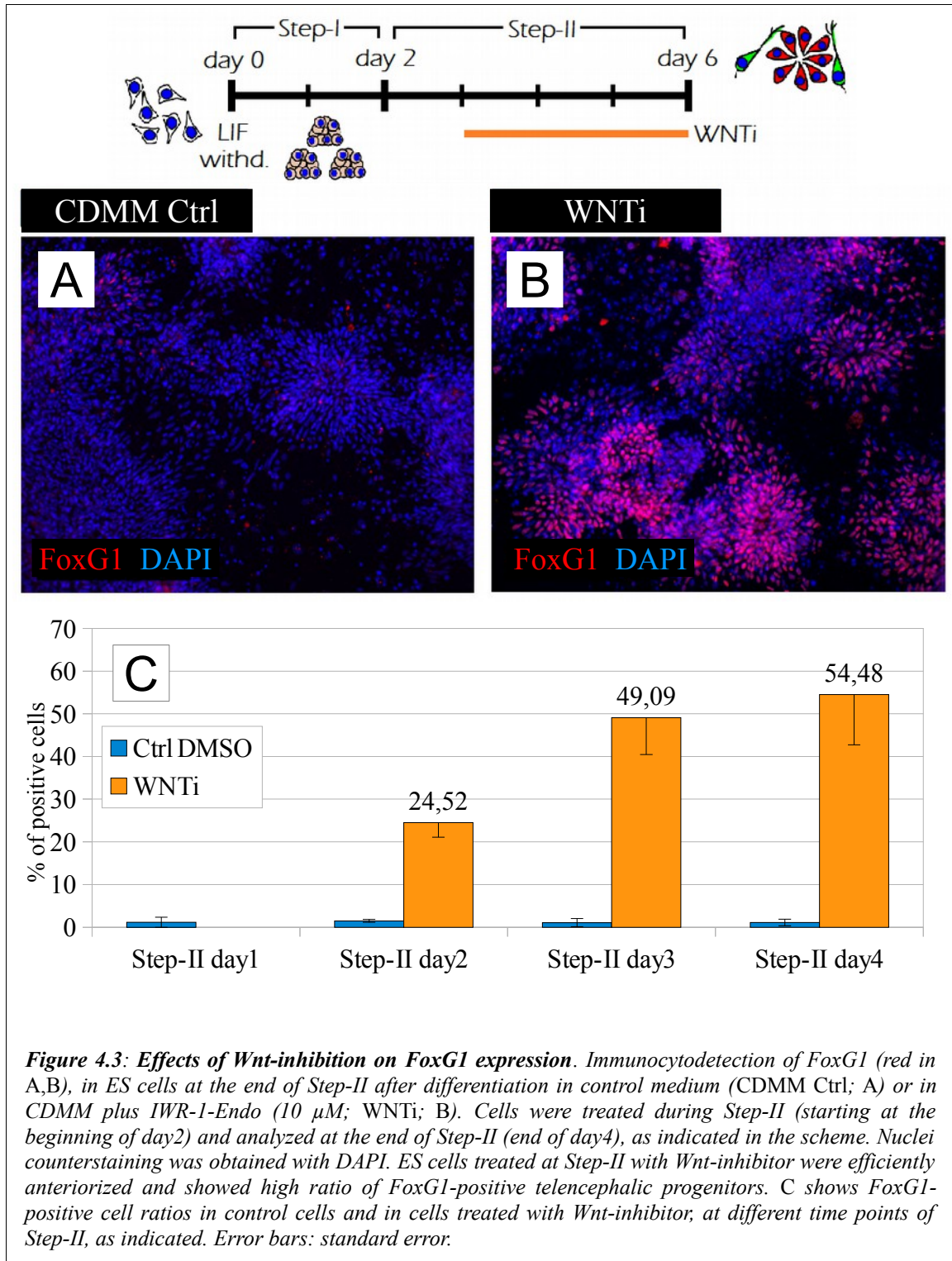
Step-II, confirming the data (**Figure 4.1**). Moreover, Dorsomorphin induced the expression of anterior markers Six3 and Emx2 (**Figure 4.1**).



Surprisingly, when the same analysis was performed after a Wnt-inhibition treatment (via treatment with 10 μ M IWR-1-Endo during Step-II), we noticed a very strong anteriorizing effect on ES cell differentiation fate, compared to BMP-inhibition. Posterior markers *En1* and *Irx3* were strongly down-regulated by IWR-1-Endo treatment, while anterior markers *Six3*, *FoxG1* and *Emx2* were up-regulated up to 20-folds compared to control cells (**Figure 4.2**).

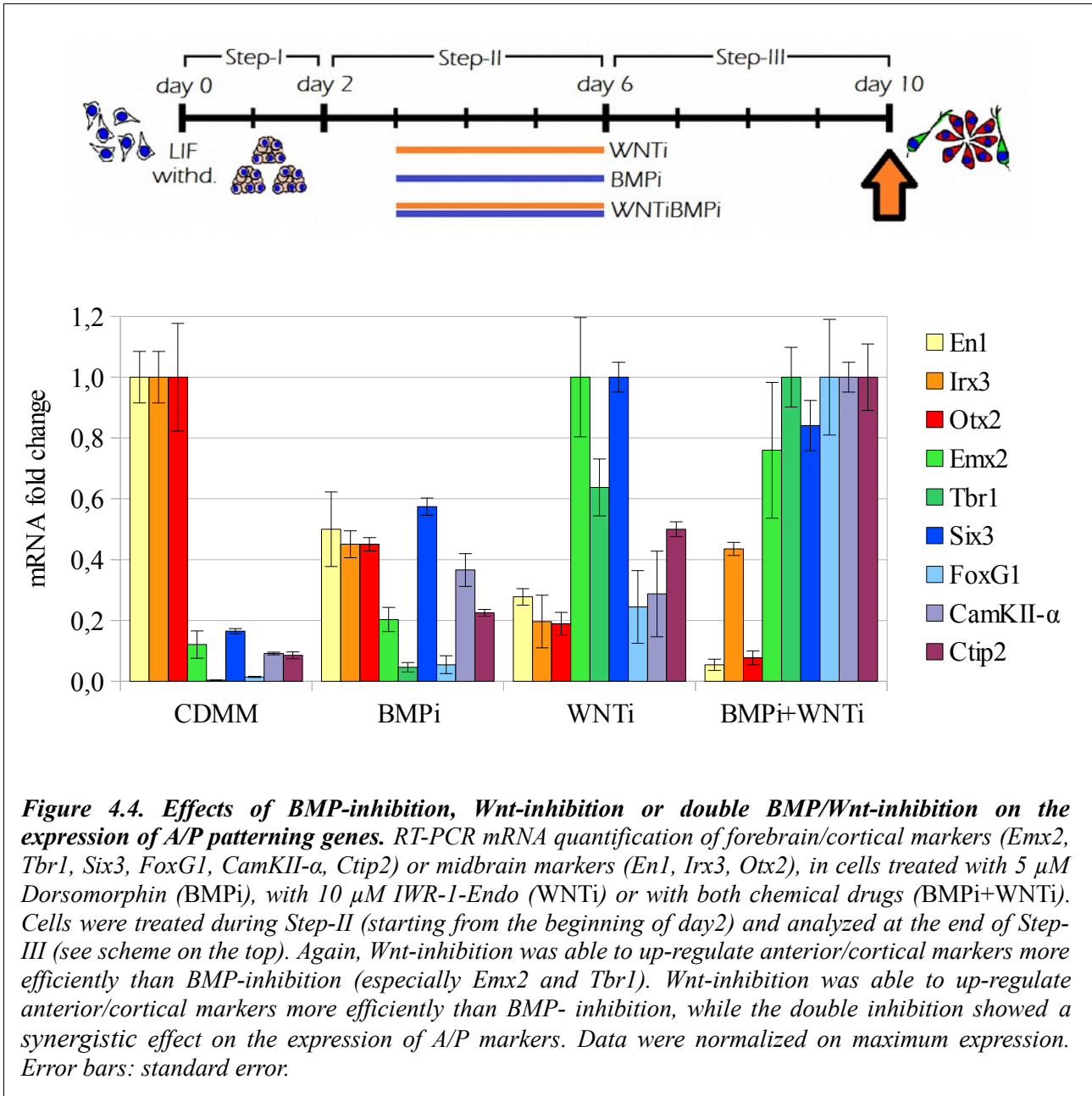


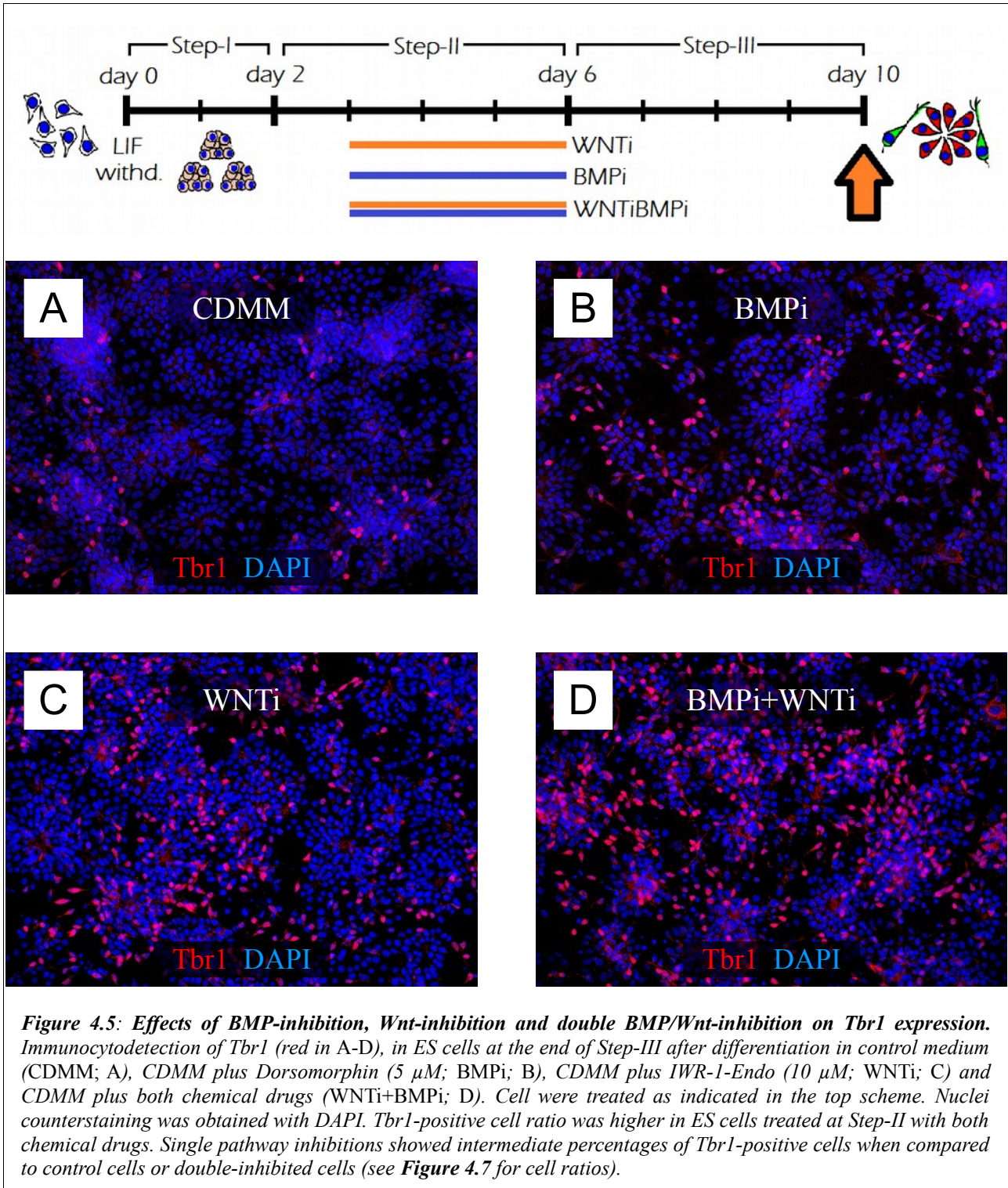
The expression of anterior/telencephalic marker *FoxG1* was also evaluated by immunocyto detection (**Figure 4.3A,B**). ES cells treated with Wnt-inhibitor during Step-II efficiently expressed *FoxG1* (54.5% *FoxG1*-positive cells; **Figure 4.3C**), while labeling was almost absent in control cells (1.1% *FoxG1*-positive cells). We found that *FoxG1* expression rapidly switched-on during Step-II: at the end of Step-II day2, only 24-hours after the starting point of Wnt-inhibition treatment, 24.2% of cells were already showing *FoxG1* nuclear staining (**Figure 4.3C**).



Then, we tested whether a double inhibition of BMP and Wnt pathways could strengthen ES cell cortical conversion (**Figure 4.4**). Cells were treated during Step-II with 5 μ M Dorsomorphin (BMP-inhibition, BMPi), with 10 μ M IWR-1-Endo (Wnt-inhibition, WNTi) or with the combination of both chemical compounds (BMP/Wnt double inhibition, BMPi+WNTi), and A/P marker expression was evaluated at the end of Step-III. Single inhibitions were both efficient for ES cell corticalization, as seen by midbrain markers down-regulation and forebrain marker up-regulation. Again, Wnt-inhibition was able to up-regulate anterior/cortical markers more efficiently than BMP-inhibition (see FoxG1, Emx2, Tbr1 and Six3 expression levels). However, double BMP/Wnt-inhibition showed a even stronger down-regulation of En1 and Otx2 and more efficient up-regulation of cortical markers FoxG1, Ctip2, Tbr1 and CamKII- α , compared to single treatments. These results suggest a synergistic effect of BMP and Wnt pathway inhibition for the acquisition of a telencephalic fate (**Figure 4.4**).

To investigate in detail the nature of neural cells generated by ES cells treated with BMP/Wnt-inhibition, we analyzed the expression of the cortical marker Tbr1, which specifically identifies a sub-set of early-generated cortical neurons, at the end of Step-III. Control cells were compared with Dorsomorphin-treated cells (BMPi), IWR-1-Endo-treated cells (Wnti) and double treated cells (BMPi+WNTi). We found that, compared to control cells, ES cells treated with Dorsomorphin or with IWR-1-Endo during Step-II produced a higher ratio of Tbr1-positive cells at the end of Step-III (10% and 14,7%, respectively, compared to 3% of control). Tbr1-positive cell ratio was even higher after double BMP/Wnt-inhibition (28.2% Tbr1-positive cells) (**Figure 4.5** and **4.7**).





We obtained consistent results by analyzing the expression of another cortical marker, *Ctip2*, which labels medium/early-generated cortical neurons of layer 5. *Ctip2*-positive cells were only 1.5% in control cells and increased to 14.8% in cells treated with double BMP/Wnt-inhibition (**Figure 4.6**).

Again, single BMP or Wnt-inhibitions showed intermediate results (3.5% Ctip2-positive cells after BMP-inhibition, 9.7% positive cells after Wnt-inhibition) (**Figure 4.7**).

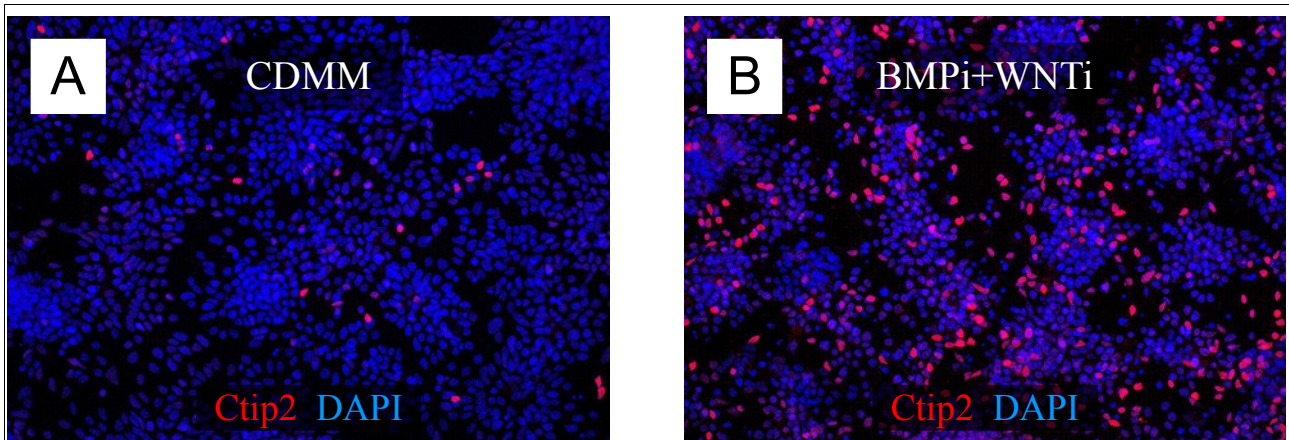


Figure 4.6: Effects of double BMP/Wnt-inhibition on Ctip2 expression. Immunocytochemistry of Ctip2 (red in A and B), in ES cells at the end of Step-III after differentiation in control medium (CDMM; A) or double pathway inhibition (WNTi+BMPi; B). Cells were treated as indicated in **Figure 4.5**. Nuclei counterstaining was obtained with DAPI. Ctip2-positive cell ratio was higher in ES cells treated at Step-II with both chemical drugs (see **Figure 4.7** for cell ratios).

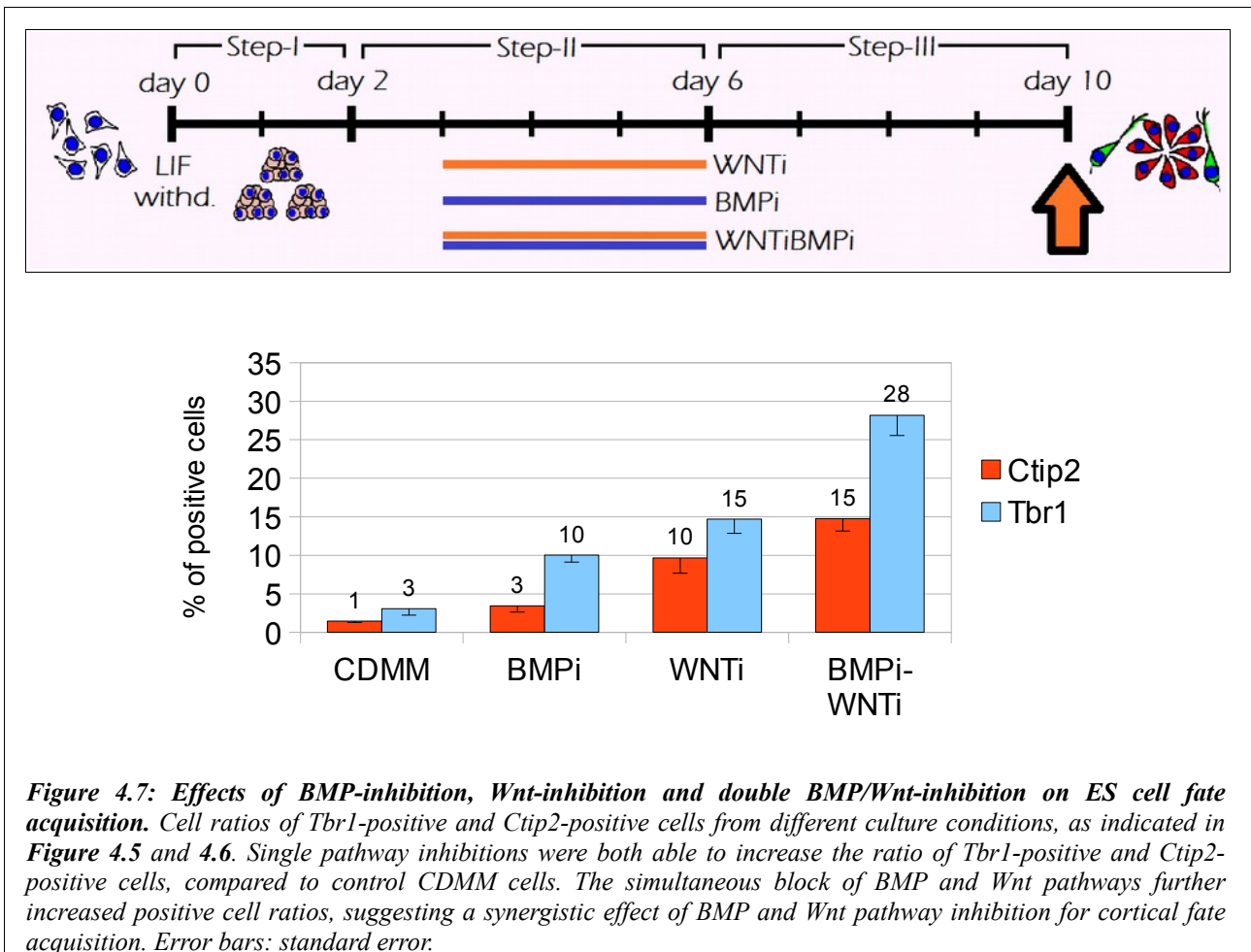


Figure 4.7: Effects of BMP-inhibition, Wnt-inhibition and double BMP/Wnt-inhibition on ES cell fate acquisition. Cell ratios of Tbr1-positive and Ctip2-positive cells from different culture conditions, as indicated in **Figure 4.5** and **4.6**. Single pathway inhibitions were both able to increase the ratio of Tbr1-positive and Ctip2-positive cells, compared to control CDMM cells. The simultaneous block of BMP and Wnt pathways further increased positive cell ratios, suggesting a synergistic effect of BMP and Wnt pathway inhibition for cortical fate acquisition. Error bars: standard error.

Notably, ES cells treated with double BMP/Wnt-inhibition followed a differentiation schedule similar to that of *in vivo* cortical neurons. The expression of Tbr1, which marks earlier cortical neurons, was followed by the activation of Ctip2, which labels medium/early-generated cortical neurons of layer 5. Ctip2-positive cells reached their peak at Step-III+4 days of culture. To obtain neurons positive for SatB2, which marks late-generated cortical neurons of layers 2/3, cells were cultured for a longer period (up to a total of 18 days); N2 medium used for Step-III was gradually replaced with N2B27 starting from Step-III+4 days, to promote cell survival in long-term culture (**Figure 4.8**).

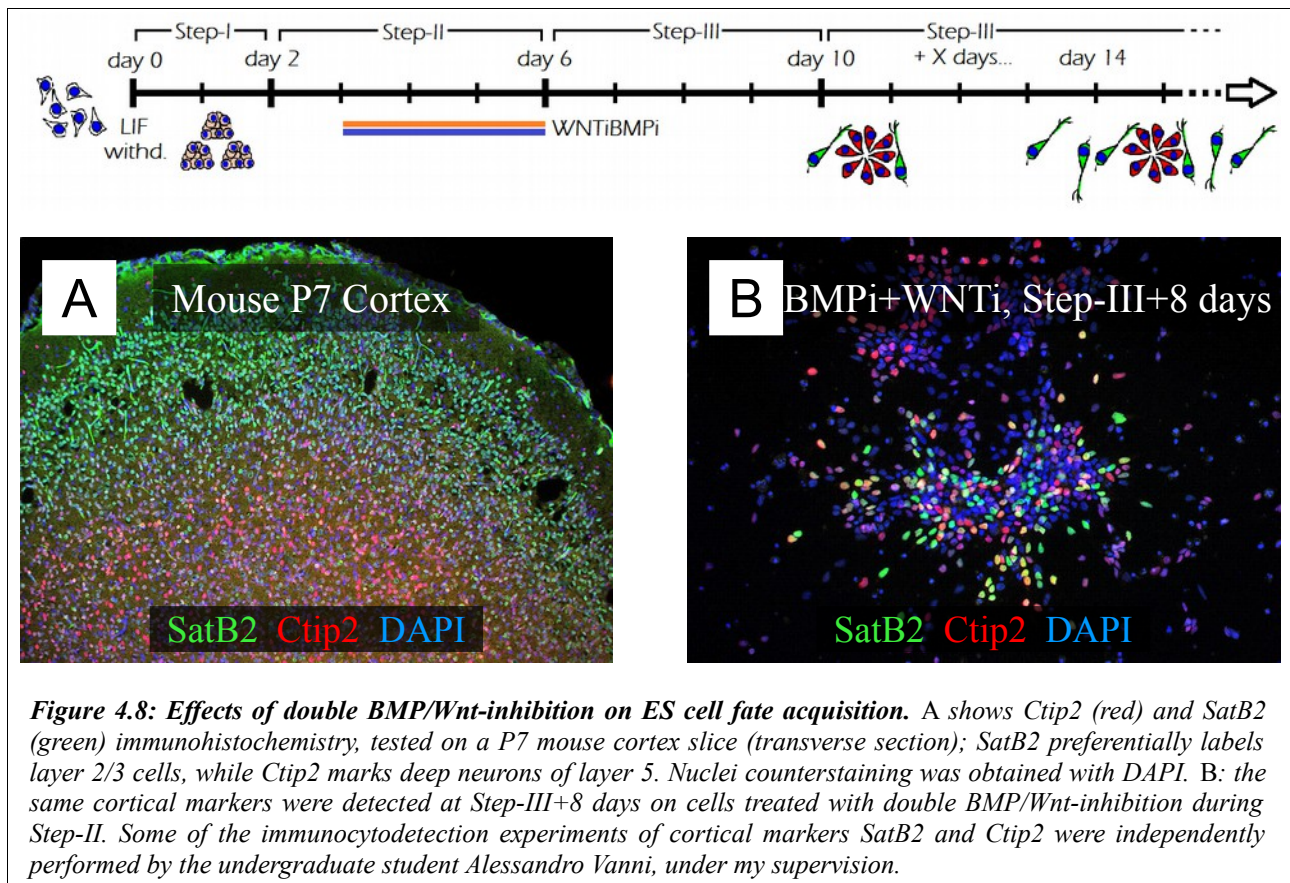
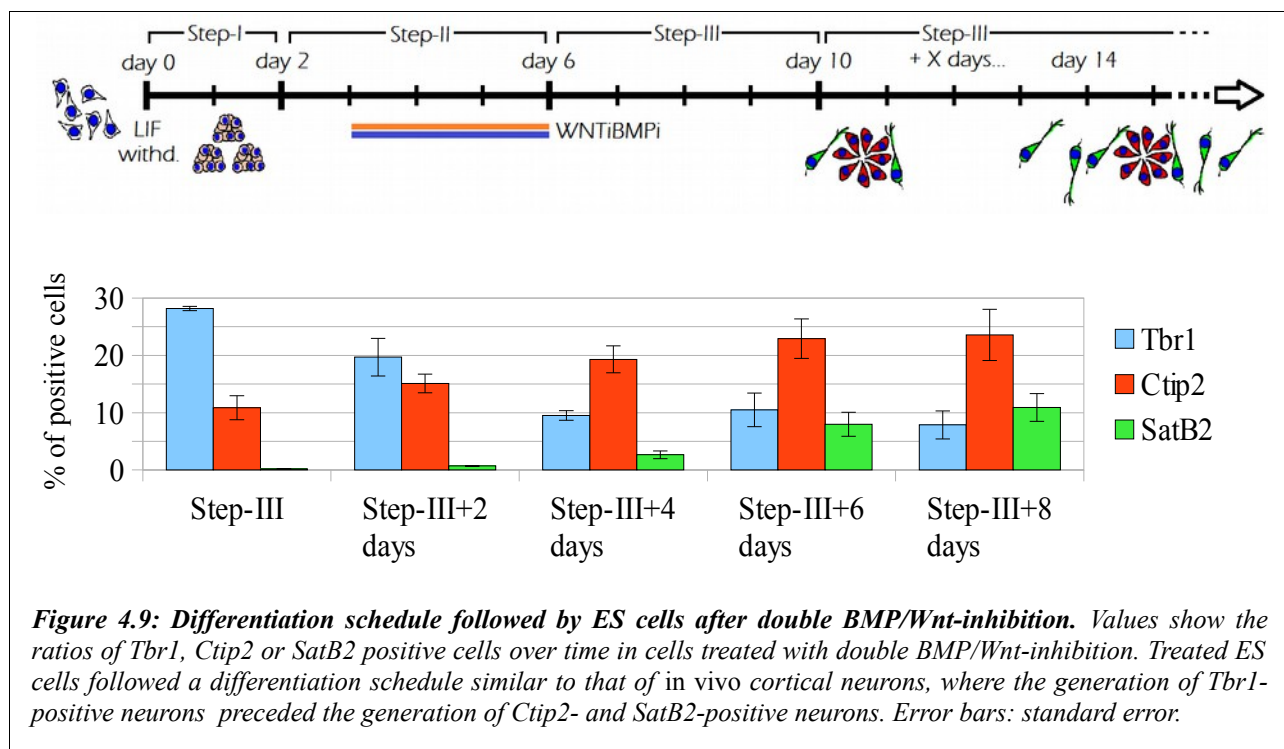


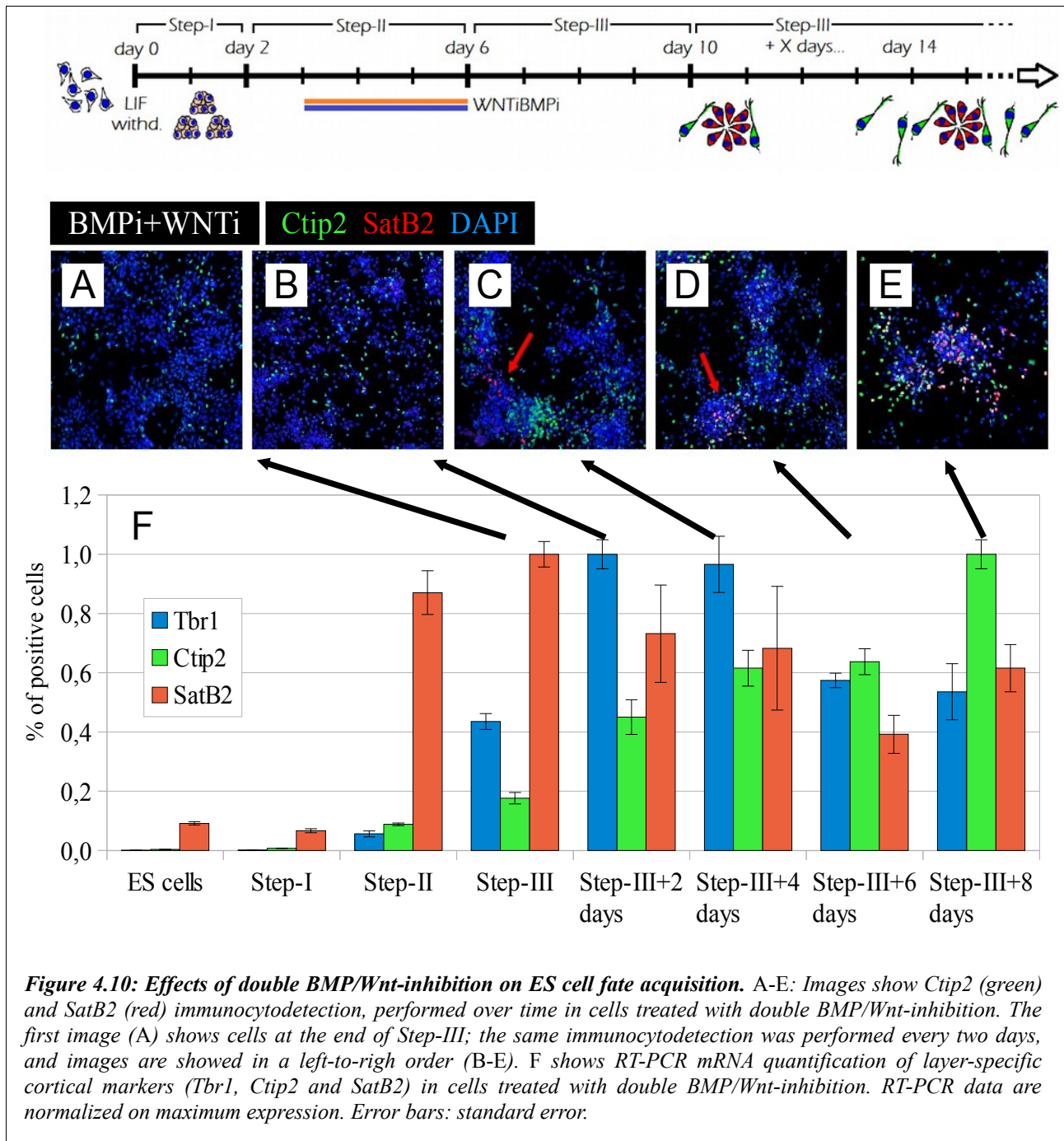
Figure 4.8: Effects of double BMP/Wnt-inhibition on ES cell fate acquisition. A shows Ctip2 (red) and SatB2 (green) immunohistochemistry, tested on a P7 mouse cortex slice (transverse section); SatB2 preferentially labels layer 2/3 cells, while Ctip2 marks deep neurons of layer 5. Nuclei counterstaining was obtained with DAPI. B: the same cortical markers were detected at Step-III+8 days on cells treated with double BMP/Wnt-inhibition during Step-II. Some of the immunocytochemistry experiments of cortical markers SatB2 and Ctip2 were independently performed by the undergraduate student Alessandro Vanni, under my supervision.

SatB2-positive cell ratio (late-generated neurons) increased over time, as the culture matured, at the expense of Tbr1-positive cell ratio (early-generated neurons) (**Figure 4.9**).



Notably, when we analyzed by RT-PCR the expression of cortical markers during differentiation, we found that some of them were already highly expressed at the end of Step-III (Ctip2, green columns in **Figure 4.10**) and even at the end of Step-II (SatB2, red columns in **Figure 4.10**). The case of SatB2 was particularly interesting, because the expression of this marker was already detectable at Step-II, a developing time where SatB2-positive neurons cannot be detected by immunocytochemistry (**Figure 4.10**). SatB2-positive neurons, as shown before, first appeared in our culture only after a total of 14 days of differentiation, that is 8 days after the appearance of SatB2 mRNA expression (**Figure 4.9** and **Figure 4.10C,D**). These data show that SatB2 mRNA is prematurely expressed by differentiating cortical progenitors, but SatB2 protein expression is switched-on only at a later differentiation phase. This temporal difference between mRNA expression and the generation of SatB2-positive neurons could be possibly due to a post-transcriptional regulation of SatB2 mRNA. A translational regulation of SatB2 mRNA was already hypothesized *in vivo* (Britanova et al., 2005).

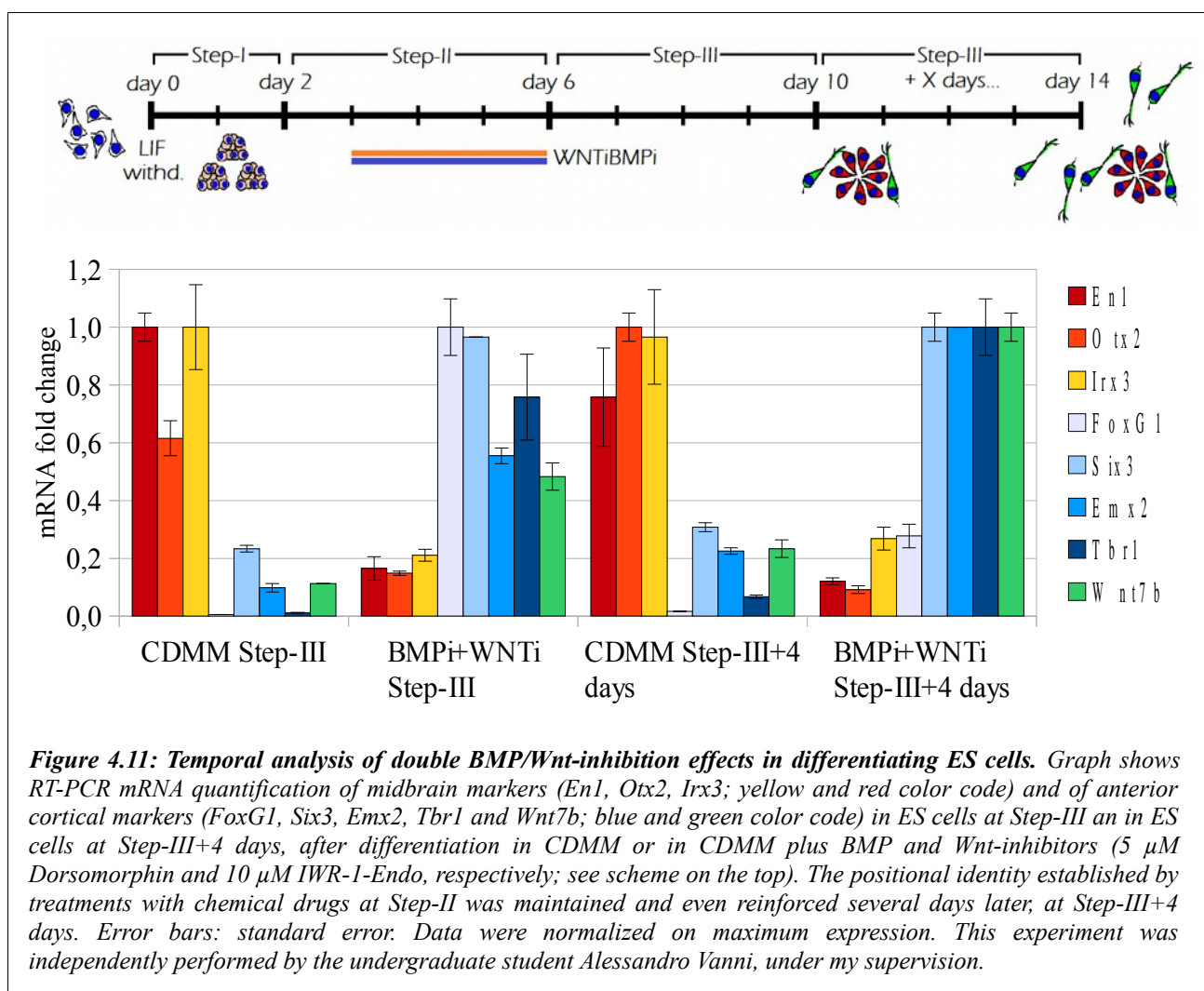
A possible mechanism of SatB2 mRNA post-transcriptional regulation has not been investigated in my PhD work, but this topic will deserve attention in future experiments in our Lab.



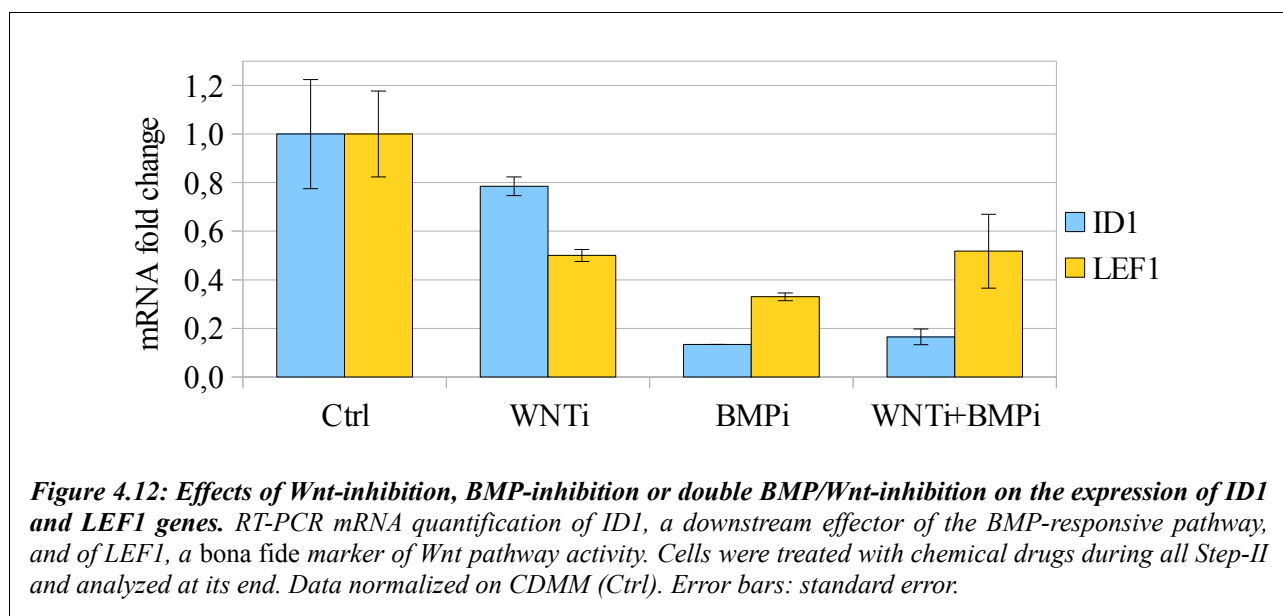
As the positional markers analyzed by RT-PCR and by immunocytochemistry can change very rapidly their expression during neural differentiation, both *in vitro* and *in vivo*, we decided to analyze cell identity at earlier and later times of differentiation (end of Step-III or Step-III+4 days) to test the maintenance of cell positional identity. Control CDMM-cultured cells were compared to cells treated with double BMP/Wnt-inhibition; the expression level of midbrain genes (*Otx2*, *En1*

and *Irx3*) and that of anterior/cortical genes (*FoxG1*, *Six3*, *Emx2*, *Tbr1*, *Wnt7b*) was analyzed. Cells anteriorized by double BMP/Wnt-inhibition expressed high level of anterior genes, and this expression was further increased at Step-III+4 days, with the only exception of *FoxG1* gene (this was not surprising, as *FoxG1* is a early marker that decreases its expression during neural differentiation). On the contrary, control cells maintained a high expression of midbrain genes during differentiation, and never switched-on the expression of anterior/cortical markers (**Figure 4.11**).

As similar results were obtained by analyzing two different time points, we excluded the possibility that the effect of double BMP/Wnt-inhibition on positional identity may be the result of an enhancement/acceleration in neural fate induction: Differentiating ES cells acquire a specific A/P fate after treatments with chemical drugs (always performed at Step-II) and maintain their identity during differentiation, without losing their positional memory.



To confirm the specificity of action of chemical drug treatments, we quantified by RT-PCR the expression of ID1, a downstream effector of the BMP-responsive pathway, and the expression of LEF1, a *bona fide* marker of the canonical Wnt pathway activity. Cells were treated during Step-II (starting at the beginning of day2) and analyzed at the end of Step-II. As expected, Dorsomorphin-mediated BMP-inhibition, both in single and in double treatment, resulted in a strong decrease of ID1 expression, compared to control cells. Similarly, LEF1 expression decreased when cells were treated with IWR-1-Endo (both in single Wnt-inhibition and in double BMP/Wnt-inhibition). Surprisingly, LEF1 expression showed a marked decrease also in Dorsomorphin-treated cells, indicating that BMP-inhibition caused a secondary down-regulation of Wnt pathway activity (**Figure 4.12**). This suggested a cross-talk mechanisms between the two pathways.



To better understand this phenomenon, we cultured ES cells until the end of Step-II, then performed an acute (12 hours) treatment with chemical drugs. In this condition, LEF1 and ID1 levels decreased in cells treated with IWR-1-Endo and Dorsomorphin, respectively, but LEF1 expression level in Dorsomorphin-treated cells was comparable to that of control cells. The acute treatment isolated the early effect on BMP and Wnt pathways, and avoided late regulations/cross-talks of the two pathways (**Figure 4.13**).

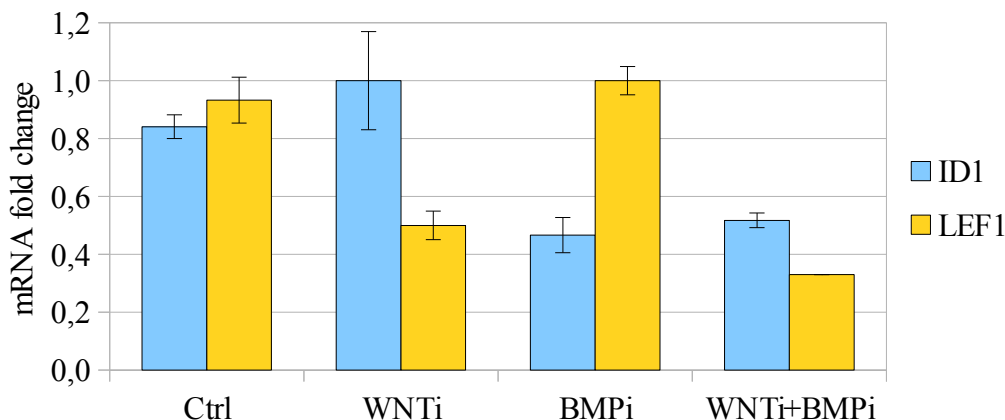
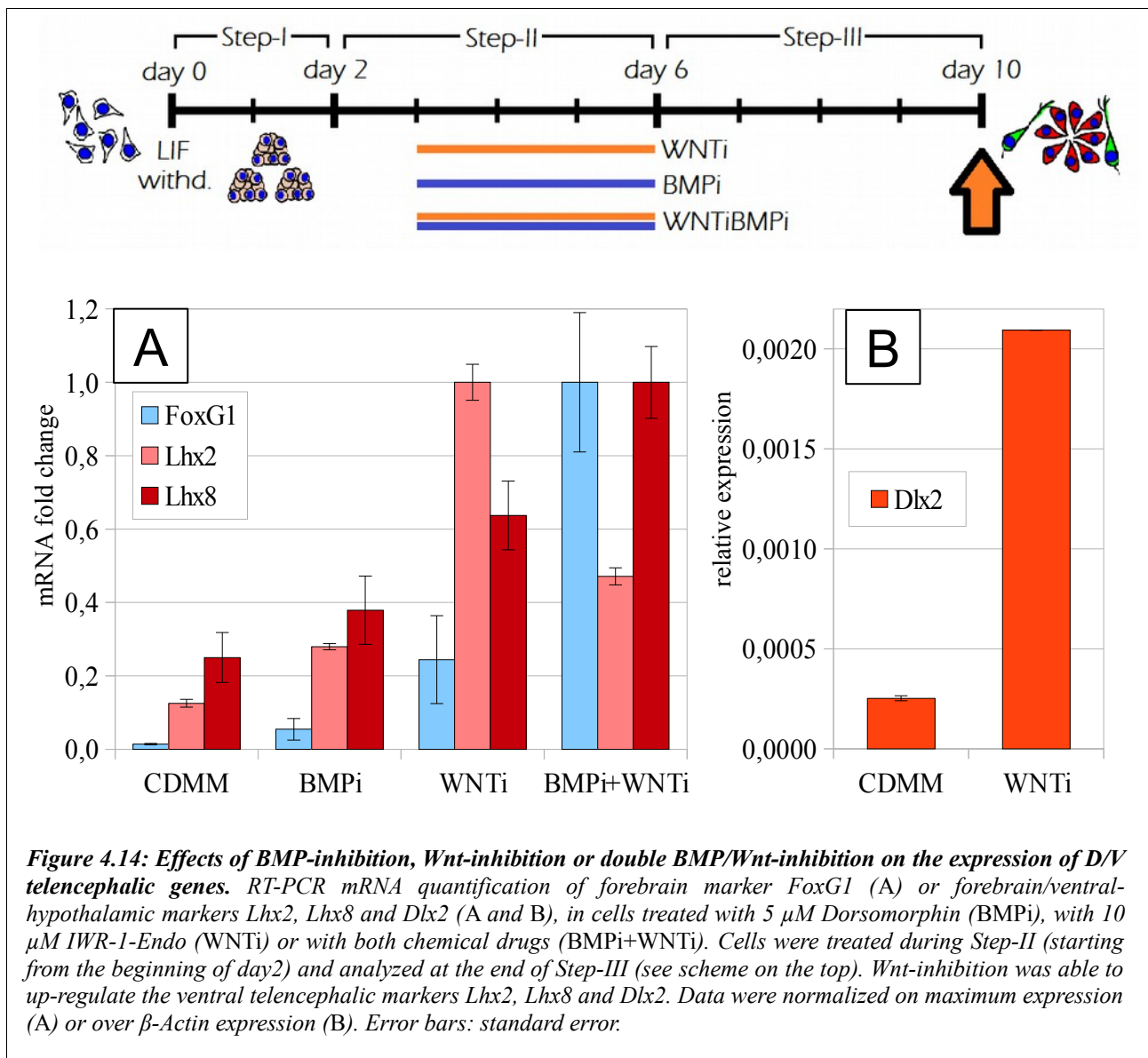


Figure 4.13: Effects of transient Wnt-, BMP- or double BMP/Wnt-inhibition (acute 12 hours treatment) on the expression of ID1 and LEF1 genes. RT-PCR mRNA quantification of ID1, a downstream effector of the BMP-responsive pathway, and of LEF1, a bona fide marker of Wnt pathway activity. Cells were treated with chemical drugs only during the last 12 hours of Step-II. Data normalized on CDMM (Ctrl). Error bars: standard error.

The dissection of BMP and Wnt pathways and the study of possible cross-talks between the two signaling pathways will require further investigation. At this point of the analysis, the results suggest that some of the *corticalizing* effects previously seen with Noggin-mediated BMP-inhibition (Results, Chapter 3), may be, at least in part, due to a secondary modulation of the Wnt signaling pathway. However, the molecular nature of the interaction between BMP and Wnt pathway was not further investigated in my work.

All in all, we concluded that Wnt-inhibition plays a fundamental role in establishing an anterior, cortical fate during ES cell neural differentiation *in vitro*, consistently with previous findings (Eiraku et al., 2008).

However, some of the markers we used in our analysis (FoxG1 and Six3, for example) are expressed *in vivo* both in the ventral and in the dorsal area of the telencephalon. Thus, we can not exclude that Wnt-inhibition steered ES cell differentiation fate towards a mixed dorsal (Cortical, Emx2 and Tbr1-positive) and ventral (Subpallial, Dlx2-positive) telencephalic differentiation fate. In fact, we detected by RT-PCR the expression of ventral/telencephalic (Dlx2) and specifically hypothalamic (Lhx2 and Lhx8) markers, after Wnt-inhibition (**Figure 4.14**).



In conclusion, we can state that WNT-inhibition during ES cell neural differentiation *in vitro* induces a telencephalic fate, generating a mixed cortical and subpallial cell population, that is consistent with previous findings (Ikeda et al., 2005; Verani et al., 2007; Nicoleau et al., 2013).

5– Anterior Brain Patterning

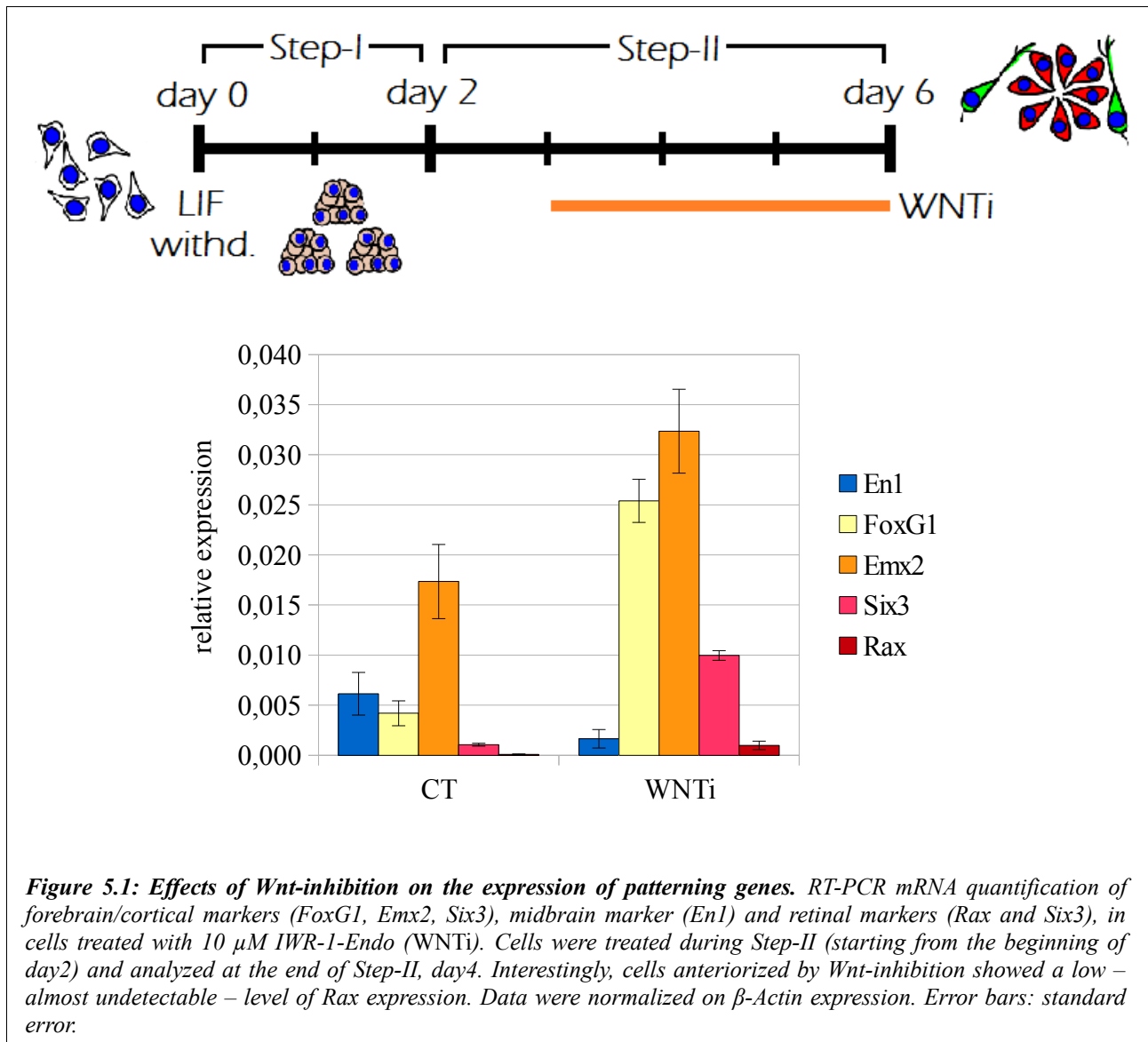
How to Make a Retina

Playing with BMP, Wnt and Activin/Nodal Pathways.

While much information can be found about cortical fate acquisition, the cellular and molecular mechanisms that regulate the regionalization of the forebrain are largely unknown. As an example, the molecular mechanisms controlling the diversification of the presumptive telencephalon and the eye field have not been elucidated so far (Wilson and Houart, 2004; Andonadiou et al., 2013).

We therefore decided to exploit the plasticity of our differentiation protocol to steer stem cell fate choice between dorsal telencephalon (Cortex) and lateral diencephalon (Retina). We reasoned that the first step to achieve for retinal differentiation was necessarily to anteriorize differentiating ES cells (forebrain fate), as retinal cells arise from the most anterior aspect of neural plate *in vivo* (Wilson and Houart, 2004). We previously demonstrated that endogenously produced Wnts and BMPs can affect ES cell regional fate acquisition; control ES cells, under the effect of high amounts of endogenously produced BMP and Wnt morphogens, expressed mesencephalic markers such as Otx2 and En1 (Results, Chapter 3). On the contrary, ES cells treated with double BMP and Wnt-inhibition were *anteriorized*, expressed high levels of FoxG1, Emx2 and Six3, and specifically acquired a genuine cortical/telencephalic identity (Results, Chapters 3 and 4).

The need for an anteriorization *via* Wnt and/or BMP-inhibition, in order to obtain retinal cells, was supported by our experimental observation that ES cells treated with Wnt-inhibition expressed the eye field marker Rax (Furukawa et al., 1997), even if at very low level (**Figure 5.1A**).



After the first step of ES cell anteriorization, in which a low expression of *Rax* was already present, the question was how to switch-off telencephalic genes (*FoxG1*, *Emx2*) and how to efficiently switch-on eye field genes (*Six6* and *Rax*), steering stem cell fate choice towards retinal fate at the expense of cortical fate (**Figure 5.2**).

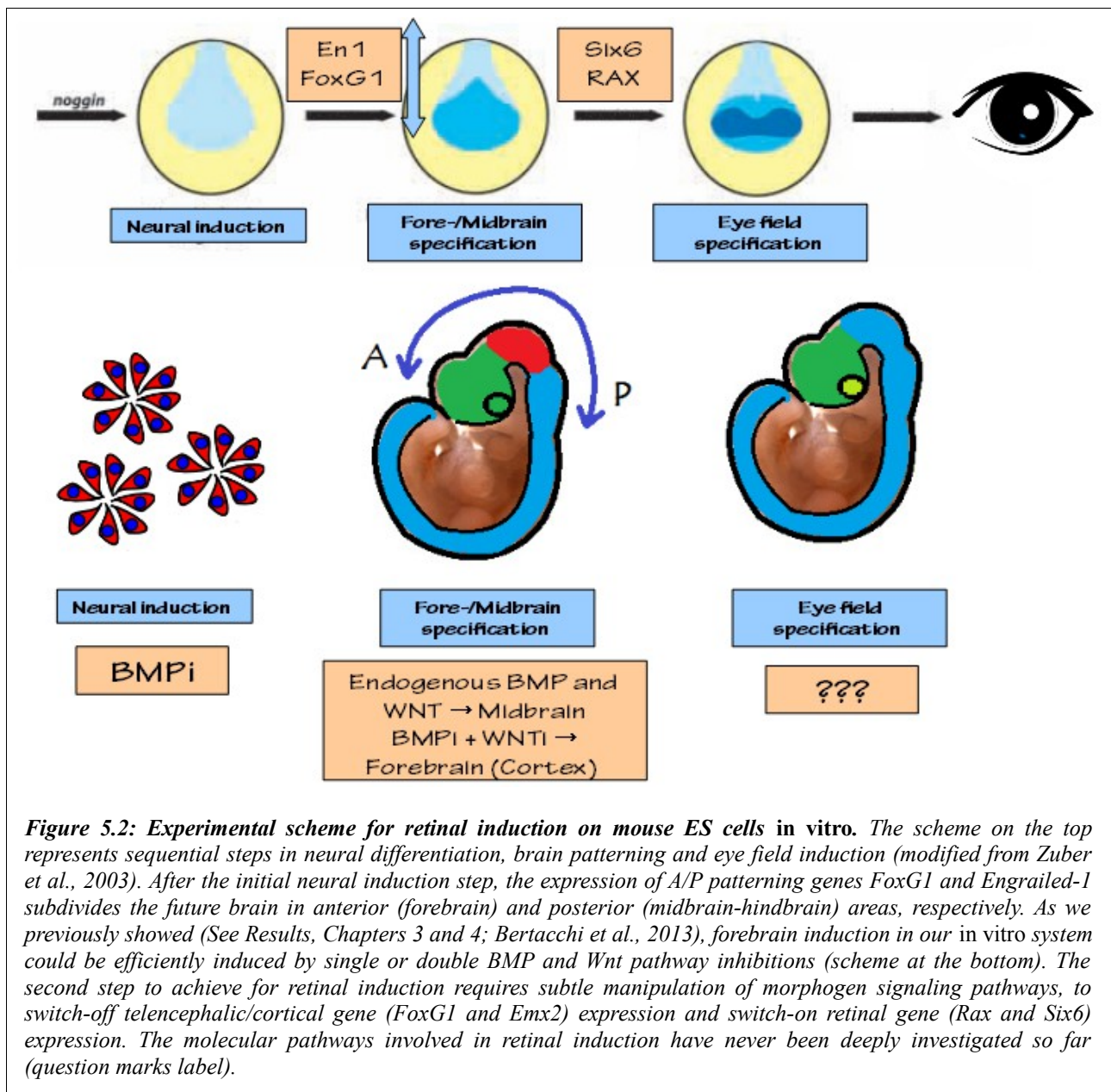
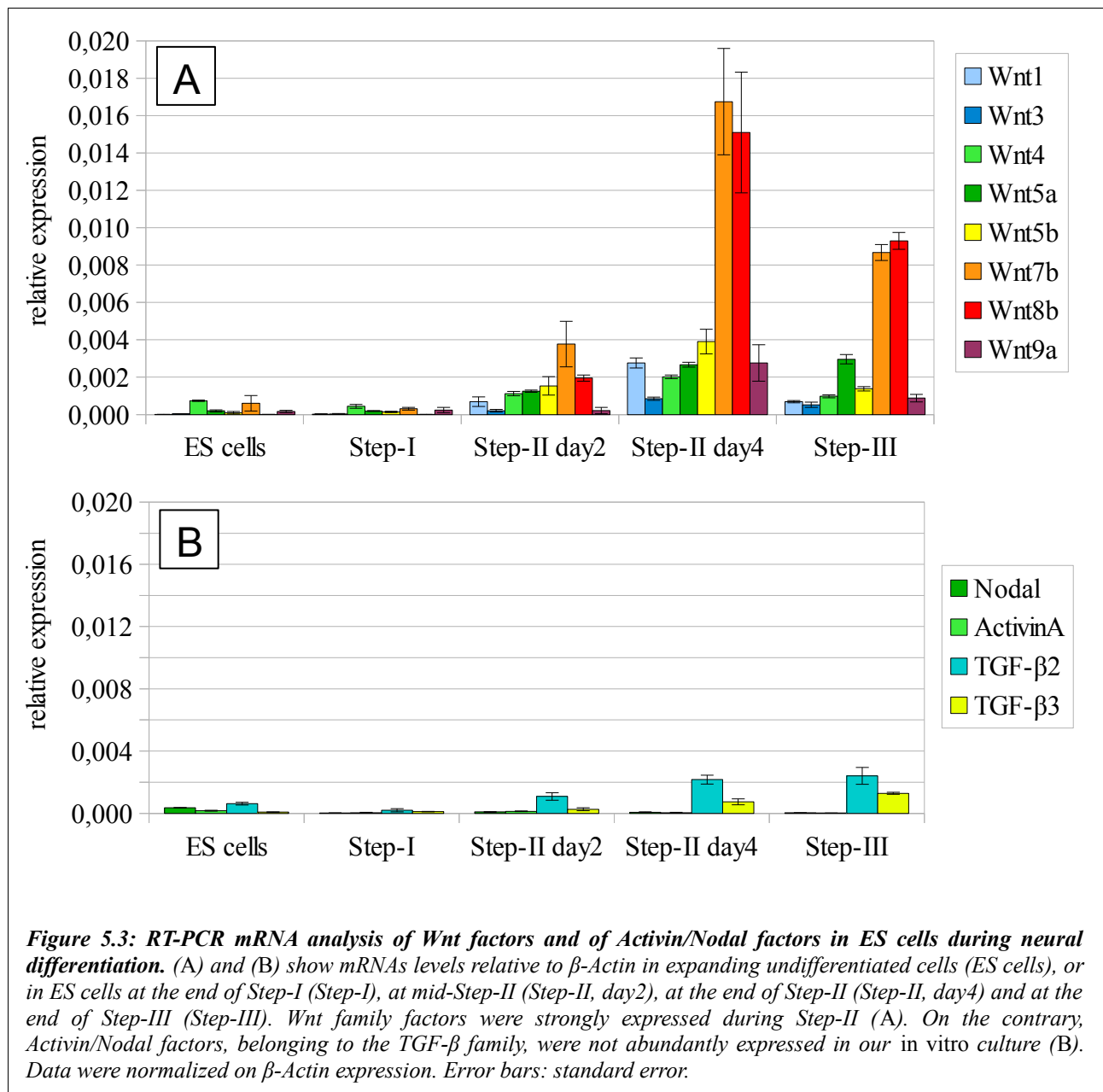
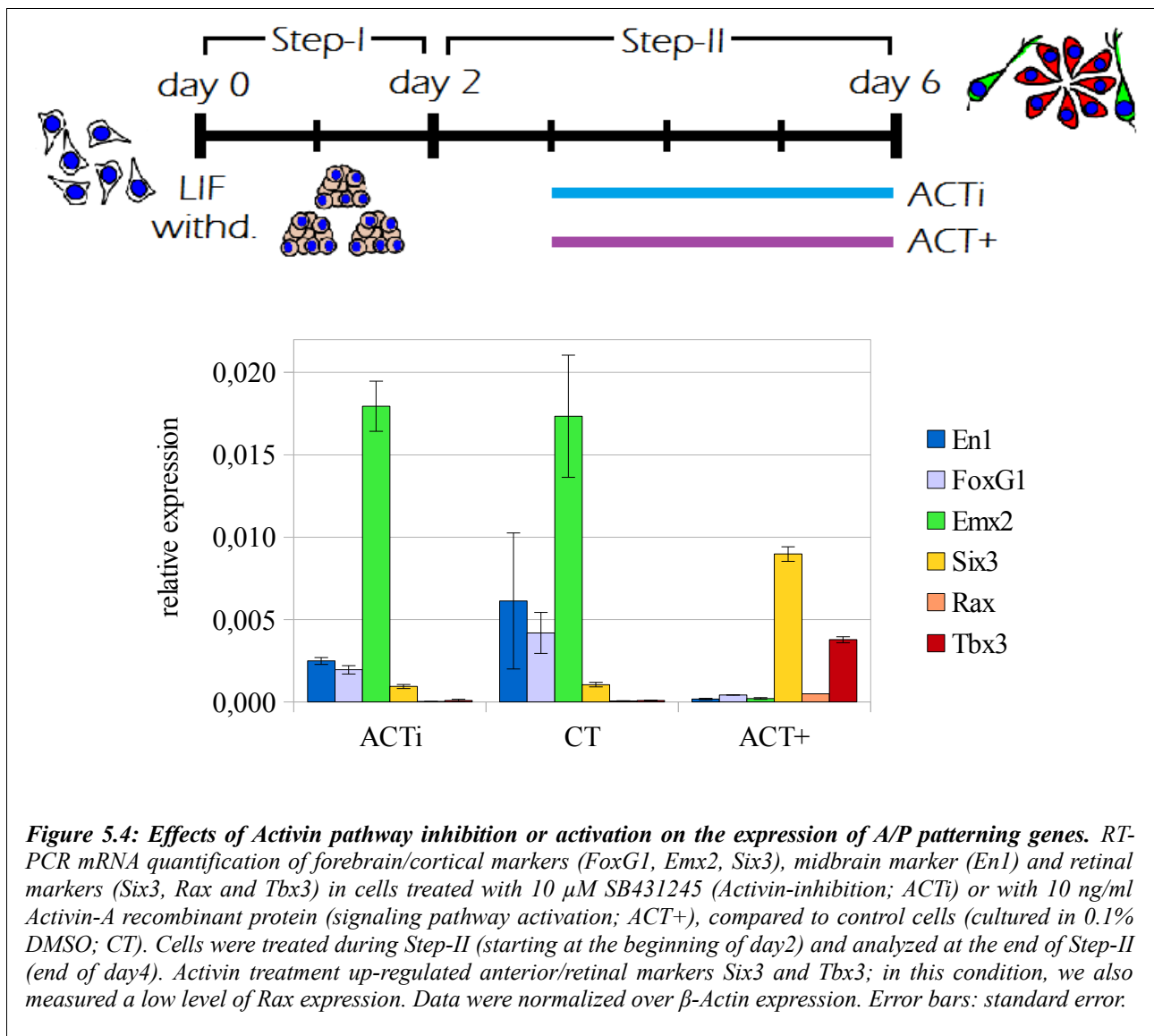


Figure 5.2: Experimental scheme for retinal induction on mouse ES cells in vitro. The scheme on the top represents sequential steps in neural differentiation, brain patterning and eye field induction (modified from Zuber et al., 2003). After the initial neural induction step, the expression of A/P patterning genes *FoxG1* and *Engrailed-1* subdivides the future brain in anterior (forebrain) and posterior (midbrain-hindbrain) areas, respectively. As we previously showed (See Results, Chapters 3 and 4; Bertacchi et al., 2013), forebrain induction in our in vitro system could be efficiently induced by single or double BMP and Wnt pathway inhibitions (scheme at the bottom). The second step to achieve for retinal induction requires subtle manipulation of morphogen signaling pathways, to switch-off telencephalic/cortical gene (*FoxG1* and *Emx2*) expression and switch-on retinal gene (*Rax* and *Six6*) expression. The molecular pathways involved in retinal induction have never been deeply investigated so far (question marks label).

We previously showed that mouse ES cells expressed high levels of BMPs and Wnts during neural differentiation *in vitro* (See Results, Chapter 2). Notably, in our system of neural differentiation, ES cells do not express a large amount of Activin/Nodal signals compared to Wnts and BMPs (See Results, Chapter 2; compare RT-PCR data in **Figure 5.3**). This prompted us to consider the possibility of manipulating Activin/Nodal signaling pathway, by adding exogenous Activin-A. Additionally, a recently published work on human ES cells showed the importance of Activin/Nodal signaling for eye field gene induction (Lupo et al., 2013).



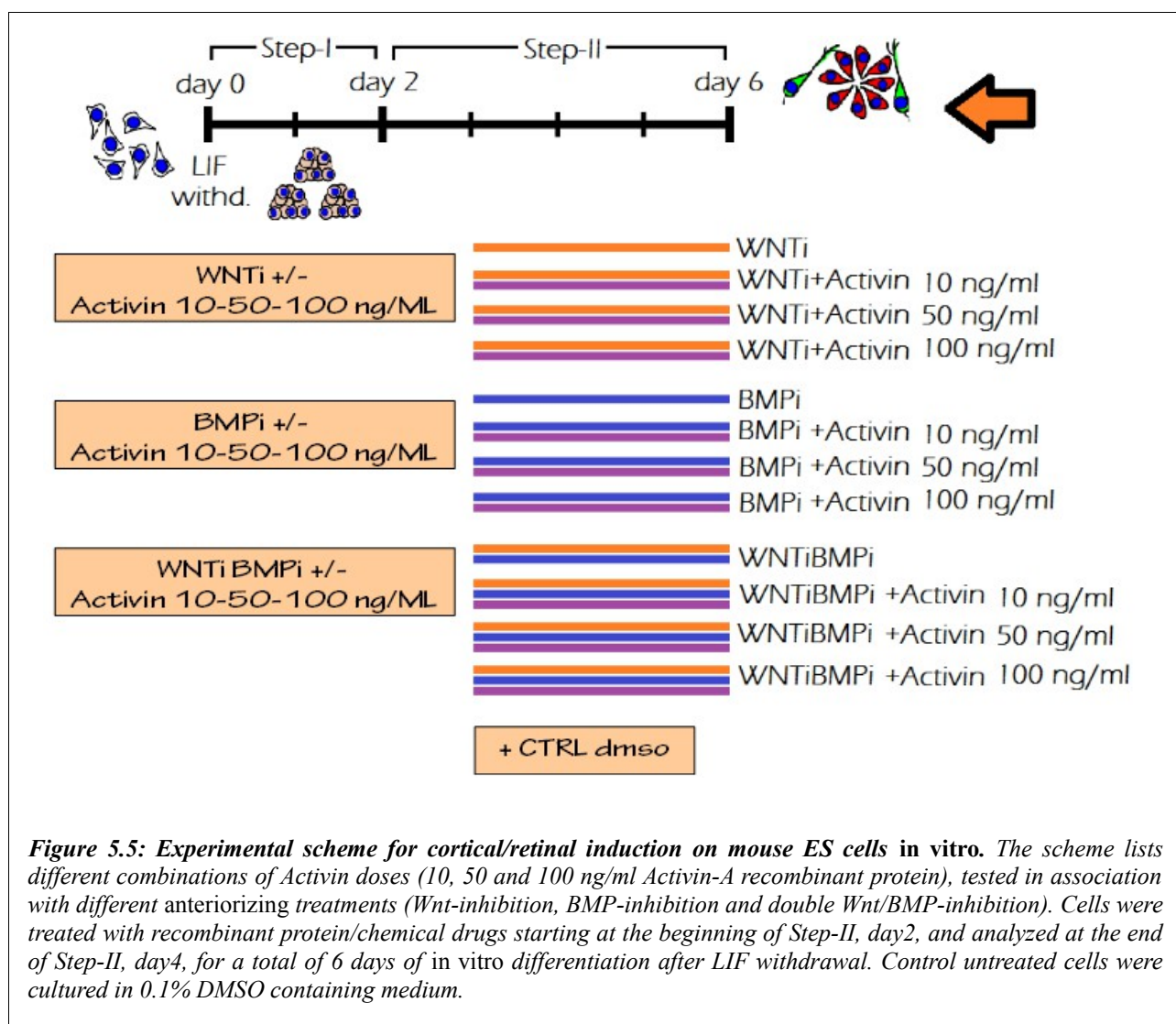
The induction of Activin/Nodal pathway alone down-regulated both anterior/cortical markers (Emx2 and FoxG1) and midbrain marker (En1), and up-regulated the retinal marker Tbx3 and the anterior/retinal marker Six3. However, this effect was associated with a very low expression of the eye field gene Rax (**Figure 5.4**). Activin/Nodal-inhibition via SB431245 treatment did not affect the expression of the positional markers analyzed, consistently with the absence of endogenous Activin/Nodal production in our culture system (**Figure 5.4**).



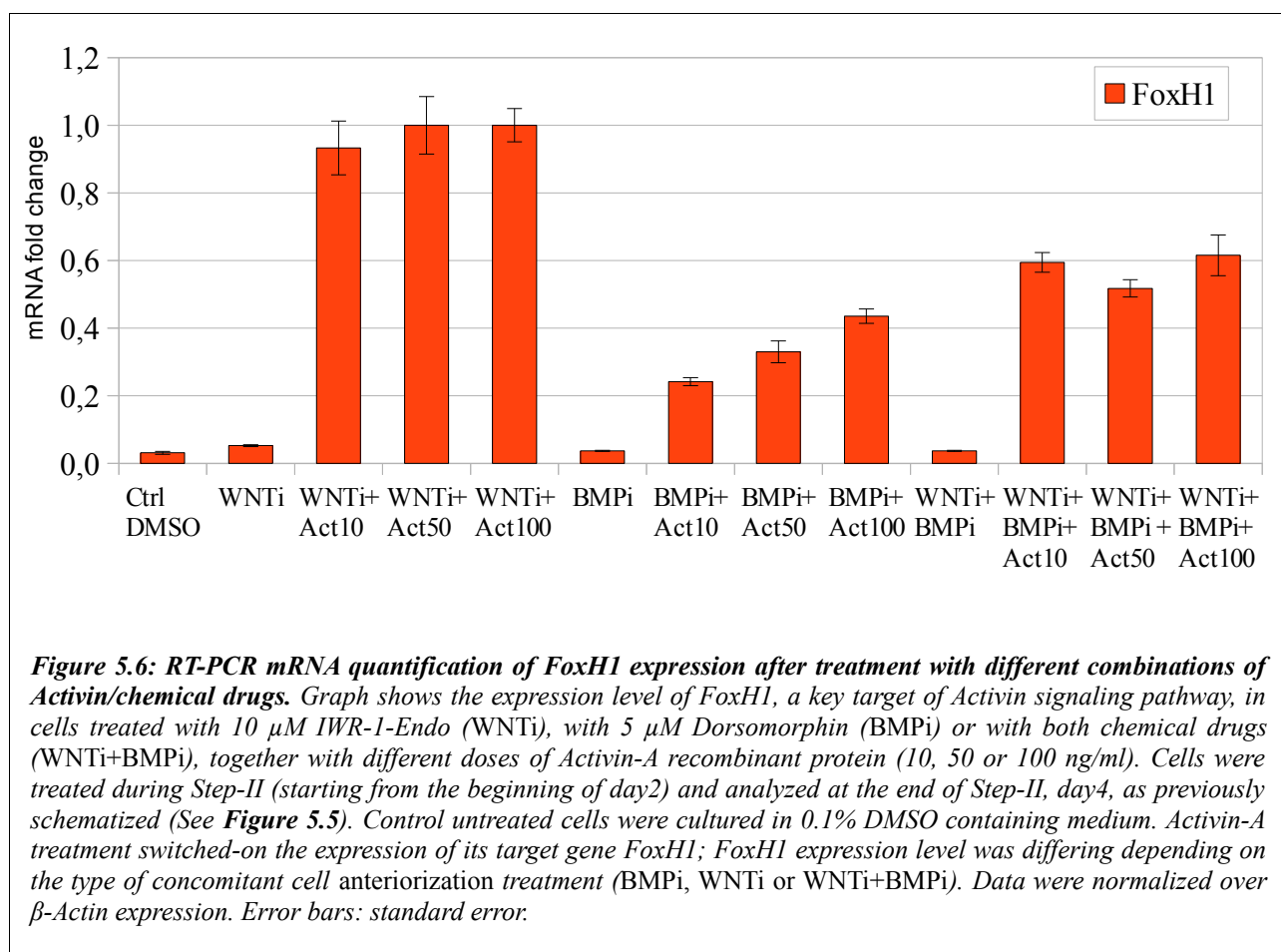
Finally, as reported in the literature (Tomizawa et al., 2013; Sakaki-Yumoto et al., 2013), Activin treatment alone promoted the maintenance of pluripotency and strongly inhibited ES cell neuralization (see also **Figures 5.9, 5.10, 5.19-5.21, 5.45, 5.46** and text below), making very difficult to understand the identity of the few neural progenitors differentiated in this culture condition.

We thus decided to use different doses of Activin in combination with ES cell *anteriorizing* treatments, obtained by means of BMP, Wnt or double Wnt/BMP-inhibitions (**Figure 5.5**).

The ED50 of Activin protein (that is the ability to induce hemoglobin expression in K562 cells, as reported on R&D Systems information sheet) is 0.5-2 ng/ml. Three different doses of Activin (10, 50 and 100 ng/ml) were associated with three different *anteriorizing* treatments: Wnt-inhibition via IWR-1-Endo treatment (10 μ M; WNTi), BMP-inhibition via Dorsomorphin treatment (5 μ M; BMPi) and double Wnt/BMP-inhibition, previously used for optimal anteriorization and cortical induction (See Results, Chapter 4; WNTi+BMPi). Cells were always treated during Step-II (see scheme in **Figure 5.5**), starting from day2 of Step-II until the analysis point at the end of Step-II, day4. Control cells were always cultured in CDMM supplemented with the same amount of DMSO used for treatments (CTRL 0.1% DMSO). The effects of different treatments on gene expression were evaluated by RT-PCR.



As a read-out of Activin/Nodal signaling pathway activation, we measured the expression of FoxH1 by RT-PCR (**Figure 5.6**). FoxH1 is a key target gene of Activin/Nodal signaling pathway and consistently its expression was switched-on by the addition of Activin-A protein in culture medium. The activation of Activin/Nodal signaling pathway (FoxH1 expression) showed different efficiencies when Activin treatment was associated with Wnt-inhibition, BMP-inhibition or double Wnt/BMP-inhibition. This suggested that ES cell responsiveness to Activin treatment can be strongly influenced by the type of *anteriorizing* protocol used at the same time. Higher FoxH1 expression levels were obtained by associating Activin treatment together with Wnt-inhibitor alone. FoxH1 expression reached high levels even after treatment with the lower Activin dose tested (10 ng/ml). As FoxH1 expression level was already high in cells treated with 10 ng/ml Activin, we reasoned that this dose could be considered already saturating for signaling pathway activation in our culture system.



We then focused our attention on cell identity, measuring by RT-PCR the expression of regional markers among the different combinations of treatments (**Figure 5.7**). Single Wnt- or BMP-inhibitions were both efficient for ES cell corticalization, as seen by midbrain marker *En1* down-regulation (dark red columns in **Figure 5.7**) and forebrain markers up-regulation (*Emx2*, *FoxG1*; yellow and orange columns, respectively), when compared to control cells. Wnt-inhibition was able to up-regulate anterior/cortical markers more efficiently than BMP-inhibition, and the best *corticalizing* treatment was the combination of double Wnt/BMP-inhibition (as previously seen in Results, Chapter 4). Activin treatment was able to silence cortical gene expression and to efficiently switch-on the expression of eye field genes, such as *Rax*, *Six6*, *Tbx3*, *Six3*, *Vsx2* and *Otx2* (**Figure 5.7**). The prosencephalic marker *Six3* and the forebrain/midbrain marker *Otx2* have also been demonstrated to have a key-role as eye field transcription factors, and were used here as a read-out of retinal induction; see Zuber et al., 2003.

Among different Activin doses tested, the 10 ng/ml dose was sufficient to inhibit cortical genes and efficiently induce retinal gene expression. Higher doses (50 ng/ml and 100 ng/ml) had similar effects on global gene expression, but were less efficient when compared to 10 ng/ml in terms of retinal gene expression level (compare the expression level of retinal genes – green and blue color code – in WNTi+BMPi+10 ng/ml Activin to that of same genes in WNTi+BMPi+100 ng/ml Activin). This was presumably due to high Activin doses interfering with ES cell neural differentiation (see below in this Chapter, **Figures 5.9**, **5.10** and **5.40**) and thus reducing the number of differentiating neural progenitors inside the cell culture.

As an exception to this, BMP-inhibition associated with higher Activin doses (50 and 100 ng/ml) showed high retinal gene expression levels, giving better results if compared to BMP-inhibition plus low dose (10 ng/ml) of Activin. This difference between Wnt-inhibition and BMP-inhibition in terms of response to Activin treatments was not further investigated. However, BMP-inhibition alone was not used as a treatment in later experiments because of the high expression of mesodermal markers in this condition (see below in this chapter, **Figure 5.19**).

Concerning retinal markers, their expression levels were quite similar in different conditions except *Tbx3*, whose expression was highest in Wnt-inhibition plus high Activin doses (see violet columns in **Figure 5.7**). The key gene for retinal development, *Rax*, showed its highest expression level in cells treated with WNTi+10 ng/ml Activin.

We detected some residual cortical marker (FoxG1 and Emx2) expression even after Activin treatment. This was particularly evident with low Activin dose treatment (see cortical marker expression – yellow and orange color code in **Figure 5.7** – in WNTi, BMPi or WNTi+BMPi+10 ng/ml Activin); higher Activin doses completely silenced FoxG1 and Emx2 expression, but we do not know to what extent this was due to an effect on cell positional fate or rather to a simple inhibition of the neuralization process (see the effect of high Activin doses on neural marker expression Nestin and Pax6, below in this chapter, **Figures 5.9** and **5.10**).

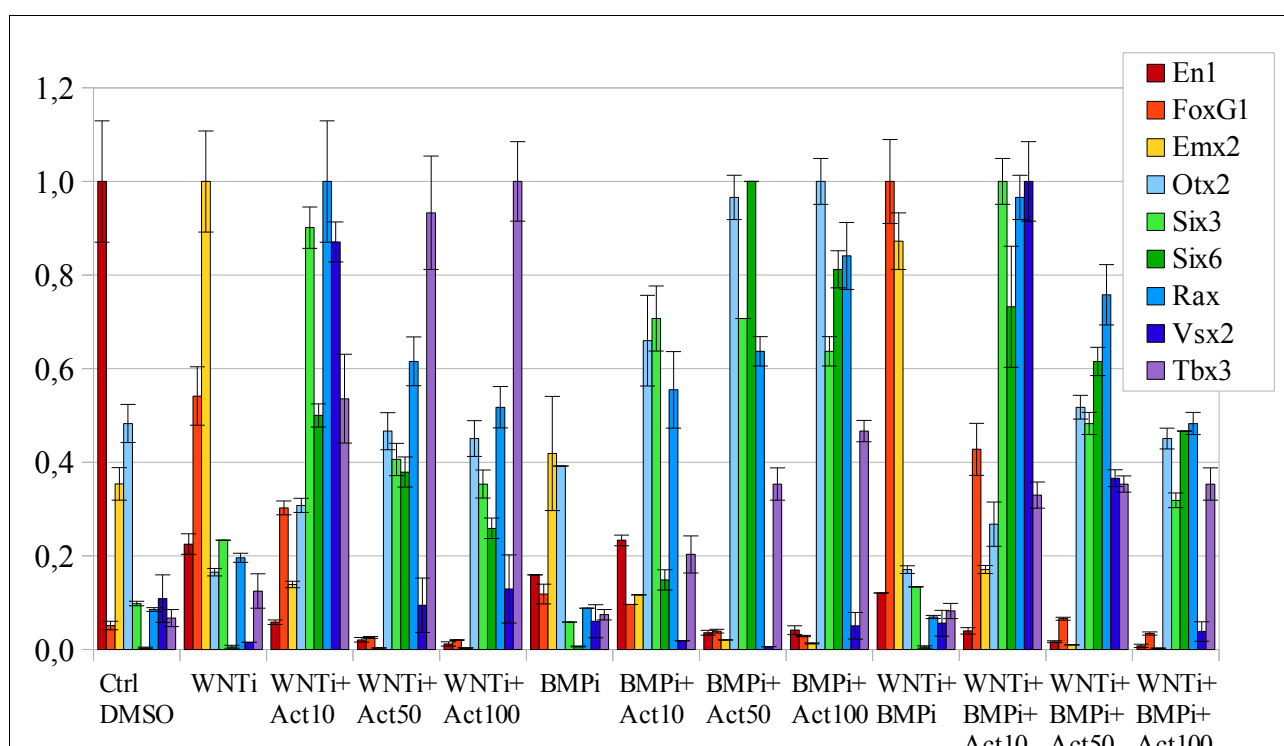
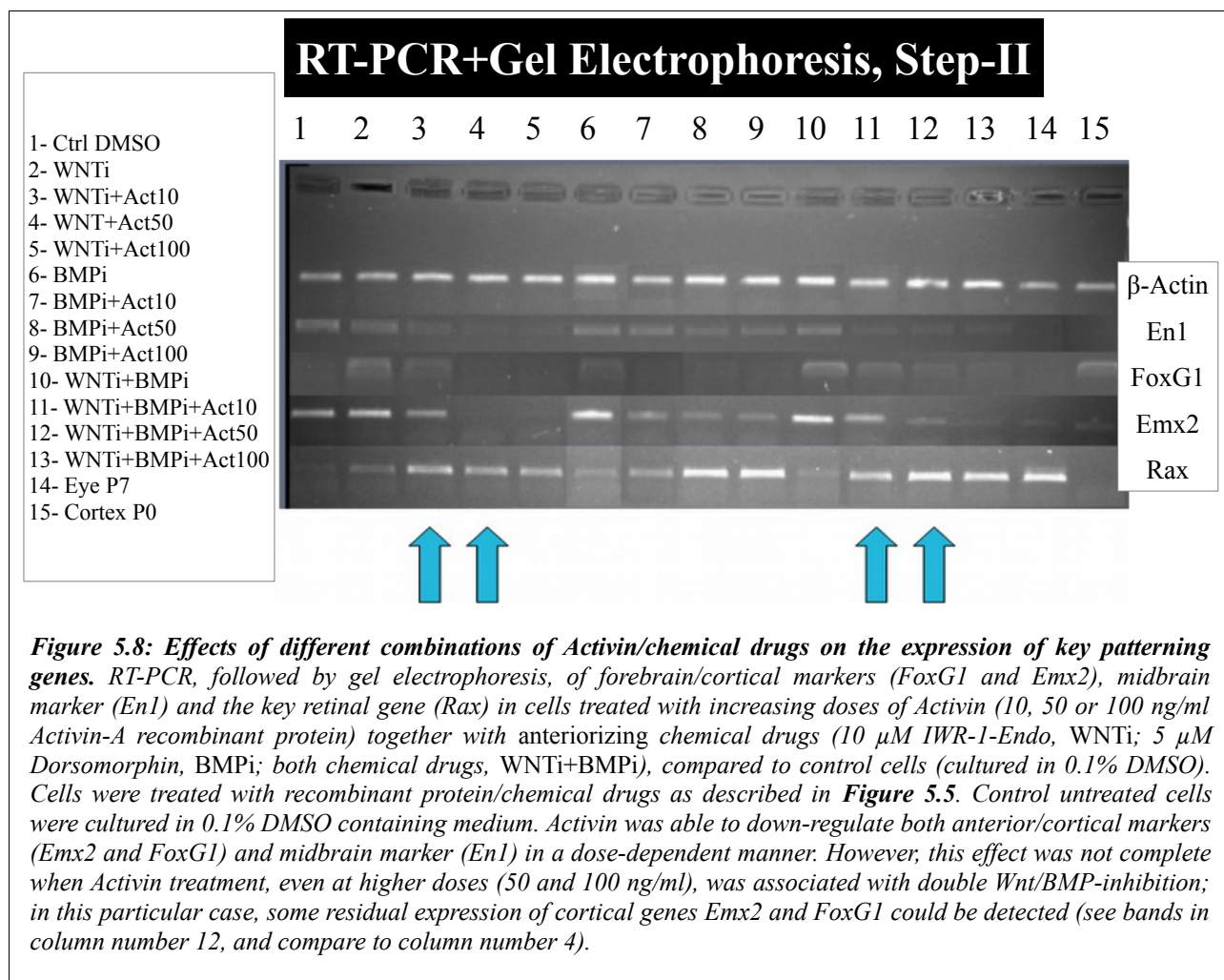


Figure 5.7: Effects of different Activin/chemical drugs combinations on the expression of key patterning genes. RT-PCR mRNA quantification of forebrain/cortical markers (FoxG1, Emx2, Six3), midbrain marker (En1, Otx2) and retinal markers (Otx2, Six3, Six6, Rax, Vsx2 and Tbx3) in cells treated with increasing doses of Activin (10, 50 or 100 ng/ml Activin-A recombinant protein) together with anteriorizing chemical drugs (10 μ M IWR-1-Endo, WNTi; 5 μ M Dorsomorphin, BMPi; both chemical drugs, WNTi+BMPi), compared to control cells (cultured in 0.1% DMSO). Cells were treated with recombinant protein/chemical drugs starting at the beginning of Step-II, day2, and analyzed at the end of Step-II, day4, for a total of 6 days of in vitro differentiation after LIF withdrawal (see **Figure 5.5** for a scheme of the experiment). Activin was able to down-regulate both anterior/cortical markers (Emx2 and FoxG1) and midbrain marker (En1) in a dose-dependent manner. On the contrary, Activin treatment efficiently up-regulated anterior/retinal markers Six3, Otx2, Rax, Six6, Vsx2 and Tbx3. Data were normalized on maximum expression. Error bars: standard error. Y axis: mRNA fold change.

Even if it was not easy to understand which was the best option to obtain retinal cells among all these combinations, we concluded that Activin treatment, when associated with anteriorization via Wnt/BMP-inhibition, was able to switch-on the expression of retinal markers, while suppressing the expression of cortical/telencephalic genes, steering stem cell fate choice towards retinal fate at the expense of cortical fate.

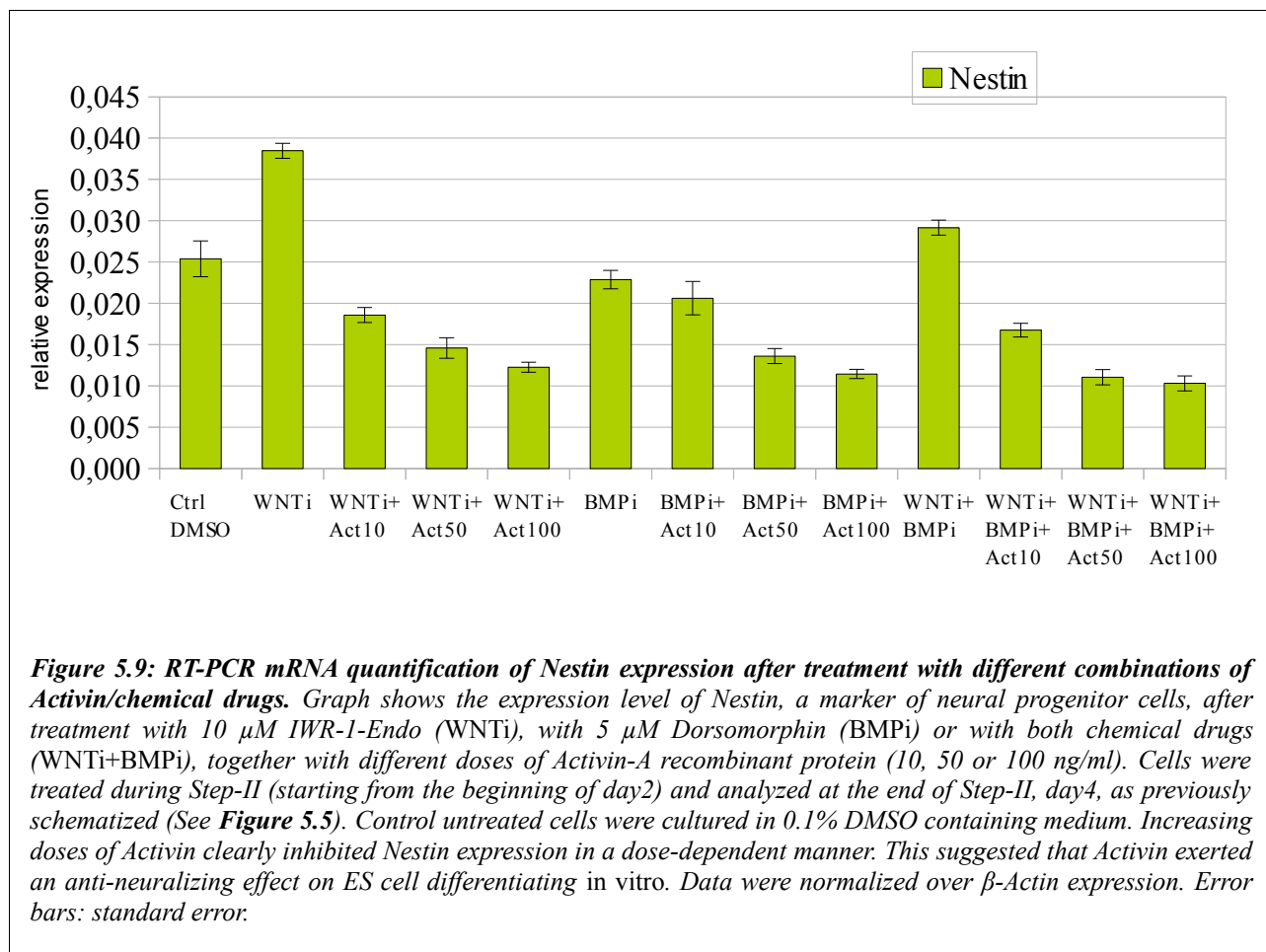


We performed RT-PCR followed by gel electrophoresis to better visualize the residual expression of cortical genes *FoxG1* and *Emx2* after Activin treatments (**Figure 5.8**). This experiment showed again that *FoxG1* and *Emx2* expression were down-regulated by Activin treatment. However, this down-regulation was more efficient in cells treated with Wnt-inhibitor alone, than in cells treated with double inhibition, where *Emx2* and *FoxG1* bands were still detectable after treatment with

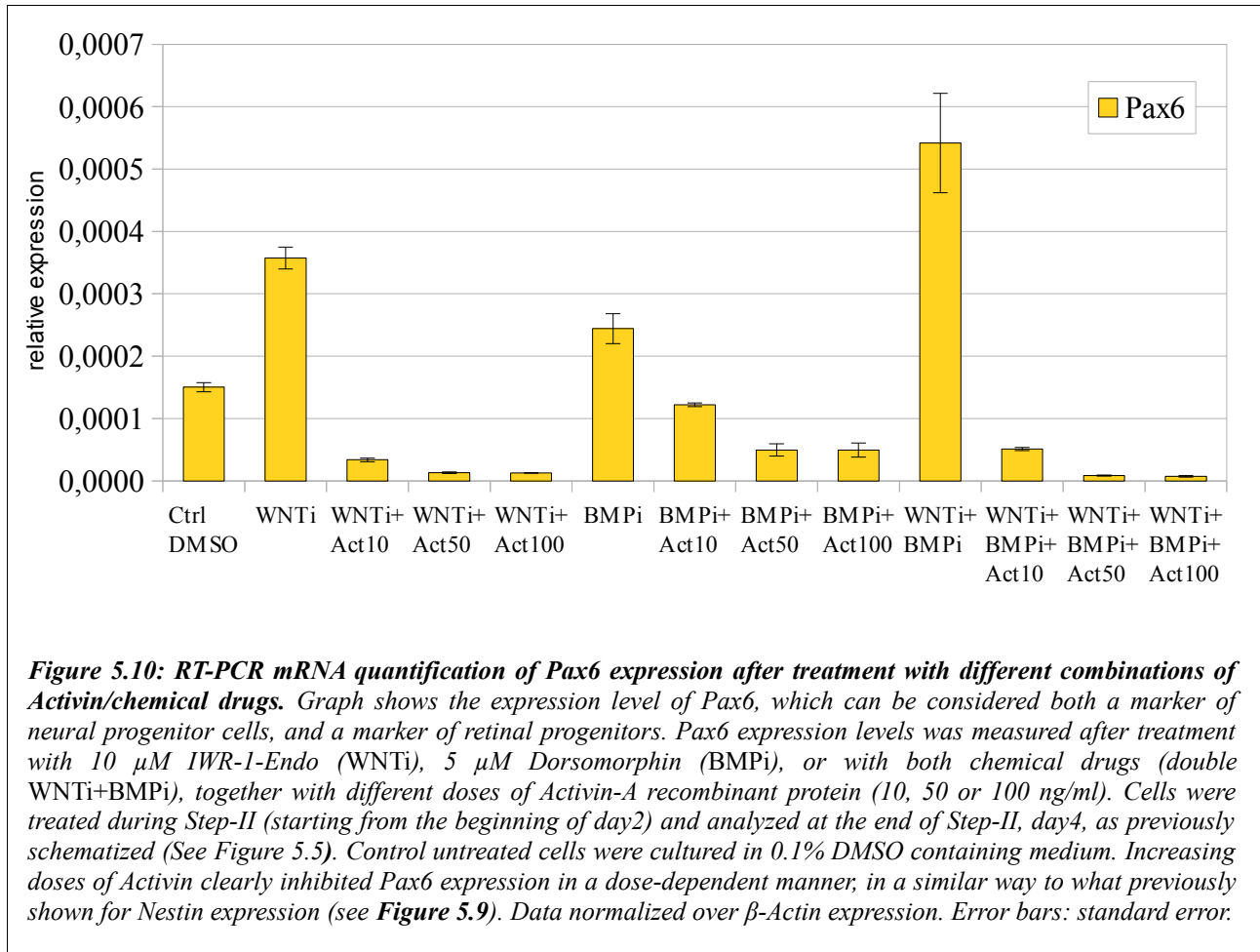
high doses of Activin (compare columns marked by blue arrows in **Figure 5.8**). This is consistent with a higher FoxG1 and Emx2 expression in cells treated with double Wnt/BMP-inhibition, when compared to single Wnt pathway inhibition; we reasoned that ES cell anteriorization/corticalization obtained with double Wnt/BMP-inhibition might specify a cortical fate that can not be re-directed toward retina by Activin. For this reason, we decided to focus on WNTi+Activin as an optimal combination for subsequent experiments.

Activin is known to support the pluripotency of both ES and induced pluripotent stem (IPS) cell (Tsuneyoshi et al., 2012; Tomizawa et al., 2013) and to induce endoderm/mesoderm fate during early fate choice of ES cell differentiation (Teo et al., 2012; Cerdan et al., 2012). For these reasons, we asked whether Activin treatment in our protocol could be responsible for slowing-down or impairing neural conversion of differentiating ES cells. In fact, the down-regulation of the neural markers Nestin and Pax6 after Activin treatment observed by RT-PCR analysis confirmed an Activin anti-neuralizing action (see **Figure 5.9** and **Figure 5.10**).

Cells treated with Wnt-inhibition and double Wnt/BMP-inhibition showed a higher Nestin expression level when compared to control (CDMM+0.1% DMSO cultured) cells, while increasing doses of Activin (ranging from 10 ng/ml to 100 ng/ml) clearly inhibited Nestin expression in a dose-dependent manner (**Figure 5.9**). Cells treated with BMP-inhibition alone showed a Nestin expression level comparable to that of control cells, but also in this case increasing Activin doses gradually silenced Nestin expression. This suggested that Activin treatment *per se* inhibits the appearance of Nestin-positive neural progenitors *in vitro*.

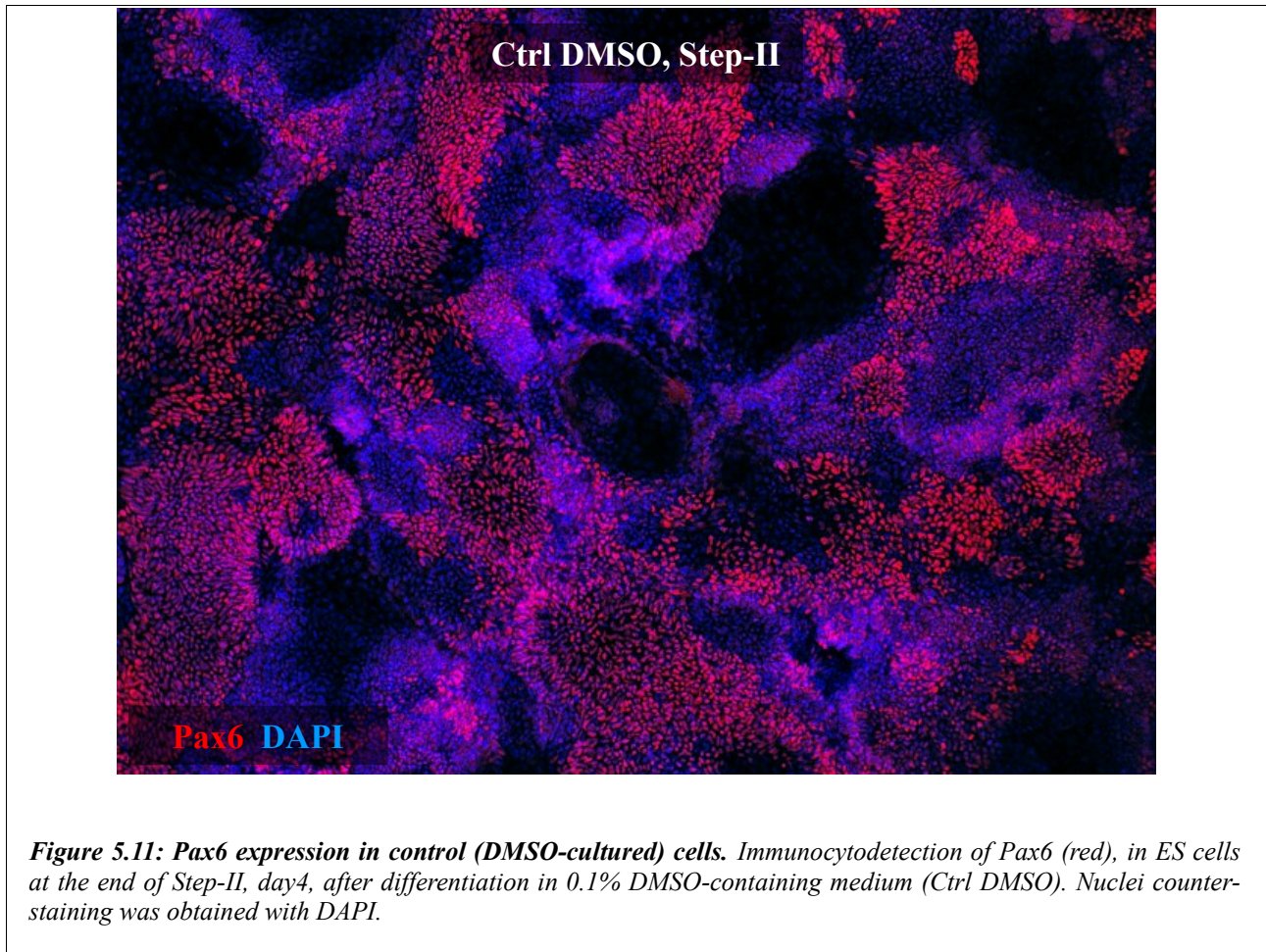


The RT-PCR analysis of neural marker Pax6 gave similar results, showing a relevant collapse of Pax6 expression after Activin treatment (**Figure 5.10**). Pax6 deserves particular attention not only as a pan-neuronal marker, but also in the quality of its role as a eye field transcription factor (Zuber et al., 2003), which must be expressed by early retinal progenitors (See Introduction; Ikeda et al., 2005). Pax6 expression was up-regulated by BMP-inhibition, Wnt-inhibition and particularly by double Wnt/BMP-inhibition, compared to control cells. Activin treatment, even at the lower dose tested (10 ng/ml), caused a marked reduction of Pax6 expression. Taken together with RT-PCR data on Nestin expression, this data suggested that Activin treatment prevented the neural conversion that ES cells normally undergo when cultured in a minimal medium.



Nestin and Pax6 were studied also at the protein level, by performing immunocytochemistry experiments (**Figure 5.11-5.14**). Only Pax6 nuclear staining was quantified by cell counting (**Figure 5.13**), due to difficulty to count Nestin labeling, whose signal was distributed along the soma of partially overlapping cells (**Figure 5.14**).

Figure 5.11 shows Pax6 labeling on control (CDMM+0.1% DMSO cultured) cells, where Pax6 antibody staining revealed a salt-and-pepper mosaic of positive and negative groups of cells (as previously seen in Results, Chapter 3); Pax6-positive cells were 37% among total cell number.



Wnt-inhibition (both alone and together with BMP-inhibition) caused a strong increase of Pax6-positive cells (Wnt-inhibition: 55.5% Pax6-positive cells; double Wnt/BMP-inhibition: 66.4% positive cells; **Figure 5.12A,B**), and this was consistent with RT-PCR results (**Figure 5.10**). Activin treatment dramatically repressed Pax6, which ranged from 1.5 to 12% of total cell number in different treatment combinations (**Figure 5.13** and **Figure 5.12B**). A clear dose-dependent effect of Activin treatment on Pax6 inhibition was evident: WNTi+BMPi+10 ng/ml Activin scored 12% Pax6-positive cells, WNTi+BMPi+50 ng/ml Activin scored 4% Pax6-positive cells and WNTi+BMPi+100 ng/ml Activin scored only 3% Pax6-positive cells (**Figure 5.13**).

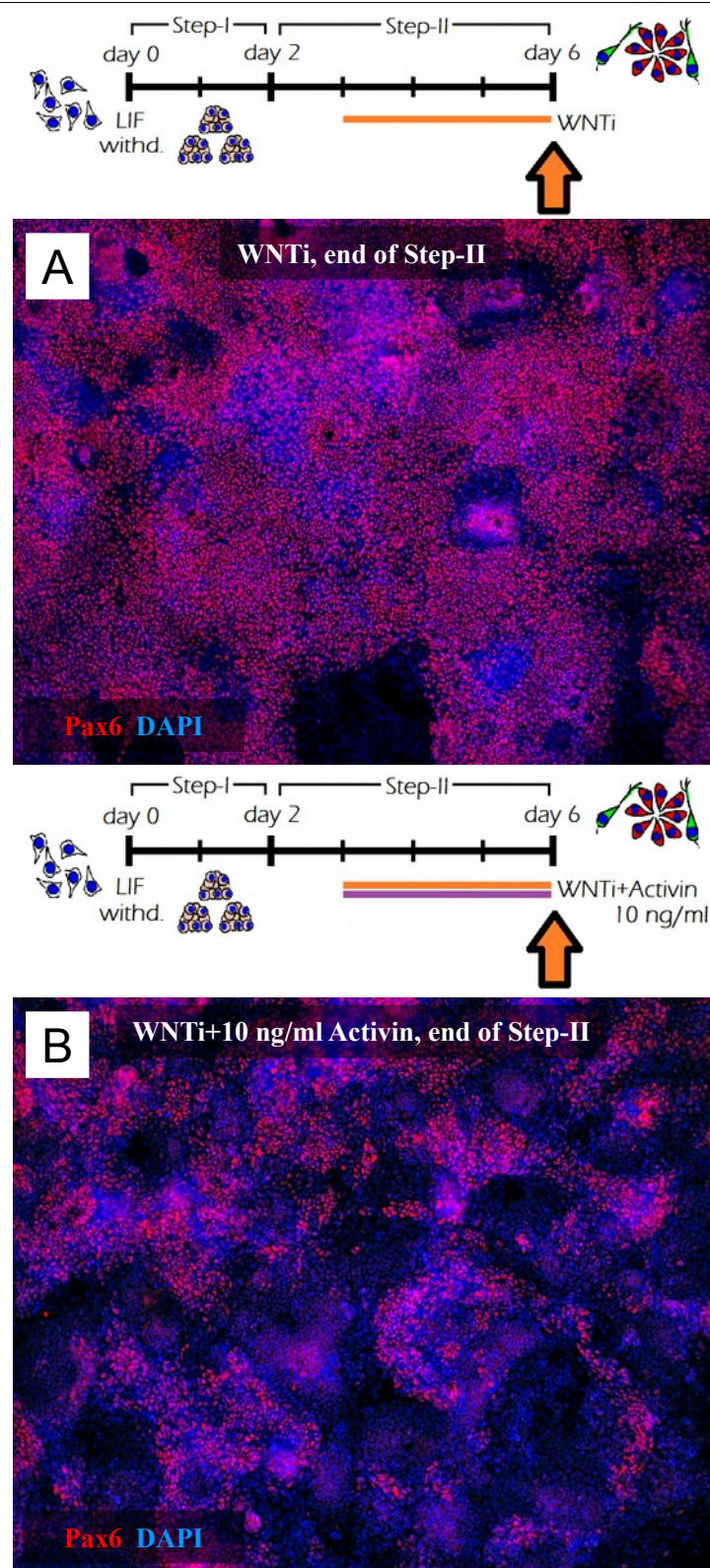
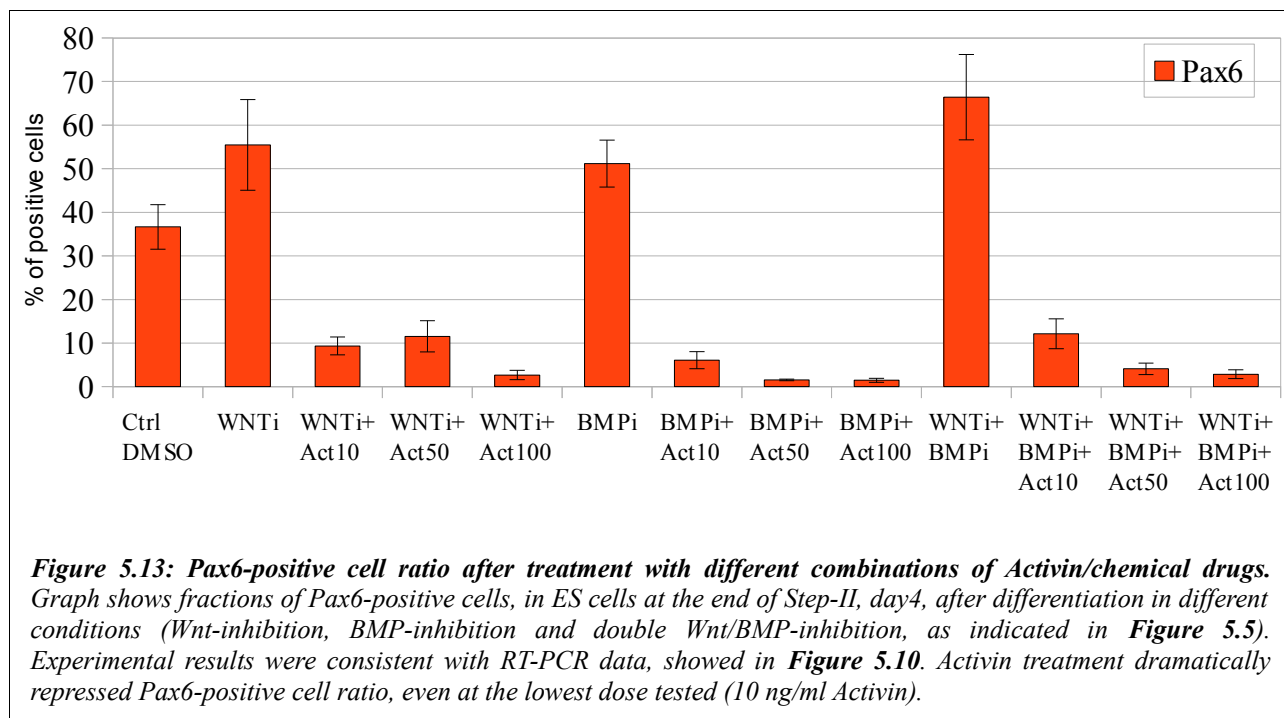
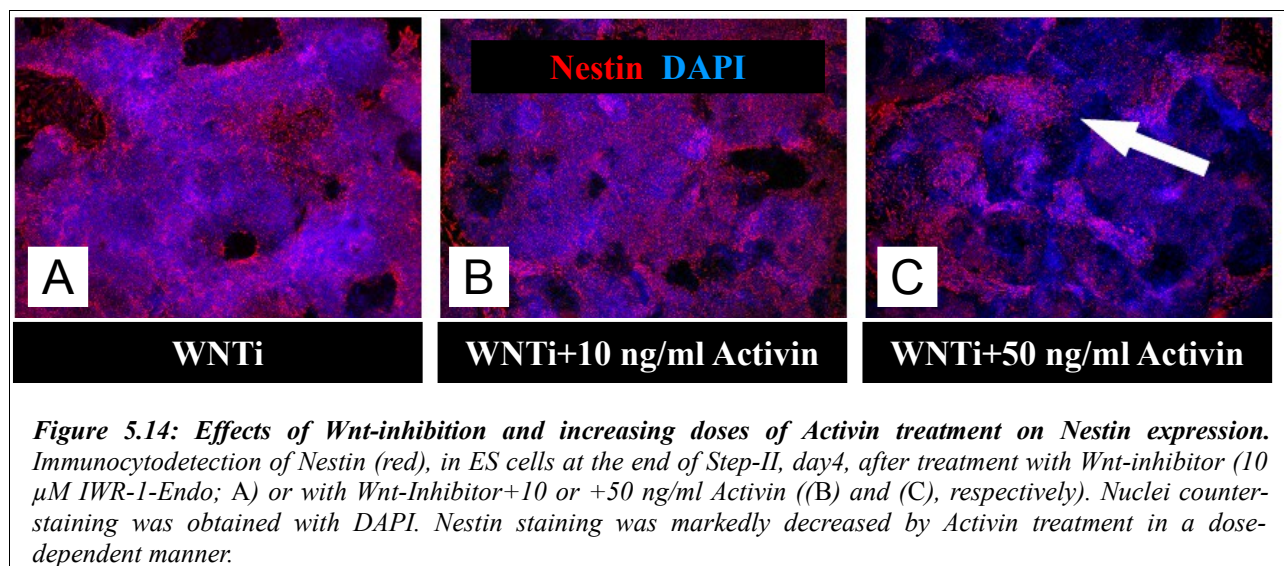


Figure 5.12: Effects of Wnt-inhibition and Activin treatment on Pax6 expression. Immunocyto detection of Pax6 (red), in ES cells at the end of Step-II, day4, after treatment with Wnt-inhibitor (10 μ M IWR-1-Endo; A) or with Wnt-inhibitor plus 10 ng/ml Activin; B). Nuclei counter-staining was obtained with DAPI. Activin treatment dramatically repressed Pax6, as few Pax6-positive cell clusters were present in culture after Activin treatment.



Nestin immunostaining was analyzed only from the qualitative point of view. However, **Figure 5.14** shows very clearly that Nestin staining followed a general trend consistent with RT-PCR data. A strong staining was detected at the end of Step-II on control cells and on Wnt, BMP or double Wnt/BMP inhibited cells (**Figure 5.14** and data not shown), but the staining was markedly decreased by Activin treatment in a dose-dependent manner. In cells treated with high Activin doses, only few cell clusters maintained a strong Nestin staining (white arrow in **Figure 5.14**).



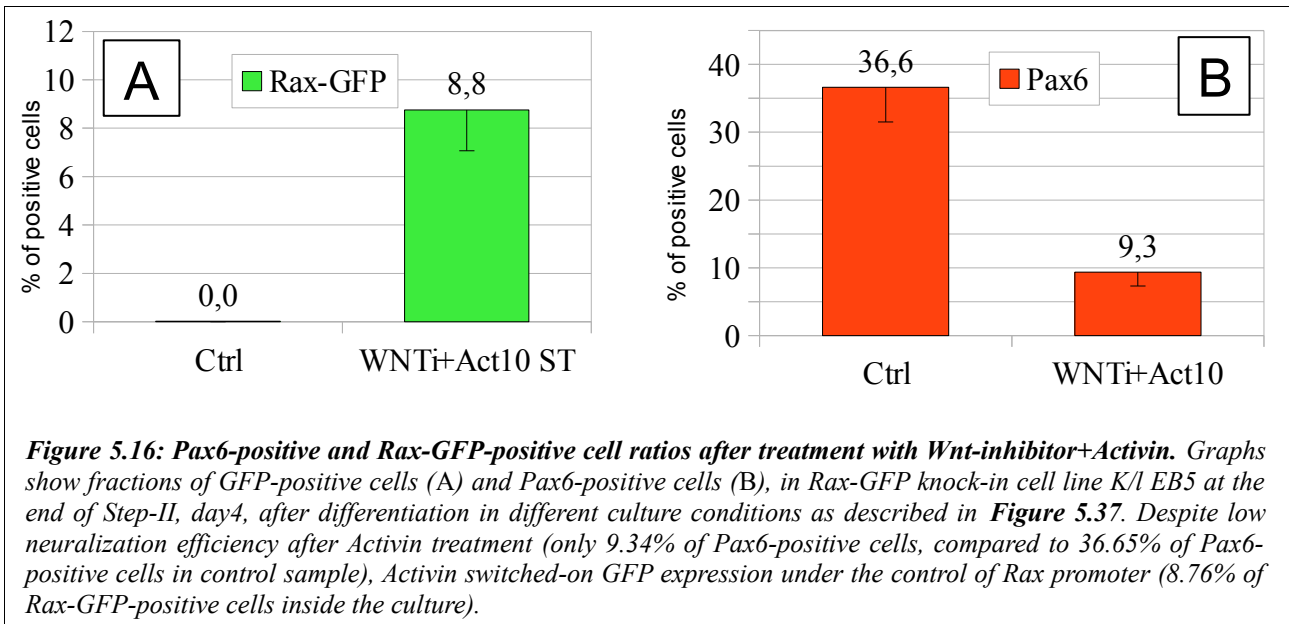
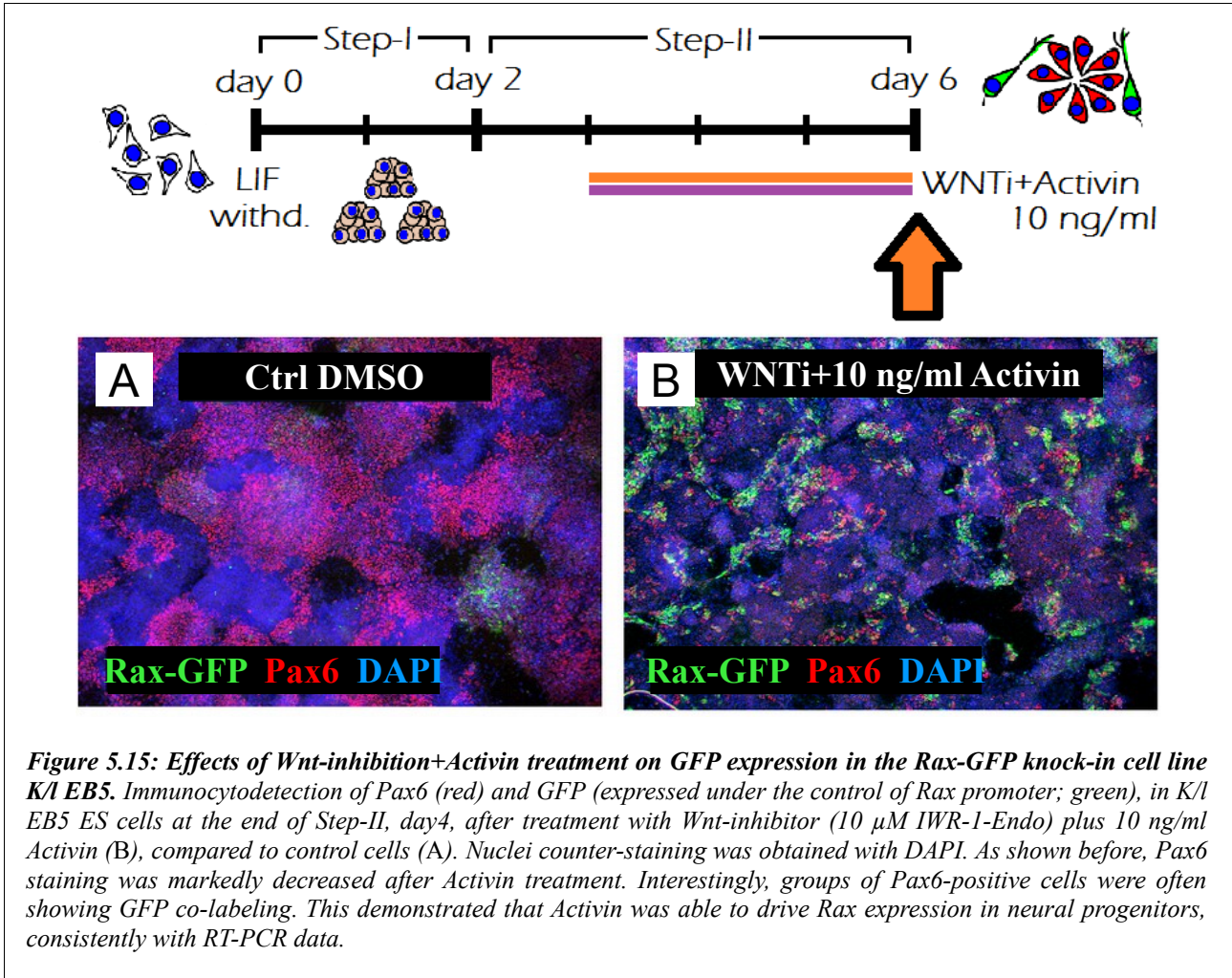
Taken all together, these data indicated that Activin had two different effects on our cultures:

- Activin treatment, when associated together with Wnt- and/or BMP-inhibition, was able to inhibit cortical gene expression and sustain retinal gene expression, as seen by RT-PCR.
- ES cell neural conversion was partially prevented by Activin treatment, as seen by both RT-PCR and immunocytochemistry analysis of Nestin and Pax6 expression. This means that Activin treatment reduced the neuralization efficiency of our protocol, and the inductive effect of Activin on retinal marker expression could be consequently underestimated.

A better characterization of Activin effect on ES cell neural conversion, and the modifications to our protocol to reduce Activin side-effect on neuralization will be discussed later in this Chapter.

To directly visualize Rax-positive cells, we took advantage of a Rax-GFP knock-in ES cell line (K/I EB5, a kind gift of Professor Yoshiki Sasai). Cells were treated with WNTi+10 ng/ml Activin during Step-II, then fixed at the end of Step-II and analyzed by immunocytochemistry. Rax-GFP-positive neural progenitors were not present in our control culture; on the contrary, we found GFP-positive cells in WNTi+10 ng/ml Activin condition (**Figure 5.37**).

This first attempt to use K/I EB5 ES cell line was successful, as we obtained Rax-GFP staining after WNTi+Activin treatment (10ng/ml), but this experiment highlighted again the low efficiency of our protocol when associated with Activin treatment, both in terms of neuralization (only 9.3 % of Pax6-positive cells, compared to 36.7 % of Pax6-positive cells in control sample) and in terms of Rax expression (only 8.8 % of Rax-GFP-positive cells inside the culture) (**Figure 5.16**).

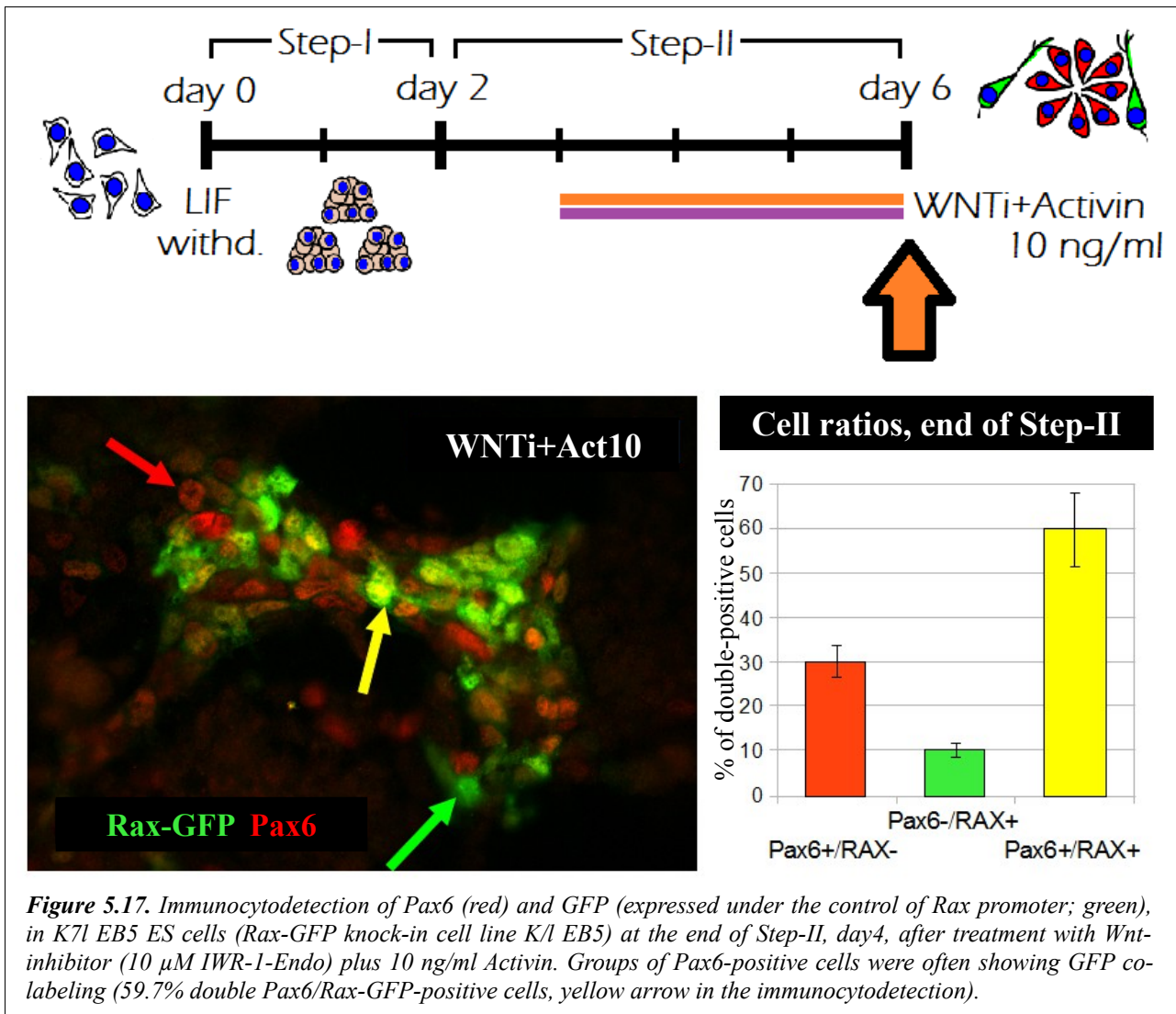


Previous studies demonstrated that cells co-expressing the eye field marker Rax and the neural marker Pax6 are *bona fide* retinal progenitors (Zuber et al., 2003; Ikeda et al., 2005). We performed a double immunocytochemical detection of Rax-GFP together with Pax6, to test for a possible co-expression also in our differentiation culture.

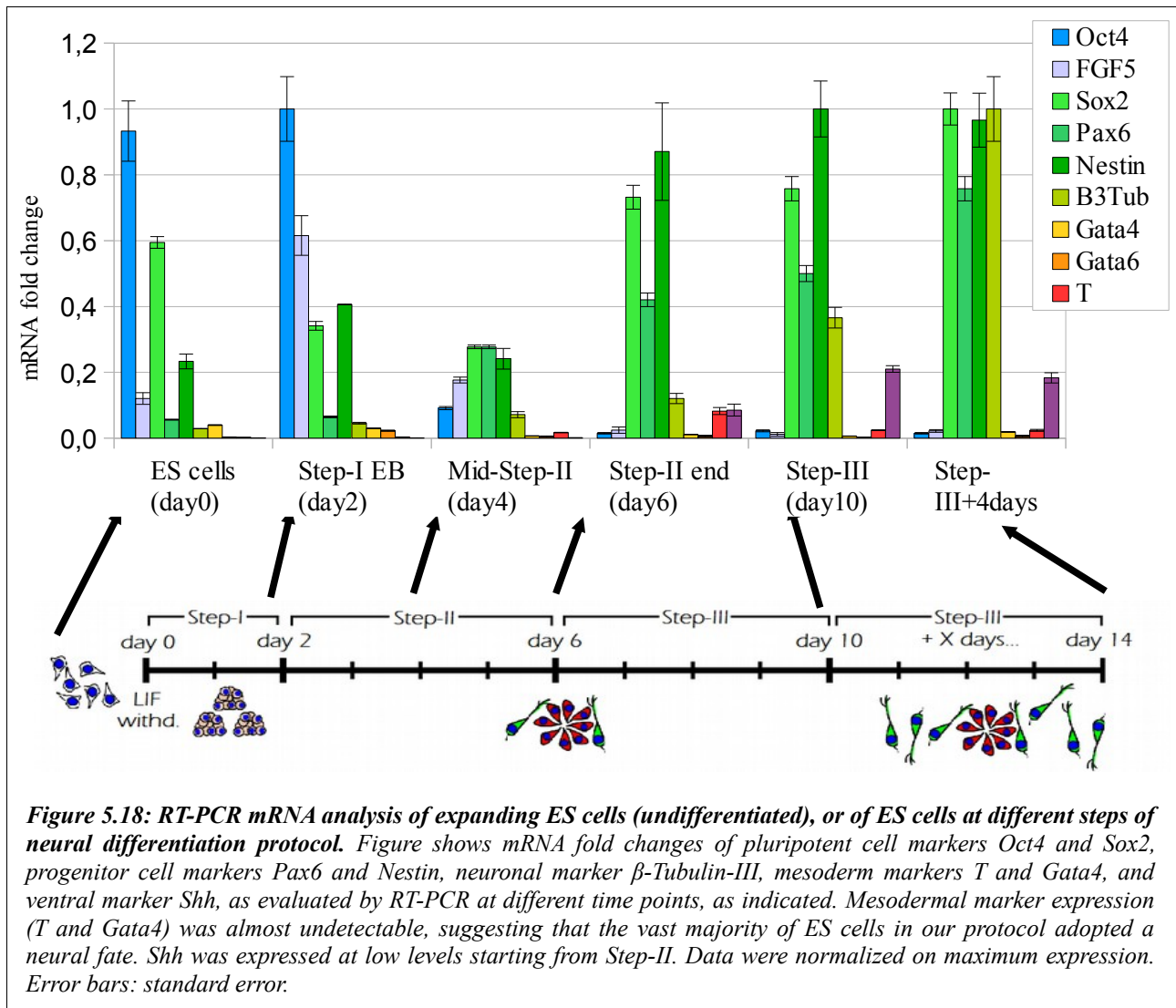
After treatment with WNTi+10 ng/ml Activin, the most represented population inside the culture among immunolabeled cells (Pax6-positive cells, GFP-positive cells, or double Pax6/GFP-positive cells) was the one expressing both proteins. Pax6-positive/GFP-negative cells (red column in **Figure 5.17**) were 30.15% over labeled cells, which correspond to 4.2% positive cells over total cell population. Pax6-negative/GFP-positive cells (green column in **Figure 5.17**) were only 10.15% over labeled cells, which correspond to a very small percentage (1.3% positive cells) of total cell population. Finally, double Pax6/GFP-positive cells (yellow column in **Figure 5.17**) were 59.7% over labeled cells, which correspond to 7.5% positive cells over total cell population. Thus, Pax6 and Rax-GFP were often co-expressed (in the 59.7% of case). This result demonstrated that Activin is able to induce the differentiation of *bona fide* Rax(+)/Pax6(+) retinal progenitors. However, the ratio of double Rax/Pax6-positive neural progenitors among total cell population was quite low, scoring only 7.5% positive cells.

To improve the protocol efficiency, we addressed the problem of inefficient neuralization, starting with a more detailed characterization of the markers of pluripotency/neural identity by RT-PCR in different conditions.

As already described in Results, Chapter 1, differentiating ES cells gradually switched-off the expression of pluripotency/epiblast markers (Oct4 and FGF5), and up-regulated the expression of neural markers (Nestin, Pax6 and Sox2) during differentiation in chemically defined minimal medium (CDMM) (**Figure 5.18**).



Oct4 was strongly down-regulated between Step-I and Step-II, as differentiation started (**Figure 5.18**). Sox2, which is considered both an embryonic stem cell pluripotency marker and a neural progenitor marker, behaved consistently with this definition, being strongly expressed by both undifferentiated ES cells and neural progenitors. Nestin and Pax6 expression became strong during Step-II, while β -Tubulin-III expression increased at Step-III. The expression of mesodermal and endodermal markers Gata4, Gata6 and Brachyury (T) was very low, almost undetectable, indicating the absence of meso/endodermal differentiation inside our protocol. Shh, which is produced by ventral neural progenitors (Jessell, 2000) and lately in development acts as a mitogen for cortical progenitors (Komada et al., 2008; 2012), was expressed at low levels starting at Step-II.



When the same genes were analyzed after treatments with different combinations of Activin/chemical drugs, we found that Activin presence in culture medium dramatically affected the process of ES cell neuralization (**Figure 5.19A,B**). As a general trend, neuralization was achieved spontaneously in our control condition (ES cell differentiation in CDMM+0.1% DMSO; first column group on the left in **Figure 5.19B**), and was even strengthened after Wnt-, BMP- or double Wnt/BMP-inhibition (see Sox2, Pax6 and Nestin expression, green color code in **Figure 5.19B**). This was confirmed also by measuring the expression of pluripotency markers (blue color code in **Figure 5.19B**): pluripotent stem cell marker Oct4 and epiblast marker FGF5 were silenced after ES cell differentiation, both in control condition (CDMM DMSO) and in cells treated with Wnt, BMP or Wnt/BMP inhibitors. Meso/endodermal marker Gata4, Gata6 and Brachyury (T) expression level was almost undetectable in these conditions.

The situation after treatment with Activin was markedly different. Activin treatment switched-off the expression of neural progenitor markers Pax6, Nestin and Sox2 in a dose-dependent manner (see how green columns, corresponding to the expression level of neural markers, were lower when compared to control CDMM condition). *Vice versa*, the presence of Activin in the medium impeded the down-regulation of the pluripotency markers Oct4 and FGF5, which are normally silenced as differentiation starts *in vitro*. Oct4 expression level was particularly high in cells treated with Wnt-inhibitor+Activin or with double Wnt/BMP-inhibition+Activin, while FGF5 expression peaked in cells treated with BMPi+Activin.

Concerning the meso/endodermal markers Gata4, Gata6 and Brachyury (T) (yellow and red columns in **Figure 5.19B**), their expression was switched-on by Activin treatment, accordingly with an Activin role in mesodermal and endodermal induction (Cerdan et al., 2012). Brachyury (T) expression was particularly high in cells treated with BMP-inhibition+10 ng/ml Activin. This sample was also characterized by a high expression level of the ventral marker Shh (violet columns in **Figure 5.19B**).

Dissecting the characteristics of each combination of treatments was far from easy. Anyhow, some general trends were deduced:

- ES neural conversion was increased by Wnt, BMP or double Wnt/BMP-inhibition, compared to control cells, but was strongly prevented by Activin treatment, as seen by the dramatic down-regulation of Sox2, Nestin and Pax6 in cells treated with increasing doses of Activin.
- Activin acted mainly by slowing down the neuralization process that normally ES cells undergo in our protocol when cultured in a minimal medium. This was suggested by the high expression levels of the pluripotency markers Oct4 and FGF5 in Activin-treated cells.
- As another side-effect of Activin treatment, the expression of mesodermal markers Gata4 and Brachyury was induced. The “*mesodermal contamination*” of our culture was particularly evident in cells treated with BMPi plus low Activin dose. This particular combination also showed a high degree of ventralization, as suggested by the high level of Shh expression. For this reason, BMP-inhibition alone was not used as a retinal inducing treatment in later experiments.

The effect of Activin on ES cell neuralization was also investigated by immunocyto detection of the neural progenitor marker Musashi-1 (red staining in **Figure 5.20**, Panels A-D) and of the pluripotency marker Oct4 (green staining in **Figure 5.20**, Panels A-D), as detected at the end of Step-II.

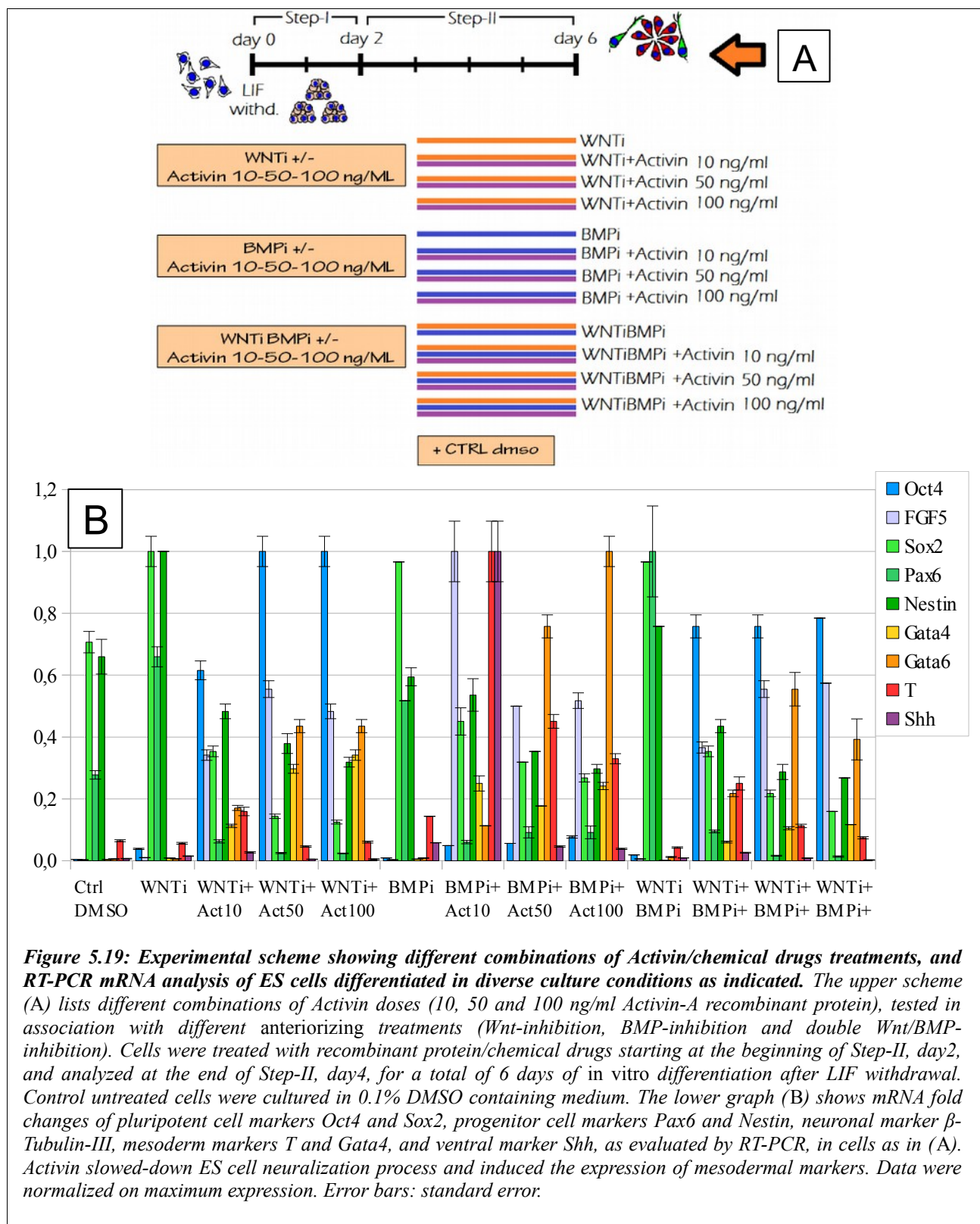


Figure 5.19: Experimental scheme showing different combinations of Activin/chemical drugs treatments, and RT-PCR mRNA analysis of ES cells differentiated in diverse culture conditions as indicated. The upper scheme (A) lists different combinations of Activin doses (10, 50 and 100 ng/ml Activin-A recombinant protein), tested in association with different anteriorizing treatments (Wnt-inhibition, BMP-inhibition and double Wnt/BMP-inhibition). Cells were treated with recombinant protein/chemical drugs starting at the beginning of Step-II, day2, and analyzed at the end of Step-II, day4, for a total of 6 days of in vitro differentiation after LIF withdrawal. Control untreated cells were cultured in 0.1% DMSO containing medium. The lower graph (B) shows mRNA fold changes of pluripotent cell markers Oct4 and Sox2, progenitor cell markers Pax6 and Nestin, neuronal marker β -Tubulin-III, mesoderm markers T and Gata4, and ventral marker Shh, as evaluated by RT-PCR, in cells as in (A). Activin slowed-down ES cell neuralization process and induced the expression of mesodermal markers. Data were normalized on maximum expression. Error bars: standard error.

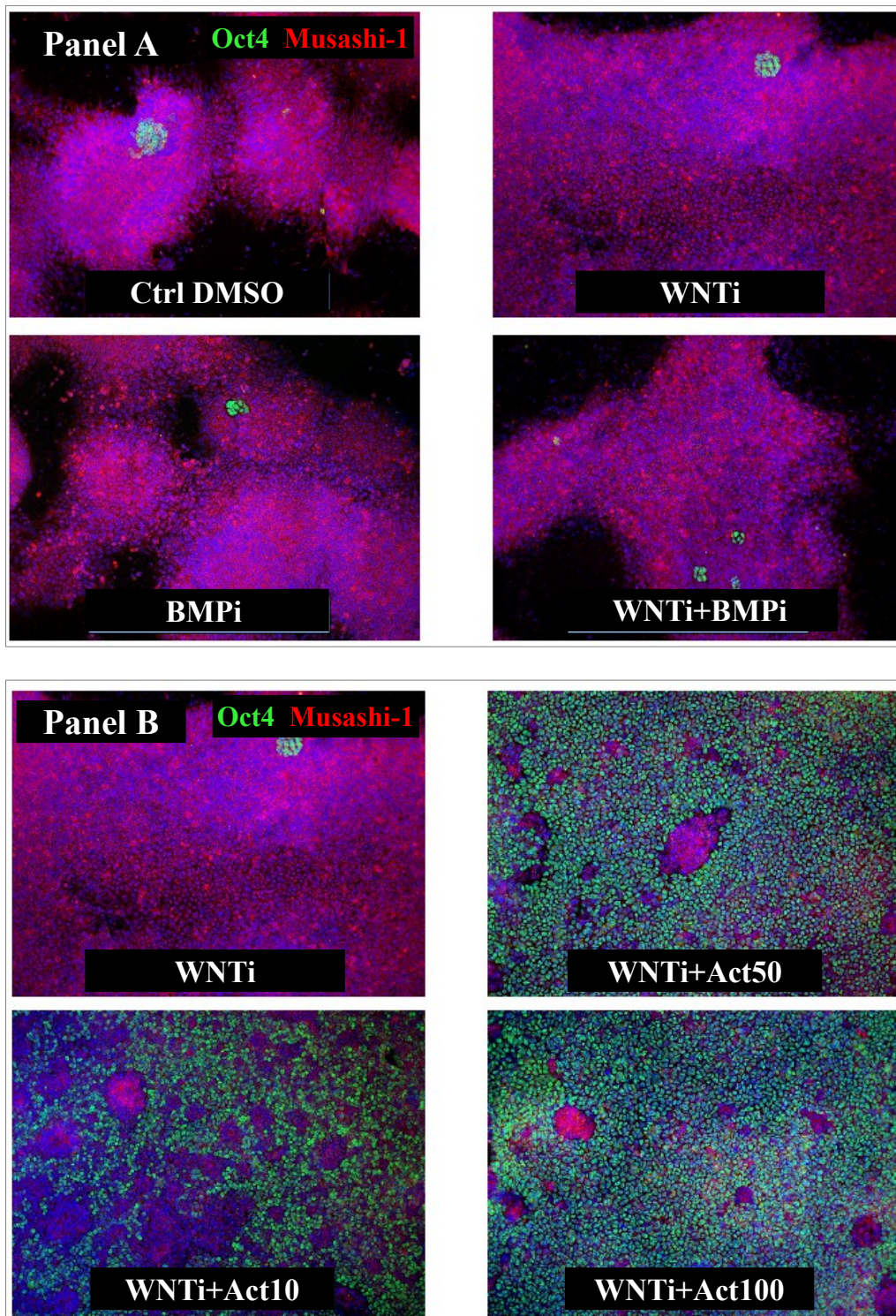
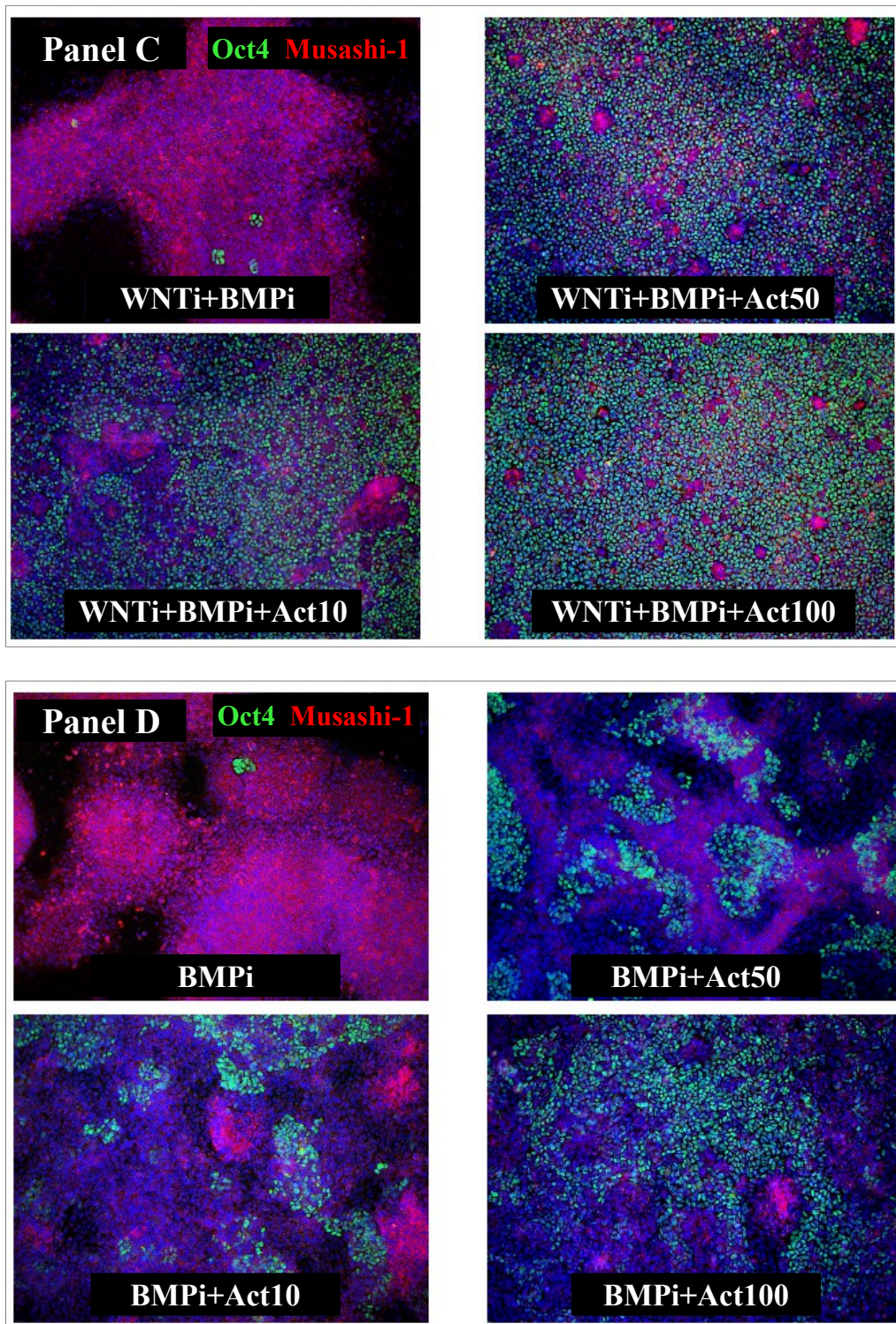


Figure 5.20: Effects of different combinations of Activin/chemical drugs on ES cell neural differentiation. Panels A-D show immunocyto detection of neural marker Musashi-1 (red) and stem cell marker Oct4 (green), in ES cells at the end of Step-II, day4, after treatment with different combinations of Activin/chemical drugs, as schematized in **Figure 5.5** and **Figure 5.19**. Nuclei counter-staining was obtained with DAPI. As showed before by RT-PCR (**Figure 5.19**), the expression level of neural markers was markedly reduced after Activin treatment, while that of pluripotency markers was increased.



*This effect of Activin on neural differentiation was confirmed here by Oct4 and Musashi-1 immunostaining: the vast majority of cell population remained in a undifferentiated (Oct4-positive) state after treatment with high doses of Activin (50 and 100 ng/ml). Musashi-1 immunostaining showed a signal intensity and distribution which were complementary to those of Oct4. Concerning Activin effect on neural differentiation markers, see also **Figure 5.12**, **Figure 5.13** and **Figure 5.14**.*

The result was perfectly consistent with RT-PCR data, showing high ratio of Oct4-positive cells in Activin-treated samples (**Figure 5.20** and **Figure 5.21**). Oct4-positive cell ratio was low in control cells (0.71% Oct4-positive cells) and was not strongly affected by Wnt-inhibition, BMP-inhibition and double Wnt/BMP-inhibition (3.24%, 0.2% and 4.7% Oct4-positive cells, respectively); this indicated that ES cells switched-off Oct4 expression when differentiated using our protocol. On the contrary, Activin treatment dramatically increased Oct4-positive cell ratio. As an example, Wnt-inhibition+10 ng/ml Activin treated cultures scored 51.13% Oct4-positive cells, Wnt-inhibition+50 ng/ml Activin treated cultures scored 80.7% Oct4-positive cells and this percentage was further increased in Wnt-inhibition+100 ng/ml Activin treated cultures, with 91.6% Oct4-positive cells. This indicated that the vast majority of cell population was still in a undifferentiated state at the fourth day of Step-II, after treatment with high doses of Activin (**Figure 5.20** and **Figure 5.21**). Moreover, this result is consistent with the reduced neuralization observed at later stages of *in vitro* differentiation after Activin treatment (see above). Musashi-1 immunostaining showed signal intensity and distribution that were complementary to those of Oct4 immunostaining (**Figure 5.20**). Oct4-positive cell ratio in BMP-inhibition alone was not so high if compared to other conditions (ranging from 15.3% in BMPi+10 ng/ml Activin treated cells to 57.2% in BMPi+100 ng/ml Activin treated cells); this, together with RT-PCR data showing high Gata4, Gata6 and Brachyury expression levels, suggested that cells treated with BMP-inhibition+Activin followed a meso/endodermal differentiation fate instead of simply being slowed-down in differentiation.

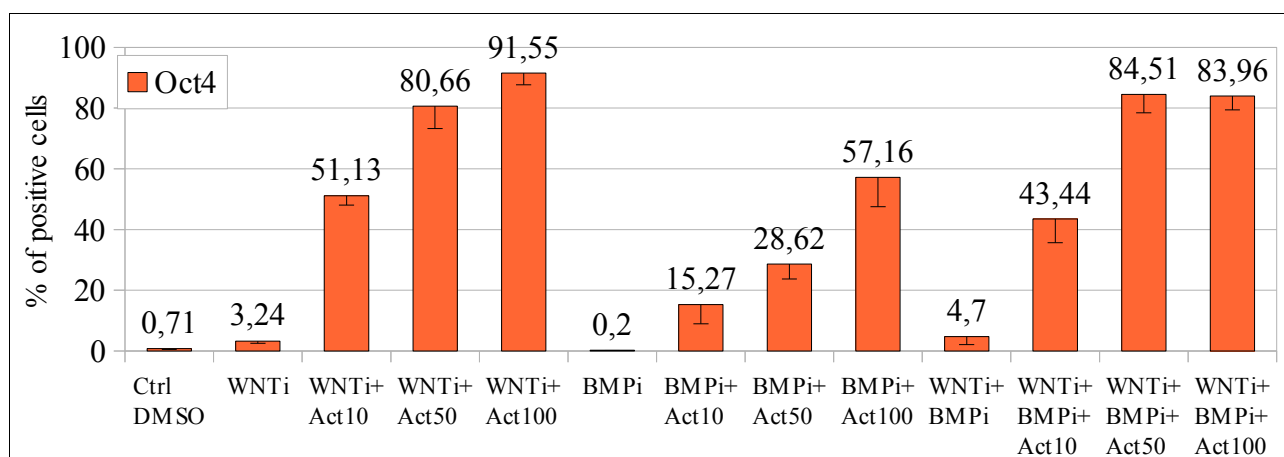
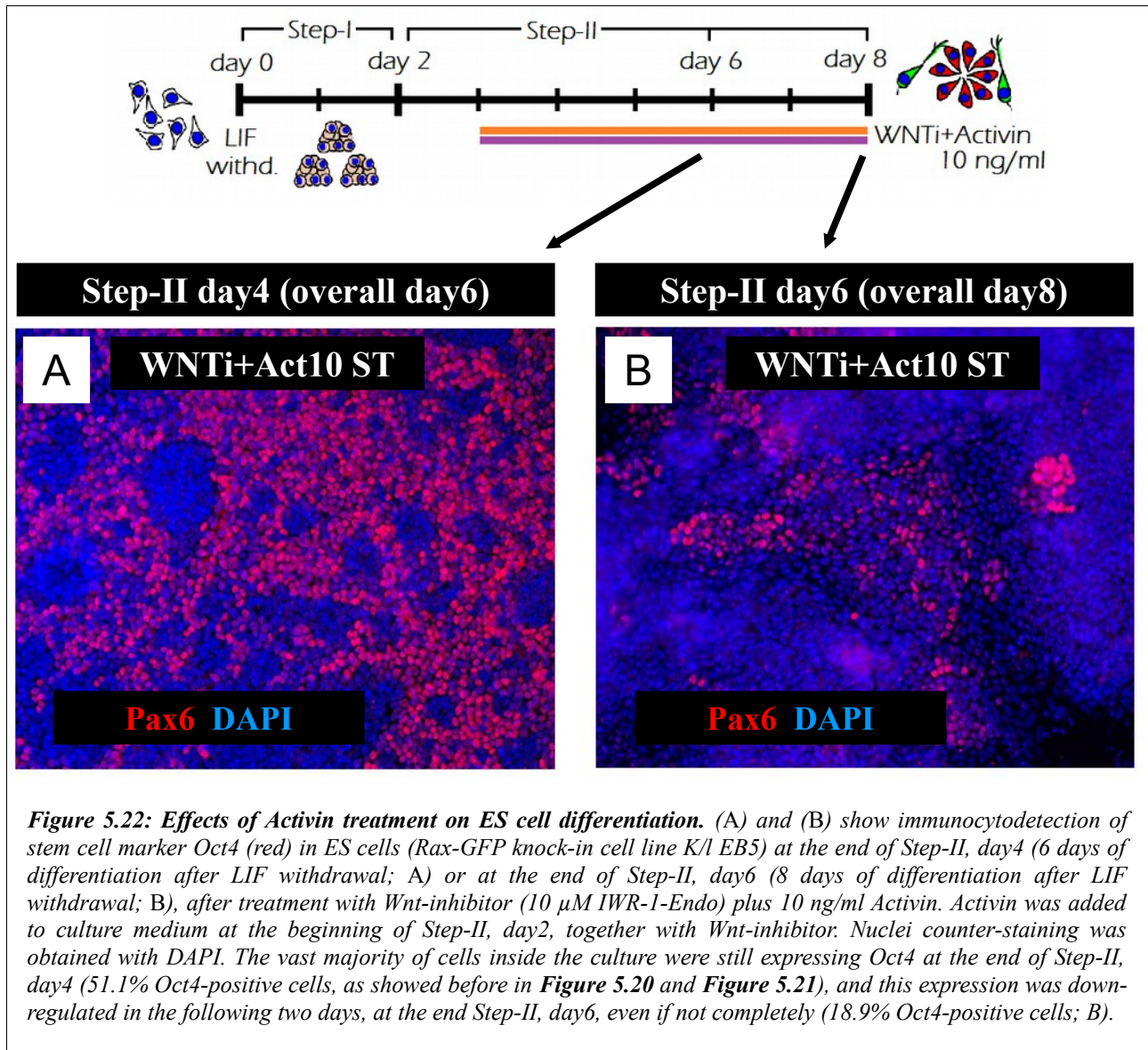


Figure 5.21: Effects of different combinations of Activin/chemical drugs on ES cell neural differentiation. Graph shows Oct4-positive cell ratio in ES cells at the end of Step-II, day4, after differentiation in different conditions as indicated in **Figure 5.5** and **Figure 5.19**. Images are shown in **Figure 5.20**. Oct4-positive cell ratio was low in control cells (0.71% Oct4-positive cells). On the contrary, Activin treatment dramatically increased Oct4-positive cell ratio, even at the lowest dose tested (51.13% Oct4-positive cells after WNTi+10 ng/ml Activin, as an example). This suggested that ES cell neural conversion was partially prevented by Activin treatment in a dose-dependent manner. Error bars: standard error.

Taken together, all these data highlighted the effect of Activin on ES cell neuralization and possibly explained the reason for the low efficiency of Rax-GFP-positive cell induction in our protocol (as showed before in **Figure 5.37** and **Figure 5.16**).

To investigate whether, after an initial delay, Activin-treated cells could efficiently undergo neuralization, we cultured cells for a longer period during Step-II, without any additional dissociation/replating. For subsequent experiments, cells were then cultured until the end of Step-II as a first analysis time point (fourth day of the canonical Step-II, for a total of 6 days of differentiation after LIF withdrawal) and simultaneously until a new analysis time point (two additional days of culture in a prolonged Step-II, for a total of 8 days of differentiation after the starting point of the protocol), to allow for more cells to gradually convert into neural progenitors and express neuronal/regional markers.

Rax-GFP knock-in ES cell line was treated with WNTi+10 ng/ml Activin during Step-II, then fixed and analyzed by immunocytochemistry. This time some samples were cultured until the additional analysis point at Step-II, day6, which corresponded to a total of 8 days of differentiation after LIF withdrawal. A comparison between cells treated with Wnt-inhibitor+10 ng/ml Activin, analyzed by immunocytochemistry at the two different time points during neural differentiation, showed how the vast majority of cells inside the culture were still expressing Oct4 at the end of Step-II, day4 (51.1% Oct4-positive cells, as showed before in **Figure 5.20** and **Figure 5.21**), and this expression was down-regulated in the following two days, at the end Step-II, day6, even if not completely (18.9% Oct4-positive cells) (**Figure 5.22**). Rax-GFP-positive cell ratio increased three-fold at Step-II, day6 (longer protocol, 8 days of differentiation; 24.4% Rax-GFP-positive cells), when compared to Step-II, day4 (shorter protocol, 6 days of differentiation; 8.8% Rax-GFP-positive cells) (**Figure 5.23**).



This was accompanied by a more than two-fold increase of the neuronal/retinal marker Pax6 (9.3% Pax6-positive cells in WNTi+Activin at Step-II, day4; 21.7% Pax6-positive cells at Step-II, day6) (**Figure 5.24**). This experiment suggested that Activin treatment delayed but did not completely impair neural differentiation. In fact, two additional days of differentiation allowed more efficient neural conversion (as seen by Pax6-positive cell ratio increase and by Oct4-positive cell ratio decrease) and higher retinal marker expression (evaluated by the increase of Rax-GFP-positive cell ratio).

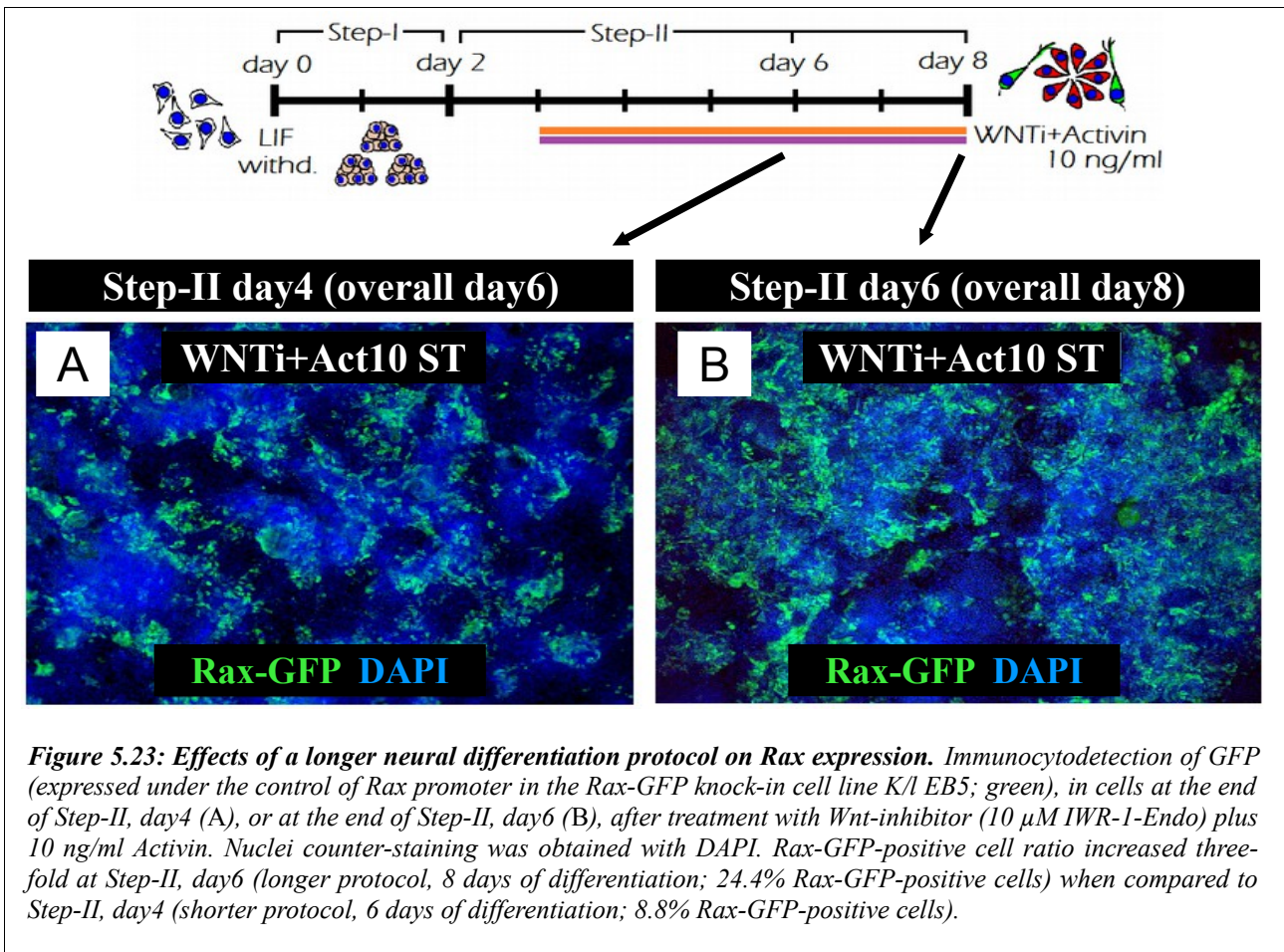


Figure 5.23: Effects of a longer neural differentiation protocol on Rax expression. Immunocyto detection of GFP (expressed under the control of Rax promoter in the Rax-GFP knock-in cell line K/l EB5; green), in cells at the end of Step-II, day4 (A), or at the end of Step-II, day6 (B), after treatment with Wnt-inhibitor (10 μ M IWR-1-Endo) plus 10 ng/ml Activin. Nuclei counter-staining was obtained with DAPI. Rax-GFP-positive cell ratio increased three-fold at Step-II, day6 (longer protocol, 8 days of differentiation; 24.4% Rax-GFP-positive cells) when compared to Step-II, day4 (shorter protocol, 6 days of differentiation; 8.8% Rax-GFP-positive cells).

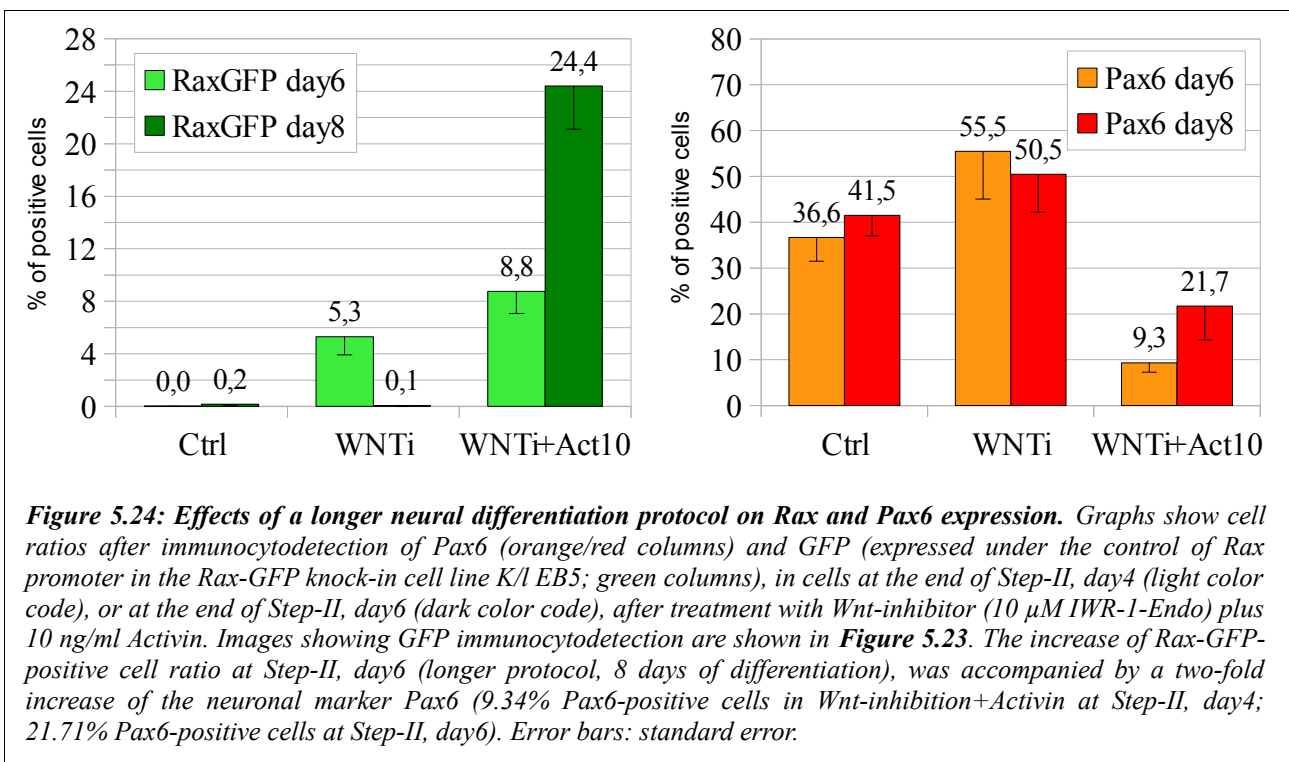


Figure 5.24: Effects of a longer neural differentiation protocol on Rax and Pax6 expression. Graphs show cell ratios after immunocyto detection of Pax6 (orange/red columns) and GFP (expressed under the control of Rax promoter in the Rax-GFP knock-in cell line K/l EB5; green columns), in cells at the end of Step-II, day4 (light color code), or at the end of Step-II, day6 (dark color code), after treatment with Wnt-inhibitor (10 μ M IWR-1-Endo) plus 10 ng/ml Activin. Images showing GFP immunocyto detection are shown in **Figure 5.23**. The increase of Rax-GFP-positive cell ratio at Step-II, day6 (longer protocol, 8 days of differentiation), was accompanied by a two-fold increase of the neuronal marker Pax6 (9.34% Pax6-positive cells in Wnt-inhibition+Activin at Step-II, day4; 21.71% Pax6-positive cells at Step-II, day6). Error bars: standard error.

The analysis of Rax activation in the K/l EB5 ES cell line at late time of differentiation was repeated for all the combinations of Activin doses plus Wnt and/or BMP pathway inhibitions. Wnt-inhibition+10 ng/ml Activin turned out to be the best treatment to induce Rax-GFP-positive cells (**Figure 5.25A,B**).

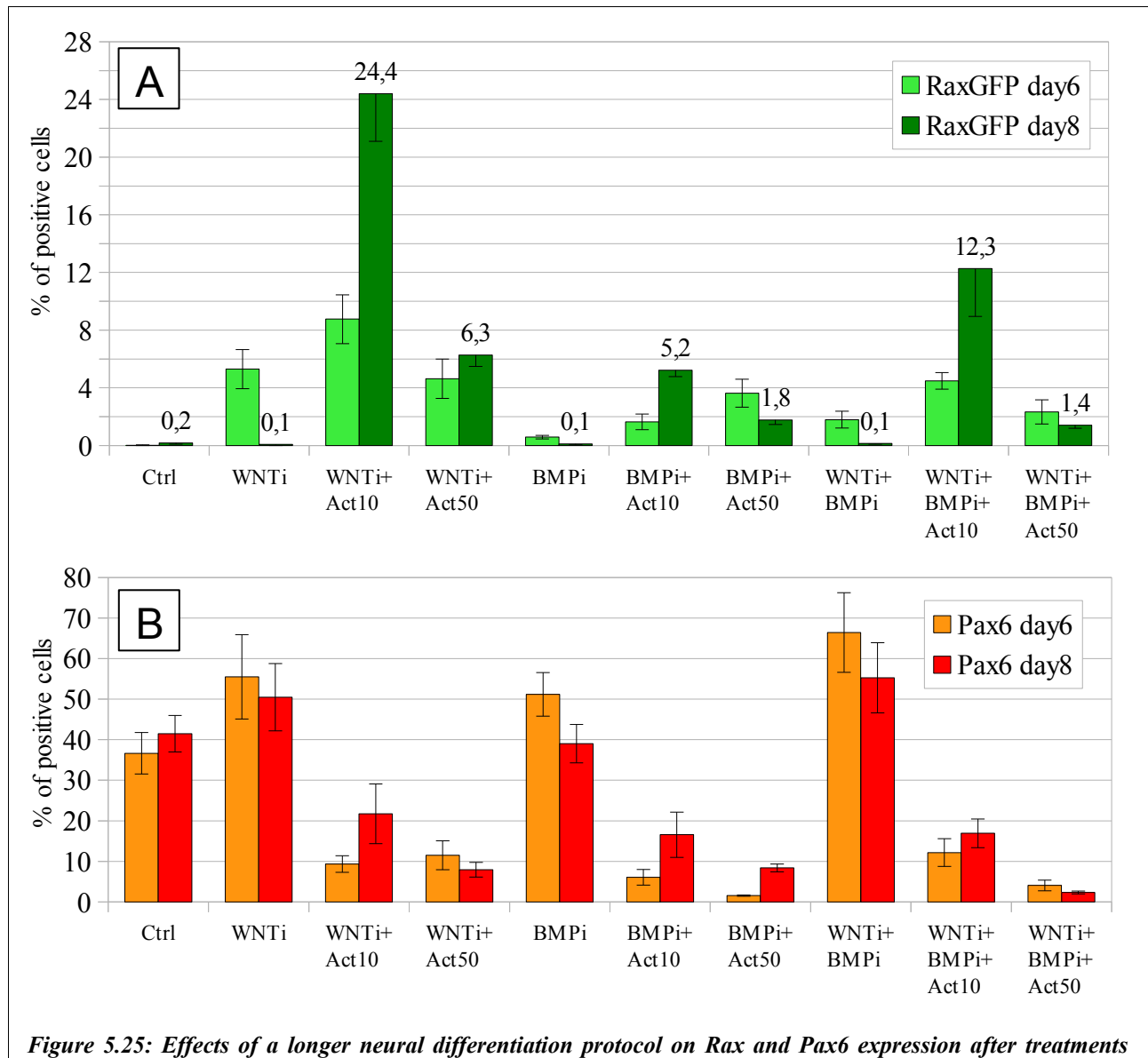
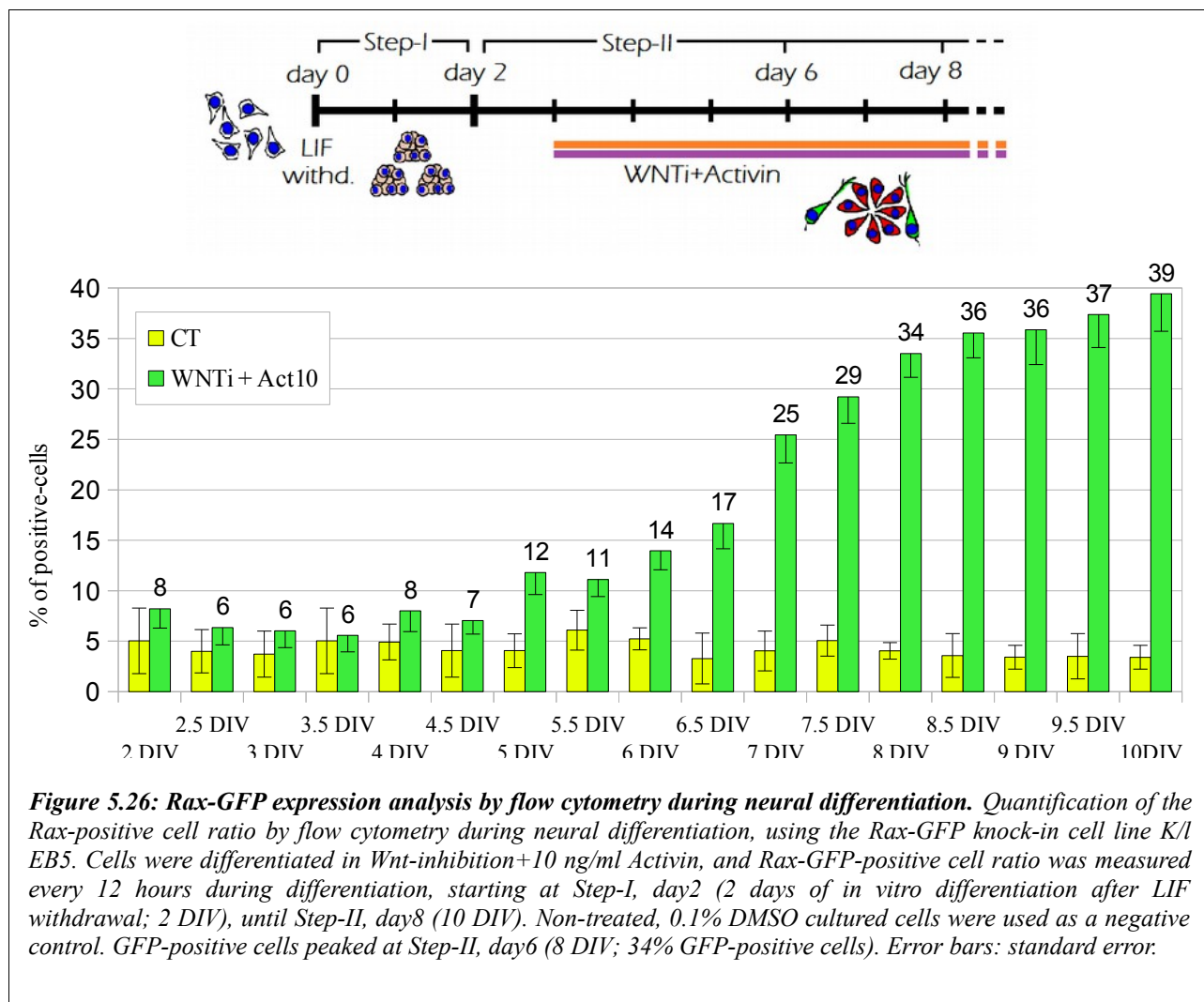


Figure 5.25: Effects of a longer neural differentiation protocol on Rax and Pax6 expression after treatments with different combinations of Activin/chemical drugs. Graphs (A) and (B) show cell ratios after immunocyto detection of Pax6 (orange/red columns, B) and GFP (expressed under the control of Rax promoter in the Rax-GFP knock-in cell line K/l EB5; green columns, A), in ES cells at the end of Step-II, day4 (6 days of differentiation; light color code), or at the end of Step-II, day6 (8 days of differentiation; dark color code), after treatment with different combinations of Activin/chemical drugs. Wnt-inhibition+10 ng/ml Activin turned out to be the best treatment to induce Rax-GFP-positive cells (24.4% Rax-GFP-positive cells at Step-II, day6). Error bars: standard error.

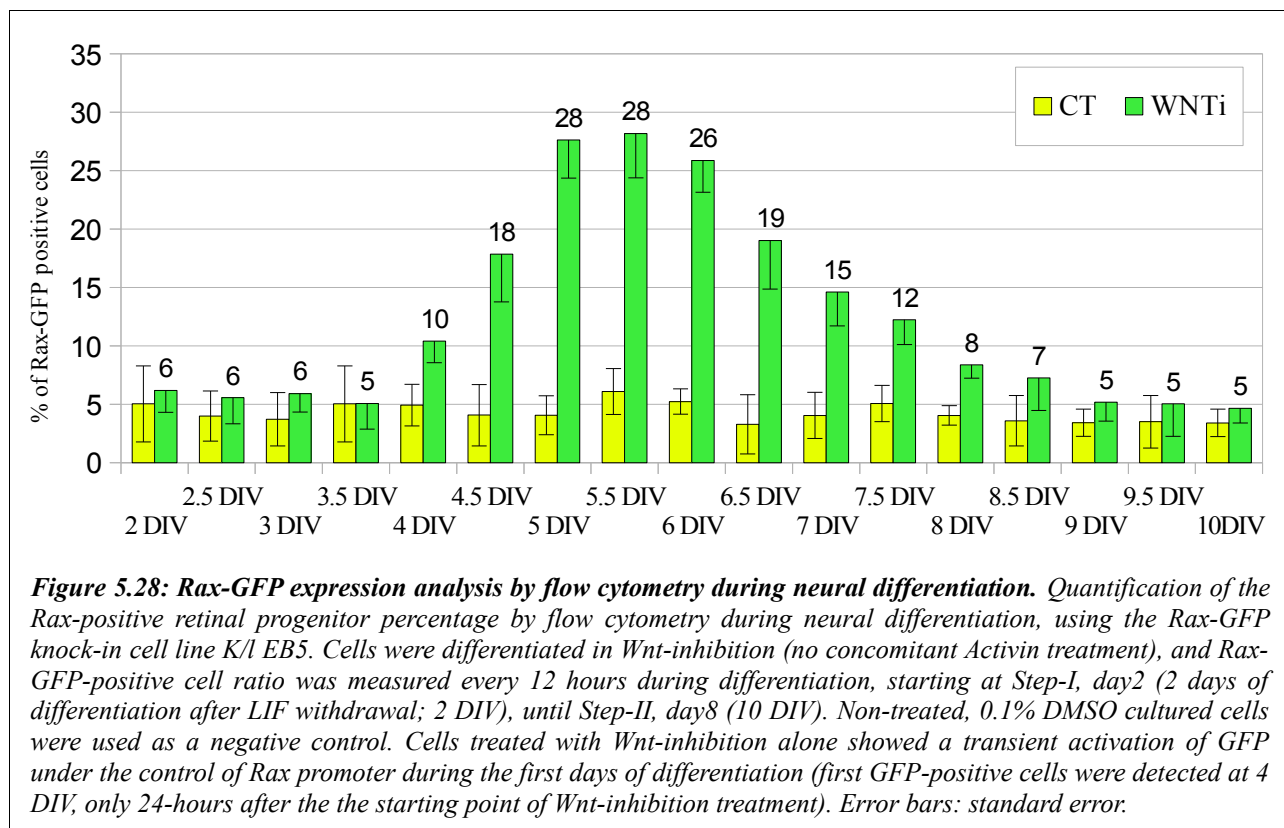
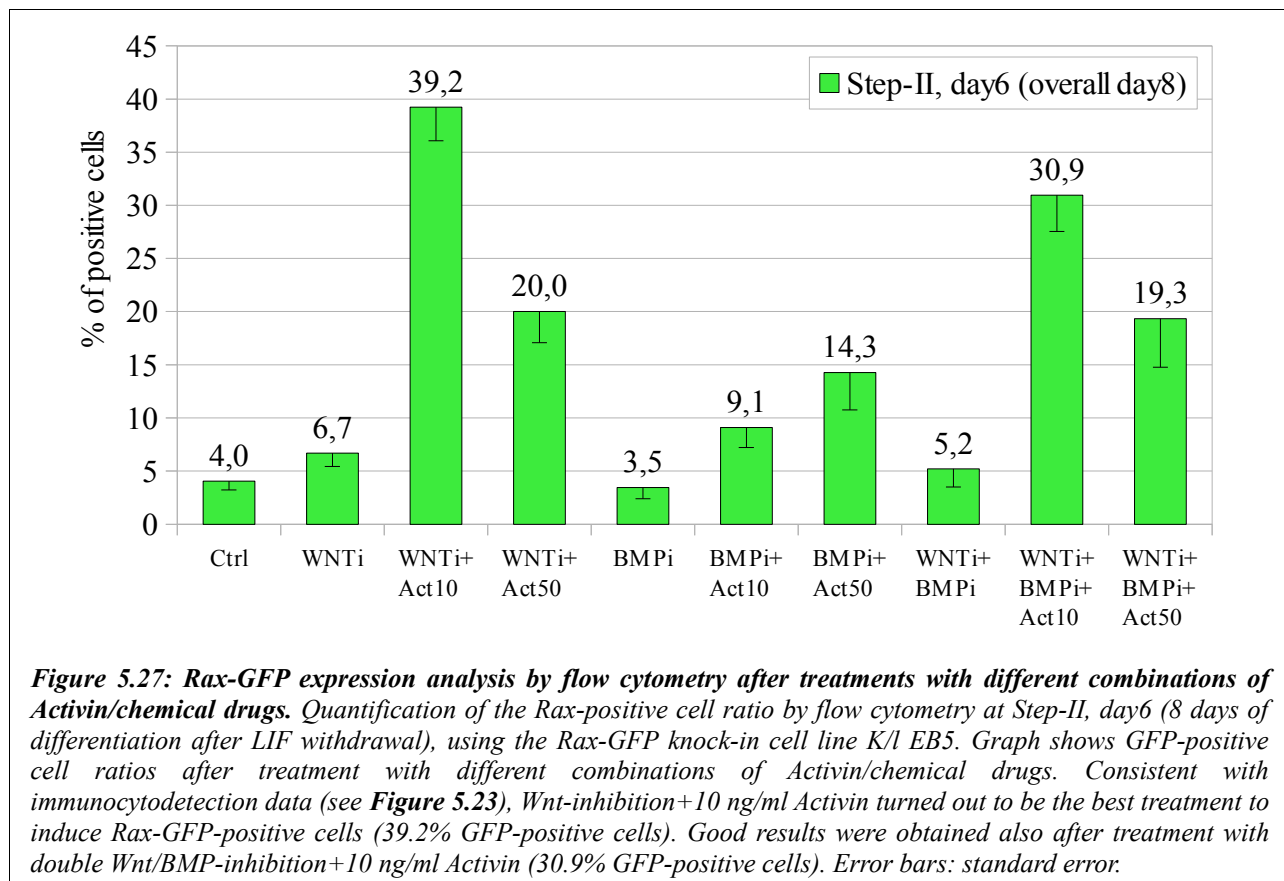
To better quantify the ratio of Rax-GFP-positive cells over time, and to explore the dynamic of Rax-GFP expression at later time of differentiation, we analyzed GFP expression by flow cytometry during a differentiation protocol where Step-II was further prolonged (**Figure 5.26**).

Cells were treated with Wnt-inhibitor +10 ng/ml Activin, and Rax-GFP-positive cell ratio was measured every 12 hours, starting from Step-I, day2 (2 days of differentiation *in vitro* after LIF withdrawal; 2 DIV), until Step-II, day8 (10 DIV). Non-treated cells, cultured in 0.1% DMSO, were used as a negative control. GFP expression switched-on at Step-II, day3 (5 DIV; 15% GFP-positive cells), increased at Step-II, day5 (7 DIV; 25% GFP-positive cells), peaking at Step-II, day6 (8 DIV; 34% GFP-positive cells). After Step-II, day6, GFP-positive cell ratio remained constant (39% GFP-positive cells at 10 DIV; **Figure 5.26**). CDM culture condition (control) induced no Rax-positive neural progenitor (this is consistent with the predominantly mesencephalic identity of our control cells, see Results, Chapter 3). This data reconfirmed the necessity for a longer time of differentiation when treating cells with Activin, to overcome for slow neural conversion in Activin-treated samples.

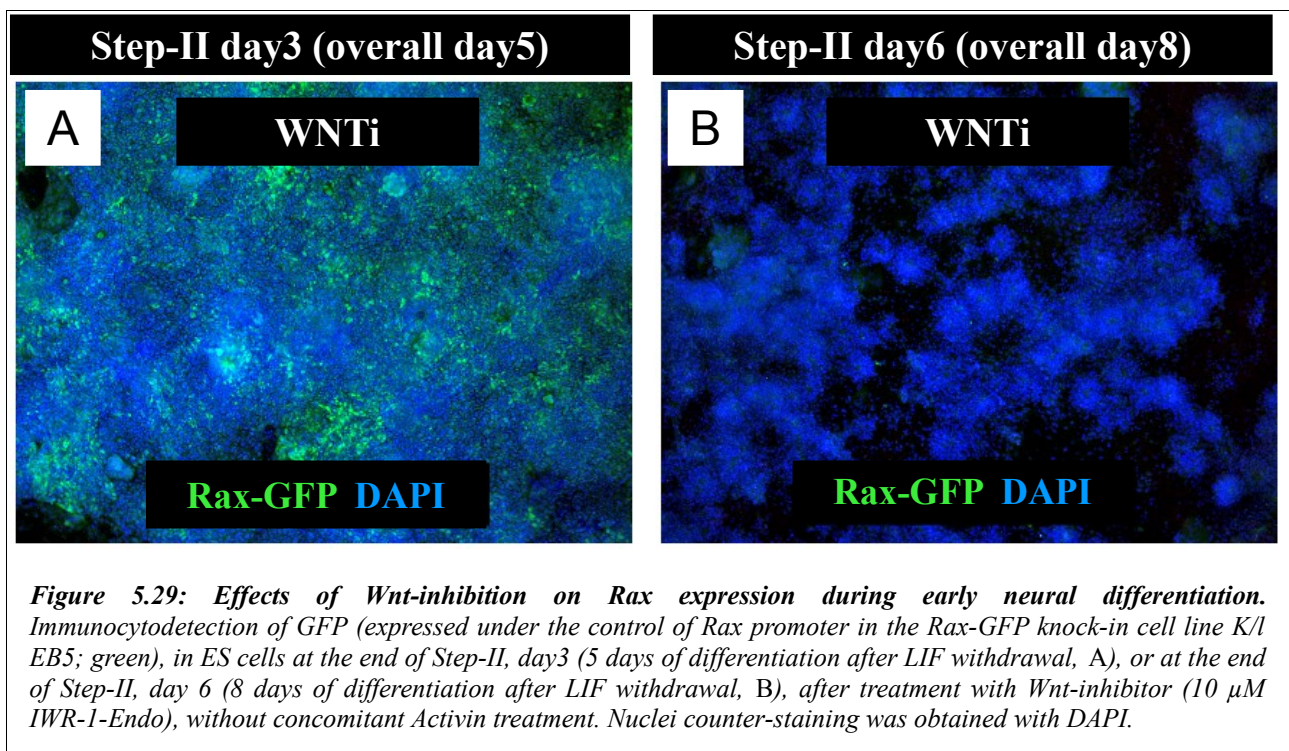
We directly compared the retinal inducing activity of different culture conditions (Wnt and/or BMP-inhibition, plus increasing doses of Activin) in terms of percentage of Rax-positive neural progenitors generated by ES cells. The analysis by flow cytometry was repeated for all the combinations of Activin doses (10 ng/ml and 50 ng/ml) plus chemical drugs (Wnt-inhibition, BMP-inhibition and double Wnt/BMP-inhibition), processing samples at Step-II, day6 (longer protocol, 8 days of differentiation after LIF withdrawal) (**Figure 5.27**). Again, Wnt-inhibition+10 ng/ml Activin was the best treatment to induce Rax-GFP expression (39.2% Rax-GFP-positive cells). The lowest dose of Activin (10 ng/ml) gave good results also when associated together with double Wnt/BMP-inhibition, scoring 30.9% Rax-GFP-positive cells at Step-II, day6.



During the analysis of the Rax-GFP-positive cell ratio by flow cytometry, we noticed an interesting phenomenon concerning Rax gene expression. Cells treated with Wnt-inhibition alone (without concomitant Activin treatment) showed a transient activation of GFP under the control of Rax promoter during the first days of differentiation (**Figure 5.15**). Rax-GFP-positive cells appeared at Step-II, day2 (4 days of differentiation after LIF withdrawal, and only 24 hours after the starting point of Wnt-inhibition treatment; 4 DIV; 10% Rax-GFP-positive cells). Rax-GFP-positive cells scored their maximum percentage at Step-II, day3 (5.5 DIV; 28% Rax-GFP-positive cells), then they started decreasing at Step-II, day4 (6.5 DIV; 19% Rax-GFP-positive cells). At later time points of the analysis (Step-II, day6 and following days) Rax-GFP expression was almost disappeared and was not significantly differing if compared to that of control untreated cells (**Figure 5.15**).



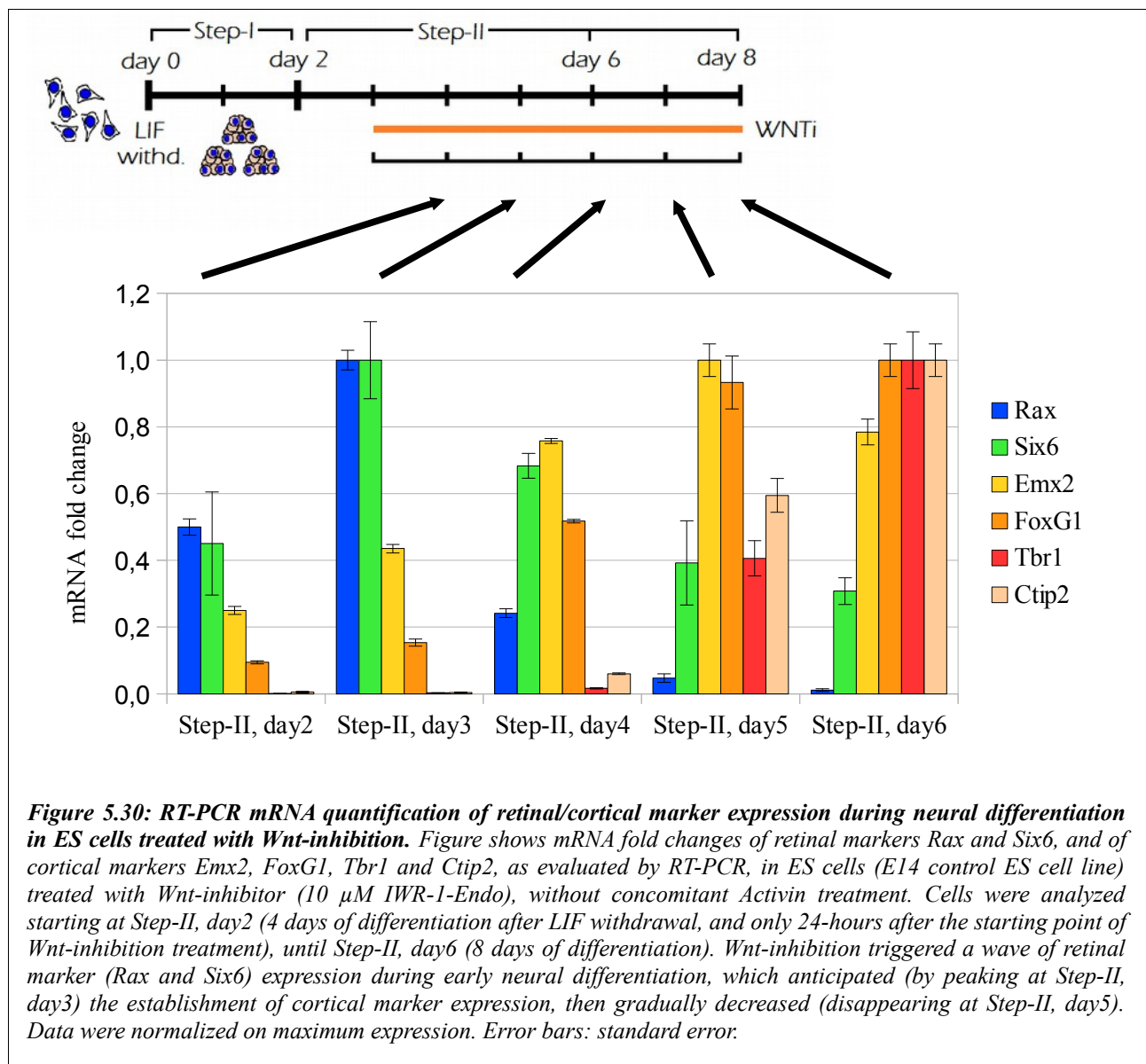
The precocious and transient Rax expression during ES neural differentiation in Wnt-inhibition treatment was confirmed by both Rax-GFP immunocytochemistry, performed on Rax-GFP knock-in ES cell line, and RT-PCR, performed on control E14 ES cell line. Cells treated with Wnt-inhibition showed a widespread Rax-GFP signal at Step-II, day3 (5 days of differentiation after the starting point of the protocol; **Figure 5.29A**); three days later Rax-GFP signal was almost completely disappeared (**Figure 5.29B**).



Early Rax expression during differentiation of ES cell treated with Wnt-inhibition was also detectable by RT-PCR, performed on control E14 ES cell line (**Figure 5.30**). As showed before (see Results, Chapter 4), Wnt-inhibition established an anterior, cortical fate in ES cells differentiated *in vitro*; consistently, cortical markers were gradually up-regulated during neural differentiation and cortical fate acquisition. Interestingly, Wnt-inhibition triggered a wave of Rax expression, which anticipated the establishment of cortical marker expression. The wave of Rax expression started at the end of Step-II, day2, after the first 24 hours of Wnt-inhibition treatment, and reached the highest level at Step-II, day3. Rax was then rapidly down-regulated, and this was accompanied by robust up-regulation of cortical gene markers (FoxG1, Tbr1, Ctip2 and Emx2). The expression of Six6 (a

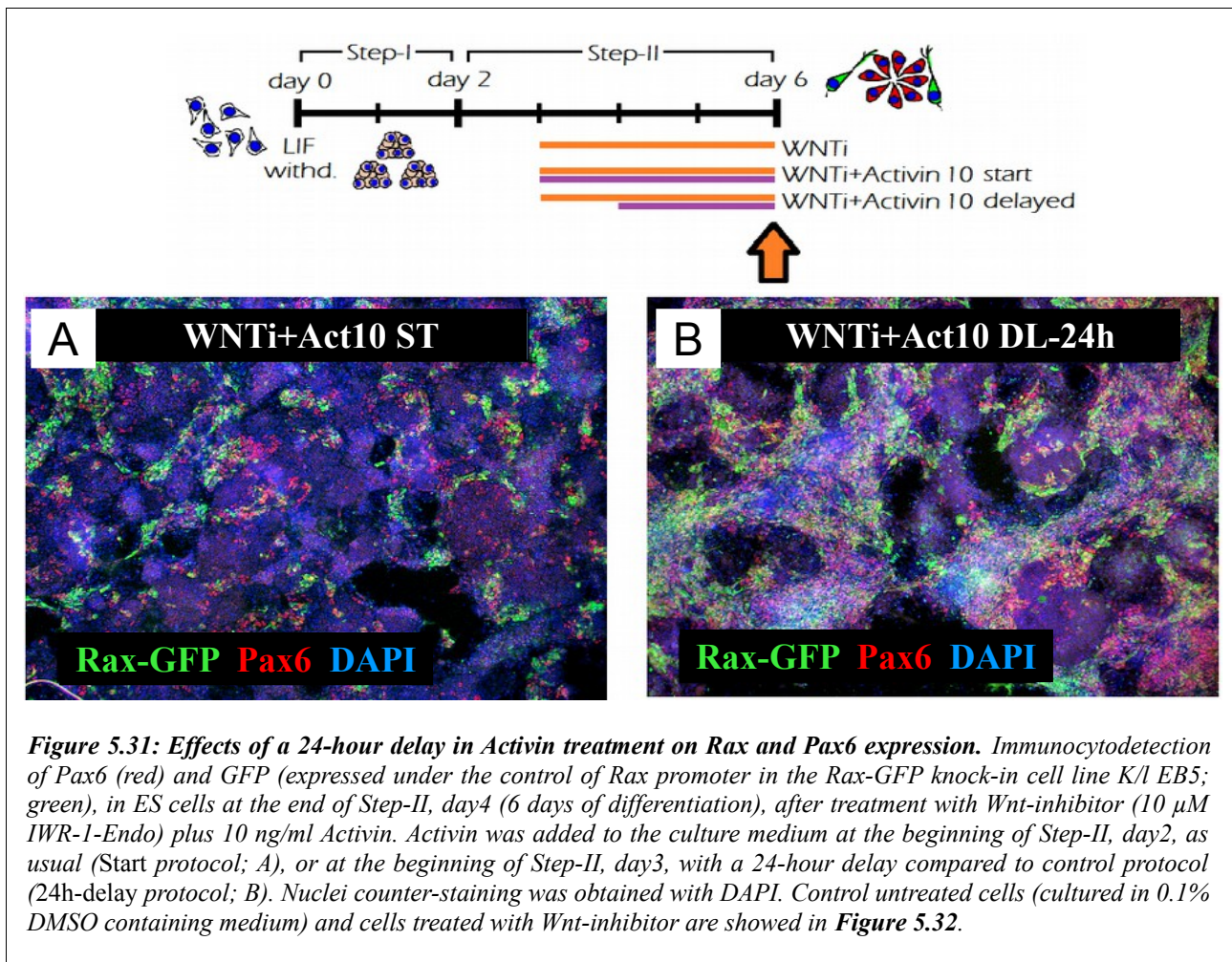
retinal marker) followed the same dynamic of Rax expression.

These results indicate that early Rax expression was not an artifact regarding Rax-GFP knock-in cell line, but could be detected even by using an unmodified ES cell line (E14 cell line).

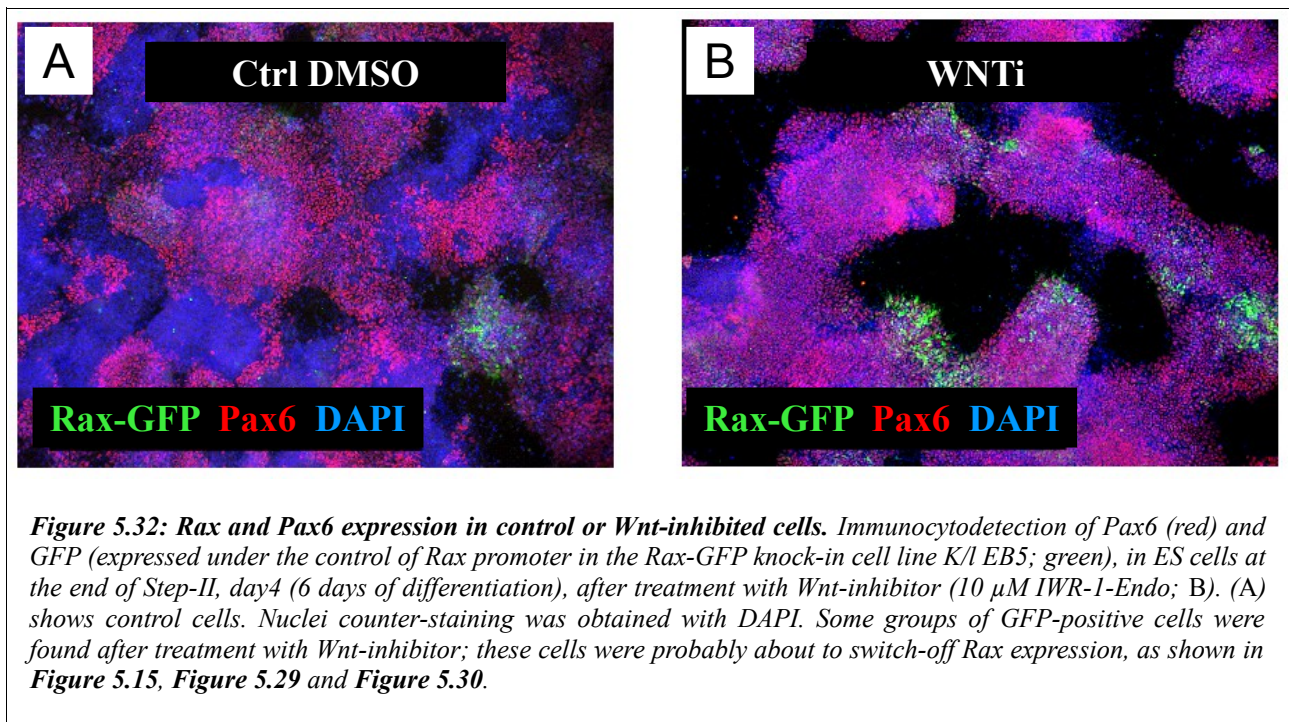


As previously described, Wnt-inhibited cells followed an anterior (cortical) differentiation fate (see Results, Chapter 4). The reason for an early transient *wave* of Rax expression in cells that will then follow a cortical differentiation fate was not further investigated. Anyhow, it should be noticed that early Rax expression in early FoxG1-positive telencephalon has been reported both in lower vertebrates and mouse (Furukawa et al., 1997; Lupo et al., 2002), and this suggest that early Rax expression in our culture system might mimic a mechanism actually present in neural development *in vivo*. This hypothesis is now the topic of an undergoing project in our Lab.

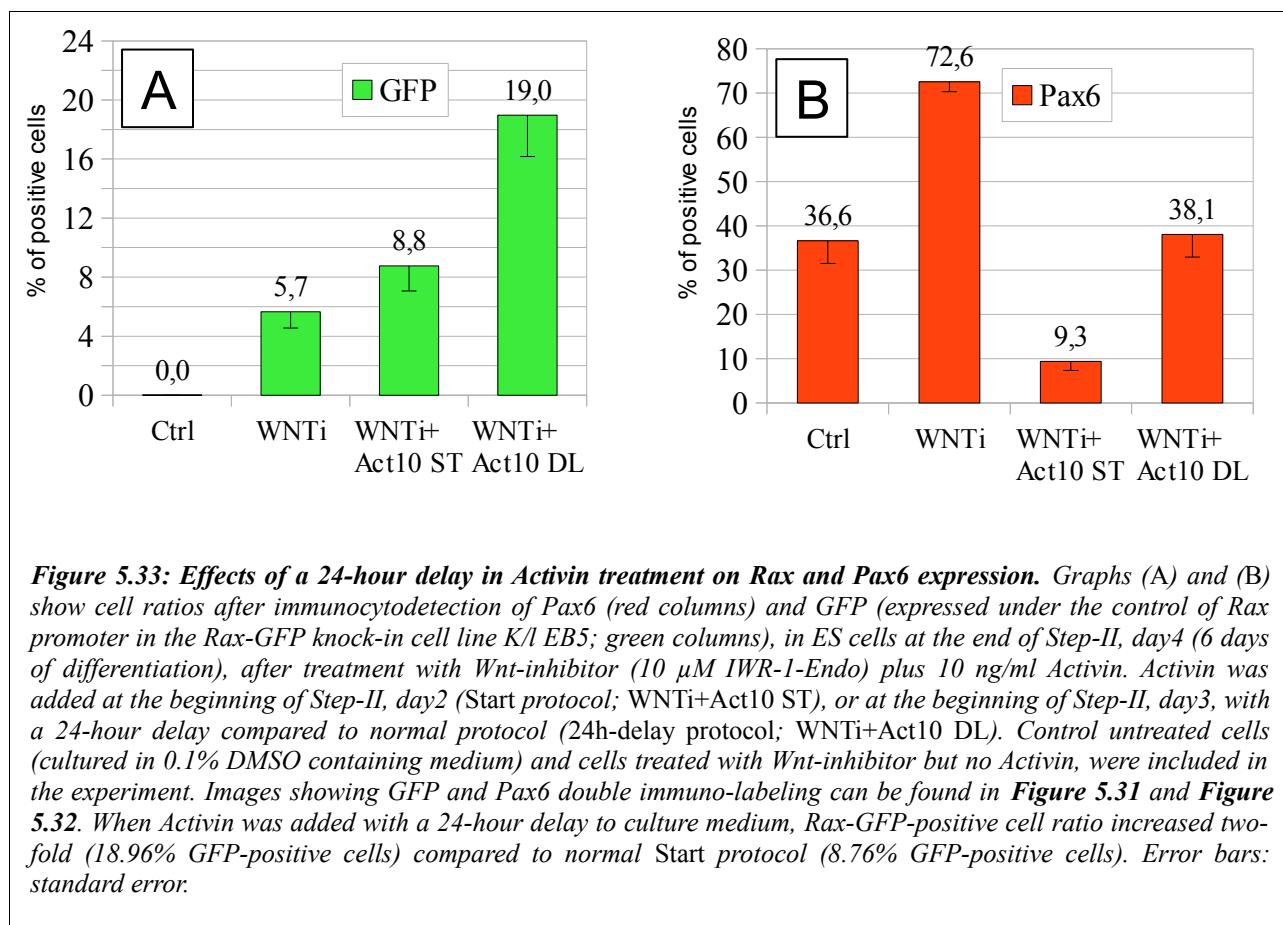
As the *side-effect* of Activin on neural differentiation efficiency is concerned, we tested if a change of the starting point of Activin treatment could improve the neuralization efficiency. As showed before (see Results, Chapter 1), Sox1-positive and Nestin-positive neural progenitors started to accumulate at mid-Step-II, after 4 days of ES cell differentiation. The presence of Activin in the culture medium starting from the Step-II, day2, could interfere with this early phase of neural induction, sustaining Oct4 and FGF5 expression (as showed in **Figure 5.19**). We reasoned that this effect could be possibly prevented or reduced by simply delaying Activin treatment during the differentiation period. We first treated cells with 10 ng/ml Activin starting at mid-Step-II (beginning of the fifth day of total differentiation time), with a 24-hour delay when compared to normal Activin treatment. Wnt-inhibition was performed as usual, starting at the beginning of Step-II, day2. We then immunodetected Pax6 and Rax-GFP at the end of Step-II, day4 (**Figure 5.31**). We found that a 24-hour delay of Activin treatment increased the ratio of both Pax6-positive and Rax-GFP-positive cells (**Figure 5.31** and **Figure 5.33**).



Rax-GFP signal was almost absent in control cells (0.02% Rax-GFP-positive cells; **Figure 5.32**). In cells treated with Wnt-inhibition, Rax-GFP-positive cell ratio was 5.7%. These GFP-positive cells were probably the queue of the early wave of Rax expression showed before (see **Figure 5.15**, **Figure 5.29** and **Figure 5.30**).

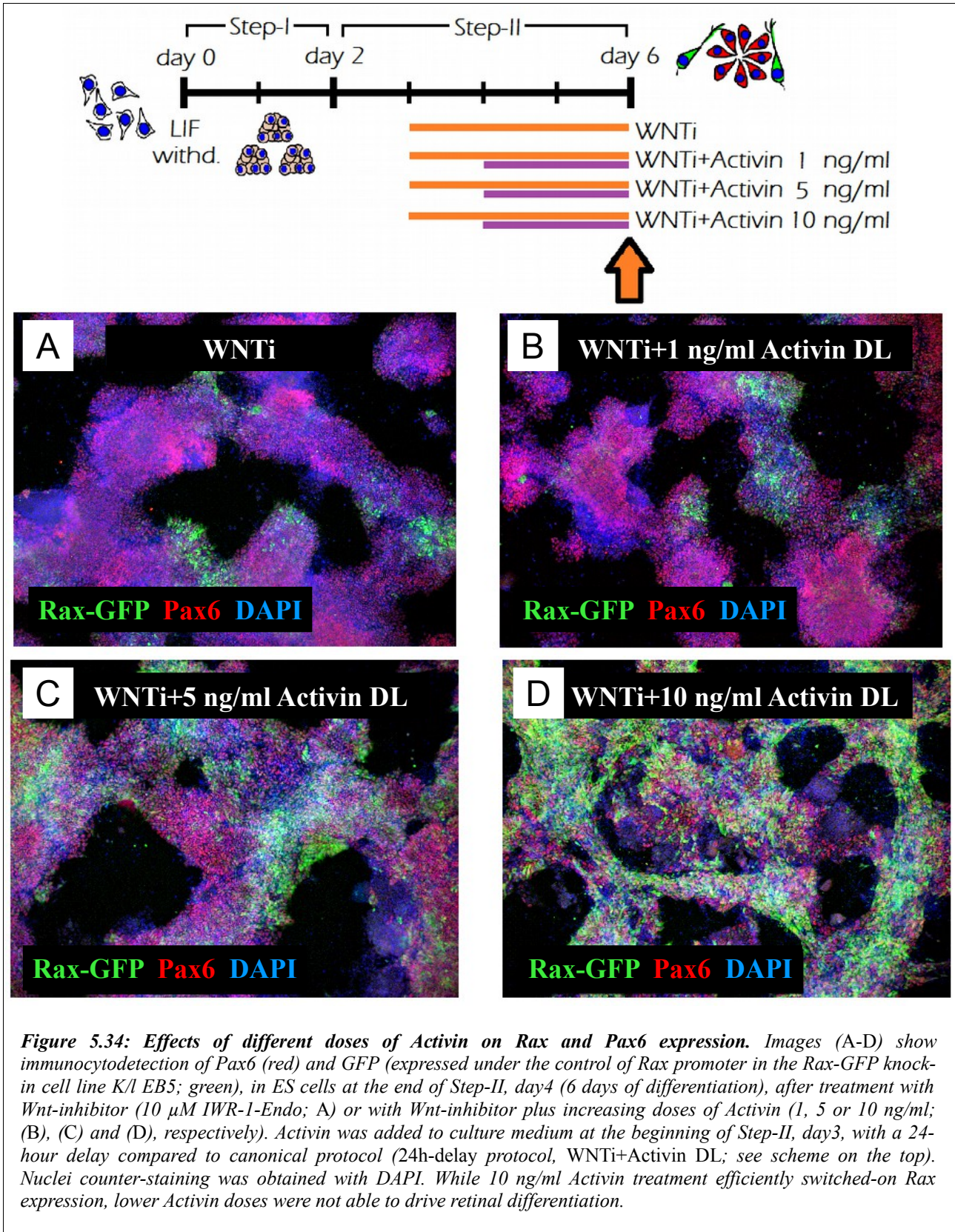


The Rax-GFP-positive cell ratio, which was 8.8% in normal protocol – Activin at the beginning of second day of Step-II; *Start* protocol – underwent a two-fold increase and reached a score of 19% positive cells when Activin was added later (*24-hour Delay* protocol – Activin at Step-II, beginning of day3) (**Figure 5.33A**). Pax6-positive cells were also increased by the 24-hour delay in Activin treatment (9.3% Pax6-positive cells in normal condition, 38.1% Pax6-positive cells in *24-hour delayed* treatment), suggesting a higher neuralization (**Figure 5.33B**). The improvement of protocol efficiency due to delay of Activin treatment was particularly relevant, especially considering that the total time of treatment was shorter (only two days, while normal Activin treatment lasted for 3 days).

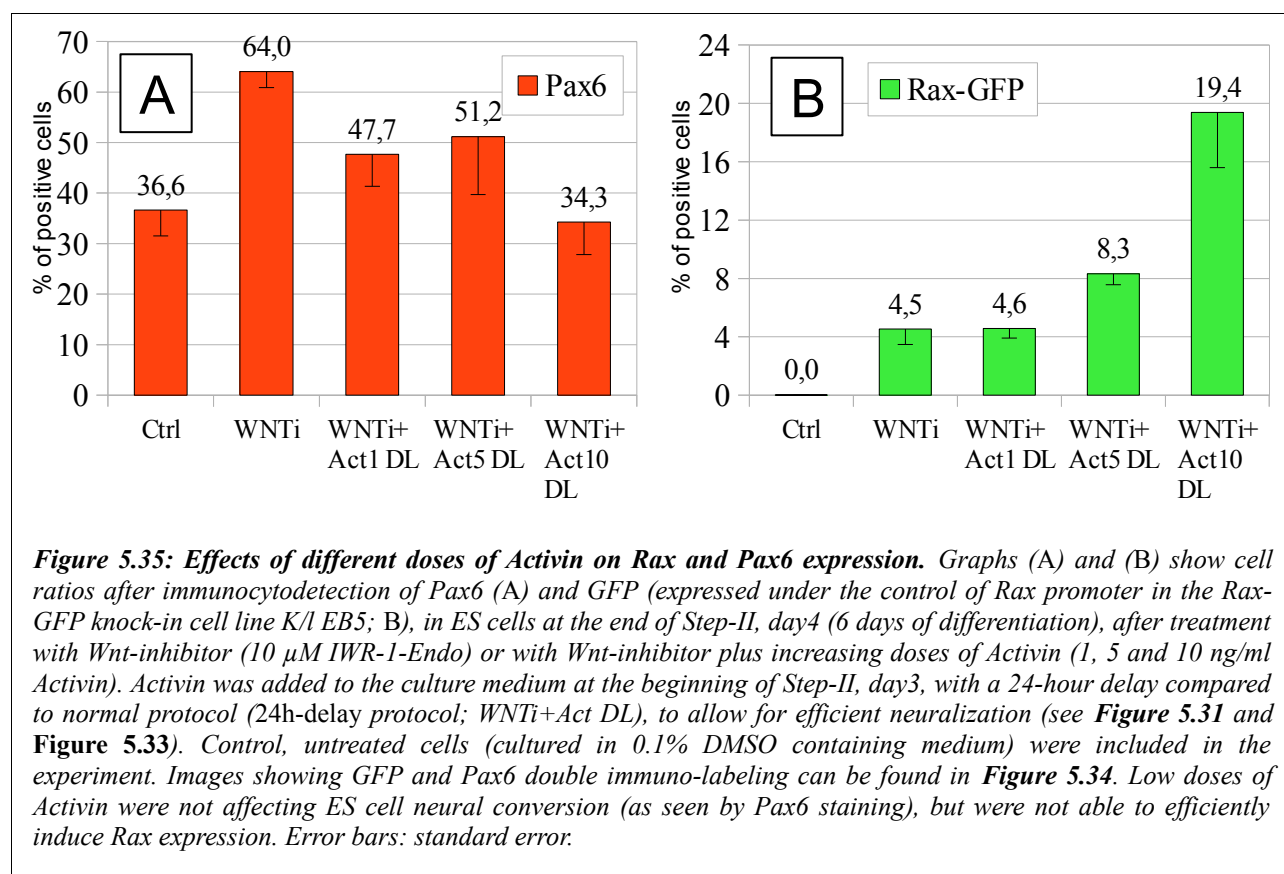


In parallel, we decided to test different doses of Activin on ES differentiating cells. As showed before (**Figure 5.6**), Activin/Nodal pathway target gene FoxH1 was strongly up-regulated by the presence of Activin in the culture medium. FoxH1 expression did not increase with Activin doses higher than 10 ng/ml, suggesting that this was already a saturating dose. Thus, we reasoned that another possible way to improve our retinal differentiation protocol was to reduce the dose of Activin in culture medium. Our idea was to test if lower doses of Activin were still able to induce a retinal differentiation fate, without affecting ES cell neural conversion. Cells were then treated during Step-II with lower Activin doses, ranging from 1 ng/ml to 10 ng/ml, including an intermediate dose of 5 ng/ml. Cells were analyzed after Rax-GFP/Pax6 immunocyto detection at Step-II, day4. In this experiment, Activin doses were added with a 24-hour delay to allow for efficient neuralization.

Unfortunately, lower Activin doses were less efficient in switching-on Rax-GFP expression (**Figure 5.34**).

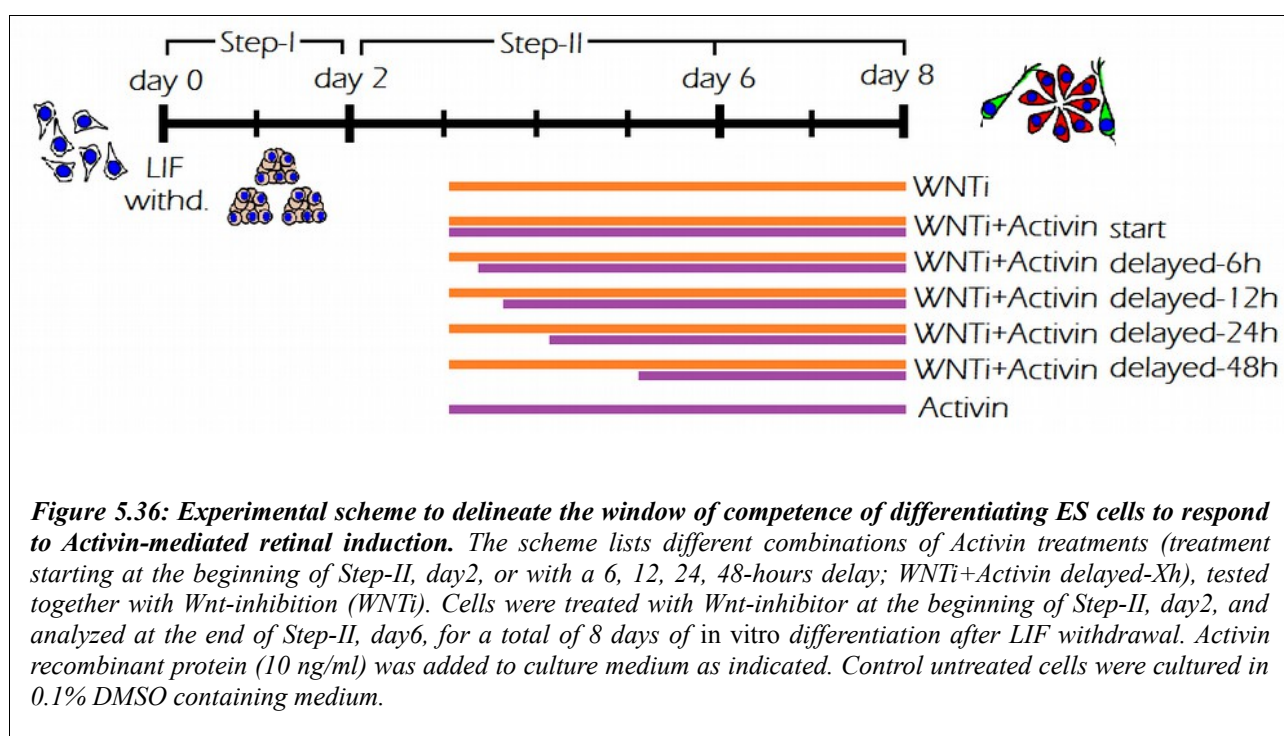


Pax6-positive cell ratio was increased when cells were treated with low Activin doses, compared to 10 ng/ml Activin treatment (47.8% Pax6-positive cells after 1 ng/ml Activin treatment, and a similar percentage in cells treated with 5 ng/ml Activin; **Figure 5.35A**), but Rax-GFP-positive cells were only 4.6% after 1 ng/ml Activin treatment and 8.3% after 5 ng/ml Activin treatment (**Figure 5.35B**). We decided to keep 10 ng/ml Activin as the lowest effective dose for retinal induction in our protocol.

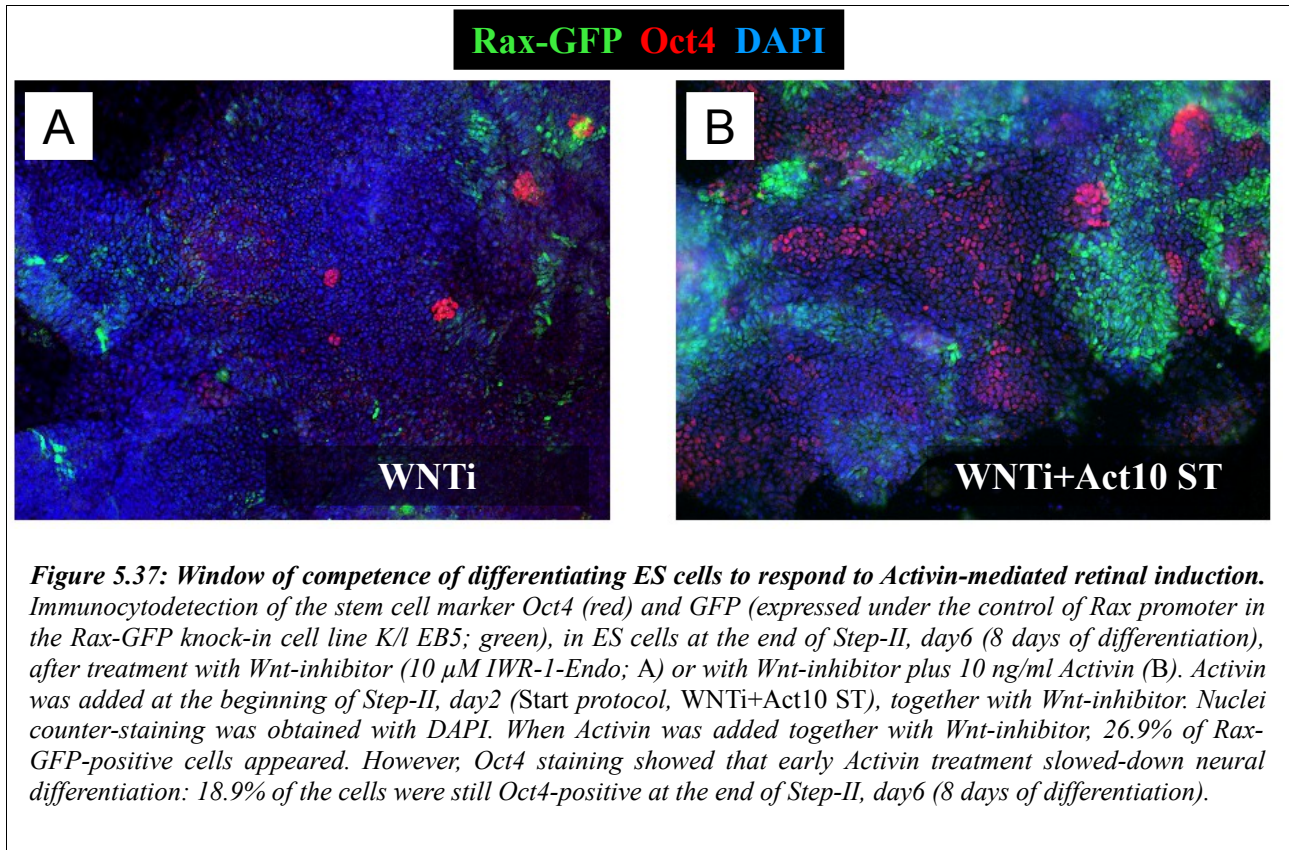


We decided to better characterize the timing of Activin retinal induction properties, by analyzing Rax-GFP expression after Activin treatment performed at different time windows. This was useful not only to improve the protocol efficiency, but especially to delineate the window of competence of differentiating ES cells to respond to Activin signal. Control cells were treated with 10 ng/ml Activin as usual, starting at the second day of Step-II, together with 10 μ M of Wnt-inhibitor IWR-1-Endo. Some replicates samples were treated with 10 ng/ml Activin starting with a delay of 6, 12, 24 or 48 hours with respect to normal treatment (**Figure 5.36**). Wnt-inhibition always started at the

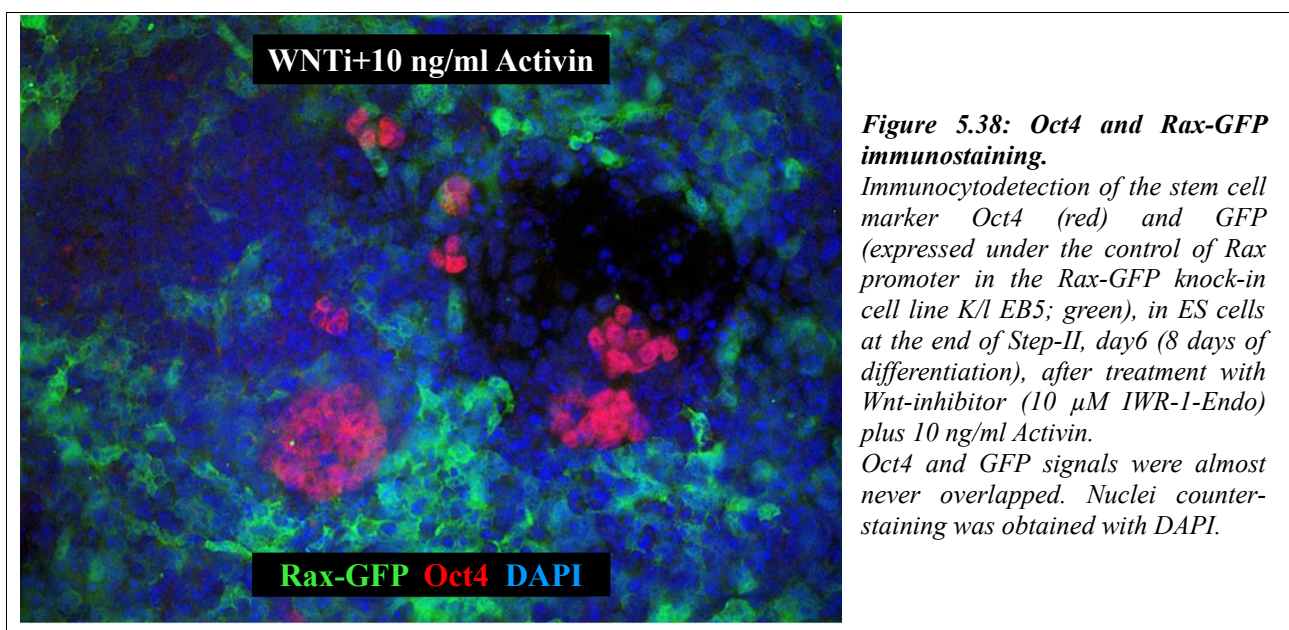
beginning of the second day of Step-II. Cells were cultured until the sixth day of Step-II (8 days of differentiation after LIF withdrawal), then fixed and processed by Rax-GFP and Oct4 double immunocytochemistry, to quantify the ratios of Rax-positive neural progenitors and of Oct4-positive undifferentiated cells, respectively. Cells treated with IWR-1-Endo but no Activin, together with cells treated with 10 ng/ml Activin but no Wnt-inhibitor, were included as a negative control (**Figure 5.36**).



Cells anteriorized by Wnt-inhibition treatment showed no, or rare, Rax-GFP-positive cells, as already seen before. When Activin was added together with Wnt-inhibitor, 26.9% of Rax-GFP-positive cells appeared. However, Oct4 staining showed how the neuralization efficiency was inhibited by Activin early treatment (Activin added at the beginning of the second day of Step-II): 18.9% of the cells were still Oct4-positive at the end of Step-II, day6 (8 days of differentiation).



Oct4 and Rax-GFP signals were almost never overlapped, as can be easily appreciated at a higher magnification (40X) (**Figure 5.38**).



These data confirmed again that Activin treatment at early differentiation time was strongly interfering with neural conversion that ES cell normally undergo when cultured in a minimal medium (see the first experiment on Activin *24-hour delay* treatment showed in **Figure 5.31** and **Figure 5.33**; see also the RT-PCR data about Oct4 and FGF5 expression in **Figure 5.19B** and immunostaining of Musashi-1 and Oct4 in **Figure 5.20-5.22**). Activin treatment slowed-down ES cell neural differentiation, sustaining Oct4 expression.

Interestingly, the persistence of Oct4-positive cells inside the culture system after Activin treatment could be prevented by adding Activin with a delay (*Delayed* treatments) compared to the start of Wnt-inhibition (*Start* treatment) (**Figure 5.39**). A delay of only 6 hours was already enough to prevent Activin to inhibit neuralization (44.8% Rax-GFP-positive retinal cells and only 6.1% Oct4-positive cells, that is a three-fold decrease of undifferentiated Oct4-positive cell ratio). The best option as a retinal induction treatment was to add Activin at the second half of day2, Step-II, with a 12-hours delay compared to normal treatment (45.2% Rax-GFP-positive retinal cells and only 3% Oct4-positive undifferentiated cells). Notably, when cells were treated with an excessive delay (Activin 10 ng/ml at the beginning of Step-II, day4, 48 hours after the beginning of Wnt-inhibition treatment), Activin was no more able to efficiently induce the formation of Rax-positive retinal progenitors (5.5% Rax-GFP-positive retinal cells) (**Figure 5.39** and **Figure 5.40**).

This analysis allowed us to identify a precise time window for Activin treatment to induce Rax expression. The best option to induce retinal neural progenitors without interfering with ES cell neural conversion was to add Activin in a period included between the second half of day2, Step-II, and the beginning of day3, Step-II.

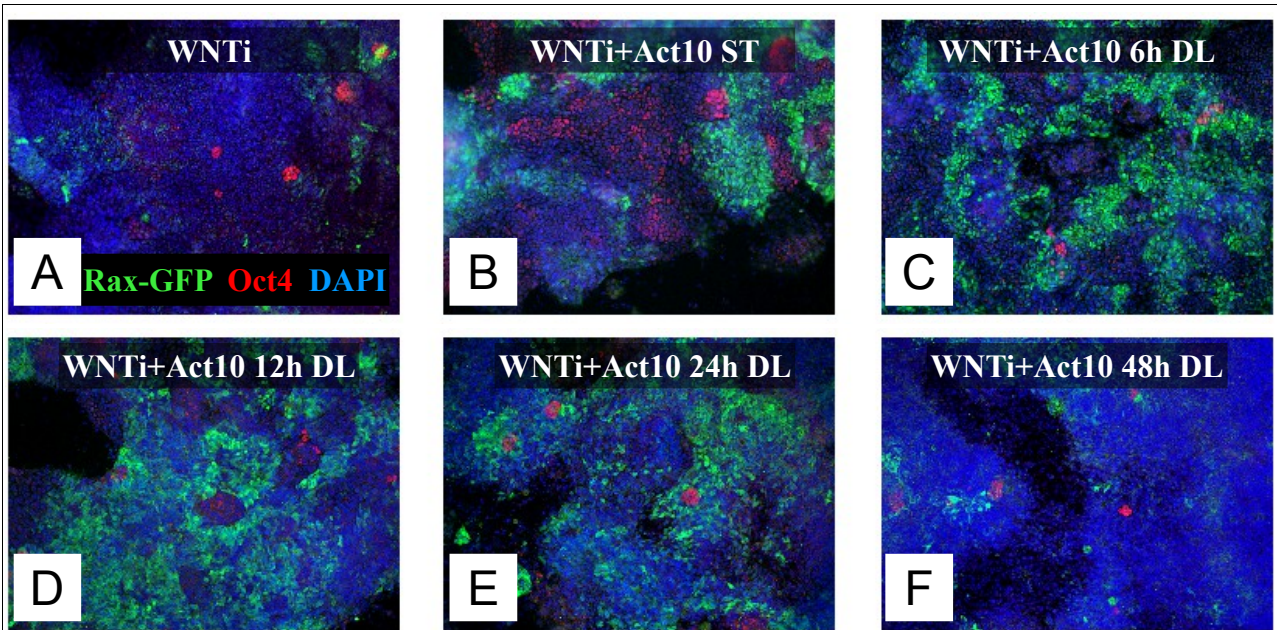


Figure 5.39: Window of competence of differentiating ES cells to respond to Activin-mediated retinal induction. Immunocytochemical detection of stem cell marker Oct4 (red) and GFP (expressed under the control of Rax promoter in the Rax-GFP knock-in cell line K/l EB5; green), in ES cells at the end of Step-II, day6 (8 days of differentiation), after treatment with Wnt-inhibitor (10 μ M IWR-1-Endo; A) or with Wnt-inhibitor plus 10 ng/ml Activin (B-F). Activin was added to culture medium at the beginning of Step-II, day2 (Start protocol; B), or with a 6, 12, 24 or 48-hour delay (Delay – DL – protocol, as indicated here and schematized in Figure 5.36; C-F). Nuclei counter-staining was obtained with DAPI. The best option as a retinal induction treatment was to add Activin at the second half of day2 Step-II, with a 12-hours delay compared to normal treatment (45.2% Rax-GFP-positive retinal cells and only 3% Oct4-positive undifferentiated cells).

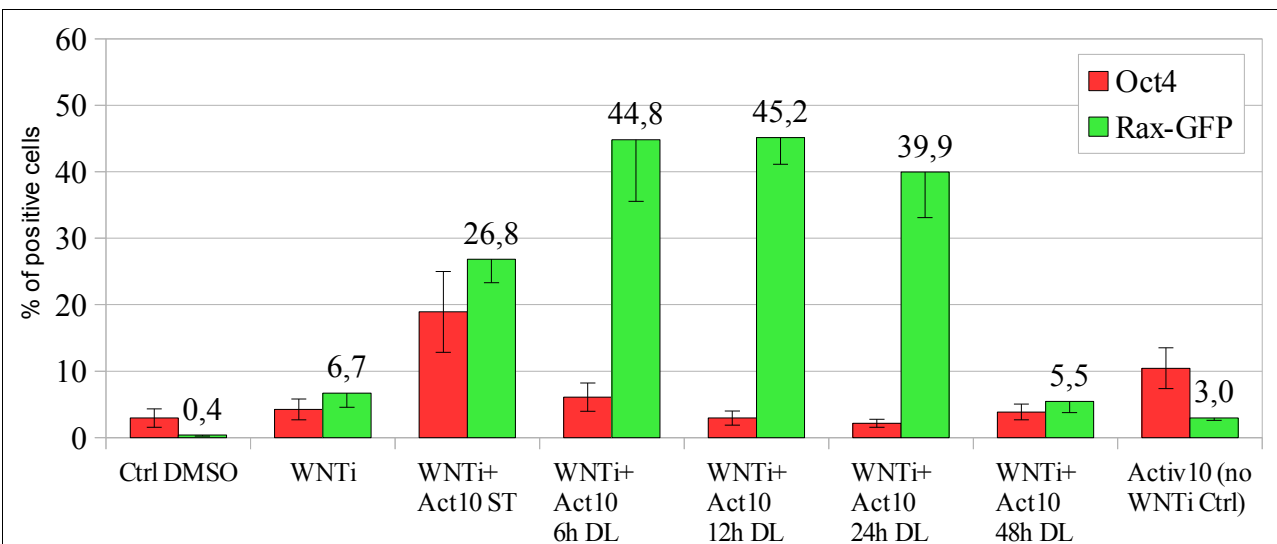


Figure 5.40: Window of competence of differentiating ES cells to respond to Activin-mediated retinal induction. Graph shows cell ratios after immunocytochemical detection of the stem cell marker Oct4 (red columns) and GFP (expressed under the control of Rax promoter in the Rax-GFP knock-in cell line K/l EB5; green columns), in ES cells treated as indicated in Figure 5.36. Non treated cells and cells treated with Activin alone were included in the experiment as negative control. Error bars: standard error.

RT-PCR analysis of neural differentiation/stem cell markers confirmed these findings. Oct4 and FGF5 expression levels (undifferentiated stem cell and epiblast markers, respectively) were particularly high when Activin was added to culture medium at the beginning of the second day of Step-II (*Start* treatment); the expression of Oct4 and FGF5 was decreased when cells were allowed to differentiate without Activin for a longer period (**Figure 5.41**). Activin also acted as an inducer of mesodermal and endodermal identity: Gata4, Gata6, T and FoxA2 expression levels were particularly high when Activin was used alone (no concomitant Wnt-inhibition treatment).

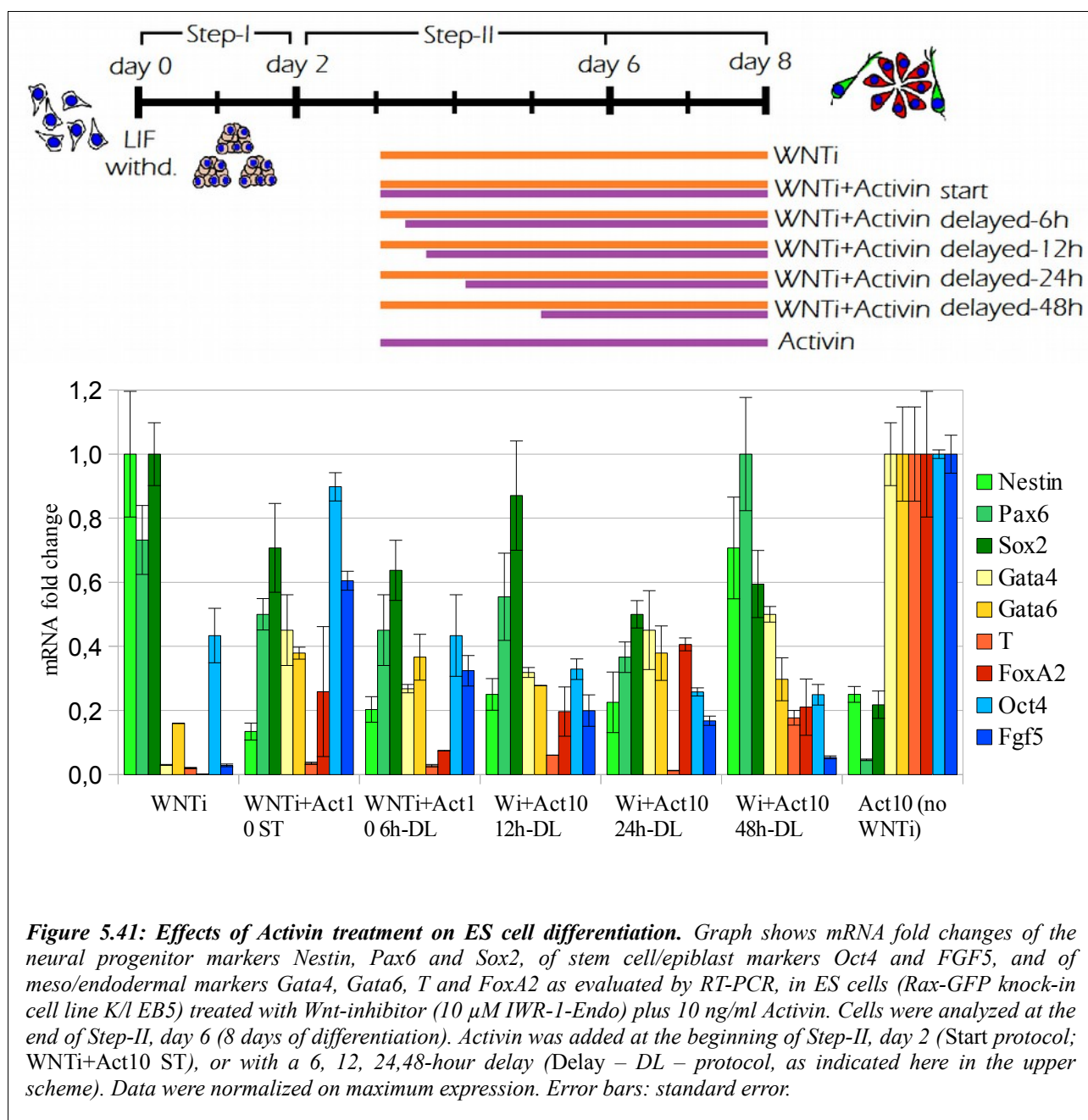
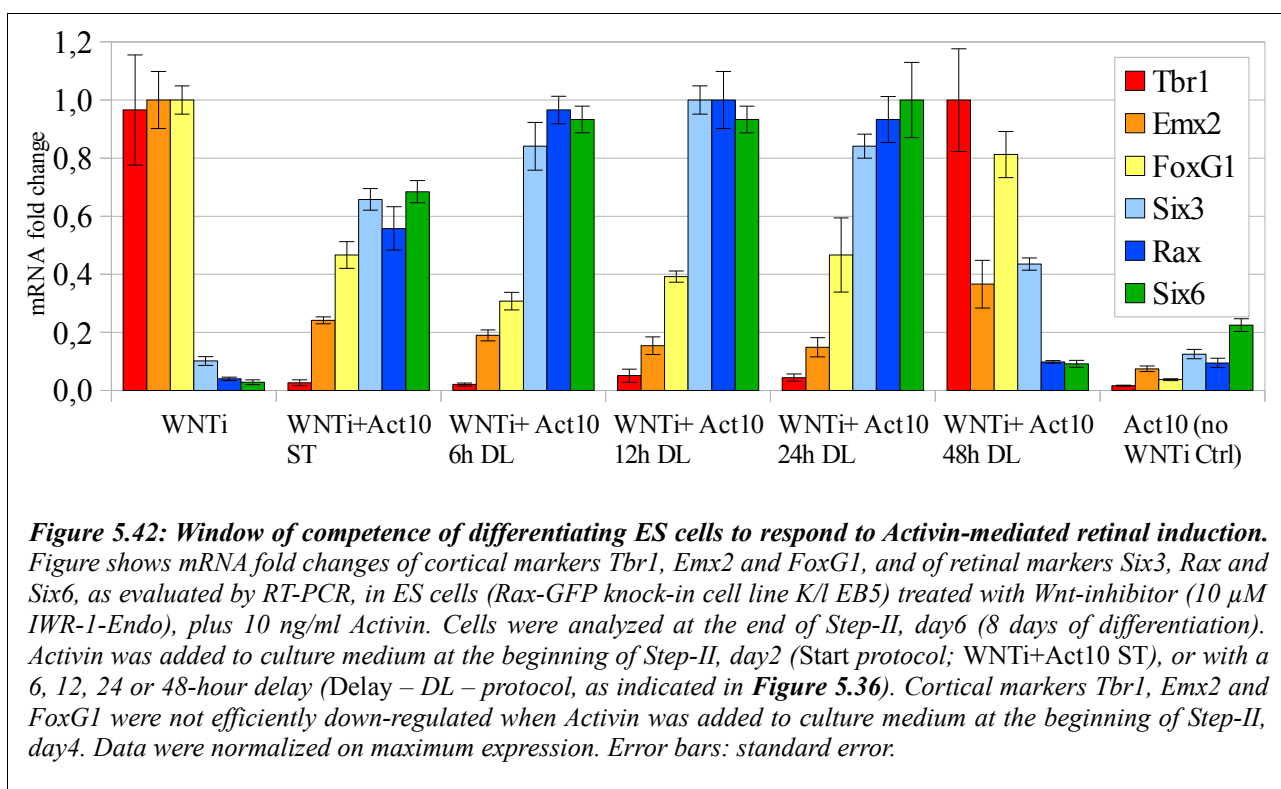


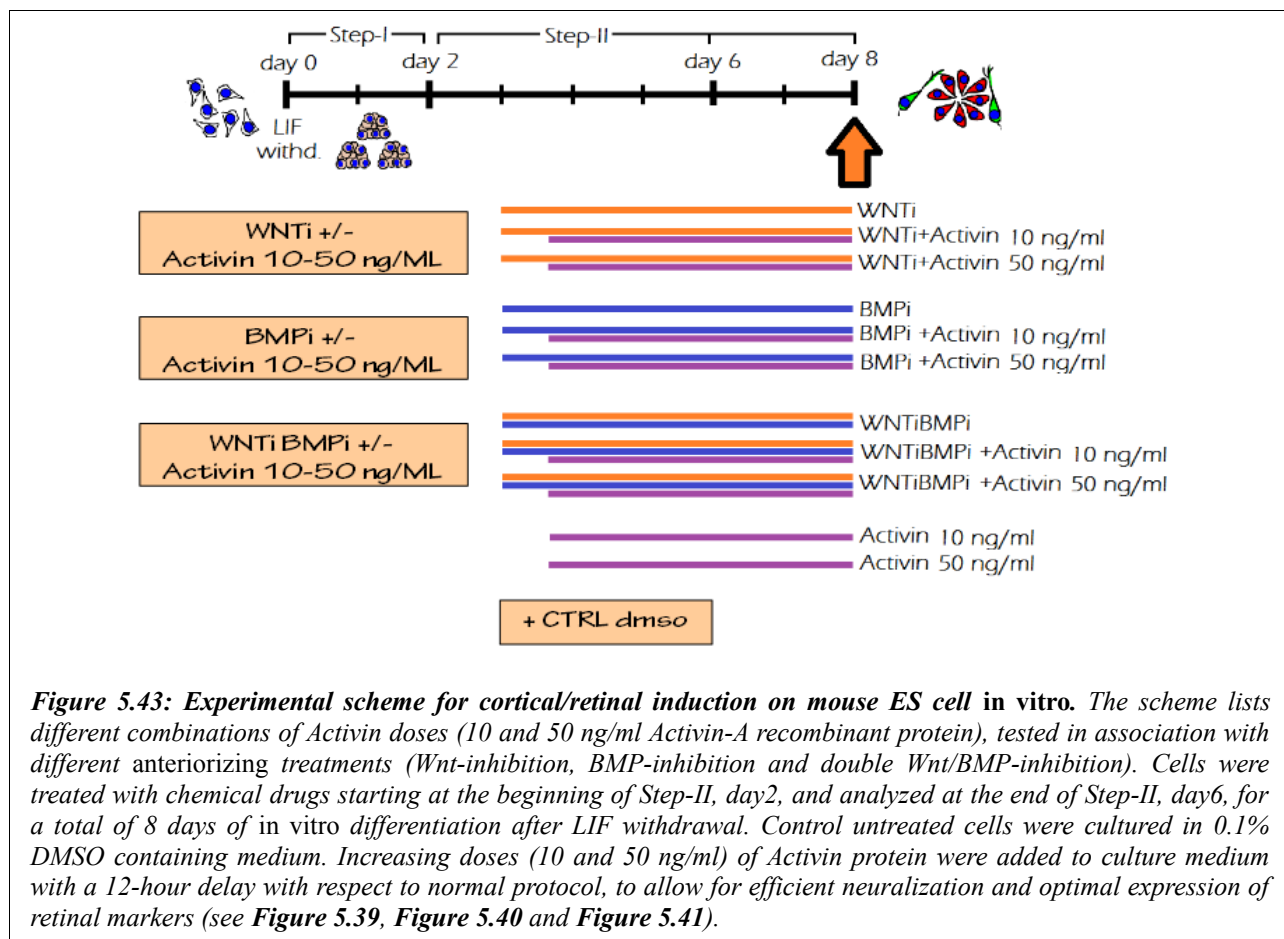
Figure 5.41: Effects of Activin treatment on ES cell differentiation. Graph shows mRNA fold changes of the neural progenitor markers Nestin, Pax6 and Sox2, of stem cell/epiblast markers Oct4 and FGF5, and of meso/endodermal markers Gata4, Gata6, T and FoxA2 as evaluated by RT-PCR, in ES cells (Rax-GFP knock-in cell line K/l EB5) treated with Wnt-inhibitor (10 μ M IWR-1-Endo) plus 10 ng/ml Activin. Cells were analyzed at the end of Step-II, day 6 (8 days of differentiation). Activin was added at the beginning of Step-II, day 2 (Start protocol; WNTi+Act10 ST), or with a 6, 12, 24,48-hour delay (Delay – DL – protocol, as indicated here in the upper scheme). Data were normalized on maximum expression. Error bars: standard error.

The analysis of regional/identity markers by RT-PCR showed that retinal markers Six3, Rax and Six6 (blue and green color code in **Figure 5.42**) were strongly expressed when Activin was added to culture medium with a 6, 12 or 24-hours delay compared to normal *Start* treatment. Cortical markers Tbr1, Emx2 and FoxG1 were not efficiently down-regulated when Activin was added lately to culture medium (Activin 10 ng/ml at the beginning of day4, Step-II, 48-hours later compared to normal *Start* treatment; **Figure 5.42**). This suggested that two days of Wnt-inhibition without concomitant Activin treatment irreversibly led cells toward cortical fate, and also explained why cells treated with Activin with a 48-hours delay were no more capable of switching-on Rax expression (**Figure 5.39**, **Figure 5.40**).



We concluded that Activin has a retinal induction effect on differentiating ES cells. Activin can also inhibit/slow down ES cell neural differentiation, but this effect can be prevented by delaying Activin treatment (around the fourth day of differentiation *in vitro*) and by allowing cells to differentiate for a longer period (8 days of culture *in vitro* after LIF withdrawal).

Bearing these observations in mind, we repeated some combinations of Activin doses (10 ng/ml and 50 ng/ml) plus chemical drugs (BMP-inhibition, Wnt-inhibition and double Wnt/BMP-inhibition). Cells were allowed to differentiate 8 days *in vitro*; Activin treatment was performed with a 12-hour delay compared to chemical drug treatments. ES cells were then analyzed by Rax-GFP and Oct4 double immunocyto detection. Non-treated (0.1% DMSO-cultured) cells and cells treated with Activin but no chemical drugs were included as negative controls (**Figure 5.43**).



Cells anteriorized by Wnt-inhibition or by double Wnt/BMP-inhibition, then treated with 10 ng/ml Activin, gave rise to retinal progenitor-enriched cultures (44.8% and 31.8% Rax-GFP-positive cells, respectively; Panels in **Figure 5.44**). The high (50 ng/ml) dose of Activin strongly impaired neural differentiation (26.8% and 25.8% Oct4-positive cells in WNTi and double WNTi/BMPi cells+50 ng/ml Activin, respectively), despite of the longer differentiation period and of Activin treatment delay. This suggested that high doses of Activin were deleterious for ES cell neural conversion *in vitro* and were instead promoting the maintenance of pluripotency (**Figure 5.44**; cell countings in **Figure 5.45**).

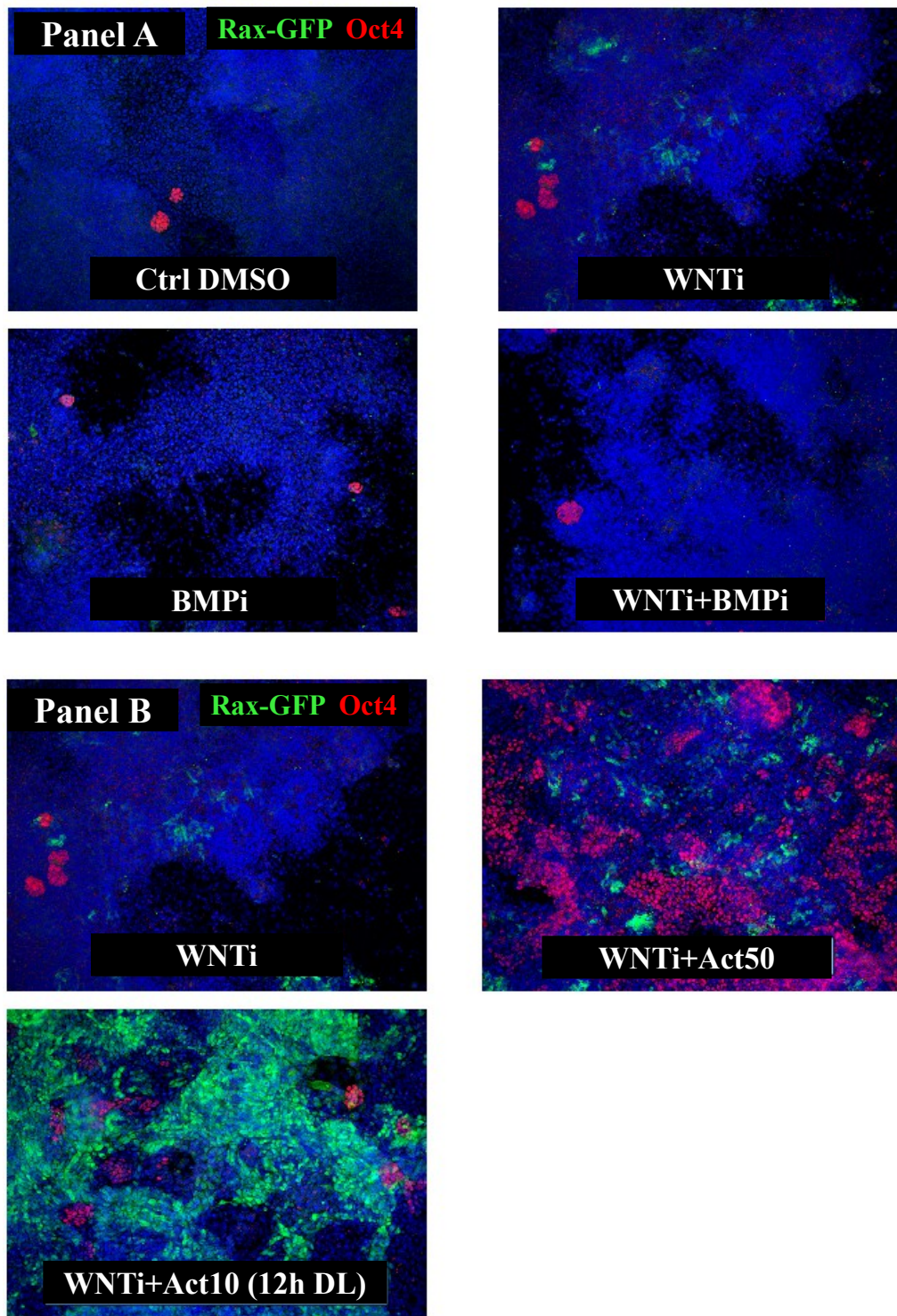
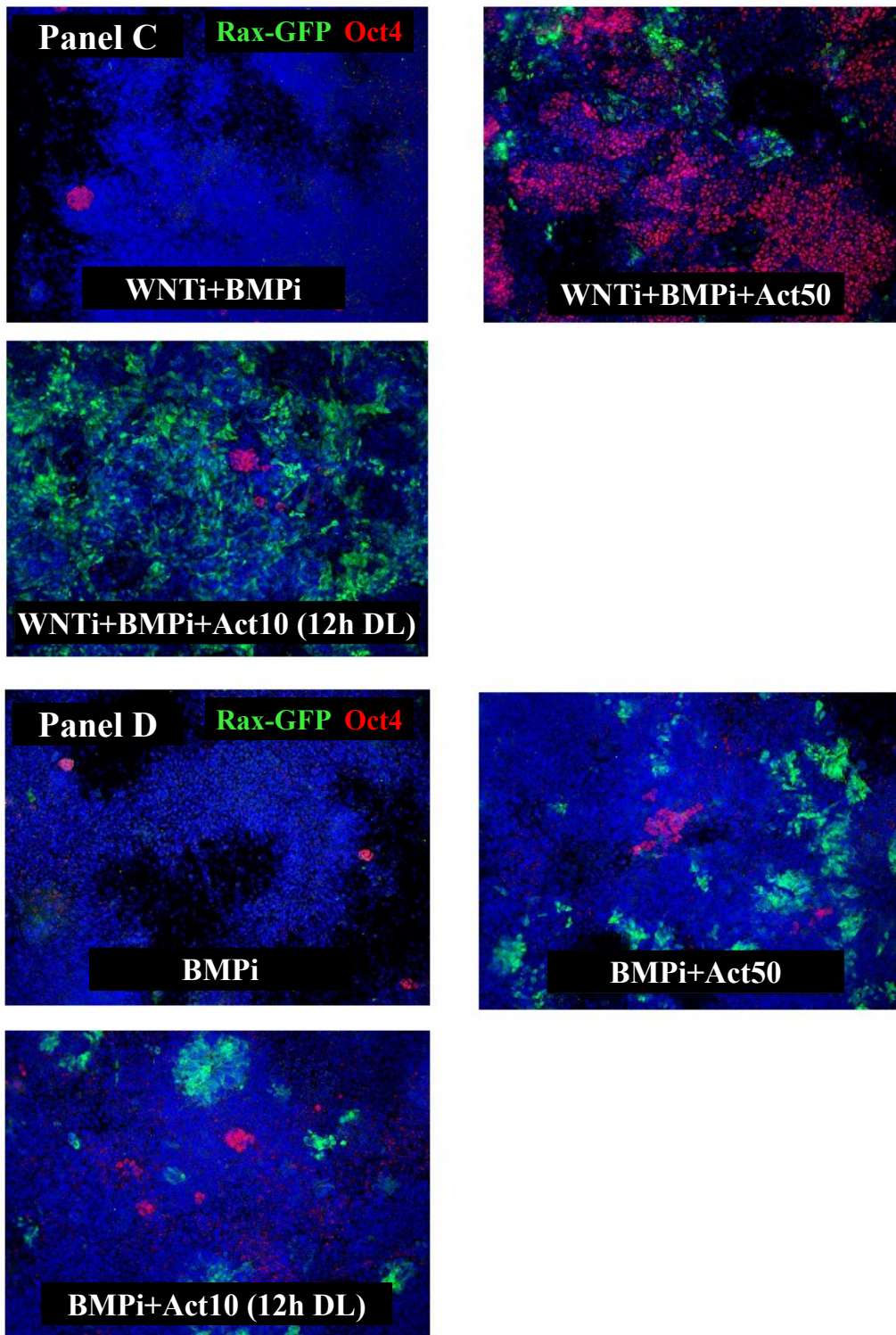
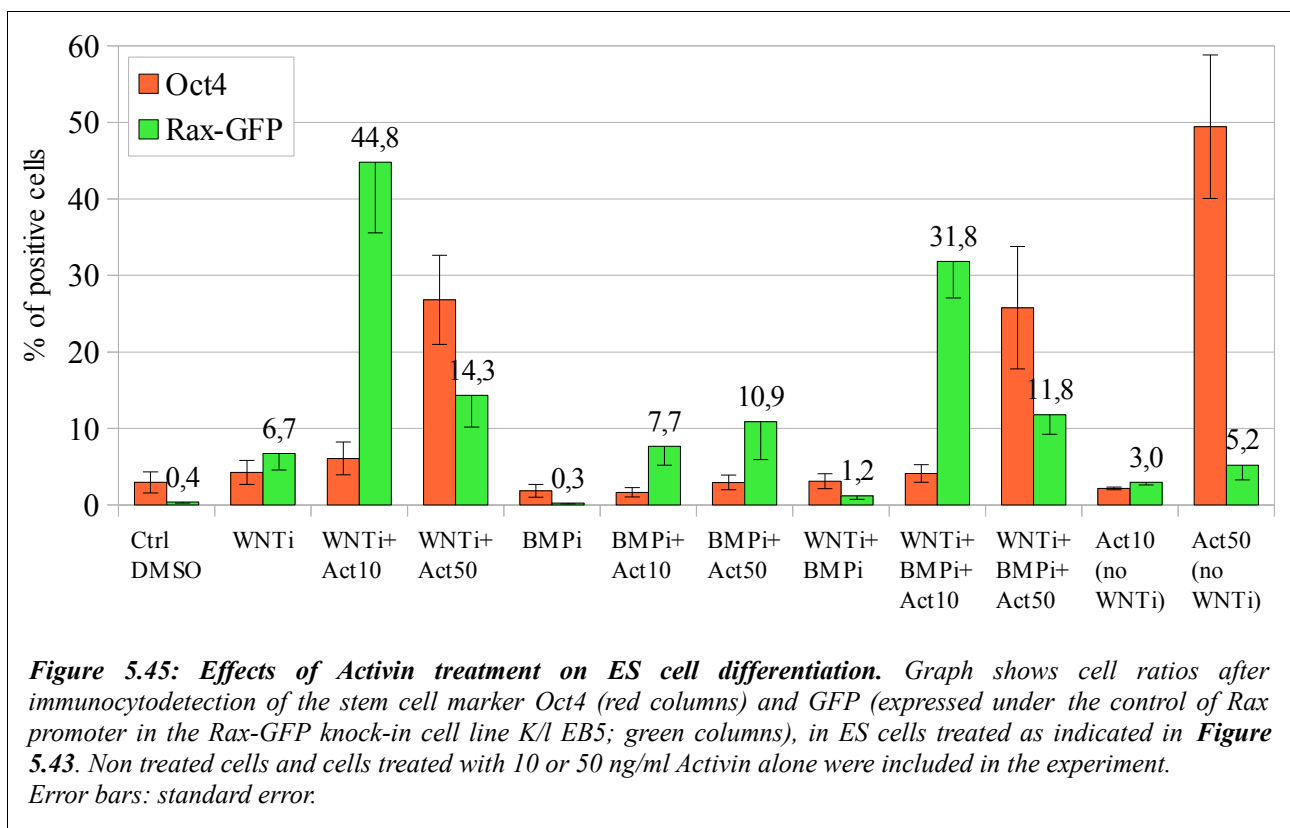


Figure 5.44: Effects of Activin treatment on ES cell differentiation. Panels A-D show immunocyto detection of the stem cell marker Oct4 (red) and GFP (expressed under the control of Rax promoter in the Rax-GFP knock-in cell line K/1 EB5; green), in ES cells at the end of Step-II, day6 (8 days of in vitro differentiation after LIF withdrawal), after treatment with different combinations of Activin doses (10 and 50 ng/ml Activin-A recombinant protein), tested in association with different anteriorizing treatments (Wnt-inhibition, BMP-inhibition and double Wnt/BMP-inhibition).



Activin was added to the culture medium at Step-II, day2, with a 12-hour delay with respect to the starting point for chemical drug treatments (see scheme in **Figure 5.43**). Nuclei counter-staining was obtained with DAPI. The best option to drive Rax expression was to add 10 ng/ml Activin in combination with Wnt-inhibition or double Wnt/BMP-inhibition (44.8% and 31.8% GFP-positive cells, respectively).

As noticed before (see **Figure 5.20**), Activin treatment was not affecting ES cell neural differentiation in a strong way when associated to BMP-inhibition, compared to what happened in other combinations. Oct4-positive cells were only 2.95% in BMP-inhibition plus 50 ng/ml Activin. The reason for this difference was not further investigated; anyhow, RT-PCR data showed before (see **Figure 5.19**) suggested that this particular treatment combination (BMP-inhibition+Activin) steered stem cell fate towards meso/endodermal differentiation, instead of simply slowing-down neural conversion, and additionally lead to a ventralization of cell culture, as seen by high level of Shh expression (**Figure 5.19**).



Control cells were treated with Activin (10 ng/ml and 50 ng/ml) but no concomitant chemical drug-mediated anteriorization (**Figure 5.46**). Oct4 staining revealed the anti-neuralizing effect of high dose (50 ng/ml) Activin treatment (49.4% Oct4-positive cells). Furthermore, it was clear that Activin alone was not able to efficiently induce Rax-GFP-positive cells (only 2.9% and 5.2% Rax-GFP-positive cells after 10 ng/ml and 50 ng/ml Activin treatment, respectively).

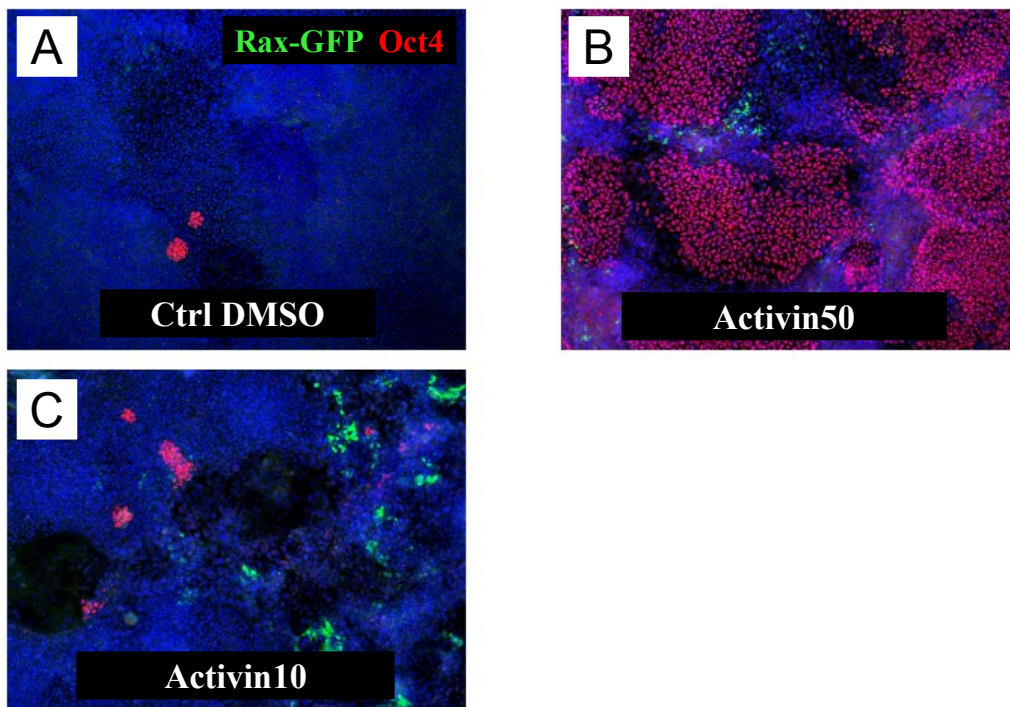


Figure 5.46: Effects of Activin treatment on ES cell differentiation. Images (A-C) show immunocyto detection of stem cell marker Oct4 (red) and GFP (expressed under the control of Rax promoter in the Rax-GFP knock-in cell line K/I EB5; green), in ES cells at the end of Step-II, day6 (8 days of in vitro differentiation after LIF withdrawal). Nuclei counter-staining was obtained with DAPI. Here are shown non-treated (0.1% DMSO cultured) cells (A) and cells treated with 10 or 50 ng/ml Activin alone (without concomitant treatment with chemical drugs; (B) and (C)). Activin alone was not able to efficiently induce Rax-positive retinal cells when used at low dose (10 ng/ml; 2.97% GFP-positive cells); the higher dose (50 ng/ml) dramatically inhibited ES cell neural differentiation (49.4% Oct4-positive cells).

Taken all together, these data strongly suggest a role for Activin as a retinal inducer during ES cell neural differentiation.

Activin itself can play other roles during differentiation, first of all as an anti-neuralizing, stemness-promoting, factor; this effect can be prevented by allowing ES cells to differentiate in absence of Activin during the first 3.5 days of culture after LIF withdrawal.

Activin retinal inducing action was exerted only on cells that acquired a forebrain fate via Wnt-inhibition or double Wnt/BMP-inhibition; Activin was not effective as a retinal inducer when used alone. This suggests that a previous anteriorization to a forebrain fate was necessary to acquire the competence to respond to Activin-mediated retinal induction, consistently to what happens *in vivo*.

6– BMP and Anterior Brain Patterning

A Possible Role for BMP as a Retinal Inducer.

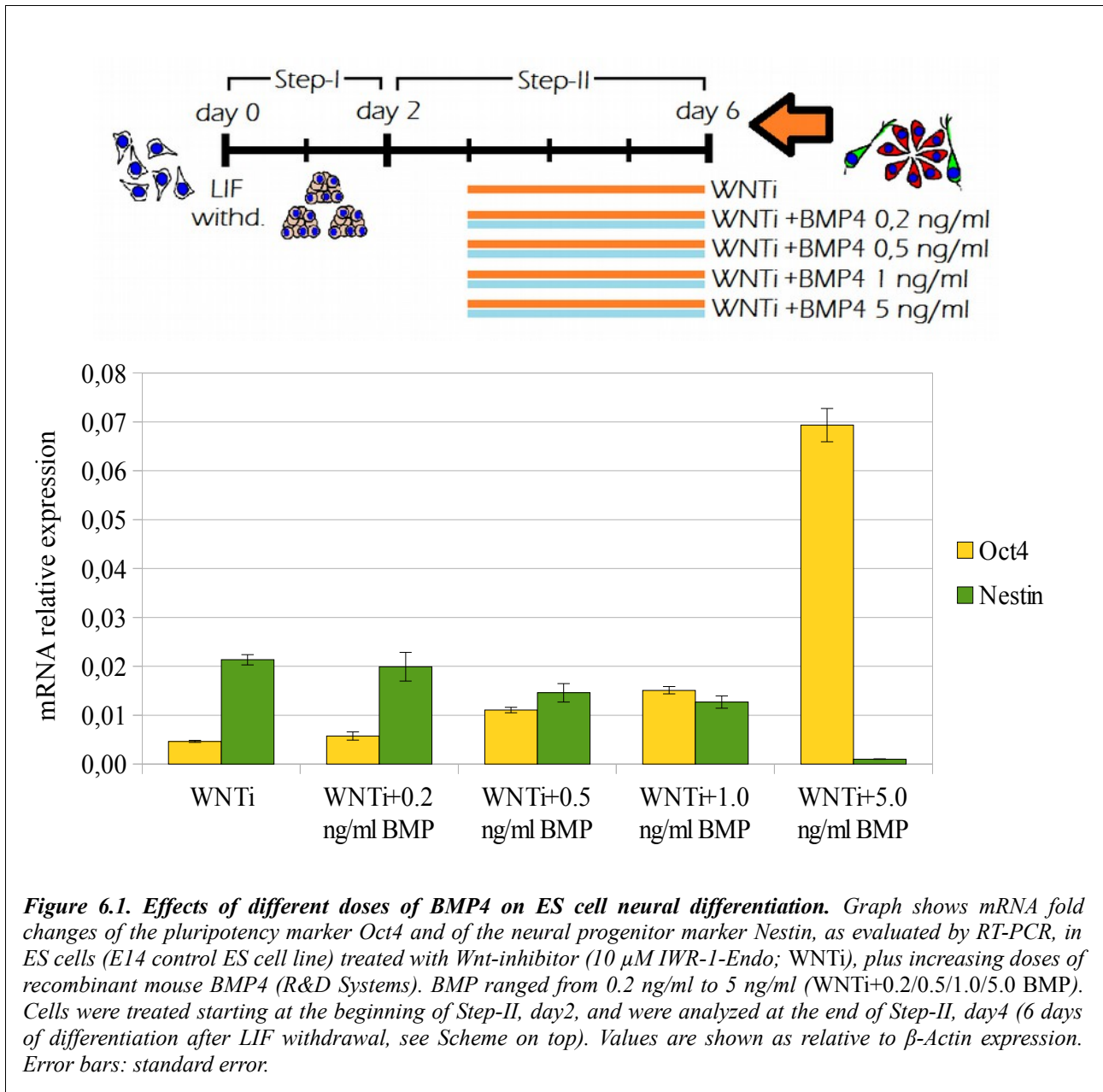
A recently published work on human ES cells showed the involvement of both Activin/Nodal and BMP signaling for the induction of eye field genes (Lupo et al., 2013). We demonstrated that Activin play a pivotal role in retinal induction also in our *in vitro* system of mouse ES cell neural differentiation (Results, Chapter 5, and Bertacchi et al., manuscript in preparation). Next, we wanted to test a possible role for BMP signaling in retinal induction.

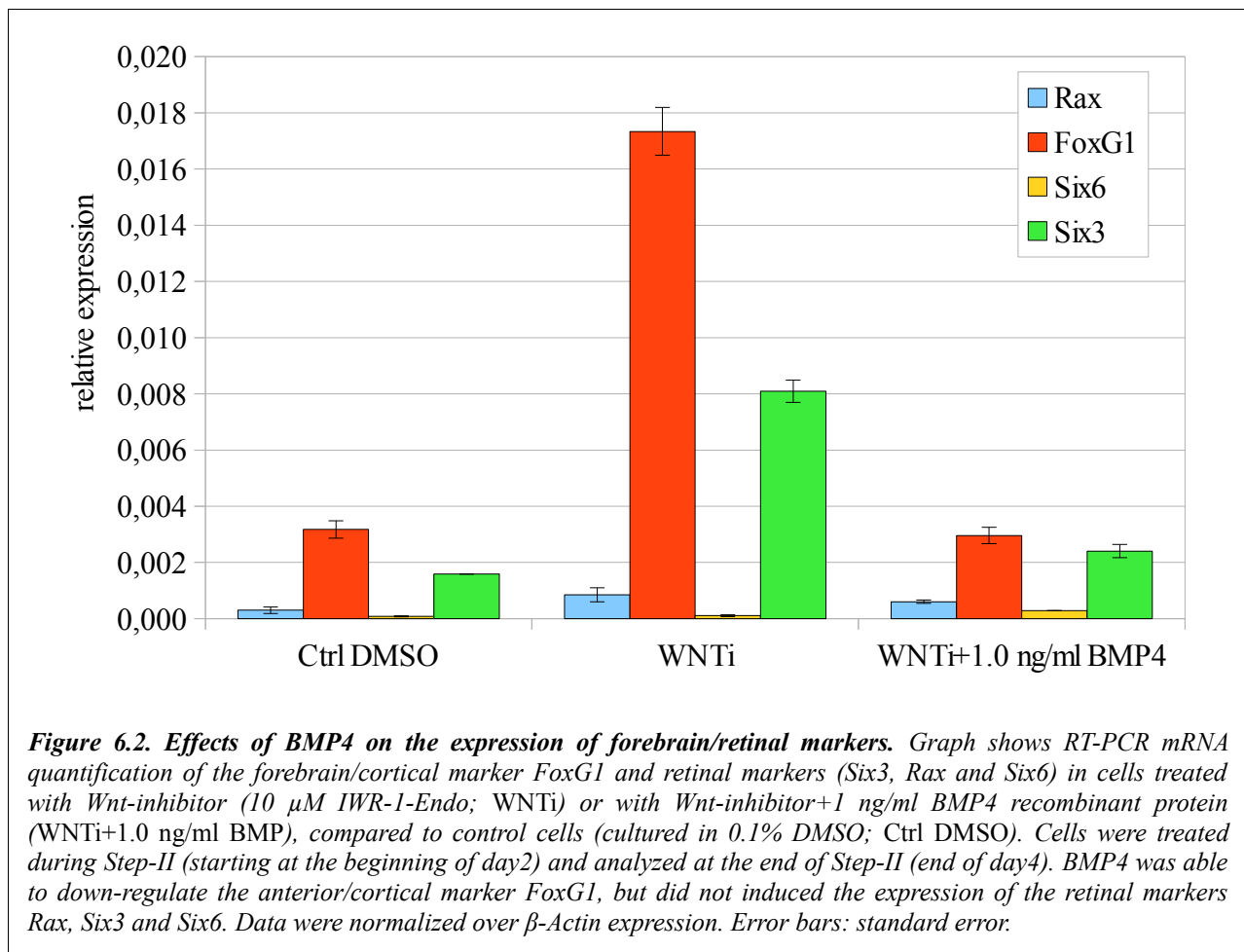
We previously showed that mouse ES cells expressed morphogens belonging to the BMP family during neural differentiation *in vitro* (see Results, Chapters 2 and 3). We also demonstrated that endogenously produced BMPs can affect ES cells regional fate acquisition; Noggin-mediated BMP inhibition was necessary and sufficient to acquire a telencephalic identity in our culture system (see Results, Chapter 3).

We decided to test if BMP factors could play a role in retinal induction in cells anteriorized by Wnt-inhibition. To this purpose, we used a purified recombinant mouse BMP4 protein (R&D System); Wnt-inhibition was performed by treating cells with 10 μ M IWR-1-Endo, as described for treatments with Activin.

BMP factors play an important role in sustaining the stemness of pluripotent ES cells (Silva et al., 2008). We tried to identify the right dose of BMP to treat our cells without blocking their spontaneous neural differentiation. Cells were treated during Step-II (starting at the beginning of day2) with increasing doses of BMP4, ranging from 0.2 ng/ml to 5 ng/ml; at the same time, cells were anteriorized by Wnt-inhibition, starting treatment at the beginning of Step-II, day2. ES cell neural differentiation was investigated by RT-PCR at the end of Step-II, day4 (total of 6 days of *in vitro* differentiation after LIF withdrawal) (**Figure 6.4**). We found that the higher BMP4 dose (5 ng/ml) was strongly inhibiting neural differentiation, as seen by the high expression level of Oct4 and the low expression level of Nestin (**Figure 6.4**). Nestin expression was clearly inhibited by increasing doses of BMP4 in a dose-dependent manner; we thus choose the dose of 1 ng/ml BMP4 as an optimal compromise to treat cells while maintaining a good level of Nestin expression (neural conversion).

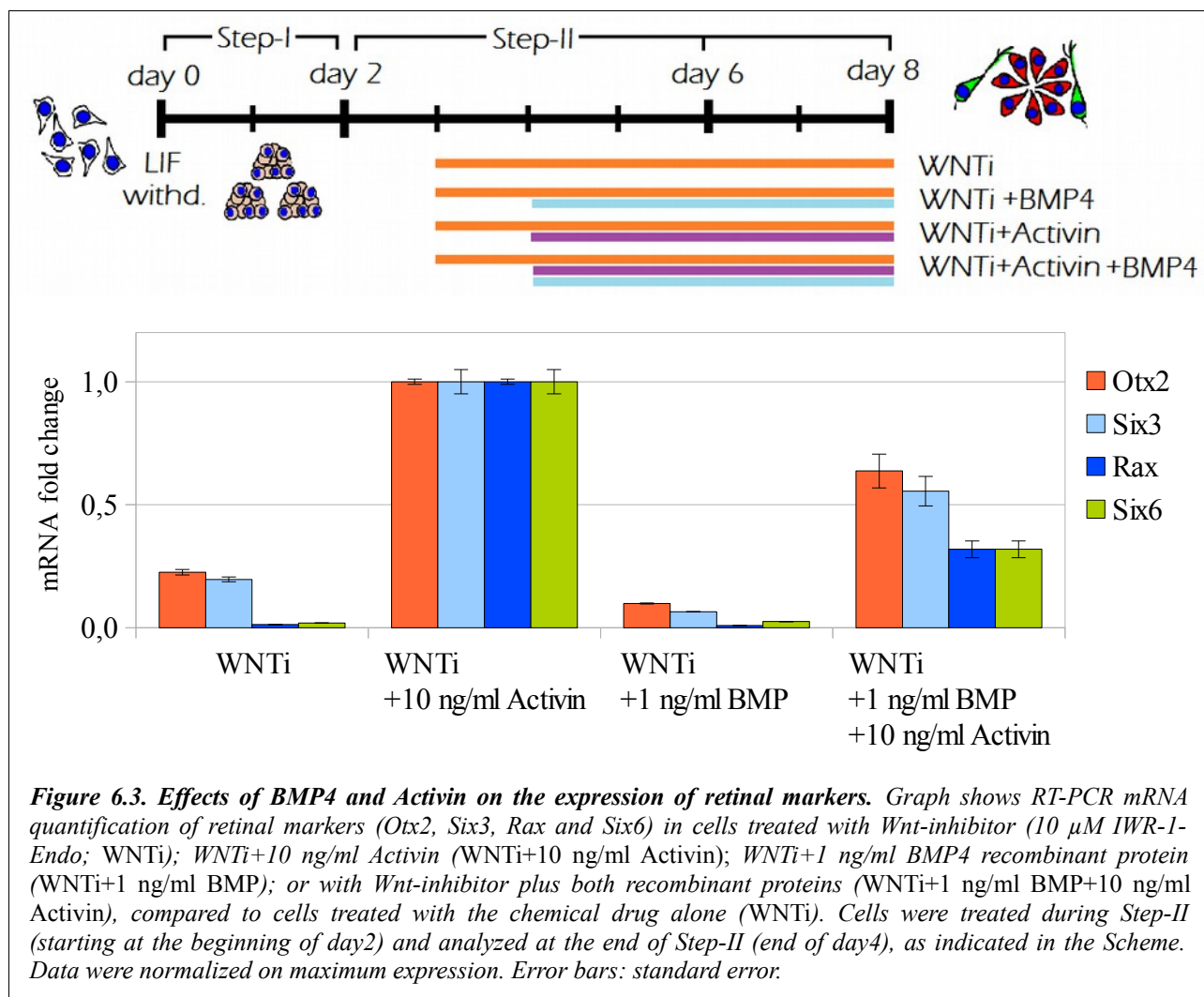
Unfortunately, when we analyzed the expression levels of anterior/retinal markers, we found that the presence of BMP4 in culture medium was not promoting retinal differentiation. BMP4 switched-off the expression of FoxG1, consistently with our previous findings (see Results, Chapter 3; Bertacchi et al., 2013), but was not able to efficiently induce the expression of the retinal markers Rax and Six6 (**Figure 6.2**).





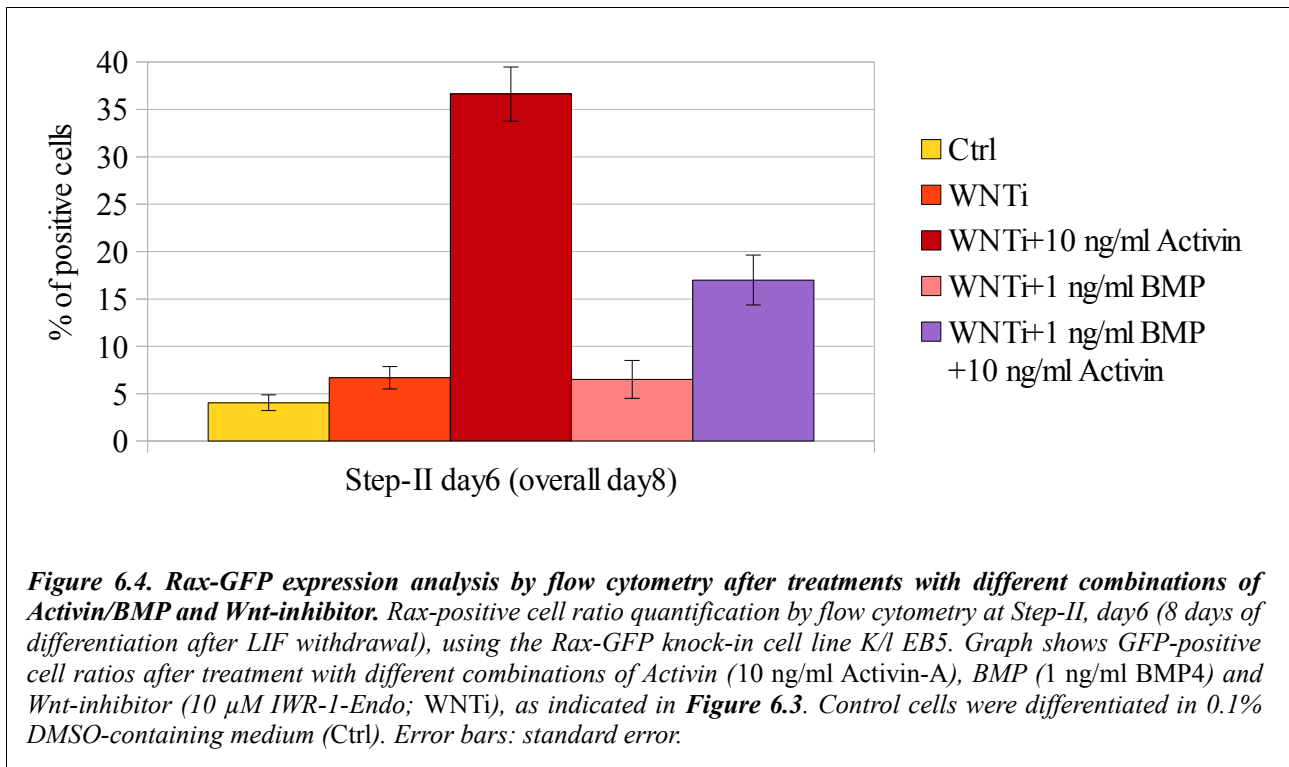
To consolidate our results, we performed a further experiment, testing a possible synergistic effect of BMP4 when used in combination with Activin (**Figure 6.3**).

Cells were anteriorized by *Wnt*-inhibition and treated with 10 ng/ml Activin, with 1 ng/ml BMP4, or with both recombinant proteins. Retinal marker expression was investigated by RT-PCR at Step-II, day6 (8 days of differentiation). Again, BMP4 was not able to up-regulated the expression level of retinal markers (*Otx2*, *Six3*, *Rax* and *Six6*). The compresence of BMP4 together with Activin was not efficient in terms of retinal induction properties: we obtained intermediate levels of retinal marker expression, compared to control and to Activin-treated conditions, and this suggested that BMP4 interfered with the retinal inducing action of Activin (**Figure 6.3**). We do not know if BMP4 acted by specifically inhibiting retinal gene expression or if it simply interfered with neural differentiation.



The analysis by flow cytometry using Rax-GFP knock-in cell line confirmed the results obtained by RT-PCR. Cells were treated with the conditions described above (**Figure 6.3**) and samples were processed at the end of Step-II, day6 (8 days of differentiation after LIF withdrawal). Treatment with Wnt-inhibitor+10 ng/ml Activin+1 ng/ml BMP4 produced an intermediate percentage of GFP-positive cells (17% GFP-positive cells), when compared to control untreated cells and to Wnt-inhibitor+Activin treated cells (4.1% and 36.6% GFP-positive cells, respectively) (**Figure 6.4**).

We concluded that, differently from what was demonstrated in human ES cell differentiation (Lupo et al., 2013), BMPs were not efficient *retinal inducing signals* for differentiating mouse ES cells, at least in the concentration and conditions tested in our protocol.



7– Dorso-Ventral Patterning of the Diencephalon

How to Control the Dorso-Ventral Identity of Diencephalic Progenitors Playing with Shh Pathway.

As Rax gene is also expressed in the ventral diencephalon (Beccari et al., 2013), we decided to better investigate Rax expression in our culture system and to dissect ES cell dorso/ventral (D/V) identity in the context of forebrain patterning/differentiation (**Figure 7.1**).

Retinal progenitors originate from the lateral wall of diencephalon, and are both Rax-positive and Pax6-positive (Wilson and Houart, 2004; Ikeda et al., 2005). They are also positive for the anterior/dorsal marker Otx2 and for the forebrain marker Six3 (Ikeda et al., 2005). Neural progenitor cells in the ventral diencephalon, on the contrary, are Rax-positive but Pax6-negative (Ikeda et al., 2005); they are positive for ventral markers such as Nkx2.1 (which is expressed in the ventral forebrain) and Vax1 (whose name stands for *ventral anterior homeobox* and clearly describes its expression pattern) (**Figure 7.1**; See also gene expression patterns on www.emouseatlas.org).

Neural progenitor D/V identity can be efficiently manipulated by modulating Shh pathway, as we previously demonstrated also in our protocol (Bertacchi et al., 2013). Shh pathway can be activated

by SAG treatment (Smoothened agonist, 100-150 nM) and blocked by Cyclopamine treatment (Cyc, 5 μ M; it must be noticed that our cells produced only few amounts of endogenous Shh during their differentiation, see Results, Chapter 2).

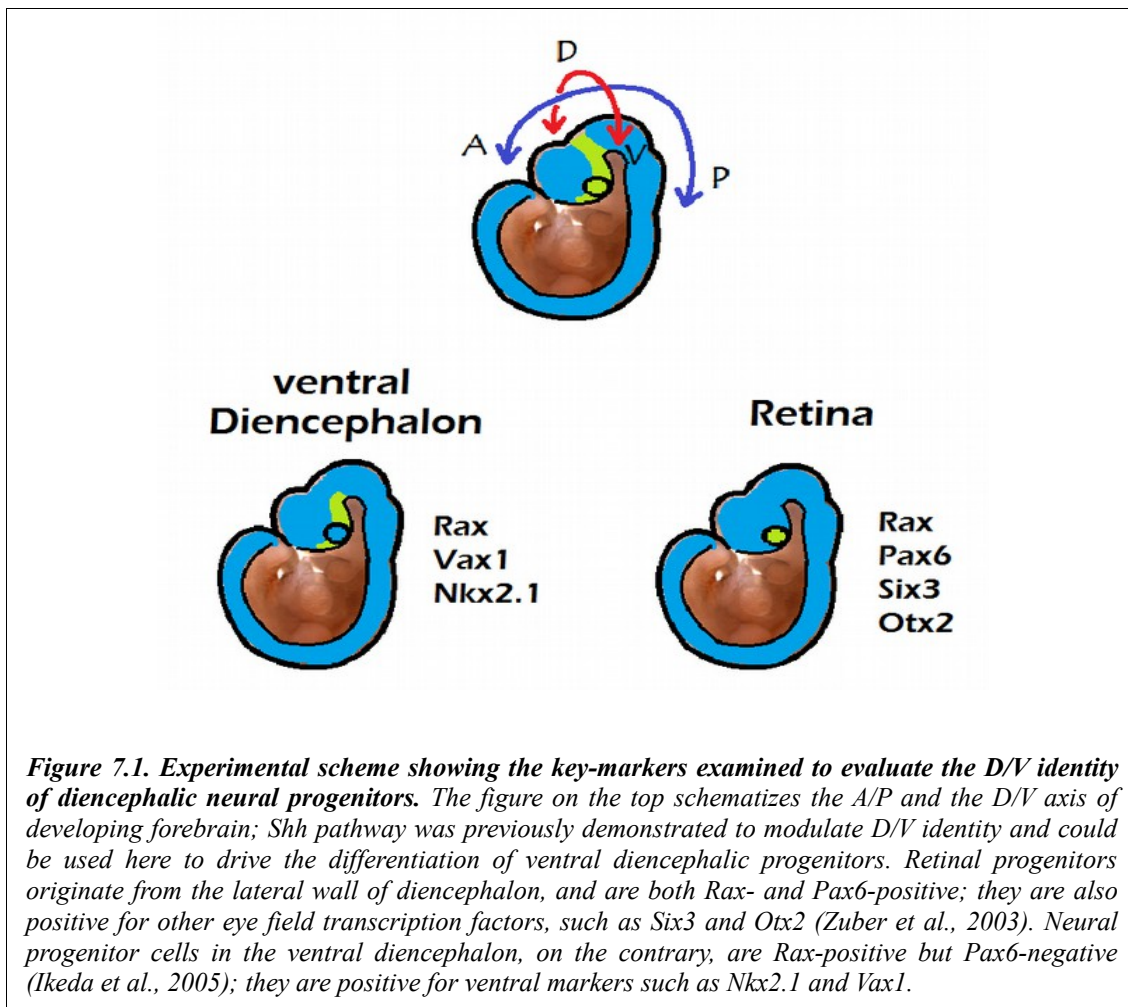


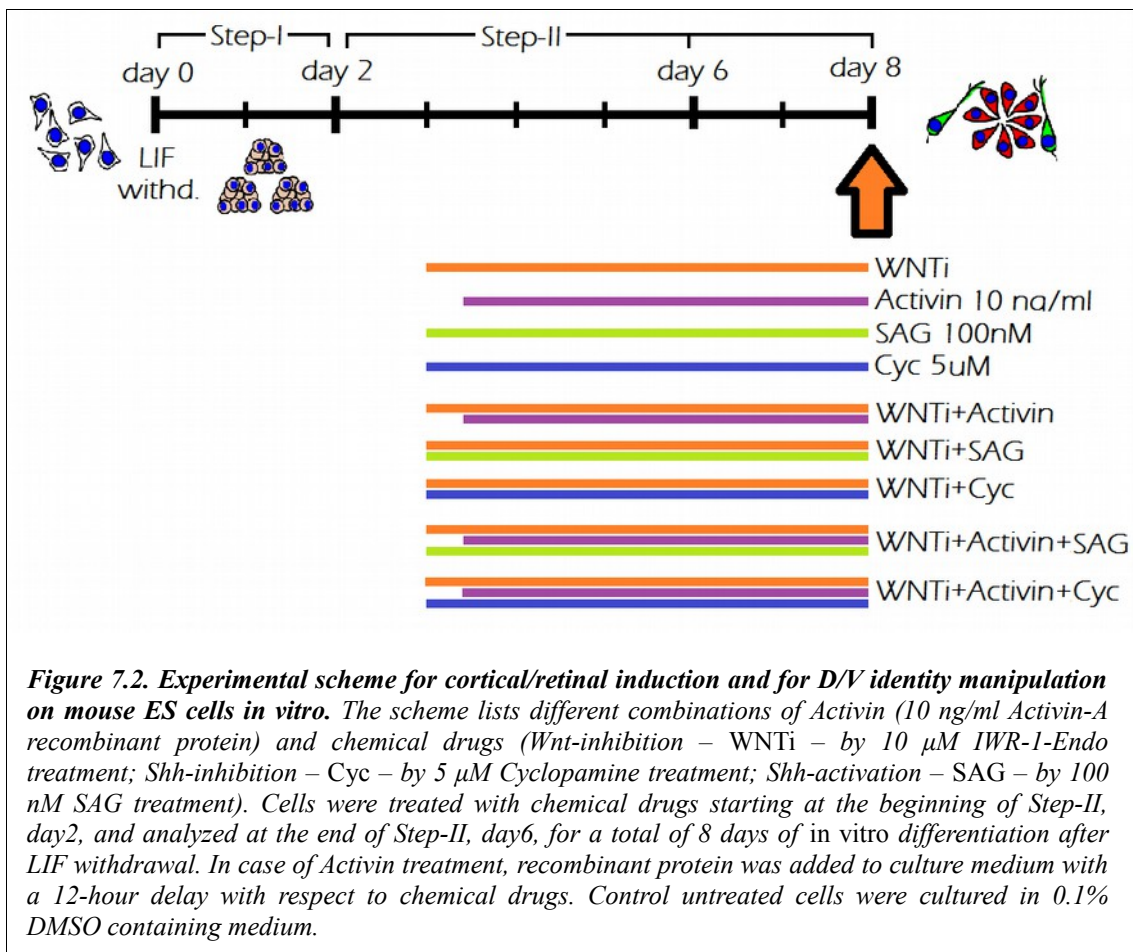
Figure 7.1. Experimental scheme showing the key-markers examined to evaluate the D/V identity of diencephalic neural progenitors. The figure on the top schematizes the A/P and the D/V axis of developing forebrain; Shh pathway was previously demonstrated to modulate D/V identity and could be used here to drive the differentiation of ventral diencephalic progenitors. Retinal progenitors originate from the lateral wall of diencephalon, and are both Rax- and Pax6-positive; they are also positive for other eye field transcription factors, such as Six3 and Otx2 (Zuber et al., 2003). Neural progenitor cells in the ventral diencephalon, on the contrary, are Rax-positive but Pax6-negative (Ikeda et al., 2005); they are positive for ventral markers such as Nkx2.1 and Vax1.

We decided to test if our ES cells were able to exhibit both types of Rax expression, in the context of dorsal identity (Pax6-positive retinal cells) or ventral identity (Nkx2.1-positive ventral diencephalon cells).

Cells were anteriorized by Wnt-inhibition (10 μ M IWR-1-Endo starting at the beginning of Step-II, day2, as previously described for Activin and BMP treatments). At the same time, D/V identity was controlled by SAG and Cyclopamine treatment. SAG and Cyclopamine were added to culture medium together with Wnt-inhibitor (cortical induction condition; see Results, Chapter 4) or together with Wnt-inhibitor and Activin (retinal induction condition; see Results, Chapter 5)

(**Figure 7.2**). Control samples were untreated (DMSO-cultured) cells, or cells treated separately with single chemical drugs (**Figure 7.2**).

At the end of Step-II, day6 (after a total of 8 days of differentiation *in vitro*), cells were fixed and analyzed by double Rax-GFP/Pax6 and Rax-GFP/Nkx2.1 immunostainings, to investigate the production of Pax6/Rax-positive retinal progenitors and Nkx2.1/Rax-positive ventral diencephalic progenitors, respectively.



Control untreated cells showed no staining for Rax-GFP, consistently with their regional identity that we previously showed to be predominantly mesencephalic (see Results, Chapter 3; Bertacchi et al., 2013; **Figure 7.3A**). Only little clusters of Nkx2.1-positive cells were present in control condition at Step-II, day6 (3.6% Nkx2.1-positive cells). A similar situation was found in cells treated with Wnt-inhibitor (7.4% Nkx2.1-positive cells; **Figure 7.3B**).

Nkx2.1 expression could be efficiently modulated by performing SAG and Cyclopamine treatments to activate/repress Shh pathway, respectively. Cyclopamine treatment abolished Nkx2.1 expression, as the already low number of Nkx2.1-positive cell clusters completely disappeared (0.2% Nkx2.1-positive cells; **Figure 7.3D**). On the contrary, SAG treatment robustly switched-on Nkx2.1 expression (65.3% Nkx2.1-positive cells), leading to a massive ventralization of the cell culture (**Figure 7.3G,F**).

Rax expression was efficiently induced in cells treated with Wnt-inhibitor+10 ng/ml Activin (40.7% GFP-positive cells; **Figure 7.3E**); cells labeled by GFP staining were very rarely co-labeled by Nkx2.1 staining (only 2.2% Nkx2.1/GFP-double positive cells). We concluded that the *retinal induction* treatment was driving Rax expression in cells with a lateral/dorsal identity. This was further confirmed by the high proportion of Pax6/Rax-GFP double positive cells (32.4%, see below, **Figure 7.6**).

Blocking the endogenously produced Shh by the use of Cyclopamine, together with the addition of Wnt-inhibitor and Activin, caused the complete disappearance of the few double positive Rax/Nkx2.1-positive cells that were present in our retinal culture (0.07% Nkx2.1/GFP-double positive cells; **Figure 7.3H**). However, also the efficiency of Rax induction was generally affected (38.5% GFP-positive cells in Wnt-inhibitor+Activin, 20.9% GFP-positive cells in Wnt-inhibitor+Activin+Cyclopamine; compare **Figure 7.3E** and **Figure 7.3H**). Further analysis will be necessary to understand if this was caused by a possible toxicity after treatment with Cyclopamine, or if this phenomenon was specific and due to the effect of a complete block of Shh pathway on Rax-positive cell differentiation. Cell ratios are shown in **Figure 7.4**.

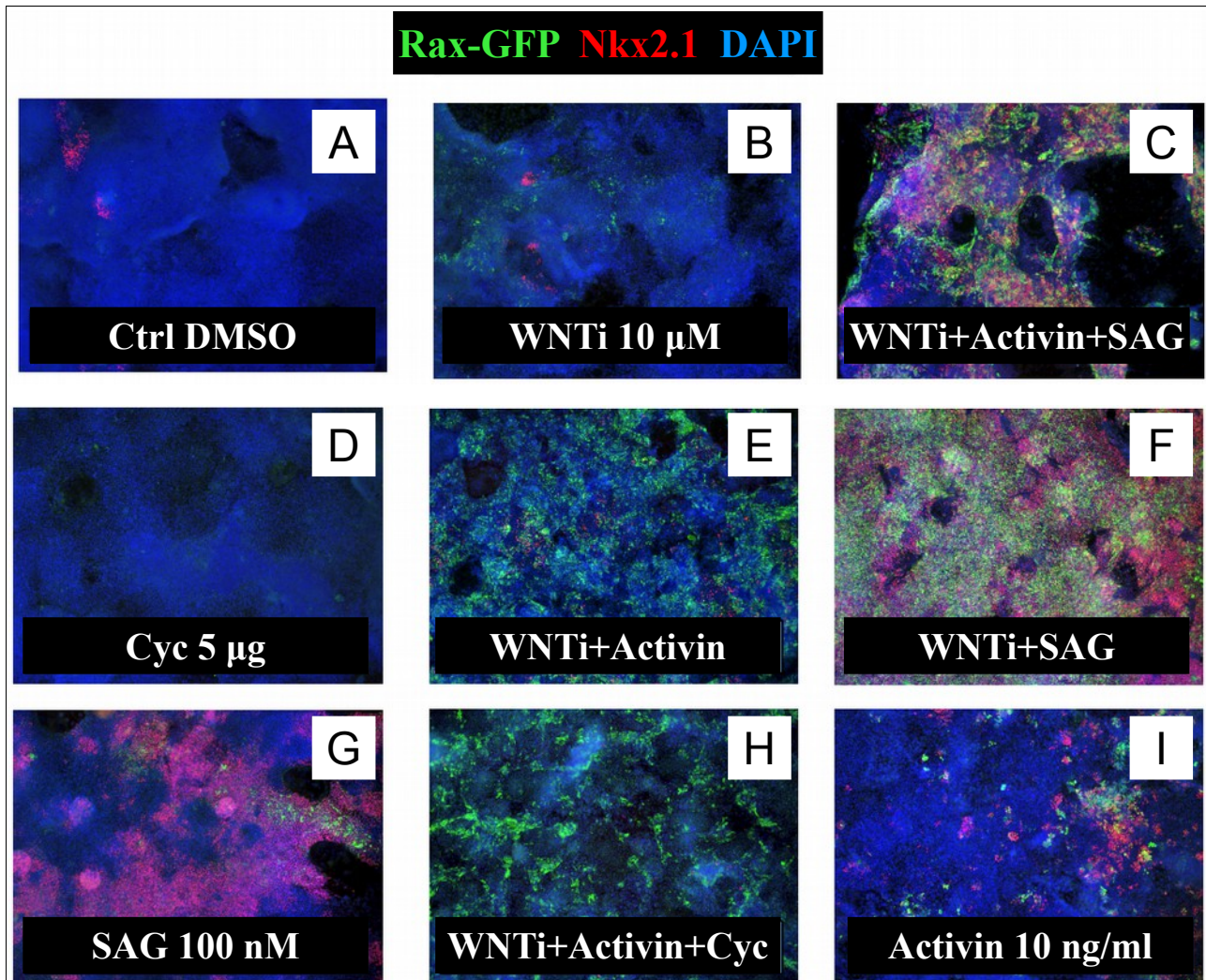
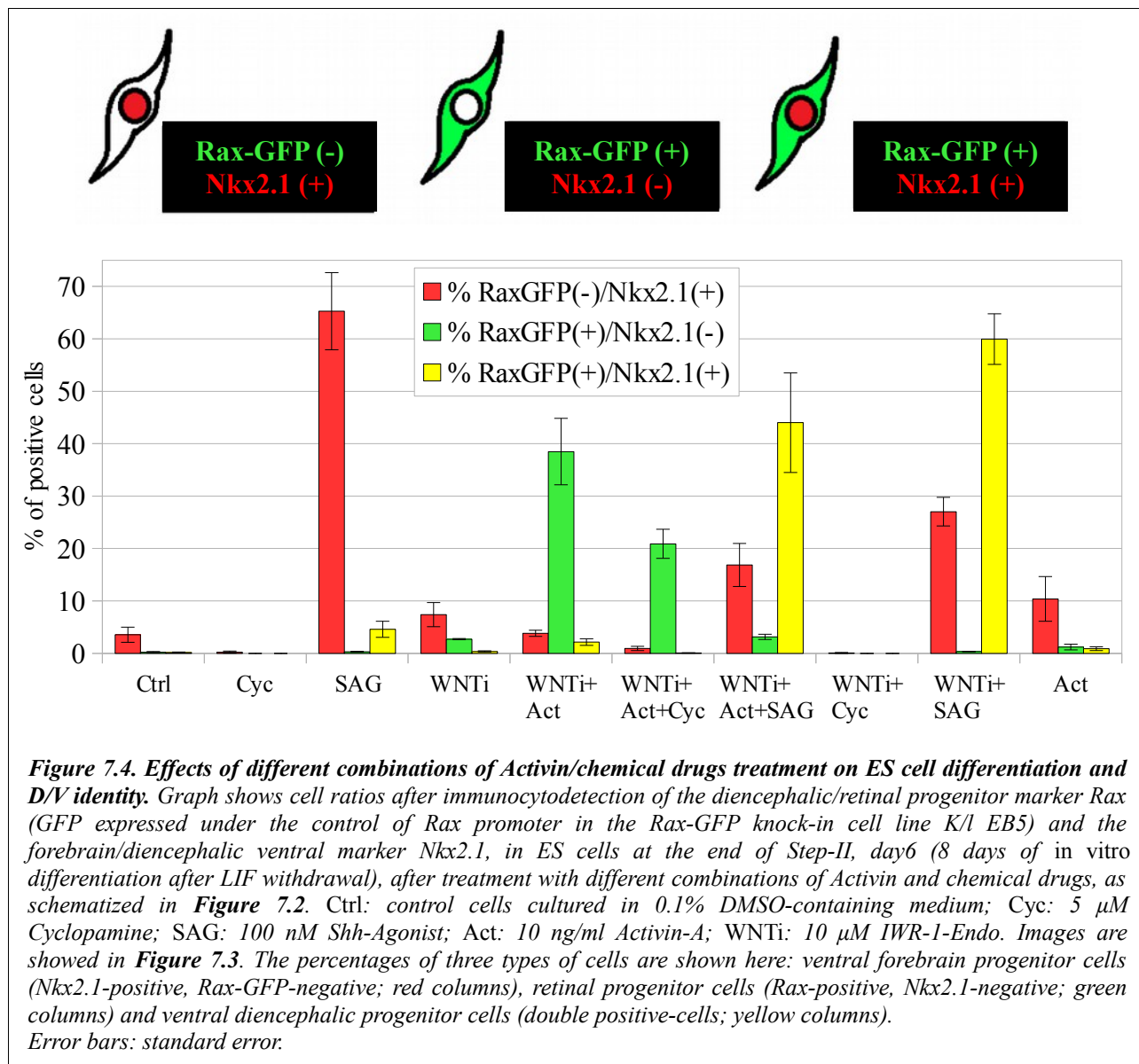


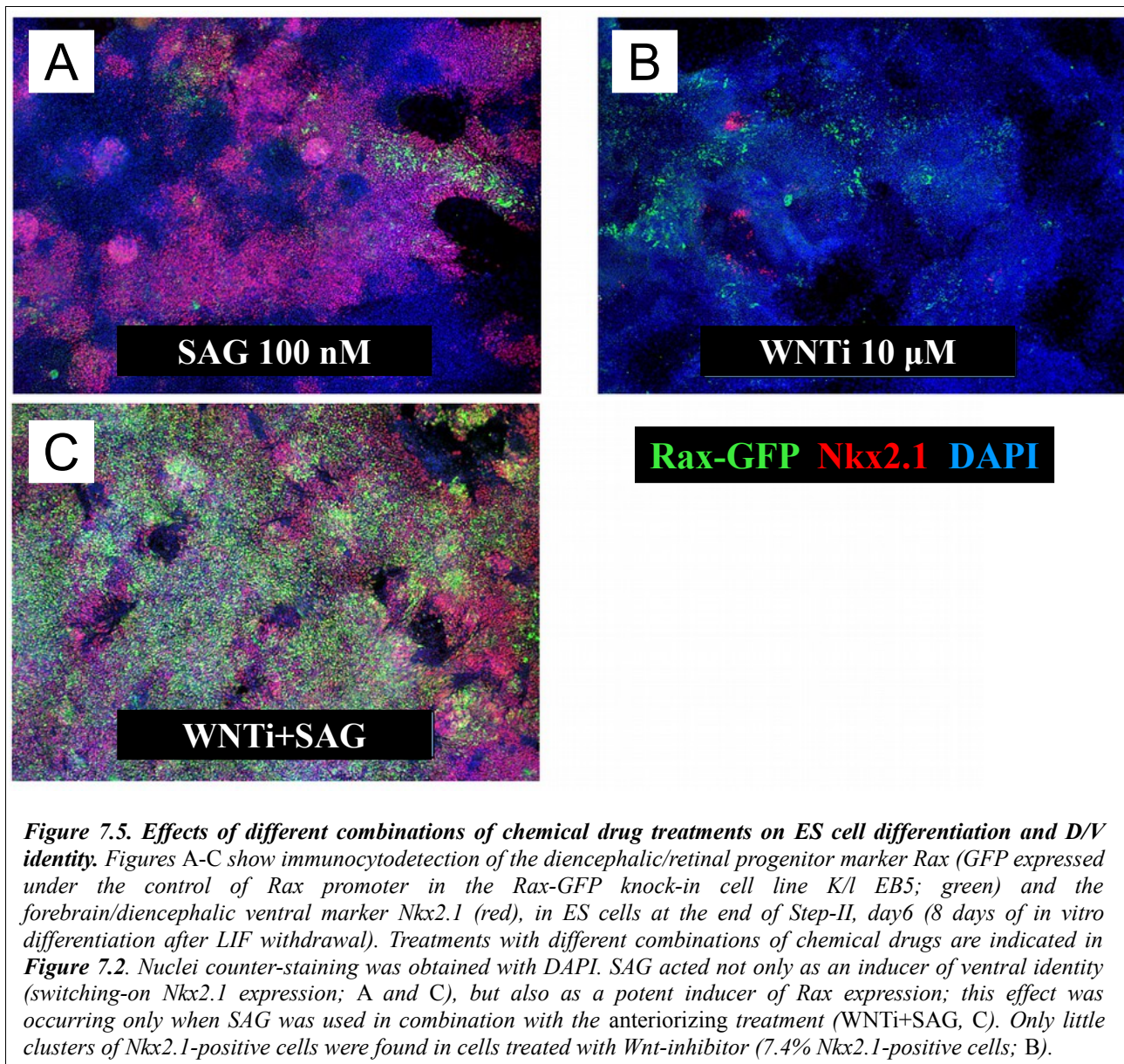
Figure 7.3. Effects of different combinations of Activin/chemical drugs treatment on ES cell differentiation and D/V identity. Figures A-I show immunocyto detection of the diencephalic/retinal progenitor marker *Rax* (GFP expressed under the control of *Rax* promoter in the *Rax*-GFP knock-in cell line *K/l EB5*; green) and of the forebrain/diencephalic ventral marker *Nkx2.1* (red), in ES cells at the end of Step-II, day6 (8 days of in vitro differentiation after LIF withdrawal), after treatment with different combinations of Activin and chemical drugs as indicated in **Figure 7.2**. Activin was added to the culture medium at Step-II, day2, with a 12-hour delay with respect to the starting point for chemical drug treatments. Nuclei counter-staining was obtained with DAPI. *Nkx2.1* expression could be efficiently modulated by performing SAG and Cyclopamine treatments to activate/repress *Shh* pathway, respectively (C,D,F-H). SAG acted not only as an inducer of ventral identity (switching-on *Nkx2.1* expression; C,F,G), but also as a potent inducer of *Rax* expression; this effect was occurring only when SAG was used in combination with the anteriorizing treatment (*Wnt*-inhibition) (F). Activin showed a light ventralizing effect when used alone (I). Ctrl DMSO: control cells cultured in 0.1% DMSO-containing medium; Cyc: 5 μ M Cyclopamine; SAG: 100 nM *Shh*-Agonist; Activin: 10 ng/ml Activin-A; WNTi: 10 μ M IWR-1-Endo.

Activin alone was not able to induce *Rax*-positive neural progenitors (only 2.1% GFP-positive cells) and showed to have a slight ventralizing effect (10.4% *Nkx2.1*-positive cells) (**Figure 7.3I**).



Interestingly, SAG acted not only as an inducer of ventral identity (switching-on Nkx2.1 expression), but also as a potent inducer of Rax expression (**Figure 7.5C**); this effect was occurring only when SAG was used in combination with the *anteriorizing* treatment (Wnt-inhibition) (compare **Figure 7.5A** and **Figure 7.5C**). Cells treated with Wnt-inhibitor together with SAG were both ventralized (87% Nkx2.1-positive cells) and expressing Rax (60.4% Rax-GFP-positive cells), with a high degree of co-labeling of the two markers (60% Nkx2.1/GFP-double positive cells). This suggested that Shh pathway was able to switch-on Rax expression, but this action could be exerted only on *anteriorized* (forebrain) cells, which were competent to respond to this Shh-

mediated Rax induction. Shh activation alone, performed on control cells with a midbrain identity, was not able to drive efficient Rax expression (only 4.6% double Nkx2.1/GFP-positive cells; **Figure 7.5A**).



The analysis of Pax6 expression in GFP positive cells (**Figure 7.6**) was consistent with that of Nkx2.1, as the two markers showed a quite good reciprocity of staining (**Figure 7.3**).

Pax6-positive cell percentage was increased after Wnt-inhibition compared to control cells (55.8% and 44.5% Pax6-positive cells, respectively; **Figure 7.6A** and **Figure 7.6B**) and was strongly decreased by SAG treatment (2.1% Pax6-positive cells; **Figure 7.6G**).

The highest inductive efficiency of Rax-GFP expression was found in cells treated by Wnt-inhibition plus SAG (61.6% GFP-positive cells; **Figure 7.6F**), but few of these cells were marked by Pax6, whose expression was dramatically inhibited (3.1% Pax6-positive cells, and only 0.6% GFP/Pax6 double positive cells). This finding confirmed the ventral identity of Rax-positive cells obtained by Wnt-inhibition plus SAG treatment. Cell ratios are shown in **Figure 7.8**.

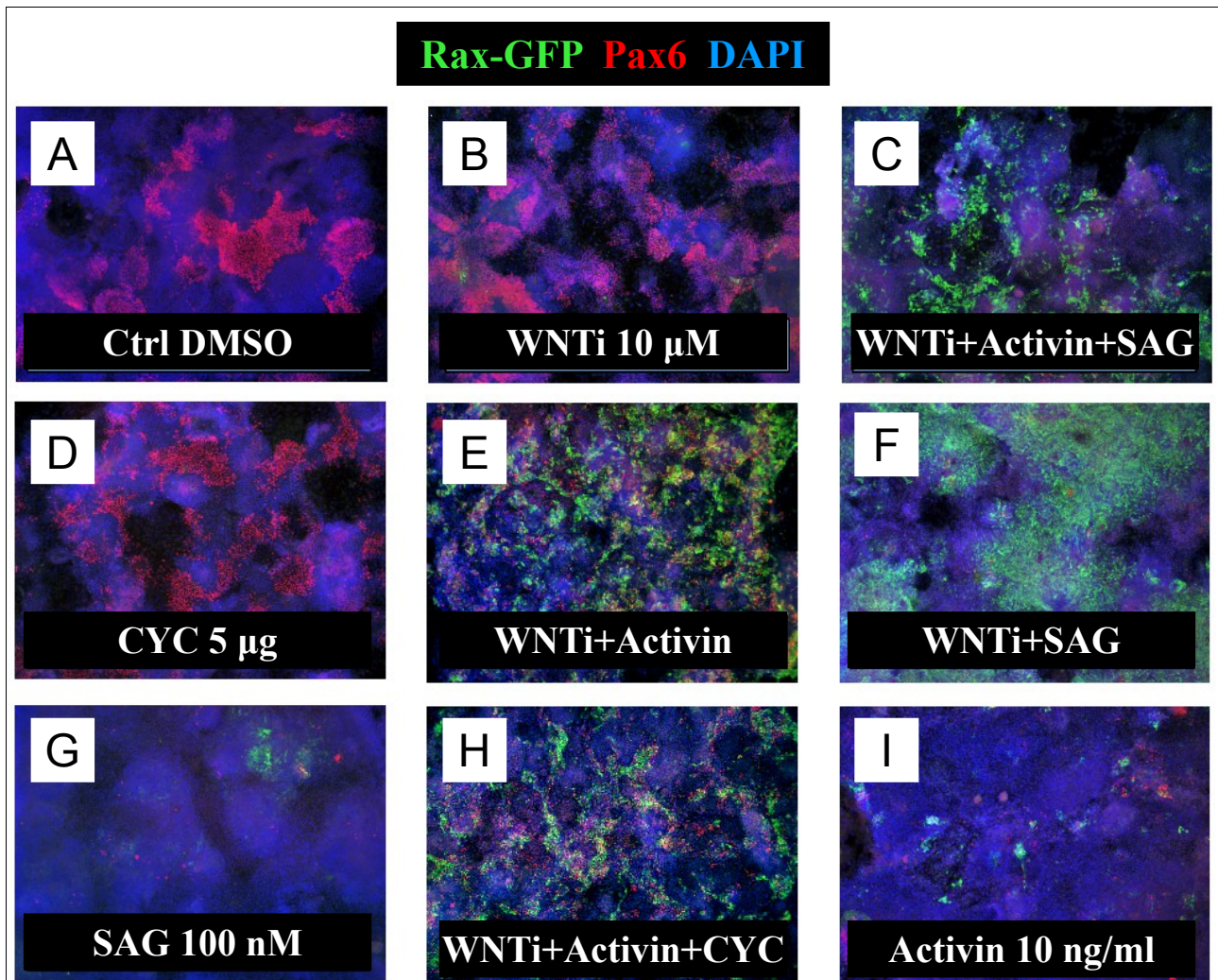
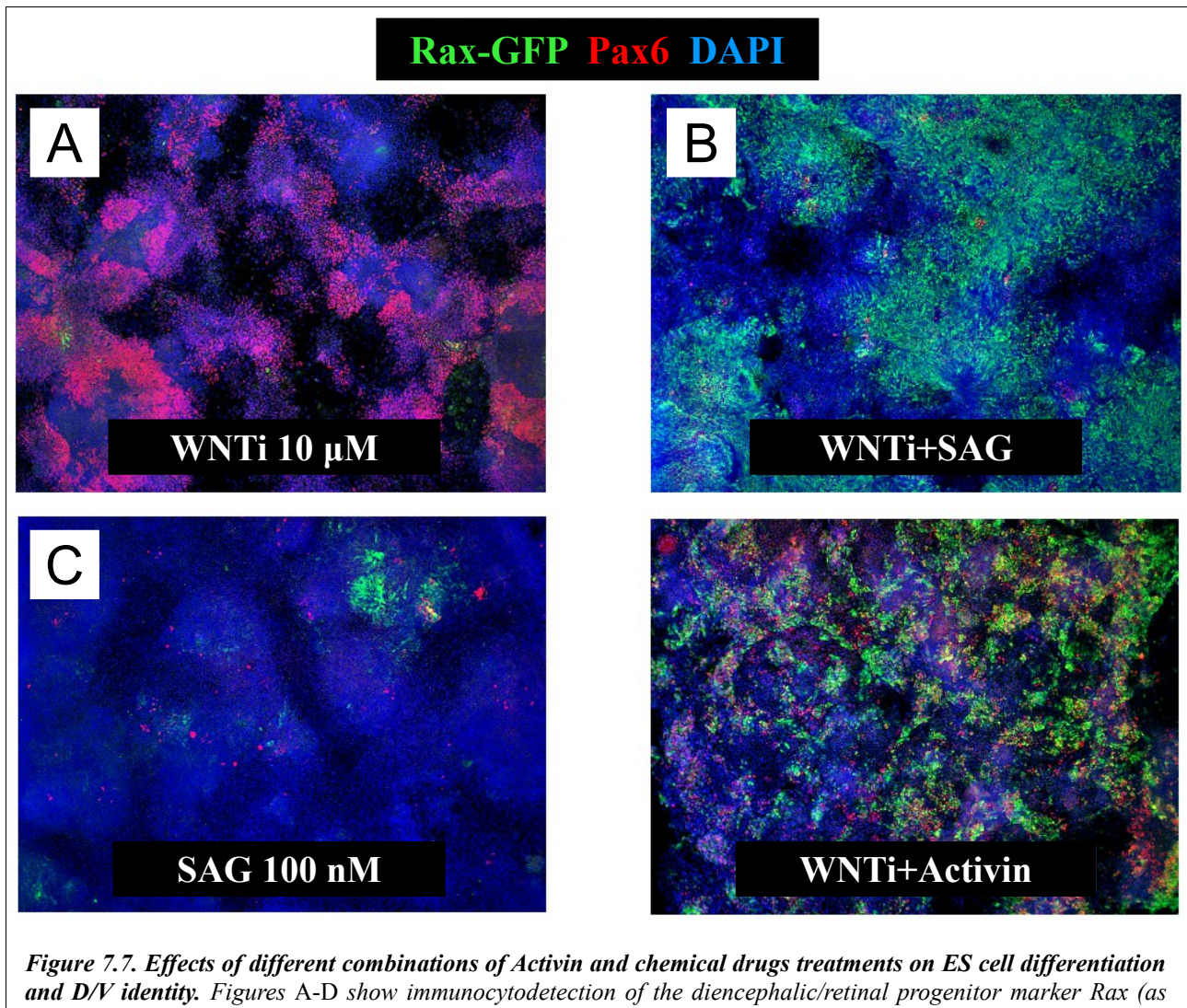
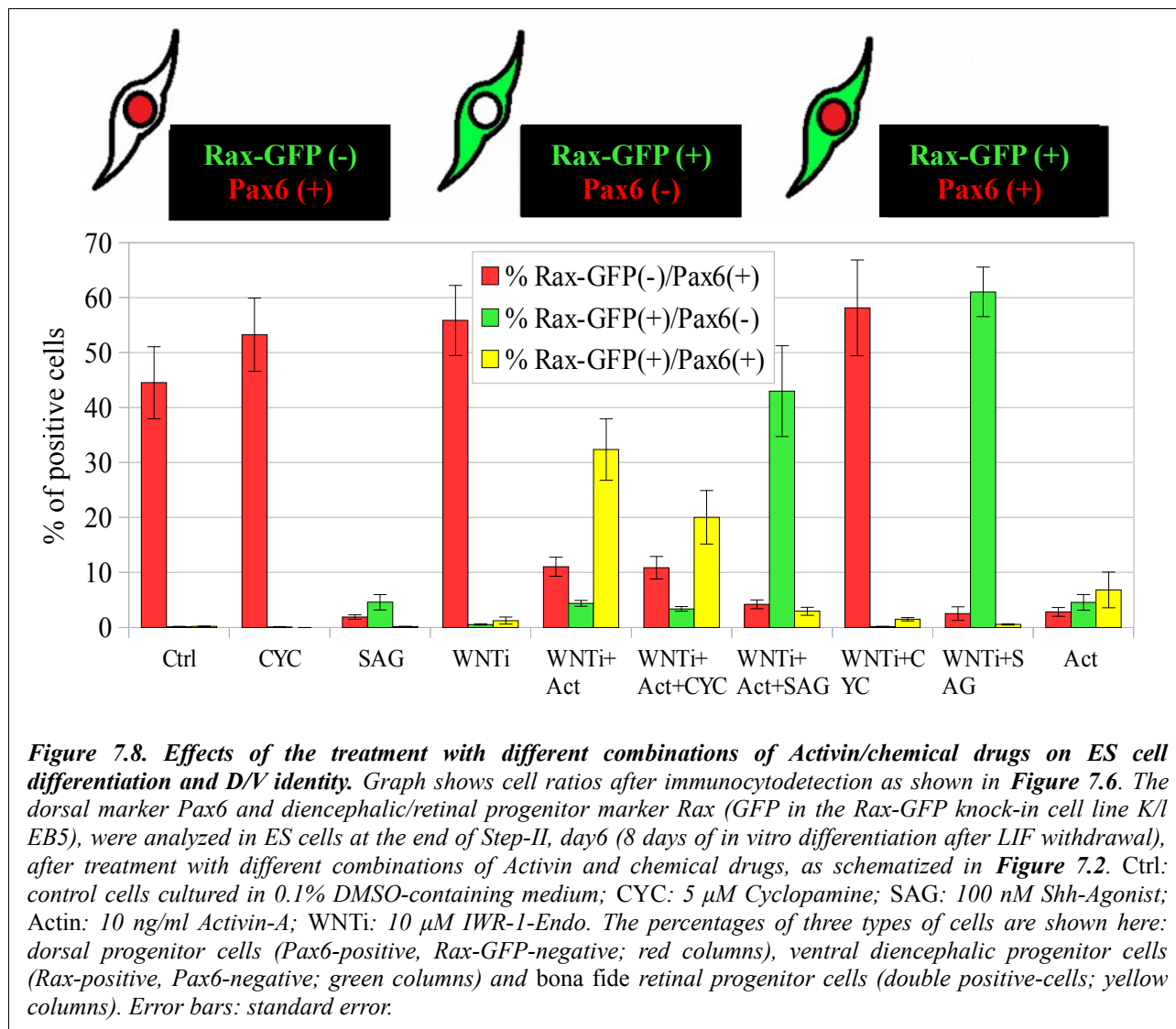


Figure 7.6. Effects of the treatment with different combinations of Activin/chemical drugs on ES cell differentiation and D/V identity. Figures A-I show immunocytochemical detection of the diencephalic/retinal progenitor marker Rax (as GFP expressed in the Rax-GFP knock-in cell line K/l EB5; green) and the dorsal marker Pax6 (red), in ES cells at the end of Step-II, day6 (8 days of *in vitro* differentiation after LIF withdrawal), after treatment with different combinations of Activin and chemical drugs as indicated in **Figure 7.2**. Ctrl DMSO: control cells cultured in 0.1% DMSO-containing medium; CYC: 5 μ M Cyclopamine; SAG: 100 nM Shh-Agonist; Activin: 10 ng/ml Activin-A; WNTi: 10 μ M IWR-1-Endo. Activin was added to culture medium at Step-II, day2, with a 12-hour delay with respect to the starting point for chemical drug treatments. Nuclei counter-staining was obtained with DAPI. Pax6 expression could be efficiently modulated by performing SAG and Cyclopamine treatments to activate/repress Shh pathway, respectively (C,D,F-H).

Basically, the only condition promoting the co-expression of Rax together with Pax6 (an index for *bona fide* retinal progenitors) was found in cells treated with Wnt-inhibitor plus Activin (36.8% GFP-positive cells, and 32.4% of GFP/Pax6 co-labeled cells; **Figure 7.7**). Adding Cyclopamine to cells treated with Wnt-inhibitor plus Activin slightly decreased the efficiency of retinal induction (20% GFP/Pax6-double positive cells; **Figure 7.6H**).

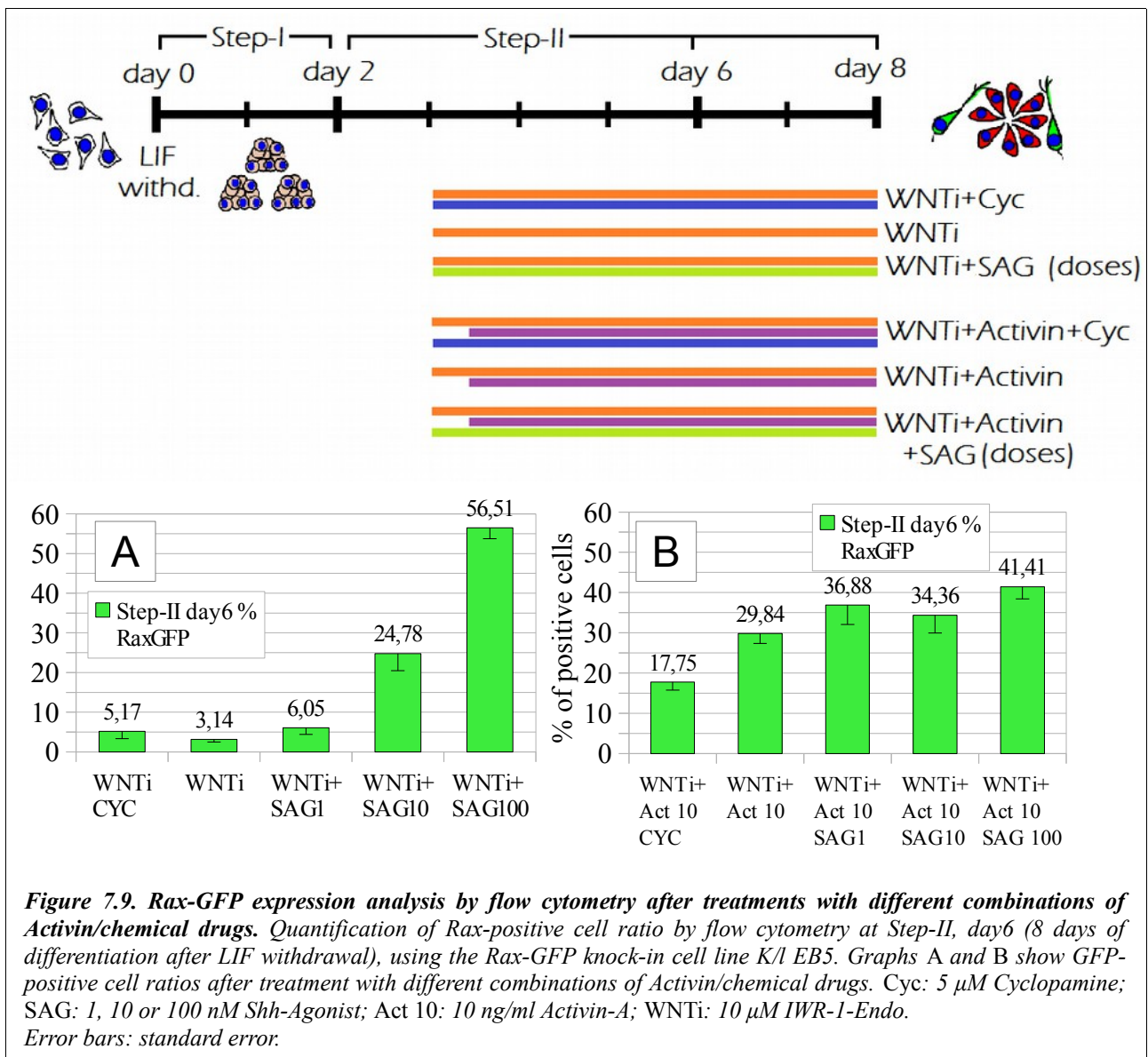




The results on Rax expression were confirmed by flow cytometry (Figure 7.9). Rax-GFP knock-in cell line was treated with different combinations and doses of chemical drugs and Activin, as indicated; cells were analyzed at Step-II, day6 (that is after 8 days of differentiation *in vitro*).

SAG strongly induced Rax expression (Wnt-inhibitor+100 nM SAG; 56.5% GFP-positive cells) and its effect was partially preserved even when using a ten-time lower dose (Wnt-inhibitor+10 nM SAG; 24.8% GFP-positive cells). Activin worked as a good inducer of Rax expression (Wnt-inhibitor+10 ng/ml Activin; 29.8% GFP-positive cells); Compared to Wnt-inhibitor+Activin treatment, Rax expression was enhanced by the compresence of SAG (Wnt-inhibitor+10 ng/ml Activin+100 nM SAG; 41.4% GFP-positive cells) and inhibited by the compresence of Cyclopamine (Wnt-inhibitor+10 ng/ml Activin+5 μ M Cyclopamine; 17.8% GFP-positive cells) in the cell culture medium (Figure 7.9).

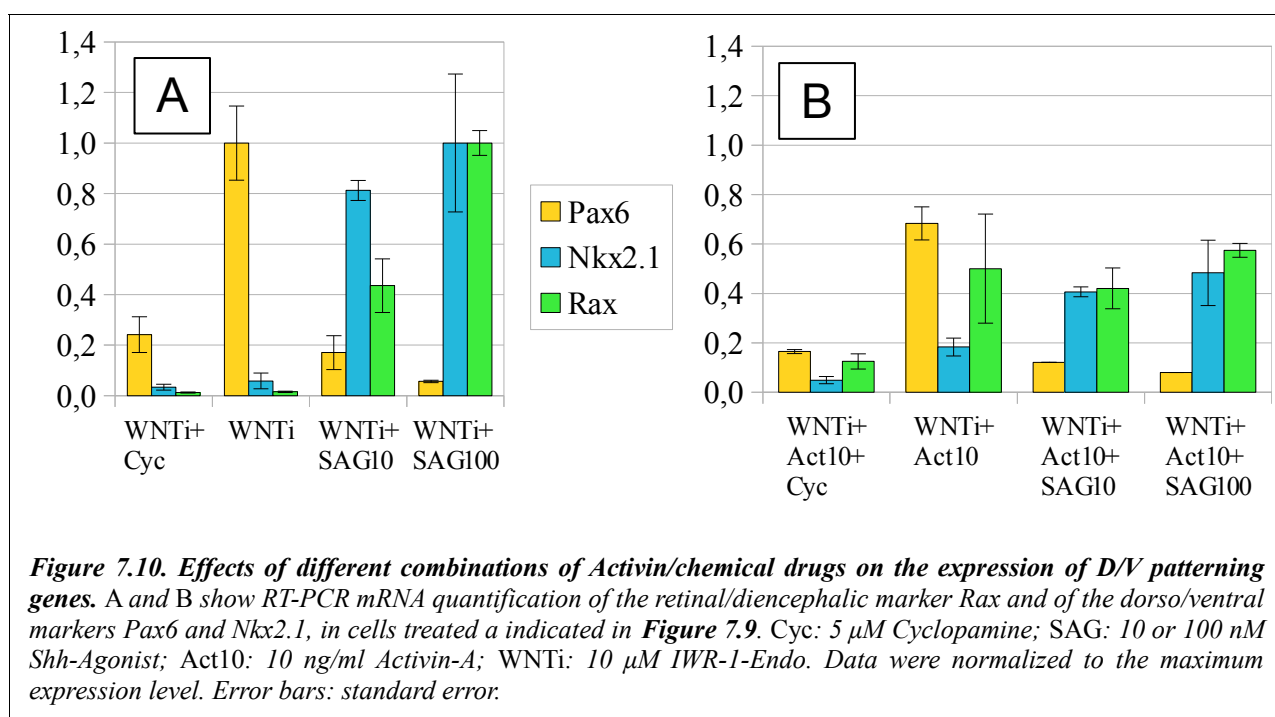
Although this aspect was not further investigated, we speculate that Activin could partially counteract the action of SAG in inducing Nkx2.1/Rax-positive cells.



By comparing cells treated with Wnt-inhibitor+100 nM SAG to cells treated with Wnt-inhibitor+SAG+Activin, we noticed a slight decrease of Rax-GFP-positive cell percentage in the latter condition (56.5% and 41.4% GFP-positive cells, respectively).

This was also evident by the observation of Nkx2.1/Rax-GFP double immunostaining after the same two treatments; cells treated with Wnt-inhibitor+SAG scored 60% Nkx2.1/GFP-double positive cells, while cells treated with Wnt-inhibitor+SAG+Activin were 44% double positive for Nkx2.1/GFP-double.

The D/V identity of Rax-positive neural progenitor was also investigated by RT-PCR, measuring Pax6 (dorsal) and Nkx2.1 (ventral) expression levels (**Figure 7.10**). Rax expression was strongly induced by SAG treatment, even when this Shh agonist was used at a lower dose (see Rax expression – green columns – after 10 nM or 100 nM SAG treatment, **Figure 7.10A**). This effect was accompanied by a strong induction of Nkx2.1 expression (blue columns) and a marked silencing of Pax6 expression (yellow columns), compared to control levels in cells treated with Wnt-inhibitor (**Figure 7.10A**). Wnt-inhibitor+Activin treatment was the only condition where Rax expression was associated with a good level of Pax6 expression (**Figure 7.10B**). Additionally, the RT-PCR data demonstrated that Activin could partially block SAG effect on Rax and Nkx2.1 expression (**Figure 7.10A** and **Figure 7.10B**), somehow counteracting the Shh-mediated induction of Rax-positive ventral cells.



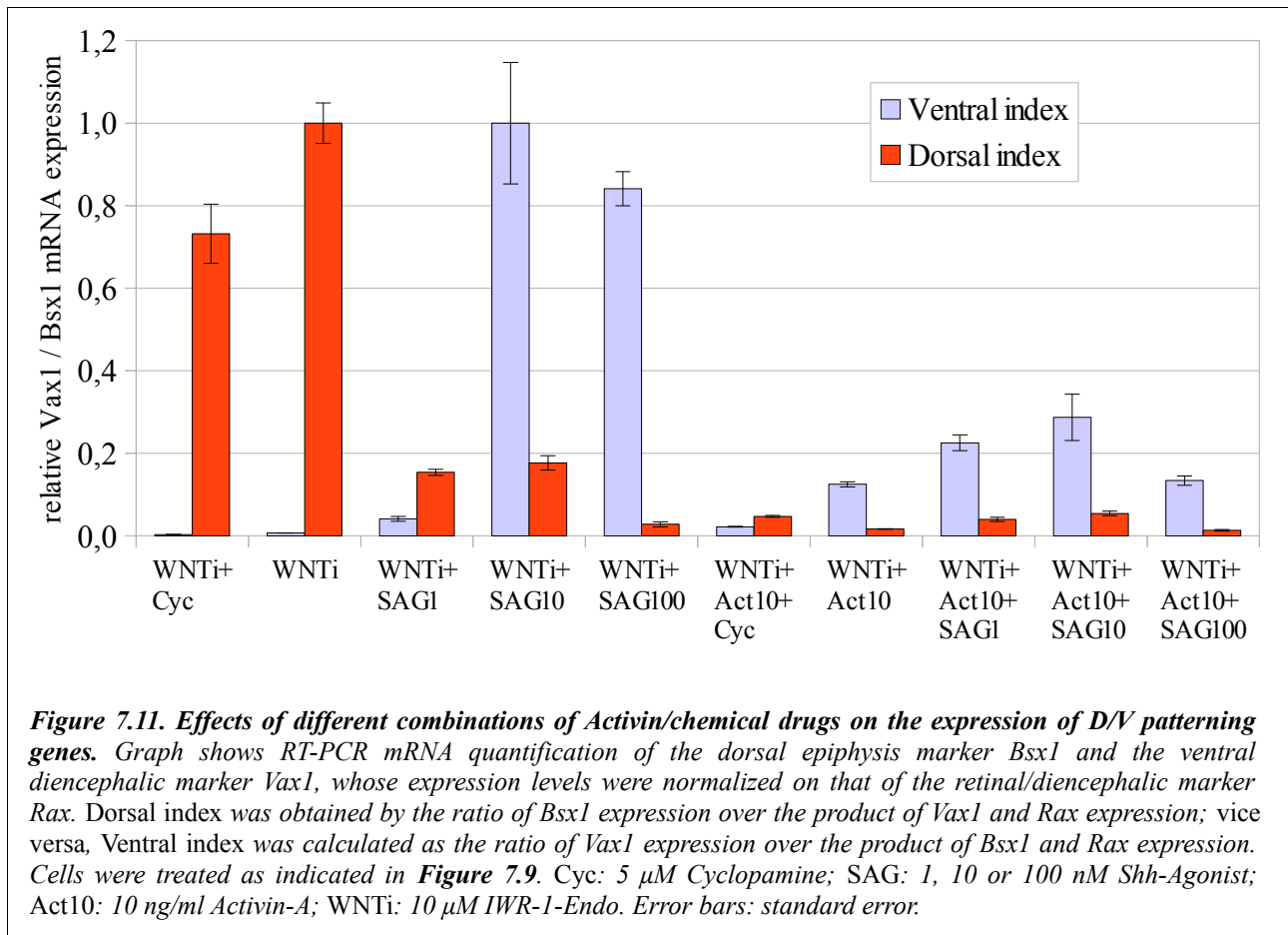
It must be noticed that Cyclopamine treatment repressed Pax6 expression, when compared to the expression level in cells treated with Wnt-inhibition (**Figure 7.10**). This was not consistent with the data from immunocytochemistry experiment, where cells treated with Wnt-inhibitor + Cyclopamine scored a higher ratio of Pax6-positive cells compared to control Wnt-inhibited cells (53.2% and

44.5% Pax6-positive cells, respectively; **Figure 7.8**). After a careful observation at the microscope, we noticed that Pax6-positive cells in samples treated with Wnt-inhibitor+Cyclopamine were more numerous, but were labeled with a lower staining intensity, when compared to control – Wnt-inhibition – cells. We speculate that Pax6 could display different level of expression, and this could be detected by immunostaining at the single cell level but not by RT-PCR, which returns an average level of expression. We still do not know the meaning (and the possible implications for cell differentiation) for different levels of Pax6 expression inside the cell.

We better determined the identity of our cells along the D/V axis, by measuring the expression of the dorsal epiphysis marker Bsx1 and that of the ventral diencephalic marker Vax1 (**Figure 7.11**). Bsx1 and Vax1 expression levels were normalized on Rax expression level, and are shown here as ratios; this was necessary to compensate for differences of Rax-positive cell percentage inside culture after diverse treatments. For this reason, *dorsal index* was obtained by the ratio of Bsx1 expression over the product of Vax1 and Rax expression; *vice versa*, *ventral index* was calculated as the ratio of Vax1 expression over the product of Bsx1 and Rax expression (**Figure 7.11**).

Dorsal index was higher in cells treated with Wnt-inhibitor alone or with Wnt-inhibitor+Cyclopamine. On the contrary, SAG treatment (both at 10 nM and at 100 nM), when performed together with Wnt-inhibition, caused a marked decrease of dorsal index and a strong increase of ventral index. This was consistent with a ventral diencephalic identity (**Figure 7.11**). Interestingly, dorsal and ventral indexes were both quite stable when Activin was present in the culture medium. Ventral index, in particular, was not responding to SAG treatment when cells were simultaneously treated by Activin (**Figure 7.11**).

These results raised an intriguing hypothesis, that will surely deserve further investigation in our Lab: Activin seemed to act here as a specific inducer of retinal identity (lateral diencephalon), able to bypass normal mechanisms of dorsal (Bsx1-positive) vs. ventral (Vax1-positive) specification.



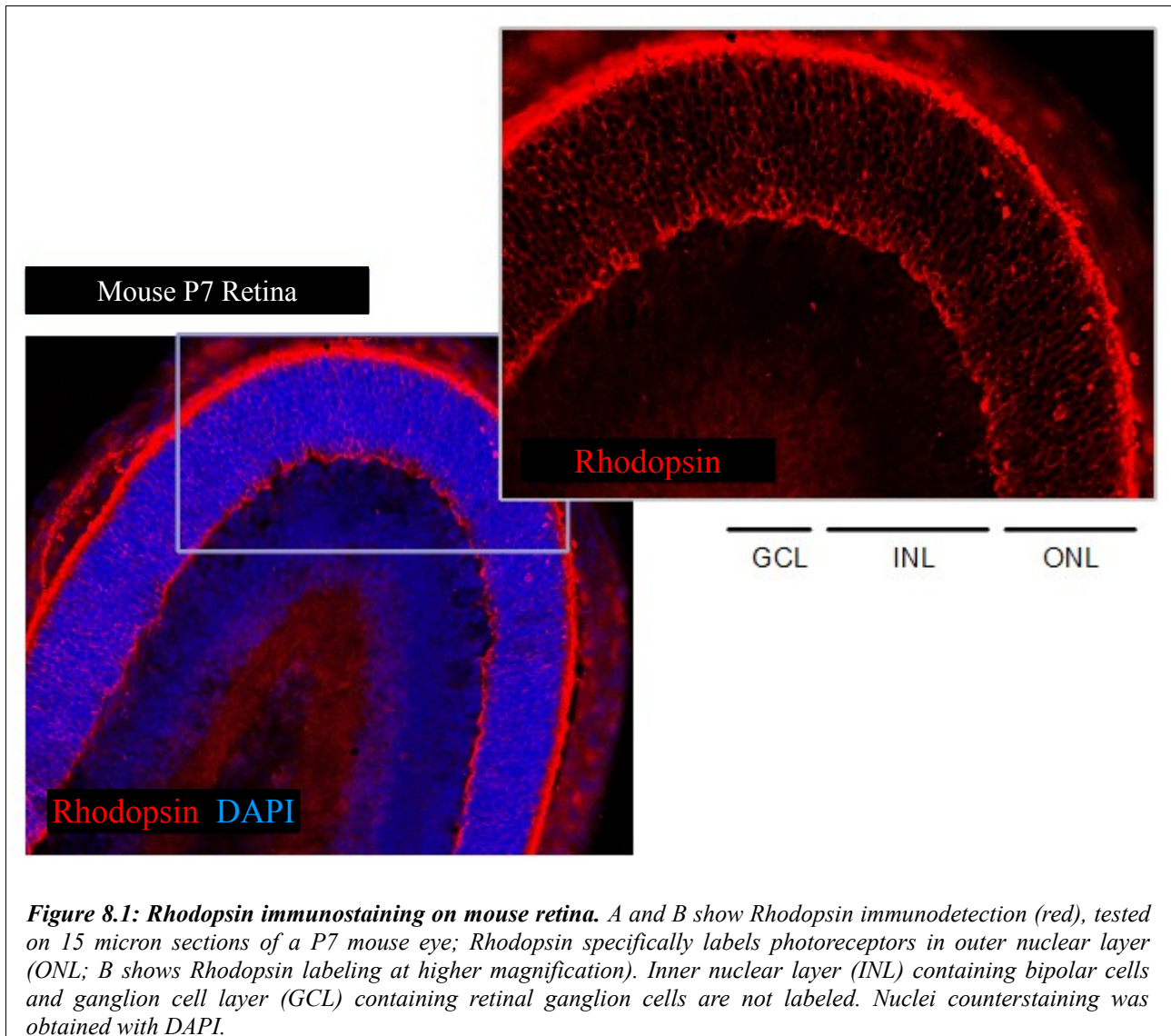
All in all, we concluded that *Rax* expression can be switched-on during ES cell neural differentiation in a Petri dish. Both Activin and Shh are able to drive *Rax* expression in forebrain neural progenitors. However, while Activin can induce a retinal differentiation fate (*Rax/Pax6* double positive neural progenitors), Shh pathway activation mainly steers stem cell fate towards a ventral diencephalic identity (*Rax/Nkx2.1* double positive neural progenitors, also expressing the ventral marker *Vax1*). The dorsal-most fate, which is epiphysis, can be preserved by inhibiting endogenous Shh, via Cyclopamine treatment (*Rax*-positive progenitors expressing the dorsal-most diencephalic marker *Bsx1*).

8– Terminal Differentiation of Retinal Cells

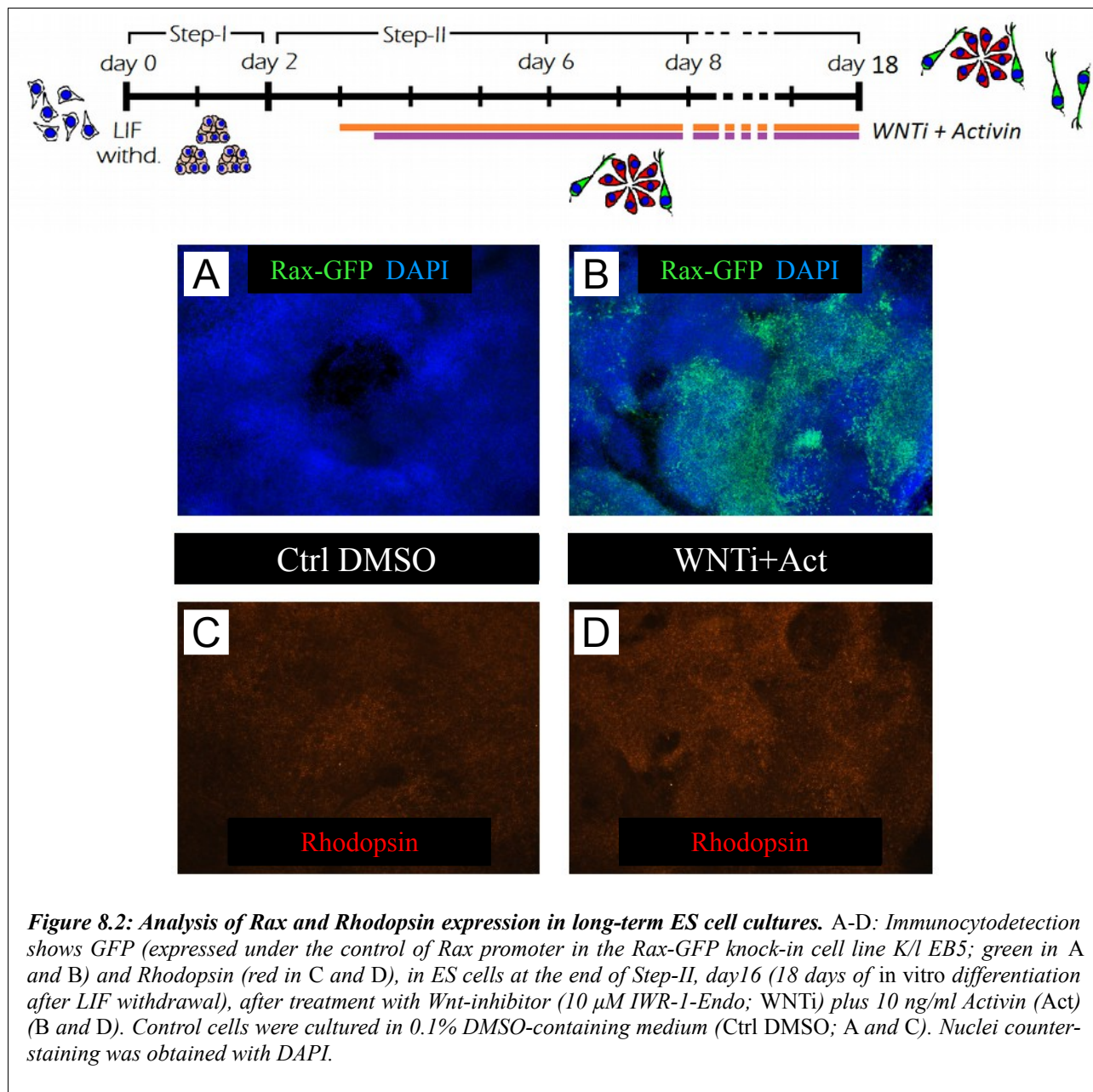
Efficient Differentiation of Retinal Cells by Prolonged Manipulation of Wnt and Activin/Nodal Pathways.

As Rax gene is also expressed both in the ventral diencephalon and in the neural retina, we decided to better define the identity card of Rax-expressing cells by culturing them for a longer period and investigating for the expression of late retinal markers.

ES cells were treated with Wnt-inhibitor+10 ng/ml Activin, starting at Step-II, day2, until Step-II day16, for a total of 18 days of differentiation. This time was previously shown to be the minimal culture time necessary to drive terminal differentiation of mouse retinal cells starting from pluripotent stem cells (Ikeda et al., 2005). Then, cells were fixed and analyzed by double GFP (Rax-GFP-positive retinal progenitors) and Rhodopsin (photoreceptors; Olsson et al., 1992) immunocyto detection. No additional cell dissociation/replating was performed during the long culture protocol. An antibody specific for Rhodopsin was tested on mouse P7 retinas (**Figure 8.1**).



We found that Rax-GFP-positive neural progenitors were still present in culture after 18 days of differentiation, forming wide cell clusters inside the culture. However, no strong Rhodopsin staining was detected.



In parallel, we tested some different culture conditions previously shown to enhance retinal progenitor proliferation and/or retinal differentiation (Hicks and Courtois, 1992; Lamba et al., 2006; Ikeda et al., 2005; Kelley et al., 1994; Levine et al., 1997). Cells were treated with Wnt-inhibitor+10 ng/ml Activin during Step-II, then (starting at the end of Step-II, day 6) cells were cultured in control N2B27 medium (supplemented with 0.1% DMSO), or in Wnt-inhibitor+10 ng/ml Activin medium, or in medium supplemented with Retinoic acid (100 nM), KSR (Knock-out Serum Replacement, 1.5%) or Wnt-inhibitor+10 ng/ml Activin+1 ng/ml BMP4. We found that only the presence of Activin (or of Activin together with BMP4, to a lesser extent) was able to sustain the

proliferation of Rax-GFP-positive progenitors. Cells treated with Wnt-inhibitor+Activin, but then cultured in KSR, in Retinoic acid or even in control medium showed low level of Rax-GFP staining (**Figure 8.3**). Again, no Rhodopsin staining was detected in all the different conditions (data not shown).

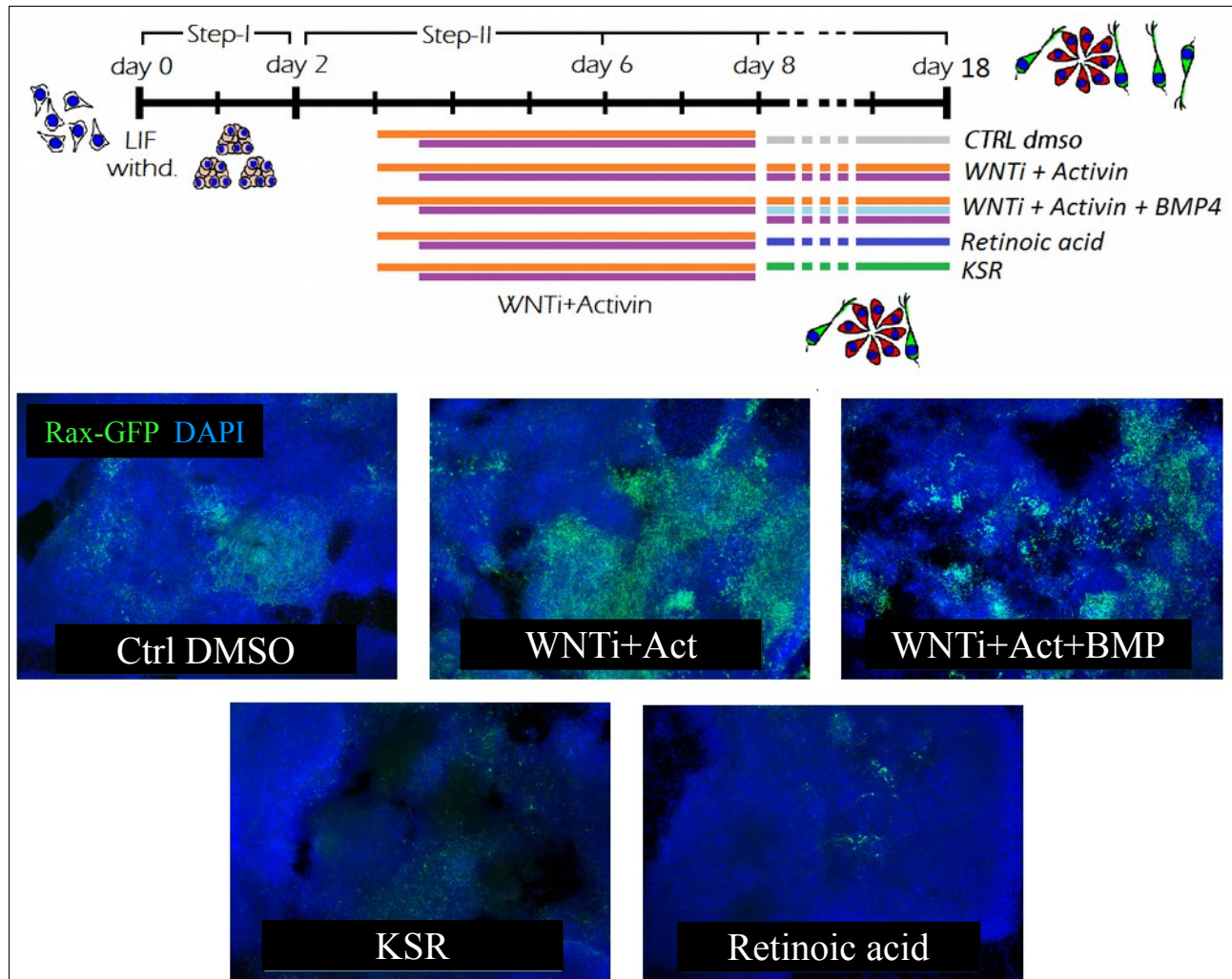
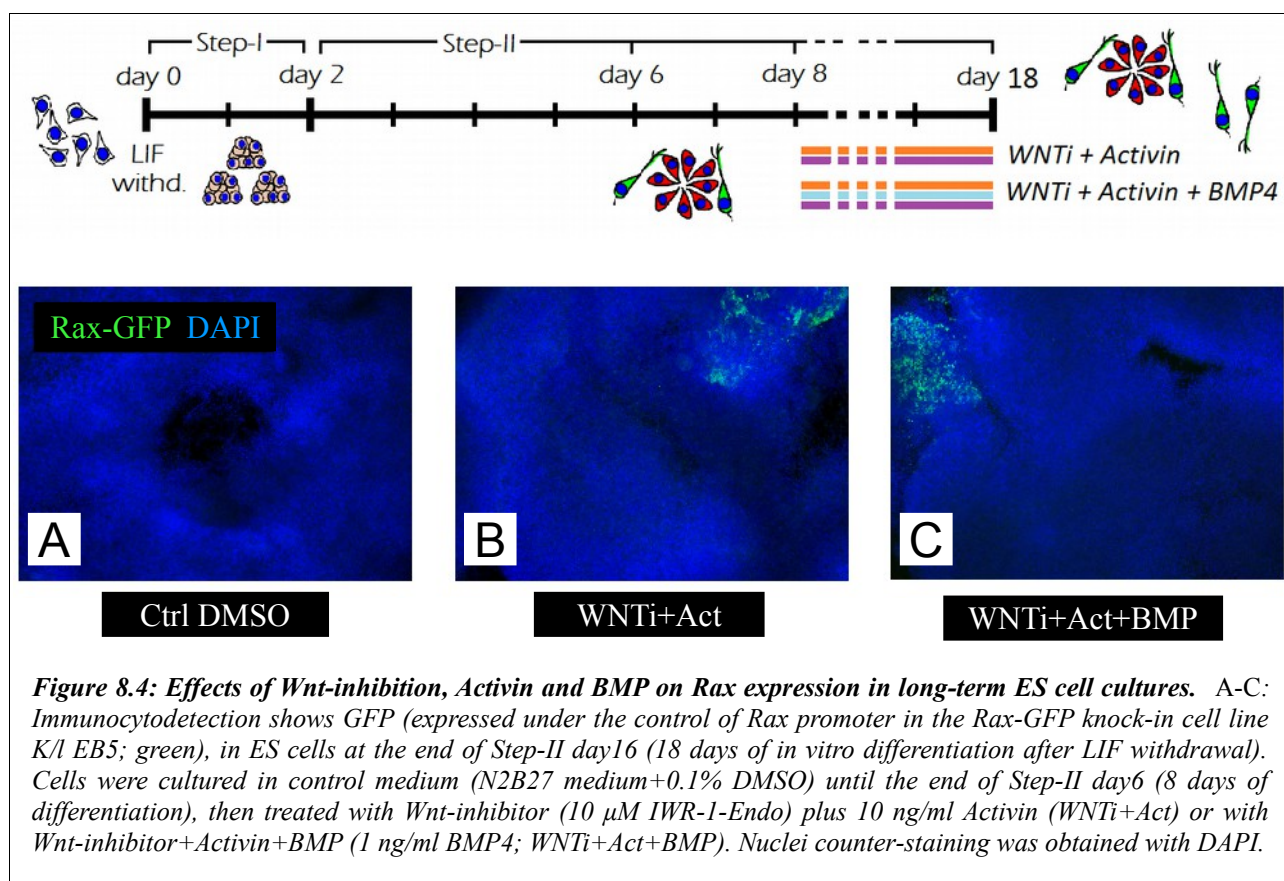


Figure 8.3: Effects of Wnt-inhibition, Activin, KSR, Retinoic acid and BMP on Rax expression in long-term ES cell cultures. A-E: Immunocytochemistry shows GFP (expressed under the control of Rax promoter in the Rax-GFP knock-in cell line K/1 EB5; green), in ES cells at the end of Step-II day 16 (18 days of in vitro differentiation after LIF withdrawal). Cells were treated with Wnt-inhibitor (10 μ M IWR-1-Endo; WNTi) plus 10 ng/ml Activin until the end of Step-II day 6 (8 days of differentiation), then different culture media were tested: control 0.1% DMSO-containing medium (Ctrl DMSO, A); medium with Wnt-inhibitor+10 ng/ml Activin (same medium used in the first 10 days of culture; WNTi+Act, B); medium with Wnt-inhibitor and Activin supplemented with 1 ng/ml BMP4 (WNTi+Act+BMP, C); medium supplemented with 1.5% KSR (KSR, D); finally, medium with 500 nM Retinoic acid (Retinoic acid, E). Rax-GFP-positive neural progenitors were still present in culture after 18 days of differentiation, but only when Activin was maintained during long-term culture. Nuclei counter-staining was obtained with DAPI.

We suggest that prolonged Activin treatment was responsible for Rax-GFP-positive retinal progenitor maintenance rather than for new retinal cell induction, because cells cultured in control medium during Step-II, then treated by WNTi+Activin at a later time windows, were not able to respond to Activin retinal inducing action (**Figure 8.4**). This was consistent with the identification of a narrow time window where cells are sensitive to Activin treatment, located at the beginning of Step-II (see Figures 39-42 in Chapter 5).

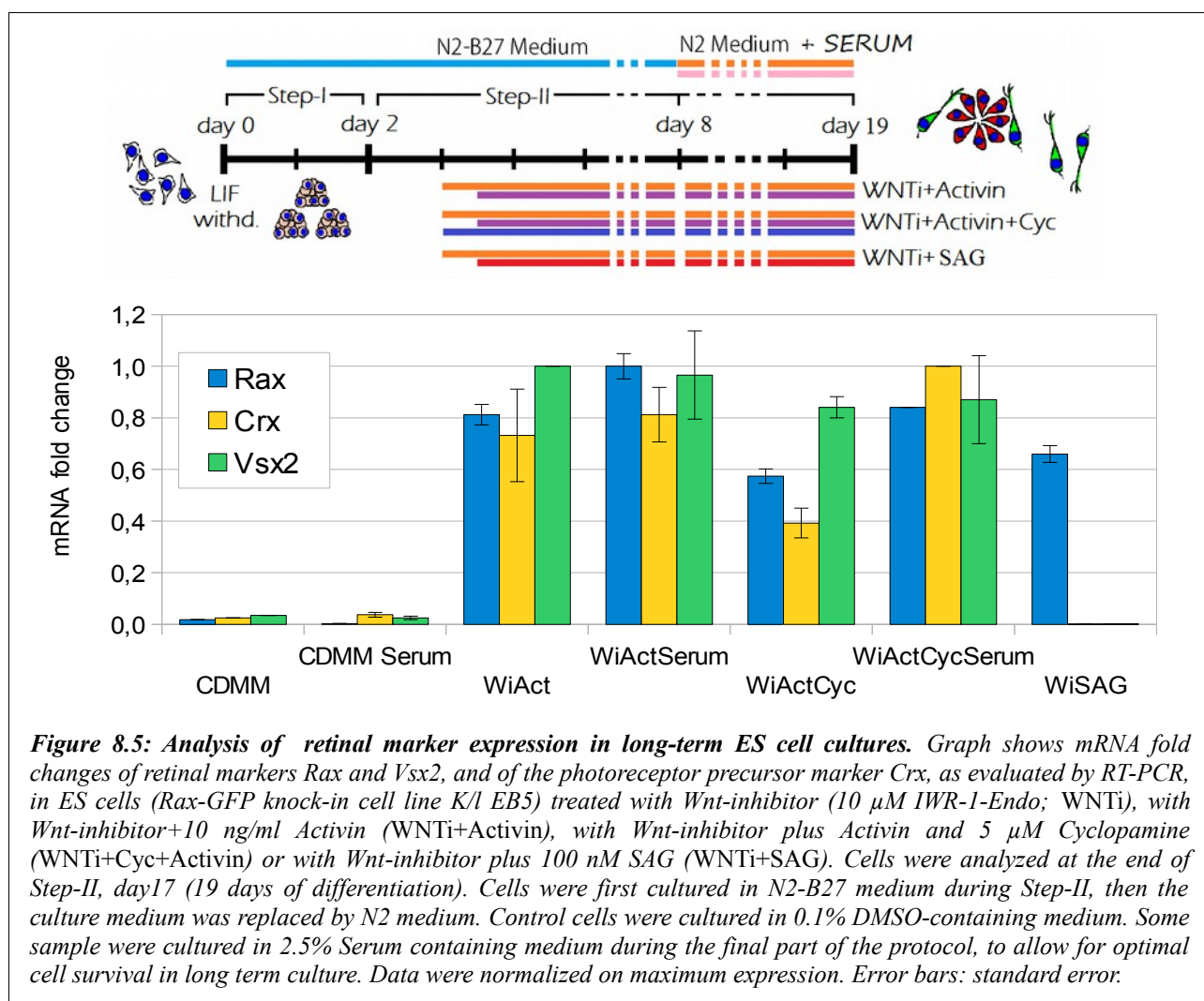


We concluded that Activin signal plays a role in retinal progenitor induction, but is also required for their maintenance and proliferation *in vitro* for longer culture periods.

We thus decided to force retinal progenitor differentiation. Neural progenitors can be forced toward terminal differentiation by culturing them in a minimal medium; chemically defined minimal medium (containing N2 and B27 supplements) can be further depleted by removing B27 supplement. Therefore, cells were first treated with Wnt-inhibitor+Activin in N2-B27 medium during Step-II, then the culture medium was replaced by N2 medium (always containing Wnt-

inhibitor and Activin). Moreover, the culture protocol was further prolonged (up to 22 days of culture *in vitro*) to allow for terminal differentiation. In some experiments we found useful to add 2.5% Serum to culture medium, to allow for cell survival during the final days of culture.

Long-term ES cultures treated with Wnt-inhibitor+Activin or with Wnt-inhibitor+Activin+Cyclopamine continued to express retinal markers Rax and Vsx2 after 18/19 days of differentiation *in vitro* (**Figure 8.5**). Cells additionally started to express Crx, a transcription factor which is essential for photoreceptor differentiation (**Figure 8.5**); the expression level of Crx was particularly high in cells treated with Wnt-inhibitor+Activin and Cyclopamine. Serum allowed better cell survival in long term culture, without strongly affecting the differentiation identity of ES cells (data not shown and **Figure 8.5**). Notably, cells treated with Wnt-inhibitor+ SAG expressed Rax at Step-II, day 16, but failed to express retinal markers Vsx2 and Crx, consistently with their ventral diencephalic identity (See Results, Chapter 7).



Rhodopsin-positive cells, which can be considered as *bona fide* photoreceptors (Olsson et al., 1992), appeared when ES cells were cultured until Step-II, day20 (22 days of differentiation). Rhodopsin-positive photoreceptors were almost always negative for GFP signal, and this is consistent with the fact that retinal progenitors switch-off Rax expression when they terminally differentiate (Furukawa et al., 1997).

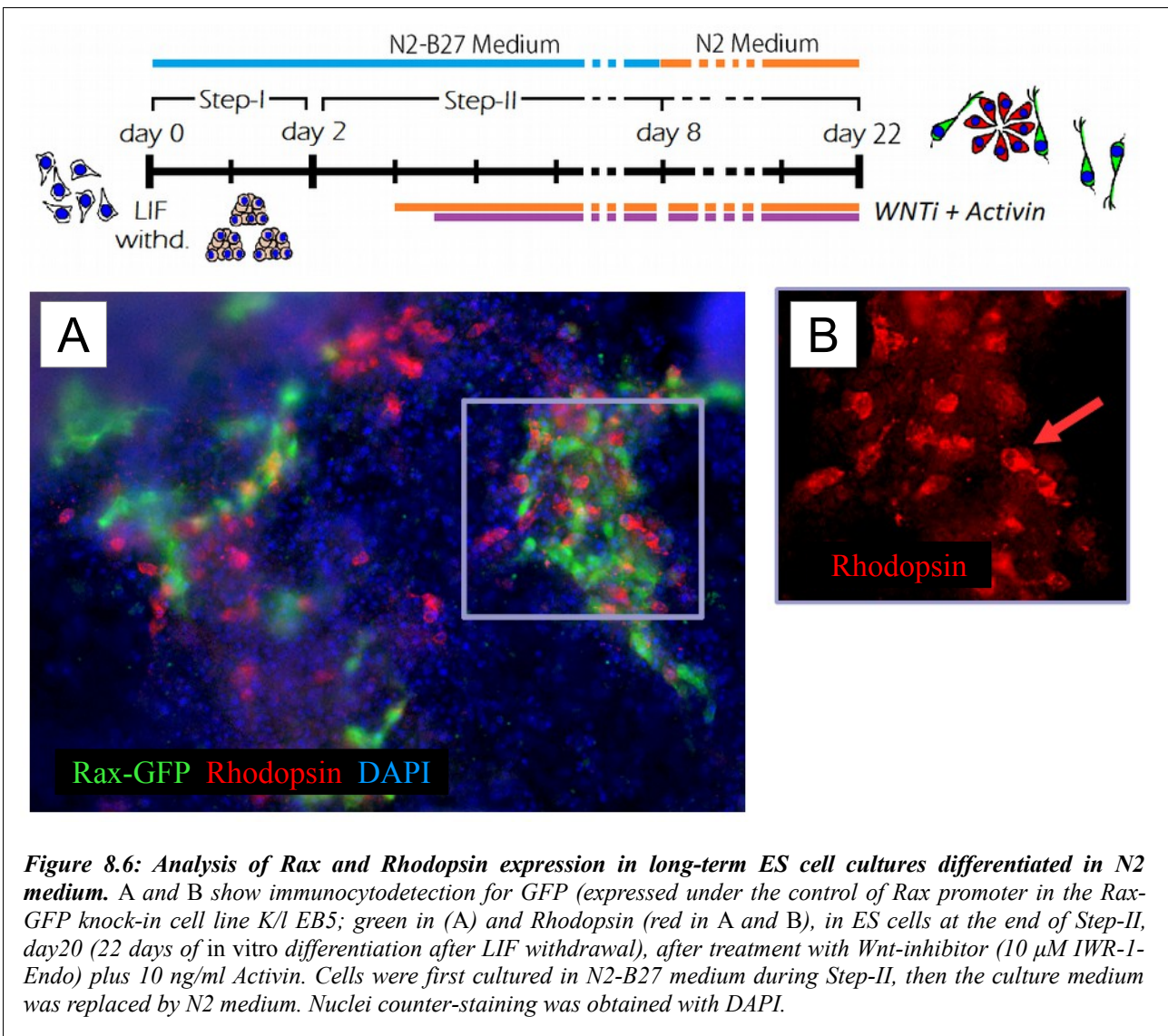
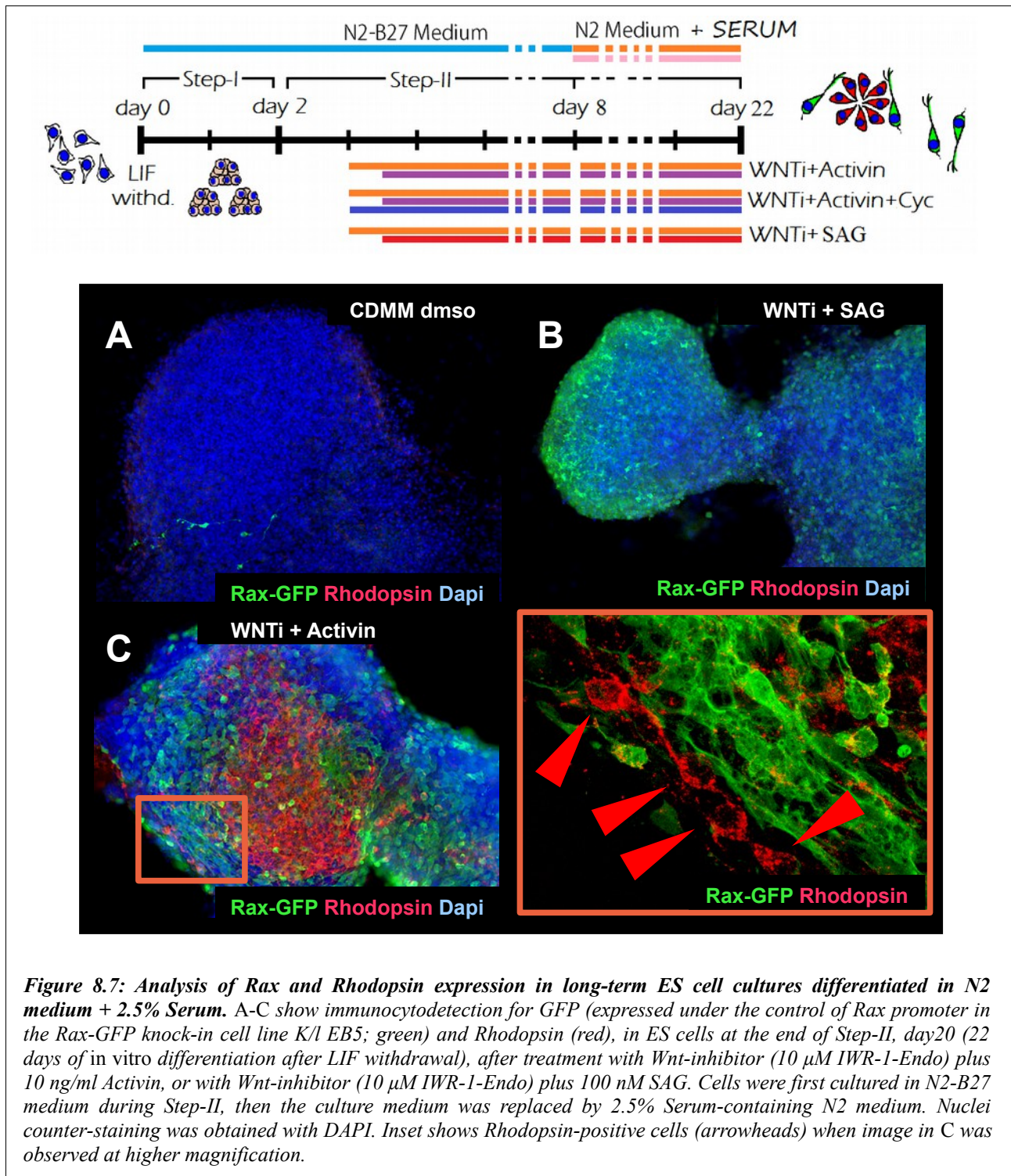
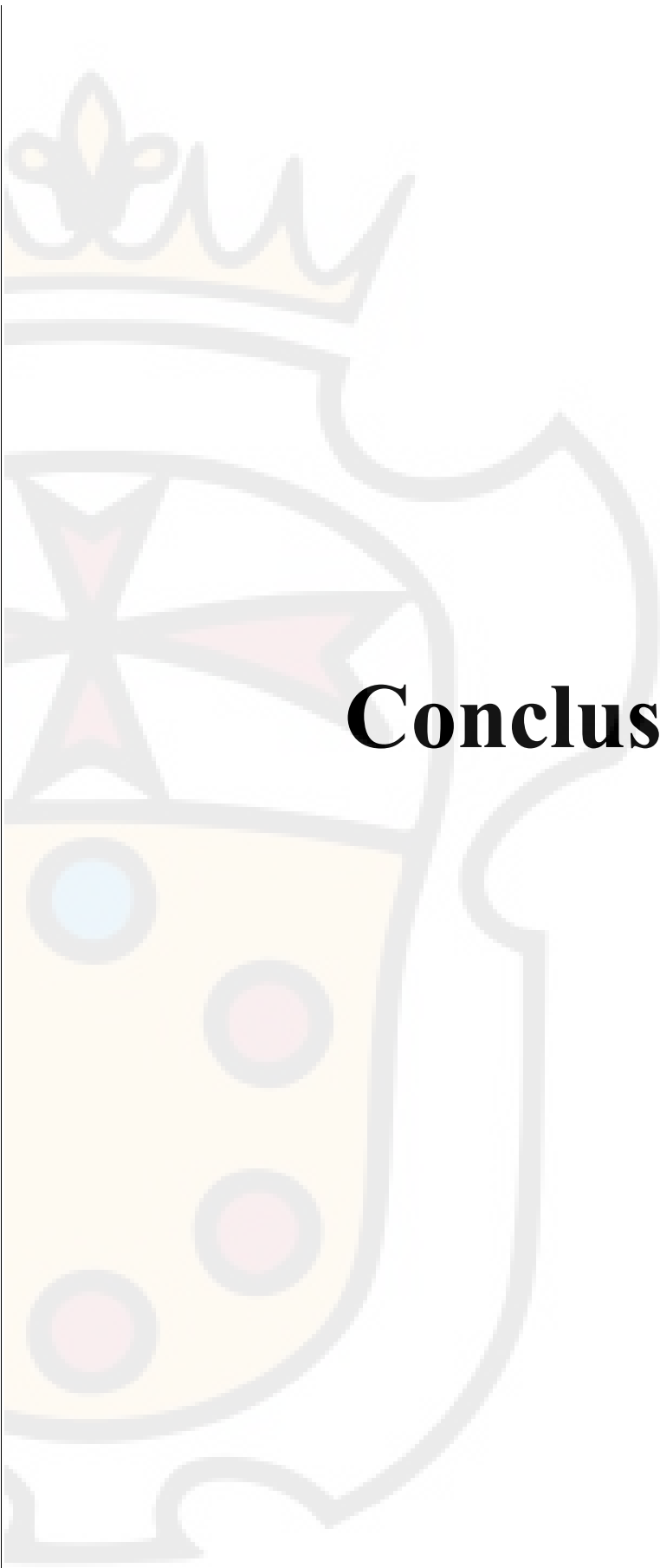


Figure 8.6: Analysis of Rax and Rhodopsin expression in long-term ES cell cultures differentiated in N2 medium. A and B show immunocytochemistry for GFP (expressed under the control of Rax promoter in the Rax-GFP knock-in cell line K/l EB5; green in (A) and Rhodopsin (red in A and B), in ES cells at the end of Step-II, day20 (22 days of in vitro differentiation after LIF withdrawal), after treatment with Wnt-inhibitor (10 μ M IWR-1-Endo) plus 10 ng/ml Activin. Cells were first cultured in N2-B27 medium during Step-II, then the culture medium was replaced by N2 medium. Nuclei counter-staining was obtained with DAPI.

Notably, Rhodopsin-positive cells were placed in close proximity to clusters of Rax-GFP-positive retinal progenitors (**Figure 8.7C and inset**), or sometimes were mixed together with them (**Figure 8.6A**). No Rhodopsin staining was detected in cells treated with WNT-inhibitor or with WNT-inhibitor+SAG (**Figure 8.7A,B**).



We concluded that Activin treatment during ES cell neural differentiation triggered a retinal differentiation program, leading to the formation of Rax-positive neural progenitors and lately Rhodopsin-positive photoreceptors.



Conclusions

1– Conclusions

Translating the Notion of the *Default Model* into an *in Vitro* Model of Neural Induction and Patterning.

I established an original method of ES cell *in vitro* neuralization that allows to obtain neural progenitors that undergo all the known sequential steps of neural development – neural induction, specification of positional identity and histological cell type, terminal differentiation – in a chemically defined minimal medium (CDMM).

We found that ES cells cultured as adherent cells in CDMM without any added exogenous factor differentiated as neurons more efficiently than ES cells cultured in serum-containing medium (SCM) during the early phase of differentiation (Step-I) (**Figure 1.1**). This is consistent with similar observations reported in the literature (Eiraku et al., 2008; Gaspard et al., 2009; Gratsch & O'Shea, 2002; Watanabe et al., 2005; Wataya et al., 2008) and confirms the notion that a default program of neuronal differentiation of ES cells exists and can be inhibited by factors contained in serum. We do not know to what extent BMPs, which are present in serum (Kodaira et al., 2006), or other morphogens, may account for its inhibitory effects.

Even when differentiated in a chemically defined, *morphogen-free* culture medium, we found that mouse ES cells expressed themselves different morphogens during neural differentiation *in vitro*, especially BMPs and Wnts. We reasoned that endogenously produced BMPs could affect ES cell neuralization. In fact, Noggin-mediated BMP-inhibition further strengthened their spontaneous neural differentiation in a minimal medium. The expression of *Zfp521*, a key gene for the priming of neuralization (Kamiya et al., 2011), was highest in Noggin treated cultures compared to any other culture condition, confirming the crucial role of Noggin in ES cell neural conversion. Furthermore,

we found that adding increasing doses of Noggin to CDMM during Step-II supported the expression of the pan-neuronal markers Ncam and Pax6 and increased the ratios of Pax6-, Nestin- and Sox1-positive neural progenitors.

We concluded that ES cells, when cultured in the absence of any added morphogen, efficiently acquired a neuronal fate; this was perfectly in line with the well-known *Default model of neural induction* (See Introduction, Wilson and Houart, 2004; Gaspard et al., 2008; Smukler et al., 2006).

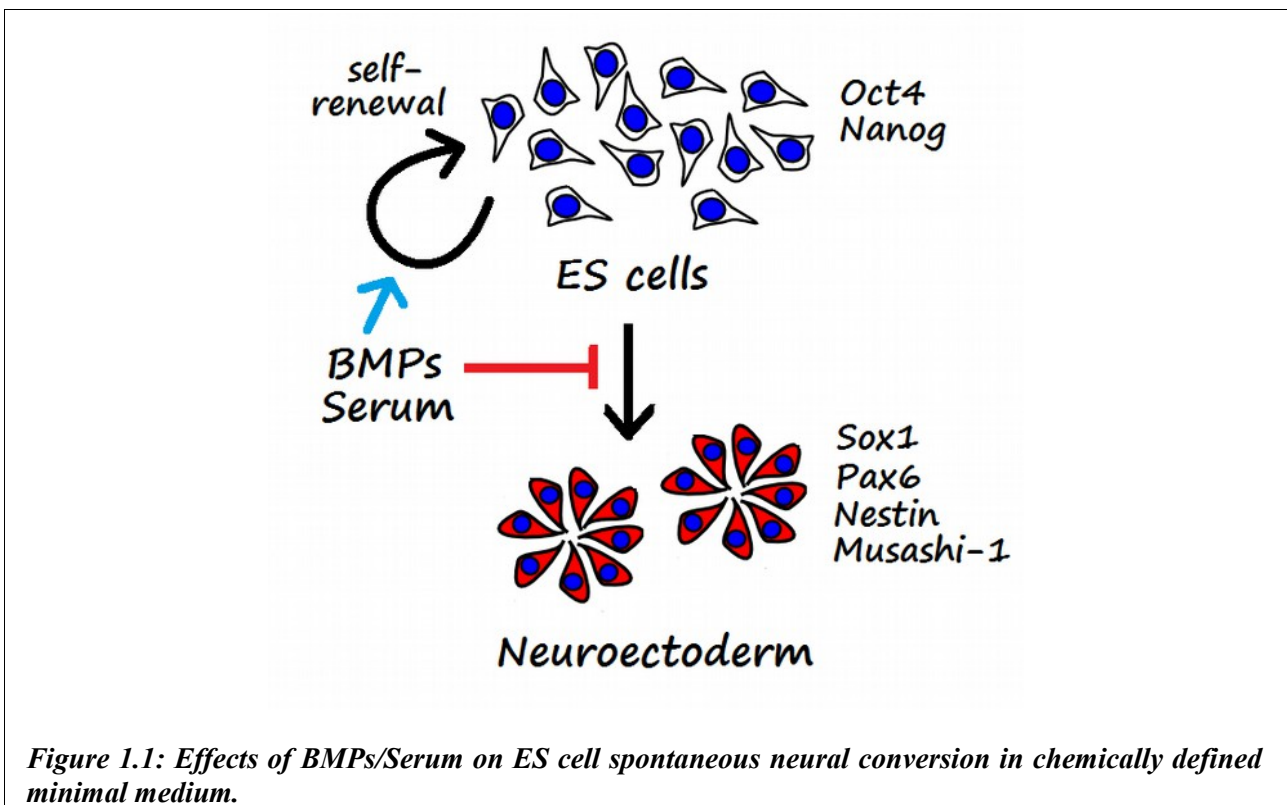


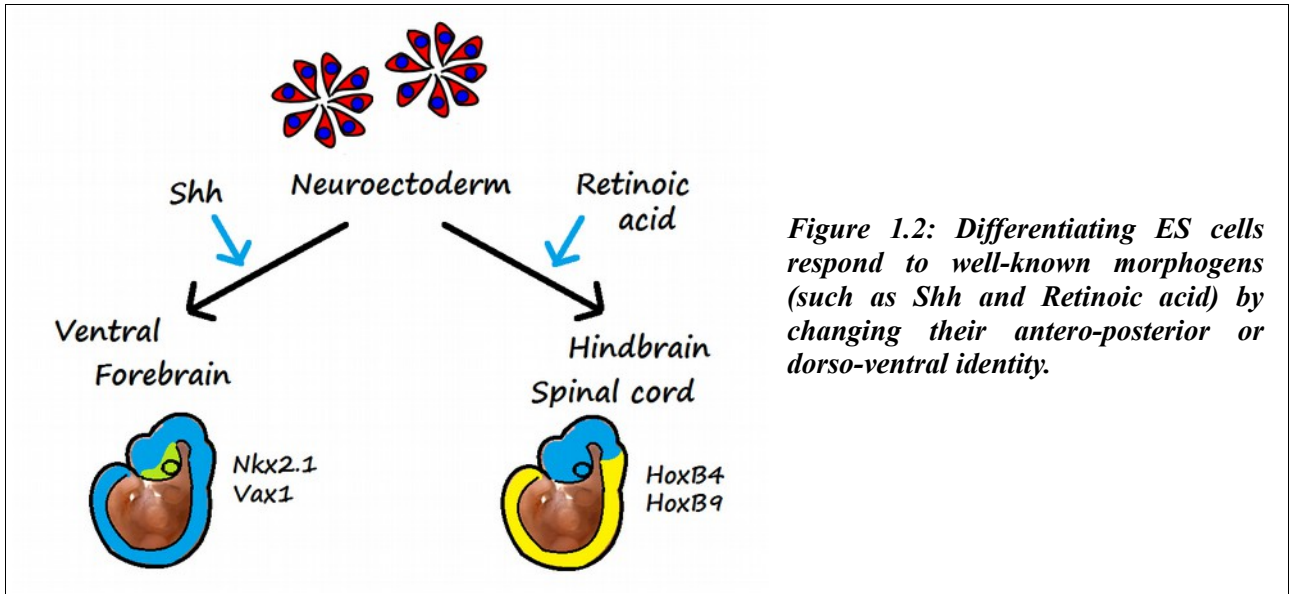
Figure 1.1: Effects of BMPs/Serum on ES cell spontaneous neural conversion in chemically defined minimal medium.

**A Plastic and Handy System to Work with:
ES Cells Recapitulate *in vitro* the Major Milestones of Brain Development *in vivo*.**

ES cells neuralized in CDMM showed to be capable of acquiring different positional identities, similarly to the early neural progenitors during the embryonic patterning of the central nervous system. This sort of “*in vitro* patterning” of ES-derived neural progenitors was affected by morphogens and growth factors - either added to CDMM during the differentiation protocol or produced by the neuralizing ES themselves - or by their agonists and antagonists. Notably, the effects on patterning were different depending on the time of activation (or inhibition) of the different pathways. Most importantly, the type of effect exerted by the manipulation of the protocol was often consistent with the role of a given type of signaling in embryonic development, if it was known by *in vivo* studies.

ES cells responded to Retinoic acid (RA) and SAG (Shh agonist) by activating posterior and ventral pathways of differentiation, respectively (**Figure 1.2**). SAG efficiently caused a strong ventralization of our cultures, switching-on Nkx2.1 expression in the vast majority of the cells (65-80% Nkx2.1-positive cells, varying from experiment to experiment). RA had a strong posteriorizing effect and led to high expression levels of posterior Hox genes HoxB4 and HoxB9, which are mainly expressed in hindbrain and spinal cord, respectively. By employing these well-known morphogens, we obtained strong evidence that ES cells *in vitro* follow and respond to the same signals found during *in vivo* embryonic development.

Our observations suggest that the protocol of ES neuralization in CDMM I established might be an useful alternative to the embryo as model to investigate the role of different morphogens and growth factors at different times of the neural differentiation process in establishing distinct positional and cell identities.



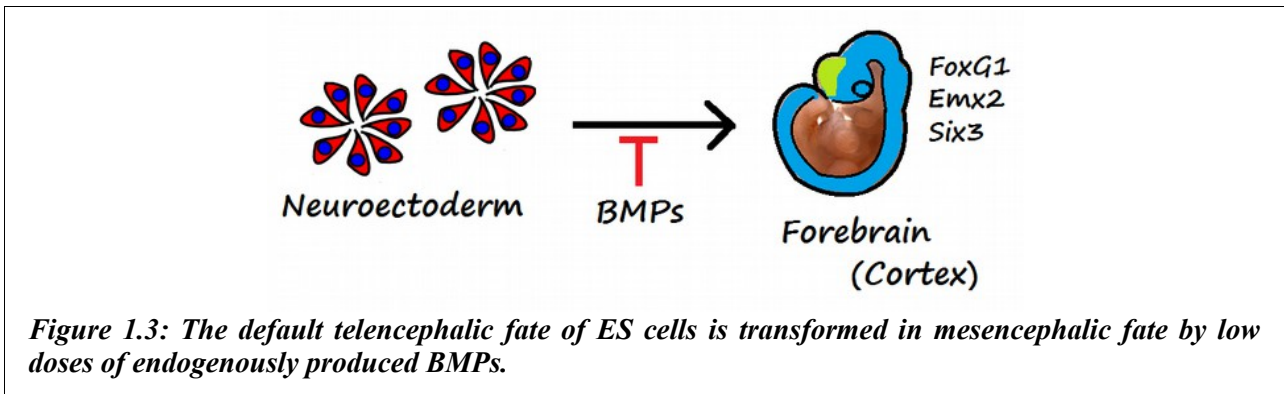
**Endogenously Produced BMPs and Brain Patterning:
BMP Activity Regulates Regional Differences in Embryonic Fore-Midbrain.**

I have addressed the role of BMPs in the anterior-posterior neural patterning. BMP and Noggin have been deeply studied in early development as important players for neural induction (Wilson and Houart, 2004). BMP is a the key player of the choice among the primordial embryonic tissues during the earliest steps of embryonic development and BMP inhibitors, including Noggin, orchestrate the spatio-temporal occurrence of neural induction.

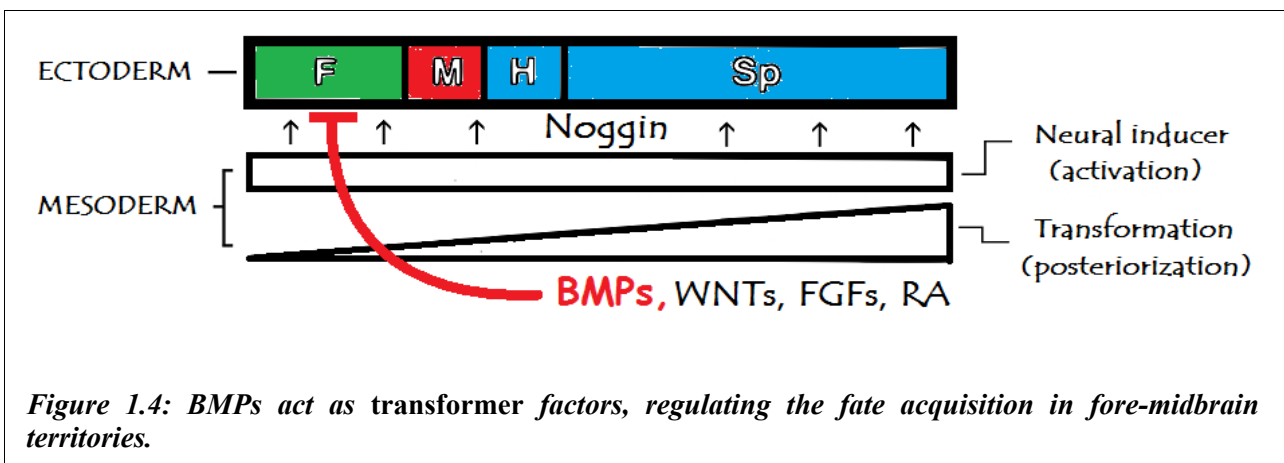
Moreover, a later role for BMP has been suggested in brain patterning, consisting in the inhibition of an anterior, default, identity. In fact, classical studies in lower vertebrates showed that BMP antagonism on *Xenopus* animal caps generates anterior neural structures (Hawley et al., 1995; Lamb et al., 1993; Sasai et al., 1995). In mouse, specific forebrain defects in mice mutant for BMP antagonists were shown (Bachiller et al., 2000). However, my work is the first study that directly addresses this issue in a systematic way in neuralized ES cells (Bertacchi et al., 2013, and this Thesis).

We found that Noggin acted at two distinct levels of ES cell differentiation: at the level of neural induction Noggin induced only a slight increase of neural progenitor ratio compared to control cells, while at the level of neural patterning it supported a dramatic increase of cells expressing the telencephalic marker FoxG1. Noggin had a profound effect on the positional identity of ES cell-generated neurons, as it up-regulated the global gene expression of cortical genes and down-regulated that of midbrain and hindbrain genes. This indicates that BMPs endogenously produced by differentiating ES cell directly act on the positional identity of the neural progenitors they spontaneously generate in a minimal medium, by influencing the anterior-posterior neural identity (**Figure 1.3**).

A crucial role for BMP in patterning neural structures has been recently suggested *in vitro*, as pluripotent cells of *Xenopus* animal caps acquired anterior neural fate when treated with high doses of Noggin (Lan et al., 2009; Viczian et al., 2009). In fact, my results are consistent with this observation and point to the existence of a default, intrinsic program of differentiation of pluripotent cells that has been conserved through vertebrate evolution and is both neuronal and anterior.



A revisited analysis of mammalian neural induction points to a model in which neural inducing signals called *activators* are proposed to impart both neural and anterior identity to the ectoderm. In this view, events that posteriorize the anterior neural tissue to generate the full range of CNS structures would occur later, by *transformer* molecules (Levine & Brivanlou, 2007; Wilson & Houart, 2004). According to such a classical model, we speculate that a primitive neuronal-telencephalic fate of ES cells might be further transformed in midbrain by a secondary signaling of BMP *transformers* (**Figure 1.4**), in a similar way to what has been demonstrated for Retinoic acid (RA) in hindbrain patterning.



A Novel Protocol for Cortical Induction: A Comparison with Already Established Protocols.

To induce a cortical fate, some procedures make use of a feeder layer of stromal cells (Ideguchi et al., 2010), or cell aggregation (Eiraku et al., 2008). In these studies, the factors that were endogenously produced by cells in culture and that might have influenced ES cell differentiation were not identified. In one of these studies, ES cell cultured in a minimal medium at a very low density generated cells with morphological, electrophysiological and molecular features of anterior neurons (Gaspard et al., 2008). These could be directed toward a cortical fate by treatment with the Shh antagonist Cyclopamine, although neither Shh secretion nor autocrine action of Shh were directly investigated (Gaspard et al., 2008). I did not observe any strong effect of Cyclopamine on ES cell dorso-ventral fate. However, we can confirm that ES cell can activate Shh signaling, as shown by the ventralizing effect described when adding a Shh agonist during Step-II. I hypothesize that under the low density culture conditions employed by Gaspard et al., an endogenous production of Shh that was not present in our culture condition was induced.

Eiraku et al. developed a three-dimensional aggregation culture for the self-organized generation of apico-basally polarized cortical tissues (Eiraku et al., 2008). The generated cortical neurons are functional, transplantable, and capable of forming proper long-range connections *in vivo* and *in vitro*. However, the formation of a three-dimensional structure (the embryoid body) could lead to the uncontrolled generation of intrinsic gradient of autocrine factors produced by differentiating cells themselves. A 3D structure could also obstacle the treatment with exogenous morphogens added to culture medium. Additionally, the Authors made use of KSR (knock-out serum replacement supplement) in their protocol; the composition of this patented supplement is not completely known, and its possible contribution to neural tissue patterning has never been thoroughly investigated.

In any case, ES cells differentiating as a monolayer of adherent cells in a minimal medium devoid of external signals were never able, to our knowledge, to induce a genuine cortical gene expression profile, as we on the contrary observed by means of Noggin-mediated BMP-inhibition in our culture system (Bertacchi et al., 2013).

The Inhibition of Endogenously Produced Wnts: A Must for Optimal ES Cell Cortical Conversion.

Inhibition of BMP signaling appears to be a crucial step in forebrain induction, as shown by the severe defects in the development of the prosencephalon of mice double mutants for of the BMP inhibitors Chordin and Noggin (Bachiller et al., 2000). However, dual inhibition of Wnt and BMP signals has been proposed to be necessary to confer head organizer activity both in Zebrafish (Houart et al., 2002), *Xenopus* (Glinka et al., 1997; Lupo et al., 2002; Bayramov et al., 2011) and mouse (del Barco Barrantes et al., 2003).

Although we observed a robust activation of cortical markers and a strong repression of midbrain genes with the sole inhibition of BMP (Bertacchi et al., 2013), we could not exclude that Wnt-inhibition might be synergistic with BMP-inhibition in inducing a cortical fate in ES cells. Endogenous Wnt activity might explain why the ratios of ES cells treated with high doses of Noggin that express markers of cortical progenitors (FoxG1, 22%) and of cortical neurons (Tbr1 and Satb2, 30% in total) at the end of Step-III did not account for the total number of Sox1-positive cells neuralized at step II (90,5 %). Additionally, by analyzing the expression level of key target genes of BMP and Wnt pathways (ID1 and LEF1 genes, respectively), we found evidence for a possible crosstalk between the two pathways. This suggested that the *corticalizing* effects previously seen with Noggin-mediated BMP-inhibition, could be, at least in part, due to a secondary modulation of Wnt signaling pathway.

We then asked whether endogenously produced Wnts in our culture system could contribute to mask an intrinsic cortical fate of neuralizing ES cells.

For these reasons, I investigated for endogenous Wnt production in our cultures and for possible effects of Wnt-inhibition via treatment with specific chemical drug IWR-1-Endo. Members of the Wnt family were expressed during Step-II, and this was clearly correlated with the appearance of neural progenitors inside the culture. We found that Wnt-inhibition was extremely efficient for ES cell cortical induction, as we obtained high percentages of both cortical progenitors (54% FoxG1-positive cells) and cortical post-mitotic neurons (Tbr1 and Ctip2, more than 40% in total). Considering that FoxG1 exclusively labels Nestin-positive neural progenitors, while Tbr1 and Ctip2

preferentially mark β -Tubulin-III-positive post-mitotic neurons, we can state that the vast majority of cells in culture were telencephalic/cortical cells after double Wnt/BMP-inhibition.

Additionally, we highlighted a synergistic effect of BMP and Wnt pathway inhibitions for the acquisition of a cortical fate: double BMP- and Wnt-inhibition showed a stronger down-regulation of the midbrain markers *En1* and *Otx2* and a more efficient up-regulation of the cortical markers *FoxG1*, *Ctip2* and *Tbr1*, compared to single treatments.

We concluded that Wnt-inhibition plays a fundamental role in establishing an anterior, telencephalic fate during ES cells neural differentiation *in vitro* (**Figure 1.5**). Our findings are consistent with the use of Wnt antagonists (such as Dkk-1 recombinant protein) in many neural induction protocols available in literature, both alone or in association with BMP- or Activin/Nodal-inhibitors, for the induction of neural tissues showing an anterior default identity (Eiraku et al., 2008; Ikeda et al., 2005; Verani et al., 2007; Nicoleau et al., 2013).

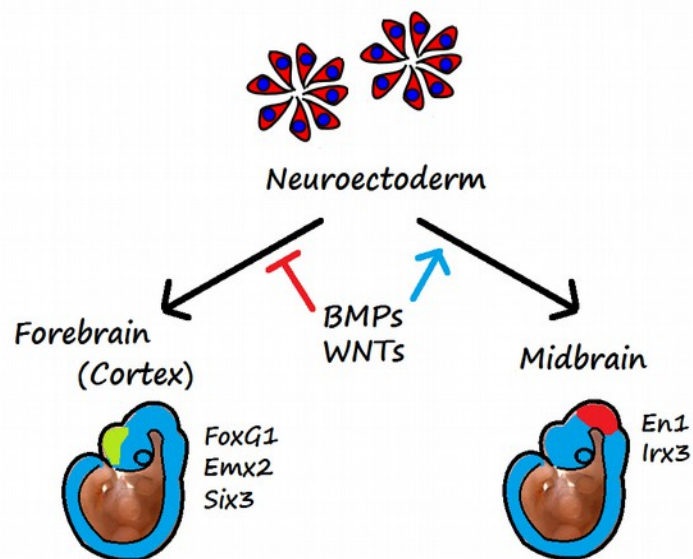


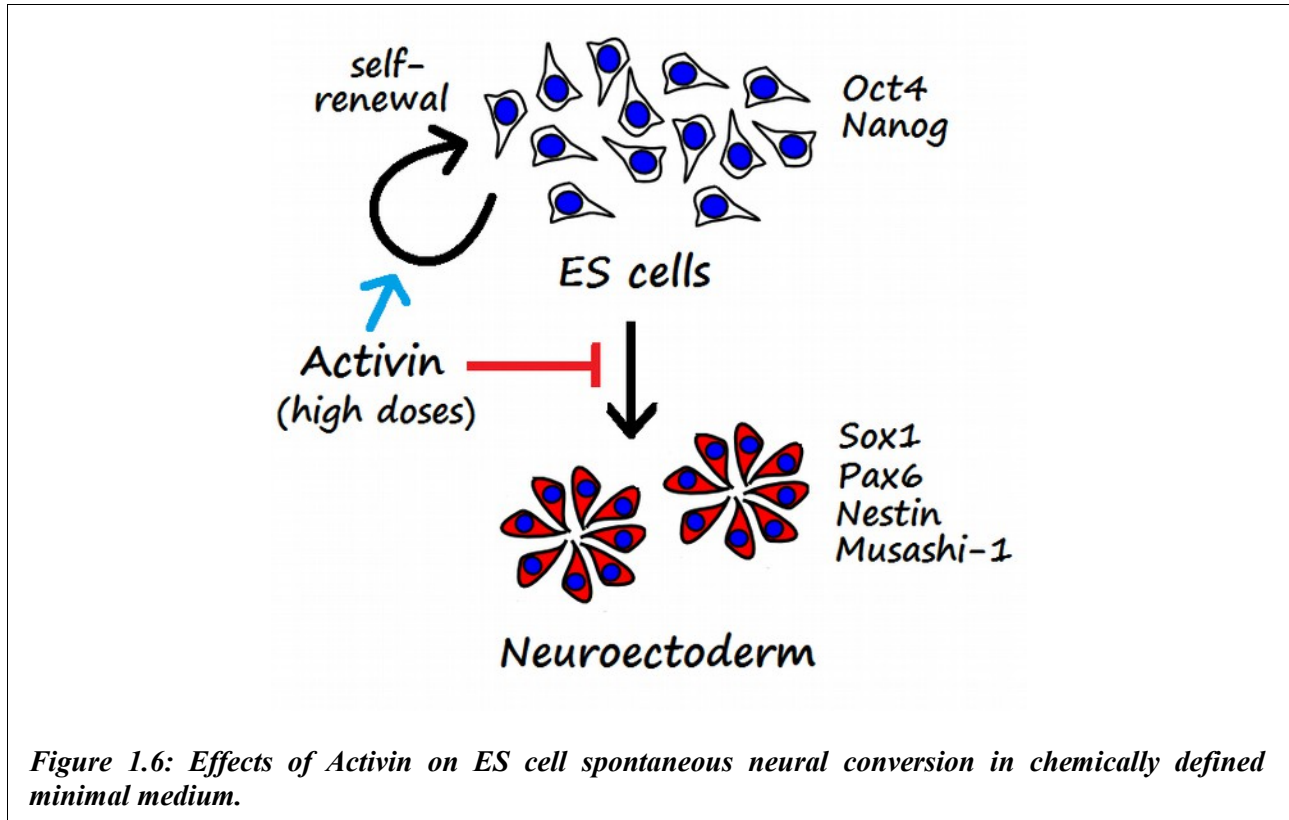
Figure 1.5: BMP and Wnt pathway inhibitions play a synergistic role for the acquisition of a cortical fate.

What is Old and What is New: Activin as an Inducer of Retinal Identity.

Classical studies showed that Activin plays a pivotal role in mesodermal development. At moderate concentrations, Activin activates the expression of the key gene for mesodermal induction, Brachyury, while at higher concentrations it induces organizer genes to become expressed. For this reason, Activin is used in ES cell differentiation protocols as an efficient inducer of mesoderm identity (Cerdan et al., 2012). Additionally, Activin was found to be crucial for endoderm induction *in vitro* (Teo et al., 2012; Iwao et al., 2013; Vosough et al., 2013). We detected minimal expression of early endodermal/mesodermal markers Gata4 and Gata6 in our system after treatment with low doses of Activin in association with WNT-inhibition. Activin strongly induced the expression of Gata4 and Gata6 only when used alone or when added at very high doses. This assured us on the marginal contribution of mesodermal/endodermal cells to the cultures, at least in our Retinal inducing condition.

In our hands, Activin induced instead a high expression level of stem cell marker Oct4. We found that Activin acted by slowing-down neural differentiation (**Figure 1.6**). This was particularly evident when Activin was used in the early phase of neural conversion of the protocol (before the fourth day of differentiation) or at very high doses (50 and 100 ng/ml). This effect is consistent with Activin role in maintenance of stem cell pluripotency (Tomizawa et al., 2013; Sakaki-Yumoto et al., 2013).

We asked whether Activin could play additional roles in ES cell differentiation and possibly in ES cell patterning. To date, few evidence has been provided for a possible role of Activin as an inducer of retinal identity. A cue in this direction has been given by Sasai's Lab (Ikeda et al., 2005); their protocol for the *in vitro* generation of retinal progenitors makes use of Activin-A in the culture medium. Unfortunately, the experimental procedures described in this work did not allow to infer neither the exact role for each of molecules used nor the temporal competence of cells to specifically respond to the different signals. In particular, the role of Activin in patterning neural fate toward a retinal identity was not dissected.



Conversely Lupo et al. showed the importance of both BMP and Activin/Nodal signaling for eye field gene induction in differentiating human ES cells, separately investigating their contribution and time of action on the transcription of early retinal markers (Lupo et al., 2013).

Our experiments (this Thesis and Bertacchi et al., manuscript in preparation) are the first description and full characterization of a new role of Activin as an inducer of retinal identity in mouse ES cells (**Figure 1.7**). The expression of retinal markers was investigated by RT-PCR, immunocytochemistry and flow cytometry. We found that low doses (10 ng/ml) of Activin were able to drive the expression of retinal markers Rax, Six3, Pax6, Otx2, Vsx2 and Six6, some of which were previously shown to play a fundamental role as eye field transcription factors (Zuber et al., 2003). At the same time, Activin could inhibit the expression of cortical (Emx2 and FoxG1) and midbrain (En1 and Irx3) genes.

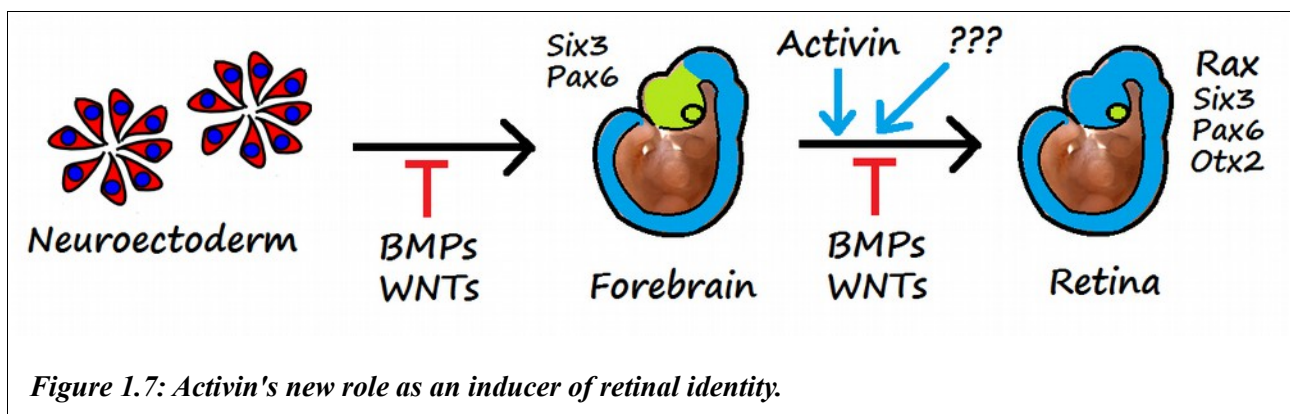
The retinal inducing action of Activin was exerted only on cells that acquired a forebrain fate via Wnt-inhibition or double Wnt/BMP-inhibition; Activin was not effective as a retinal inducer when used alone. This suggests that a previous anteriorization to a forebrain fate was necessary to acquire the competence to respond to Activin-mediated retinal induction (**Figure 1.7**), consistently to what happens in *in vivo* development.

Further studies will be necessary both to dissect molecular mechanisms controlling Rax expression in response to Activin treatment, and to unravel the role of Activin in retinal induction *in vivo*.

It must be also noticed that cell culture after our protocol of retinal induction did not reached complete uniformity (45% Rax-positive cells in the best condition of Activin treatment, after optimization of the protocol). Some other protocol of retinal induction / retinal culture and differentiation have been shown to be more efficient, but they often make use of cell sorting (Ikeda et al., 2005; Eiraku et al., 2011) or they use already differentiated retinal precursors coming from the embryo eye primordium or from eye ciliary margin (see as a review Lamba et al., 2008). In our case, we can hypothesize that some other, still unidentified signals, possibly acting in a synergistic way together with Activin, might be necessary to obtain a more efficient retinal induction. Insulin-like growth factor-1 (IGF-1) has already been used as a retinal inducer (Lamba et al., 2010) and could be a useful morphogen to be tested, both alone or in combination with Activin.

All in all, we concluded that Activin functions as a retinal inducer during ES cell neural differentiation (**Figures 1.7 and 1.10**).

Lupo and collaborators additionally showed the importance of BMP signaling for eye field gene induction in differentiating human ES cells, together with Activin (Lupo et al., 2013). Unfortunately, in our system we found that the presence of BMP4 in culture medium was not promoting retinal differentiation, as BMP4 was not able to efficiently induce Rax expression. We speculate that intrinsic differences between mouse and human ES cells could be responsible for some discrepancies when comparing different studies.



**Retina vs. Ventral Diencephalon:
Shh and Activin Switch-on Different Kinds of Rax Expression.**

An interesting finding of my Thesis is that different morphogens are able to switch-on Rax expression (**Figure 1.8**).

Retinal progenitors originate from the lateral wall of diencephalon, and are both Rax-positive and Pax6-positive (Wilson and Houart, 2004; Ikeda et al., 2005). They are also positive for the anterior/dorsal marker Otx2 and for the forebrain marker Six3 (Ikeda et al., 2005). Neural progenitor cells in the ventral diencephalon, on the contrary, are Rax-positive but Pax6-negative (Ikeda et al., 2005); they are positive for ventral markers such as Nkx2.1 (which is expressed in the ventral forebrain) and Vax1 (*ventral anterior homeobox*).

Interestingly, we found that Activin was able to induce the formation of Pax6/Rax double positive cells, which can be considered as *bona fide* retinal progenitors, while SAG (Shh-agonist) was driving efficient Rax co-expression together with Nkx2.1 and Vax1 (**Figure 1.8**). Notably, both morphogens (Activin and Shh) were able to induce the expression of Rax only if used in combination with Wnt-inhibitor. This suggested that only *anteriorized* forebrain cells were competent to respond to Activin- or Shh-mediated Rax induction.

Cells treated with Wnt-inhibition together with SAG were both ventralized (87% Nkx2.1-positive cells) and expressed Rax (60.4% Rax-GFP-positive cells), showing high degree of co-labeling of the two markers (60% Nkx2.1/GFP-double positive cells). This means that almost all Rax-positive cells in this condition were also Nkx2.1-positive. A better characterization of the expression of regional markers will be necessary to complete the identity card of these cells. However, the co-expression of Rax together with Nkx2.1 and Vax1 is consistent with a ventral diencephalic identity (rostral hypothalamus cells; Wataya et al, 2008).

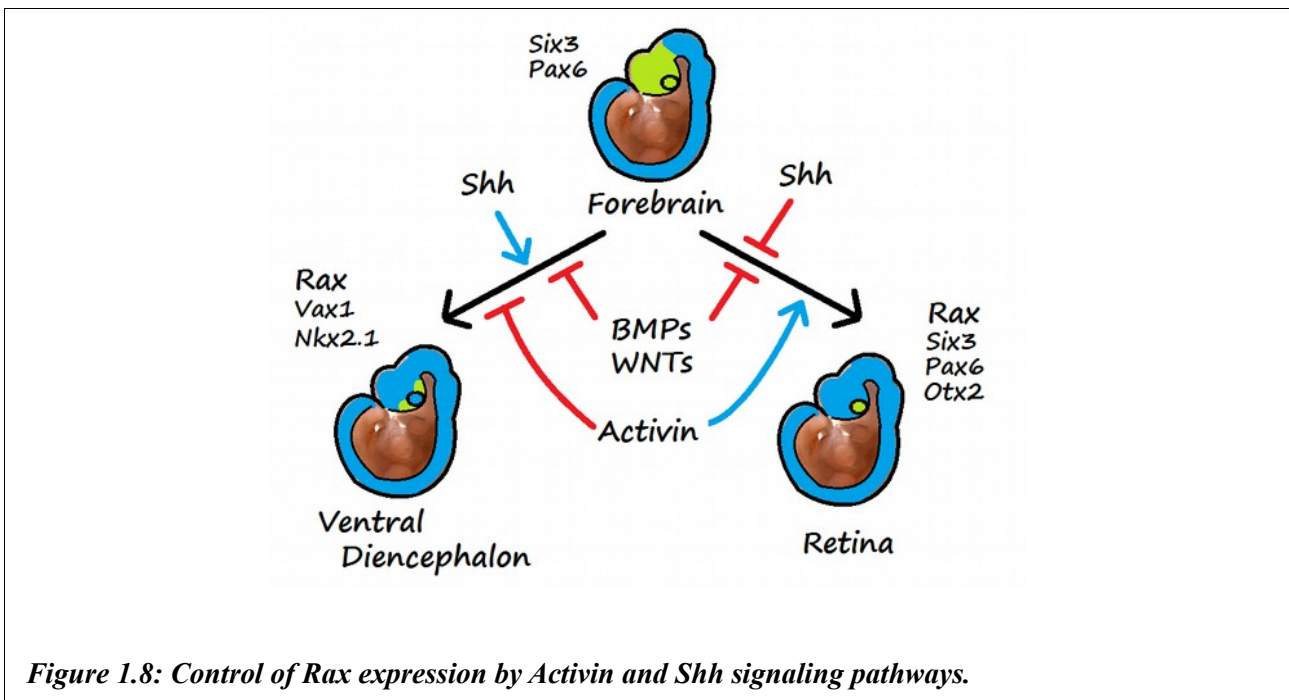


Figure 1.9 and **Figure 1.10** schematize the principal findings described in my Thesis. Some of these findings are consistent with previous observations present in the literature. We found that ES cells cultured in the absence of any added morphogen efficiently acquired a neuronal fate, and that the positional identity of ES-derived neural progenitors can be steered by distinct growth factors present in the culture medium, according to the role that these growth factors exert during the embryonic development of the central nervous system. This is in line with the classical *Default model* of neural differentiation (see Introduction). Some data were completely new findings. We demonstrated that low doses of endogenously produced BMPs and Wnts act as morphogens on differentiating ES cells and dampen an intrinsic cortical fate. Additionally, we discovered that Activin is a useful morphogen to induce retinal identity during mouse ES cell neuralization. Finally, we identified a Shh-mediated induction of Rax expression in the context of forebrain cells. Taken all together, my data contribute to add some little pieces to the huge enigmatic puzzle of mouse brain development and patterning.

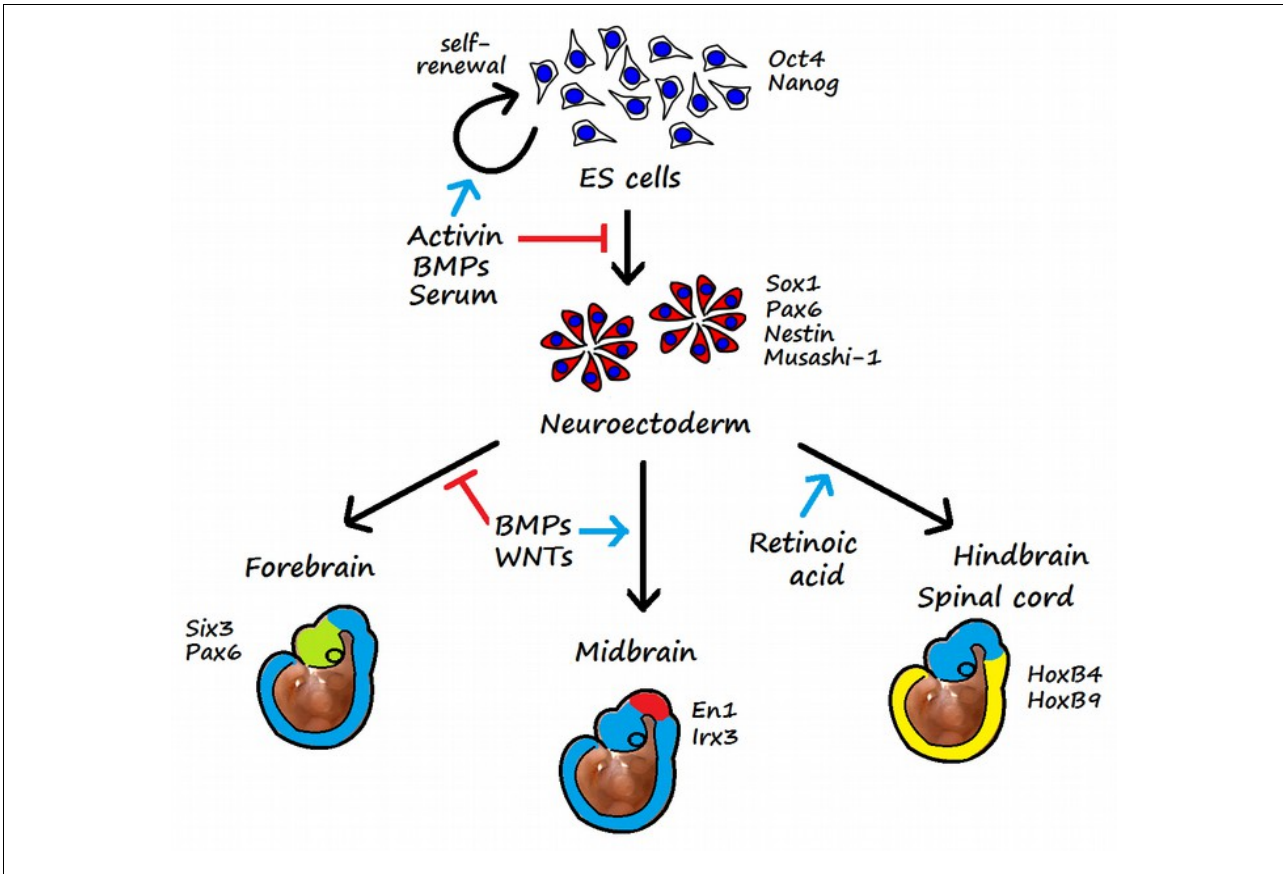


Figure 1.9: Early steps in mouse ES cell neural conversion and antero-posterior patterning: Principal findings in my Thesis.

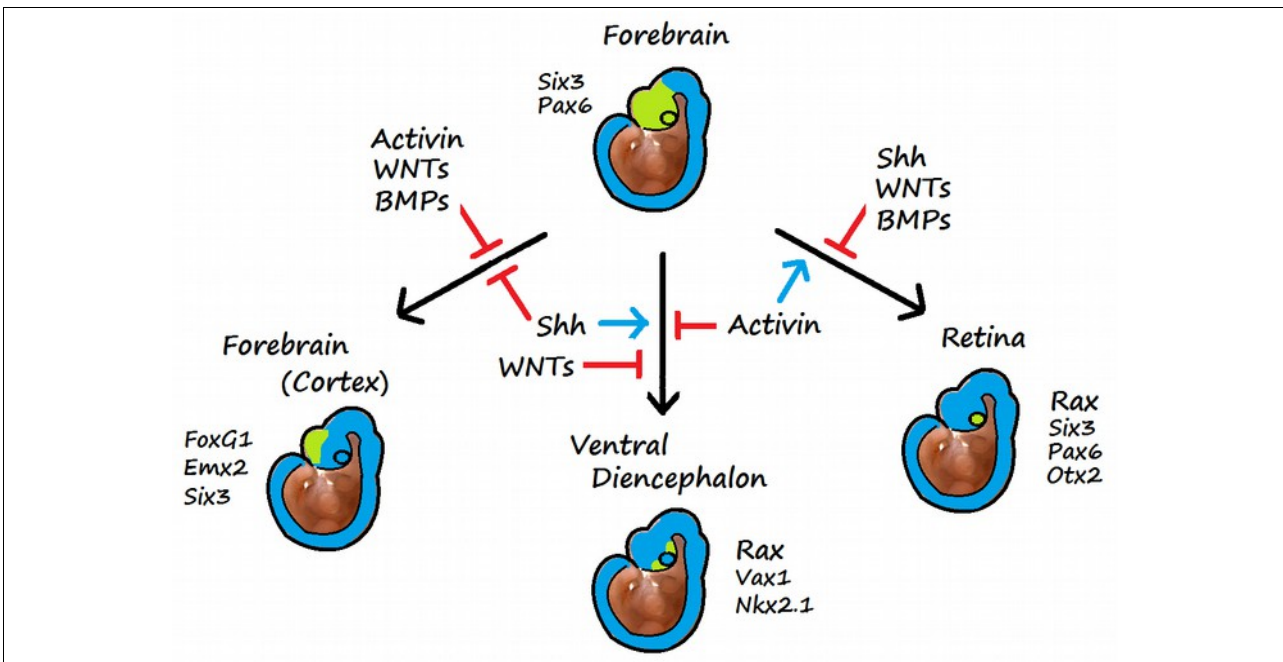


Figure 1.10: Mouse ES cells as a model for the study of forebrain patterning: Principal findings in my Thesis.



Bibliography

1- References

Abe, E., M. Yamamoto, Y. Taguchi, B. Lecka-Czernik, C. A. O'Brien, A. N. Economides, N. Stahl, R. L. Jilka and S. C. Manolagas. "Essential Requirement of Bmps-2/4 for Both Osteoblast and Osteoclast Formation in Murine Bone Marrow Cultures from Adult Mice: Antagonism by Noggin." *J Bone Miner Res* 15, no. 4 (2000): 663-73.

Acampora, D., V. Avantaggiato, F. Tuorto, P. Barone, H. Reichert, R. Finkelstein and A. Simeone. "Murine *Otx1* and *Drosophila Otd* Genes Share Conserved Genetic Functions Required in Invertebrate and Vertebrate Brain Development." *Development* 125, no. 9 (1998): 1691-702.

Amaya, E., T. J. Musci and M. W. Kirschner. "Expression of a Dominant Negative Mutant of the Fgf Receptor Disrupts Mesoderm Formation in *Xenopus* Embryos." *Cell* 66, no. 2 (1991): 257-70.

Andoniadou, C. L. and J. P. Martinez-Barbera. "Developmental Mechanisms Directing Early Anterior Forebrain Specification in Vertebrates." *Cell Mol Life Sci* 70, no. 20 (2013): 3739-52.

Ariizumi, T. and M. Asashima. "In Vitro Induction Systems for Analyses of Amphibian Organogenesis and Body Patterning." *Int J Dev Biol* 45, no. 1 (2001): 273-9.

Aubert, J., H. Dunstan, I. Chambers and A. Smith. "Functional Gene Screening in Embryonic Stem Cells Implicates Wnt Antagonism in Neural Differentiation." *Nat Biotechnol* 20, no. 12 (2002): 1240-5.

Bachiller, D., J. Klingensmith, C. Kemp, J. A. Belo, R. M. Anderson, S. R. May, J. A. McMahon, A. P. McMahon, R. M. Harland, J. Rossant and E. M. De Robertis. "The Organizer Factors Chordin and Noggin Are Required for Mouse Forebrain Development." *Nature* 403, no. 6770 (2000): 658-61.

Barberi, T., P. Klivenyi, N. Y. Calingasan, H. Lee, H. Kawamata, K. Loonam, A. L. Perrier, J. Bruses, M. E. Rubio, N. Topf, V. Tabar, N. L. Harrison, M. F. Beal, M. A. Moore and L. Studer. "Neural Subtype Specification of Fertilization and Nuclear Transfer Embryonic Stem Cells and Application in Parkinsonian Mice." *Nat Biotechnol* 21, no. 10 (2003): 1200-7.

Bayramov, A. V., F. M. Eroshkin, N. Y. Martynova, G. V. Ermakova, E. A. Solovieva and A. G. Zaraisky. "Novel Functions of Noggin Proteins: Inhibition of Activin/Nodal and Wnt Signaling." *Development* 138, no. 24 (2011): 5345-56.

Beccari, L., R. Marco-Ferreres and P. Bovolenta. "The Logic of Gene Regulatory Networks in Early Vertebrate Forebrain Patterning." *Mechanisms of Development* 70, no. 130 (2013): 95-111.

Bertacchi, M., L. Pandolfini, E. Murenu, A. Viegi, S. Capsoni, A. Cellerino, A. Messina, S. Casarosa and F. Cremisi. "The Positional Identity of Mouse Es Cell-Generated Neurons Is Affected by Bmp Signaling." *Cell Mol Life Sci* 70, no. 6 (2013): 1095-111.

Bibel, M., J. Richter, E. Lacroix and Y. A. Barde. "Generation of a Defined and Uniform Population of Cns Progenitors and Neurons from Mouse Embryonic Stem Cells." *Nat Protoc* 2, no. 5 (2007): 1034-43.

Blumberg, B., J. Bolado, Jr., T. A. Moreno, C. Kintner, R. M. Evans and N. Papalopulu. "An Essential Role for Retinoid Signaling in Anteroposterior Neural Patterning." *Development* 124, no. 2 (1997): 373-9.

Bosse, A., A. Zulch, M. B. Becker, M. Torres, J. L. Gomez-Skarmeta, J. Modolell and P. Gruss. "Identification of the Vertebrate Iroquois Homeobox Gene Family with Overlapping Expression During Early Development of the Nervous System." *Mech Dev* 69, no. 1-2 (1997): 169-81.

Bouhon, I. A., H. Kato, S. Chandran and N. D. Allen. "Neural Differentiation of Mouse Embryonic Stem Cells in Chemically Defined Medium." *Brain Res Bull* 68, no. 1-2 (2005): 62-75.

- Bouwmeester, T., S. Kim, Y. Sasai, B. Lu and E. M. De Robertis. "Cerberus Is a Head-Inducing Secreted Factor Expressed in the Anterior Endoderm of Spemann's Organizer." *Nature* 382, no. 6592 (1996): 595-601.
- Briscoe, J. and J. Ericson. "The Specification of Neuronal Identity by Graded Sonic Hedgehog Signalling." *Semin Cell Dev Biol* 10, no. 3 (1999): 353-62.
- Briscoe, J., A. Pierani, T. M. Jessell and J. Ericson. "A Homeodomain Protein Code Specifies Progenitor Cell Identity and Neuronal Fate in the Ventral Neural Tube." *Cell* 101, no. 4 (2000): 435-45.
- Britanova, O., S. Akopov, S. Lukyanov, P. Gruss and V. Tarabykin. "Novel Transcription Factor Satb2 Interacts with Matrix Attachment Region DNA Elements in a Tissue-Specific Manner and Demonstrates Cell-Type-Dependent Expression in the Developing Mouse Cns." *Eur J Neurosci* 21, no. 3 (2005): 658-68.
- Bulfone, A., S. M. Smiga, K. Shimamura, A. Peterson, L. Puelles and J. L. Rubenstein. "T-Brain-1: A Homolog of Brachyury Whose Expression Defines Molecularly Distinct Domains within the Cerebral Cortex." *Neuron* 15, no. 1 (1995): 63-78.
- Cai, C. and L. Gabel. "Directing the Differentiation of Embryonic Stem Cells to Neural Stem Cells." *Dev Dyn* 236, no. 12 (2007): 3255-66.
- Cerdan, C., B. A. McIntyre, R. Mechael, M. Levadoux-Martin, J. Yang, J. B. Lee and M. Bhatia. "Activin a Promotes Hematopoietic Fated Mesoderm Development through Upregulation of Brachyury in Human Embryonic Stem Cells." *Stem Cells Dev* 21, no. 15 (2012): 2866-77.
- Chambers, S. M., C. A. Fasano, E. P. Papapetrou, M. Tomishima, M. Sadelain and L. Studer. "Highly Efficient Neural Conversion of Human Es and Ips Cells by Dual Inhibition of Smad Signaling." *Nat Biotechnol* 27, no. 3 (2009): 275-80.
- Chatzi, C., T. Brade and G. Duester. "Retinoic Acid Functions as a Key Gabaergic Differentiation Signal in the Basal Ganglia." *PLoS Biol* 9, no. 4 (2011): e1000609.
- Chen, F. and M. R. Capecchi. "Targeted Mutations in Hoxa-9 and Hoxb-9 Reveal Synergistic Interactions." *Dev Biol* 181, no. 2 (1997): 186-96.

Chen, Y., L. Huang and M. Solursh. "A Concentration Gradient of Retinoids in the Early *Xenopus Laevis* Embryo." *Dev Biol* 161, no. 1 (1994): 70-6.

Chenn, A. and S. K. McConnell. "Cleavage Orientation and the Asymmetric Inheritance of Notch1 Immunoreactivity in Mammalian Neurogenesis." *Cell* 82, no. 4 (1995): 631-41.

Chiba, S., M. S. Kurokawa, H. Yoshikawa, R. Ikeda, M. Takeno, M. Tadokoro, H. Sekino, T. Hashimoto and N. Suzuki. "Noggin and Basic Fgf Were Implicated in Forebrain Fate and Caudal Fate, Respectively, of the Neural Tube-Like Structures Emerging in Mouse Es Cell Culture." *Exp Brain Res* 163, no. 1 (2005): 86-99.

Cho, K. W., E. A. Morita, C. V. Wright and E. M. De Robertis. "Overexpression of a Homeodomain Protein Confers Axis-Forming Activity to Uncommitted *Xenopus* Embryonic Cells." *Cell* 65, no. 1 (1991): 55-64.

Cox, W. G. and A. Hemmati-Brivanlou. "Caudalization of Neural Fate by Tissue Recombination and Bfgf." *Development* 121, no. 12 (1995): 4349-58.

Dale, L., G. Howes, B. M. Price and J. C. Smith. "Bone Morphogenetic Protein 4: A Ventralizing Factor in Early *Xenopus* Development." *Development* 115, no. 2 (1992): 573-85.

Dale, L. and J. M. Slack. "Fate Map for the 32-Cell Stage of *Xenopus Laevis*." *Development* 99, no. 4 (1987): 527-51.

DeCamp, D. L., T. M. Thompson, F. J. de Sauvage and M. R. Lerner. "Smoothed Activates Galphai-Mediated Signaling in Frog Melanophores." *J Biol Chem* 275, no. 34 (2000): 26322-7.

del Barco Barrantes, I., G. Davidson, H. J. Grone, H. Westphal and C. Niehrs. "Dkk1 and Noggin Cooperate in Mammalian Head Induction." *Genes Dev* 17, no. 18 (2003): 2239-44.

Dubrulle, J. and O. Pourquie. "Fgf8 Mrna Decay Establishes a Gradient That Couples Axial Elongation to Patterning in the Vertebrate Embryo." *Nature* 427, no. 6973 (2004): 419-22.

Durston, A. J., J. P. Timmermans, W. J. Hage, H. F. Hendriks, N. J. de Vries, M. Heideveld and P. D. Nieuwkoop. "Retinoic Acid Causes an Anteroposterior Transformation in the Developing Central Nervous System." *Nature* 340, no. 6229 (1989): 140-4.

- Echelard, Y., D. J. Epstein, B. St-Jacques, L. Shen, J. Mohler, J. A. McMahon and A. P. McMahon. "Sonic Hedgehog, a Member of a Family of Putative Signaling Molecules, Is Implicated in the Regulation of Cns Polarity." *Cell* 75, no. 7 (1993): 1417-30.
- Edmondson, J. C., R. K. Liem, J. E. Kuster and M. E. Hatten. "Astrotactin: A Novel Neuronal Cell Surface Antigen That Mediates Neuron-Astroglial Interactions in Cerebellar Microcultures." *J Cell Biol* 106, no. 2 (1988): 505-17.
- Eiraku, M., N. Takata, H. Ishibashi, M. Kawada, E. Sakakura, S. Okuda, K. Sekiguchi, T. Adachi and Y. Sasai. "Self-Organizing Optic-Cup Morphogenesis in Three-Dimensional Culture." *Nature* 472, no. 7341 (2011): 51-6.
- Eiraku, M., K. Watanabe, M. Matsuo-Takasaki, M. Kawada, S. Yonemura, M. Matsumura, T. Wataya, A. Nishiyama, K. Muguruma and Y. Sasai. "Self-Organized Formation of Polarized Cortical Tissues from Escs and Its Active Manipulation by Extrinsic Signals." *Cell Stem Cell* 3, no. 5 (2008): 519-32.
- Eisen, M. B., P. T. Spellman, P. O. Brown and D. Botstein. "Cluster Analysis and Display of Genome-Wide Expression Patterns." *Proc Natl Acad Sci U S A* 95, no. 25 (1998): 14863-8.
- Fishell, G. and M. E. Hatten. "Astrotactin Provides a Receptor System for Cns Neuronal Migration." *Development* 113, no. 3 (1991): 755-65.
- Foley, A. C. and C. D. Stern. "Evolution of Vertebrate Forebrain Development: How Many Different Mechanisms?" *J Anat* 199, no. Pt 1-2 (2001): 35-52.
- Frantz, G. D. and S. K. McConnell. "Restriction of Late Cerebral Cortical Progenitors to an Upper-Layer Fate." *Neuron* 17, no. 1 (1996): 55-61.
- Fujita, S., M. Horii, T. Tanimura and H. Nishimura. "H3-Thymidine Autoradiographic Studies on Cytokinetic Responses to X-Ray Irradiation and to Thio-Tepa in the Neural Tube of Mouse Embryos." *Anat Rec* 149, (1964): 37-48.
- Fujita, S., M. Shimada and T. Nakamura. "H3-Thymidine Autoradiographic Studies on the Cell Proliferation and Differentiation in the External and the Internal Granular Layers of the Mouse Cerebellum." *J Comp Neurol* 128, no. 2 (1966): 191-208.

Furue, M., Y. Myoishi, Y. Fukui, T. Ariizumi, T. Okamoto and M. Asashima. "Activin a Induces Craniofacial Cartilage from Undifferentiated *Xenopus* Ectoderm in Vitro." *Proc Natl Acad Sci U S A* 99, no. 24 (2002): 15474-9.

Furukawa, T., C. A. Kozak and C. L. Cepko. "Rax, a Novel Paired-Type Homeobox Gene, Shows Expression in the Anterior Neural Fold and Developing Retina." *Proc Natl Acad Sci U S A* 94, no. 7 (1997): 3088-93.

Furuta, Y., D. W. Piston and B. L. Hogan. "Bone Morphogenetic Proteins (Bmps) as Regulators of Dorsal Forebrain Development." *Development* 124, no. 11 (1997): 2203-12.

Gallera, J. "Primary Induction in Birds." *Adv Morphog* 9, (1971): 149-80.

Gaspard, N., T. Bouschet, A. Herpoel, G. Naeije, J. van den Aemele and P. Vanderhaeghen. "Generation of Cortical Neurons from Mouse Embryonic Stem Cells." *Nat Protoc* 4, no. 10 (2009): 1454-63. Gaspard, N., T. Bouschet, R. Hourez, J. Dimidschstein, G. Naeije, J. van den Aemele, I. Espuny-Camacho, A. Herpoel, L. Passante, S. N. Schiffmann, A. Gaillard and P. Vanderhaeghen. "An Intrinsic Mechanism of Corticogenesis from Embryonic Stem Cells." *Nature* 455, no. 7211 (2008): 351-7.

Gaspard, N., A. Gaillard and P. Vanderhaeghen. "Making Cortex in a Dish: In Vitro Corticogenesis from Embryonic Stem Cells." *Cell Cycle* 8, no. 16 (2009): 2491-6.

Gaspard, N. and P. Vanderhaeghen. "Mechanisms of Neural Specification from Embryonic Stem Cells." *Curr Opin Neurobiol* 20, no. 1 (2010): 37-43.

Gerhart, J., M. Danilchik, T. Doniach, S. Roberts, B. Rowing and R. Stewart. "Cortical Rotation of the *Xenopus* Egg: Consequences for the Anteroposterior Pattern of Embryonic Dorsal Development." *Development* 107 Suppl, (1989): 37-51.

Gimlich, R. L. "Cytoplasmic Localization and Chordamesoderm Induction in the Frog Embryo." *J Embryol Exp Morphol* 89 Suppl, (1985): 89-111.

Gimlich, R. L. "Acquisition of Developmental Autonomy in the Equatorial Region of the *Xenopus* Embryo." *Dev Biol* 115, no. 2 (1986): 340-52.

- Gimlich, R. L. and J. C. Gerhart. "Early Cellular Interactions Promote Embryonic Axis Formation in *Xenopus Laevis*." *Dev Biol* 104, no. 1 (1984): 117-30.
- Glaser, T., L. Jepeal, J. G. Edwards, S. R. Young, J. Favor and R. L. Maas. "Pax6 Gene Dosage Effect in a Family with Congenital Cataracts, Aniridia, Anophthalmia and Central Nervous System Defects." *Nat Genet* 7, no. 4 (1994): 463-71.
- Glinka, A., W. Wu, H. Delius, A. P. Monaghan, C. Blumenstock and C. Niehrs. "Dickkopf-1 Is a Member of a New Family of Secreted Proteins and Functions in Head Induction." *Nature* 391, no. 6665 (1998): 357-62.
- Glinka, A., W. Wu, D. Onichtchouk, C. Blumenstock and C. Niehrs. "Head Induction by Simultaneous Repression of Bmp and Wnt Signalling in *Xenopus*." *Nature* 389, no. 6650 (1997): 517-9.
- Godsave, S. F., C. H. Koster, A. Getahun, M. Mathu, M. Hooiveld, J. van der Wees, J. Hendriks and A. J. Durston. "Graded Retinoid Responses in the Developing Hindbrain." *Dev Dyn* 213, no. 1 (1998): 39-49.
- Godsave, S. F. and J. M. Slack. "Clonal Analysis of Mesoderm Induction in *Xenopus Laevis*." *Dev Biol* 134, no. 2 (1989): 486-90.
- Graff, J. M., R. S. Thies, J. J. Song, A. J. Celeste and D. A. Melton. "Studies with a *Xenopus* Bmp Receptor Suggest That Ventral Mesoderm-Inducing Signals Override Dorsal Signals in Vivo." *Cell* 79, no. 1 (1994): 169-79.
- Grant, S. "Ara-C: Cellular and Molecular Pharmacology." *Adv Cancer Res* 72, (1998): 197-233.
- Gratsch, T. E. and K. S. O'Shea. "Noggin and Chordin Have Distinct Activities in Promoting Lineage Commitment of Mouse Embryonic Stem (Es) Cells." *Dev Biol* 245, no. 1 (2002): 83-94.
- Green, J. B., H. V. New and J. C. Smith. "Responses of Embryonic *Xenopus* Cells to Activin and Fgf Are Separated by Multiple Dose Thresholds and Correspond to Distinct Axes of the Mesoderm." *Cell* 71, no. 5 (1992): 731-9.
- Grophe, J., J. Greenwald, E. Wiater, J. Rodriguez-Leon, A. N. Economides, W. Kwiatkowski, M. Affolter, W. W. Vale, J. C. Izpisua Belmonte and S. Choe. "Structural Basis of Bmp Signalling Inhibition by the Cystine Knot Protein Noggin." *Nature* 420, no. 6916 (2002): 636-42.

Grunz, H. and L. Tacke. "Neural Differentiation of *Xenopus Laevis* Ectoderm Takes Place after Disaggregation and Delayed Reaggregation without Inducer." *Cell Differ Dev* 28, no. 3 (1989): 211-7.

Guan, K., H. Chang, A. Rolletschek and A. M. Wobus. "Embryonic Stem Cell-Derived Neurogenesis. Retinoic Acid Induction and Lineage Selection of Neuronal Cells." *Cell Tissue Res* 305, no. 2 (2001): 171-6.

Guthrie, S. and A. Lumsden. "Formation and Regeneration of Rhombomere Boundaries in the Developing Chick Hindbrain." *Development* 112, no. 1 (1991): 221-9.

Halder, G., P. Callaerts and W. J. Gehring. "New Perspectives on Eye Evolution." *Curr Opin Genet Dev* 5, no. 5 (1995): 602-9.

Hatten, M. E. "Riding the Glial Monorail: A Common Mechanism for Glial-Guided Neuronal Migration in Different Regions of the Developing Mammalian Brain." *Trends Neurosci* 13, no. 5 (1990): 179-84.

Hawley, S. H., K. Wunnenberg-Stapleton, C. Hashimoto, M. N. Laurent, T. Watabe, B. W. Blumberg and K. W. Cho. "Disruption of Bmp Signals in Embryonic *Xenopus* Ectoderm Leads to Direct Neural Induction." *Genes Dev* 9, no. 23 (1995): 2923-35.

Hebert, J. M., Y. Mishina and S. K. McConnell. "Bmp Signaling Is Required Locally to Pattern the Dorsal Telencephalic Midline." *Neuron* 35, no. 6 (2002): 1029-41.

Hedgcoth, C. and M. Jacobson. "Determination of Nucleoside Composition of Ribonucleic Acid by Thin-Layer Chromatography." *Anal Biochem* 25, no. 1 (1968): 55-60.

Hemmati-Brivanlou, A., O. G. Kelly and D. A. Melton. "Follistatin, an Antagonist of Activin, Is Expressed in the Spemann Organizer and Displays Direct Neuralizing Activity." *Cell* 77, no. 2 (1994): 283-95.

Hemmati-Brivanlou, A. and D. Melton. "Vertebrate Embryonic Cells Will Become Nerve Cells Unless Told Otherwise." *Cell* 88, no. 1 (1997): 13-7.

Hemmati-Brivanlou, A. and D. A. Melton. "A Truncated Activin Receptor Inhibits Mesoderm Induction and Formation of Axial Structures in *Xenopus* Embryos." *Nature* 359, no. 6396 (1992): 609-14.

- Hemmati-Brivanlou, A. and D. A. Melton. "Inhibition of Activin Receptor Signaling Promotes Neuralization in *Xenopus*." *Cell* 77, no. 2 (1994): 273-81.
- Hemmati-Brivanlou, A., D. A. Wright and D. A. Melton. "Embryonic Expression and Functional Analysis of a *Xenopus* Activin Receptor." *Dev Dyn* 194, no. 1 (1992): 1-11.
- Hendrickx, M., X. H. Van and L. Leyns. "Anterior-Posterior Patterning of Neural Differentiated Embryonic Stem Cells by Canonical Wnts, Fgfs, Bmp4 and Their Respective Antagonists." *Dev Growth Differ* 51, no. 8 (2009): 687-98.
- Hevner, R. F., L. Shi, N. Justice, Y. Hsueh, M. Sheng, S. Smiga, A. Bulfone, A. M. Goffinet, A. T. Campagnoni and J. L. Rubenstein. "Tbr1 Regulates Differentiation of the Preplate and Layer 6." *Neuron* 29, no. 2 (2001): 353-66.
- Hicks, D. and Y. Courtois. "Fibroblast Growth Factor Stimulates Photoreceptor Differentiation in Vitro." *J Neurosci* 12, no. 6 (1992): 2022-33.
- Hollnagel, A., V. Oehlmann, J. Heymer, U. Ruther and A. Nordheim. "Id Genes Are Direct Targets of Bone Morphogenetic Protein Induction in Embryonic Stem Cells." *J Biol Chem* 274, no. 28 (1999): 19838-45.
- Houart, C., L. Caneparo, C. Heisenberg, K. Barth, M. Take-Uchi and S. Wilson. "Establishment of the Telencephalon During Gastrulation by Local Antagonism of Wnt Signaling." *Neuron* 35, no. 2 (2002): 255-65.
- Ideguchi, M., T. D. Palmer, L. D. Recht and J. M. Weimann. "Murine Embryonic Stem Cell-Derived Pyramidal Neurons Integrate into the Cerebral Cortex and Appropriately Project Axons to Subcortical Targets." *J Neurosci* 30, no. 3 (2010): 894-904.
- Idelson, M., R. Alper, A. Obolensky, E. Ben-Shushan, I. Hemo, N. Yachimovich-Cohen, H. Khaner, Y. Smith, O. Wisner, M. Gropp, M. A. Cohen, S. Even-Ram, Y. Berman-Zaken, L. Matzrafi, G. Rechavi, E. Banin and B. Reubinoff. "Directed Differentiation of Human Embryonic Stem Cells into Functional Retinal Pigment Epithelium Cells." *Cell Stem Cell* 5, no. 4 (2009): 396-408.

Iemura, S., T. S. Yamamoto, C. Takagi, H. Uchiyama, T. Natsume, S. Shimasaki, H. Sugino and N. Ueno. "Direct Binding of Follistatin to a Complex of Bone-Morphogenetic Protein and Its Receptor Inhibits Ventral and Epidermal Cell Fates in Early *Xenopus* Embryo." *Proc Natl Acad Sci U S A* 95, no. 16 (1998): 9337-42.

Ikeda, H., F. Osakada, K. Watanabe, K. Mizuseki, T. Haraguchi, H. Miyoshi, D. Kamiya, Y. Honda, N. Sasai, N. Yoshimura, M. Takahashi and Y. Sasai. "Generation of Rx+/Pax6+ Neural Retinal Precursors from Embryonic Stem Cells." *Proc Natl Acad Sci U S A* 102, no. 32 (2005): 11331-6.

Isaacs, H. V., D. Tannahill and J. M. Slack. "Expression of a Novel Fgf in the *Xenopus* Embryo. A New Candidate Inducing Factor for Mesoderm Formation and Anteroposterior Specification." *Development* 114, no. 3 (1992): 711-20.

Iwao, T., M. Toyota, Y. Miyagawa, H. Okita, N. Kiyokawa, H. Akutsu, A. Umezawa, K. Nagata and T. Matsunaga. "Differentiation of Human Induced Pluripotent Stem Cells into Functional Enterocyte-Like Cells Using a Simple Method." *Drug Metab Pharmacokinet*, (2013).

Jacobson, C. O. "Reactivation of DNA Synthesis in Mammalian Neuron Nuclei after Fusion with Cells of an Undifferentiated Fibroblast Line." *Exp Cell Res* 53, no. 1 (1968): 316-8.

Jessell, T. M. "Neuronal Specification in the Spinal Cord: Inductive Signals and Transcriptional Codes." *Nat Rev Genet* 1, no. 1 (2000): 20-9.

Jones, C. M., K. M. Lyons, P. M. Lapan, C. V. Wright and B. L. Hogan. "Dvr-4 (Bone Morphogenetic Protein-4) as a Posterior-Ventralizing Factor in *Xenopus* Mesoderm Induction." *Development* 115, no. 2 (1992): 639-47.

Jordan, T., I. Hanson, D. Zaletayev, S. Hodgson, J. Prosser, A. Seawright, N. Hastie and V. van Heyningen. "The Human Pax6 Gene Is Mutated in Two Patients with Aniridia." *Nat Genet* 1, no. 5 (1992): 328-32.

Kamiya, D., S. Banno, N. Sasai, M. Ohgushi, H. Inomata, K. Watanabe, M. Kawada, R. Yakura, H. Kiyonari, K. Nakao, L. M. Jakt, S. Nishikawa and Y. Sasai. "Intrinsic Transition of Embryonic Stem-Cell Differentiation into Neural Progenitors." *Nature* 470, no. 7335 (2011): 503-9.

- Kawasaki, H., K. Mizuseki, S. Nishikawa, S. Kaneko, Y. Kuwana, S. Nakanishi, S. I. Nishikawa and Y. Sasai. "Induction of Midbrain Dopaminergic Neurons from Es Cells by Stromal Cell-Derived Inducing Activity." *Neuron* 28, no. 1 (2000): 31-40.
- Keller, R., J. Shih, A. K. Sater and C. Moreno. "Planar Induction of Convergence and Extension of the Neural Plate by the Organizer of *Xenopus*." *Dev Dyn* 193, no. 3 (1992): 218-34.
- Keller, S., J. Nickel, J. L. Zhang, W. Sebald and T. D. Mueller. "Molecular Recognition of Bmp-2 and Bmp Receptor Ia." *Nat Struct Mol Biol* 11, no. 5 (2004): 481-8.
- Kelley, M. W., J. K. Turner and T. A. Reh. "Retinoic Acid Promotes Differentiation of Photoreceptors in Vitro." *Development* 120, no. 8 (1994): 2091-102.
- Khokha, M. K., J. Yeh, T. C. Grammer and R. M. Harland. "Depletion of Three Bmp Antagonists from Spemann's Organizer Leads to a Catastrophic Loss of Dorsal Structures." *Dev Cell* 8, no. 3 (2005): 401-11.
- Kinney, J. W., C. N. Davis, I. Tabarean, B. Conti, T. Bartfai and M. M. Behrens. "A Specific Role for Nr2a-Containing Nmda Receptors in the Maintenance of Parvalbumin and Gad67 Immunoreactivity in Cultured Interneurons." *J Neurosci* 26, no. 5 (2006): 1604-15.
- Knoth, R., I. Singec, M. Ditter, G. Pantazis, P. Capetian, R. P. Meyer, V. Horvat, B. Volk and G. Kempermann. "Murine Features of Neurogenesis in the Human Hippocampus across the Lifespan from 0 to 100 Years." *PLoS One* 5, no. 1 (2010): e8809.
- Kodaira, K., M. Imada, M. Goto, A. Tomoyasu, T. Fukuda, R. Kamijo, T. Suda, K. Higashio and T. Katagiri. "Purification and Identification of a Bmp-Like Factor from Bovine Serum." *Biochem Biophys Res Commun* 345, no. 3 (2006): 1224-31.
- Kolm, P. J., V. Apekin and H. Sive. "Xenopus Hindbrain Patterning Requires Retinoid Signaling." *Dev Biol* 192, no. 1 (1997): 1-16.
- Kolm, P. J. and H. L. Sive. "Retinoids and Posterior Neural Induction: A Reevaluation of Nieuwkoop's Two-Step Hypothesis." *Cold Spring Harb Symp Quant Biol* 62, (1997): 511-21.

Komada, M. "Sonic Hedgehog Signaling Coordinates the Proliferation and Differentiation of Neural Stem/Progenitor Cells by Regulating Cell Cycle Kinetics During Development of the Neocortex." *Congenit Anom (Kyoto)* 52, no. 2 (2012): 72-7.

Komada, M., H. Saitsu, M. Kinboshi, T. Miura, K. Shiota and M. Ishibashi. "Hedgehog Signaling Is Involved in Development of the Neocortex." *Development* 135, no. 16 (2008): 2717-27.

Komuro, H. and P. Rakic. "Selective Role of N-Type Calcium Channels in Neuronal Migration." *Science* 257, no. 5071 (1992): 806-9.

Lamb, T. M. and R. M. Harland. "Fibroblast Growth Factor Is a Direct Neural Inducer, Which Combined with Noggin Generates Anterior-Posterior Neural Pattern." *Development* 121, no. 11 (1995): 3627-36.

Lamb, T. M., A. K. Knecht, W. C. Smith, S. E. Stachel, A. N. Economides, N. Stahl, G. D. Yancopoulos and R. M. Harland. "Neural Induction by the Secreted Polypeptide Noggin." *Science* 262, no. 5134 (1993): 713-8.

Lamba, D. A., J. Gust and T. A. Reh. "Transplantation of Human Embryonic Stem Cell-Derived Photoreceptors Restores Some Visual Function in Crx-Deficient Mice." *Cell Stem Cell* 4, no. 1 (2009): 73-9.

Lamba, D. A., M. O. Karl, C. B. Ware and T. A. Reh. "Efficient Generation of Retinal Progenitor Cells from Human Embryonic Stem Cells." *Proc Natl Acad Sci U S A* 103, no. 34 (2006): 12769-74.

Lamba, D. A., A. McUsic, R. K. Hirata, P. R. Wang, D. Russell and T. A. Reh. "Generation, Purification and Transplantation of Photoreceptors Derived from Human Induced Pluripotent Stem Cells." *PLoS One* 5, no. 1 (2010): e8763.

Lamba, D., M. Karl and T. Reh. "Neural Regeneration and Cell Replacement: A View from the Eye." *Cell Stem Cell* 2, no. 6 (2008): 538-49.

Lan, L., A. Vitobello, M. Bertacchi, F. Cremisi, R. Vignali, M. Andreazzoli, G. C. Demontis, G. Barsacchi and S. Casarosa. "Noggin Elicits Retinal Fate in Xenopus Animal Cap Embryonic Stem Cells." *Stem Cells* 27, no. 9 (2009): 2146-52.

- Lee, J. E., S. M. Hollenberg, L. Snider, D. L. Turner, N. Lipnick and H. Weintraub. "Conversion of *Xenopus* Ectoderm into Neurons by Neurod, a Basic Helix-Loop-Helix Protein." *Science* 268, no. 5212 (1995): 836-44.
- Lee, S. H., N. Lumelsky, L. Studer, J. M. Auerbach and R. D. McKay. "Efficient Generation of Midbrain and Hindbrain Neurons from Mouse Embryonic Stem Cells." *Nat Biotechnol* 18, no. 6 (2000): 675-9.
- Levine, A. J. and A. H. Brivanlou. "Proposal of a Model of Mammalian Neural Induction." *Dev Biol* 308, no. 2 (2007): 247-56.
- Levine, E. M., H. Roelink, J. Turner and T. A. Reh. "Sonic Hedgehog Promotes Rod Photoreceptor Differentiation in Mammalian Retinal Cells in Vitro." *J Neurosci* 17, no. 16 (1997): 6277-88.
- Leyns, L., T. Bouwmeester, S. H. Kim, S. Piccolo and E. M. De Robertis. "Frzb-1 Is a Secreted Antagonist of Wnt Signaling Expressed in the Spemann Organizer." *Cell* 88, no. 6 (1997): 747-56.
- Li, E., H. M. Sucov, K. F. Lee, R. M. Evans and R. Jaenisch. "Normal Development and Growth of Mice Carrying a Targeted Disruption of the Alpha 1 Retinoic Acid Receptor Gene." *Proc Natl Acad Sci U S A* 90, no. 4 (1993): 1590-4.
- Liem, K. F., Jr., G. Tremml and T. M. Jessell. "A Role for the Roof Plate and Its Resident Tgfbeta-Related Proteins in Neuronal Patterning in the Dorsal Spinal Cord." *Cell* 91, no. 1 (1997): 127-38.
- Liem, K. F., Jr., G. Tremml, H. Roelink and T. M. Jessell. "Dorsal Differentiation of Neural Plate Cells Induced by Bmp-Mediated Signals from Epidermal Ectoderm." *Cell* 82, no. 6 (1995): 969-79.
- Livesey, F. J. and C. L. Cepko. "Vertebrate Neural Cell-Fate Determination: Lessons from the Retina." *Nat Rev Neurosci* 2, no. 2 (2001): 109-18.
- Lupo, G., W. A. Harris, G. Barsacchi and R. Vignali. "Induction and Patterning of the Telencephalon in *Xenopus Laevis*." *Development* 129, no. 23 (2002): 5421-36.

- Lupo, G., C. Novorol, J. R. Smith, L. Vallier, E. Miranda, M. Alexander, S. Biagioni, R. A. Pedersen and W. A. Harris. "Multiple Roles of Activin/Nodal, Bone Morphogenetic Protein, Fibroblast Growth Factor and Wnt/Beta-Catenin Signalling in the Anterior Neural Patterning of Adherent Human Embryonic Stem Cell Cultures." *Open Biol* 3, no. 4 (2013): 120167.
- MacLaren, R. E., R. A. Pearson, A. MacNeil, R. H. Douglas, T. E. Salt, M. Akimoto, A. Swaroop, J. C. Sowden and R. R. Ali. "Retinal Repair by Transplantation of Photoreceptor Precursors." *Nature* 444, no. 7116 (2006): 203-7.
- Malatesta, P., M. Gotz, G. Barsacchi, J. Price, R. Zoncu and F. Cremisi. "Pc3 Overexpression Affects the Pattern of Cell Division of Rat Cortical Precursors." *Mech Dev* 90, no. 1 (2000): 17-28.
- Mangale, V. S., K. E. Hirokawa, P. R. Satyaki, N. Gokulchandran, S. Chikbire, L. Subramanian, A. S. Shetty, B. Martynoga, J. Paul, M. V. Mai, Y. Li, L. A. Flanagan, S. Tole and E. S. Monuki. "Lhx2 Selector Activity Specifies Cortical Identity and Suppresses Hippocampal Organizer Fate." *Science* 319, no. 5861 (2008): 304-9.
- Mathers, P. H., A. Grinberg, K. A. Mahon and M. Jamrich. "The Rx Homeobox Gene Is Essential for Vertebrate Eye Development." *Nature* 387, no. 6633 (1997): 603-7.
- Matsunami, H. and M. Takeichi. "Fetal Brain Subdivisions Defined by R- and E-Cadherin Expressions: Evidence for the Role of Cadherin Activity in Region-Specific, Cell-Cell Adhesion." *Dev Biol* 172, no. 2 (1995): 466-78.
- McConnell, S. K. and C. E. Kaznowski. "Cell Cycle Dependence of Lamina Determination in Developing Neocortex." *Science* 254, no. 5029 (1991): 282-5.
- McGrew, L. L., S. Hoppler and R. T. Moon. "Wnt and Fgf Pathways Cooperatively Pattern Anteroposterior Neural Ectoderm in *Xenopus*." *Mech Dev* 69, no. 1-2 (1997): 105-14.
- McGrew, L. L., C. J. Lai and R. T. Moon. "Specification of the Anteroposterior Neural Axis through Synergistic Interaction of the Wnt Signaling Cascade with Noggin and Follistatin." *Dev Biol* 172, no. 1 (1995): 337-42.

- McNeish, J., M. Roach, J. Hambor, R. J. Mather, L. Weibley, J. Lazzaro, J. Gazard, J. Schwarz, R. Volkman, D. Machacek, S. Stice, L. Zawadzke, C. O'Donnell and R. Hurst. "High-Throughput Screening in Embryonic Stem Cell-Derived Neurons Identifies Potentiators of Alpha-Amino-3-Hydroxyl-5-Methyl-4-Isoxazolepropionate-Type Glutamate Receptors." *J Biol Chem* 285, no. 22 (2010): 17209-17.
- Mitsui, K., Y. Tokuzawa, H. Itoh, K. Segawa, M. Murakami, K. Takahashi, M. Maruyama, M. Maeda and S. Yamanaka. "The Homeoprotein Nanog Is Required for Maintenance of Pluripotency in Mouse Epiblast and Es Cells." *Cell* 113, no. 5 (2003): 631-42.
- Munoz-Sanjuan, I. and A. H. Brivanlou. "Neural Induction, the Default Model and Embryonic Stem Cells." *Nat Rev Neurosci* 3, no. 4 (2002): 271-80.
- Nadri, S., M. Soleimani, R. H. Hosseini, M. Massumi, A. Atashi and R. Izadpanah. "An Efficient Method for Isolation of Murine Bone Marrow Mesenchymal Stem Cells." *Int J Dev Biol* 51, no. 8 (2007): 723-9.
- Nicoleau, C., C. Varela, C. Bonnefond, Y. Maury, A. Bugi, L. Aubry, P. Viegas, F. Bourgois-Rocha, M. Peschanski and A. L. Perrier. "Embryonic Stem Cells Neural Differentiation Qualifies the Role of Wnt/Beta-Catenin Signals in Human Telencephalic Specification and Regionalization." *Stem Cells* 31, no. 9 (2013): 1763-1774.
- Niehrs, C. "Regionally Specific Induction by the Spemann-Mangold Organizer." *Nat Rev Genet* 5, no. 6 (2004): 425-34.
- Niwa, H., J. Miyazaki and A. G. Smith. "Quantitative Expression of Oct-3/4 Defines Differentiation, Dedifferentiation or Self-Renewal of Es Cells." *Nat Genet* 24, no. 4 (2000): 372-6.
- Nordgard, O., J. T. Kvaloy, R. K. Farnen and R. Heikkila. "Error Propagation in Relative Real-Time Reverse Transcription Polymerase Chain Reaction Quantification Models: The Balance between Accuracy and Precision." *Anal Biochem* 356, no. 2 (2006): 182-93.
- O'Rourke, N. A., M. E. Dailey, S. J. Smith and S. K. McConnell. "Diverse Migratory Pathways in the Developing Cerebral Cortex." *Science* 258, no. 5080 (1992): 299-302.

- Okabayashi, K. and M. Asashima. "Tissue Generation from Amphibian Animal Caps." *Curr Opin Genet Dev* 13, no. 5 (2003): 502-7.
- Okano, H., H. Kawahara, M. Toriya, K. Nakao, S. Shibata and T. Imai. "Function of Rna-Binding Protein Musashi-1 in Stem Cells." *Exp Cell Res* 306, no. 2 (2005): 349-56.
- Oliver, G., A. Mailhos, R. Wehr, N. G. Copeland, N. A. Jenkins and P. Gruss. "Six3, a Murine Homologue of the Sine Oculis Gene, Demarcates the Most Anterior Border of the Developing Neural Plate and Is Expressed During Eye Development." *Development* 121, no. 12 (1995): 4045-55.
- Olsson, J. E., J. W. Gordon, B. S. Pawlyk, D. Roof, A. Hayes, R. S. Molday, S. Mukai, G. S. Cowley, E. L. Berson and T. P. Dryja. "Transgenic Mice with a Rhodopsin Mutation (Pro23his): A Mouse Model of Autosomal Dominant Retinitis Pigmentosa." *Neuron* 9, no. 5 (1992): 815-30.
- Osakada, F., H. Ikeda, M. Mandai, T. Wataya, K. Watanabe, N. Yoshimura, A. Akaike, Y. Sasai and M. Takahashi. "Toward the Generation of Rod and Cone Photoreceptors from Mouse, Monkey and Human Embryonic Stem Cells." *Nat Biotechnol* 26, no. 2 (2008): 215-24.
- Papalopulu, N., J. D. Clarke, L. Bradley, D. Wilkinson, R. Krumlauf and N. Holder. "Retinoic Acid Causes Abnormal Development and Segmental Patterning of the Anterior Hindbrain in *Xenopus* Embryos." *Development* 113, no. 4 (1991): 1145-58.
- Parr, B. A., M. J. Shea, G. Vassileva and A. P. McMahon. "Mouse Wnt Genes Exhibit Discrete Domains of Expression in the Early Embryonic Cns and Limb Buds." *Development* 119, no. 1 (1993): 247-61.
- Pera, E. M. and M. Kessel. "Patterning of the Chick Forebrain Anlage by the Prechordal Plate." *Development* 124, no. 20 (1997): 4153-62.
- Pera, E. M., O. Wessely, S. Y. Li and E. M. De Robertis. "Neural and Head Induction by Insulin-Like Growth Factor Signals." *Dev Cell* 1, no. 5 (2001): 655-65.
- Perea-Gomez, A., F. D. Vella, W. Shawlot, M. Oulad-Abdelghani, C. Chazaud, C. Meno, V. Pfister, L. Chen, E. Robertson, H. Hamada, R. R. Behringer and S. L. Ang. "Nodal Antagonists in the Anterior Visceral Endoderm Prevent the Formation of Multiple Primitive Streaks." *Dev Cell* 3, no. 5 (2002): 745-56.

- Pfaffl, M. W., G. W. Horgan and L. Dempfle. "Relative Expression Software Tool (Rest) for Group-Wise Comparison and Statistical Analysis of Relative Expression Results in Real-Time Pcr." *Nucleic Acids Res* 30, no. 9 (2002): e36.
- Piao, X., R. S. Hill, A. Bodell, B. S. Chang, L. Basel-Vanagaite, R. Straussberg, W. B. Dobyns, B. Qasrawi, R. M. Winter, A. M. Innes, T. Voit, M. E. Ross, J. L. Michaud, J. C. Descarie, A. J. Barkovich and C. A. Walsh. "G Protein-Coupled Receptor-Dependent Development of Human Frontal Cortex." *Science* 303, no. 5666 (2004): 2033-6.
- Piccolo, S., E. Agius, L. Leyns, S. Bhattacharyya, H. Grunz, T. Bouwmeester and E. M. De Robertis. "The Head Inducer Cerberus Is a Multifunctional Antagonist of Nodal, Bmp and Wnt Signals." *Nature* 397, no. 6721 (1999): 707-10.
- Piccolo, S., Y. Sasai, B. Lu and E. M. De Robertis. "Dorsoventral Patterning in Xenopus: Inhibition of Ventral Signals by Direct Binding of Chordin to Bmp-4." *Cell* 86, no. 4 (1996): 589-98.
- Pierani, A., S. Brenner-Morton, C. Chiang and T. M. Jessell. "A Sonic Hedgehog-Independent, Retinoid-Activated Pathway of Neurogenesis in the Ventral Spinal Cord." *Cell* 97, no. 7 (1999): 903-15.
- Placzek, M., M. Tessier-Lavigne, T. Yamada, T. Jessell and J. Dodd. "Mesodermal Control of Neural Cell Identity: Floor Plate Induction by the Notochord." *Science* 250, no. 4983 (1990): 985-8.
- Pownall, M. E., A. S. Tucker, J. M. Slack and H. V. Isaacs. "Efgf, Xcad3 and Hox Genes Form a Molecular Pathway That Establishes the Anteroposterior Axis in Xenopus." *Development* 122, no. 12 (1996): 3881-92.
- Quiring, R., U. Walldorf, U. Kloter and W. J. Gehring. "Homology of the Eyeless Gene of Drosophila to the Small Eye Gene in Mice and Aniridia in Humans." *Science* 265, no. 5173 (1994): 785-9.
- Rakic, P. "Mode of Cell Migration to the Superficial Layers of Fetal Monkey Neocortex." *J Comp Neurol* 145, no. 1 (1972): 61-83.
- Rakic, P. "Neurons in Rhesus Monkey Visual Cortex: Systematic Relation between Time of Origin and Eventual Disposition." *Science* 183, no. 4123 (1974): 425-7.

Rakic, P. "Role of Cell Interaction in Development of Dendritic Patterns." *Adv Neurol* 12, (1975): 117-34.

Rakic, P. "Evolution of the Neocortex: A Perspective from Developmental Biology." *Nat Rev Neurosci* 10, no. 10 (2009): 724-35.

Rakic, P. and R. L. Sidman. "Weaver Mutant Mouse Cerebellum: Defective Neuronal Migration Secondary to Abnormality of Bergmann Glia." *Proc Natl Acad Sci U S A* 70, no. 1 (1973): 240-4.

Ralph, P. and I. Nakoinz. "Direct Toxic Effects of Immunopotentiators on Monocytic, Myelomonocytic, and Histiocytic or Macrophage Tumor Cells in Culture." *Cancer Res* 37, no. 2 (1977): 546-50.

Ramirez-Solis, R., H. Zheng, J. Whiting, R. Krumlauf and A. Bradley. "Hoxb-4 (Hox-2.6) Mutant Mice Show Homeotic Transformation of a Cervical Vertebra and Defects in the Closure of the Sternal Rudiments." *Cell* 73, no. 2 (1993): 279-94.

Regad, T., M. Roth, N. Breidenkamp, N. Illing and N. Papalopulu. "The Neural Progenitor-Specifying Activity of Foxg1 Is Antagonistically Regulated by Cki and Fgf." *Nat Cell Biol* 9, no. 5 (2007): 531-40.

Reversade, B., H. Kuroda, H. Lee, A. Mays and E. M. De Robertis. "Depletion of Bmp2, Bmp4, Bmp7 and Spemann Organizer Signals Induces Massive Brain Formation in *Xenopus* Embryos." *Development* 132, no. 15 (2005): 3381-92.

Roelink, H., A. Augsburger, J. Heemskerk, V. Korzh, S. Norlin, A. Ruiz i Altaba, Y. Tanabe, M. Placzek, T. Edlund, T. M. Jessell and et al. "Floor Plate and Motor Neuron Induction by Vhh-1, a Vertebrate Homolog of Hedgehog Expressed by the Notochord." *Cell* 76, no. 4 (1994): 761-75.

Roelink, H., J. A. Porter, C. Chiang, Y. Tanabe, D. T. Chang, P. A. Beachy and T. M. Jessell. "Floor Plate and Motor Neuron Induction by Different Concentrations of the Amino-Terminal Cleavage Product of Sonic Hedgehog Autoproteolysis." *Cell* 81, no. 3 (1995): 445-55.

Ruiz i Altaba, A. and T. Jessell. "Retinoic Acid Modifies Mesodermal Patterning in Early *Xenopus* Embryos." *Genes Dev* 5, no. 2 (1991): 175-87.

- Sakaki-Yumoto, M., J. Liu, M. Ramalho-Santos, N. Yoshida and R. Derynck. "Smad2 Is Essential for Maintenance of the Human and Mouse Primed Pluripotent Stem Cell State." *J Biol Chem* 288, no. 25 (2013): 18546-60.
- Saldanha, A. J. "Java Treeview--Extensible Visualization of Microarray Data." *Bioinformatics* 20, no. 17 (2004): 3246-8.
- Sansom, S. N. and F. J. Livesey. "Gradients in the Brain: The Control of the Development of Form and Function in the Cerebral Cortex." *Cold Spring Harb Perspect Biol* 1, no. 2 (2009): a002519.
- Sasai, Y., B. Lu, H. Steinbeisser and E. M. De Robertis. "Regulation of Neural Induction by the Chd and Bmp-4 Antagonistic Patterning Signals in *Xenopus*." *Nature* 377, no. 6551 (1995): 757.
- Sasai, Y., B. Lu, H. Steinbeisser, D. Geissert, L. K. Gont and E. M. De Robertis. "Xenopus Chordin: A Novel Dorsalizing Factor Activated by Organizer-Specific Homeobox Genes." *Cell* 79, no. 5 (1994): 779-90.
- Sato, S. M. and T. D. Sargent. "Development of Neural Inducing Capacity in Dissociated *Xenopus* Embryos." *Dev Biol* 134, no. 1 (1989): 263-6.
- Sausedo, R. A., J. L. Smith and G. C. Schoenwolf. "Role of Nonrandomly Oriented Cell Division in Shaping and Bending of the Neural Plate." *J Comp Neurol* 381, no. 4 (1997): 473-88.
- Schoenwolf, G. C. and I. S. Alvarez. "Roles of Neuroepithelial Cell Rearrangement and Division in Shaping of the Avian Neural Plate." *Development* 106, no. 3 (1989): 427-39.
- Sharpe, C. R. "Retinoic Acid Can Mimic Endogenous Signals Involved in Transformation of the *Xenopus* Nervous System." *Neuron* 7, no. 2 (1991): 239-47.
- Silva, J., O. Barrandon, J. Nichols, J. Kawaguchi, T. W. Theunissen and A. Smith. "Promotion of Reprogramming to Ground State Pluripotency by Signal Inhibition." *PLoS Biol* 6, no. 10 (2008): e253.
- Simeone, A., D. Acampora, M. Gulisano, A. Stornaiuolo and E. Boncinelli. "Nested Expression Domains of Four Homeobox Genes in Developing Rostral Brain." *Nature* 358, no. 6388 (1992): 687-90.

Sive, H. L. and P. F. Cheng. "Retinoic Acid Perturbs the Expression of Xhox.Lab Genes and Alters Mesodermal Determination in *Xenopus Laevis*." *Genes Dev* 5, no. 8 (1991): 1321-32.

Sive, H. L., B. W. Draper, R. M. Harland and H. Weintraub. "Identification of a Retinoic Acid-Sensitive Period During Primary Axis Formation in *Xenopus Laevis*." *Genes Dev* 4, no. 6 (1990): 932-42.

Smith, J. L. and G. C. Schoenwolf. "Notochordal Induction of Cell Wedging in the Chick Neural Plate and Its Role in Neural Tube Formation." *J Exp Zool* 250, no. 1 (1989): 49-62.

Smith, W. C. and R. M. Harland. "Expression Cloning of Noggin, a New Dorsalizing Factor Localized to the Spemann Organizer in *Xenopus* Embryos." *Cell* 70, no. 5 (1992): 829-40.

Smukler, S. R., S. B. Runciman, S. Xu and D. van der Kooy. "Embryonic Stem Cells Assume a Primitive Neural Stem Cell Fate in the Absence of Extrinsic Influences." *J Cell Biol* 172, no. 1 (2006): 79-90.

Stoykova, A. and P. Gruss. "Roles of Pax-Genes in Developing and Adult Brain as Suggested by Expression Patterns." *J Neurosci* 14, no. 3 Pt 2 (1994): 1395-412.

Subramanian, A., P. Tamayo, V. K. Mootha, S. Mukherjee, B. L. Ebert, M. A. Gillette, A. Paulovich, S. L. Pomeroy, T. R. Golub, E. S. Lander and J. P. Mesirov. "Gene Set Enrichment Analysis: A Knowledge-Based Approach for Interpreting Genome-Wide Expression Profiles." *Proc Natl Acad Sci U S A* 102, no. 43 (2005): 15545-50.

Suzuki, A., R. S. Thies, N. Yamaji, J. J. Song, J. M. Wozney, K. Murakami and N. Ueno. "A Truncated Bone Morphogenetic Protein Receptor Affects Dorsal-Ventral Patterning in the Early *Xenopus* Embryo." *Proc Natl Acad Sci U S A* 91, no. 22 (1994): 10255-9.

Taipale, J., J. K. Chen, M. K. Cooper, B. Wang, R. K. Mann, L. Milenkovic, M. P. Scott and P. A. Beachy. "Effects of Oncogenic Mutations in Smoothed and Patched Can Be Reversed by Cyclopamine." *Nature* 406, no. 6799 (2000): 1005-9.

Taira, M., J. P. Saint-Jeannet and I. B. Dawid. "Role of the *Xlim-1* and *Xbra* Genes in Anteroposterior Patterning of Neural Tissue by the Head and Trunk Organizer." *Proc Natl Acad Sci U S A* 94, no. 3 (1997): 895-900.

- Takahashi, K. and S. Yamanaka. "Induction of Pluripotent Stem Cells from Mouse Embryonic and Adult Fibroblast Cultures by Defined Factors." *Cell* 126, no. 4 (2006): 663-76.
- Teo, A. K., Y. Ali, K. Y. Wong, H. Chipperfield, A. Sadasivam, Y. Poobalan, E. K. Tan, S. T. Wang, S. Abraham, N. Tsuneyoshi, L. W. Stanton and N. R. Dunn. "Activin and Bmp4 Synergistically Promote Formation of Definitive Endoderm in Human Embryonic Stem Cells." *Stem Cells* 30, no. 4 (2012): 631-42.
- Toivonen, S. and L. Saxen. "The Simultaneous Inducing Action of Liver and Bone-Marrow of the Guinea-Pig in Implantation and Explantation Experiments with Embryos of *Triturus*." *Exp Cell Res*, no. Suppl 3 (1955): 346-57.
- Tomizawa, M., F. Shinozaki, T. Sugiyama, S. Yamamoto, M. Sueishi and T. Yoshida. "Activin a Is Essential for Feeder-Free Culture of Human Induced Pluripotent Stem Cells." *J Cell Biochem* 114, no. 3 (2013): 584-8.
- Tropepe, V., S. Hitoshi, C. Sirard, T. W. Mak, J. Rossant and D. van der Kooy. "Direct Neural Fate Specification from Embryonic Stem Cells: A Primitive Mammalian Neural Stem Cell Stage Acquired through a Default Mechanism." *Neuron* 30, no. 1 (2001): 65-78.
- Tsuneyoshi, N., E. K. Tan, A. Sadasivam, Y. Poobalan, T. Sumi, N. Nakatsuji, H. Suemori and N. R. Dunn. "The Smad2/3 Corepressor Snon Maintains Pluripotency through Selective Repression of Mesendodermal Genes in Human Es Cells." *Genes Dev* 26, no. 22 (2012): 2471-6.
- Turner, D. L. and C. L. Cepko. "A Common Progenitor for Neurons and Glia Persists in Rat Retina Late in Development." *Nature* 328, no. 6126 (1987): 131-6.
- Veien, E. S., J. S. Rosenthal, R. C. Kruse-Bend, C. B. Chien and R. I. Dorsky. "Canonical Wnt Signaling Is Required for the Maintenance of Dorsal Retinal Identity." *Development* 135, no. 24 (2008): 4101-11.
- Verani, R., I. Cappuccio, P. Spinsanti, R. Gradini, A. Caruso, M. C. Magnotti, M. Motolese, F. Nicoletti and D. Melchiorri. "Expression of the Wnt Inhibitor Dickkopf-1 Is Required for the Induction of Neural Markers in Mouse Embryonic Stem Cells Differentiating in Response to Retinoic Acid." *J Neurochem* 100, no. 1 (2007): 242-50.

Viczian, A. S., E. C. Solessio, Y. Lyou and M. E. Zuber. "Generation of Functional Eyes from Pluripotent Cells." *PLoS Biol* 7, no. 8 (2009): e1000174.

Vosough, M., E. Omidinia, M. Kadivar, M. A. Shokrgozar, B. Pournasr, N. Aghdami and H. Baharvand. "Generation of Functional Hepatocyte-Like Cells from Human Pluripotent Stem Cells in a Scalable Suspension Culture." *Stem Cells Dev* 22, no. 20 (2013): 2693-2705.

Walsh, C. and C. L. Cepko. "Clonally Related Cortical Cells Show Several Migration Patterns." *Science* 241, no. 4871 (1988): 1342-5.

Wang, S., M. Krinks, K. Lin, F. P. Luyten and M. Moos, Jr. "Frzb, a Secreted Protein Expressed in the Spemann Organizer, Binds and Inhibits Wnt-8." *Cell* 88, no. 6 (1997): 757-66.

Wassarman, P. M., T. E. Ukena, W. J. Josefowicz, G. E. Letourneau and M. J. Karnovsky. "Cytochalasin B-Induced Pseudo-Cleavage of Mouse Oocytes in Vitro. Ii. Studies of the Mechanism and Morphological Consequences of Pseudocleavage." *J Cell Sci* 26, (1977): 323-37.

Watanabe, K., D. Kamiya, A. Nishiyama, T. Katayama, S. Nozaki, H. Kawasaki, Y. Watanabe, K. Mizuseki and Y. Sasai. "Directed Differentiation of Telencephalic Precursors from Embryonic Stem Cells." *Nat Neurosci* 8, no. 3 (2005): 288-96.

Wataya, T., S. Ando, K. Muguruma, H. Ikeda, K. Watanabe, M. Eiraku, M. Kawada, J. Takahashi, N. Hashimoto and Y. Sasai. "Minimization of Exogenous Signals in Es Cell Culture Induces Rostral Hypothalamic Differentiation." *Proc Natl Acad Sci U S A* 105, no. 33 (2008): 11796-801.

Wichterle, H., I. Lieberam, J. A. Porter and T. M. Jessell. "Directed Differentiation of Embryonic Stem Cells into Motor Neurons." *Cell* 110, no. 3 (2002): 385-97.

Wilson, P. A. and A. Hemmati-Brivanlou. "Induction of Epidermis and Inhibition of Neural Fate by Bmp-4." *Nature* 376, no. 6538 (1995): 331-3.

Wilson, S. W. and C. Houart. "Early Steps in the Development of the Forebrain." *Dev Cell* 6, no. 2 (2004): 167-81.

- Wurst, W., A. B. Auerbach and A. L. Joyner. "Multiple Developmental Defects in Engrailed-1 Mutant Mice: An Early Mid-Hindbrain Deletion and Patterning Defects in Forelimbs and Sternum." *Development* 120, no. 7 (1994): 2065-75.
- Xuan, S., C. A. Baptista, G. Balas, W. Tao, V. C. Soares and E. Lai. "Winged Helix Transcription Factor Bf-1 Is Essential for the Development of the Cerebral Hemispheres." *Neuron* 14, no. 6 (1995): 1141-52.
- Yamada, T., S. L. Pfaff, T. Edlund and T. M. Jessell. "Control of Cell Pattern in the Neural Tube: Motor Neuron Induction by Diffusible Factors from Notochord and Floor Plate." *Cell* 73, no. 4 (1993): 673-86.
- Yamada, T., M. Placzek, H. Tanaka, J. Dodd and T. M. Jessell. "Control of Cell Pattern in the Developing Nervous System: Polarizing Activity of the Floor Plate and Notochord." *Cell* 64, no. 3 (1991): 635-47.
- Yang, Y. P. and J. Klingensmith. "Roles of Organizer Factors and Bmp Antagonism in Mammalian Forebrain Establishment." *Dev Biol* 296, no. 2 (2006): 458-75.
- Ying, Q. L. and A. G. Smith. "Defined Conditions for Neural Commitment and Differentiation." *Methods Enzymol* 365, (2003): 327-41.
- Ying, Q. L., J. Wray, J. Nichols, L. Batlle-Morera, B. Doble, J. Woodgett, P. Cohen and A. Smith. "The Ground State of Embryonic Stem Cell Self-Renewal." *Nature* 453, no. 7194 (2008): 519-23.
- Yu, P. B., C. C. Hong, C. Sachidanandan, J. L. Babitt, D. Y. Deng, S. A. Hoynig, H. Y. Lin, K. D. Bloch and R. T. Peterson. "Dorsomorphin Inhibits Bmp Signals Required for Embryogenesis and Iron Metabolism." *Nat Chem Biol* 4, no. 1 (2008): 33-41.
- Zhang, R. L., Z. G. Zhang, L. Zhang and M. Chopp. "Proliferation and Differentiation of Progenitor Cells in the Cortex and the Subventricular Zone in the Adult Rat after Focal Cerebral Ischemia." *Neuroscience* 105, no. 1 (2001): 33-41.
- Zimmerman, L. B., J. M. De Jesus-Escobar and R. M. Harland. "The Spemann Organizer Signal Noggin Binds and Inactivates Bone Morphogenetic Protein 4." *Cell* 86, no. 4 (1996): 599-606.
- Zuber, M. E., G. Gestri, A. S. Viczian, G. Barsacchi and W. A. Harris. "Specification of the Vertebrate Eye by a Network of Eye Field Transcription Factors." *Development* 130, no. 21 (2003): 5155-67.



Acknowledgments

1– Special Thanks

I still don't understand if PhD stands for “Philosophiae Doctor” or rather for “Permanent head Damage”, as I read on the Internet. Sure enough it has been pretty hard! And writing this Thesis did not improve the fitness of my past Summer. Anyhow, my sincere thanks goes...

To Elena and Silvia, sharing caffeine and... (mis)adventures. To Giuseppe, Michele, Roberto, Nicola and Luca, sharing caffeine and... chats. Then to Matteo, sharing train trips, mountains and photographs. To my dear Ombretta, sharing home, post-it notes, movies and everyday life. To Emiliano, sharing laughs. And to Tanya, sharing colors and smiles.

To Federico, a very good boss (after all). To Simona, for the same reason.

To Aurora, who showed me the darkness all around, and to Daniele, who helped me understand that there's light everywhere, as well.

To Elisa (twin), who's always next to me, even being so distant.

To Lorena, Francesca and Daria, 'cause having lunch on the grass in a sunny day can be a very special moment. To Milena, who's never upset. And to Manuela, sharing fun at congresses (and even back to normal routine).

To everyone in the Lab, especially Cristina, Valentina and Antonella.

And to my Family, for being so patient with me.

Thanks.

